Double Differential Thick Target Yields of Secondary Light-Ion Transport from Intermediate-Energy Hadron Experiments

A Dissertation Presented for the

Doctor of Philosophy

Degree

The University of Tennessee, Knoxville

Ashwin Paul Srikrishna

May 2018

Copyright © 2018 by Ashwin P. Srikrishna
All Rights Reserved.

To my mother, my father, and everyone back home who sacrificed everything for me

Acknowledgements

This work was made possible through funding by NASA: grants NNX12Al51A, NNX15AD90A and NNX17AI10A.

I would especially like to thank Dr. Lawrence Heilbronn for mentoring and advising me throughout this entire project – his patience in helping me transition from chemical engineering to nuclear engineering, as well as his academic help on this project has been incredible and it is impossible to put it into words.

I would also like to thank Dr. Lawrence Townsend, Dr. Maik Lang, and Dr. Pete Counce for serving on my committee and providing additional guidance and feedback on my dissertation and throughout graduate school.

I am grateful for all of the assistance from Dr. Michael Sivertz, Dr. Adam Rusek, and the rest of the staff at the NASA Space Radiation Laboratory and Brookhaven National Laboratory, Dr. Chiara La Tessa at the University of Trento, Dr. Cary Zeitlin from Leidos, and Dr. Martha Clowdsley, Dr. Steve Blattnig, Dr. John Norbury, Dr. Ryan Norman, Dr. Tony Slaba, Dr. Charlie Werneth and Mr. Dave Moore from the NASA-Langley Research Center for all of their help over the course of this project.

The help from members of the Heilbronn Research Group, past and present, was invaluable throughout this entire process – Dr. Pi-En Tsai, Dr. Matthew Beach, Dr. Natalie McGirl, Dr. Luis Castellanos, Mr. Hunter Ratliff, and Ms. Hui-Chen Wang.

Abstract

Understanding the effects due to the space radiation environment is an important step as space missions become longer and more complex – there is a major risk to both astronauts and their equipment, and optimizing the shielding is the best way to ensure the safety and success of such long-term missions to the Moon or Mars. Galactic Cosmic Rays (GCR) and Solar Energetic Particles (SEP) are the two main sources that comprise the space radiation field. At Earth-based testing facilities, it is impossible to fully replicate the conditions astronauts will face, so the use of particle transport codes to model the physics associated with shielding strategies are necessary, and these transport codes (both stochastic and deterministic) are dependent on relevant experimental data. Thus, the models help better understand the radiation physics in outer space, and experimental results help improve the models. Most recent model predictions of the effective dose in an enclosed shielding design (looking at radiation dose within a front surface and a back surface) suggested an optimal shielding thickness for aluminium, and an experiment to test these simulation results was conducted at the NASA Space Radiation Laboratory (NSRL) at Brookhaven National Laboratory (BNL). It is believed that a secondary radiation field is produced via interactions of initial GCR and SEP radiation within the shielding material, and this secondary field is directed inwards (towards the human environment on a spacecraft or lunar habitat) and is responsible for the predicted optimal shielding thickness. This thesis contains the energy- and spatial-dependent ("double differential") yield of Z = 1 and 2 light ions measured from the accelerator-based experiments at NSRL. Three nuclei (hydrogen, helium and iron) were accelerated to 400 and 800 MeV/n and fired at three thicknesses of aluminium shielding (20/40/60 g/cm2), and to detect the secondary light ions produced by beam interactions in the shielding, sodium iodide scintillation detector arrays were placed at 10 and 30 degrees off beam axis.

Table of Contents

CHAPTER 1: Background Information 1
1.1: Radiation 1
1.1.1: Ionizing Radiation 1
1.1.2: Radiation Concerns 2
1.2: Space Radiation Environment 3
1.2.1: Galactic Cosmic Rays 3
1.2.2: Solar Energetic Particles 7
1.3: Simulation Results 9
1.3.1: Dose Contribution Results 9
1.3.2: Secondary Radiation Field 11
CHAPTER 2: Literature Review and Original Work 13
2.1: Literature Summary 13
2.2: Original Work 16
CHAPTER 3: Experimental Design 18
3.1: Complete Experimental Overview 18
3.2: Sodium Iodide (NaI) Detectors 19
3.2.1: NaI Detector Layout 19
3.2.2: NaI Detector Workings 22
3.3: BNL Beamline Facility 23
3.4: Data Acquisition System 24
CHAPTER 4: Analysis Methodology 28
4.1: Data Cuts 28
4.1.1: Good-Beam Cut 28
4.1.2: Self-Time Cut 29
4.1.3: Time-of-Flight Cut 31
4.1.4: Energy Deposition Cut 32
4.1.5: Combining Cuts for Particle Identification 33
4.2: Time-Energy Conversion 35
CHAPTER 5: Data Analysis and Discussion 38
5.1: Timing Issues 38
5.1.1: Data Acquisition System – Timing 38
5.1.2: Mistimed Signals 38
5.1.3: Shifting the Signals 41
5.2: Data Corrections 44
5.2.1: Overlap Regions 44
5.2.2: Nuclear Attenuation Corrections 47
5.3: Unit Conversions 51

5.3.1: Channel-Time-Energy 51
5.3.2: Yield Normalizations 51
5.4: Data Removal 54
5.4.1: CS4-CS8 Threshold Issues 54
5.4.2: Minimum Data Requirements 57
5.5: Double-Differential Light Ion Yields 57
5.5.1: Yield Influences from variation in Incoming Beam Energy 58
5.5.2: Yield Influences from variation in Incoming Beam Species 69
5.5.3: NaI vs OLS – Fe 400 MeV/n 80
5.5.4: NaI vs MCNP – Fe400 MeV/n 87
5.6: Uncertainties and Error Propagation 99
5.6.1: Statistical Uncertainties 99
5.6.2: Systematic Uncertainties 99
CHAPTER 6: Conclusions and Future Work 106
LIST OF REFERENCES 108
APPENDICES 113
Appendix A: Raw Data 114
Appendix B: PHITS Input Script 326
Appendix C: Additional MCNP Comparisons 329
Appendix D: Additional OLS Comparisons 348
VITA 363

List of Tables

Table 1 – Existing angular- and energy-dependent data for proton-induced reactions..... 14

Table 2 – Existing angular- and energy-dependent data for alpha-induced reactions..... 15

Table 3 – Existing angular- and energy-dependent data for all Z > 2 induced reactions..... 15

Table 4 – Summary of Incoming Beam Species, Energies, and Target Configurations. The colours indicate the dates when the experiments were performed..... 19

Table 5 – Summary of Particle Detection as a function of shielding thickness and incoming beam species/energy..... 37

Table 6. Solid Angle Measurements for each Charged Scintillator Paddle..... 53

Table 7. Summary of light ion detection from 400 and 800 MeV/n iron systems for all three aluminium shielding thicknesses and corresponding figures for each light ion yield comparison..... 58

Table 8. Summary of light ion detection from 400 MeV/n iron, helium, and hydrogen nuclei systems for all three aluminium shielding thicknesses and corresponding figures for each light ion yield comparison 69

Table 9. Flight Path Distance Measurements for each Charged Scintillator Paddle..... 103

Table 10. Solid Angle Calculations..... 103

Table 11. Solid Angle Uncertainties..... 104

List of Figures

Figure 1. Elemental Nuclei Abundances of Galactic Cosmic Rays (GCR) at 2 GeV/n 4

Figure 2. Flux distribution for select GCR nuclei as a function of energy as measured near the Earth's orbit 6

Figure 3. SEP Abundances relative to Oxygen 8

Figure 4. Differential Effective Dose rate from different particle species as a function of kinetic energy behind 20 g/cm^2 Al shielding exposed to BON2010 GCR model at solar minimum conditions 10

Figure 5. Fractional contribution to effective dose as a function of aluminum shielding thickness for solar min (L) and solar max (R) for two different GCR models 10

Figure 6. Equivalent Dose contributions from neutrons and light ions in a water target between two aluminum shields over a series of simulations as a function of aluminum shielding thicknesses 12

Figure 7. 10° Sodium Iodide detector array (with phototubes) with three plastic scintillator paddles in front 20

Figure 8. Visual representation of upstream target, three sodium iodide arrays, and the downstream target within the target room at the NSRL facility at BNL 21

Figure 9. Data Acquisition System Trigger Logic Mapping 25

Figure 10A. Constant Fraction Discrimination at a 50% level with associated digital signals 26

Figure 10B. Constant Fraction Triggering technique: input pulse V_a, delayed signal V_d, inverted pulse V_c and flat constant k 27

Figure 11. 2D histogram illustrating charge deposition in the two scintillator paddles prior to an Fe 400 MeV/n beam hitting upstream 20 g/cm^2 target 29

Figure 12. 1D histogram of Charged Scintillator Paddle 5 timing values on a logarithmic scale 30

Figure 13. Time-of-Flight plot using timing values from start scintillator S1 and charge deposition from the front detector of the 10° sodium iodide array NaI 3 from Fe400 MeV/n particles on a 20 g/cm^2 Al upstream target 31

Figure 14. dE-dE plot comparing energy deposition in the front detector (NaI 3) with the energy deposition in the back detector (NaI 4) of the 10° sodium iodide detector array from Fe400 MeV/n particles on a 20 g/cm^2 Al upstream target 32

Figure 15. The proton particle identification cuts from the TOF plot (L) and dE-dE plot (R) for the 10° sodium iodide detector array from Fe400 MeV/n particles on a 20 g/cm^2 Al upstream target 33

Figure 16. Both TOF and dE-dE proton cuts added together in disjunction and displayed on the time-of-flight plot using timing values from start scintillator S1 and charge deposition from the front detector of the 10° sodium iodide array NaI 3 from Fe400 MeV/n particles on a 20 g/cm^2 Al upstream target 34

Figure 17. One-dimensional histogram of proton events projected on to the time (S1 TDC) axis 34

Figure 18. Comparison between signal/gate information between a properly timed (L) event, and a mistimed (R) event from a faster particle. 39

Figure 19. Unshifted (raw) data for Run 45 (Fe400 on Al 20) for the CS5 self-time peak 40

Figure 20. 10 deg NaI detector Time-of-Flight plot with the raw (uncorrected) data 41

Figure 21. Shifted (corrected) data for Run 45 (Fe400 on Al 20) for the CS5 self-time peak 43

Figure 22. 10 deg NaI detector Time-of-Flight plot with the shifted (corrected) data..... 43

Figure 23. Time-of-Flight plot at 10 degrees of 400 MeV/n iron nuclei incident upon a 20 g/cm^2 aluminium target illustrating isotope overlap regions 44

Figure 24. Selected portion of proton and deuteron spectra illustrating overlap region corrections 46

Figure 25. Nuclear Attenuation Yield Correction Factors as a function of incident particle energy via PHITS simulations..... 49

Figure 26. Nuclear Attenuation Yield Correction Factors as a function of incident particle energy via MCNP simulations..... 50

Figure 27. Proton Double Differential Yields as a function of incoming energy per nucleon from the 400 MeV/n Iron on the 20g/cm^2 (left) Aluminium shielding thicknesses detected at 10° and 30° NaI and OLS detectors. 56

Figure 28. Proton Double Differential Yields as a function of incoming energy per nucleon from the 400 and 800 MeV/n Iron beams on the 10° NaI Array at the 20g/cm^2 (left), 40 g/cm^2 (middle), and 60 g/cm^2 (right) Aluminium shielding thicknesses 62

Figure 29. Proton Double Differential Yields as a function of incoming energy per nucleon from the 400 and 800 MeV/n Iron beams on the 30° NaI Array at the 20g/cm^2 (left), 40 g/cm^2 (middle), and 60 g/cm^2 (right) Aluminium shielding thicknesses 63

Figure 30. Deuteron Double Differential Yields as a function of incoming energy per nucleon from the 400 and 800 MeV/n Iron beams on the 10° NaI Array at the 20g/cm^2 (left), 40 g/cm^2 (middle), and 60 g/cm^2 (right) Aluminium shielding thicknesses 64

Figure 31. Deuteron Double Differential Yields as a function of incoming energy per nucleon from the 400 and 800 MeV/n Iron beams on the 30° NaI Array at the 20g/cm^2 (left), 40 g/cm^2 (middle), and 60 g/cm^2 (right) Aluminium shielding thicknesses 65

Figure 32. Triton Double Differential Yields as a function of incoming energy per nucleon from the 400 and 800 MeV/n Iron beams on the 10° NaI Array at the 20g/cm^2 (left), 40 g/cm^2 (middle), and 60 g/cm^2 (right) Aluminium shielding thicknesses 66

Figure 33. Helion (3-He) Double Differential Yields as a function of incoming energy per nucleon from the 400 and 800 MeV/n Iron beams on the 10° NaI Array at the 20g/cm^2 (left), 40 g/cm^2 (middle), and 60 g/cm^2 (right) Aluminium shielding thicknesses 67

Figure 34. Alpha (4-He) Double Differential Yields as a function of incoming energy per nucleon from the 400 and 800 MeV/n Iron beams on the 10° NaI Array at the 20g/cm^2 (left), 40 g/cm^2 (middle), and 60 g/cm^2 (right) Aluminium shielding thicknesses 68

Figure 35. Proton Double Differential Yields as a function of incoming energy per nucleon from the 400 MeV/n Iron, Helium, and Hydrogen beams on the 10° NaI Array at the 20g/cm^2 (left), 40 g/cm^2 (middle), and 60 g/cm^2 (right) Aluminium shielding thicknesses 73

Figure 36. Proton Double Differential Yields as a function of incoming energy per nucleon from the 400 MeV/n Iron, Helium, and Hydrogen beams on the 30° NaI Array at the 20g/cm^2 (left), 40 g/cm^2 (middle), and 60 g/cm^2 (right) Aluminium shielding thicknesses 74

Figure 37. Deuteron Double Differential Yields as a function of incoming energy per nucleon from the 400 MeV/n Iron, Helium, and Hydrogen beams on the 10° NaI Array at the 20g/cm^2 (left), 40 g/cm^2 (middle), and 60 g/cm^2 (right) Aluminium shielding thicknesses 75

Figure 38. Deuteron Double Differential Yields as a function of incoming energy per nucleon from the 400 MeV/n Iron and Helium beams on the 30° NaI Array at the 20g/cm^2 (left), 40 g/cm^2 (middle), and 60 g/cm^2 (right) Aluminium shielding thicknesses 76

Figure 39. Triton Double Differential Yields as a function of incoming energy per nucleon from the 400 MeV/n Iron and Helium beams on the 10° NaI Array at the 20g/cm^2 (left), 40 g/cm^2 (middle), and 60 g/cm^2 (right) Aluminium shielding thicknesses 77

Figure 40. Helion (3-He) Double Differential Yields as a function of incoming energy per nucleon from the 400 MeV/n Iron and Helium beams on the 10° NaI Array at the 20g/cm^2 (left), 40 g/cm^2 (middle), and 60 g/cm^2 (right) Aluminium shielding thicknesses 78

Figure 41. Alpha (4-He) Double Differential Yields as a function of incoming energy per nucleon from the 400 MeV/n Iron and Helium beams on the 10° NaI Array at the 20g/cm^2 (left), 40 g/cm^2 (middle), and 60 g/cm^2 (right) Aluminium shielding thicknesses 79

Figure 42. Proton Double Differential Yields as a function of incoming energy per nucleon from the 400 MeV/n Iron beam on the 20g/cm^2 (left), 40 g/cm^2 (middle), and 60 g/cm^2 (right) Aluminium shielding thicknesses detected at 10° and 30° NaI and OLS detectors 82

Figure 43. Deuteron Double Differential Yields as a function of incoming energy per nucleon from the 400 MeV/n Iron beam on the 20g/cm^2 (left), 40 g/cm^2 (middle), and 60 g/cm^2 (right) Aluminium shielding thicknesses detected at 10° and 30° NaI and OLS detectors 83

Figure 44. Triton Double Differential Yields as a function of incoming energy per nucleon from the 400 MeV/n Iron beam on the 20g/cm^2 (left), 40 g/cm^2 (middle), and 60 g/cm^2 (right) Aluminium shielding thicknesses detected at 10° and 30° NaI and OLS detectors 84

Figure 45. Helion (3-He) Double Differential Yields as a function of incoming energy per nucleon from the 400 MeV/n Iron beam on the 20g/cm^2 (left), 40 g/cm^2 (middle), and 60 g/cm^2 (right) Aluminium shielding thicknesses detected at 10° NaI and OLS detectors 85

Figure 46. Alpha (4-He) Double Differential Yields as a function of incoming energy per nucleon from the 400 MeV/n Iron beam on the 20g/cm^2 (left), 40 g/cm^2 (middle), and 60 g/cm^2 (right) Aluminium shielding thicknesses detected at 10° NaI and OLS detectors 86

Figure 47. Comparison of proton yields at 10 deg NaI detector array with MCNP simulated yields at same angles from 400 MeV/n iron nuclei incident upon 20 g/cm^2 (left), 40 g/cm^2 (middle), and 60 g/cm^2 (right) Aluminium shielding 91

Figure 48. Comparison of proton yields at 30 deg NaI detector array with MCNP simulated yields at same angles from 400 MeV/n iron nuclei incident upon 20 g/cm^2 (left), 40 g/cm^2 (middle), and 60 g/cm^2 (right) Aluminium shielding 92

Figure 49. Comparison of deuteron yields at 10 deg NaI detector array with MCNP simulated yields at same angles from 400 MeV/n iron nuclei incident upon 20 g/cm^2 (left), 40 g/cm^2 (middle), and 60 g/cm^2 (right) Aluminium shielding 93

Figure 50. Comparison of deuteron yields at 30 deg NaI detector array with MCNP simulated yields at same angles from 400 MeV/n iron nuclei incident upon 20 g/cm^2 (left), 40 g/cm^2 (middle), and 60 g/cm^2 (right) Aluminium shielding 94

Figure 51. Comparison of triton yields at 10 deg NaI detector array with MCNP simulated yields at same angles from 400 MeV/n iron nuclei incident upon 20 g/cm^2 (left), 40 g/cm^2 (middle), and 60 g/cm^2 (right) Aluminium shielding..... 95

Figure 52. Comparison of triton yields at 30 deg NaI detector array with MCNP simulated yields at same angles from 400 MeV/n iron nuclei incident upon 20 g/cm^2 (left), 40 g/cm^2 (middle), and 60 g/cm^2 (right) Aluminium shielding..... 96

Figure 53. Comparison of helion yields at 10 deg NaI detector array with MCNP simulated yields at same angles from 400 MeV/n iron nuclei incident upon 20 g/cm^2 (left), 40 g/cm^2 (middle), and 60 g/cm^2 (right) Aluminium shielding..... 97

Figure 54. Comparison of alpha yields at 10 deg NaI detector array with MCNP simulated yields at same angles from 400 MeV/n iron nuclei incident upon 20 g/cm^2 (left), 40 g/cm^2 (middle), and 60 g/cm^2 (right) Aluminium shielding..... 98

Figure 55. Proton Time-of-Flight Calibration curves for the 10° NaI array across all three production points for the 20 g/cm^2 (top), 40 g/cm^2 (middle), and 60 g/cm^2 (bottom) shielding thicknesses 101

Figure 56. Nuclear attenuation correction factor percent errors across the five light ion species as a function of incident energy..... 105

CHAPTER 1
BACKGROUND INFORMATION

A major challenge to long-term manned space travel and exploration is understanding and characterizing the shielded radiation environment in space. Effective shielding strategies against the primary radiation in the solar system (galactic cosmic rays and solar energetic particles) are necessary to protect both the astronauts as well as the electronic equipment from radiative damage. Because the full GCR environment is impossible to replicate on Earth, transport codes are developed and used to simulate the radiative environment in space, and experiments are then designed to both verify model predictions and improve cross section models and data bases used in transport codes. These transport codes are used to transport radiation through proposed shielding environments. Currently there are some discrepancies amongst the models, but not enough experimental data to compare with and use to resolve those discrepancies. Both deterministic and Monte Carlo based models suggest that the major contribution to dose in moderate to heavily shielded environments in space comes from light ions – not necessarily from primary radiation sources, but instead from interactions within the shielding material itself. Understanding this secondary field is important both for the shielding implications for humans and equipment, but also to improve and verify model data through sensitivity analysis and uncertainty quantification. This novel experiment is one of the first to study secondary production (double-differential light ion yields) in thick shielding configurations beyond thin stopping targets, as well as including a second "back" target (representing the rear shielding of a spacecraft or habitat. This thesis measured the double-differential thick target yield of charged secondary light ions across a wide dynamic range of kinetic energies with high angular fidelity in an effort to understand production within the upstream target of an enclosed radiation shielding environment.

1.1 Radiation

1.1.1 Ionizing Radiation

Ionizing radiation refers to the specific types of radiation that carry enough energy to knock electrons out from either individual atoms or molecules. By removing electrons, the targeted atom or molecule becomes ionized. There are two types of such radiation – directly, and indirectly ionizing radiation. Directly ionizing radiation consists of charged particles that interact via the

Coulombic force – these include charged nuclei and high-energy beta particles. Neutrons are categorized as indirectly ionizing radiation because of their inability to directly ionize (electrically neutral) when interacting with matter – thus, they induce ionization by producing charged secondary particles (such as proton radiation) that then directly ionize a target material. Similarly, high-energy photons (x-rays and gamma rays) indirectly ionize atoms through physical processes like the photelectric effect and Compton scattering. And while beta particles are directly ionizing particles, the induced bremsstrahlung can be classified as indirectly ionizing radiation, as the resulting x-rays then ionize the surrounding matter. [1]

Radiation can be measured in 'dose' – and there are three different related calculations. Absorbed dose measures the amount of energy deposited per unit mass in a region (generally human tissue). This is a purely physical definition and does not represent a way to categorize radiation biological effects, as neither the type of radiation nor the material properties are factored in. Equivalent dose attempts to incorporate biological effects by applying a radiation weighting factor to the absorbed dose to account for differences in ionizing radiation. According to ICRP 103 report, photons have a weighting factor of 1, protons have a weighting factor of 2, alpha particles and other such heavy nuclei/fission fragments have a weighting factor of 20, and neutrons have a continuous interval ranging from 5 to 20 depending on energy. But the third type of calculated dose – effective dose – adds in a further weighting factor. Just as different ionizing radiation types have different levels of effect at a given dose, different body tissues have different reactions to radiation. Effective dose applies a tissue weighting factor to the equivalent dose to improve the mathematical correlations between dose and biological radiative effects. These weighting factors mathematically sum to unity and are defined such that the higher the value, the higher the risk of stochastic effects. [1]

1.1.2 Radiation Concerns

Understanding the nature of space radiation is a crucial component to planning a long-term space exploration mission – the harsh risks that both astronauts and the associated spaceflight equipment would be subject to is impossible to exactly reproduce on Earth, so a combination of both deterministic and Monte Carlo simulations as well as specific experimental results are necessary to understand the space radiation environment. Ionizing radiation can lead to the creation of free radicals within biological tissue, and the subsequent damage created by those radicals has major health effects for humans – radiation sickness, cataracts, and increased risk of cancer. There are

radiative concerns for electronic equipment too – ionizing radiation can lead to the creation of charge within an instrument, leading to an unexpected induced current. This can cause minor issues – false signals registering – as well as more permanent damage – abnormally high currents or voltage spikes that may not be easily fixed on-board. These events are known as Single Event Effects (SEE) and include upsets (SEU – a change of state within an electronic device), latch-ups (SEL – an unintended short-circuit of a power supply within the electronic device), gate ruptures (SEGR – destruction of thin oxide layers) and burnouts (SEB – permanent destruction of the MOSFET transistors). The SEU is an example of a minor (fixable) failure, whereas the SEL, SEGR and SEB are all examples of more permanent failures. Radiation-hardening techniques are used to help prevent SEE by incorporating different materials into the chips (like different insulation or different RAM) or the logical signals (adding redundancies to check for corrupted data). Any of these techniques used to reduce the effect of radiation on electronics requires an accurate description and understanding of the radiation incident upon such technologies. [2]

1.2 Space Radiation Environment

1.2.1 Galactic Cosmic Rays

In the solar system, there are two major sources of radiation – galactic cosmic rays (GCR), and solar energetic particles (SEP). In low- and near-Earth orbit there is an additional radiation source of protons and electrons in the trapped Van Allen belts surrounding the planet. The GCR is composed of high-energy nuclei that originate from deep space (i.e. outside of the heliosphere) and can be treated as an isotropic source. It is primarily composed of hydrogen and helium nuclei (83% and 13% respectively), with the nuclei elements $Z > 2$ composing roughly 1% of the overall spectra, and the remaining 3% coming from charged leptons (electrons, positrons, etc.). The GCR energy spectra is also quite wide – ranging from 10^6 to 10^{20} eV. [3]

Figure 1 shows the elemental abundances within the GCR spectra (expressed as fluence rates). There are two major drop points – at $Z = 2$ and $Z = 26$. The former illustrates the dominance of proton and alpha particles, while the latter represents the point at which nuclear fusion becomes energetically unviable and heavier elements require galactic “explosions” (i.e. supernovae) to be produced. [4]

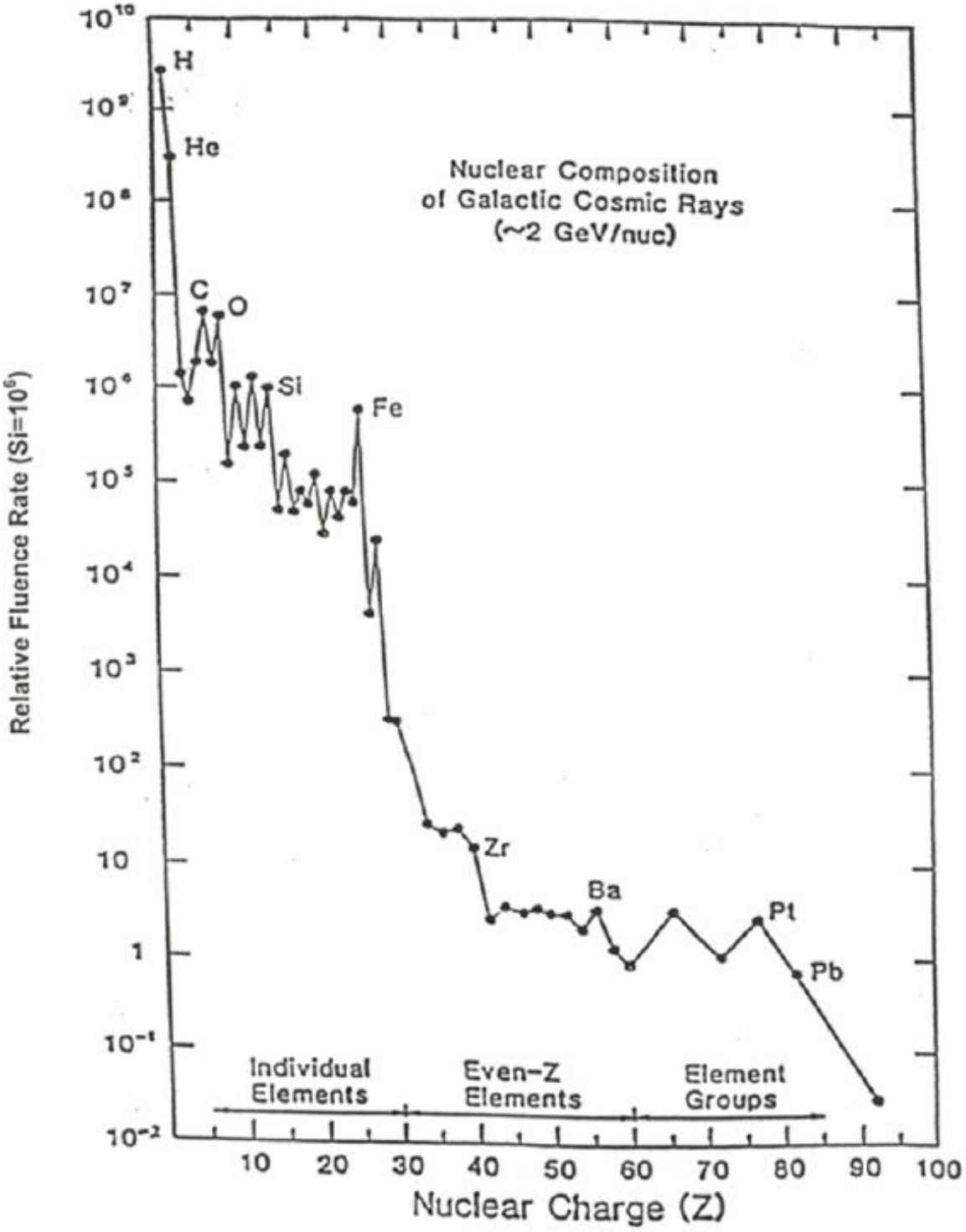


Figure 1. Elemental Nuclei Abundances of Galactic Cosmic Rays (GCR) at 2 GeV/n [4]

Figure 2 shows the flux distribution for select major nuclei as a function of energy as measured near Earth's orbit. As the energies decrease along the *x*-axis, a few "branches" in measured flux occur. This is a result of the effect of the solar modulation on galactic cosmic rays – depending on the solar cycle, the flux of the lower-energy cosmic rays varies. At high solar activity ("solar maximum"), the increased production of charged ions in the solar wind increases the strength of the magnetic field around the solar system. This increased magnetic field strength modulates the incoming galactic cosmic ray energy spectra. Similarly, at the other extreme of the solar cycle ("solar minimum"), cosmic rays encounter less magnetic "resistance" and the measured fluxes are higher. Solar wind modulation on galactic cosmic rays is most notable at the lower end of the GCR energy spectra, explaining why the branches in Figure 2 can only be seen through portions of the plot. The higher curves illustrate the corresponding flux during solar minimum, and the lower curve represents the flux at solar maximum. The hydrogen data has been multiplied by a factor of 5 to provide curve differentiation.

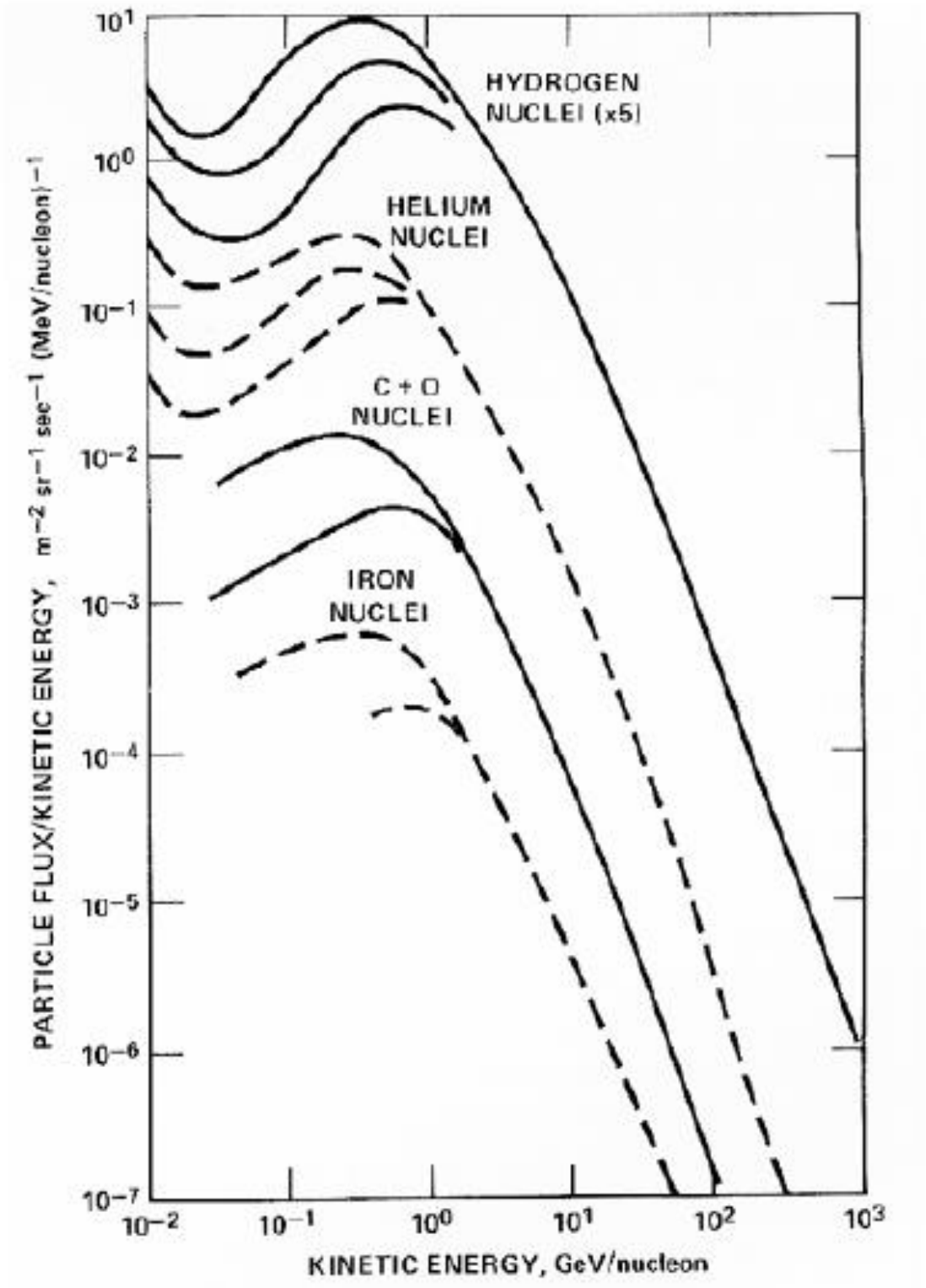


Figure 2. Flux distribution for select GCR nuclei as a function of energy as measured near the Earth's orbit [5]

1.2.2 Solar Energetic Particles

The other components of the radiation environment in deep space are the solar energetic particles (SEP) that are generated from the sun. The primary source of these particles are solar flares and coronal mass ejections. SEP events have less consistency in their relative elemental abundances as a result of the variability in factors influencing solar events such as the Earth's position relative to the Sun, the length of flares, the intensity of flares, or the frequency of flares. There seem to be no consistencies that indicate a preferred mechanism with regards to specific particles or energy ranges. But despite this, the base composition of SEP events seems to match the composition of elements within the solar atmosphere (corona and photosphere). Impulsive SEP events have higher nuclei abundancies relative to the corona (higher helium and iron/oxygen nuclei presence) and are also accompanied by the release of electrons and high energy photons (gamma and x-rays). Figure 3 shows the abundance of elements in solar flares (relative to oxygen), and shows that much like GCR, the bulk of SEP events are hydrogen and helium nuclei. The filled circles represent abundances in the solar corona, the asterisks represent abundances in the photosphere, and the solid line shows the abundances in solar flare events. The boxes show the variability in 'normal' SPE events versus iron/helion-rich SEP events. [3]

However, unlike the GCR spectrum in Figure 1, there is a much stronger cutoff at Z = 26 because of the fusion energy threshold at iron. Because it is energetically unfavorable to fuse nuclei heavier than iron, the Sun is not capable of producing heavier nuclei on its own at its current stellar age.

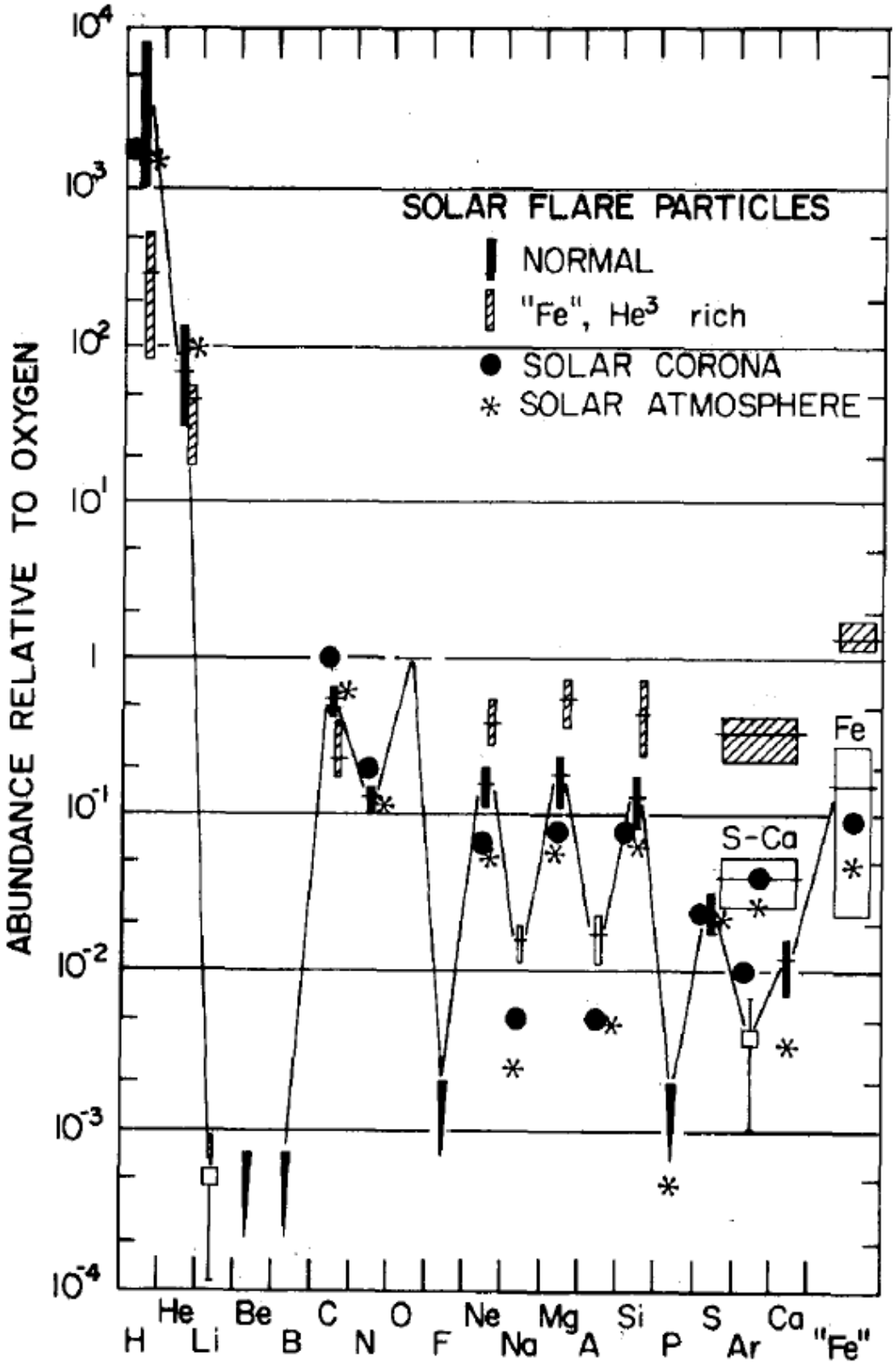


Figure 3. SEP Abundances relative to Oxygen [3]

1.3 Simulation Results

1.3.1 Dose Contribution Results

Building models for both the GCR and SEP environments are important steps towards being able to fully understand, predict and prepare for a manned long-term space mission, because being able to incorporate the information in Figures 1-3 into a computer model will allow for a better understanding of the radiation environment as it pertains to radiation shielding design. The standard GCR model used by NASA is the Badhwar-O'Neill (BON) model, and validation and further developments are based on comparisons with measurements taken from the Advanced Composition Explorer/Cosmic Ray Isotope Spectrometer instrument. However, it is important to quantify the individual influences of ion type and energies on the overall effective dose calculations, which is the important result from GCR model calculations with regards to space travel. The deterministic NASA code HZETRN was used to model the effective dose rate contributions from the major ions present in the GCR spectrum (all scaled to provide visible comparisons between curve shapes). As can be seen in Figure 4, the majority of the dose contribution comes from the proton and alpha particles, and for the most part, the ions have a fairly narrow peak with respect to their boundary kinetic energies. Protons are the exception – they have a broad peak extending across several orders of magnitude (100 MeV/n through 10 GeV/n), suggesting that proton contribution to dose is highest in comparison to other ions as well as the energy spectra. Integrating each curve results in the cumulative effective dose (including contributions from any secondary reaction products). [6]

This information is further summarized in Figure 5, where dose contributions from $Z = 1$, $Z = 2$ and $Z > 2$ from a BON GCR model at both solar min and solar max are compared across varying aluminium thicknesses for two discrete energy bins ($E > 500$ MeV/n and $E < 500$ MeV/n). The contributions to dose from $Z > 2$ nuclei naturally decreases (across both energy bins), as they collide with the aluminium shielding and create biologically less damaging secondary ions. Similarly, this secondary field is why the influence from protons incident on the shielding increases with more aluminium – there is more shielding material to create secondary and tertiary particles via nuclear collisions. The impact of solar activity can be seen for maximum GCR activity (left) and minimum (right) – at solar max, the lower energy GCR nuclei are modulated by solar winds, and the contribution from more energetic ions increases (~45% from $Z > 2$ at solar max versus

~35% from Z > 2 at solar min). This is most visible in the Z > 2 block (blue lines). Perhaps the most glaring trend, though, is that at increased levels of aluminium shielding, the effective dose contribution of high energy protons and alpha particles continues to rise while the other four bins (low energy proton, low energy alpha, and both high and low energy heavy ions) all slowly decrease. [6]

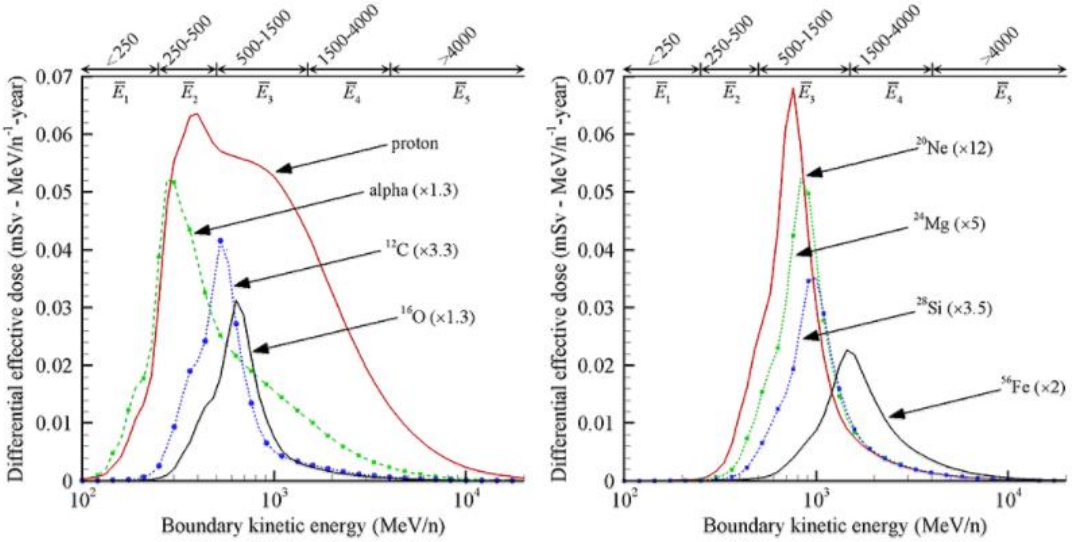


Figure 4. Differential Effective Dose rate from different particle species as a function of kinetic energy behind 20 g/cm^2 Al shielding exposed to BON2010 GCR model at solar minimum conditions [6]

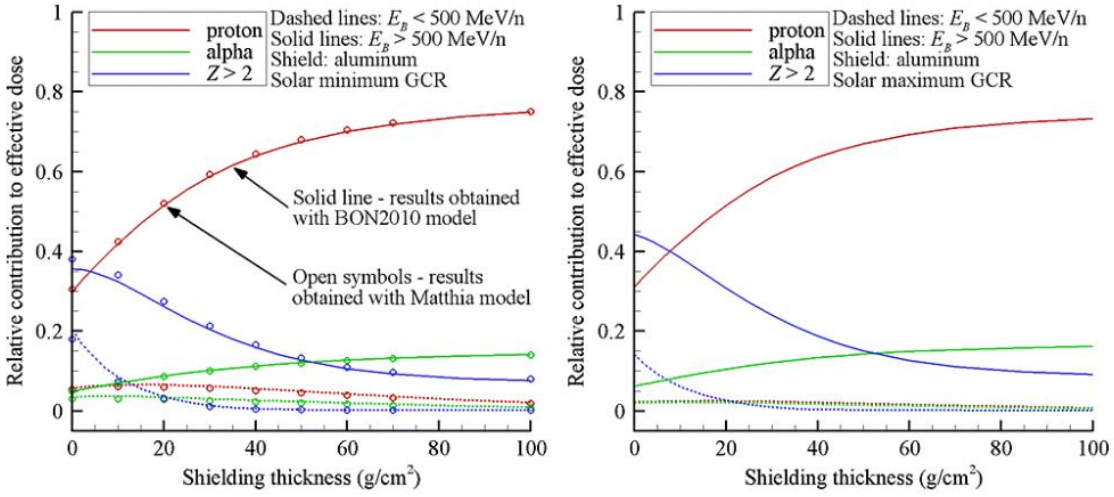


Figure 5. Fractional contribution to effective dose as a function of aluminum shielding thickness for solar min (L) and solar max (R) for two different GCR models [6]

1.3.2 Secondary Radiation Field

In an effort to better understand the physics and influence of the secondary radiation field produced by the primary field (GCR and SEP) interacting within the shielding material, NASA performed more simulations to specifically study the total dose equivalent from the space shielding environment using both deterministic and Monte Carlo codes. The introduction of a "back slab" of aluminium shielding, with a water sample (representing generic human body tissue) in the middle, more accurately represents the shielding setup of both spacecraft and surface habitats. Radiation from an external source (GCR and SEP) may not only interact within the front shielding but penetrate and interact again in the back shielding of the spacecraft. Additionally, the secondaries produced from such nuclear collisions may also interact further within the back shielding. Figure 6 shows the equivalent dose within the water target from neutrons and light ions ($Z \leq 2$), because as seen earlier, the primary charged nuclei are hydrogen and helium, and the primary dose contributors are hydrogen and helium nuclei. The percentages shown at each data point represent the differences between the Monte Carlo codes, and the deterministic NASA code 3DHZETRN (N = 34). The variations in HZETRN (N=1, N=2, N=34) represent the number of "directions" that the code can transport particles through. As N increases, the number of calculable directions increases. Because it is a deterministic code, particle movements can only be directly calculated (as opposed to a Monte Carlo code, which can randomly sample from a full range of motion) and thus, as N approaches infinity, HZETRN approaches a Monte Carlo simulation. The associated errors (with each data point) were computed as a percentage representing half the difference between the extreme data points (maximum minus minimum) and the average of the extreme data points. There is a minimum roughly around 20 g/cm^2 in nearly every completed simulation, which suggests that there is an optimal shielding thickness, and that increasing the shielding does not necessarily increase overall radiation protection. The increased shielding blocks the incoming GCR/SEP particles, but also provides more material for them to interact with. Of the increased dose due to charged secondary ions – the bulk of this rise (~70%) is from proton contributions with the remaining light ions (deuteron, triton, helion, alpha) providing an additional 10 to 20% contribution. [7]

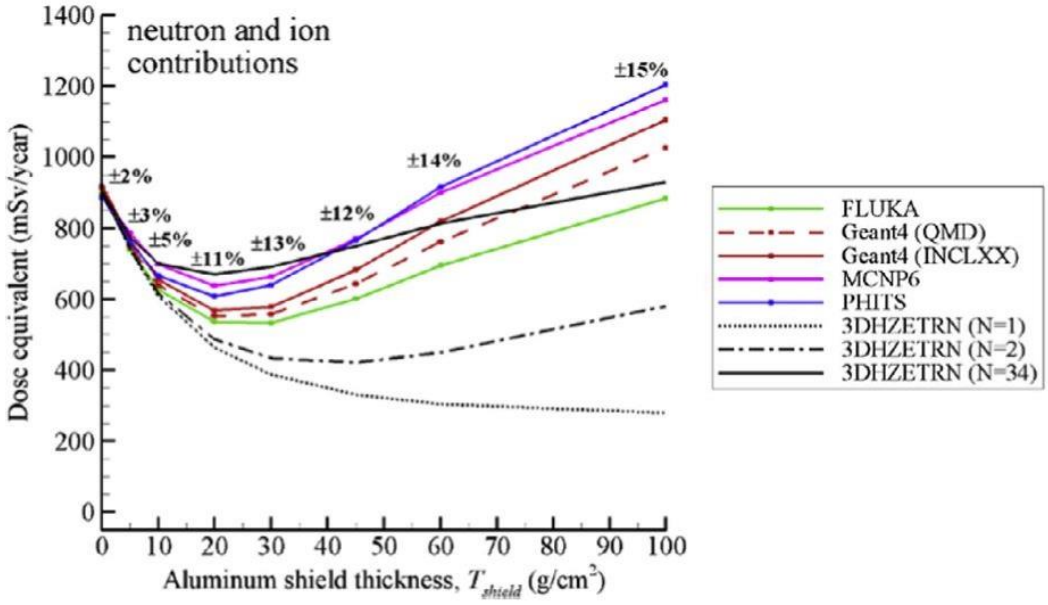


Figure 6. Equivalent Dose contributions from neutrons and light ions in a water target between two aluminum shields over a series of simulations as a function of aluminum shielding thicknesses [7]

Understanding the dynamics of this secondary field, as well as corroborating the differences amongst the codes at increased thicknesses is of major interest for future manned deep-space travel. The presence of an "optimal" shielding thickness has ramifications for spacecraft and habitat design – excess shielding can increase the cost of travel spacecraft, increase space flight challenges and increase the radiation threat to both astronauts and the equipment within the habitat modules. It also suggests that there is a minimum and unavoidable dose, which has additional implications in mission design – specifically mission duration. Furthermore, finding such patterns for other shielding materials can lead to hybrid solutions designed to mitigate these radiative effects by artificially increasing the shielding ability whilst still working within optimal thickness ranges. One such example would be to combine a hydrogen-rich material with a strong and lightweight material – the metal would be durable enough to withstand the heat and stress of spaceflight, and the hydrocarbon would be effective at neutron attenuation as well as limiting the amount of secondary production due to the lack of target fragments produced in interactions with hydrogen nuclei.

CHAPTER 2
LITERATURE REVIEW AND ORIGINAL CONTRIBUTION

The goal of this research is to produce yield spectra for the five major charged light ion contributors to the effective dose from space radiation in an enclosed environment: protons (^{1}H), deuterons (^{2}H), tritons (^{3}H), helions (^{3}He), and alphas (^{4}He). Specifically, this research focuses on double-differential thick target yields dependent on angular (steradian) and energy (MeV/n) differentials. Because this is the first nuclear physics experiment focused on space radiation transport to incorporate a second target (the "back" downstream target of an enclosed system), the initial calculations are all designed towards developing these energy- and angular-dependent thick target yields. The original contribution of this research is to determine the double-differential thick target yields of the secondary light ions produced within an enclosed shielding (i.e. between a front and rear shield) setup, and to help NASA and other code developers validate the physics models. And for the latter, specifically with model uncertainty quantification and sensitivity analysis. [12]

2.1 Literature Summary

The majority of previous nuclear physics experimental work has been about measuring cross-sectional values for the production of light ions from interactions between heavy nuclei and lighter materials, and those measurements that incorporate similar energy and angular double-differentials are summarized in Tables 1-3. The italicized information represents any commonalities between the existing experimental data and our March 2016 experimental data set. Tracking the fragmentation products as a function of both incoming the incoming beam and the target itself is tantamount to understanding this secondary radiation field – and most of the experimental data summarized in Tables 1-3 are with thin or stopping (i.e. designed for the initial incoming beam to exactly attenuate in the material) targets. These are thin targets intentionally, because the experiments have been designed to determine certain particle production pathways. As such, the experimental work summarized ensure that every other reaction type is minimized – to focus on the cross-sectional measurements of the specific reaction. This is also done by using lower incoming particle energies. The lower energies can help mitigate fragmentation, and instead focus on particular scattering types. As a result, the measurements listed in Tables 1-3 were not focused on experimentally mimicking galactic cosmic ray interactions with thick targets.

Table 1. Existing angular- and energy-dependent data for proton-induced reactions

Beam	Energy (MeV/n)	Target	Produced Ions	Angles (°)	Source
1H	600	Be, C, Na, *Al*, Ca, Fe, Au	*1H, 2H, 3H, 3He, 4He*	*30*, 45, 75, 105	[13]
1H	29, 39, 62	C, *Al*, Fe, Sn, Au, Bi	*1H, 2H, 3H, 3He, 4He*	25-60	[14]
1H	1200, 1900, 2500	Au	*1H, 2H, 3H, 3He, 4He*, 6Li, 7Li, 8Li, 9Li, 7Be, 9Be, 10Be, 10B, 11B, 12B	16, 65, 100	[15]
1H	*800*	Li, C, *Al*, Ca, V, Zr, Pb	*1H*	5, *7*, 9, 11, *13*, 15, 20, 25, *30*	[16]
1H	100	Ni	*1H*	8-25	[17]
1H	392	Ca	*1H*	N/A	[18]
1H	30	Li	*1H, 2H. 3H. 4He*, 5He, 5Li, 6Li	10-90	[19]
1H	27, 49, 63	Si	*1H, 2H, 3H, 3He, 4He*	10-165	[20]
1H	1000, 2000, 3000	Be, C, Cu, Pb	*1H*	0, 17, 32	[21]
1H	210, 300, 480	Ag	Li-Na	20, 90, 160	[22]
1H	62.9	Pb	*1H, 2H, 3H, 3He, 4He*	25-155 (increments of 10)	[23]
1H	300, 392	O, V, Tb, Ta, Au, Pb, Bi	*1H*	N/A	[24]
1H	2200	C, *Al*, Cu, Ag, Au, U	8Li	N/A	[25]
1H	300, 392	C, *Al*, Nb	*1H*	20-105	[26]
1H	240-2100	*Al*, Ca, Ag, U	*1H, 2H, 3H*	N/A	[27]
1H	100, 164	*Al*, Ni, Pb	*1H, 2H, 3H, 3He, 4He*	25-150	[28]
1H	90	*Al*, Ni, Zr, Bi	*1H, 2H, 3H, 3He, 4He*	15-155	[29]
1H	100	Ni	*1H, 2H, 3H, 3He, 4He*	15-155	[29]

Table 2. Existing angular- and energy-dependent data for alpha-induced reactions

Beam	Energy (MeV/n)	Target	Produced Ions	Angles (°)	Source
4He	15	*Al*	Li-O	20-130	[30]
4He	2-6	Co	*1H, 4He*	N/A	[31]
4He	180	*Al*, Ag, Ta	*1H, 2H, 3H, 3He, 4He*	60, 90, 120	[32]
4He	6, 12, 15	Si	*1H, 2H, 3H, 3He, 4He*, 6Li, 7Li, 7Be	10-165	[20]
4He	240-2100	*Al*, Ca, Ag, U	*1H, 2H, 3H*	N/A	[27]

Table 3. Existing angular- and energy-dependent data for all Z>2 induced reactions

Beam	Energy (MeV/n)	Target	Produced Ions	Angles (°)	Source
7Li	5	Mg	Be-F	15-120	[33]
7Li	6	Ni	*1H, 2H, 3H, 3He, 4He*, 7Li	20, 39, 45, 50, 53, 55, 60	[34]
12C	13	Al	7Be, 9Be, B-Si	10-50	[35]
12C	35	Au	*1H, 2H, 3H, 3He, 4He*, 6He	40, 60, 75, 90, 105, 120, 140	[36]
14N	35	C, Ni, Ho	Li-N	7-23	[37]
14N	9, 11, 15	Nb	*1H, 2H, 3H, 3He, 4He*	N/A	[38]
14N	35	Ho, Ni	Li, Be, B, C	7-30	[39]
16O	52, 100, 147	*Al*, Ni, Sn, Au	*1H, 2H, 3H, 3He, 4He*	N/A	[40]
18Ar	240-2100	*Al*, Ca, Ag, U	*1H, 2H, 3H*	N/A	[27]
20Ne	43	Ni, Ag, Ta	*1H, 2H, 3H, 3He, 4He*	N/A	[41]
20Ne	240-2100	*Al*, Ca, Ag, U	*1H, 2H, 3H*	N/A	[27]
20Ne	100, 156	Au	*1H, 2H, 4He*	N/A	[42]
27Al	13	C	7Be, 9Be, B-Si	10-50	[35]
28Si	200, 300	H	*4He*, 12C, 14N, 16O, 18F, 20Ne, 22Na, 26Al, 28Si	0-11, 60-120	[43]
86Kr	5.5-8.5	Cu	H-Cr	N/A	[44]

2.2 Original Work

This experiment uses thicker targets than those referenced in Tables 1-3 to allow for multiple interactions by both the primary beam ions and the secondaries (and tertiaries, and so on). Using a very thick target allows for investigating more realistic scenarios for space shielding – focusing on every possible interaction, and not just specific individual pathways. Hydrogen, helium, and iron nuclei provide a sampling of the galactic cosmic ray and solar energetic particle spectra, and beam energies on the order of 400-800 MeV/n provide the most relevant boundary energies of the cosmic ray energy spectrum. This research goes beyond understanding the specific cross-sectional measurements and investigates the types of interactions that would occur in the space radiation environment. Furthermore, this work starts to fill in some gaps in the intermediate energy ranges for all three data sets. There are even more gaps in thick-target experiments (mainly due to their scarcity in general), and all three experimental runs aim to expand this in a way that promotes further experimentation for both model validation as well as the shielding implications in high radiation environments. Furthermore, aluminium serves as a popular shielding material, whereas most targets used in previous experiments were unfeasible as shielding materials in space – a lot were either too heavy (high Z materials) or too expensive to fabricate.

Thus, the originality of these experimental runs at the NASA Space Radiation Laboratory comes from the implementation of a secondary "back" target, the usage of relevant space shielding materials, the usage of relevant space shielding thicknesses, the selection of nuclei within space radiation charge distribution, and the selection of energies within the space radiation energy distribution. The experimental design was chosen to mimic the conditions of the computer simulations executed across several transport codes by NASA (Figure 6). However, the focus with this experiment is on the double-differential thick target yield, as opposed to calculated dose equivalent. The collected data presented in this dissertation does not directly factor in production within the rear shielding, but instead provides yield measurements within the enclosed shielding for the secondary radiation field. Additionally, the light ions produced within the upstream target will provide a boundary condition for production within the rear shielding. These interactions from the secondary field can lead to backscattered neutrons and tertiary light ions. [12]

Furthermore, the usage of sodium iodide (NaI) detectors is a unique addition to this experiment. Thallium-doped sodium iodide scintillation detectors are primarily used for the detection of high

energy photons – gamma rays, for instance. But NaI detectors have high density, high atomic number and higher light output compared to other inorganic scintillators. The first two qualities lead to a greater stopping power than organic detectors – critical for providing high stopping power for the Z = 1 and 2 light ions. The third quality is crucial for energy resolution. And because the resolution of a detector increases with higher energy deposition, this experiment also showed that NaI detectors can be also be used as effective charged particle detectors. [8]

The data and methods presented in this thesis are a portion of a much larger set of measurements that are necessary to understand and quantify secondary light ion production. Thus, the presented results will also be compared with both current transport code results as well as similar light ion yields measured during the same experiment using organic liquid scintillator detectors.

CHAPTER 3
EXPERIMENTAL DESIGN

In an effort to both understand this secondary radiation field, as well as resolve computation differences amongst the codes, an experiment was designed with similar setup parameters to the twin shields water target model simulations.

3.1 Complete Experimental Overview

The experimental work was performed at the NASA Space Radiation Laboratory (NSRL) at Brookhaven National Laboratory (BNL) in conjunction with their accelerator facilities to accelerate various nuclei at a series of energies for a few shielding configurations (summarized in Table 4). Protons and alpha particles make up the bulk of the GCR and SEP flux, carbon and silicon were selected from the mid-Z range of the spectra, and iron represents the heaviest ions with statistical importance. The energies these nuclei were accelerated to span the peaks of both the GCR fluxes (Figure 2) and the effective dose rates (Figure 4). There were three shielding configurations considered – pure aluminium, a high-density polyethylene polymer ($[\text{-}CH_2\text{-}]_n$), and a hybrid combination of the two. These were chosen because of their current popularity in space shielding designs. The hybrid targets were designed to see if the high density of hydrogen atoms (polyethylene) in tandem with the higher Z of the aluminium could work concurrently to modulate incoming radiation more efficiently than either shielding material could individually.

Three different total thicknesses were used for the front (upstream) target, and one fixed thickness for the back (downstream) target. The upstream shielding varied across three targets of 20 g/cm^2, 40 g/cm^2 and 60 g/cm^2 for the individual aluminium and polyethylene, and two hybrid targets consisting of a 'thin' hybrid (10 g/cm^2 of each) and a 'thick' hybrid (10 g/cm^2 aluminum + 50 g/cm^2 polyethylene) shielding target. The downstream target was fixed at 60 g/cm^2 of polythene for the polyethylene runs, and 60 g/cm^{2}of aluminium for both the aluminium and hybrid targets. The two targets were centered along the beam axis and were placed 3.5 meters (target center to target center) away from each other. The upstream targets were 30 cm (high) x 100 cm (wide), and the downstream targets were 100 cm x 100 cm.

Table 4 – Summary of Incoming Beam Species, Energies, and Target Configurations. The colours indicate the dates when the experiments were performed.

Species / Energy	Hydrogen	Helium	Carbon	Silicon	Iron
400 MeV/n	Al , CH_2 , Al+CH_2	Al , CH_2 , Al+CH_2	Al , CH_2 , Al+CH_2	Al , CH_2 , Al+CH_2	Al , CH_2 , Al+CH_2
800 MeV/n	Al , CH_2 , Al+CH_2	Al , CH_2 , Al+CH_2	Al , CH_2 , Al+CH_2	Al , CH_2 , Al+CH_2	Al , CH_2 , Al+CH_2
1500 MeV/n	-	Al , CH_2 , Al+CH_2	Al , CH_2 , Al+CH_2	Al , CH_2 , Al+CH_2	Al , CH_2 , Al+CH_2
2500 MeV/n	Al , CH_2 , Al+CH_2	-	-	-	-

Blue	Dec-16	Al	Aluminium
Red	Mar-16	$[-CH_2-]_n$	Polyethylene
Green	Nov-17	Al+CH_2	Hybrid

3.2 Sodium Iodide (NaI) Detectors

3.2.1 NaI Detector Layout

To determine the light ion yield in the space between the upstream and downstream shielding targets, a pair of sodium iodide detector arrays were placed on the beamline, 10° off beam axis and 30° off beam axis, each 3 meters away from center of the upstream target. Each sodium iodide array composed of two 4 x 4 x 16 in^3 (10.16 x 10.16 x 40.64 cm^3) detectors, with the widest face of the detector being open towards the upstream target. And by using a second sodium iodide, the 'depth' of the detector can be essentially doubled while also providing additional energy deposition data to be used in the data analysis. Each 16" face is covered by three plastic scintillation paddles to set the trigger on events within the sodium iodide. In addition to setting the timing, the paddles also help with particle identification as well as segmentation of the sodium iodide array, allowing for finer granularity on the angular distributions spanned by the arrays. By specifically focusing on the incoming light ions that traverse only through one paddle into the sodium iodide detectors (instead of all three added in disjunction), angular yields can be calculated for three different angles centered around 10° and 30°. Figure 7 shows the three plastic scintillator paddles set up in front of a sodium iodide array. As can be seen, the middle paddle is centered on 10°, and the paddles

on either side are offset by 2.7° respectively. The same is true for the 30° array (not pictured, but similarly set up).



Figure 7. 10° Sodium Iodide detector array (with phototubes) with three plastic scintillator paddles in front.

A schematic of the beam room at NSRL with the sodium iodide detectors in relation to the upstream and downstream targets, the beam dump, and the layout of the target room can be seen in Figure 8. The beam enters in from the bottom of the diagram, travelling upwards through the red upstream target first (the 20 g/cm^2 target is shown), then the green sodium iodide detector arrays are shown in the middle (0°, 10° and 30° arrays from left to right) before the 60 g/cm^2 red back target (and the opening in the back wall represents the opening to the beam dump). Not shown are a pair of scintillators along the beamline, and in front of the first (upstream) target. These two plastic scintillators were placed there to verify the quality of the beam by ensuring that the beam particles that initiate the data acquisition sequence did not have any interactions in the air, resulting in the fragmentation into different nuclei. Furthermore, these scintillators were used to keep track of the number of incoming beam particles incident upon the target – an important statistic for data normalization. Not shown are six organic liquid scintillators that were placed on the opposite side of the target room from the sodium iodide arrays – these detectors were used to collect both neutron and light ion yields, and were outside of the purview of this thesis, and thus are excluded from further discussion.

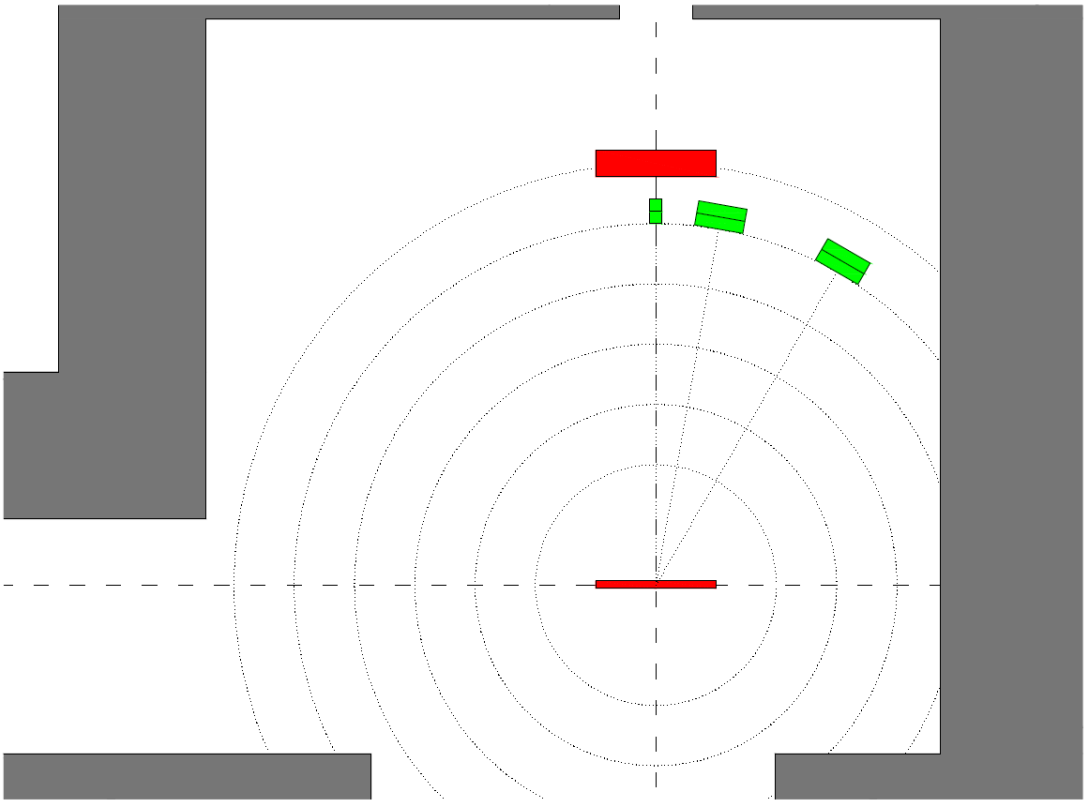


Figure 8. Visual representation of upstream target, three sodium iodide arrays, and the downstream target within the target room at the NSRL facility at BNL. [9]

3.2.2 NaI Detector Workings

Thallium-doped sodium iodide (NaI) detectors (as illustrated in Figure 7) are scintillation detectors. As radiation enters the detector and interacts, photons are produced (scintillation). This is done via coulombic interactions within the detector – as the charged light ion traverses the detector crystal, atoms along the direction of travel get excited. As they return to a ground state, the excess energy is released in the form of the scintillation photons. Photomultiplier tubes are used to convert the light signal into a current of photoelectrons. Further multiplication is done to amplify the current into a more stable electronic pulse that contains information about the energy of that specific incident radiation. The thallium is used as an impurity activator – to help extend the emission time of the photons. The main benefits of using inorganic crystals – like sodium iodide – are the greater stopping power (higher density) and the high light output (greater energy resolution). These qualities are very helpful when trying to detect Z = 1 and Z = 2 nuclei. [8]

The resolution of a detector is a function of the energy deposited within the detector, and generally improves as more energy is deposited. Sodium iodide detectors are generally used for detecting high-energy photons (like gamma rays), but their properties suggest that detection of charged particles is possible as well. And because of the detector layout, the utilization of two NaI detectors per array provides ample stopping power (leading to high energy deposition within the detectors), which then increases the dynamic energy range of the collected charged particle data. Light output refers to the efficiency of the scintillation material at converting the incoming radiation ionization energy into photons. Thus, to properly identify the incoming radiation particle energy, full deposition within the detector is a necessity – and unlike lighter particles (e.g. electrons, photons, etc.), the ions of interest are massive enough that backscattering out of the detectors is not a concern. Scintillation detectors are generally less productive with the detection of heavy ions (relative to photons and electrons) due to reduced light output from quenching effects. The high ionization power of these charged particles leads to a reduced scintillation light output signal – in inorganic scintillators, the light output from charged particles varies from 50-70% of the light output from electrons of the same energy. But of the inorganic crystals, NaI detectors offer the highest light output along with higher stopping power. And this energy deposition is critical towards calculating the energy spectra of each incoming particle species. [8]

3.3 BNL Beamline Facility

The ions used at NSRL come from two different sources: the Tandem Van de Graaff facility, and the Electron Beam Ion Source (EBIS). The former, as the name suggests, uses an electrostatic Tandem to strip electrons off ions ranging in mass from hydrogen up to gold. It has since been replaced by the EBIS, a more reliable linear accelerator ("linac") based system. However, the Tandem Van de Graaff is still used to provide hydrogen nuclei (protons) to NSRL, and was the source used for the proton experimental runs performed in accordance with Table 1. The major benefit of the upgrade to EBIS is the removal of the stripping foils used by electrostatic generators (like the Tandem Van de Graaff) – solving issues with the instability in electron stripping efficiency. Furthermore, because EBIS can directly produce high charge states, NSRL (and other accelerator divisions at BNL) can accelerate heavy ions of all species up to uranium. The electron beam used by EBIS is subjected to a superconducting solenoid, and the high magnetic field greatly compresses the electron beam to a very high density. Drift tubes are used to control the intensity of the magnetic field. The desired cations are produced by bombarding the targeted [neutral] atoms with this dense electron beam at an orthogonal angle. It is primarily a gas phase reaction which relies upon the energy of the electrons being greater than the ionizing energy of the targeted atom. Naturally, as the charge state builds up, the efficiency of electron ionization decreases – thus, for higher mass ion beams, EBIS is not always able to achieve the highest charge state. The EBIS is categorized as a 'pre-injector' and is fed into a booster synchrotron. The booster is used to accelerate the ions and does so using a radio-frequency quadrupole accelerator (RFQ). The RFQ both accelerates and focuses the beam of charged ions. The booster feeds into the Alternating Gradient Synchrotron (AGS) ring, where hundreds of magnets are placed facing inward and outward ("alternating-gradient focusing") such that the beam is further focused in both the horizontal and vertical planes. Simultaneous focusing is impossible, but by alternating the orientation of the quadrupole magnets, focusing can be done in the horizontal plane and then vertical plane. The RFQ serves as a conduit between the source (EBIS) and the primary accelerator (AGS). From AGS, particles can be delivered either to the Relativistic Heavy Ion Collider (RHIC) facility at BNL, or to NSRL. Both EBIS and AGS can be operated such that RHIC and NSRL can operate simultaneously, but there can be slight losses in beam quality whenever both RHIC and NSRL are used concurrently. [10]

These beam imperfections – beam instabilities, beam loss in quality, or an inability to produce the desired high charge states (for heavier nuclei) – can directly impact the experimental runs. To offset these issues, changes to the beam spill structure are implemented. The spill length represents the time duration in which the beam particles are delivered and changing this length can improve the ratio of desired triggers to total triggers. Similarly, the beam shape (structure) itself can be modified to control the distribution of the beam and how evenly the particles are extracted.

3.4 Data Acquisition System

The data acquisition logic electronics is plotted in Figure 9. The signal from the sodium iodide detectors are at the very bottom, and as it can be seen, are not in the trigger logic. What that means is events detected by the sodium iodide arrays do not start, or "trigger", the acquisition logic system – instead, that is done by the nine charged scintillator paddles ("CS 1-9") in front of each of the three sodium iodide detector arrays. The beam particles, as they enter the target room, traverse through the initial two scintillator paddles ("S1" and "S2"), and in doing so, create a "common start" signal. This ensures that the initial timing for every acquired data point is the same. However, by delaying this signal by a quarter of a microsecond (250 ns), data acquisition is instead stopped when the delayed signal is registered – a "common stop." This ensures that each signal processed (both live triggers and any erroneous triggers) is ended. However, this also means that there is reverse timing information within the system – higher timing values (TDC – "time-to-digital convertor") would imply a shorter timing signal. Successful triggers could come from any of the nine paddles in front of the sodium iodide arrays, or from the other six detectors in the target room (no data from those detectors was used in this thesis). Thus, any trigger initiated from a CS paddle will record the integrated charge (ADC – "analogue-to-digital convertor") data deposited within the respective sodium iodide array. Triggers from any of the other liquid detectors should lead to a pedestal (zero) signal in the sodium iodide detector, since there would be no respective scintillation and thus no signal for the ADC to process. The specific ADC modules used can be more accurately referred to as QDCs ("charge-to-digital convertor") because these units specifically convert the integrated charge pulse to a digital signal. That is, the output of the QDC is the charge deposition within the corresponding detector unit (sodium iodide detector, CS paddle, etc.). [8]

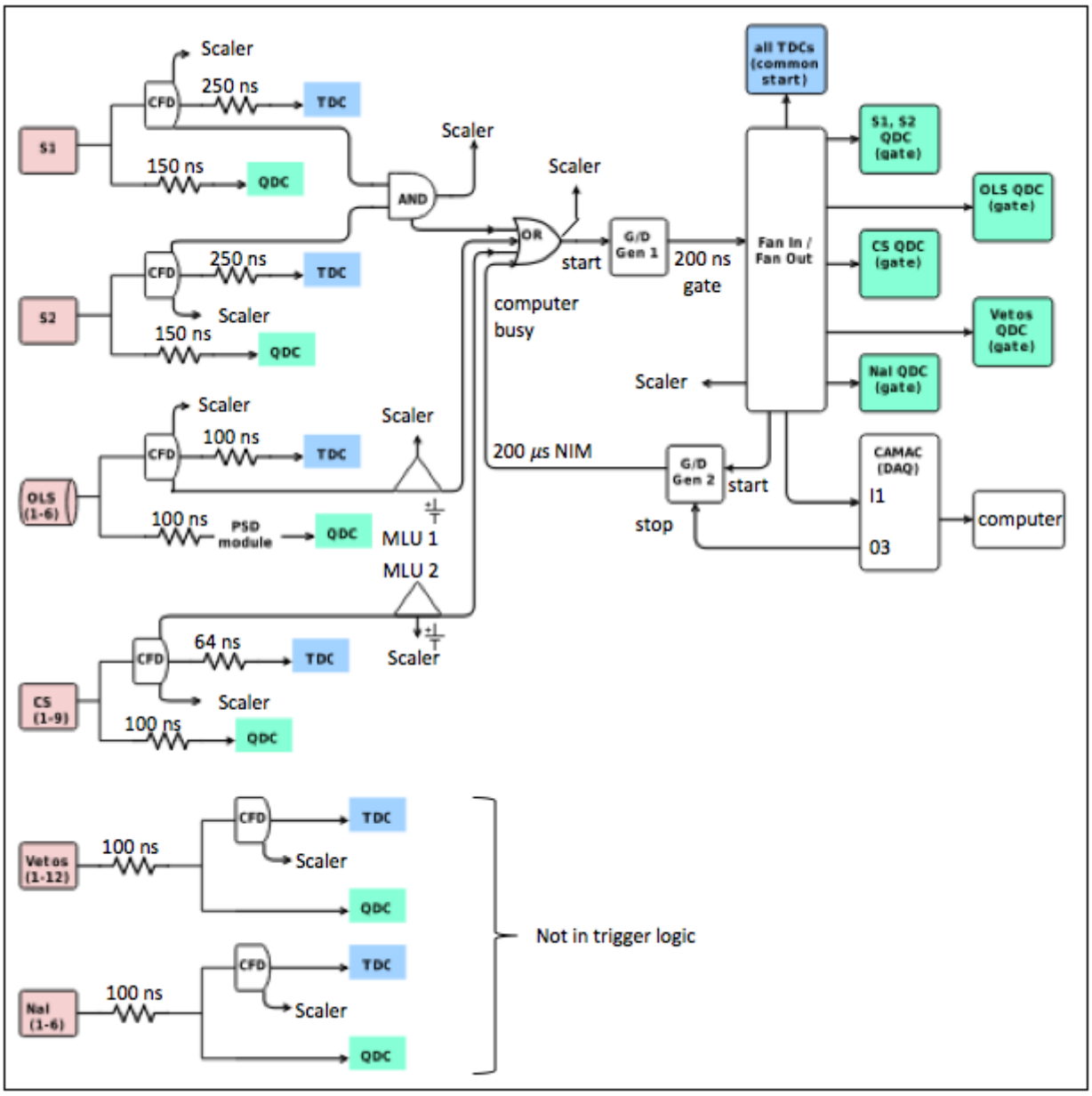


Figure 9. Data Acquisition System Trigger Logic Mapping [11]

The timing logic presents a few challenges – each incoming pulse does not always have the same amplitude. As a result, two coincident signals could have different timing outputs based on differences in rise-time. Depending on the slope of the rise-time, each signal may hit the fixed trigger threshold at a different time. A threshold is used to ensure a valid pulse is recorded and is just not electronic noise. This method of generating logic signals is called Leading Edge Triggering and relies solely on rise-time to set the trigger. The associated error due to the dependence of timing with pulse height is referred to as a time "walk" and can be prevented by modifying the trigger logic. A secondary source of time walk can come from discriminators that rely upon a fixed charge (i.e. the area under the pulse curve) to set the trigger, and similarly, differences in pulse shape can lead to differing timing signals (e.g. a sharper rise may lead to a lower integrated pulse). To fix this, a more complicated version of triggering is used – and the experiments at NSRL relied on this technique – known as Constant Fraction Triggering. In this, the initial pulse is split: one part is delayed, and the other inverted. The delayed signal is offset by the time it takes the pulse to go from the constant fraction level (pre-determined and usually set at 50% – see Figure 10A) to the pulse peak. The inverted signal is multiplied by a flat constant, and then summed together. As a result, the pulse is now bipolar, and there is a zero-crossing point. This point is at the flat constant fraction of the original signal. This process is illustrated in Figure 10B, and while does not fully eliminate the time walk, that effect is significantly mitigated. [8]

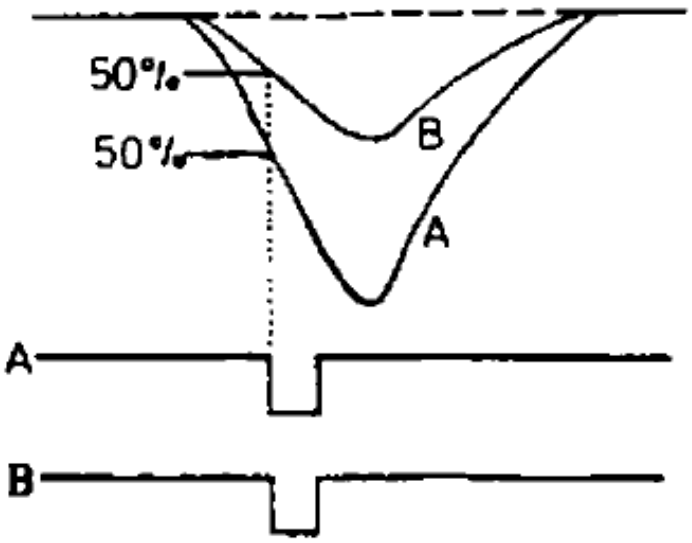


Figure 10A. Constant Fraction Discrimination at a 50% level with associated digital signals [8]

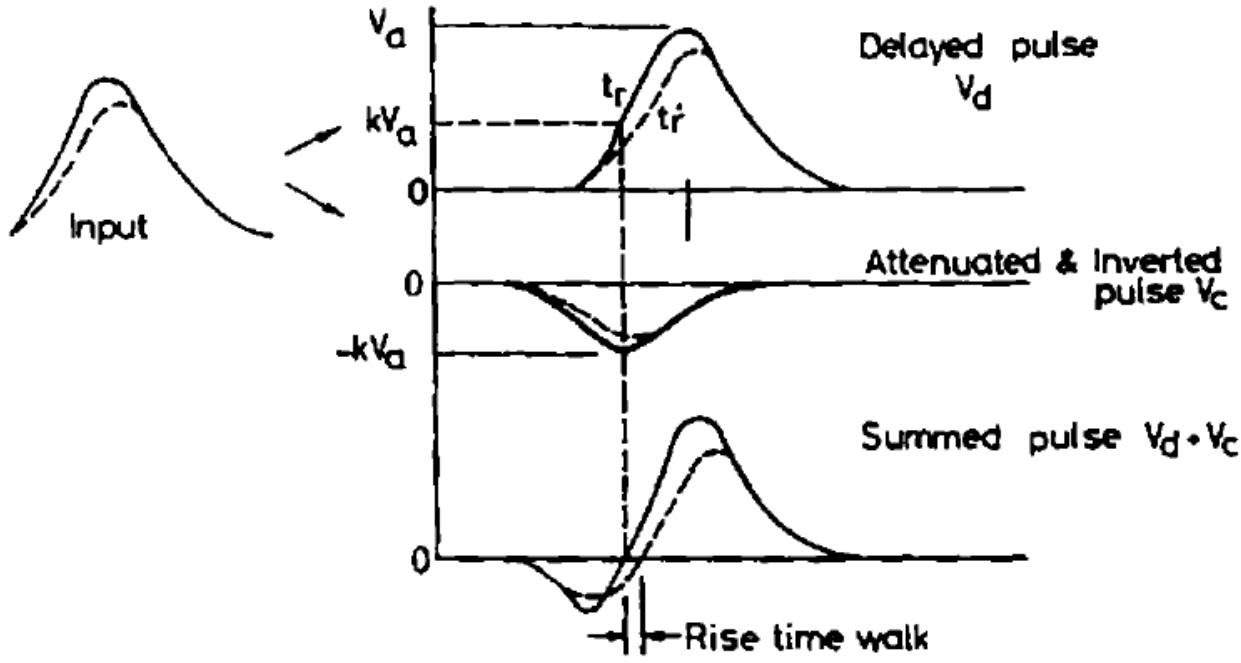


Figure 10B. Constant Fraction Triggering technique: input pulse V_a, delayed signal V_d, inverted pulse V_c and flat constant k [8]

CHAPTER 4
ANALYSIS METHODOLOGY

For each combination of energies, target types, target thicknesses and beam species (Table 1), more than hundreds of thousands of events were collected. Isolating the useful portions of the data set requires a series of cuts to cull as much of the extraneous or incomplete data points as possible. The data were analyzed using the CERN-developed data analysis software ROOT. The plots shown through this section are from the combined data set from iron beams at 400 MeV/n incident on a 20 g/cm^2 aluminium target.

4.1 Data Cuts

4.1.1 Good-Beam Cuts

The first step is to select all the initial beam particles that helped set the trigger in the two scintillators (S1 and S2). A two-dimensional histogram comparing charge deposition from each scintillators' QDC during the iron 400 MeV/n runs on a 20 g/cm^2 aluminum target is depicted in Figure 11. The two axes represent charge deposition in the upstream scintillator (*y*-axis) versus the downstream scintillator (*x*-axis) with the number of counts (*z*-axis) on a logarithmic scale. The concentrated spot in the middle is where the graphical cut was made (the black outline), and represents the events that deposited the correct amount of energy in each scintillator ("good beam"), whereas the continuing diagonal represents incoming beam events of lower energy (due to interactions in the air), and the horizontal portion (coming out of the good beam spot) represents those that deposited the correct energy in the first scintillator (the upstream paddle S1) and because of an interaction within the paddle, had less energy to deposit in the second paddle (the downstream S2). The purpose of the good beam cuts is to select events where the incoming beam particles that did not have interactions (leading to significant energy loss) prior to the upstream shielding target.

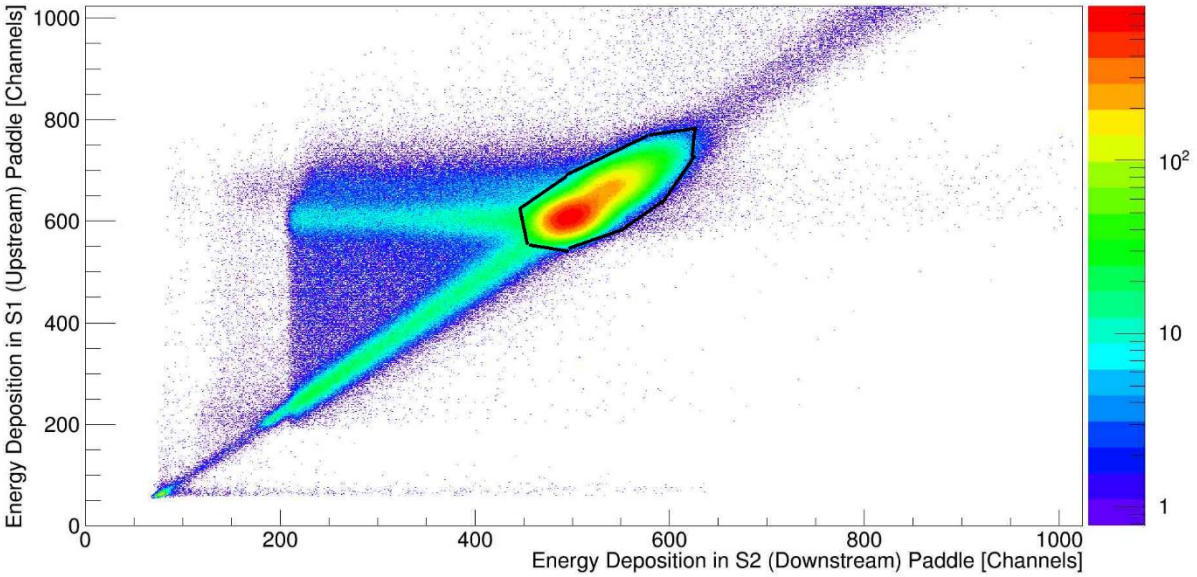


Figure 11. 2D histogram illustrating charge deposition in the two scintillator paddles prior to an Fe 400 MeV/n beam hitting the upstream 20 g/cm^2 target

4.1.2 Self-Time Cut

Events within S1 and S2 set one portion of the coincidence trigger, so the next step is to identify which particles set the other half of the coincidence. For the sodium iodide detectors, these were done with the charged scintillator (CS) paddles placed in front of the 16" face of each detector array. For the 10° array, these were the paddles labelled CS4-6, and for the 30° these were the paddles labelled CS7-9. A sample 1D timing histogram for the TDC of paddle CS5 is shown in Figure 12. There are two peaks of interest on the CS TDC plots – the peak around channel 180, and the peak past channel 4000. There are two peaks because the triggering system can be set by either one of the nine CS paddles, or one of the six organic liquid detectors. When a CS paddle sets the trigger (CS5, in the situation shown in Figure 12), the timing data is recorded by when the particle interacts with the CS paddle. When the trigger is set by anything else (i.e. not CS5), the timing data is recorded into the "pile-up" peak around channel 4000, because there was no timing signal from CS5, and therefore the value gets thrown into the maximum channel the TDC unit was capable of recording. Thus, making specific cuts on each of the CS paddles around the peak at channel 180 allows for the subsequent data analysis to be focused on particles that specifically interact with each of the relevant CS paddles. These cuts – generally a few channels wide, and

specifically centered on the peak – are referred to as "self-time" cuts, because they focus on the data points created by events triggered by that specific CS paddle. On a linear scale, the self-time cut stands out from the extraneous points more but is presented here on a logarithmic scale to show that there are other mistimed points that must be culled. The black arrow in Figure 12 points to the self-time peak for the CS5 paddle. The range of channels encompassing that peak would be defined as the "self-time cut." The orange arrow points to the aforementioned "pile-up" peak around channel 4000.

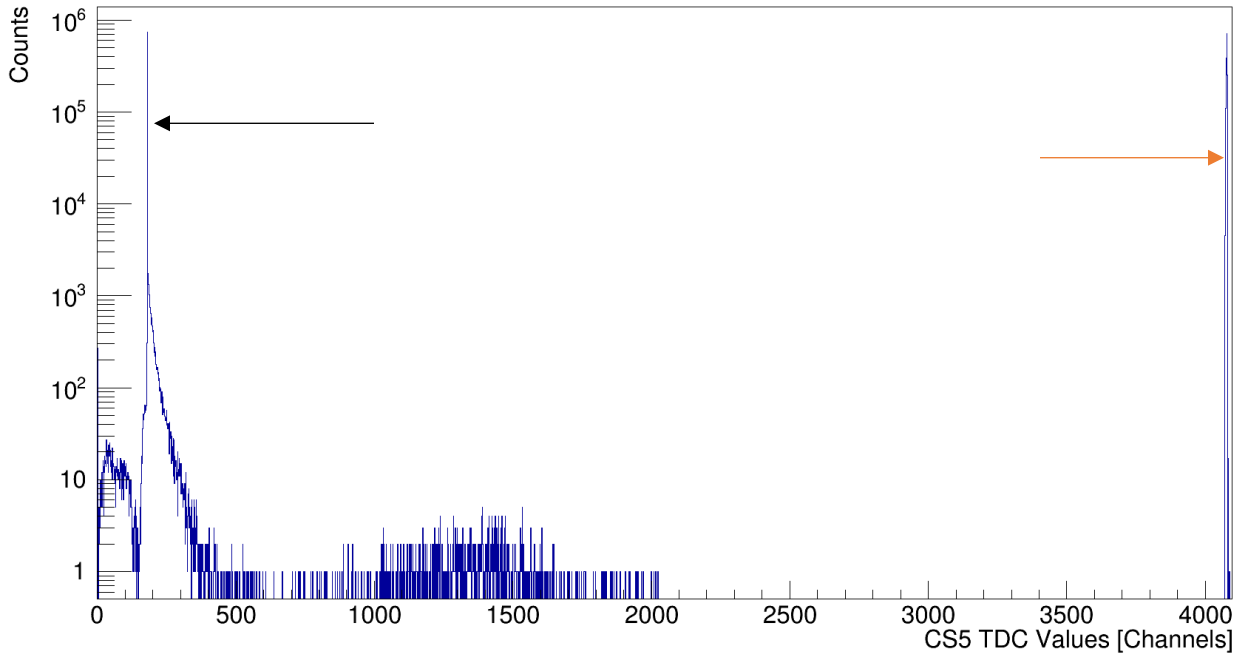


Figure 12. 1D histogram of Charged Scintillator Paddle 5 timing values on a logarithmic scale

Figure 12 is specifically for the middle paddle (CS5) associated with the 10° sodium iodide detector array. Creating self-time cuts for the other paddles (CS4, CS6) gives two options for data analysis: adding the self-time cuts in disjunction (OR gates), or treating them each individually, and artificially separating the detector into three individual detectors. The former is used to ensure there is enough visible data to create particle identification cuts, and then the latter is used when creating yield spectra for each light ion, so individual spectra can be produced from events in each paddle

4.1.3 Time-of-Flight Cut

Figure 13 shows a two-dimensional plot of Time-of-Flight (TOF) versus energy deposition (given in QDC channel number) for events in the 10° array with the two types of cuts applied to the data. The plot correlates the timing data from the start scintillators (S1 TDC) with the coincident charge deposition data in the front detector of the sodium iodide array (NaI 3 QDC). As can be seen, there are roughly 6 overlapping wishbone curves – the bottom three representing Z = 1 particles, the middle two representing Z = 2, and the relatively faint line at the top representing Z = 3. The first five are the ones of interest – proton, deuteron, triton, helion, and alpha particles (labelled p, d, t, He3 and He4 respectively). The peak in each curve represents the "punch-through" point for each particle – it represents the energy at which particles were stopped just before exiting the front detector in the sodium iodide array. Thus, points to the left of the peak represent the respective charged ions that fully deposit their energy in the detector, and points to the right represent those that the ions that made it into the back detector of each array pairing. Graphical contour cuts around each of these curves allow the data sets to be further culled to the point where individual yield data can be calculated. Five individual one-dimensional histograms can be created as a function of timing information. It is important to note that depending on the incoming beam species and energies, not all five light ions of interest are always visible. This information is summarized in Table 5.

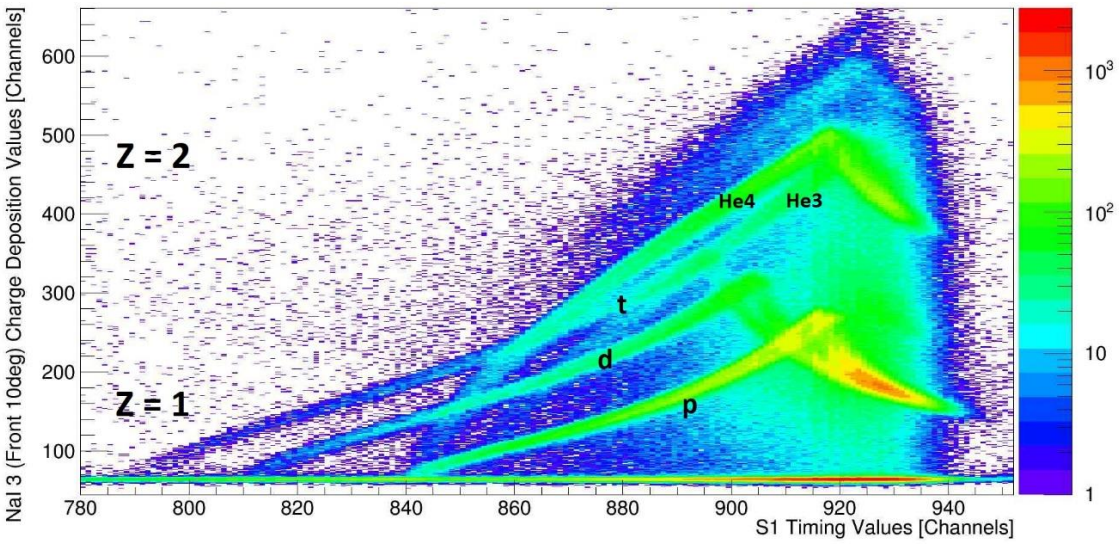


Figure 13. Time-of-Flight plot using timing values from start scintillator S1 and charge deposition from the front detector of the 10° sodium iodide array NaI 3 from Fe400 MeV/n particles on a 20 g/cm^2 Al upstream target.

4.1.4 Energy Deposition Cut

In addition to the particle identification cuts made with the TOF data in Figure 13, comparing the energy deposition (dE) in the front detector versus the back detector of each array can extend the depth of these cuts – as can be seen, the Z=1 and Z=2 particles all start to converge together past the punch-through point. Using a dE(NaI3) vs dE(NaI4) plot of the two detectors in each sodium iodide detector array (Figure 14), further identification cuts can be made to help distinguish the Z = 1 particles in the punch-through energy region of the TOF plot. Here, you can see three (rotated) wishbone curves in the lower left and one signal in the upper right representing the helium ions. By making similar graphical cuts on this data, they can be added in disjunction to the TOF particle identifying cuts, and each 1D histogram can be extended past the punch-through point of the front detector, by using the energy deposition in the back detector. And as before – the efficacy of the dE vs dE method here is even more dependent on incoming beam species and energies, because all the particles recorded in Figure 14 need to be energetic enough to deposit a statistically important amount of energy in the back detector – that is to say, they need to be able to traverse through four inches of sodium iodide, as well as three layers of stainless steel detector housing (0.04" thick).

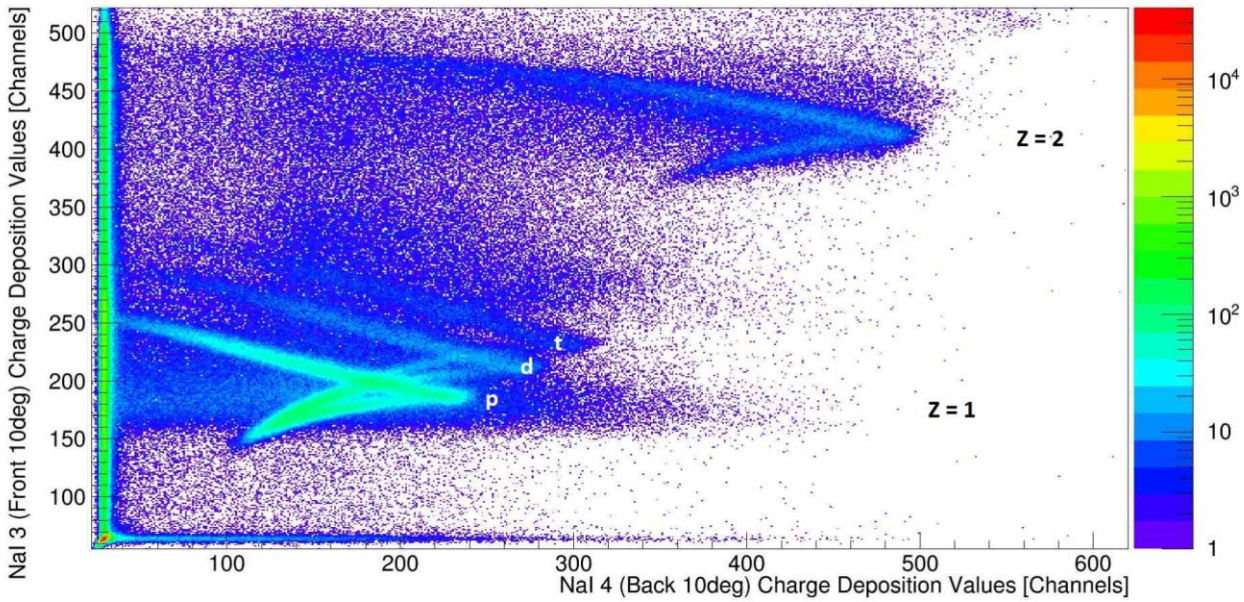


Figure 14. dE-dE plot comparing energy deposition in the front detector (NaI 3) with the energy deposition in the back detector (NaI 4) of the 10° sodium iodide detector array from Fe400 MeV/n particles on a 20 g/cm^2 Al upstream target

4.1.5 Combining Cuts for Particle Identification

Figure 15 illustrates an example particle identification cut for the proton lines from both the TOF and dE-dE plots, and Figure 16 shows what the TOF plot looks like when the two contour cuts are added together in disjunction. These two plots are used because they can most clearly be used to isolate each particle species. And because these two plots are derived from different techniques, they must be added together on the same plot to provide a consistency in the translation from the module channel numbers to an incoming particle energy. The two-dimensional time-of-flight vs energy deposition plot provides the best way to do this, as the conversion from channel timing (TDC) to incoming particle energy (in MeV/n) is more accurate than converting from the QDC data. At this point, the two-dimensional data is projected onto the time axis (S1 TDC values on the *x*-axis) to create a one-dimensional histogram of the proton data for the 400 MeV/n iron nuclei incident on a 20 g/cm^2 aluminium upstream target (Figure 17).

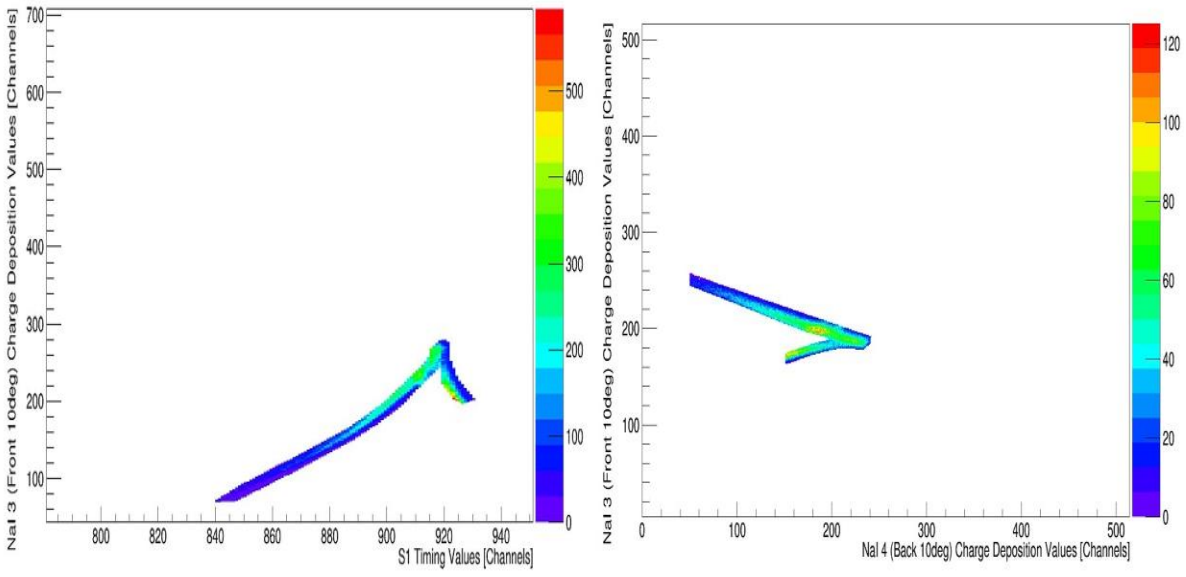


Figure 15. The proton particle identification cuts from the TOF plot (L) and dE-dE plot (R) for the 10° sodium iodide detector array from Fe400 MeV/n particles on a 20 g/cm^2 Al upstream target

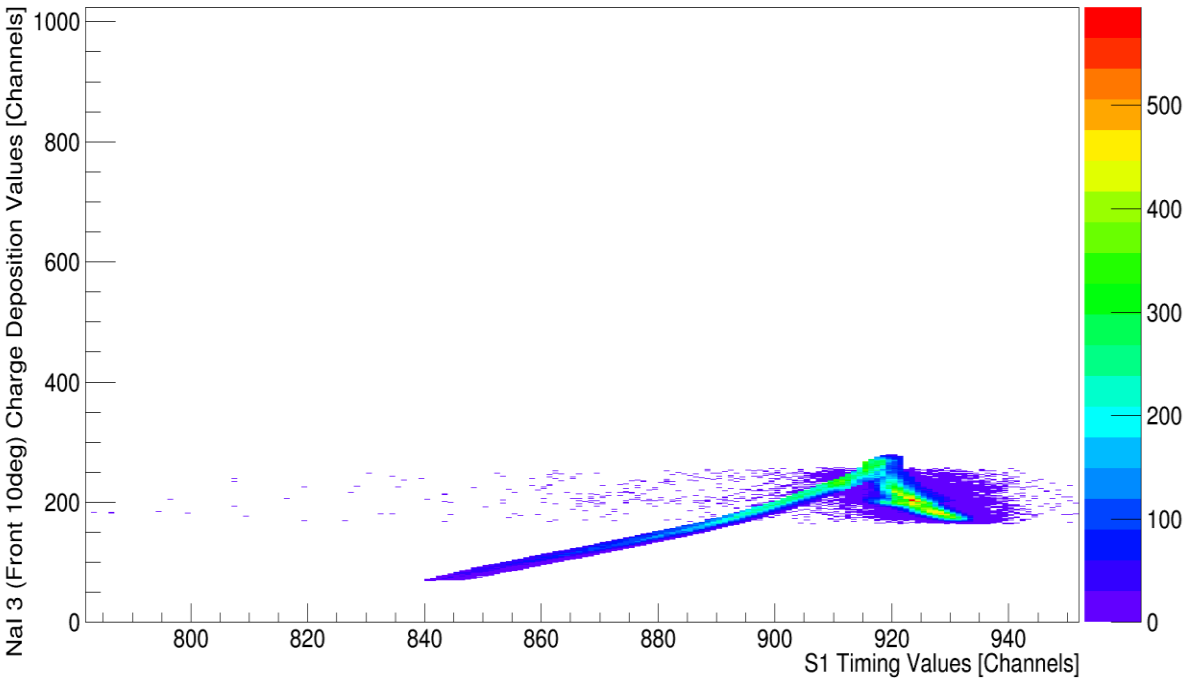


Figure 16. Both TOF and dE-dE proton cuts added together in disjunction and displayed on the time-of-flight plot using timing values from start scintillator S1 and charge deposition from the front detector of the 10° sodium iodide array NaI 3 from Fe400 MeV/n particles on a 20 g/cm^2 Al upstream target

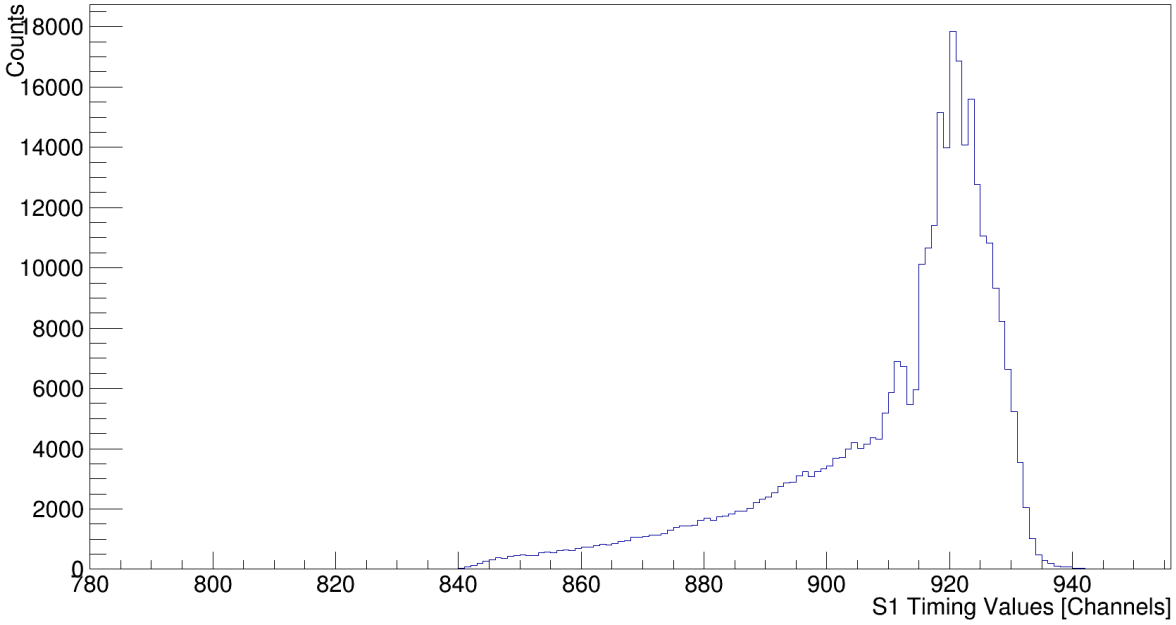


Figure 17. One-dimensional histogram of proton events projected on to the time (S1 TDC) axis.

4.2 Time-Energy Conversion

Once the individual histograms are produced for each light ion, the next step is correlating TDC channels with energy. This is done by using the punch-through points as a calibrator – the punch-through energy of each particle can be calculated by noting the corresponding particle energy that stops in four inches of sodium iodide, and thus, the TDC channel of the peak can be correlated with a particle energy. Because of the energies and narrowness of the beam, it can be assumed that the secondary light ions are born along the beamline. The variability in flight path comes from where within the target the ions are created – it is assumed that they are born in the center of the target. Thus, using the Bethe-Bloch formula (Equation 1) to step through the target, then the air, then the CS paddle, then the detector housing into the detector, a flight time can be calculated for a wide range of relevant particle energies (including, specifically, the punch-through energies).

$$-\left\langle \frac{dE}{dx} \right\rangle = \frac{4\pi}{m_e c^2} \cdot \frac{nz^2}{\beta^2} \cdot \left(\frac{e^2}{4\pi\varepsilon_0} \right)^2 \cdot \left[\ln\left(\frac{2m_e c^2 \beta^2}{I \cdot (1-\beta^2)} \right) - \beta^2 \right] \tag{1}$$

Where ε_0 is the vacuum permittivity constant, c is the speed of light, m_e is the rest mass of the electron, e is the charge of an electron, n is the electron density of the target material, I is the mean excitation potential of the target material, and the incoming particle has speed v (with corresponding β) and charge z. Equation 2 relates the Lorentz factor γ with β:

$$\gamma = \frac{1}{\sqrt{1 - \frac{v^2}{c^2}}} = \frac{1}{\sqrt{1-\beta^2}} \tag{2}$$

The Bethe-Bloch formula calculates energy loss (dE) through each step (dx) – the energy at the end of the step is used to relativistically calculate the particle velocity and is then used with the distance travelled in the step to calculate the flight time. That is, if a particle starts with kinetic energy E_k, the relativistic velocity can be calculated using Equations 2 and 3.

$$E_k = E - E_0 = (\gamma - 1) m_0 c^2 \tag{3}$$

And once the energy loss is calculated across a distance dx via Bethe-Bloch (Equation 1), the new E_k is used to calculate the new particle velocity v, and the time-of-flight across that distance can be calculated from the relationship between distance, velocity and time.

Summing these individual time calculations over the entire flight path gives a time-of-flight measurement, and summing energy loss and subtracting from initial particle energy gives the corresponding energy of each particle as it reaches the detector face. The channel scale can be turned into an energy scale using the punch-through point, and then into a timing scale using the calculated time-of-flights. And because the fidelity of the scintillator timing is known (~0.25 ns/ch), once the channel corresponding to the punch-through time-of-flight is known, every other channel can be calculated linearly. As a result, each channel's time value can be correlated with energy from the derived Bethe-Bloch time-energy tables.

Once the histogram has been fully translated from channel to energy, a few corrective steps must be incorporated – as can be seen in Figures 14 and 15, where there are regions of particle overlap. Those overlap regions are sections of the spectra where both protons and deuterons are counted together, tritons and helium-4, and so on. The corresponding intervals on the individual ions' spectra are artificially higher, because other light ions are incorporated into the histogram counts, so these must be subtracted out. There is also a nuclear attenuation correction that must be made. Light ions, as they interact within the detector through nuclear interactions, may deposit less or more energy than would be expected if the particle had only undergone electromagnetic interactions (stopping power). In general, the recorded number of counts of a particular ion will be lower than the experiment should indicate. This is corrected by applying a flat multiplicative factor (the inverse of the calculated 'efficiency') – and this factor can be calculated by running Monte Carlo simulations of light ions entering a sodium iodide detector. There are a few methods by which these factors can be generated. First, by comparing the number of particles that enter (known) with the number of particles that do anything except undergo nuclear collisions. Secondly, by comparing the flux at the start of the detector (known) with the flux at the corresponding stopping distance within the detector. Or third, by looking at an energy deposition distribution within the detector for the incoming monoenergetic light ions. All three methods are repeated for all five light ions (proton, deuteron, triton, helion, alpha) over an energy spectrum spanning the experimental data set.

Table 5 summarizes the light ions detected – with enough data points collected – across the five incoming beam species incident upon each shielding thicknesses at each NaI array. The raw data tables are available in Appendix A.

Table 5 – Summary of Particle Detection as a function of shielding thickness and incoming beam species/energy

Beam	**Shielding**	**Particle**				
		H+	*D2+*	*T3+*	*He-3*	*He-4*
He 400	*Al 20*	10 30	10 30	10	--	10
	Al 40	10 30	10 30	10	--	10
	Al 60	10 30	10 30	10	10	10
Fe 400	*Al 20*	10 30	10 30	10 30	10	10
	Al 40	10 30	10 30	10 30	10	10
	Al 60	10 30	10 30	10 30	10	10
Fe 800	*Al 20*	10 30	10 30	10 30	10	10 30
	Al 40	10 30	10 30	10	10	10
	Al 60	10 30	10 30	10	10	10
H 400	*Al 20*	10 30	10	--	--	--
	Al 40	10 30	10	--	--	--
	Al 60	10 30	10	--	--	--
H 800	*Al 20*	10 30	10	--	--	--
	Al 40	10 30	10	--	--	--
	Al 60	10 30	10	--	--	--

CHAPTER 5
DATA ANALYSIS AND DISCUSSION

This section will cover the implementation and results of the data analysis process – the corrections to the data, specific variations to analysis methodology, and external considerations in producing the light ion yields summarized in Table 5.

5.1 Timing Issues

5.1.1 Data Acquisition System – Timing

As mentioned in section 3.4, the data acquisition system directly measures two pieces of information – charge deposition, and timing information. These two bits of information are used in conjunction to calculate incoming particle energy, so incomplete timing signal information will lead to incorrect energy calculations.

These timing modules – time-to-digital convertors (TDC) – convert a time difference between two logic pulses into an output pulse with height directly corresponding to period length, which is then digitized. The incoming beam particles pass through one pair of timing modules (S1 and S2), which in coincidence create one logic pulse. The second logic pulse comes from the produced light ion as it interacts with one of six charged scintillation (CS) paddles in front of the two sodium iodide (NaI) arrays – CS 4-6 for the 10° NaI array, and CS 7-9 for the 30° NaI array. Together, the time difference between these two pulses forms the output pulse that is converted into a digital readout. However, in situations where the light ion interacts with a different detector, this second logic pulse in the CS paddles will never arrive, and thus the gate would stay open in perpetuity. To prevent this, the initial (S1 and S2) logic pulse is delayed, allowing it to serve instead as the second logic pulse, with the starting pulse coming from the CS paddles. This creates a reverse timing situation where a longer difference in time between to pulses instead correlates with a shorter time-of-flight measurement.

5.1.2 Mistimed Signals

In traditional timing, the "start" pulse would come from S1+S2, and the "stop" pulse from the corresponding CS paddle. A higher energy particle (corresponding to a higher velocity) would have a shorter TDC pulse, because the "stop" pulse would arrive faster. Thus, in reverse timing,

the S1+S2 signal forms the "stop" at a fixed time as a result of an intentional delay put into the system. This means the CS signal forms the "start" pulse instead, and the higher energy particles would have a longer timing signal, since the faster particles arrive at the paddle sooner. Slower (lower energy) particles would take longer to reach the paddles, so the CS "start" and the S1+S2 delayed "stop" would have a shorter time difference. However, an unintended result of changing this timing mechanism was, for some of the higher energy particles, the CS signal was arriving too early. Figure 18 shows two events (the analog signal is in gold) – the one on the left is a properly timed event, and the one on the right represents one of these faster (higher energy) events that leads to incorrect timing information. A 200 nanosecond (ns) gate is fired when a signal is received from any of the six CS paddles – the QDC integrates the analog signal that falls within this 200 ns gate, resulting in the determination of the charge (i.e. energy) deposition. When the S1+S2 signal arrives first, this is not an issue, because the timing information and charge information is collected properly. However, in the aforementioned situation where the CS signal arrives first (as can be seen on the right), the charge collected is still correct (because the incoming analog signal is still within the 200 ns gate), but the timing information is off, because the signal from S1+S2 generates the start signal in the TDC, instead of the stop as it normally does. So, events are recorded with an incorrect time-of-flight value.

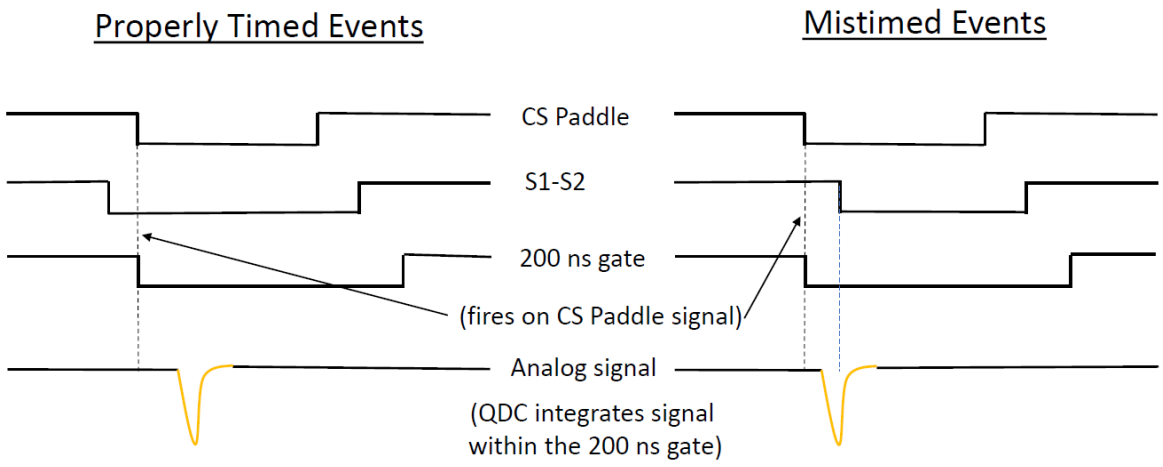


Figure 18. Comparison between signal/gate information between a properly timed (L) event, and a mistimed (R) event from a faster particle.

Rather than shifting the delayed S1-S2 TDC values to compensate, the CS TDC values were instead shifted out of synchronization with the correctly timed data. The faster the particle, the further the shift. As a result, the timing data for those events were incorrectly written, and the data was mistimed. In Figure 19, an example of the raw (uncorrected) timing information for a sample run (iron nuclei at 400 MeV/n on a 20 g/cm^2 aluminium target) is presented. This trend was seen in all six paddles across the entire experiment, regardless of incoming beam species, energy, or upstream target thickness.

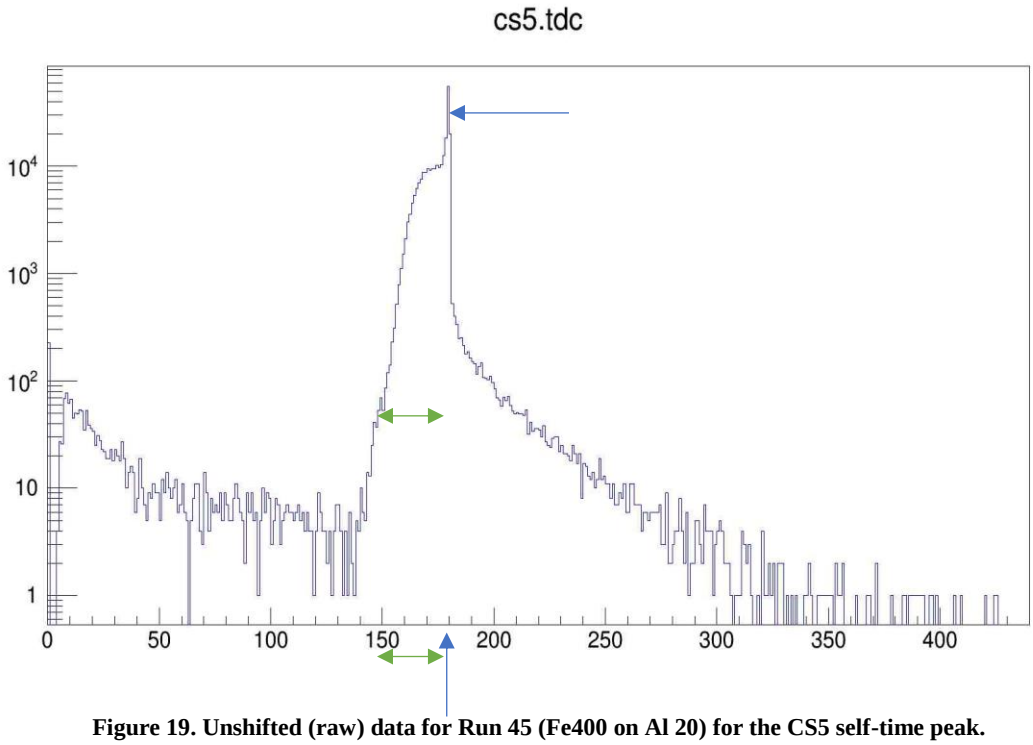


Figure 19. Unshifted (raw) data for Run 45 (Fe400 on Al 20) for the CS5 self-time peak.

The blue arrows in Figure 19 point to the 2-3 channel wide self-time peak that contains the properly timed data. The hump (of similar magnitude) immediately to the left – of width approximately 40 channels (illustrated by the green arrows) – represents all of the fast, high-energy light ions that were incorrectly timed by the data acquisition system. As can be seen for the raw data of Figure 19, there is a statistically significant amount of mistimed data, and it is important to correct the mistimed events to maximize the useful data from each experimental run. The implication for

these mistimed signals can be seen in the time-of-flight (TOF) vs charge deposition (QDC) plot of the 10° NaI detector array in Figure 20.

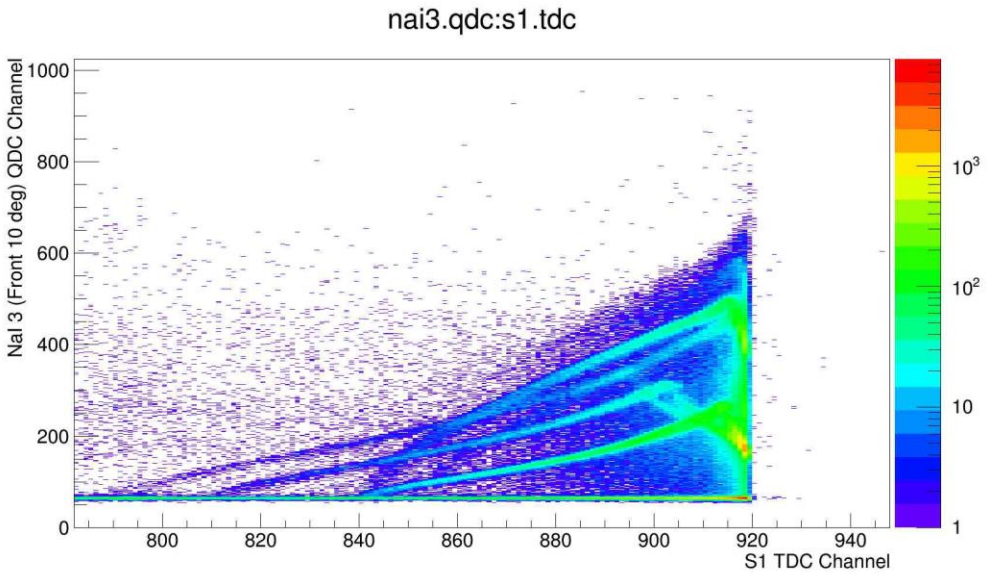


Figure 20. 10 deg NaI detector Time-of-Flight plot with the raw (uncorrected) data.

As can be seen, this lack of high-energy data is immediately noticeable as all high-energy events are incorrectly grouped together in the pile-up peak occurring around channel 920. Generally, the pile-up peak is populated by pairs of pulses that come in so quickly that the system cannot process the two individually (as it should), and instead incorrectly adds them together to create an artificially high value. It represents the extreme channel of the acquisition system. Very little data is present past this peak – it is a very distinct hard cutoff. This suggests that the lack of data for the high-energy points was not a feature of the raw data, but rather an issue with the acquisition system. For these faster events, the system had incorrectly calculated the time-of-flight values (i.e. the S1+S2 and CS Paddle TDC values), and instead an overflow issue occurred. This caused the timing data past channel 920 to be aggregated together into the pile-up peak.

5.1.3 Shifting the Signals

The solution was to calculate – on an event-by-event basis – the shift in each paddle and update the S1+S2 timing information. The shift is calculated as the difference between the self-time peak

(what the CS Paddle TDC value "should" be) and the channel where the event was actually recorded. The shift is then used to update the corresponding event history in the S1+S2 TDC values by that same value. This shifts the high-energy events out of the pile-up peak in Figure 20 into their proper channels.

It is important to note that in these CS TDC plots, the data points that make up the "background noise" of the plot are triggers initiated from one of the other five paddles. So, in addition to calculating these shifts, it is important to isolate only the relevant pulses – that is, for each individual paddle, to only focus on the triggers (logic pulses) from that specific paddle. Once the correct triggers from the overflow region (green arrows in Figure 19) are isolated, then the proper data points can be shifted. Shifting while using a trigger from a different CS paddle will lead to misappropriated data.

The shift for each event is calculated as follows: for each run, each event is cycled through. For each event, first the trigger paddle is identified. Next, the paddle TDC value for the event is determined – if it falls within the broad peak, the shift value (paddle self-time peak TDC channel minus event TDC channel) is calculated. Then, the S1 and S2 TDC values for the event are shifted by this same value.

Applying this algorithm for all six paddles across every single run leads to the corrected data. Figures 21 and 22 are the corrected version of Figures 19 and 20, and the benefit can be most clearly seen in Figure 22. The time-of-flight plot has been extended well into the high-energy region, drastically improving the energy range of the light ion yields well past the punch-through point of the front detector of each array.

The relevant CS5 triggers in the left hump have been shifted into their correct channel location, and the peak has increased five-fold. The remaining counts in the ~40 channels that were in that region correspond to triggers from any of the other five paddles. The events triggered by CS5 are now all timed correctly within the self-time peak, and a visual comparison between Figures 19 and 21 shows how much mistimed data there was, and how important it is to correct the data to be able to access it. The original data in channels 920 and up were all placed together in an "overflow" bin, and Figure 22 shows the true nature of the timing data when allowed to populate bins 920 and up.

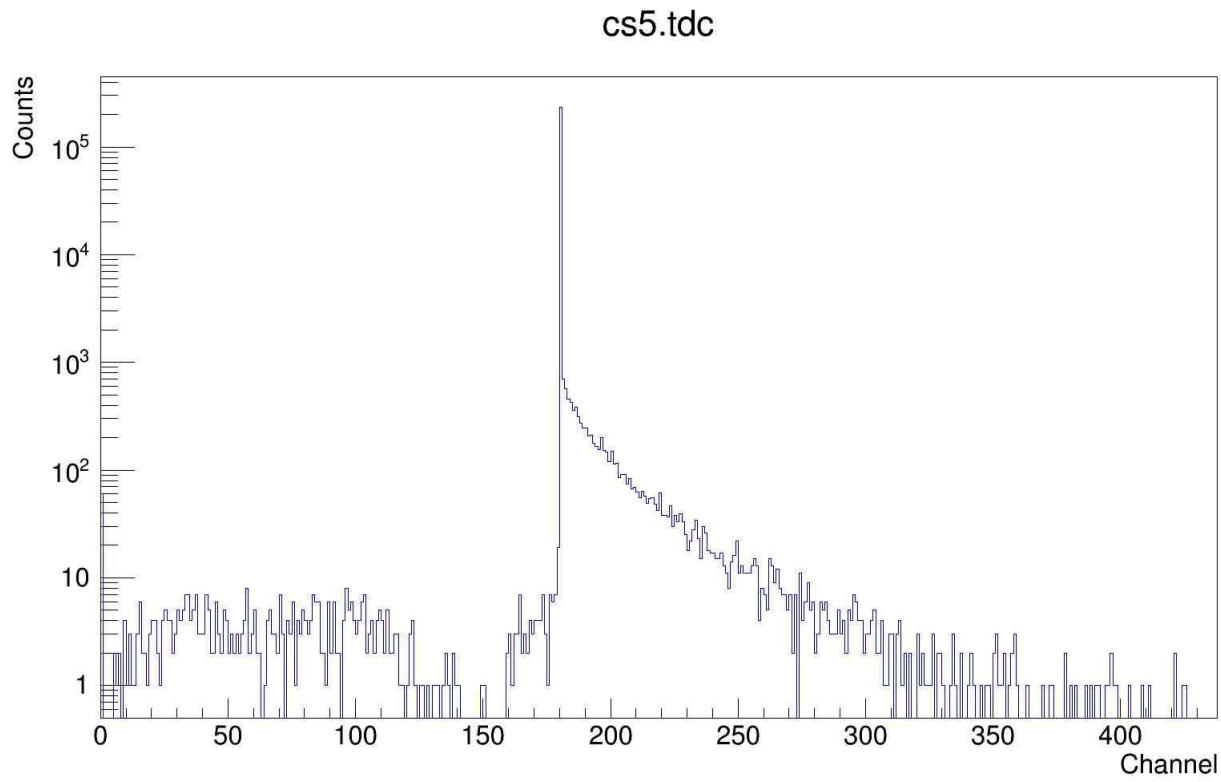


Figure 21. Shifted (corrected) data for Run 45 (Fe400 on Al 20) for the CS5 self-time peak.

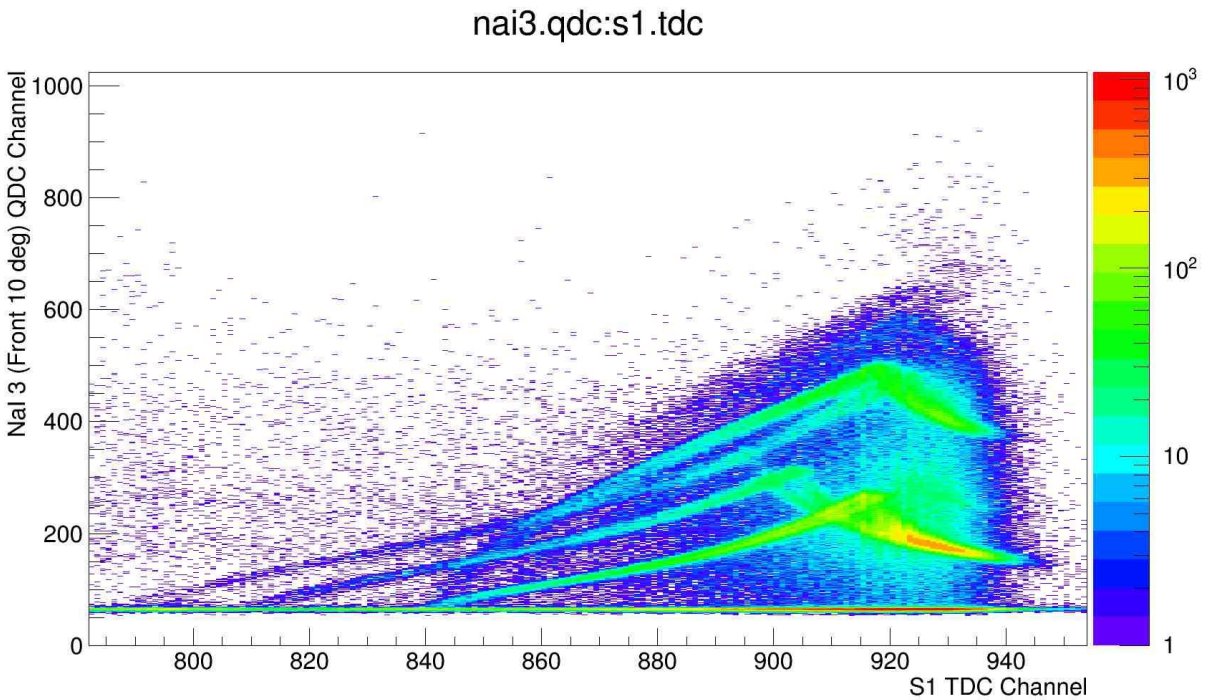


Figure 22. 10 deg NaI detector Time-of-Flight plot with the shifted (corrected) data

5.2 Data Corrections

This section entails the corrections that must be applied to the data because of issues that arise purely from the physics within the experiment, and not as the result of any external issues with the detectors or acquisition system.

5.2.1 Overlap Regions

As can be seen in Figure 23, there are regions of overlap amongst the five light ion isotope lines. These regions of overlap are important to note, because in those specific channels (bins), data is being double-counted. The black circles represent these regions in the 400 MeV/n iron incident upon a 20 g/cm^2 aluminium target at the 10° sodium iodide (NaI) array using all three timing paddles in disjunction. The lavender circle specifically illustrates the overlap between the proton and deuteron isotope lines.

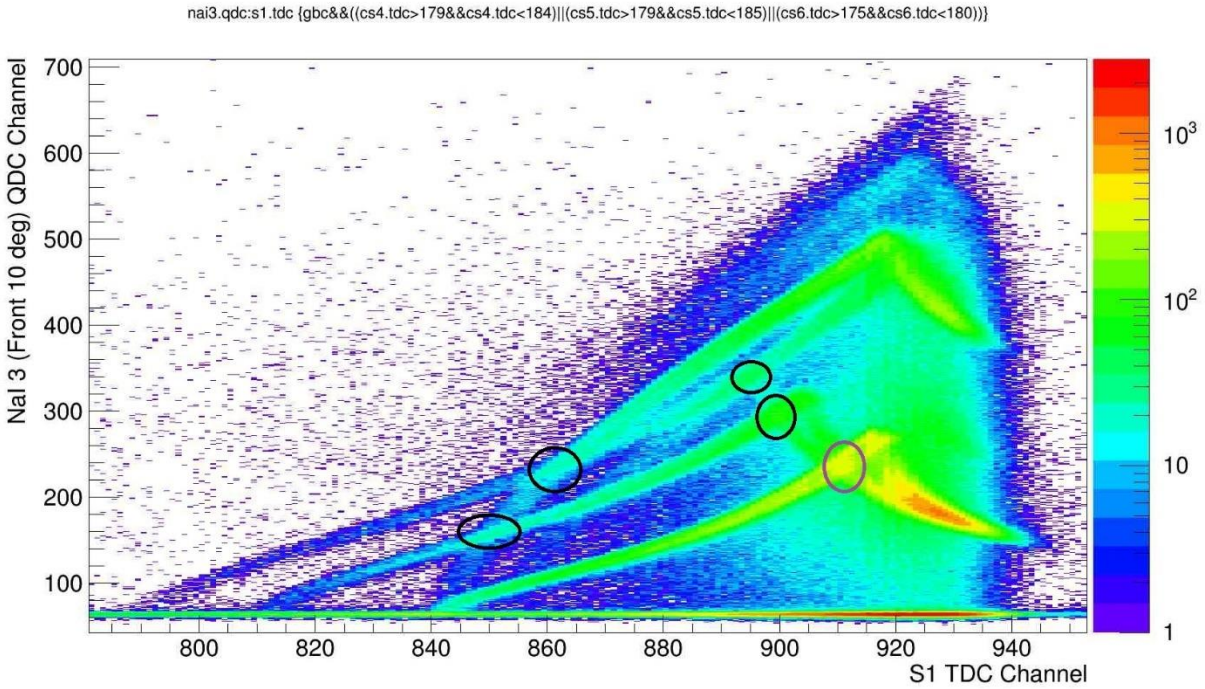


Figure 23. Time-of-Flight plot at 10 degrees of 400 MeV/n iron nuclei incident upon a 20 g/cm^2 aluminium target illustrating isotope overlap regions.

To generate the respective yields for each plot, these isotope lines are all (individually) projected onto the timing (*x*-) axis, so it follows that for these regions, the count rates will be inflated. In the

lavender region, both deuteron and proton counts will show up in the opposing spectra, so resolving these regions is an important correction.

Assumptions are made about the data – that each particle line consists solely of those particles (i.e. the particle identification cuts are accurate), and that there are no random spikes in the magnitude of the data (i.e. a level of continuity within each spectrum). The first assumption dictates that in the lavender region, if 70% of the counts are protons, then the remaining 30% would be deuterons. The second assumption allows for an estimation of these overlap ratios – they are derived from the continuity of the data, as opposed to a formulaic calculation. Thus, if 30% of the counts from the proton spectrum are removed, then 70% of the counts of the deuteron spectrum would be removed. These ratios are calculated on a channel-by-channel basis by comparing the ratio of protons to deuterons at both ends of the overlap region, and then interpolating that ratio to each channel (bin) within the region.

Using this lavender region as an example, Figure 24 shows the uncorrected normalized count rate for the proton and deuteron lines in red and blue respectively. From a graphical inspection of Figure 23, the overlap range is from channels 907-914 inclusive. Thus, the ratio of protons to deuterons at channels 906 and 915 are calculated, and the presumed ratio of protons to deuterons are interpolated for the channels in [907,914]. Using these ratios, the percentage of counts that need to be removed are calculated. The corrected regions are shown in Figure 24 – the green and orange lines show the corrected portions of the spectrum. Every overlap region across every system is handled in a similar manner.

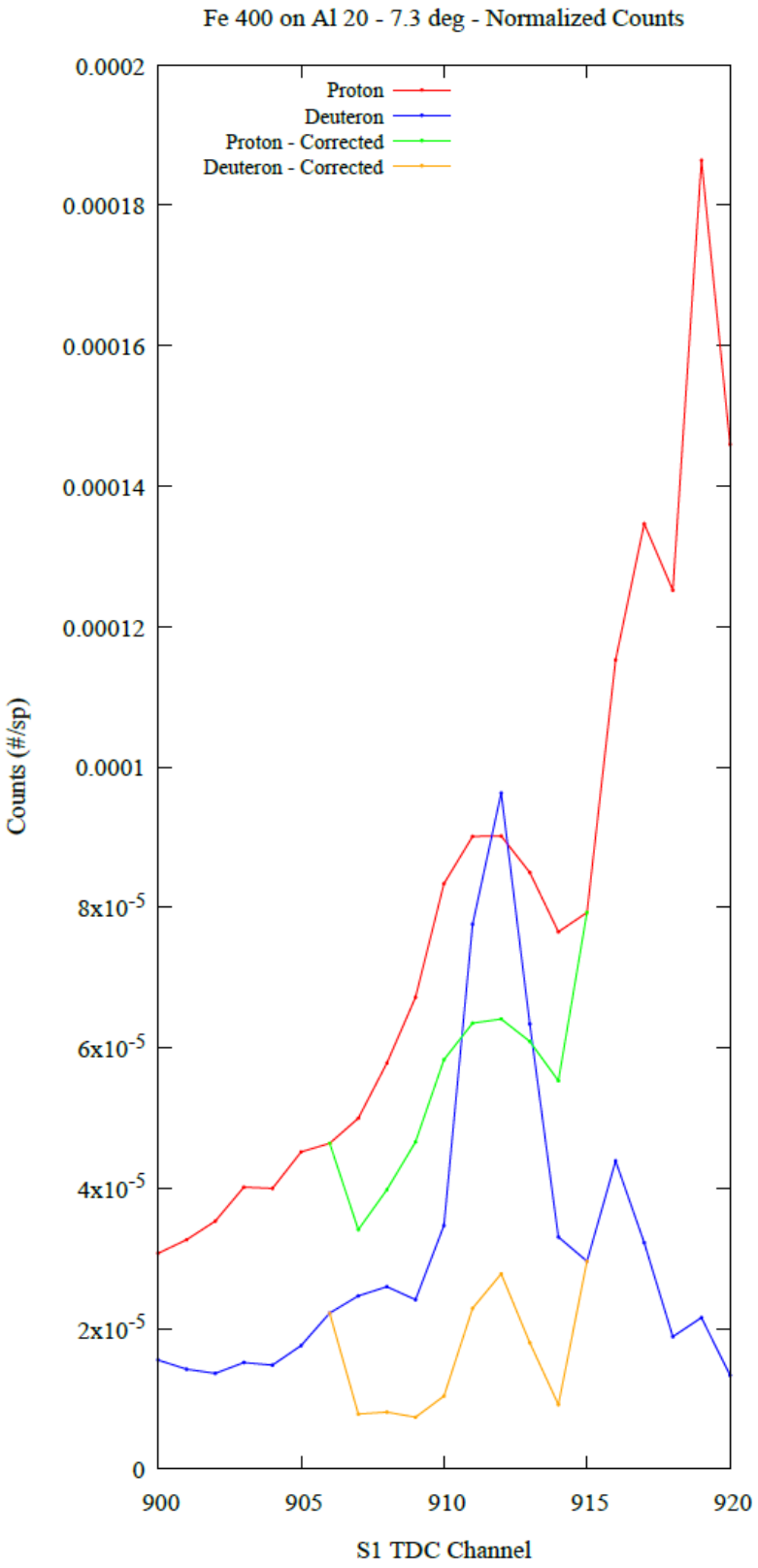


Figure 24. Selected portion of proton and deuteron spectra illustrating overlap region corrections.

5.2.2 Nuclear Attenuation Corrections

Detectors rely on coulombic interactions to obtain their signals – it's the interaction of the delta electrons that leads to the output signal from the detector. As the light ion travels through the NaI crystal, it ionizes atoms in its pathway. These ionized atoms get excited, and release scintillation photons as they return to ground state, which is how the detector registers an event. However, a nuclear interaction would lead to no such output pulse from the detector – interactions between projectile (incoming light ions) nuclei and target (sodium iodide with the detector) nuclei would cause what can be described as "non-ionizing energy loss." The incoming radiation has deposited energy within the detector, but not necessarily the full energy of the incoming particle. This means that the data recorded for that particular event will be incomplete. Thus, the yields calculated from the detector output will underestimate the true flux of light ions at the surface of the detector. A yield-correction factor is necessary to account for particles that interact within the detector but record an abnormal or absent signal.

The methodology for correcting this involves the usage of Monte Carlo-based particle transport codes that have the capacity to calculate and predict energy deposition. The Japanese code PHITS (Particle and Heavy Ion Transport code System) was used to model the sodium iodide detector array. The code followed 10^5 source particles of each light ion type (proton, deuteron, triton, helion, alpha) incident upon the detector. For each source particle, the code tracks how much energy is deposited within the detector. A full energy histogram is created over the course of the simulation. These simulations are run for each five particles individually, starting at 20 MeV/n and increasing up to 400 MeV/n in blocks of 20 MeV/n. The PHITS input file can be seen in Appendix B.

In theory, if each particle were to undergo electronic stopping, the output of the PHITS simulation would reflect that every single source particle deposited the exact same amount of energy. But instead, as a result of nuclear interactions, a range of energies is deposited within the detector. For each combination of light ion and incident energy, a histogram of energy deposited within NaI detectors was created. The peak for each run represents the number of particles that have behaved "ideally" and deposited the full energy through coulombic interactions within the detector. Thus, inverting the ratio of the integral of the peak (i.e. the number of events within the peak) to the source particle count gives a yield-correction factor.

As an example: if 80% of the incoming 120 MeV/n protons fully deposited their energy, then that indicates a multiplicative correction factor of $\frac{1}{0.8} = 1.25$. It is known that there were 10^5 source ions, but only 80% of them would have been correctly identified with the right timing signals and energy deposition. Thus, to get a proper estimate of the yield of 120 MeV/n protons, the aforementioned multiplicative correction factor would be necessary. For each of the five species, eighteen such simulations were done (40 MeV/n – 400 MeV/n, increasing by 20 MeV/n).

Figure 25 shows a plot of these PHITS corrective factors as a function of incoming particle energy. At lower energies, it is more likely that the ions fully deposit their energy, which explains why the corrective factor is so low, especially for energies that are not high enough to punch through the front detector (plus casing). But as the total energy increases, more interactions within the detector crystal occur, not to mention that the ions are starting to also deposit their energy within the back detector as well. This leads to lower counts within the "expected" energy deposition bins, which in turn increases the correction factor. But beyond a certain point, for most of the ions of interest, the correction factor tends to level out and approach a constant value.

For a comparison between models, a similar simulation setup was used in the stochastic particle transport code MCNP6 (Monte Carlo N-Particle version 6), except instead of building a histogram of energy deposition per history, the particle tracking was enabled. The resulting output for each run listed how each source particle 'died' out – the two important tallies being "energy cutoff" and "nuclear interactions." The former represents the incoming ions that lead to scintillation (until their energy drops below the minimum threshold for calculation), and the latter the ions that undergo nuclear attenuation. Figure 26 shows the same plot of the MCNP corrective factors for comparison. Because the PHITS model is a more accurate representation of what is measured in the experiment – the detector relies on energy deposition for both particle identification as well as energy conversion – those multiplicative figures were used, but the MCNP models allowed for a way to measure the uncertainty of the yield correction factors. As Figure 26 shows, the MCNP estimations show a similar trend – sharp rise into a plateau – but the corrective factors are much higher. It is believed this is because MCNP is also transporting the inelastic creation (via nuclear reaction) of additional particles (specifically the light ions being transported), which is artificially decreasing the counting efficiency of the detector.

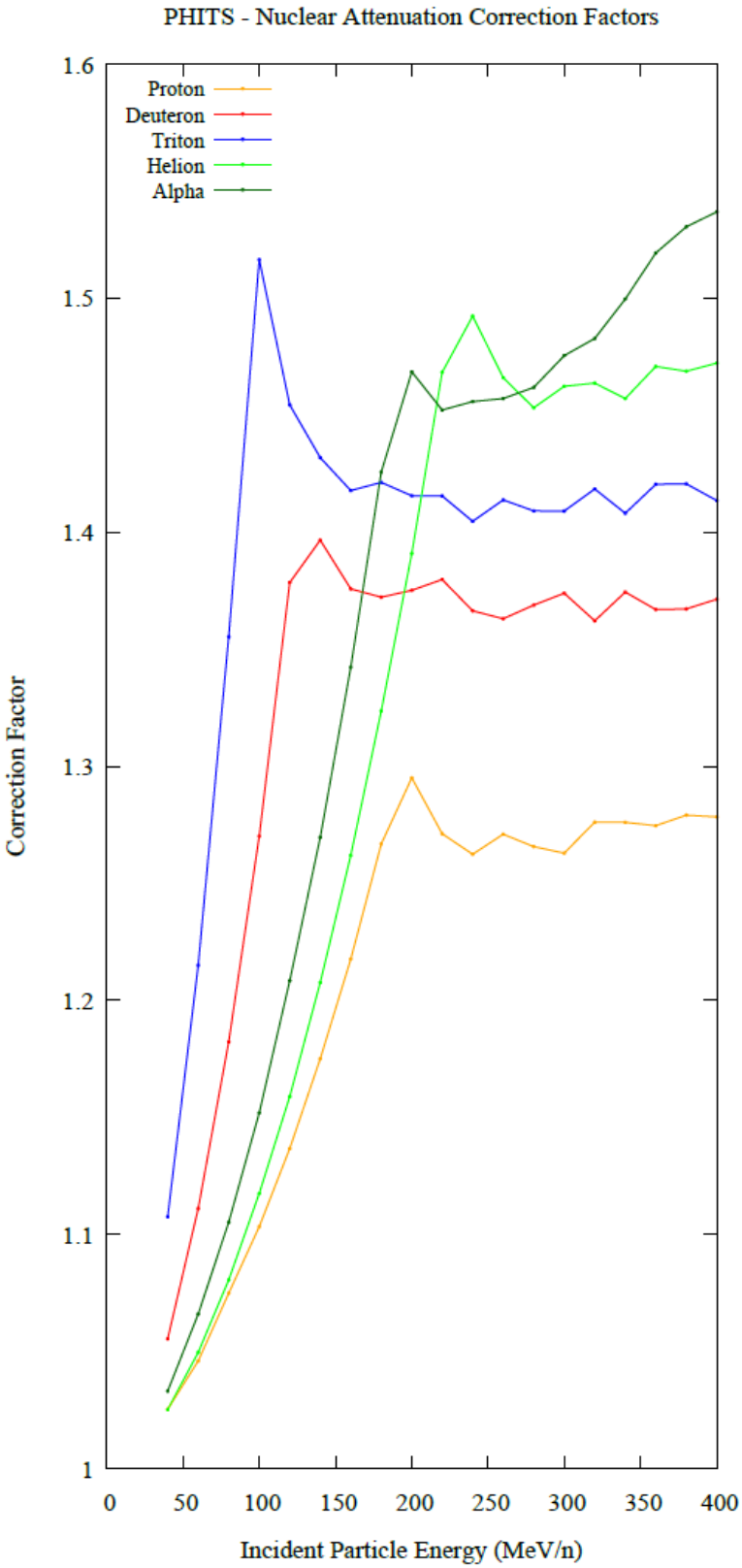


Figure 25. Nuclear Attenuation Yield Correction Factors as a function of incident particle energy via PHITS simulations.

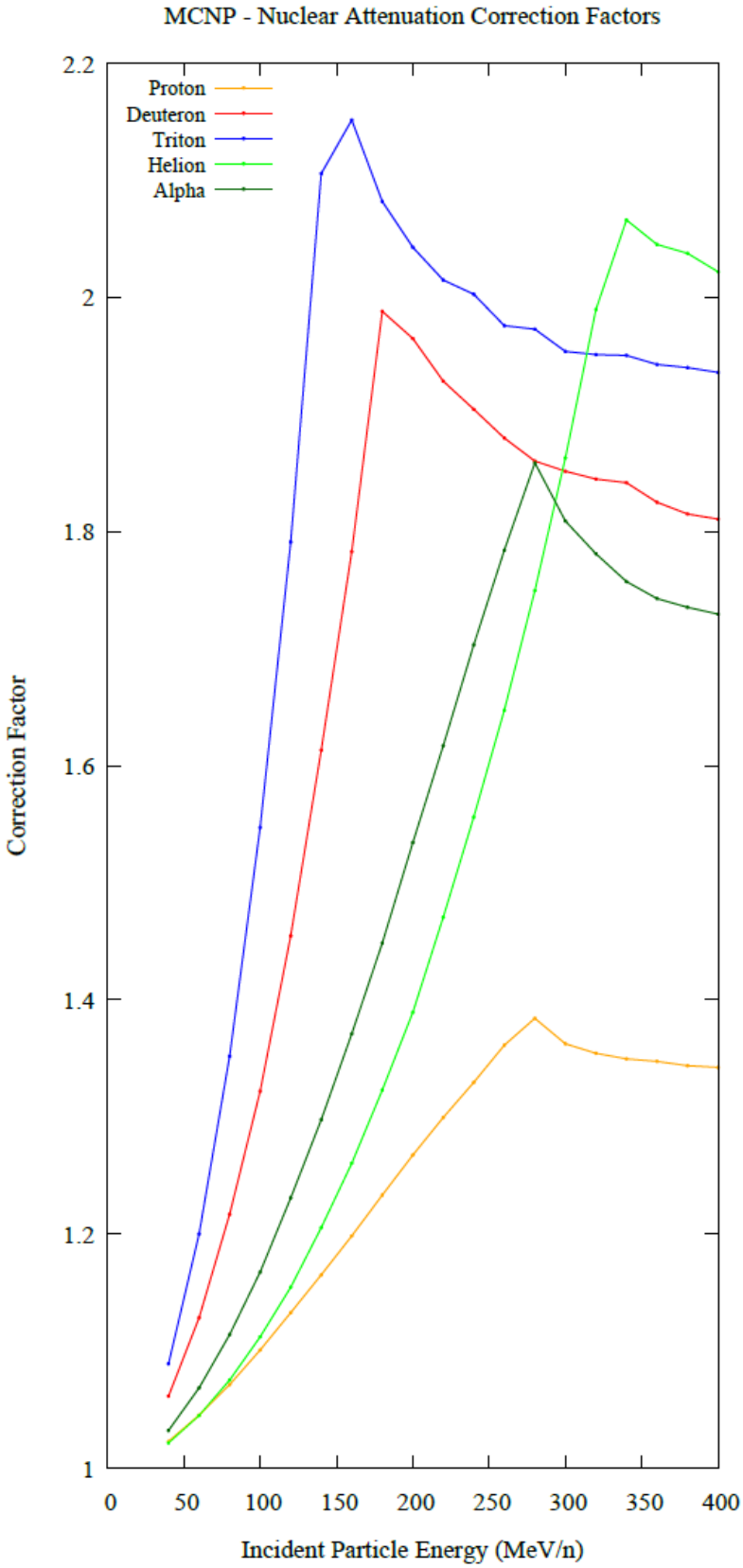


Figure 26. Nuclear Attenuation Yield Correction Factors as a function of incident particle energy via MCNP simulations

5.3 Unit Conversions

5.3.1 Channel-Time-Energy

Once the yields have been corrected, the final step in converting the data acquisition system output into useable form is to convert the TDC channels (*x*-axis) into energy via time-of-flight (ToF). The methods outlined in section 3.2 are utilized to create tables for each light ion and each target thickness configuration. The most important information is the energy at the surface of the detector, and the total time of flight of the ion from the point of creation within the target until the surface of the detector. It is assumed that the particle is born along the beamline in the center of the target, and from there travels through the aluminium target and the air until reaching the charged scintillator paddle and detector casing. The two extremes are also considered to provide a full range of energy estimation – that the particle is born along the beamline at the immediate front of the target (as the beam travels), and that the point of creation for the light ion is at the very back edge of the target.

The calibration point is the peak of each isotope line from the time-of-flight plots – this peak represents the "punch-through" energy and is a known constant value. It represents the maximum energy deposition within the front detector (of the array), which implies a specific incident particle energy. And from the time-of-flight tables (specifically those with the base assumption of mid-target origin), this energy can be converted into a time. The timing resolution for the charged scintillator paddles is known (0.23 ns/ch), which means that from the punch-through channel, the entire *x*-axis can be linearly converted into time, and again referring to the ToF tables, into units of energy. The error in the estimation can be done by repeating this process, except with the tables corresponding to the two extremes (particle birth at either end of the target), giving higher and lower estimates of the energy.

5.3.2 Yield Normalizations

On its own, the counts recorded by the data acquisition system have no meaning – context needs to be provided to understand what the histogram values mean. This has the additional benefit of allowing these results to be compared across experiments that utilize different types and sizes of detectors, different experimental facilities (with differing capabilities for ion acceleration and deliverance), etc. Thus, factors are added in to convert raw counts into double-differential yields,

where the unit is the number of light ions per source particle per energy (MeV/n) per solid angle (steradian).

In order to normalize the data per source particle, three factors need to be known: how many accelerated nuclei were fired at the target during the run, how many of those were during a time where the detectors/acquisition system were available for recording, and how many of those were acceptable incoming beam ions. The first is a measurement of the coincidence between the two beam scintillators S1 and S2 (hereon referred to as S_1S_2), the second is a measurement of the live-time (LT), and the third is a measurement of the good-beam (GB) ratio. The GB ratio, as mentioned in section 3.1.1, represents the percentage of incoming beam particles that did not lose energy or change species via interactions in the air. In order to normalize by source particle, it is necessary to calculate how many source ions there truly were. And this is done by figuring out how many primary ions arrived when the detector system was busy (LT), how many lost energy or changed species via nuclear interactions (GB), and how many ions passed through one part of the timing mechanism for the data acquisition system (S_1S_2).

For each combination of incoming beam, beam energy, and shielding thickness, there were several individual runs of data. Thus, in order to combine all of the data, they must be normalized and added together in a very specific way, as illustrated by Equation 4:

$$C_{i,p} = \frac{\sum \frac{c_{i,r,p}}{LT_r}}{\sum[(GB)_r\ (S_1S_2)_r]} \tag{4}$$

Where *c* represents the individual counts at each paddle *p* for each channel *i* for each run *r* and *C* is the cumulative total (across the respective runs for each bin across all six paddles). Equation 4 is applied on a channel-by-channel basis (*i*) for each run *r* that makes up each combination. The LT ratio is used to determine input count rate, so $\frac{c_{i,r,p}}{LT_r}$ represents the "true" number of light ion detection events. The denominator updates the total number of source events to a more accurate estimation of how many beam particles entered the target as the correct ion species with the correct incident energy. Thus, dividing the two gives the ratio of the true number of detected events to the true number of source particles. As a result, for experiments run with different beamline capabilities, or for different lengths of time, the yields can be compared against each other.

The solid angle (Ω) of an object is a way to represent a three-dimensional volume subtended by a two-dimensional surface at a given point. For this experiment, the given point would be the point of light ion production within the target, and the two-dimensional surface represents the front face of each charged scintillator paddle. Thus, the three-dimensional volume is the entire space between the light ion birth and the detector. Normalizing the yield by solid angle allows for comparisons across experiments that utilize detectors with different active areas or at different distances/angles to the beamline. Equation 5 shows the calculation of the solid angle (an approximation that works under the assumption that *r* is very large, which holds true here):

$$\Omega = \frac{A}{r^2} \tag{5}$$

where *A* is the surface area of the detector, and *r* is the distance between the production point (assumed to be the center of the target) and the front of the detector. The updated raw count calculations from Equation 4 are then normalized by the solid angle. Table 6 summarizes the solid angle measurements and calculations for each of the six charged scintillator paddles. Because each array's yield is split by paddle, the "paddle area" replaces the surface area of the detector, because the active area is specifically the portion of the 4"x16" NaI detector face covered by each 5"x5" paddle.

Table 6. Solid Angle Measurements for each Charged Scintillator Paddle

CS Paddle (°)	Target Center to CS Paddle Distance (cm)	CS Paddle to NaI Distance (cm)	Sum (cm)	Paddle Area (cm^2)	Solid Angle (steradian)
4 (12.7°)	300.28	1.26	301.54	129.032	0.001419
5 (10°)	300.28	1.00	301.28	129.032	0.001421
6 (7.2°)	300.28	1.35	301.63	129.032	0.001418
7 (32.7°)	299.97	1.65	301.62	129.032	0.001418
8 (30°)	299.97	1.20	301.17	129.032	0.001422
9 (27.2°)	299.97	1.14	301.11	129.032	0.001423

The last normalization has to do with the width of each data bin – once the timing axis has been converted from channels to energy, each data bin has a slightly different bin width. Thus, the yields need to be normalized by bin width. This has the additional benefit of removing another

inconsistency across different experiments – different acquisition software and electronics would lead to different timing fidelity, which would lead to a variation in bin widths. This removes those differences.

Equation 6 summarizes the entirety of yield normalizations:

$$Y_{i,p} = \frac{C_{i,p}}{\Omega_p * (E_{i+0.5} - E_{i-0.5})} \quad (6)$$

for each channel *i* and paddle *p* using the previous calculated counts *C* and the solid angle Ω. The individual channels are assumed to be the midpoint of each bin; thus, the bin width would come from calculating the difference in energy at each edge (i.e. half a channel above and below). With all of these normalizations, the data is finally converted into double-differential yields that can be measured as a function of incoming particle energy.

5.4 Data Removal

5.4.1 CS4-CS8 Threshold Issues

Figure 27 shows the proton yields at both the 10° (left) and 30° (right) detector arrays from the 400 MeV/n iron beam incident upon the 20 g/cm^2 aluminium shielding. Each array was covered by three charged scintillator (CS) paddles that provided the timing information for each detector, and as a result, could be individually used to provide further angular separation within each detector array. This is the same data set presented throughout section 5.4, but the focus now is on the specific "falloff" that can be seen in the 12.7° (CS4) and 30° (CS8) data sets.

As can be seen, beyond a certain point (illustrated by the black vertical line), the calculated yields are consistently lower than expected. This is an issue with the threshold setting of the paddle. The threshold of a scintillator represents the minimum energy necessary to produce a response – i.e. the corresponding pulse height to a radiation event needs to meet a certain baseline. This is done in an effort to limit the amount of noise that would incorrectly trigger a response within the data acquisition system. However, if the threshold is too high, certain signals will not be processed, which is the issue with the data sets from the CS4 and CS8 paddles. From the Bethe-Bloch formulization (Equation 1), it can be seen that the stopping power of a material decreases with energy. This means that the higher the energy of a particle, the less amount of energy deposited per unit distance. Which means that for these higher energy protons, the deposited energy by the

incoming radiation falls below this threshold setting for these two specific paddles, leading to decreased counts (and thus yields) for the higher energy range of particles.

Thus, it is important to note that the 12.7° (CS4) and 30° (CS8) higher energy yields (i.e. beyond the black lines) are not indicative of a physical phenomenon, but rather the result of a threshold setting that was too high. For any conclusions inferred from these data sets, the data for the CS4 and CS8 to the right of the vertical black bar must be ignored/removed.

For the data presented in section 5.5, none of the data has been removed from the plots in an effort to show the total collected and analyzed data. The aforementioned threshold issues with the CS4 and CS8 data (12.7° and 30° respectively) are presented, as well as the artificial decline in yield at higher energies. At these higher energies, the dynamic range of the detector is reached, so the fall-off in yield is not necessarily representative of the physics of the system, and instead is a data artifact.

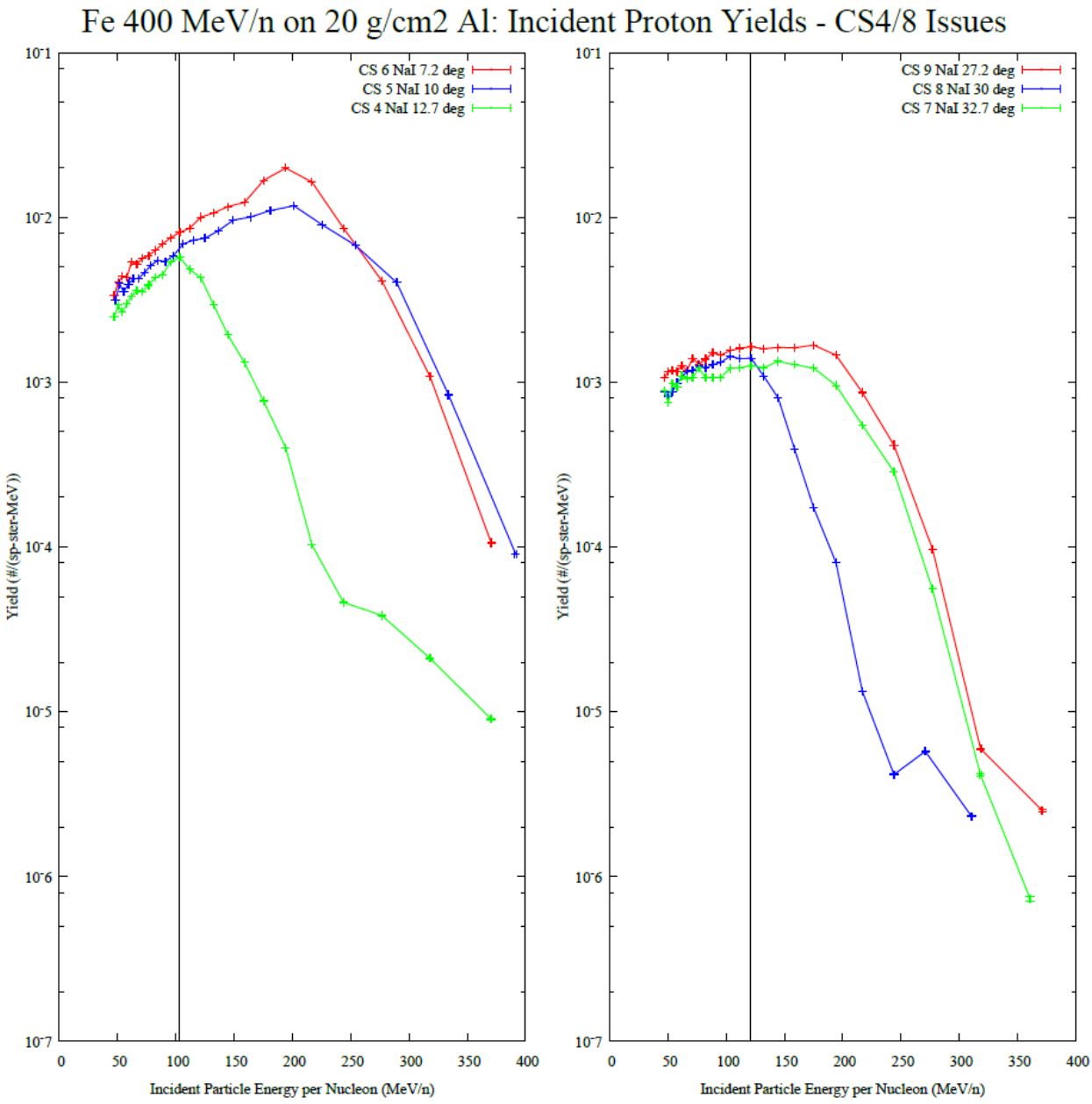


Figure 27. Proton Double Differential Yields as a function of incoming energy per nucleon from the 400 MeV/n Iron on the 20g/cm^2 (left) Aluminium shielding thicknesses detected at 10° and 30° NaI and OLS detectors.

5.4.2 Minimum Data Requirements

In order to ensure the robustness of the data collected across the runs, a requirement mandating a minimum number of data points was enforced – Table 5 summarizes the light ions seen across each system, and the gaps within illustrate that some light ion measurements did not meet this minimum. This is most notably seen with the triton and helion data sets, as certain thicknesses of shielding limited data rate – and as a result, those sets either had yields that were several orders of magnitude below any other system due to a natural low count rate or did not have enough raw data bins at all.

5.5 Double-Differential Light Ion Yields

The following sub-sections discuss a set of sampled results, to illustrate trends in the data and comparisons across the experimental runs, across the charged particle detectors used, and between experimental results and simulations. The entire collection of data tables for each individual system can be found in the sub-appendices of Appendix A.

These plots show the yield of light ions as a function of incident particle energy upon the face of the detector – that is, the energy of the ion once it reaches the detector, and not the energy of the ion at the point of creation.

These yields are referred to as "double-differential" because of the normalizations to space (solid angle) and energy (bin width).

The particles and energies chosen in this experiment were done so to sample across both the composition of the nuclei that compose the space radiation environment, as well as the range of energies these galactic cosmic rays and solar energetic particles have. It is important to compare the double-differential yields as they change across incoming beam ion, shielding thickness and space (in terms of detector angle). However, it is also important to compare these yields in each system across all five light ion species (where available), as well as the differences in the incoming nuclei (Z) and incoming energy (E). Sections 5.5.1 and 5.5.2 examines yield differences across all three target thicknesses for all five light ions and both detector arrays – the former looking at differences when the beam species is constant, but the energy differs, and the latter when the incoming energy is the same, but the nuclei changes.

5.5.1 Yield Influences from variation in Incoming Beam Energy

Table 7 summarizes what light ions are seen at each detector array for the two iron systems (400 MeV/n and 800 MeV/n), and which figures illustrate which data sets. The ensuing plots illustrate the yield differences across all three target thicknesses for each light ion of interest. In each plot: the *x*-axis is the light ion energy in MeV/n, and the *y*-axis is the light ion yield per source particle per steradian per MeV/n. The leftmost plot is for the 20 g/cm^2 aluminium thickness, the middle is for the 40 g/cm^2 shielding, and the rightmost shows the 60 g/cm^2 results.

Table 7. Summary of light ion detection from 400 and 800 MeV/n iron systems for all three aluminium shielding thicknesses and corresponding figures for each light ion yield comparison.

IRON 400					
Al Thickness (g/cm2)	**^{1}H**	**^{2}H**	**^{3}H**	**^{3}He**	**^{4}He**
20	10° / 30°	10° / 30°	10° / 30°	10°	10°
40	10° / 30°	10° / 30°	10° / 30°	10°	10°
60	10° / 30°	10° / 30°	10° / 30°	10°	10°
IRON 800					
Al Thickness (g/cm2)	**^{1}H**	**^{2}H**	**^{3}H**	**^{3}He**	**^{4}He**
20	10° / 30°	10° / 30°	10° / 30°	10°	10° / 30°
40	10° / 30°	10° / 30°	10°	10°	10°
60	10° / 30°	10° / 30°	10°	10°	10°
FIGURE #	28 / 29	30 / 31	32	33	34

It can be seen in Figures 28-34 that as angle increases (i.e. the angle of separation between the beamline and the charged scintillator paddle), the yield decreases. This is a result of the incoming momentum of the iron nuclei, as well as the mass difference between the iron nuclei and aluminium target – the secondary ions created are then mostly forward focused. Furthermore, the higher energy iron nuclei penetrate further into the aluminium targets than the lower energy nuclei, resulting in significantly more potential interactions, which naturally leads to higher secondary ion production. This also leads to light ion detection at higher energies, too, since the initial collisions between iron and aluminium leads to higher energy fragment production.

For protons (Figure 28-29), the trends in the data overlapped fairly well across both detector arrays and beam energy – the same rise, peak and fall patterns were seen throughout. A sharp rise in yield at the lower energies led to a peak around 300 MeV/n followed by a slower fall in yield at

higher energies. The yields from the lower energy runs at the 10° array decreased with thickness, suggesting that the extra shielding material did tend to provide a slight benefit in terms of reduced secondary proton creation. However, at the wider (30° array), the yields from the 400 MeV/n runs decreased while the yields from the higher energy runs slightly increased. Thus, the yield separation between the 400 MeV/n and the 800 MeV/n data noticeably increased with shielding thickness. All of these trends suggest that increased shielding may limit the production of secondary protons from lower energy incoming beams but can lead to increased proton yields from higher energy beams. This is most likely a result of higher energy beams penetrating further into the target – neither of these incoming beam species (400 MeV/n or 800 MeV/n iron) fully penetrate the target, so the 800 MeV/n iron beams produce higher yields as a result of an increased number of interactions. But across all three thicknesses, and the energy range of detected protons – as the energy of the incoming beam increased, so did the production of secondary protons.

The shape of the deuteron yield measurements (Figures 30-31) detected at the 10° array were the same regardless of source (i.e. incoming iron nuclei energy) and shielding thickness – however, there was a noticeable decline in yield at 30° for the yields from the 400 MeV/n runs. But for the 800 MeV/n runs at 30°, there was a significant jump (a full order of magnitude) at the thickest shielding. The separation between yields from the three paddles – in addition to the yields themselves – at both energies slightly decreased across thickness. At 10° the separation at lower incident particle energies fell with increased shielding but rose at the higher light ion energies. For the 30° array, the separation between the yields (i.e. between 400 MeV/n iron-induced deuterons and 800 MeV/n iron-induced deuterons) increased with thickness between the yields from the low energy iron nuclei and the higher energy. This once again illustrates that the role of additional shielding increases at the wider angles – especially noticeable from the deuterons detected at the 30° array from the 800 MeV/n iron incident upon 60 g/cm^2 aluminium shielding.

The triton yields at 10° (Figure 32) is where the difference between incident particle energy ranges from the two different iron energies is noticeable – the higher energy iron runs produced significantly more higher energy tritons than the lower energy iron runs. The low energy trends between the two different runs overlapped, but then as the triton yields from the 400 MeV/n iron fell off, a slight dip followed by a pronounced rise and [slight] peak came from the higher energy runs. At the thinnest shielding, the lower energy runs produced more low-energy tritons, but these

yields decreased with increasing shield thickness while the triton yields from the higher energy runs stayed fairly consistent with shielding thickness.

The two helium ions (Figures 33-34) had much flatter distributions from the 400 MeV/n runs, but the higher energy iron nuclei produced a sharper rise (culminating in a peak). The energy scale is slightly different for the helium ions as well – there was not as much separation in the two helium ion lines (in the time-of-flight plots) at higher energies, so helium ion separation was only detectable at lower energies. This was true for all helium nuclei regardless of the incoming beam energy – both helion and alpha yields fell off at roughly the same energy regardless of incoming beam energy. This consistent yield fall-off was not seen in the three hydrogen nuclei, as the energy range from the 800 MeV/n iron runs produced higher energy secondary ions. The effect of increased shielding was most noticeably seen with the light ions produced by the lower energy iron runs – the thicker aluminium upstream targets led to reduced secondary light ion yield measurements.

The influence of shielding thickness was the basis of this research, and Figures 28-34 show measured light ion yields at both detector arrays across all three shielding thicknesses whilst specifically comparing the differences between incoming beam energy. It can be seen that there is no definitive proof of "increased shielding leads to increased yields" but rather that the influence of shielding drastically changes the light ion yields from heavy nuclei on a more dynamic energy scale – the light ions produced by lower energies were more easily moderated by thicker shielding materials, but the higher energy iron nuclei produced yields that did not change as much across the three shielding thicknesses. The separation between the yields from 800 MeV/n- and 400 MeV/n-produced secondaries increased with both shielding and energy, showing that – especially for incoming spectra as diverse in both nuclei and energy as galactic cosmic rays – increased shielding does not necessarily decrease the overall production of charged secondary light ions, because while increased shielding moderates lower energy beams better, it also leads to increased target interactions for higher energy beams.

Sumary of Major Findings:

- Light ion yields increase with projectile energy – higher energy projectiles penetrate further into the target. An increase in projectile range leads to more interactions (via an increase in the number of projectile mean free paths) that produce more secondary light ions.

- The differences between yields from the lower energy beams (400 MeV/n) and higher energy beams (800 MeV/n) increase with shielding, as a result of the increased number of potential reactions. Increased shielding leads to increased interactions.
- The overall trends in each light ion data set – i.e. the shape of each spectra – remain the same, regardless of incident beam energy. This suggests that incoming particle energy is not a factor in creating the shape of each yield spectrum, but it just affects the magnitude of the yield itself.
- The energy range of detected secondary light ions is wider for the higher energy projectiles. This suggests that projectile fragmentation is the source of these secondary light ions, as higher energy projectiles would lead to higher energy fragments.

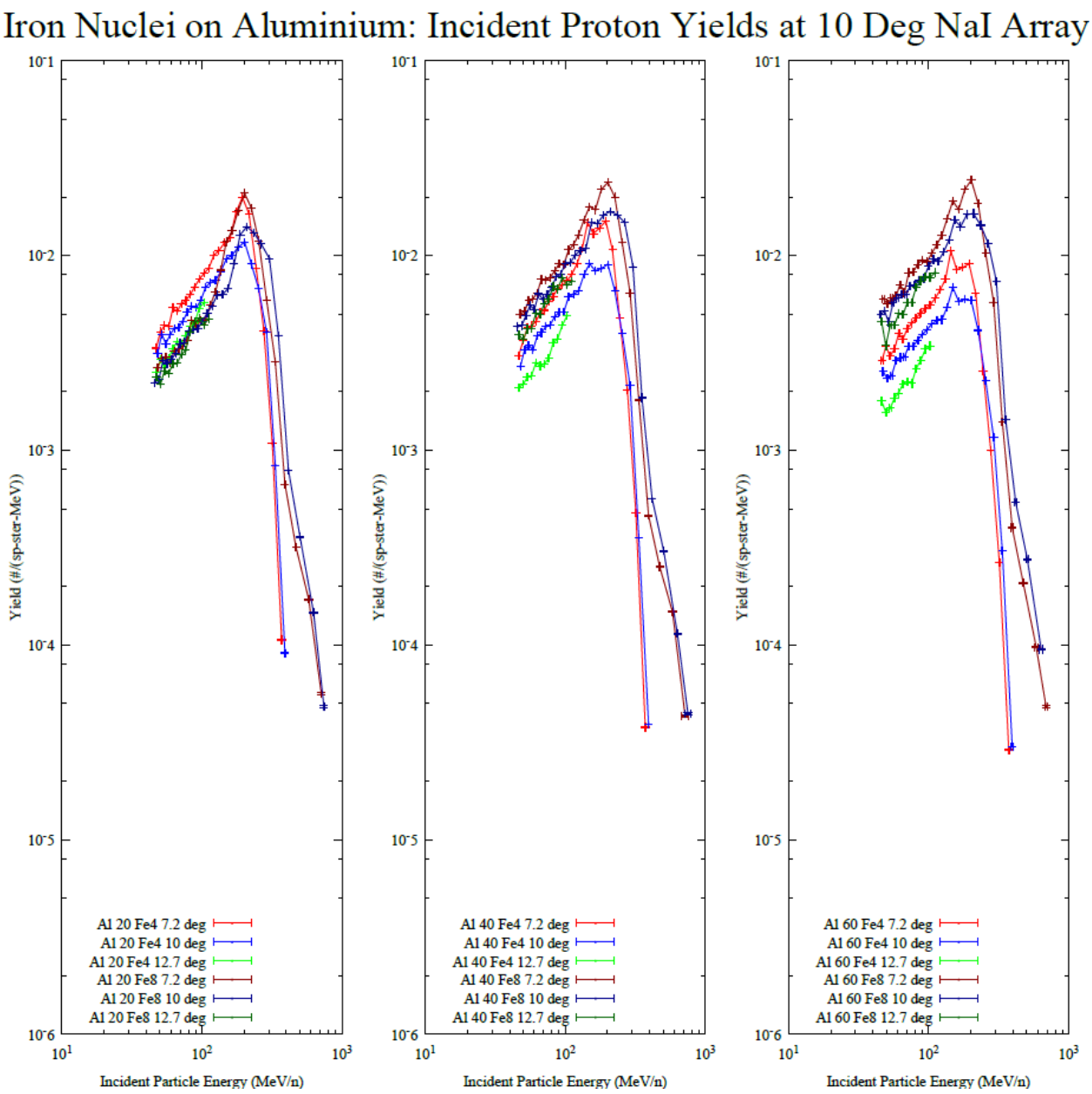


Figure 28. Proton Double Differential Yields as a function of incoming energy per nucleon from the 400 and 800 MeV/n Iron beams on the 10° NaI Array at the 20g/cm^2 (left), 40 g/cm^2 (middle), and 60 g/cm^2 (right) Aluminium shielding thicknesses

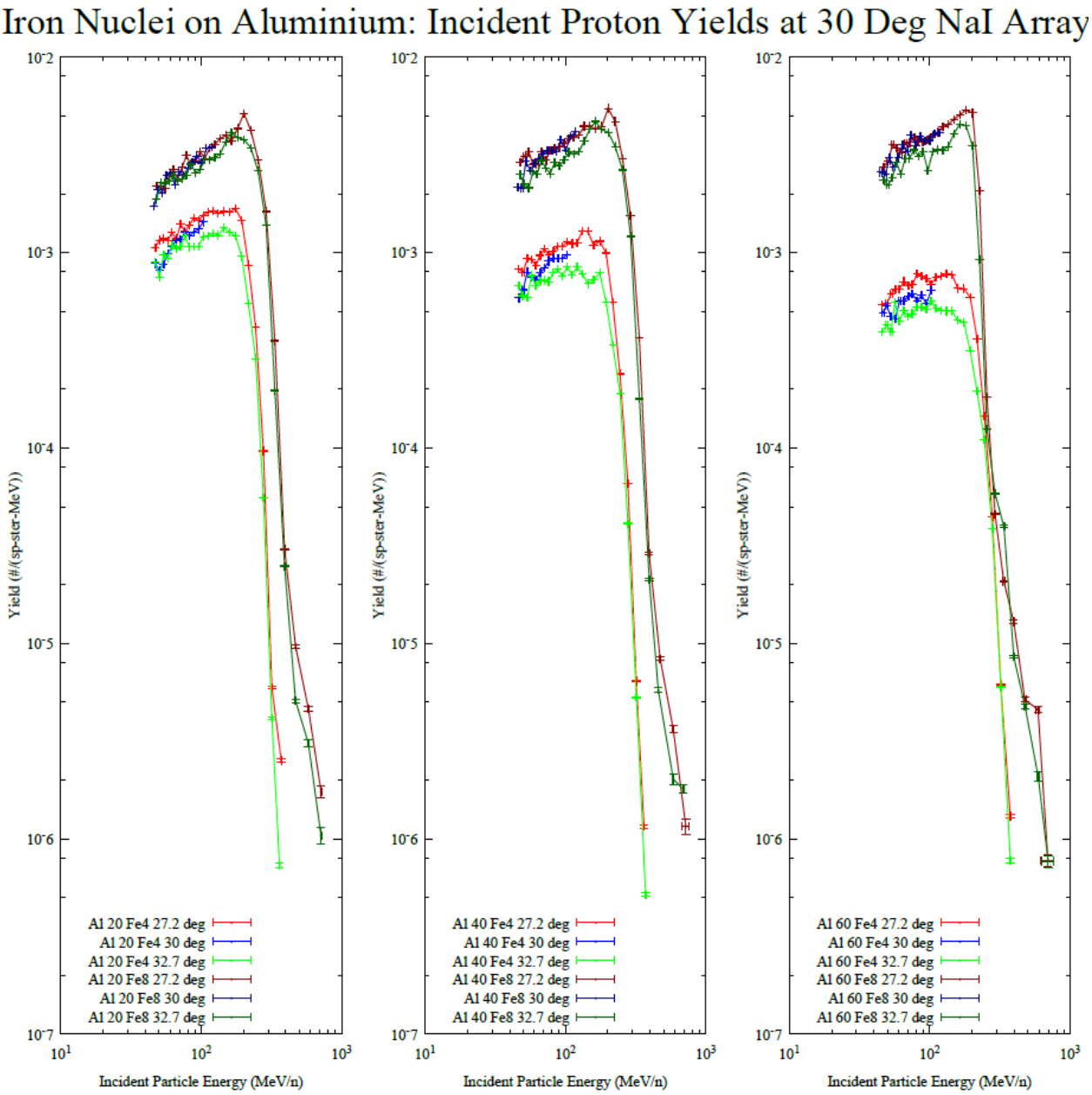


Figure 29. Proton Double Differential Yields as a function of incoming energy per nucleon from the 400 and 800 MeV/n Iron beams on the 30° NaI Array at the 20g/cm^2 (left), 40 g/cm^2 (middle), and 60 g/cm^2 (right) Aluminium shielding thicknesses

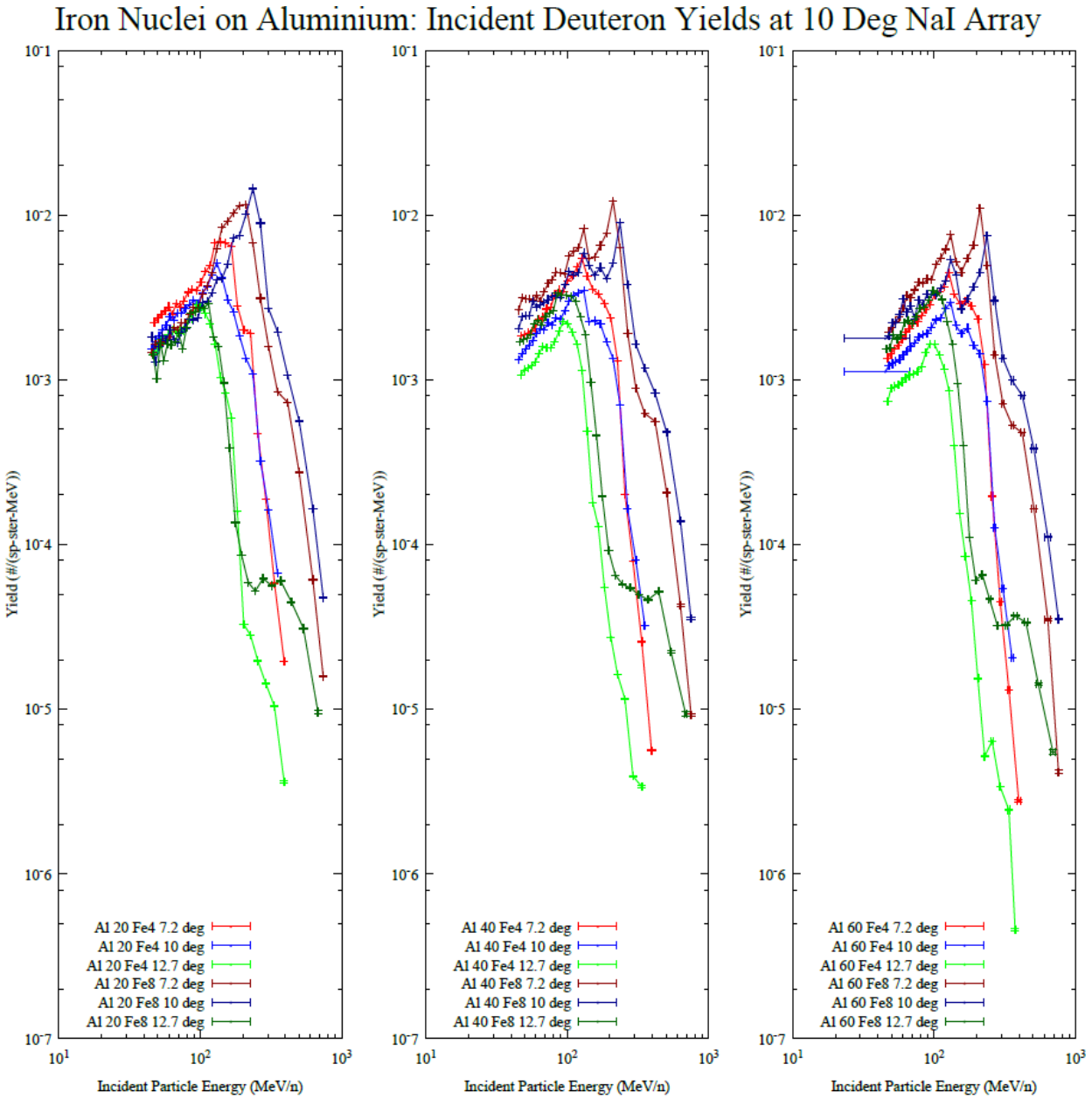


Figure 30. Deuteron Double Differential Yields as a function of incoming energy per nucleon from the 400 and 800 MeV/n Iron beams on the 10° NaI Array at the 20g/cm^2 (left), 40 g/cm^2 (middle), and 60 g/cm^2 (right) Aluminium shielding thicknesses

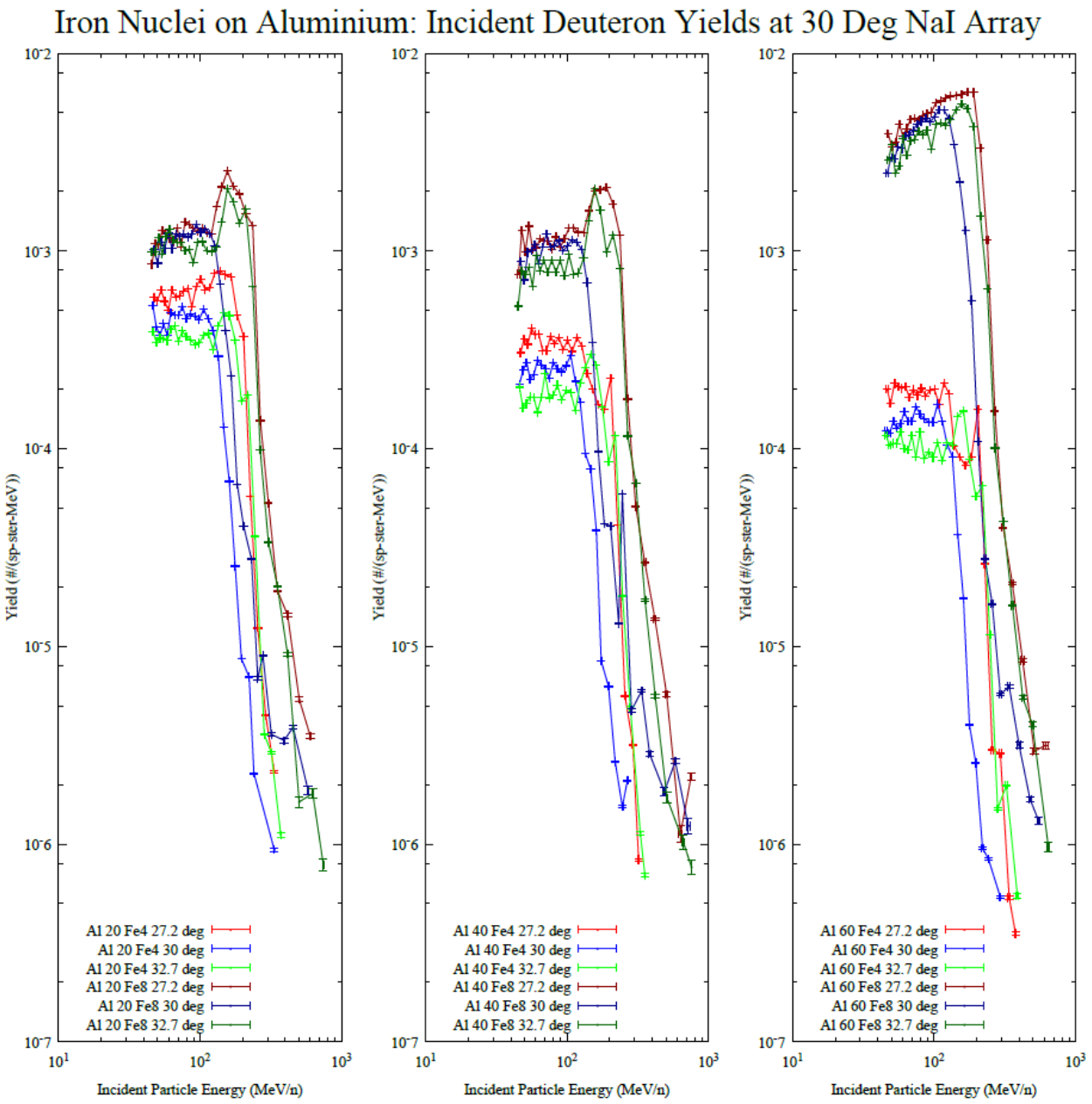


Figure 31. Deuteron Double Differential Yields as a function of incoming energy per nucleon from the 400 and 800 MeV/n Iron beams on the 30° NaI Array at the 20g/cm^2 (left), 40 g/cm^2 (middle), and 60 g/cm^2 (right) Aluminium shielding thicknesses

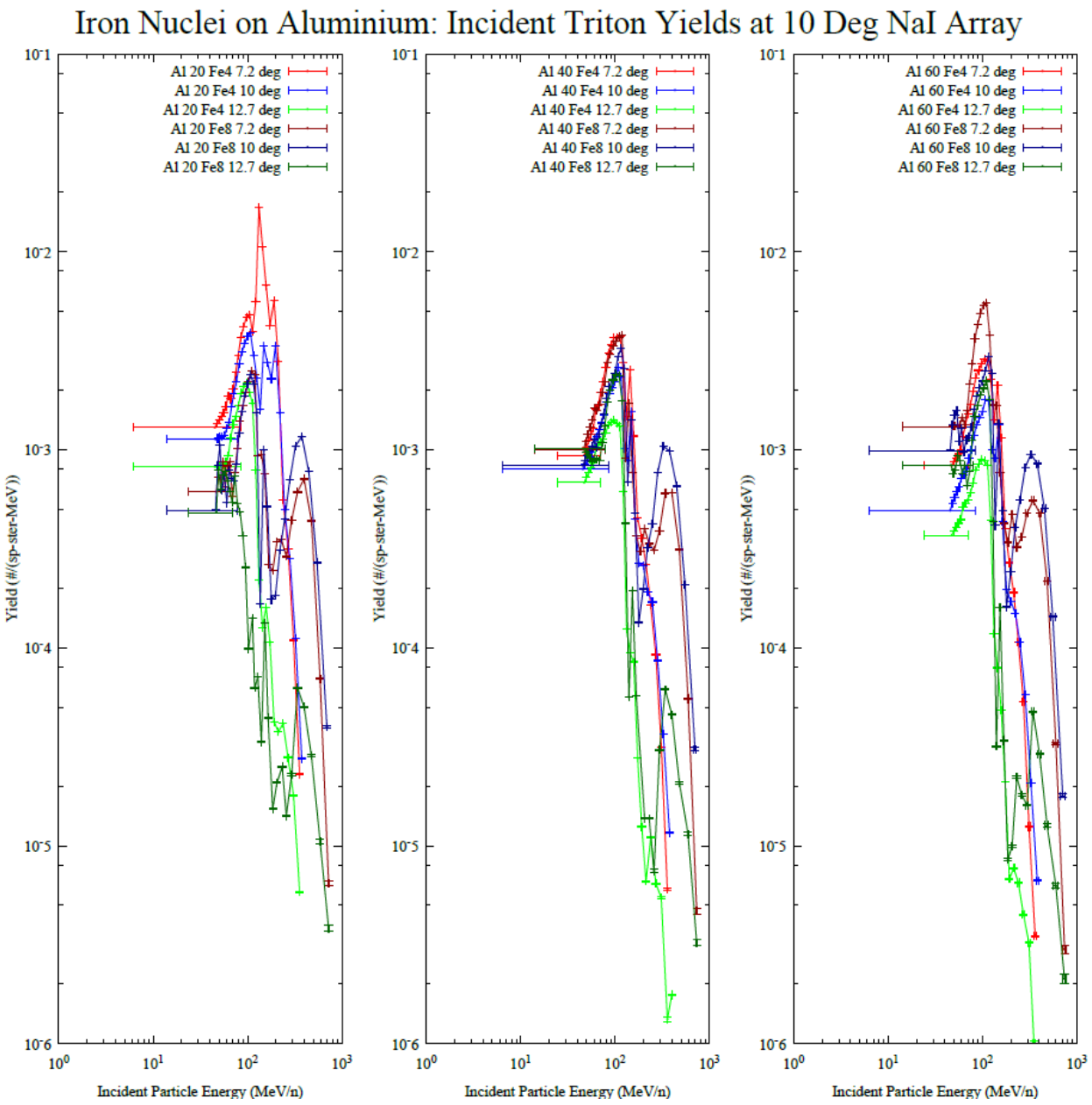


Figure 32. Triton Double Differential Yields as a function of incoming energy per nucleon from the 400 and 800 MeV/n Iron beams on the 10° NaI Array at the 20g/cm^2 (left), 40 g/cm^2 (middle), and 60 g/cm^2 (right) Aluminium shielding thicknesses

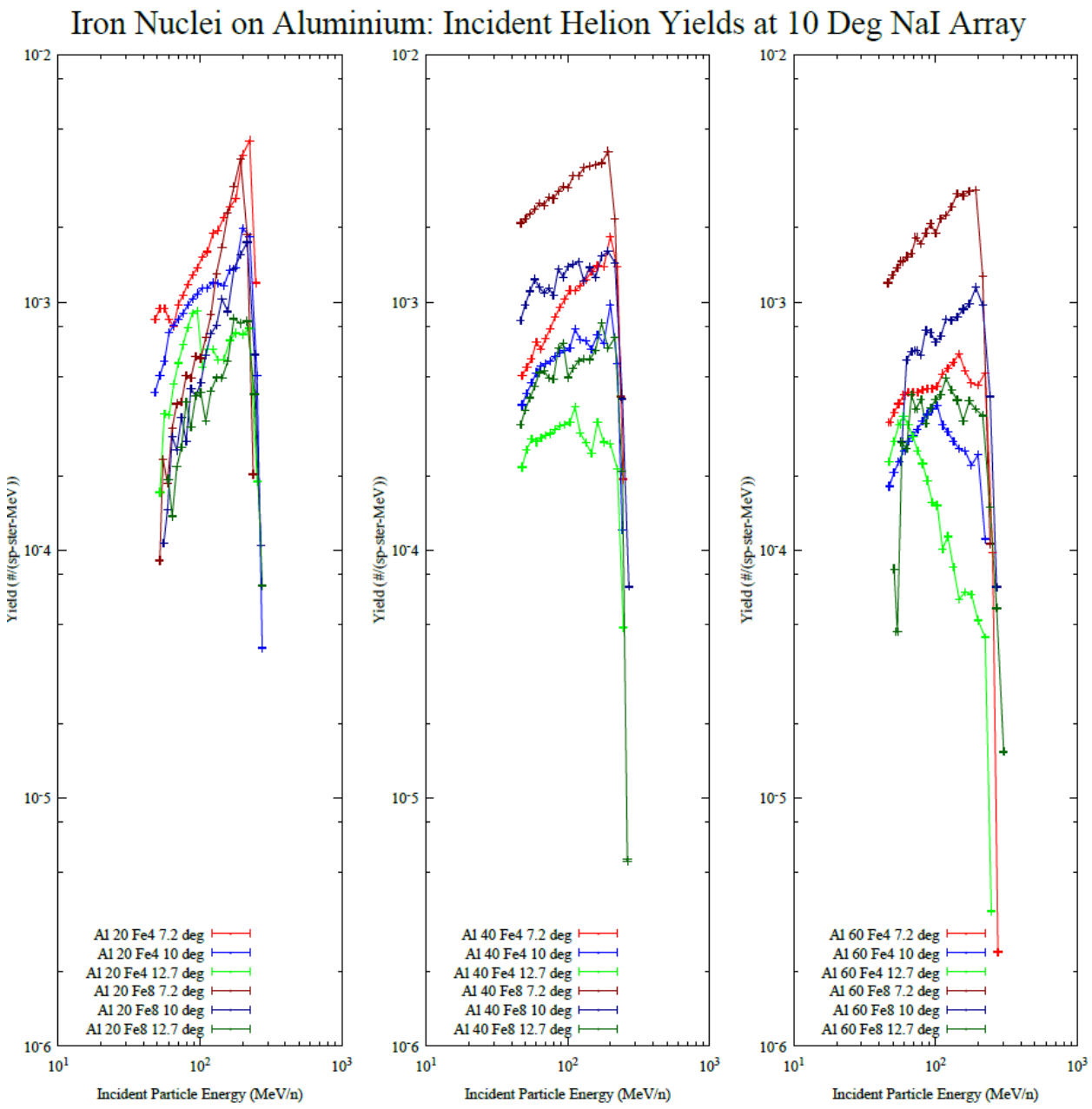


Figure 33. Helion (3-He) Double Differential Yields as a function of incoming energy per nucleon from the 400 and 800 MeV/n Iron beams on the 10° NaI Array at the 20g/cm^2 (left), 40 g/cm^2 (middle), and 60 g/cm^2 (right) Aluminium shielding thicknesses

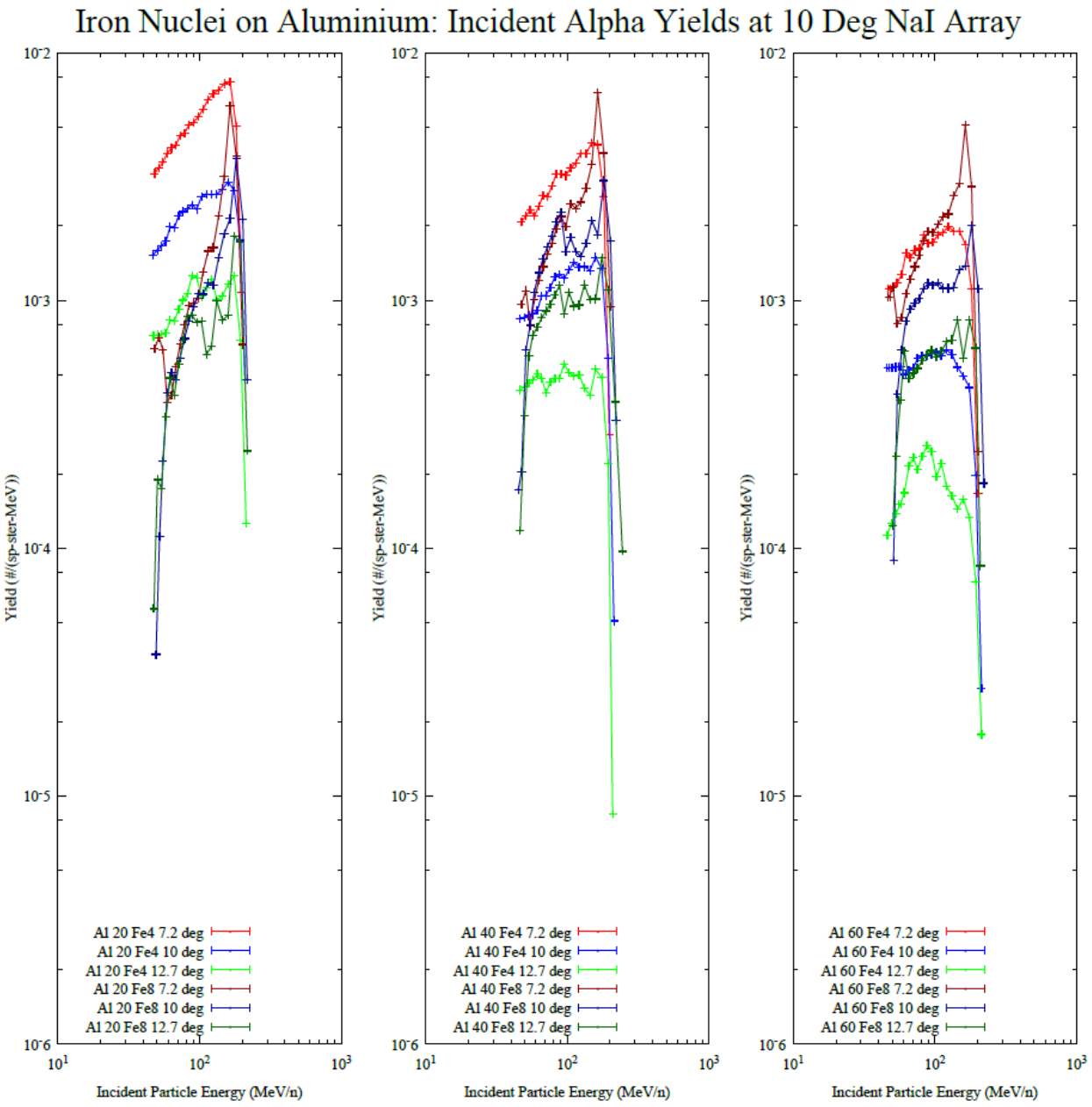


Figure 34. Alpha (4-He) Double Differential Yields as a function of incoming energy per nucleon from the 400 and 800 MeV/n Iron beams on the 10° NaI Array at the at the 20g/cm^2 (left), 40 g/cm^2 (middle), and 60 g/cm^2 (right) Aluminium shielding thicknesses

5.5.2 Yield Influences from variation in Incoming Beam Species

Table 8 summarizes what light ions are seen at each detector array for the three 400 MeV/n incoming nuclei systems (hydrogen, helium, and iron), and which figures illustrate which data sets. The ensuing plots illustrate the yield differences across all three target thicknesses for each light ion of interest. In each plot: the *x*-axis is the light ion energy in MeV/n, and the *y*-axis is the light ion yield per source particle per steradian per MeV/n. The leftmost is for the 20 g/cm^2 aluminium thickness, the middle is for the 40 g/cm^2 shielding, and the rightmost shows the 60 g/cm^2 results.

Table 8. Summary of light ion detection from 400 MeV/n iron, helium, and hydrogen nuclei systems for all three aluminium shielding thicknesses and corresponding figures for each light ion yield comparison.

IRON 400					
Al Thickness (g/cm2)	**^{1}H**	**^{2}H**	**^{3}H**	**^{3}He**	**^{4}He**
20	10° / 30°	10° / 30°	10° / 30°	10°	10°
40	10° / 30°	10° / 30°	10° / 30°	10°	10°
60	10° / 30°	10° / 30°	10° / 30°	10°	10°
HELIUM 400					
Al Thickness (g/cm2)	**^{1}H**	**^{2}H**	**^{3}H**	**^{3}He**	**^{4}He**
20	10° / 30°	10° / 30°	10°	---	10°
40	10° / 30°	10° / 30°	10°	---	10°
60	10° / 30°	10° / 30°	10°	10°	10°
HYDROGEN 400					
Al Thickness (g/cm2)	**^{1}H**	**^{2}H**	**^{3}H**	**^{3}He**	**^{4}He**
20	10° / 30°	10°	---	---	---
40	10° / 30°	10°	---	---	---
60	10° / 30°	10°	---	---	---
FIGURE #	35 / 36	37 / 38	39	40	41

Figures 35-41 compare the light ion yields as the Z of the incoming beam changes with energy. As the Z of the incoming beam increases, the resulting light ion yields are higher – this is a result of projectile fragmentation. For heavier beams, there are more nucleons, thus as the incoming beam propagates through the aluminium shielding, more light ion secondaries can be sheared off of the beam nuclei. And considering the lack of detected ions heavier than deuterons from the incoming proton beam (as compared to the helium and iron runs, as summarized in Table 8), projectile fragmentation seems to be the bigger source of secondary light ions than target fragmentation. This is also supported by comparing the relative momentum of the beam and the

target – target nuclei are stationary, whereas projectile nuclei are moving very fast in a forward direction.

For the proton yields (Figures 35-36), the separation between the detected yields decreases with thickness at both detector arrays. This is because the helium and hydrogen beams fully penetrate all three aluminum shielding thicknesses, whereas the iron beam is fully stopped within the thinnest aluminium shielding. Increased penetration depth leads to increased interactions. The iron and helium-induced proton yields share the same trends – the rise, peak, and fall all occur across the same proton energy range. The proton yields from the iron beam decrease with increased shielding, and vice versa for the helium beam. However, the change in shielding thickness does not seem to have an influence on the proton yields from the hydrogen beam runs. This could be a result of beam protons scattering directly into the detector systems in addition to target fragmentation. It is believed that projectile fragmentation is a bigger contributor to light ion yields (compared to target fragmentation), and because proton fragmentation is impossible, most of these detected protons must be coming from the scattered beam particles. Target particles are stationary, and thus target fragmentation would result in both isotropic scattering (as opposed to forward-focused beam particles) as well as fragments generally too low in energy to escape the target. A main consistency across the data from the two detector arrays is that the measured yields decrease at wider angles.

The deuteron yields are displayed in Figures 37 and 38, and these are the heaviest ions detected from the hydrogen beam experimental runs (and only at the 10° array). Pick-up reactions are the flow of nucleons (specifically neutrons) from the target nucleus to the projectile nucleus and explains the production of deuterons from the incoming proton beam. A second option would be the direct production of deuterons via knockout reactions, where the momentum of the incident proton is transferred to the deuteron ejected from the target. The deuterons from the helium runs peak at higher energies than the ones detected from the iron runs – i.e. the iron-induced deuterons are mainly lower energy ions, while the helium-induced deuterons are found more at higher energies. This happens because of differing beam penetration – if the production point for the helium-induced deuterons is further into the upstream target, then the secondary deuterons have less of the aluminium target to penetrate through, and thus lose less energy than a deuteron born closer to the upstream face of the target. At the 30° array, though, the trends for both sets of

deuteron yields are the same. The difference in yields between the data from the iron beams and helium beams decreases with thickness though, as a result of both the iron-induced deuteron yields decreasing with increased shielding and the deuterons from helium beams increasing with the extra aluminium.

The iron experimental runs are primarily the only runs where tritons are detected (Figure 39), which is most likely a result of the composition of tritons. An iron nucleus has many more nucleons than an alpha particle, so presumably it is more likely for an iron beam to fragment into triton particles than an alpha particle. But the triton yields from the incoming alpha beams increases with shielding – a result of increased opportunities for the correct knock-out reaction to convert a helium-4 nucleus into a hydrogen-3 nucleus.

Similarly, for helions (Figure 40), they are only produced (at detectable levels) from the helium beam experimental runs at the 60 g/cm^2 aluminum shielding – most likely again a result of increased material providing increased opportunities for the reactions to occur. The iron-induced helion yield has a flat distribution across the ^{3}He energy range (no real peaks or rises) but decreases with increased shielding thickness. This is also seen with the alpha particles (Figure 41) – the iron yields slightly decrease with shielding while also maintaining the "flat" trendline. However, the yields from the helium beams sharply increased with thickness. As the energy of the detected alpha ions increased, the yields had a sharp rise and peak, unlike the flatness of the iron-induced alpha trendline. The production of both helium nuclei (^{3}He and ^{4}He) from both incoming beam species had a larger dependence on angle (within each array) than from the three hydrogen nuclei. The influence of wider angles was much more noticeable, even in the small increases from 7.2° to 10° to 12.7°.

Across all five light ions, as the upstream target got thicker, the heavier beam (iron) produced fewer secondary ions, while the secondary ion production from the lighter beams (hydrogen, helium) increased. The galactic cosmic ray spectrum is dominated by hydrogen and helium nuclei, so the fact that more secondary ions are produced when lighter nuclei are bombarded at increased shielding suggests that this could be a major source of increased dose beyond thicker shielding. The increased shielding is better at reducing secondaries from the heavier beam (iron) but does result in increased light ion production from the lighter beams (hydrogen and helium). This is a result of the stopping power of the aluminium – the heavier beam (iron) is moderated by each of

the three shielding thicknesses, while the lighter beams (hydrogen and helium) punch through the upstream target. Thus, the lighter ions have more opportunities for interactions within thicker targets, leading to increased light ion production. This is reflected in the collional mean free paths for these beam particles. The mean free path is the average distance traversed by a particle between collisions and is calculated from the relevant collisional cross-section measurements. Thus, a thicker target leads to an increased number of mean free paths the incident beam will travel through, leading to increased projectile-target reactions. The data shows that finding the right shielding would need to isolate specific ion contributions to dose to find the optimal thickness that blocks out light ions from heavier sources while also minimizing the increased secondary light ion production from the lighter nuclei.

Summary of Major Findings:

- The light ion yields increase with projectile mass – larger nuclei have more nucleons, which leads to more secondary ions. This indicates that projectile fragmentation is the main source of the secondary light ions that escape the target.
- The differences in the magnitude of the light ion yields (from each of the different species) decreases with increased shielding. This shows the influence of beams that stop within the upstream target (like the incoming iron nuclei) versus those that fully punch through (hydrogen and helium). Increased shielding for the iron beams provides more material for the produced secondaries to be moderated by, while also increasing the number of potential interactions (via an increase in the mean free paths) for the hydrogen and helium beams.
- The different incoming beam species produces different spectral shapes for each light ion (most notably seen with deuterons), illustrating the influence in the incoming nuclei in the resulting measured yields.
- The different incoming beam nuclei affect what can be detected. This further shows beam fragmentation as the primary source of these detected ions – some of the larger nuclei (e.g. tritons and helions) are only detected consistently with the heaviest incoming (iron) nuclei.

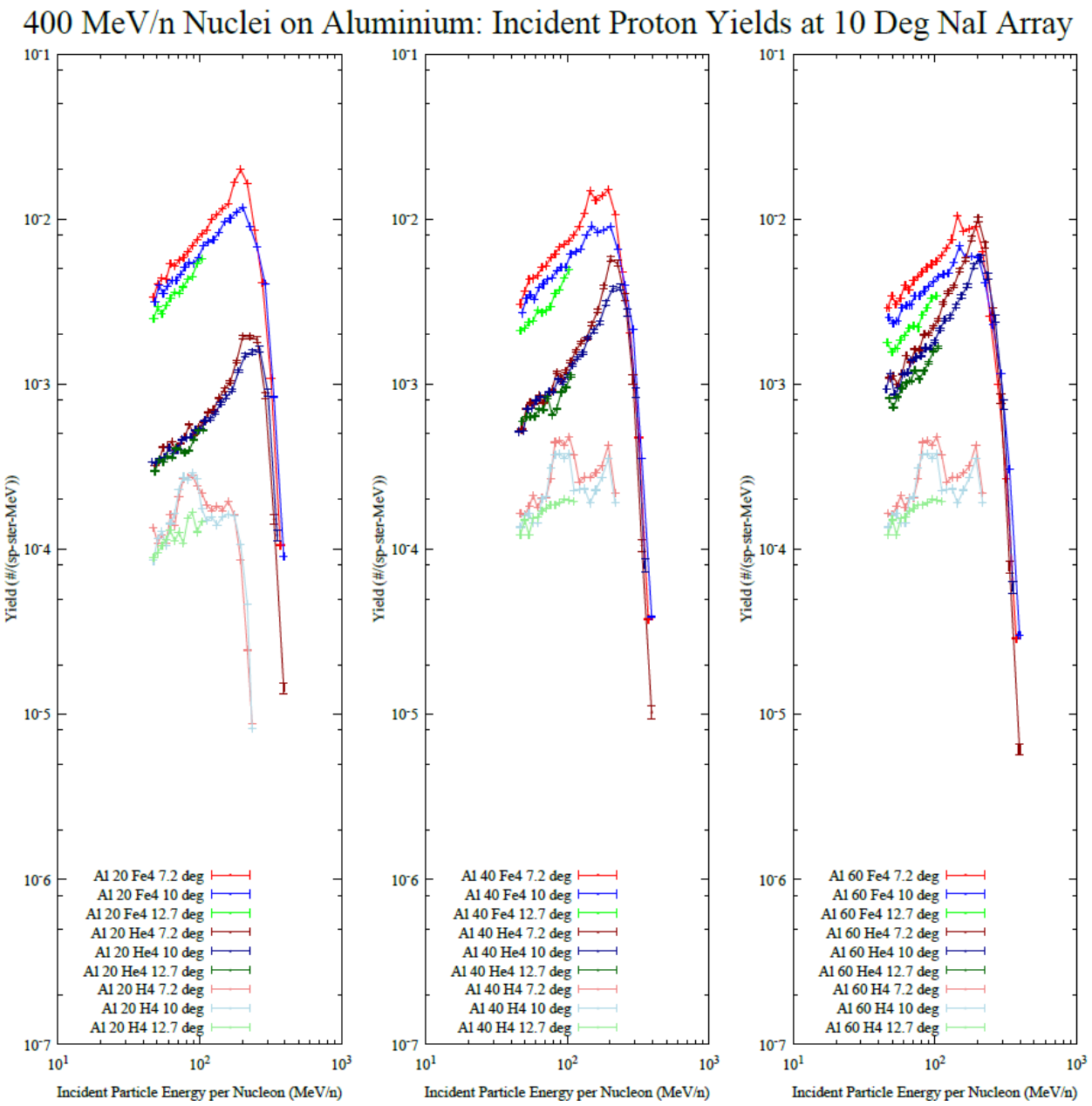


Figure 35. Proton Double Differential Yields as a function of incoming energy per nucleon from the 400 MeV/n Iron, Helium, and Hydrogen beams on the 10° NaI Array at the 20g/cm^2 (left), 40 g/cm^2 (middle), and 60 g/cm^2 (right) Aluminium shielding thicknesses

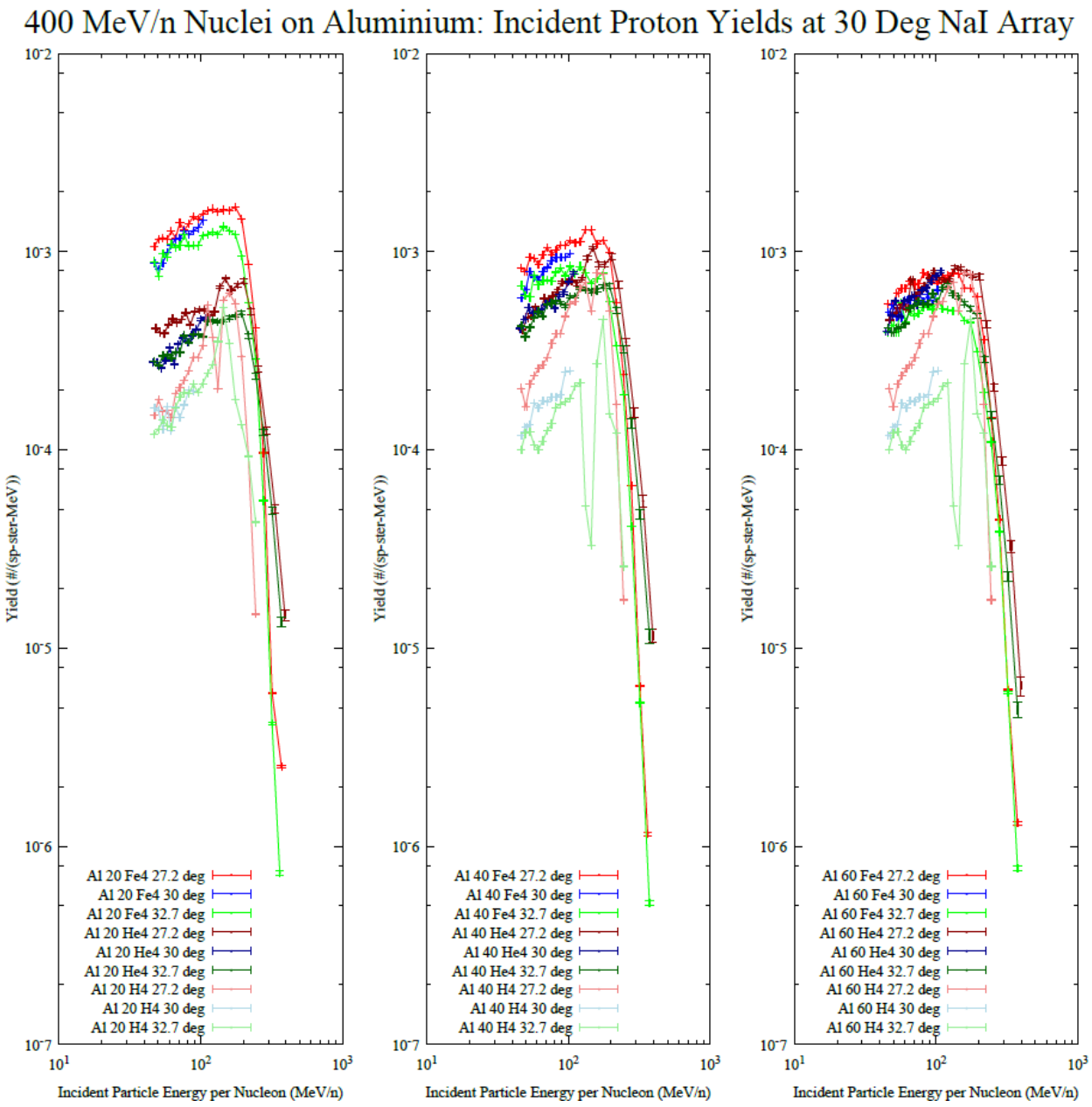


Figure 36. Proton Double Differential Yields as a function of incoming energy per nucleon from the 400 MeV/n Iron, Helium, and Hydrogen beams on the 30° NaI Array at the 20g/cm^2 (left), 40 g/cm^2 (middle), and 60 g/cm^2 (right) Aluminium shielding thicknesses

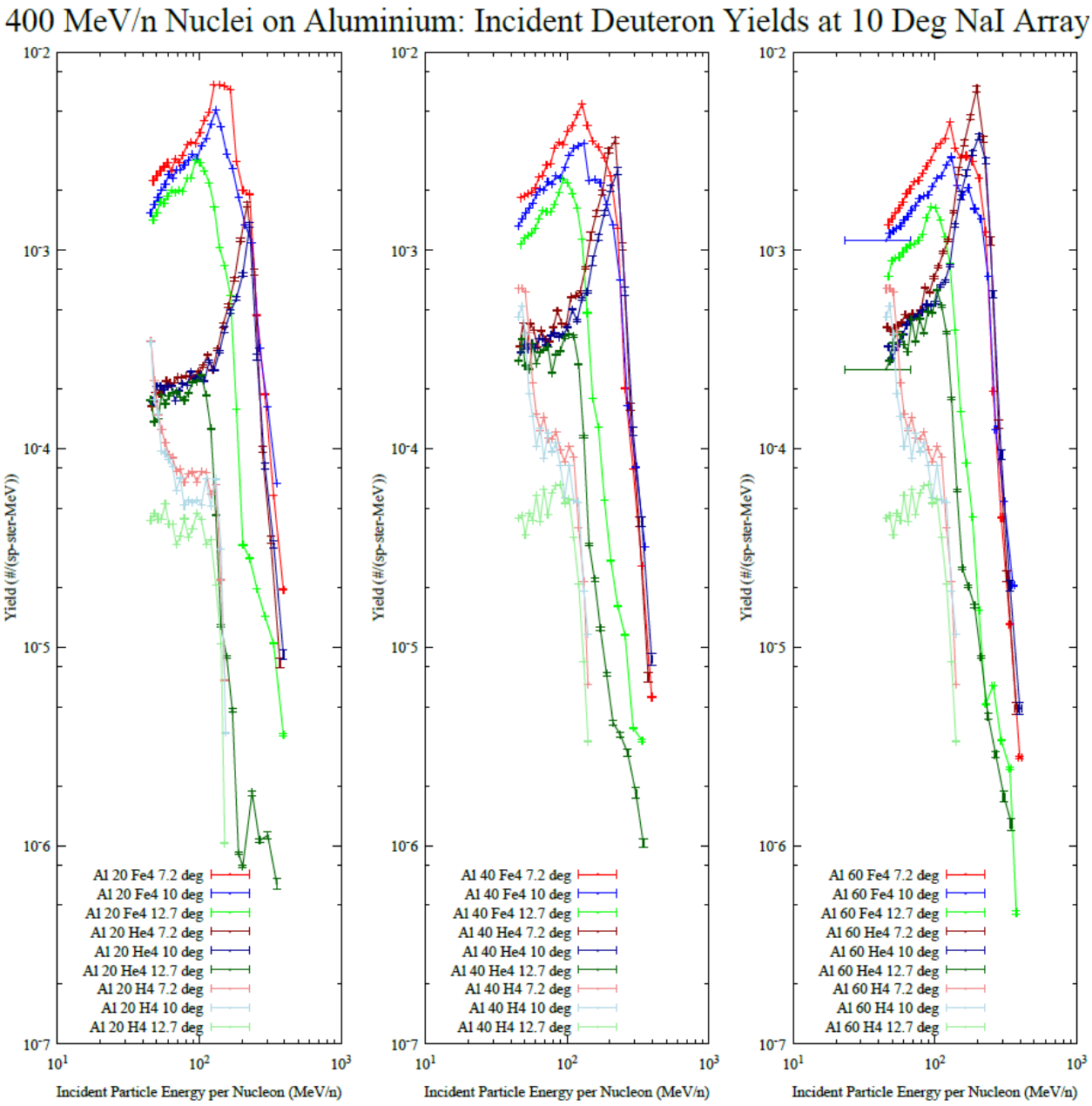


Figure 37. Deuteron Double Differential Yields as a function of incoming energy per nucleon from the 400 MeV/n Iron, Helium, and Hydrogen beams on the 10° NaI Array at the 20g/cm^2 (left), 40 g/cm^2 (middle), and 60 g/cm^2 (right) Aluminium shielding thicknesses

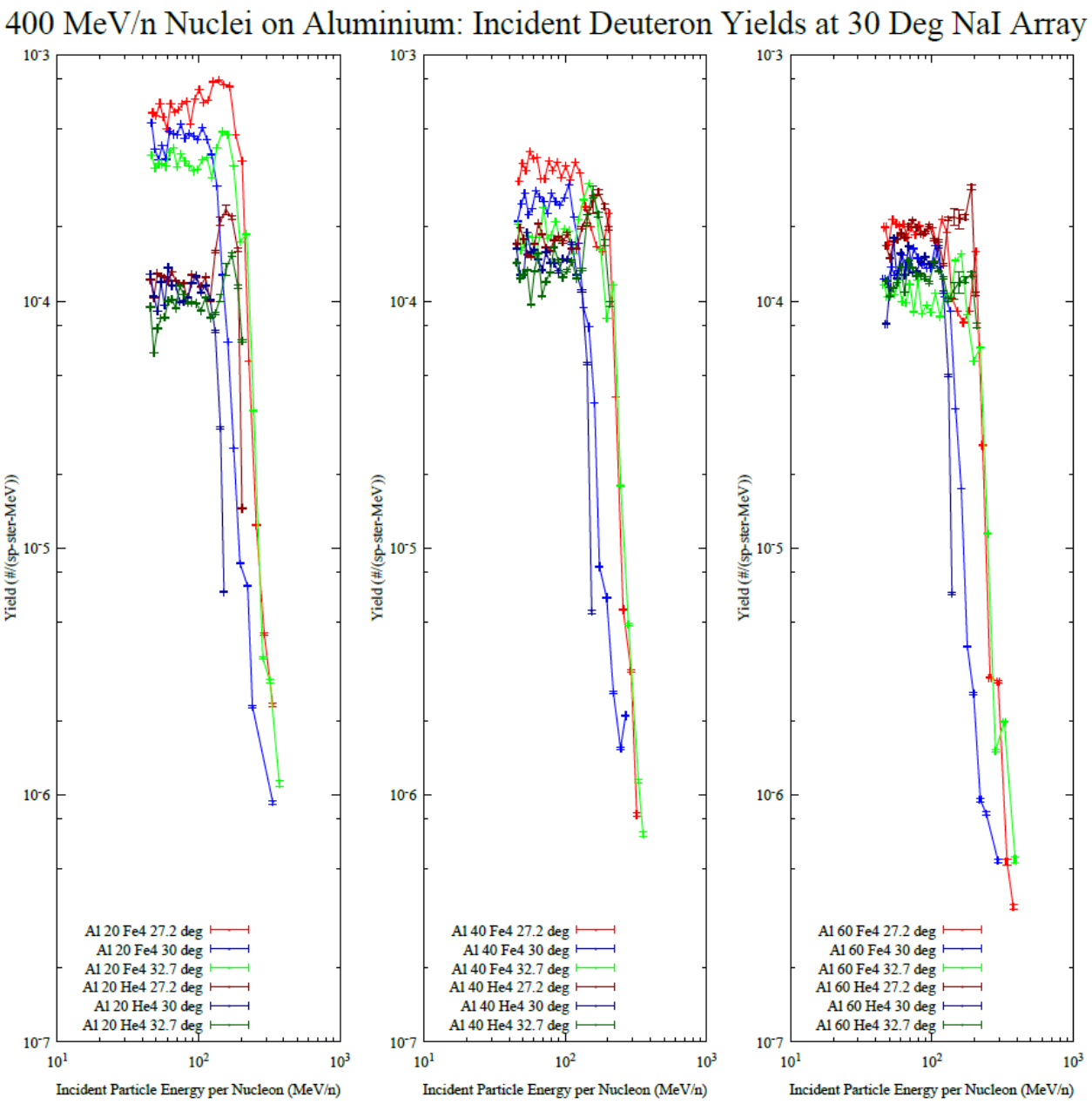


Figure 38. Deuteron Double Differential Yields as a function of incoming energy per nucleon from the 400 MeV/n Iron and Helium beams on the 30° NaI Array at the 20g/cm^2 (left), 40 g/cm^2 (middle), and 60 g/cm^2 (right) Aluminium shielding thicknesses

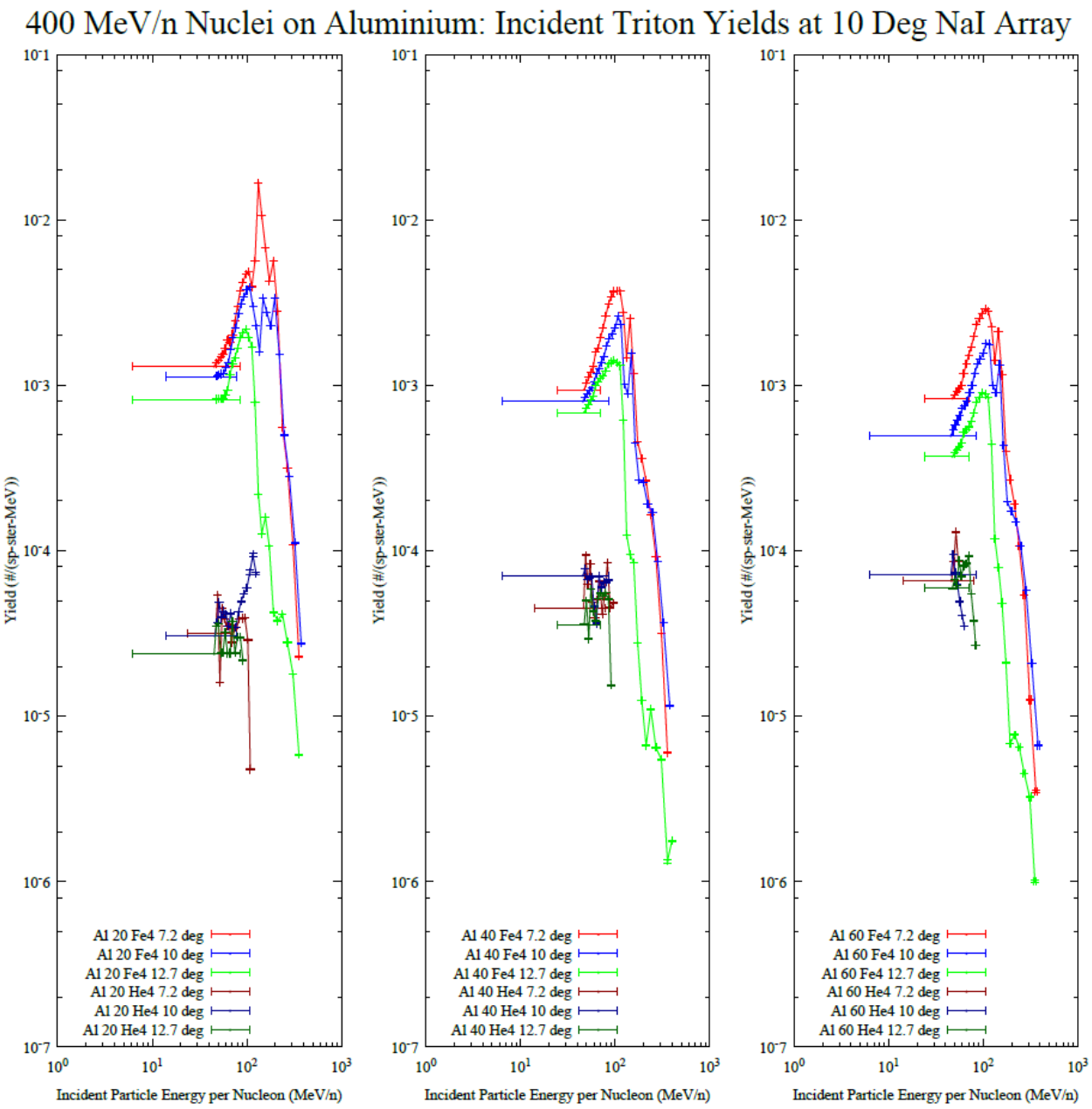


Figure 39. Triton Double Differential Yields as a function of incoming energy per nucleon from the 400 MeV/n Iron and Helium beams on the 10° NaI Array at the 20g/cm^2 (left), 40 g/cm^2 (middle), and 60 g/cm^2 (right) Aluminium shielding thicknesses

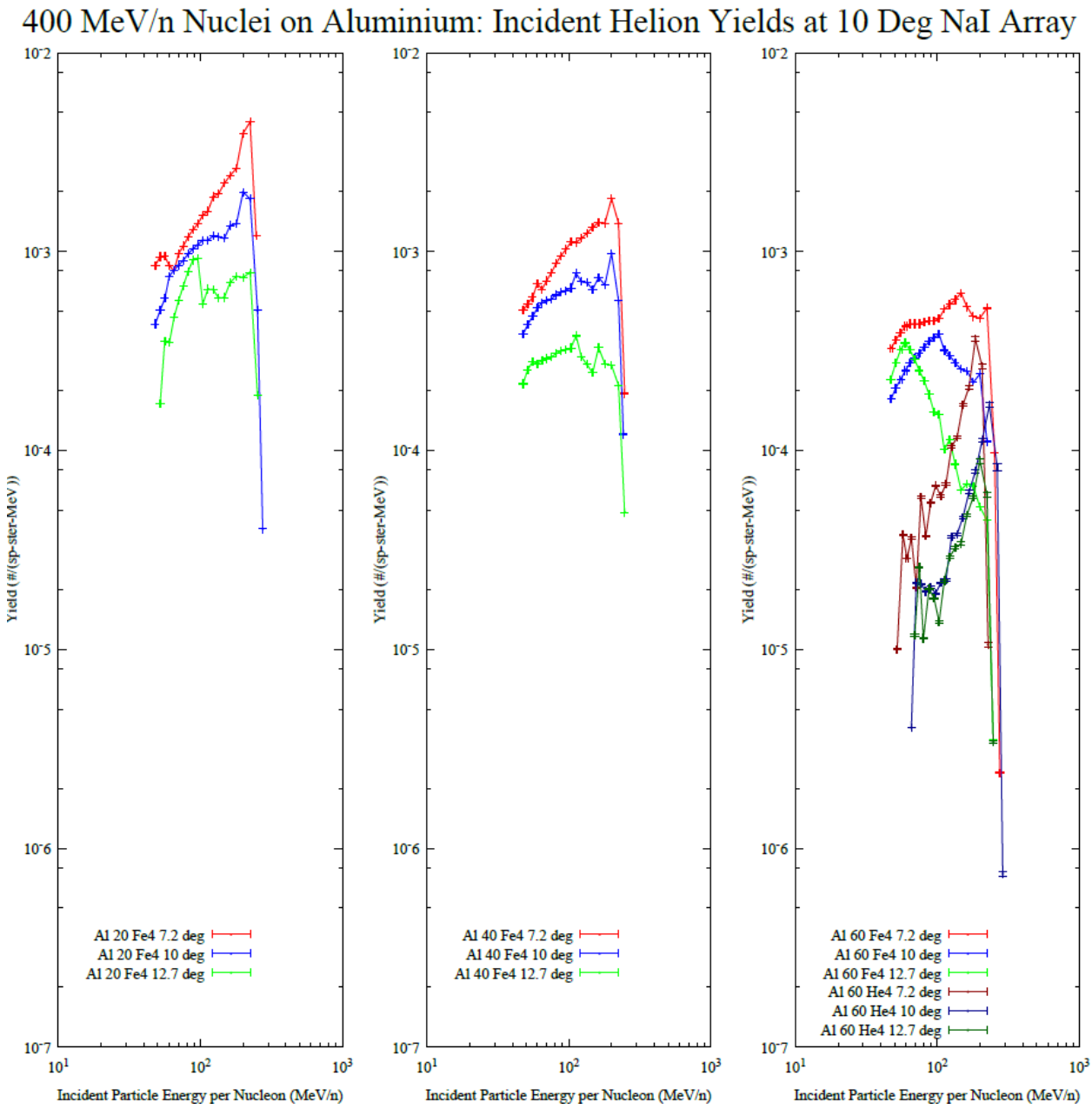


Figure 40. Helion (3-He) Double Differential Yields as a function of incoming energy per nucleon from the 400 MeV/n Iron and Helium beams on the 10° NaI Array at the 20g/cm^2 (left), 40 g/cm^2 (middle), and 60 g/cm^2 (right) Aluminium shielding thicknesses

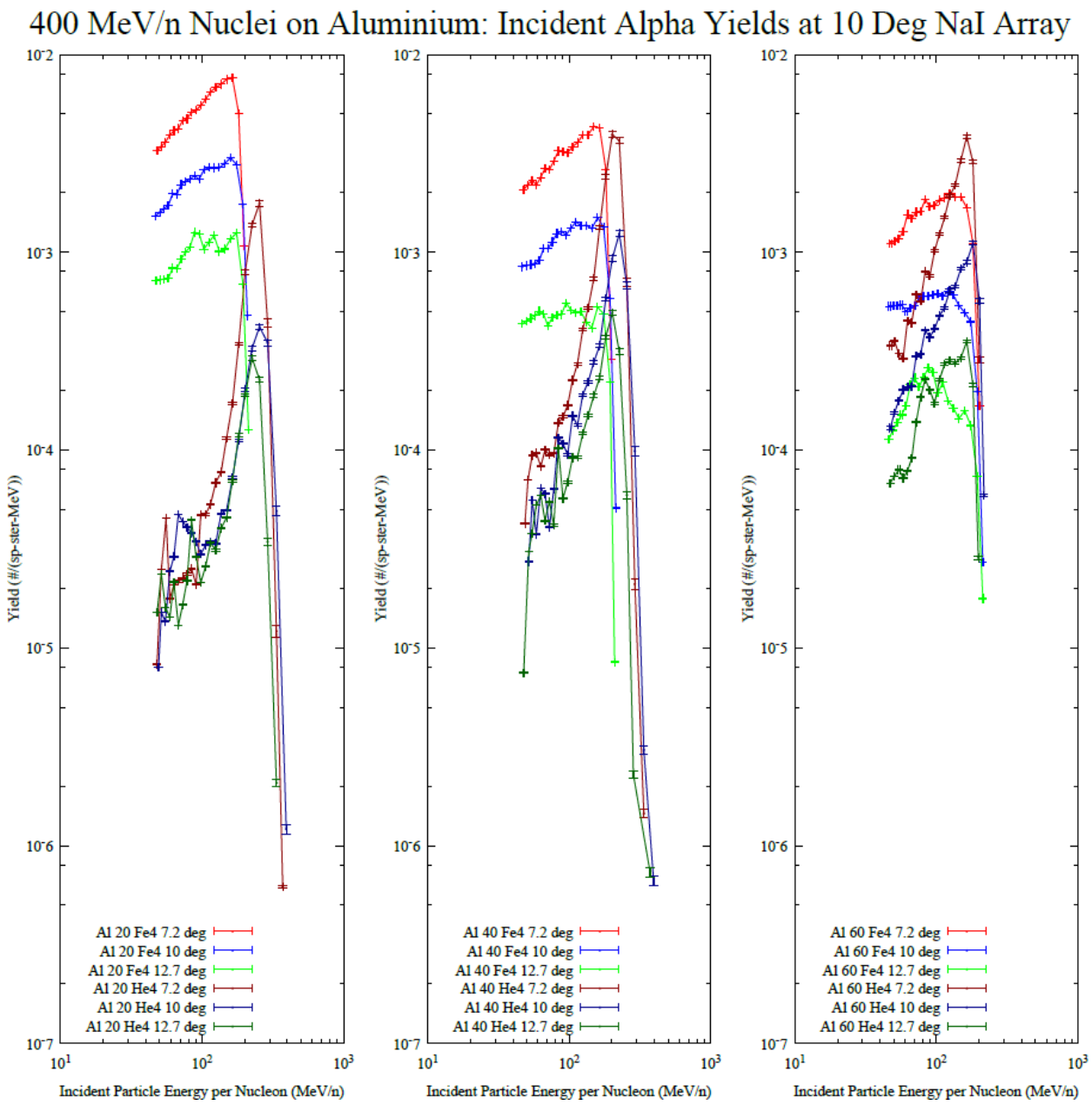


Figure 41. Alpha (4-He) Double Differential Yields as a function of incoming energy per nucleon from the 400 MeV/n Iron and Helium beams on the 10° NaI Array at the 20g/cm^2 (left), 40 g/cm^2 (middle), and 60 g/cm^2 (right) Aluminium shielding thicknesses

5.5.3 NaI vs OLS – Fe 400 MeV/n

Within this experiment, there were multiple charged particle detectors used – one with an inorganic scintillator (the sodium iodide detectors used in this research) and a series of organic liquid scintillator (OLS) detectors. Comparing the yields measured at both detectors will illustrate the benefits of utilizing both detectors in the experiment, as well as serve as a verification to see how well the sodium iodide detectors (NaI) served in this role as an additional charged particle detection system. The system presented in Figures 42-46 are the five light ions seen at the common angles (10°, 30°) from the 400 MeV/n iron nuclei incident upon all three shielding thicknesses. This OLS data comes from Luis Castellanos and can be found in his dissertation publication. [45]

Across all five light ions, the calculated yields from the OLS detectors were generally higher but the NaI yields were across a wider range of energies than the data from the OLS detectors. Because each NaI array composed of two individual sodium iodide detectors, the extra depth to the detector (in addition to the higher stopping power of the inorganic crystal compared to the organic scintillators within the OLS) allowed for the detection at higher energies, resulting in the wider energy range of detected light ions. However, the OLS detectors provided data at energies lower than the resolution of the NaI arrays allowed for. Thus, the two systems could be used in tandem to create yield measurements across a wider energy range than seen in the individual detectors.

The overlap between the NaI data and the OLS data is really promising for all three hydrogen ions – there is very little difference between the two curves at both angles. And with thicker shielding, the measurements line up even closer. For the protons (Figure 42), both detectors (at both angles) demonstrated the slight rise in yield with energy. The deuteron yields within Figure 43 show close similarities within the "overlap region" (i.e. the common energies measured by both detectors), but there is a definitive increase in measured yield. At the thinnest targets, this increase is quite minimal, but as the shielding thickness increases the disparity within the lowest energy NaI points and the highest energy OLS slightly decreases – for the thickest shielding, the two sets of yield curves overlap entirely. This trend is also seen with the triton data (Figure 44), except slightly more magnified – the sharp rise in yield at lower energies is almost exactly calculated by both the NaI and OLS detectors at 10°. For the deuteron and tritons, the overlap region is much smaller than the one for the protons, but for the common energy ranges, the two sets of data match each other. The slope of the deuteron and triton data sets from the OLS detectors in the overlap

regions matched the corresponding rises from the NaI detector, so the overall yield calculations between the two different detectors matched up well for the hydrogen isotopes. The yields were very similar, and the data showed the same trends towards a peak at higher energies (that could only be detected by the NaI arrays). Because of the strong agreement in the yields, the hydrogen isotope data from the NaI and OLS can be synchronized together – utilizing the OLS to detect the low energy secondary ions, and the NaI to detect the higher energy ions.

However, relative to secondary hydrogen measurements, there is slightly more disagreement in helion and alpha production (Figures 45 and 46). The helion and alpha data sets from both detectors have the similar trend of a slight rise at lower energies towards a plateau. However, for helions at the thinnest shielding, the OLS detector overestimates production of ^{3}He, and at the thickest shielding the NaI detector overestimates the helion yield. The intermediate shielding (40 g/cm^2) results in the best comparison between the NaI and OLS detectors. But for the detected alphas, the difference between the OLS and the NaI is reduced with the thicker targets. At the thinnest shielding, the OLS detector detects nearly twice as many secondary alpha particles as the NaI, but this difference is nearly eliminated at the thickest shielding.

The best comparisons between the two data sets comes from the 10° array, because of a threshold issue with the charged scintillator paddle in front of the 30° portion of the second NaI array. This issue was previously discussed in section 5.4, but because the NaI data at the lower energy ranges is still usable, they were presented in Figures 42-44. For the three hydrogen isotopes, stitching together the data from the OLS and NaI detectors is currently feasible. However, there are some jumps in the helium isotope yield curves (alphas at 20 g/cm^2, and helions at both 20 and 60 g/cm^2) that need resolving.

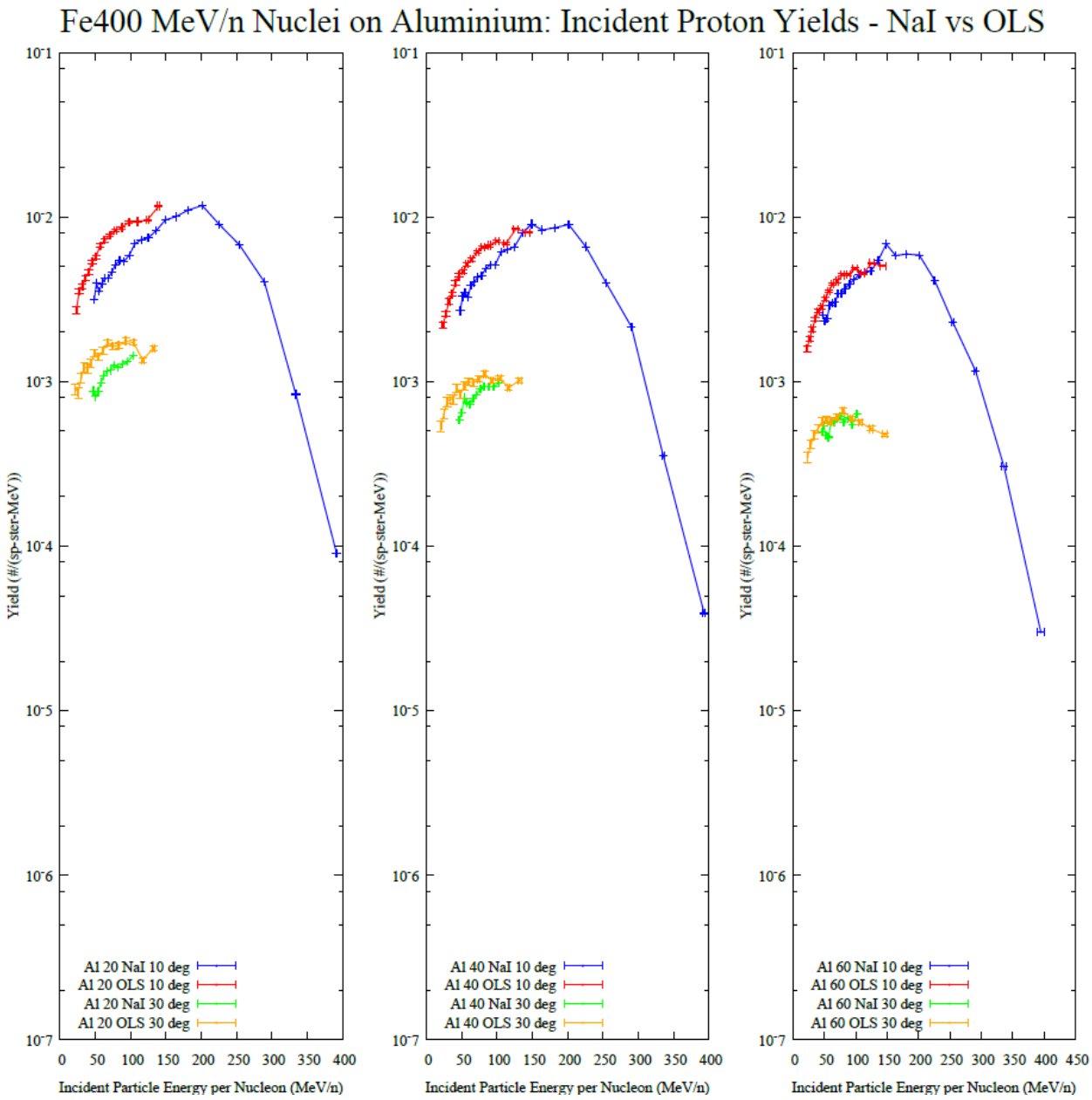


Figure 42. Proton Double Differential Yields as a function of incoming energy per nucleon from the 400 MeV/n Iron beam on the 20g/cm^2 (left), 40 g/cm^2 (middle), and 60 g/cm^2 (right) Aluminium shielding thicknesses detected at 10° and 30° NaI and OLS detectors

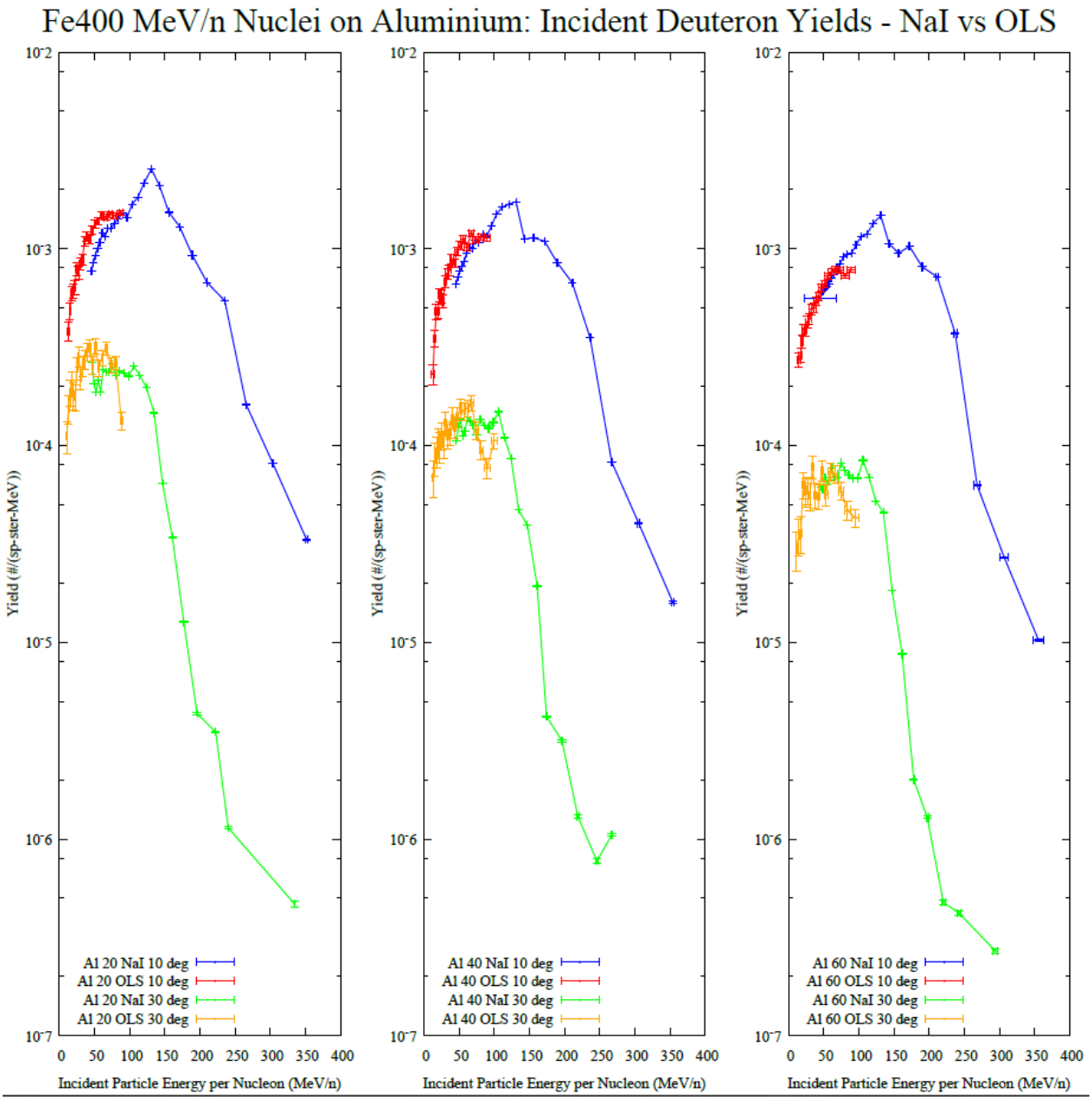


Figure 43. Deuteron Double Differential Yields as a function of incoming energy per nucleon from the 400 MeV/n Iron beam on the 20g/cm^2 (left), 40 g/cm^2 (middle), and 60 g/cm^2 (right) Aluminium shielding thicknesses detected at 10° and 30° NaI and OLS detectors

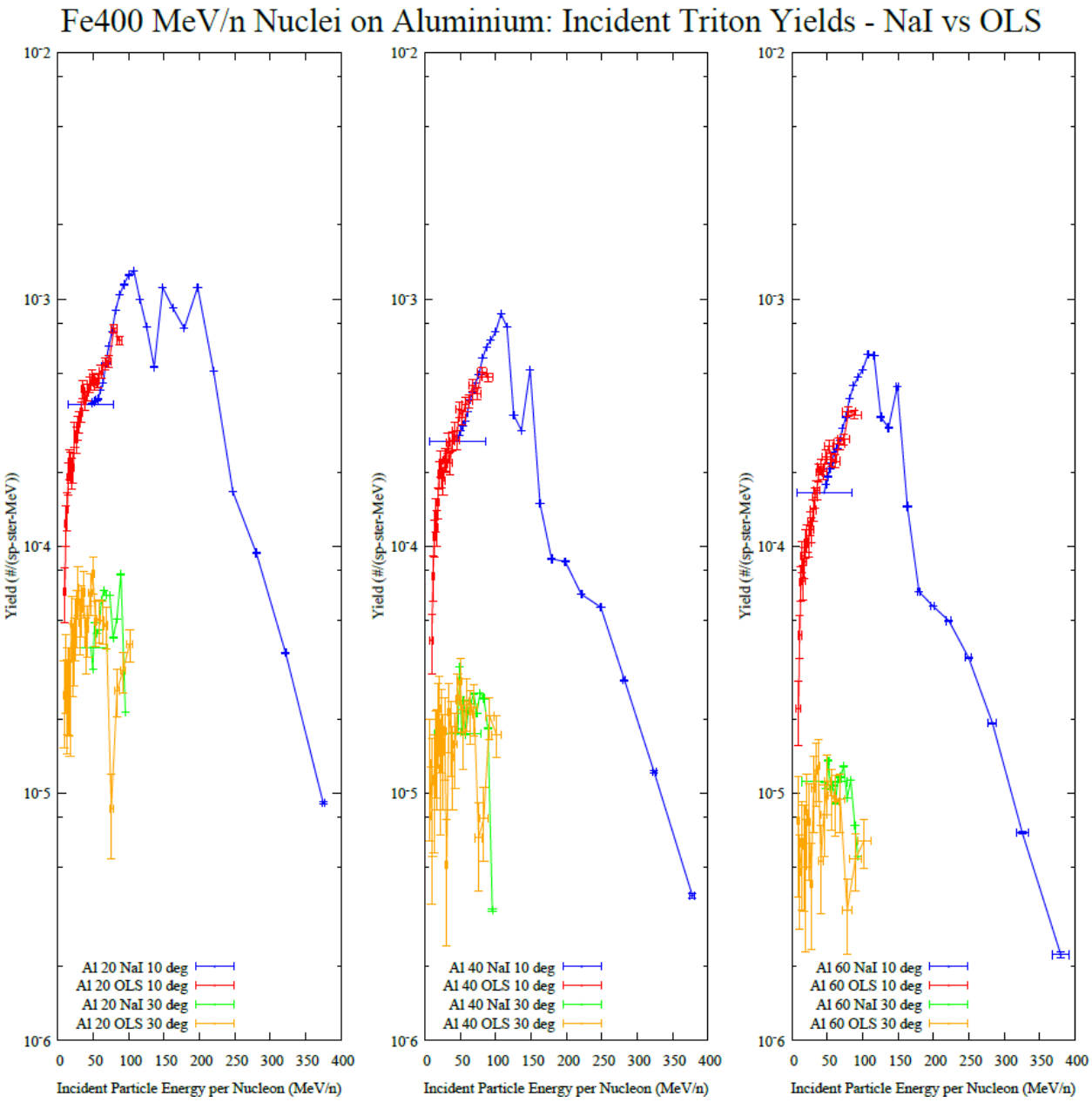


Figure 44. Triton Double Differential Yields as a function of incoming energy per nucleon from the 400 MeV/n Iron beam on the 20g/cm^2 (left), 40 g/cm^2 (middle), and 60 g/cm^2 (right) Aluminium shielding thicknesses detected at 10° and 30° NaI and OLS detectors

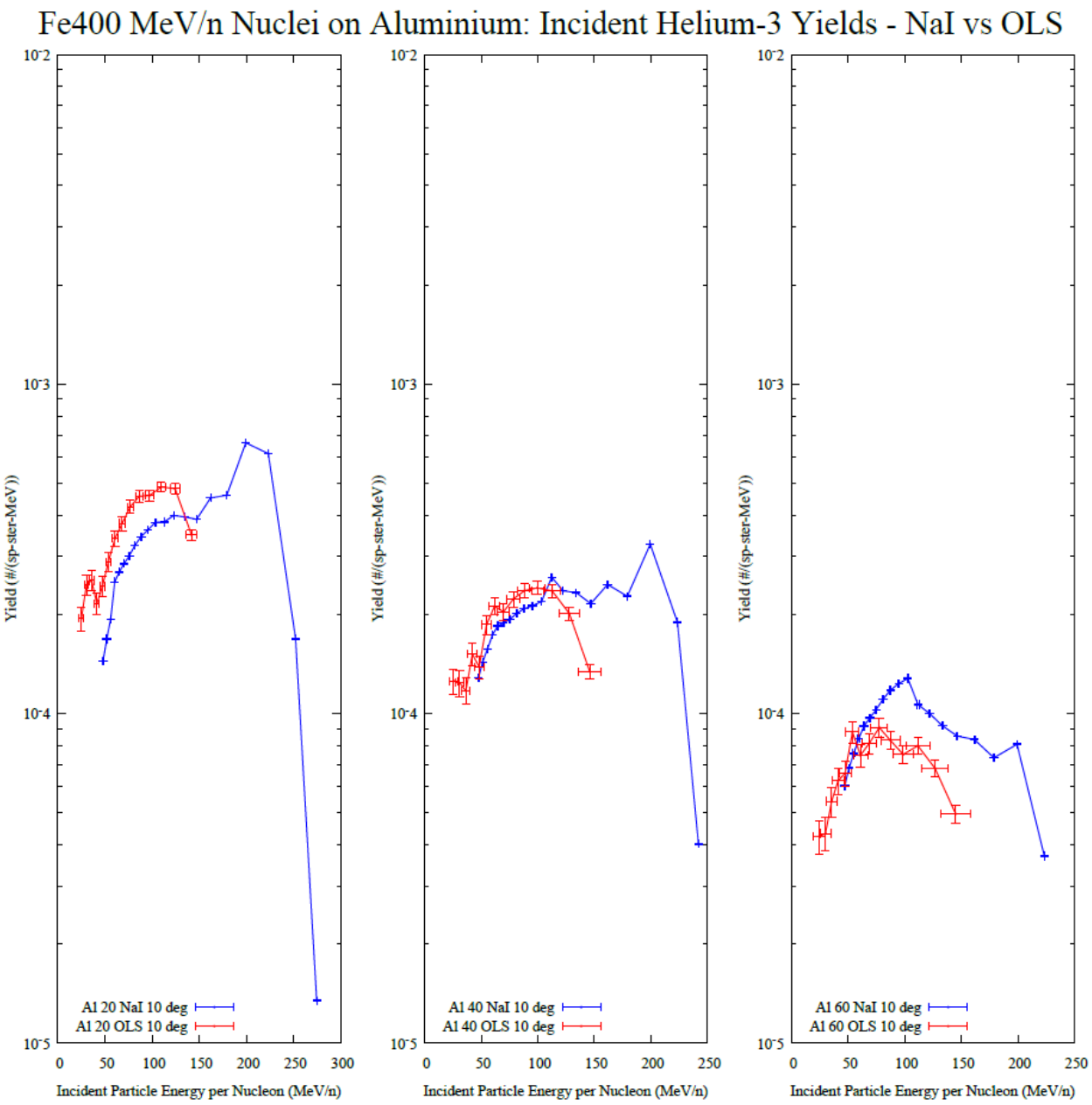


Figure 45. Helion (3-He) Double Differential Yields as a function of incoming energy per nucleon from the 400 MeV/n Iron beam on the 20g/cm^2 (left), 40 g/cm^2 (middle), and 60 g/cm^2 (right) Aluminium shielding thicknesses detected at 10° NaI and OLS detectors

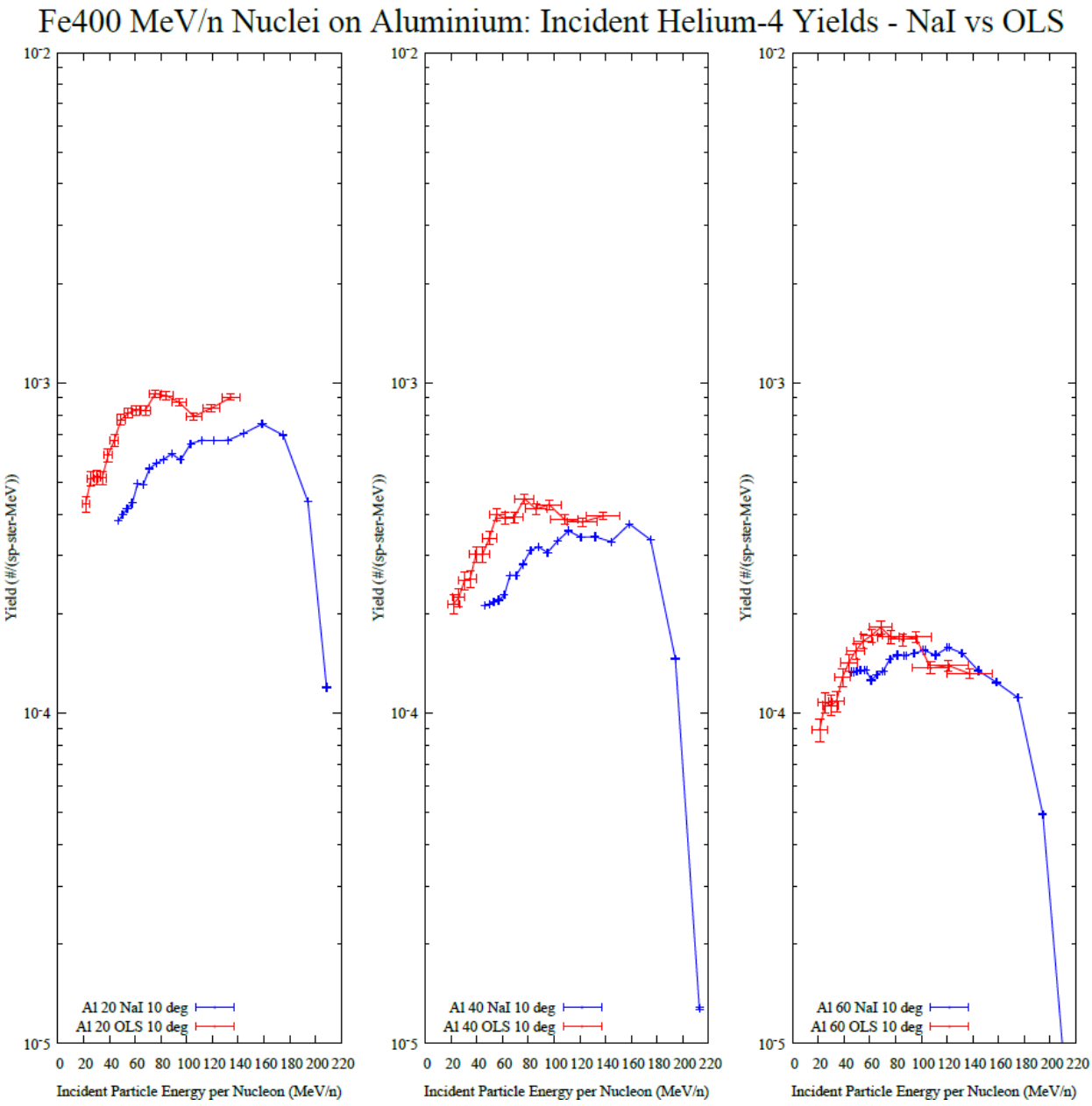


Figure 46. Alpha (4-He) Double Differential Yields as a function of incoming energy per nucleon from the 400 MeV/n Iron beam on the 20g/cm^2 (left), 40 g/cm^2 (middle), and 60 g/cm^2 (right) Aluminium shielding thicknesses detected at 10° NaI and OLS detectors

5.5.4 NaI vs MCNP – Fe 400 MeV/n

Comparisons between the stochastic modeling simulation suite MCNPX (Monte Carlo N-Particle) version 2.70 for the 400 MeV/n iron nuclei system can be seen in Figures 47-54. The beam room geometry was replicated within the MCNP6 input deck, and the same experimental systems were simulated using the physics models within the code – the output was normalized in a similar fashion to the experimental data (as in Section 5.3.2). The code relies upon physics models to simulate charged particle transport – from individual nucleons, to the secondary light ions of interest, to the incoming heavy ions interacting within the aluminium shielding. Intra-Nuclear Cascade (INC) models are used to describe reactions between nucleon/light-ion particles with target nuclei – which is very similar to the overall experiment. The two INC models used by MCNPX are the Cascade-Exciton Model (CEM) and the Los Alamos version of the Quark-Gluon String Model (LAQGSM). These models produce light fragments (like the hydrogen and helium nuclei of interest) via Fermi breakup, preequilibrium emission, and/or coalescence of cascade particles. Fermi break-up models are used to describe a process (first formulated by Enrico Fermi) to explain an excited nucleus disassembly – that is, the process in which an excited nucleus will fragment into multiple smaller nuclei. This is generally most common in high-energy nucleon collisions. These potential "channels" of break-up are randomly sampled via Monte Carlo methods, and the decay channels are chosen based on ensuring energetically-favourable methods. The second method – preequilibrium emission – is a process that occurs immediately after first contact between projectile and target, but before the formation of a compound nucleus. During this energetically unstable phase, it is believed that individual nucleons are emitted to achieve a slightly more energetically stable compound form. The third process is the evaporation of smaller and lighter particles into larger and heavier ions – these can include the coalescence of fragments emitted via Fermi break-up or the pre-emission stages. For the CEM and LAQGSM models within MCNPX, preequilibrium emission and coalescence drive the formation of light ions from the heavier residual nuclei, and the Fermi break-up models are used to produce light ions from smaller nuclei. [46]

The simulations were executed by Luis Castellanos on the computer cluster within the Department of Nuclear Engineering at the University of Tennessee, and the results provided to the author. Light ion tracks were tallied across each of the six charged scintillator paddles individually, in an effort to also mimic the event-by-event nature of the experimental setup. The particle tracks that

were crossed each paddle's surface had to be forward-focused. This was done to minimize light ion production in sources other than the upstream target (e.g. like the air within the experimental room). The results were normalized by the same factors (per incoming source particle counts, charged scintillator paddle solid angle, etc.) to provide maximum comparability with the data from the sodium iodide arrays. [9]

The comparisons between the simulated results and the detected results are shown in Figures 47-54, and across each light ion, the energy range of detected ions matches up quite well with the range predicted by the MCNPX simulations. The maximum energy for the simulations occurs at roughly the same energy as each charged scintillator (CS) paddle yield starts to fall off, which at least shows that the sodium iodide detectors energy calibration and conversion is reasonably accurate. Secondly, the angular dependence of the yields between the three paddles (at each array) appears to match the simulated results as well – the experimental data relative to itself, then, is also reasonably accurate. The net yield reduction as a function of increasing angle away from the beamline is accurate between the model and the data. But while the general separation between yields was the same, the experimental yields are larger than the predictions from the MCNP simulations.

For protons (Figures 47-48), the MCNPX simulations and the data from the NaI detectors had the strongest agreement – especially for the 10° array at low energies. At higher energies there was a bit more differentiation between the calculated and simulated yields, but the peak occurred at the same incident energy in both the model and the data, and as mentioned previously, the relative separation between the paddles was the same. For the wider angles (30° array), the agreement between the simulations and data is a lot stronger across the full range of detected energies. The highest energy data (i.e. the yield peak) is underestimated by MCNP, but the rest of the data overlaps well. Furthermore, the agreement between the data and MNCP increases with thicker shielding – that is, the data overestimation (relative to the models) decreases with thicker shielding.

For the deuteron yields (Figures 49-50), the yield peak is at a slightly higher energy relative to the model calculations for the 10° array, but the disagreement between the data and simulations decreases for the thicker experiments. The lower energy data – the data points that make up the rise portion of the spectra – overlap with model calculations, but the MCNP data across the 10° array overestimates both the location (energy) of the peak, as well as the magnitude of the yield

itself. However, at the 30° NaI array, the trends are the same across the full energy spectra, but the data is slightly higher than the model predictions.

The triton data (Figures 51-52) showed a higher uncertainty in yield from the simulations – most likely a result of low count rates for tritons. Especially at the 30° NaI array, where the error bars were largest. The trendlines were also more accurate at the wider CS paddles, but when factoring in the uncertainty of the simulated data, it is a bit harder to estimate the similarities between the experiment and the models. But even at the shallower angles, the MCNP data underestimated triton production by nearly a full order of magnitude at the thinnest shielding. This difference decreased with additional aluminium in the upstream target.

For the helium isotopes (Figures 53-54), the fairly constant yield across incident particle energies was matched by the simulations, although the calculations from the transport codes underestimates the yields across both helions and alphas from 20 g/cm^2 aluminium at all three 10° CS paddles by a factor of approximately 2-3. However, with the thicker upstream targets, the differences between the model calculations and the detector measurements dropped significantly. The data trendlines and the MCNP models did overlap pretty well though – the slope of the yield rise was matched, as well as the *x*-axis location (i.e. particle energy) of the yield maximum. Furthermore, for the helions, the differences in the MCNP and NaI results decreased for the lower energy secondary particles, and for the alphas, the NaI data was able to detect lower energy secondary ^{4}He than MCNP predicted.

The measured yields from the secondary hydrogen isotopes (primarily protons and deuterons) matched up very well with the predicted yield spectra from MCNP across all three upstream target thicknesses, all six paddles and the full energy range of each spectra. By comparison, the more complicated nuclei (triton, helions and alphas) differed more in measured versus predicted yields – most likely as a result of differences in light ion production pathways in the MCNP physics models.

Summary of Major Findings:

- The drop in detected yield across each detector (7°-12° and 27°-32°) is well-matched by the calculations from MCNPX.

- The proton yields are the most accurately estimated by the modeling across every incoming system in both the magnitude of the yield as well as the shape of each yield spectra.
- The data and MCNPX results are also consistent across deuterons with a few minor differences (the yield peaks at a slightly higher energy in the model calculations).
- MCNPX does a much better job at predicting yields of the more complex light ions (tritons, helions and alphas) from the heavier iron projectiles than the lighter helium yields.

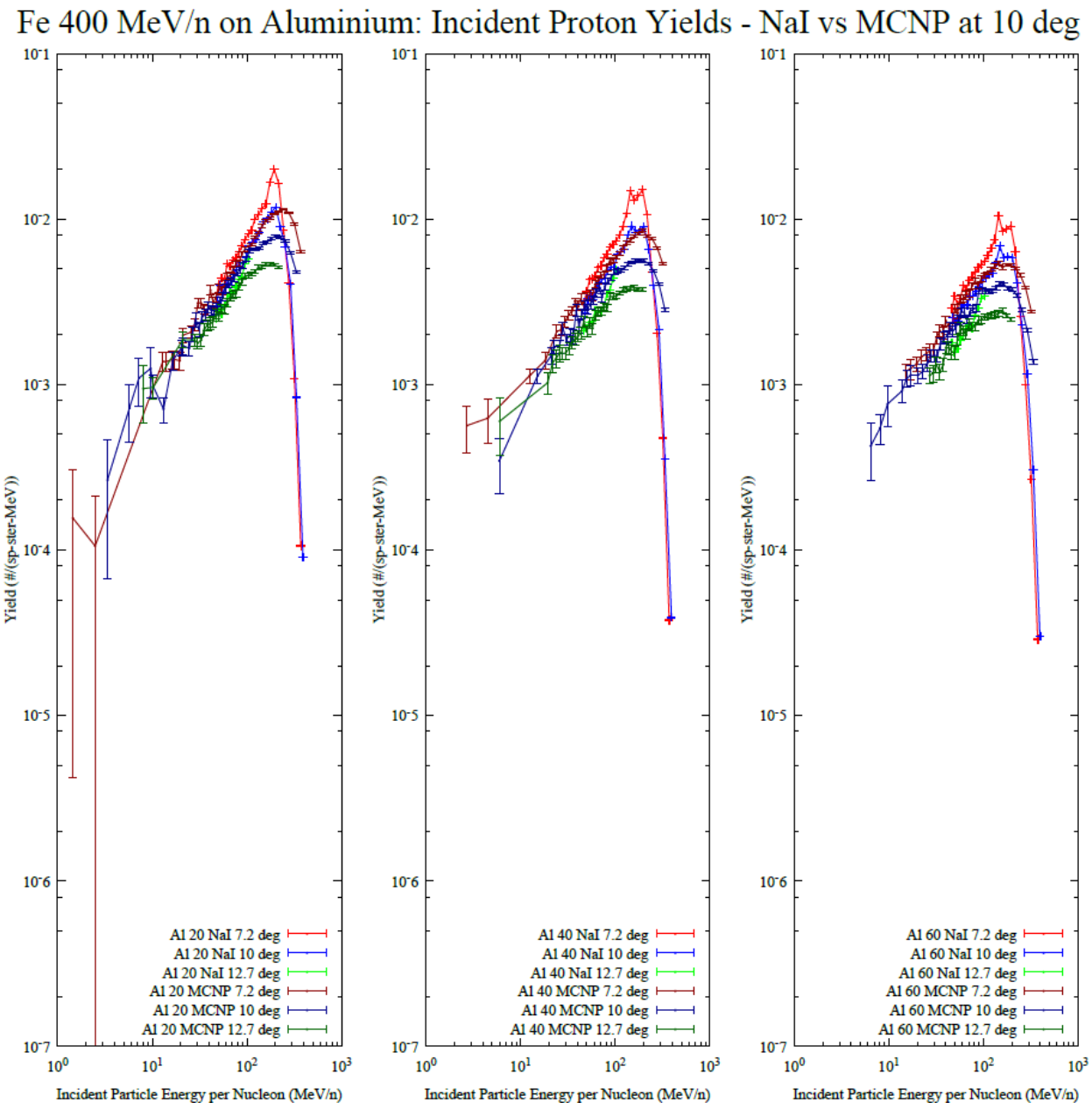


Figure 47. Comparison of proton yields at 10 deg NaI detector array with MCNP simulated yields at same angles from 400 MeV/n iron nuclei incident upon 20 g/cm^2 (left), 40 g/cm^2 (middle), and 60 g/cm^2 (right) Aluminium shielding

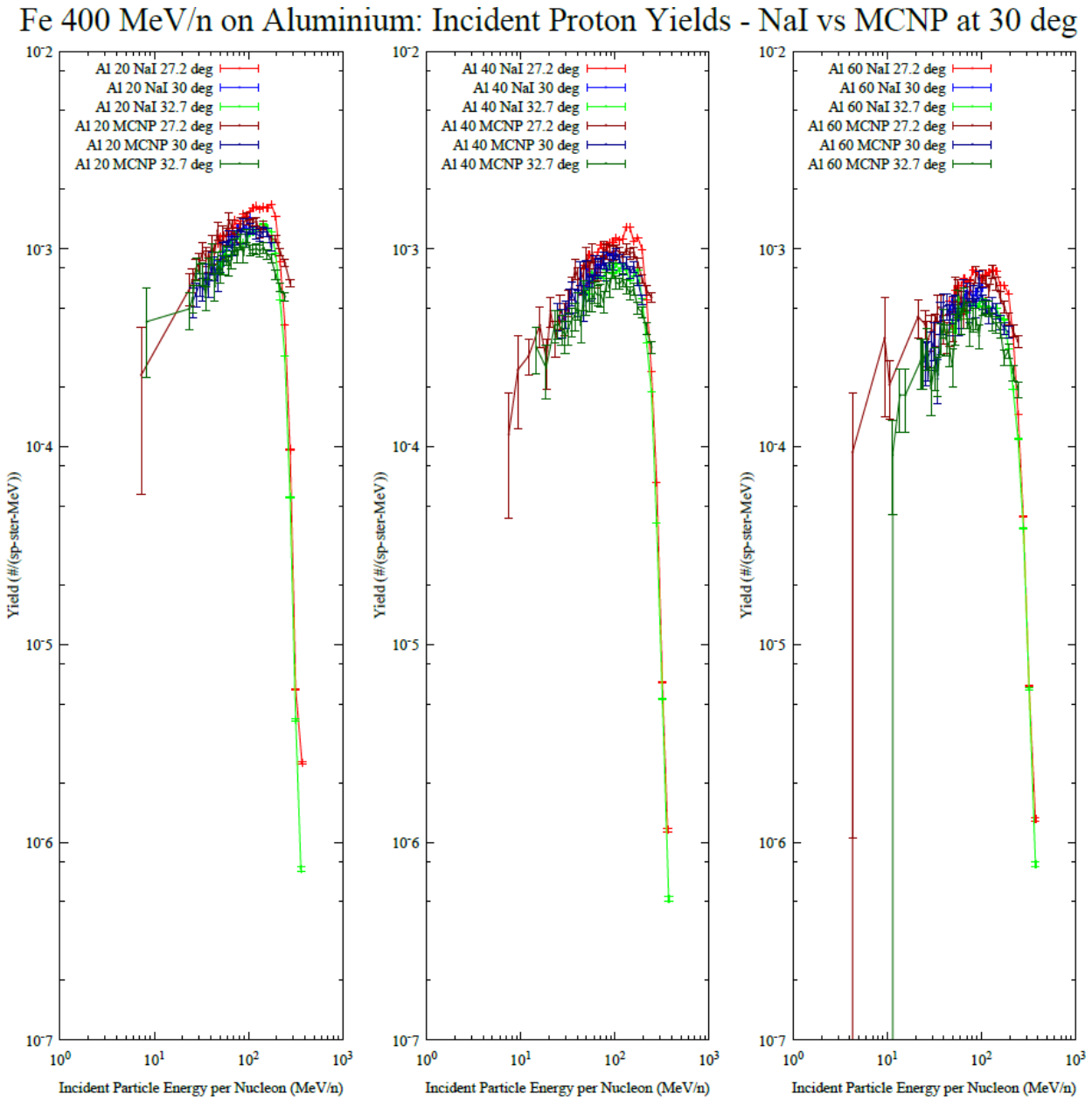


Figure 48. Comparison of proton yields at 30 deg NaI detector array with MCNP simulated yields at same angles from 400 MeV/n iron nuclei incident upon 20 g/cm^2 (left), 40 g/cm^2 (middle), and 60 g/cm^2 (right) Aluminium shielding

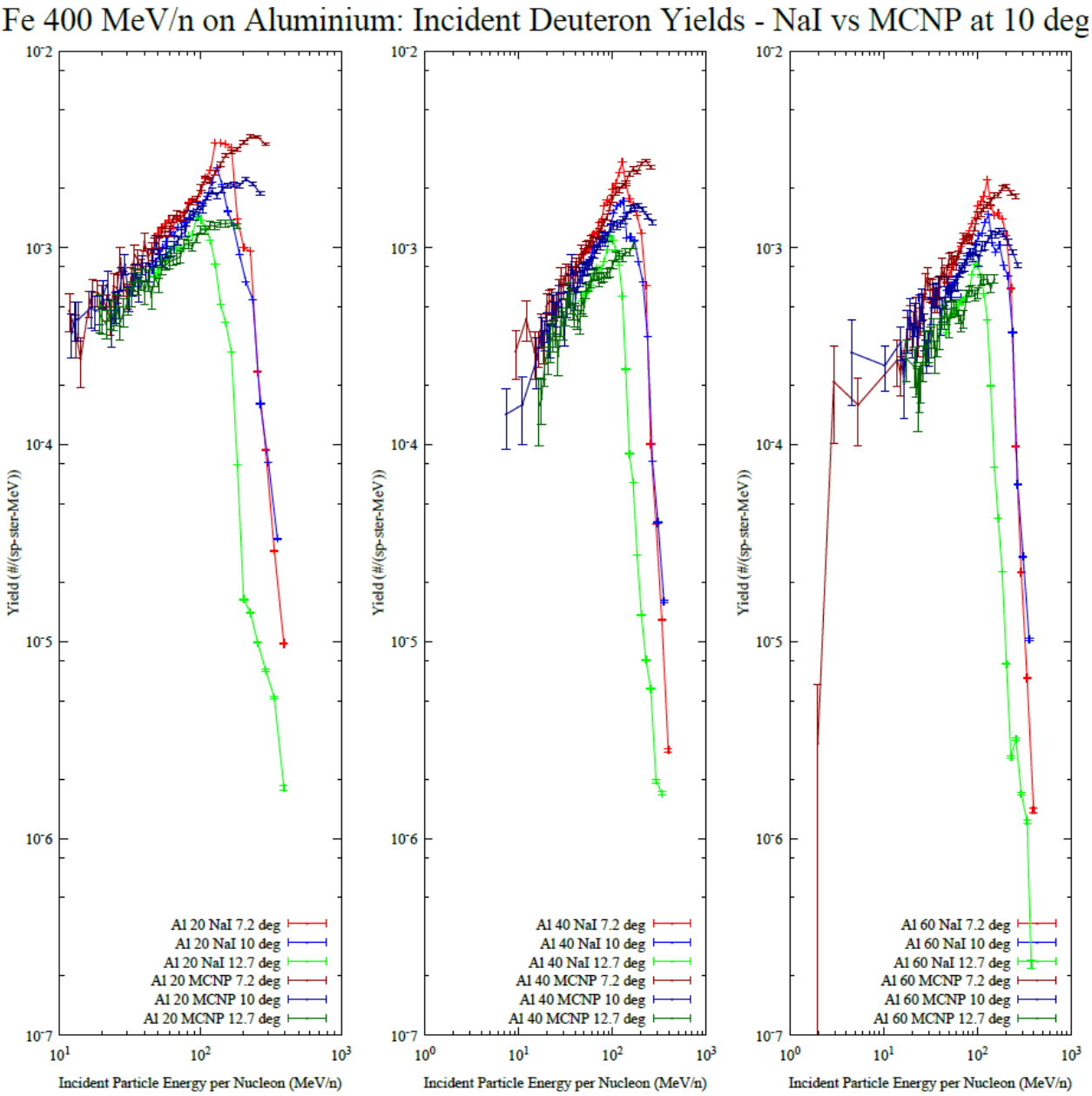


Figure 49. Comparison of deuteron yields at 10 deg NaI detector array with MCNP simulated yields at same angles from 400 MeV/n iron nuclei incident upon 20 g/cm^2 (left), 40 g/cm^2 (middle), and 60 g/cm^2 (right) Aluminium shielding

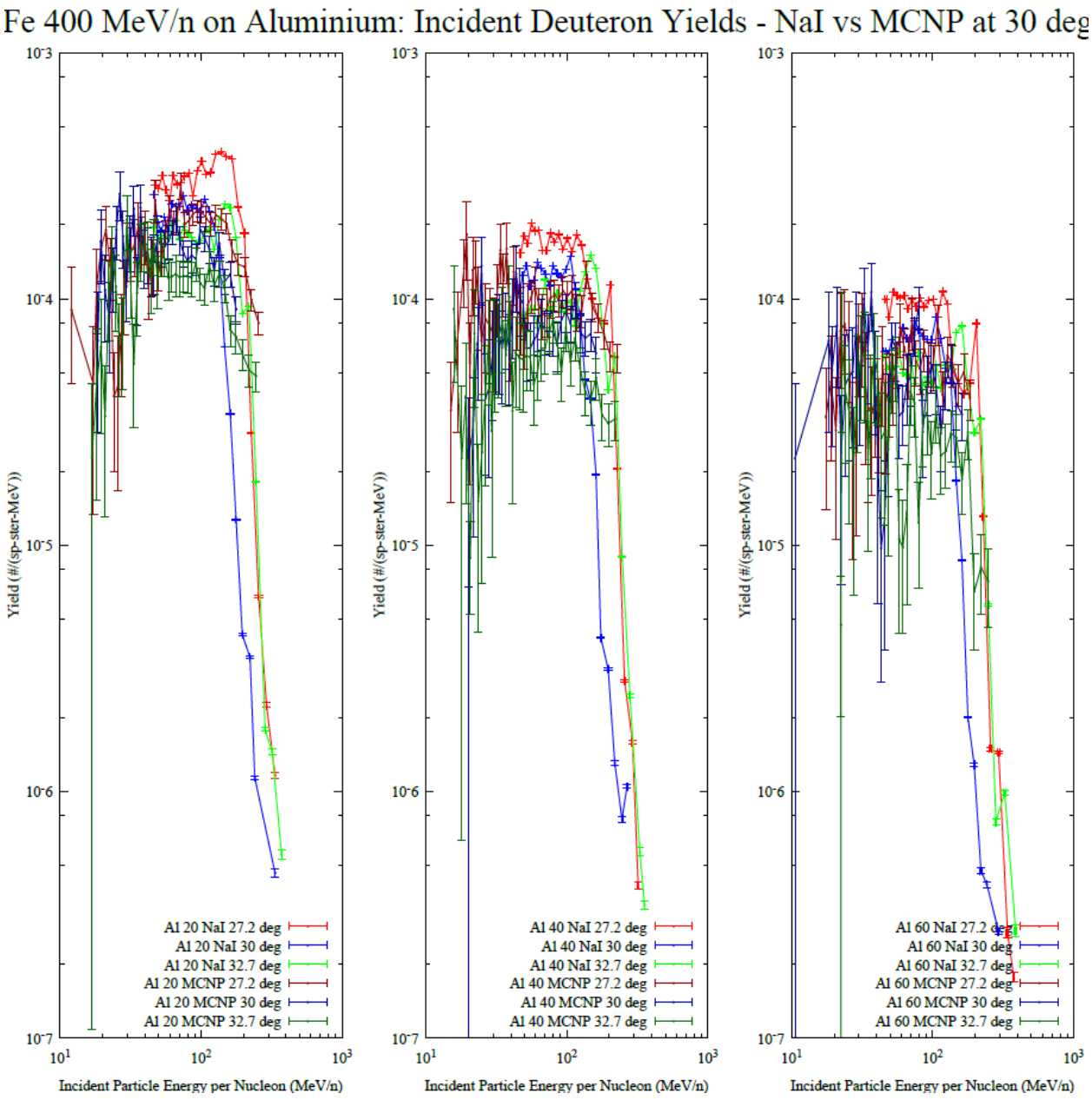


Figure 50. Comparison of deuteron yields at 30 deg NaI detector array with MCNP simulated yields at same angles from 400 MeV/n iron nuclei incident upon 20 g/cm^2 (left), 40 g/cm^2 (middle), and 60 g/cm^2 (right) Aluminium shielding

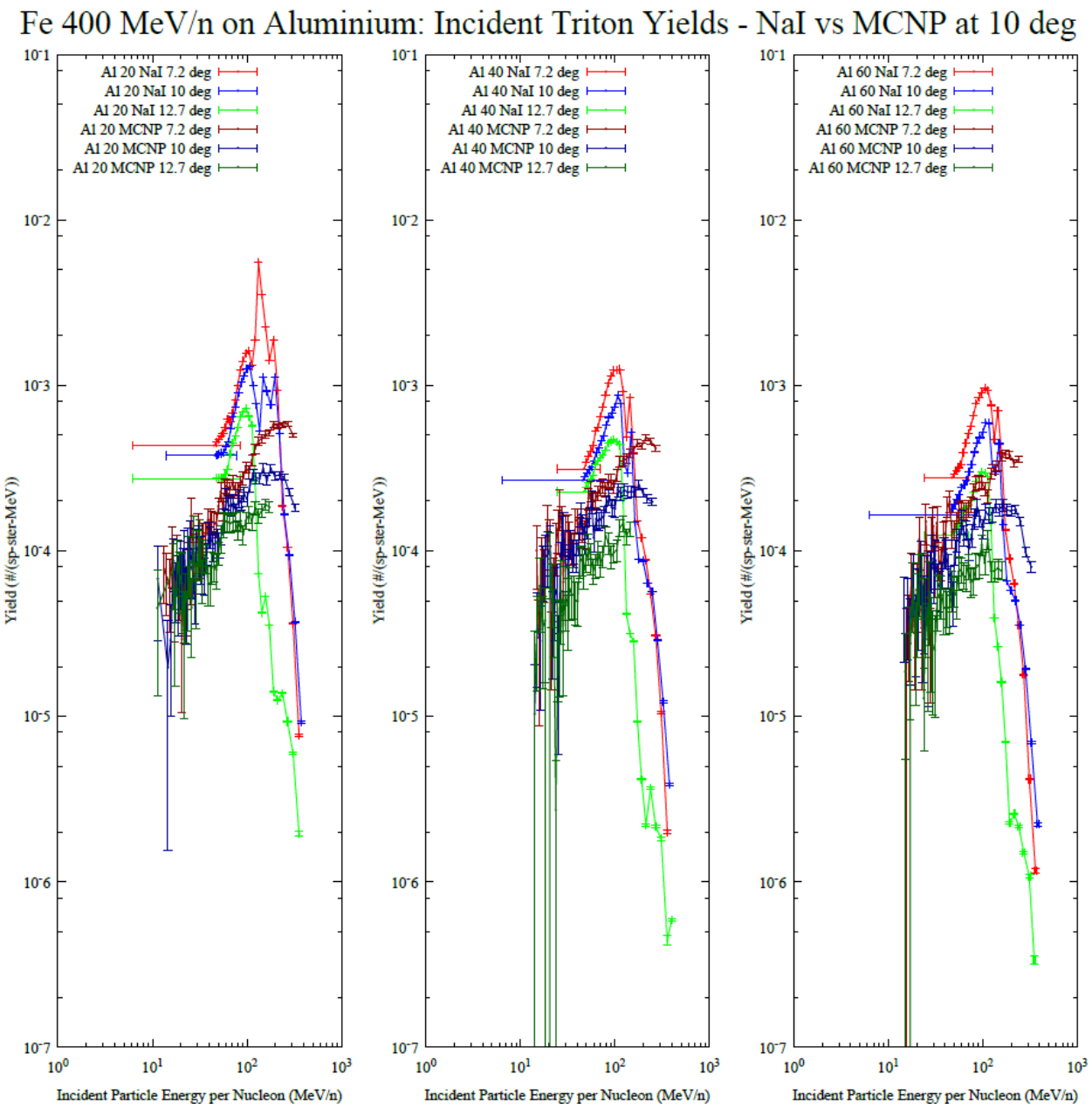


Figure 51. Comparison of triton yields at 10 deg NaI detector array with MCNP simulated yields at same angles from 400 MeV/n iron nuclei incident upon 20 g/cm^2 (left), 40 g/cm^2 (middle), and 60 g/cm^2 (right) Aluminium shielding

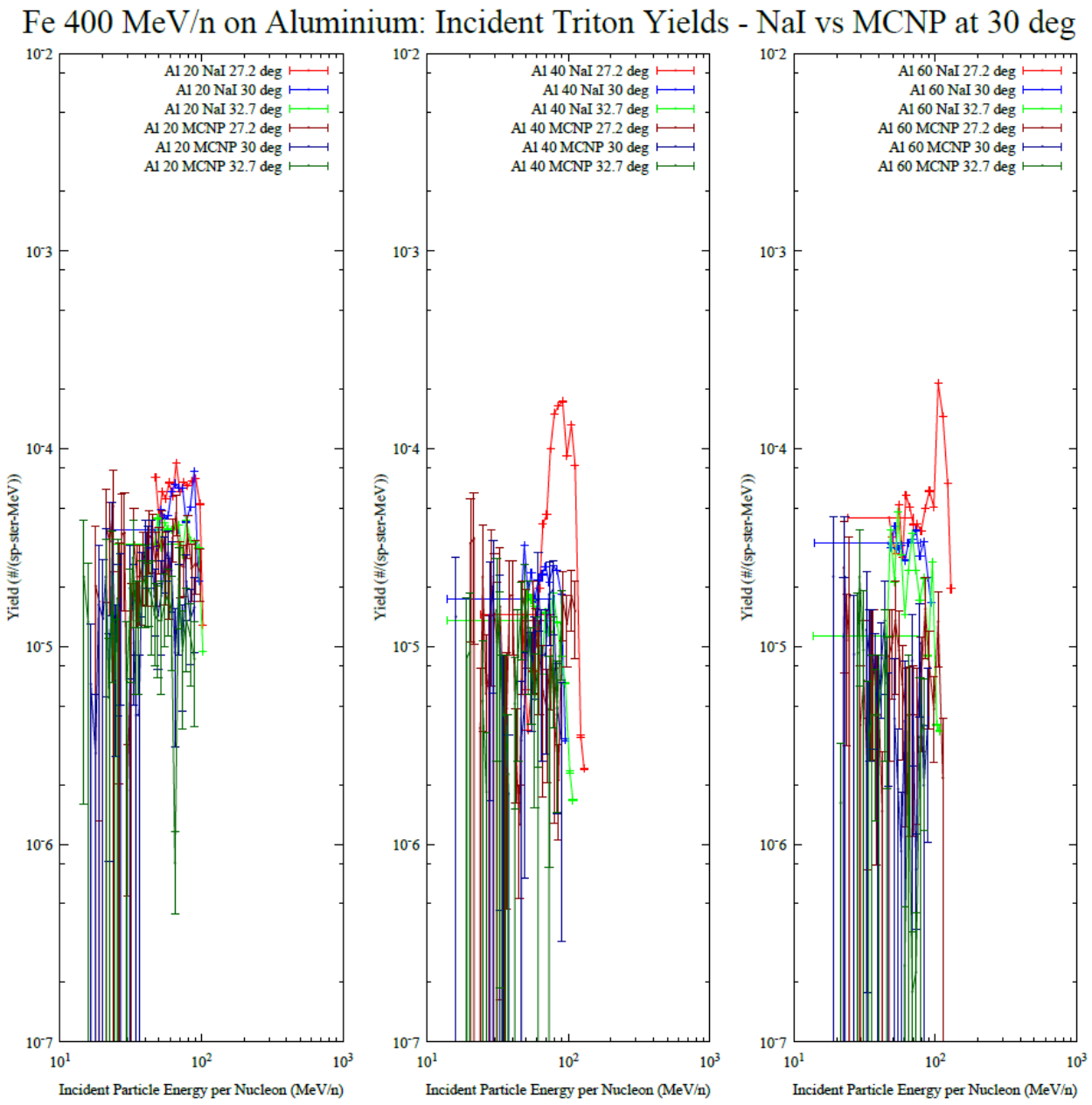


Figure 52. Comparison of triton yields at 30 deg NaI detector array with MCNP simulated yields at same angles from 400 MeV/n iron nuclei incident upon 20 g/cm^2 (left), 40 g/cm^2 (middle), and 60 g/cm^2 (right) Aluminium shielding

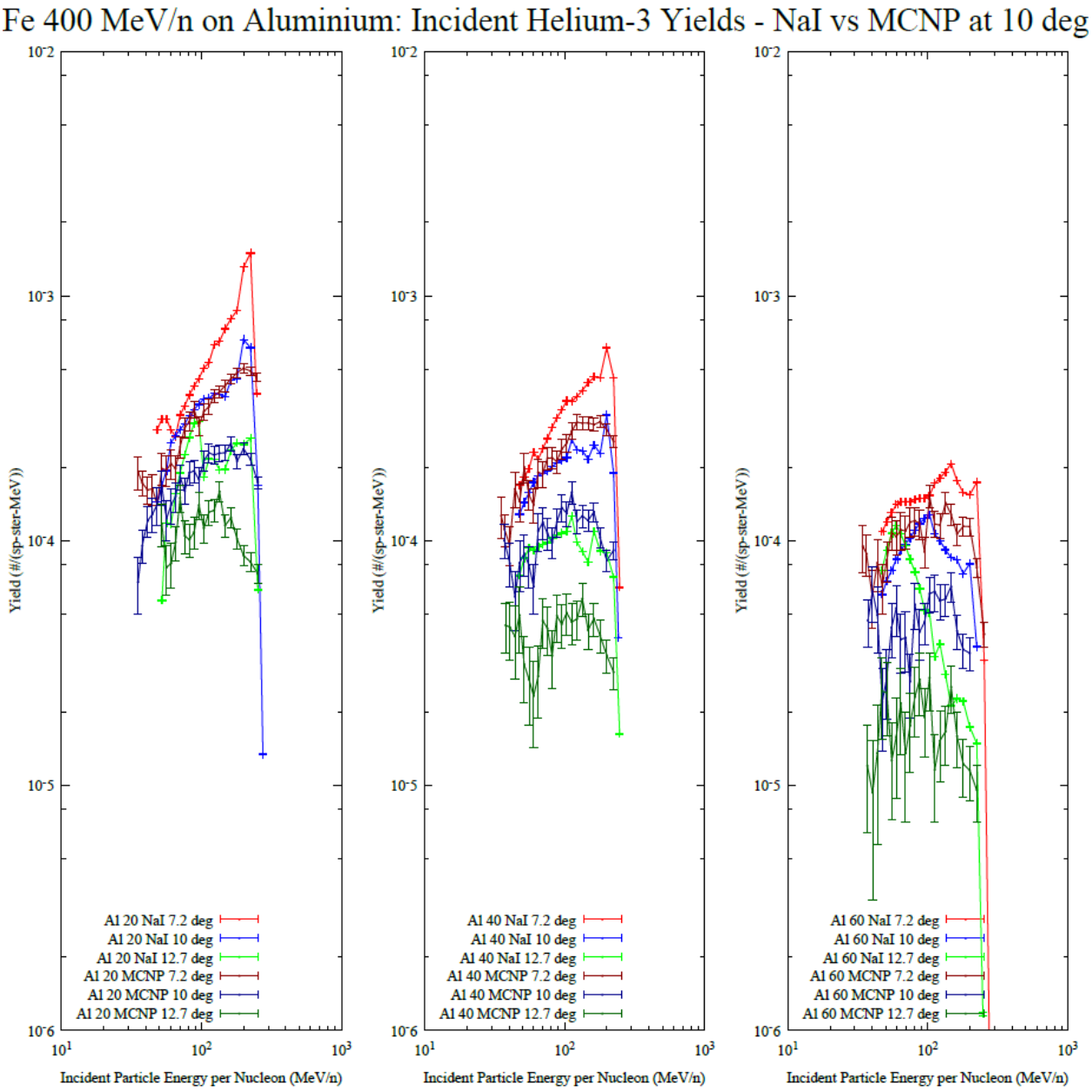


Figure 53. Comparison of helion yields at 10 deg NaI detector array with MCNP simulated yields at same angles from 400 MeV/n iron nuclei incident upon 20 g/cm^2 (left), 40 g/cm^2 (middle), and 60 g/cm^2 (right) Aluminium shielding

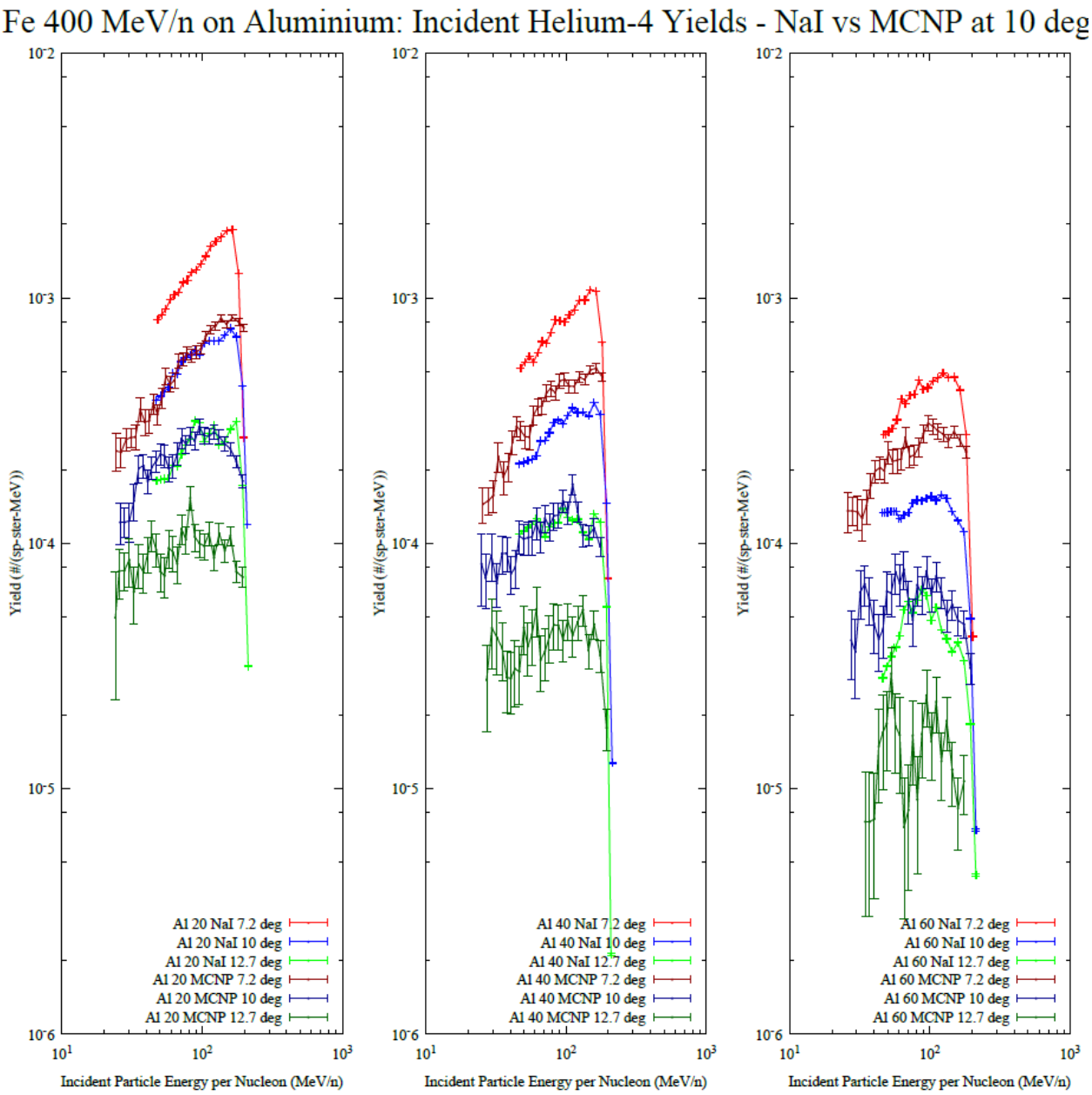


Figure 54. Comparison of alpha yields at 10 deg NaI detector array with MCNP simulated yields at same angles from 400 MeV/n iron nuclei incident upon 20 g/cm^2 (left), 40 g/cm^2 (middle), and 60 g/cm^2 (right) Aluminium shielding

5.6 Uncertainties and Error Propagation

5.6.1 Statistical Uncertainties

The base assumption for the experimental measurements is that the acquired data follows binomial statistics within each bin, allowing for the error to be calculated via Equation 7, where *c* represents the individual counts per each bin (channel):

$$\delta c = \sqrt{c} \tag{7}$$

Thus, the measurements with the best counting statistics would have the lowest corresponding statistical uncertainties. Regardless of beam species, the general trends in statistical uncertainty were consistent across detected light ions. As the charged scintillator (CS) paddle angle decreased (i.e. got closer to the beam axis), the count rate increased, with the exception of the CS4 and CS8 paddles (as mentioned previously in section 5.5.1) for some higher energy secondary ions. For the hydrogen isotopes, protons had the best counting rates, and as the hydrogen nucleus got heavier, the relative uncertainties increased – and this is noticeable especially in the triton data presented in section 5.4. Similarly, the majority of helium nuclei detected were alpha particles, so the statistical uncertainty for helions was much higher than for the detected alpha particles. The data tables in Appendix C show the overall uncertainties broken down into its component parts for each experimental run.

5.6.2 Systematic Uncertainties

The systematic uncertainties stem from the normalization calculations made to convert from raw counts to the double-differential energy- and angle-dependent yields. These include the uncertainties in the nuclear attenuation correction factor (representing the energy deposition efficiency), the solid angle corrections and the energy bin width normalizations. Equation 6 (reproduced here) illustrates the statistical conversions necessary to calculate the double differential yield from the normalized counts.

$$Y_{i,p} = \frac{C_i * \Gamma}{\Omega_p * (E_{i+0.5} - E_{i-0.5})} \tag{6}$$

Where *c* represents the adjusted number of raw counts in bin *i*, Γ is the nuclear attenuation correction factor, Ω is the solid angle measurement for each paddle *p*, and *E* is the energy measurement for the respective edge of each bin *i*. The uncertainty in the yield calculation can

thus be derived (via standard error propagation from the Gaussian equation for normally-distributed errors) as Equation 8.

$$\delta Y_{i,p} = Y_{i,p}\sqrt{\left(\frac{\delta\Gamma}{\Gamma}\right)^2 + \left(\frac{\delta C_i}{C_i}\right)^2 + \left(\frac{\delta\Omega_p}{\Omega_p}\right)^2 + \left(\frac{\sqrt{(\delta E_{i+0.5})^2 + (\delta E_{i-0.5})^2}}{(E_{i+0.5} - E_{i-0.5})}\right)^2} \quad (8)$$

The uncertainty in counts is shown in Equation 7, but the uncertainty in solid angle (δΩ) and energy (δE) can be calculated by examining the inherent uncertainties in each of those calculations – the variations in flight path. This is done by assuming that the particle is born along the beam axis at the midpoint of the target depth. Thus, the two extremes are at the beginning of the target (upstream face), and at the full depth (downstream face). The time-of-flight tables (section 5.3.1) illustrate the differences in energy loss through experimental room from each production point, and the differences between the midpoint and the two extremes is the uncertainty for each energy point. Figure 55 shows a plot of the conversion curves for protons at 10° for each of the three production points for all three shielding thicknesses. As can be seen, the separation in energy curves increases with both shielding thickness and energy – the increased separation illustrates a higher uncertainty with the time-energy calibration. These are both results of higher uncertainty in particle production location due to the thicker target for the beam to interact within. As variation in the production point increases, the amount of target material the secondary light ion traverses through increases as well – increased attenuation leads to higher variation in energy at both the point of detection as well as the point of creation.

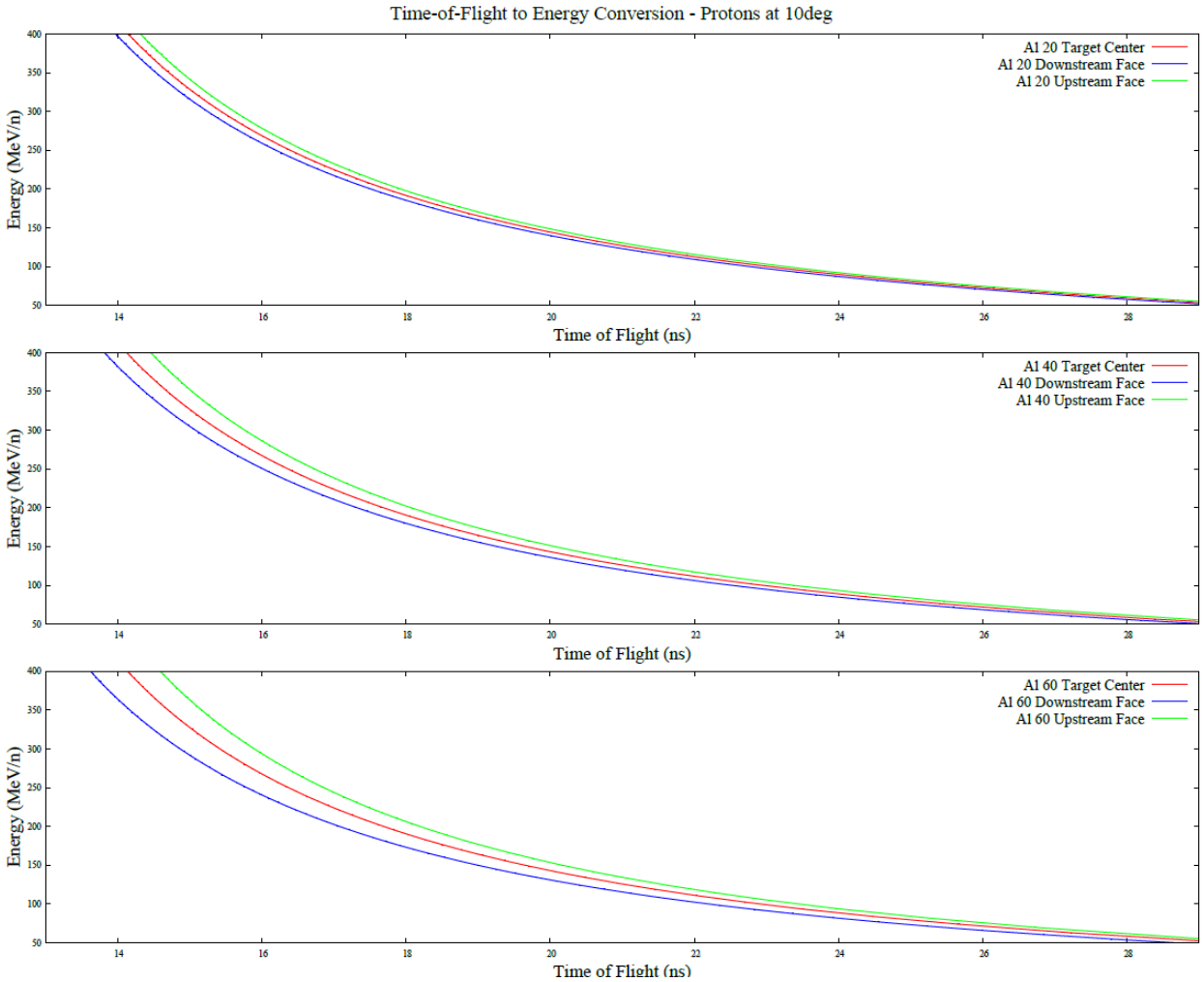


Figure 55. Proton Time-of-Flight Calibration curves for the 10° NaI array across all three production points for the 20 g/cm^2 (top), 40 g/cm^2 (middle), and 60 g/cm^2 (bottom) shielding thicknesses.

For this thick target experiment, the energy at the point of detection is of more value, because of NASA's interest in calculating the radiation (and dose) in the region between the two thick shielding targets. Thus, the timing data recorded by the charged scintillator (CS) paddles does not have to be back-calculated – those measurements represent the time between the incoming beam entering the experiment and the point of detection. However, due to the fast nature of the incoming beam, the timing calibrations can be safely done utilizing the point of production as the other timing point. The flight time from the beam scintillators (S1+S2) to the various production points adds very little variation, so the point of production can be substituted. The uncertainty for the calibration arises from the uncertainty in the production point, which is represented by the three curves in each subplot of Figure 55. And because the known value is the timing information for each bin (calibrated via the punch-through point for each detector on the two-dimensional time-of-flight data plots), the uncertainty in point-of-detection energy is represented by the vertical difference between the blue and green lines at any given time-of-flight value. The three corresponding energies for the fixed time-of-flight represent the minimum energy (blue – downstream face production point), the assumed energy (red – target center production point), and the maximum energy (green – upstream face production point). The uncertainty is calculated as the average of (assumed – minimum) and (maximum – assumed).

For the solid angle, the differences in flight path were calculated over the entirety of the full sodium iodide detector. The shortest flight path was from the deepest production point (downstream face of target) to center of the respective charged scintillator paddle, and the furthest flight path was from the front of the target (as the beam travels; the upstream face) to the center of the CS paddle. These flight path calculations for both detector arrays for all three target thicknesses are summarized in Table 9, and the resulting solid angles are shown in Table 10, and the uncertainties (as a percentage) are shown in Table 11.

Table 9. Flight Path Distance Measurements for each Charged Scintillator Paddle

CS Paddle (°)	Flight Path Target Center (cm)	Flight Path Target Max Depth (cm)			Flight Path Target Min Depth (cm)			Paddle Area (cm^2)
		Al 20	Al 40	Al 60	Al 20	Al 40	Al 60	
4 (12.7°)	301.54	297.93	294.32	290.71	305.15	308.77	312.39	129.032
5 (10°)	301.28	297.64	293.99	290.35	304.92	308.58	312.23	129.032
6 (7.2°)	301.63	297.96	294.28	290.61	305.30	308.98	312.66	129.032
7 (32.7°)	301.62	298.51	295.41	292.33	304.74	307.88	311.03	129.032
8 (30°)	301.17	297.97	294.78	291.60	304.38	307.61	310.84	129.032
9 (27.2°)	301.11	297.82	294.54	291.27	304.41	307.72	311.03	129.032

Because the variations in flight path would depend heavily on target thickness, it is expected that the thickest target would produce the highest uncertainties, and the values in Table 11 corroborate that – the highest uncertainties for both the minimum and maximum flight paths are for the 60 g/cm^2 shielding thickness, and the lowest for the 20 g/cm^2 shielding. Furthermore, it is important to note that each calculated uncertainty is well below 10%, helping minimize the overall uncertainties. The overall uncertainty in solid angle is calculated by averaging the corresponding percent differences and applying that to the base solid angle (calculated assuming mid-target particle production point).

Table 10. Solid Angle Calculations

CS Paddle (°)	Solid Angle (steradian)						
	Target Center	Target Max Flight Path			Target Min Flight Path		
		Al 20	Al 40	Al 60	Al 20	Al 40	Al 60
4 (12.7°)	0.001419	0.001454	0.001490	0.001527	0.001386	0.001353	0.001322
5 (10°)	0.001422	0.001457	0.001493	0.001531	0.001388	0.001355	0.001324
6 (7.2°)	0.001418	0.001453	0.001490	0.001528	0.001384	0.001352	0.001320
7 (32.7°)	0.001418	0.001448	0.001479	0.001510	0.001389	0.001361	0.001334
8 (30°)	0.001423	0.001453	0.001485	0.001517	0.001393	0.001364	0.001335
9 (27.2°)	0.001423	0.001455	0.001487	0.001521	0.001392	0.001363	0.001334

Table 11. Solid Angle Uncertainties

CS Paddle (°)	Aluminium Shielding Thickness (g/cm^2)		
	Al 20	Al 40	Al 60
4 (12.7°)	2.39468053	4.799763534	7.20621823
5 (10°)	2.41955771	4.849793186	7.281749525
6 (7.2°)	2.43470121	4.880265282	7.327797962
7 (32.7°)	2.06483652	4.136812915	6.206312784
8 (30°)	2.12821836	4.264125231	6.39813761
9 (27.2°)	2.1861905	4.380607078	6.573733319

The uncertainty in the nuclear attenuation correction factor ($\delta\Gamma$ – section 5.2.2) is trickier to calculate, as the two methods used to calculate the attenuation correction factor differ in both style and accuracy. However, as a way to estimate that uncertainty, $\delta\Gamma$ is calculated by the percent difference between the MCNP6 estimation and the PHITS model calculation. Figure 56 illustrates the calculated percent uncertainty across the five light ion species as a function of incident particle energy. The proton percent errors are all relatively low (below 10%), whereas the deuteron and tritons percent errors are much higher. Generally, the lower the incident energy of the secondary ion, the more likely the PHITS nuclear attenuation correction factor and the MCNP estimation are close in value. At higher energies, there is further uncertainty between the two methods, but that might be the result of the difference in the two methods. The PHITS factors are determined by calculating the simulated energy deposition totals with what the true detected data should be, while the MCNP factors are calculated by tracking each particle on an event-by-event basis (which can lead to an overestimation of nuclear attenuation as a result of extra collisions by deeper-penetrating secondary ions).

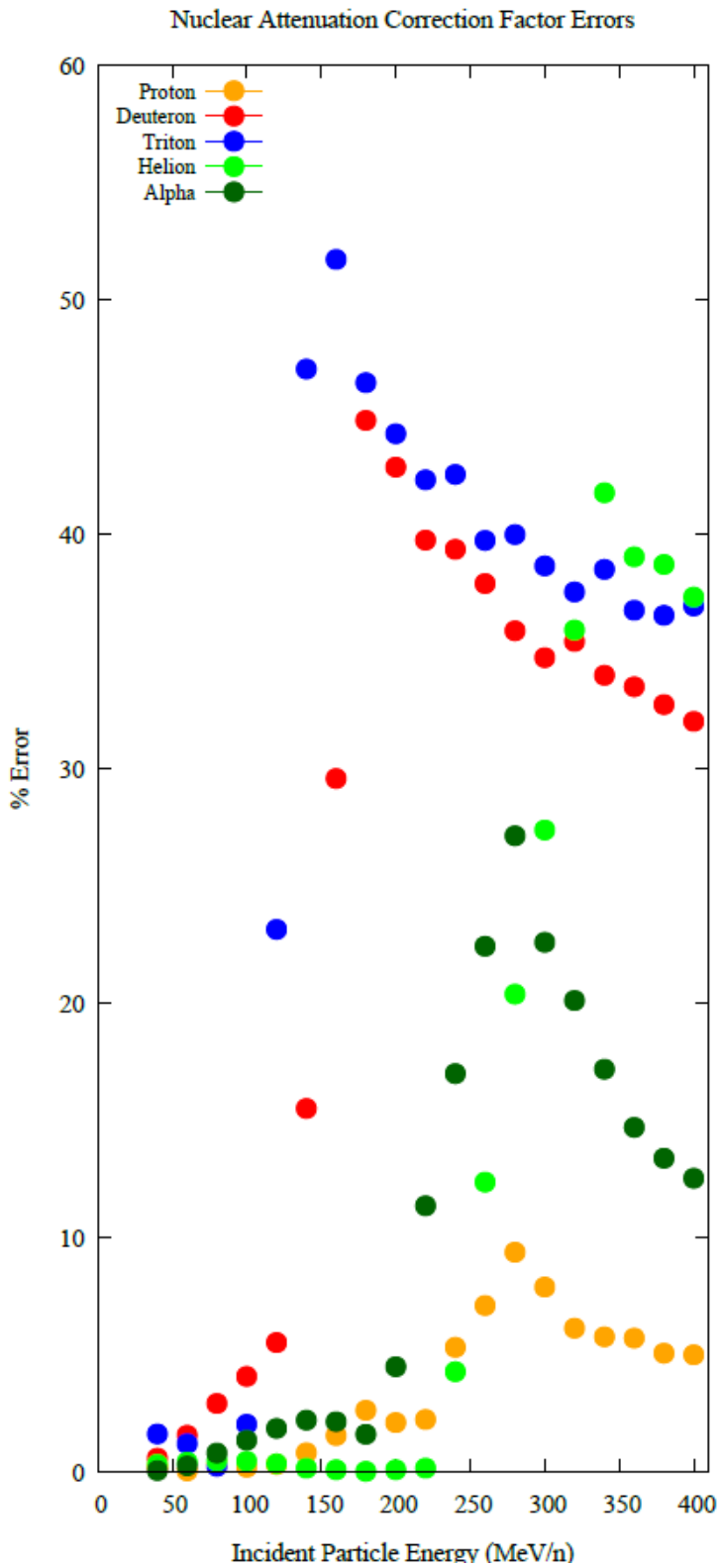


Figure 56. Nuclear attenuation correction factor percent errors across the five light ion species as a function of incident energy

CHAPTER 6
CONCLUSIONS AND FUTURE WORK

A series of experiments was conducted between March 2016 and November 2017 at the NASA Space Radiation Laboratory (NSRL) particle accelerator facility on the campus of Brookhaven National Laboratory to make thick-target light-ion measurements. Iron, helium, and hydrogen beam particles were fired at a pair of shielding targets separated by 3.5 m, with a series of detectors placed between the upstream and downstream target positions. For the data presented within this dissertation, the experimental runs consisting of 400 and 800 MeV/n iron and hydrogen beams and 400 MeV/n helium beams incident upon aluminium shielding of 20, 40, and 60 g/cm^2 thickness were analyzed. The secondary back target was aluminium and fixed at 60 g/cm^2, and four 4x4x16 in^3 sodium iodide detectors (in pairs of two) were centered at 10° and 30° along the 16" face of the detector. Double differential (spatial- and energy-) thick target yields were calculated for five major light ions (protons, deuterons, tritons, helions and alpha particles) within these two detector arrays, and those measurements were compared with predictions from transport model calculations.

The proton and deuteron measurements had the best comparisons with both Monte Carlo-based MCNPX and PHITS particle transport code simulations, as well as data collected from other detector systems within the same experiments. The differences for the other three light ions is potentially a result of particle identification issues, resulting from the issues with the detector threshold and voltage settings (specifically with the 12.7° and 30.0° data). Another potential difference could arise from the lack of light ion production cross-sections within the physics models – leading to an overreliance on cascade nuclear models to calculate light ion fragmentation.

The beam energies and species were sampled from the energy and nuclear composition spectra of the space radiation environment – specifically, galactic cosmic rays. The calculated light ion yields were compared across differences in incoming nuclear composition (hydrogen vs helium vs iron) and energy (E = 400 MeV/n vs E= 800 MeV/n) in an effort to understand the influence of shielding thickness on secondary light ion production (a necessary prelude to dose calculations) within the twin shielding structure. It was universally determined that the higher energy beams produced higher energy ions, and that angles further away from the beamline resulted in higher measured

yields. However, increased shielding seemed to moderate light ion yields from the lower energy beams more, while the increased shielding thickness led to higher yields from the more energetic beam species. For the variations in incoming beam species, the larger incoming nuclei generally produced more secondary light ions. This is most likely a result of projectile fragmentation dominating the production mechanism, so larger nuclei would have more nucleons, leading to more fragments produced. Similarly, higher energy nuclei penetrate the initial shielding more, leading to an increased number of reactions (from an increased number of mean free paths), which also results in increased light ion production. But as the thickness of the upstream target increased, the yields from the heavier iron beam decreased, while the yields from the lighter helium beams (and hydrogen, when discussing proton and deuteron production only) increased. This is a result of the stopping power of aluminium – the 400 MeV/n iron beam fully stops within the thinnest (20 g/cm^2) shielding thickness, whereas the 400 MeV/n helium and hydrogen beams punch through all three aluminium shielding thicknesses. Thus, the two lighter ions undergo many more reactions within the shielding, leading to increased secondary ion production.

This experiment was designed to better understand light ion production as it relates to the effects of shielding in the space radiation environment, and the measured data shows that there is no simplistic answer to such a question, and that understanding the production of light ions from varying energetic ions and nuclei sizes is crucial to validating improving current particle transport models.

It is recommended that measuring and/or improving current double differential light ion production cross-sections are needed to improve the physics models currently used within particle transport suites. In terms of the experiment – ensuring that the timing system for the detectors are not accidentally removing the faster particles, as well as charged scintillator thresholds are low enough to accept higher energy particles. Additionally, the energy conversion can only be done for the sodium iodides via time-of-flight using the charged scintillator paddles in front of the detector. While this did provide for the ability to separate each detector array into three individual angular subsets, it does limit the accuracy of the energy conversion. The amount of usable data is then limited by this decrease in the dynamic range of the detector.

LIST OF REFERENCES

[1] D. A. Anderson, *Absorption of Ionizing Radiation*. Baltimore: University Park Press, 1984, p. 1-14

[2] L. Townsend. 'Electronic effects – Earth,' University of Tennessee (Knoxville), 2016.

[3] D. F. Smart and M. A. Shea, *Galactic Cosmic Radiation and Solar Energetic Particles*, in *Handbook of Geophysics*, Air Force Research Laboratories, 1985, p. 6-1 – 6.29

[4] L. Townsend. 'Space Radiation Environment: Galactic Cosmic Radiation', University of Tennessee (Knoxville), 2016.

[5] P. Meyer, R. Ramaty, W.R. Webber. "Cosmic rays – astronomy with energetic particles," *Physics Today*, vol. 27, no. 10, pg. 23-33, October 1974

[6] T. C. Slaba and S. R. Blattnig, "GCR environmental models I: Sensitivity analysis for GCR environments," *Sp. Weather*, vol. 12, no. 4, pp. 217–224, April 2014.

[7] T. C. Slaba, A. A. Bahadori, B. D. Reddell, R. C. Singleterry, M. S. Clowdsley, and S. R. Blattnig, "Optimal shielding thickness for galactic cosmic ray environments," *Life Sci. Sp. Res.*, vol. 12, pp. 1–15, 2017.

[8] W. R. Leo, *Techniques for Nuclear and Particle Physics Experiments*. New Delhi, India: Springer, 2010. P. 157-178, 321-327

[9] L.A. Castellanos, Personal Communications, University of Tennessee (Knoxville), 2016.

[10] J. Alessi *et al*., "Electron Beam Source Pre-Injector Project (EBIS) Conceptual Design Report," *BNL-73700-2005-IR*. September 2005

[11] N. A. McGirl, "Double Differential Neutron Yields Produced by Proton, Helium, and Iron Interactions with Thick Aluminium Targets," Doctoral Dissertation, University of Tennessee, Knoxville, Knoxville, TN, USA, 2017.

[12] J. Norbury *et al.*, "Review of Nuclear Physics Experiments for Space Radiation," *NASA/TP-2011-217179*. September 2011

[13] Alard, J.P., *et al.*. "Light fragment production in p-Nucleus interactions at 600 MeV. Astrophysical application." Il Nuovo Cimento 30, 320-344, 1975

[14] Bertrand, F.E., Peelle, R.W." Complete hydrogen and helium particle spectra from 30 to 60 MeV proton bombardment of nuclei with A = 12 to 209 and comparison with the intranuclear cascade model." Physical Review C 8, 1045-1064. 1973

[15] Budzanowski, A., *et al.*. "Competition of coalescence and fireball processes in nonequilibrium emission of light charged particles from p + Au collisions." Physical Review C 78, 024603. 2008

[16] Chrien, R.E., Krieger, T.J., Sutters, R.J., May, M., Palevsky, H., Stearns, R.L., Kozlowski, T., Bauer, T. "Proton spectra from 800 MeV protons on selected nuclides." Physical Review C 21, 1014-1029. 1980.

[17] Cowley, A.A., Chang, C.C., Holmgren, H.D.,"Forward angle proton spectra in the continuum from the 58Ni(p, xp) reaction at 100 MeV". Physical Review C 22, 2633-2635. 1980

[18] Cowley, A.A., *et al.* "Rescattering in knockout reactions as manifested in 40Ca(p, p′p″) at an incident energy of 392 MeV." Physical Review C 57, 3185-3190. 1998

[19] Devins, D.W., Bunch, S.M., Forster, H.H., Hokhikian, J., Kim, C.C., "Charged particle reactions from 7Li+p at 30 MeV". Nuclear Physics A 126, 261-272. 1969.

[20] Dufauquez, C., El Masri, Y., Roberfroid, V., Cabrera, J., Keutgen, T., Van Mol, J., P. Demetriou, P., Charity, R.,"Light charged particle and neutron production in proton and α particle induced reactions on natSi at energies between 20 and 65 MeV". Nuclear Physics A 773, 24-55. 2006

[21] Edge, R.D., Tompkins, D.H., Glenn, J.W.,"Proton production from nuclei bombarded by protons of 1, 2 and 3 BeV". Physical Review 183, 849-853. 1969

[22] Green, R.E.L., Korteling, R.G., "Fragment production from p + Ag interactions at intermediate energies." Physical Review C 22, 1594-1611. 1980

[23] Guertin, A., *et al.*,"Neutron and light charged particle productions in proton induced reactions on 208Pb at 62.9 MeV". European Physical Journal A 23, 49-60. 2005

[24] Iwamoto, H., Imamura, M., Koba, Y., Fukui, Y., Wakabayashi, G., Uozumi, Y., Kin, T., Iwamoto, Y., Hohara, S., Nakano, M.,"Proton production double differential cross sections for 300 MeV and 392 MeV proton induced reactions". Physical Review C 82, 034604. 2010

[25] Katcoff, S., "Energy distributions of Li8 fragments emitted from C, Al, Cu, Ag, Au and U bombarded by 2.2 BeV protons". Physical Review 114, 905-911. 1995.

[26] Kin, T., *et al.*, "Proton production cross sections for reactions by 300 and 392 MeV protons on carbon, aluminum, and niobium". Physical Review C 72, 014606. 2005

[27] Sandoval, A., Gutbrod, H.H., Meyer, W.G., Stock, R., Lukner, C., "Spectra of p, d, and t from relativistic nuclear collisions". Physical Review C 21, 1321-1343. 1980

[28] Segel, R.E., Chen, T., Rutledge, L.L., Maher, J.V., Wiggins, J., Singh, P.P., Debevec, P.T., "Inclusive proton reactions at 164 MeV". Physical Review C 26, 2424-2432. 1982

[29] Wu, J.R., Chang, C.C., Holmgren, H.D., "Charged particle spectra: 90 MeV protons on 27Al, 58Ni, 90Zr, and 209Bi". Physical Review C 19, 698-713. 1979

[30] Bhattacharya, C. *et al.*, "Heavy fragment emission in alpha-induced reactions on aluminum at 60 MeV". Physical Review C 44, 1049-1056. 1991.

[31] D'Auria, J.M., Fluss, M.J., Kowalski, L., Miller, J.M., "Reaction cross section for low energy alpha particles on 59Co". Physical Review 168, 1224-1227. 1968

[32] Doering, R.R., Schweizer, T.C., Thornton, S.T., Dennis, L.C., Cordell, K.R., Ziock, K.O.H., Comiso, J.C., "Correlated energy spectra of light fragments from 720-MeV α induced reactions". Physical Review Letters 40, 1433-1435. 1978

[33] Bhattacharya, C. *et al.*, "Intermediate mass fragments emission in the reaction 47 MeV 7Li + Mg". Physical Review C 52, 798-806. 1995

[34] Gupta, D., Samanta, C., Kanungo, R., Sharan, M.K., Kailas, S., Chatterjee, A., Mahata, K., Shrivastava, A., "Measurement of 42 MeV 7Li projectile breakup on 58Ni target beyond grazing incidence". Nuclear Physics A 646, 161-174. 1999

[35] Fortsch, S.V., *et al.*, "Contributions of complete fusion and break-up fusion to intermediate mass fragment production in the low energy interaction of 12C and 27Al". Nuclear Physics A 797, 1-32. 2007

[36] Westfall, G.D., *et al.*, "Light particle spectra from 35 MeV/nucleon 12C induced reactions on 197Au". Physical Review C 29, 861-863. 1984

[37] Caskey, G., Heilbronn, L., Remington, B., Galonsky, A., Deak, F., Kiss, A., Seres, Z., "Fragment spectra from reactions induced by 35 MeV/nucleon 14N on 165Ho". Physical Review C 37, 969-975. 1988

[38] Fukuda, T., Ishihara, M., Ogata, H., Miura, I., Shimoda, T., Katori, K., Shimoura, S., Tanaka, M.K., Takada, E., Otsuka, T., "Light particle emission in the reaction 93Nb +14 N at 132, 159 and 208 MeV". Nuclear Physics A 425, 548-572. 1984

[39] Remington, B.A., *et al.*, "Neutron fragment coincidence measurements in 14N + Ho and 14N + Ni reactions at 35 MeV/nucleon". Physical Review C 34, 1685-1705. 1986

[40] Auble, R.L., *et al.*, "Light ion emission from reactions induced by 0.8 - 2.4 GeV 16O projectiles". Physical Review C 28, 1552-1564. 1983

[41] Natowitz, J.B., Namboodiri, M.N., Adler, L., Schmitt, R.P., Watson, R.L., Simon, S., Berlanger, M., Choudhury, R., "Particle emission at a 20Ne projectile velocity comparable to the Fermi velocity". Physical Review Letters 47, 1114-1117. 1981

[42] Westfall, G.D., *et al.*, "Energy dependence of nuclear matter disassembly in heavy ion collisions". Physics Letters B 116, 118-122. 1982.

[43] Jaderstrom, H., *et al.*, "200 and 300 MeV/nucleon nuclear reactions responsible for single-event effects in microelectronics." Physical Review C 77, 044601. 2008.

[44] Boger, J., Alexander, J.M., Elmaani, A., Kox, S., Lacey, R.A., Narayanan, A., Moses, D.J., McMahan, M.A., DeYoung, P.A., Gelderloos, C.J., "Intermediate mass fragments from the reactions 486, 550, 640, and 730 MeV 86Kr + 63Cu." Physical Review C 49, 1597-1602. 1994.

[45] L.A. Castellanos, “Thick-Target Measurements of Light Ion Yields Relevant to Radiation Transport Calculations,” Doctoral Dissertation, University of Tennessee, Knoxville, Knoxville, TN, USA, 2018.

[46] Mashnik, S.G., Kerby, L.M., Gudima, K.K., Sierk, A.J., Bull, J.S., James, M.R., “Production of Energetic Light Fragments in CEM, LAQGSM, and MCNP6.” Physical Review C 95, 034613. 2016.

APPENDICES

APPENDIX A

RAW DATA

The following data tables have been broken down into subsections based on the incoming beam species + energy, as well as shielding thickness:

Tables A.I – He 400 MeV/n on Al 20 g/cm^2

Tables A.II – He 400 MeV/n on Al 40 g/cm^2

Tables A.III – He 400 MeV/n on Al 60 g/cm^2

Tables A.IV – Fe 400 MeV/n on Al 20 g/cm^2

Tables A.V – Fe 400 MeV/n on Al 40 g/cm^2

Tables A.VI – Fe 400 MeV/n on Al 60 g/cm^2

Tables A.VII – Fe 800 MeV/n on Al 20 g/cm^2

Tables A.VIII – Fe 800 MeV/n on Al 40 g/cm^2

Tables A.IX – Fe 800 MeV/n on Al 60 g/cm^2

Tables A.X – H 400 MeV/n on Al 20 g/cm^2

Tables A.XI – H 400 MeV/n on Al 40 g/cm^2

Tables A.XII – H 400 MeV/n on Al 60 g/cm^2

Tables A.XIII – H 800 MeV/n on Al 20 g/cm^2

Tables A.XIV – H 800 MeV/n on Al 40 g/cm^2

Tables A.XV – H 800 MeV/n on Al 60 g/cm^2

Table A.I.1. Deuteron Yields from Helium 400 MeV/n on 20 g/cm^2 Aluminium at 12.7 deg

KE_left(MeV/n)	KE_mid(MeV/n)	KE_right(MeV/n)	Norm_Cts(#/SP*ster*MeV/n)	Y_stat(#/SP*ster*MeV/n)	Y_syst_tot(#/SP*ster*MeV/n)	X_tot(MeV/n)
44.276238	45.497400	46.718562	0.000175727119424	0.000000387689189	0.000338413499184	0.141179851673707
46.762649	48.211100	49.659551	0.000136750090813	0.000000389993947	0.000282907464491	0.163807235297529
49.659549	51.108000	52.556451	0.000142187367080	0.000000400550045	0.000290582590175	0.317316039665504
52.487751	54.050033	55.612315	0.000186339929689	0.000000626454159	0.000413281596936	0.057630784782527
55.681028	57.406433	59.131838	0.000168368519000	0.000000624162327	0.000380005004316	0.168327974570420
59.075710	60.875200	62.674690	0.000184461698221	0.000000643410837	0.000382865201331	0.182364960268825
62.730765	64.738800	66.746835	0.000191568204868	0.000000748593458	0.000391652664620	0.143426585530159
66.667922	68.823967	70.980012	0.000193660050070	0.000000825840063	0.000400630243229	0.108725444271426
71.045278	73.355633	75.665988	0.000182239335847	0.000000860126166	0.000391844577634	0.105848529299466
75.679668	78.271233	80.862798	0.000175965220207	0.000000975478300	0.000395332290614	0.112382267981875
80.808248	83.637933	86.467618	0.000190557431443	0.000001073395391	0.000398864695600	0.102154002970907
86.456720	89.563900	92.671080	0.000215643290261	0.000001287669856	0.000437346325757	0.098921607541376
92.673107	96.103567	99.534027	0.000218640819492	0.000001451840465	0.000442037139357	0.071534607096065
99.525370	103.349000	107.172630	0.000234569735758	0.000001682230205	0.000460678726501	0.056075962935304
107.164458	111.459333	115.754208	0.000185601790478	0.000001391795086	0.000342217041145	0.030908642381426
115.715352	120.521667	125.327982	0.000126552172458	0.000001003599935	0.000222307803943	0.031943571845991
125.326357	130.768667	136.210977	0.000046480702740	0.000000420433153	0.000082246234169	0.044646859311872
136.178630	142.393000	148.607370	0.000012788478422	0.000000129625226	0.000022062108120	0.074707273603177
148.590180	155.705000	162.819820	0.000008944869923	0.000000103134624	0.000014962717704	0.115959327027713
162.794725	171.066000	179.337275	0.000004798129330	0.000000081563355	0.000010724213515	0.139933969783287
182.541510	189.005500	195.469490	0.000000912885296	0.000000015318176	0.000001682730334	0.206524753763320
198.874835	202.473000	206.071165	0.000000782612044	0.000000009732000	0.000000946709000	0.176093000000000
226.096800	235.320000	244.543200	0.000001843702920	0.000000051847460	0.000003719813628	0.382152247592501
248.883400	265.783000	282.682600	0.000001060688083	0.000000019457547	0.000001217628241	0.636699968721532
282.437283	303.576333	324.715383	0.000001123715922	0.000000043497324	0.000002269455664	0.899412890150569
324.315467	351.475667	378.635867	0.000000643390331	0.000000037184737	0.000001445129748	1.277312887285649

Table A.I.2. Deuteron Yields from Helium 400 MeV/n on 20 g/cm^2 Aluminium at 10.0 deg

KE_left(MeV/n)	KE_mid(MeV/n)	KE_right(MeV/n)	Norm_Cts(#/SP*ster*MeV/n)	Y_stat(#/SP*ster*MeV/n)	Y_syst_tot(#/SP*ster*MeV/n)	X_tot(MeV/n)
45.872679	47.236300	48.599921	0.000173031817641	0.000000465850072	0.000361732122614	0.112983096112693
48.664289	50.130700	51.597110	0.000206390932653	0.000000632076515	0.000452818657533	0.312498283228884
51.597089	53.063500	54.529911	0.000207206524093	0.000000675016288	0.000483509029594	0.145047159346754
54.509122	56.231367	57.953612	0.000197638788629	0.000000721306518	0.000440845859258	0.086637556262570
57.974422	59.717467	61.460512	0.000206797706489	0.000000744995056	0.000449000047599	0.239151454070449
61.411328	63.383333	65.355338	0.000206989943346	0.000000802977807	0.000424037331936	0.081061296203860
65.379948	67.429933	69.479918	0.000174494310550	0.000000677264830	0.000346017507728	0.156276319376321
69.504478	71.818333	74.132188	0.000195501366115	0.000000978568889	0.000444169039050	0.105984157172334
74.063662	76.564867	79.066072	0.000212535800746	0.000000995317395	0.000421152749831	0.100984412977499
79.061768	81.788433	84.515098	0.000208901116549	0.000001094866873	0.000421263763049	0.091726943923419
84.522220	87.526600	90.530980	0.000244292875681	0.000001395519145	0.000486789285472	0.079354789811895
90.525208	93.852533	97.179858	0.000225935591722	0.000001467354809	0.000464795343408	0.097097286535040
97.163040	100.853600	104.544160	0.000231940923235	0.000001598118114	0.000460656603567	0.078582545510183
104.559282	108.655667	112.752052	0.000219993493983	0.000002128261031	0.000547981706637	0.037182767465992
112.744037	117.391667	122.039297	0.000275564284551	0.000002408925151	0.000541772638130	0.029616386526312
121.988192	127.211667	132.435142	0.000249143610220	0.000002307434314	0.000464565771858	0.028245887563856
132.420663	138.357333	144.294003	0.000308684449774	0.000003432081670	0.000606580282503	0.040356518192356
144.269318	151.059333	157.849348	0.000398017933066	0.000014585085835	0.002223963746187	0.102388562942645
157.842472	165.702667	173.562862	0.000489196932829	0.000010103291082	0.001379656728835	0.107614504678041
173.494568	182.685333	191.876098	0.000573802315467	0.000010362814527	0.001173166868271	0.177341516935122
191.783157	202.618667	213.454177	0.000759286712643	0.000016722683315	0.001600312283492	0.290095217402838
213.361140	226.329000	239.296860	0.001337884809531	0.000037626742637	0.002995284967228	0.382804702945249
239.159800	254.935000	270.710200	0.000291253288592	0.000009902302399	0.000686853049321	0.510686299071162
270.497250	290.068000	309.638750	0.000081928143521	0.000003174952931	0.000173366898831	0.724251650624974
309.309333	334.215333	359.121333	0.000032968325561	0.000001539583952	0.000067978625619	1.022015273791933
358.555233	391.292333	424.029433	0.000009175260058	0.000000493692738	0.000016991649331	1.463622376577374

Table A.I.3. Deuteron Yields from Helium 400 MeV/n on 20 g/cm^2 Aluminium at 7.20 deg

KE_left(MeV/n)	KE_mid(MeV/n)	KE_right(MeV/n)	Norm_Cts(#/SP*ster*MeV/n)	Y_stat(#/SP*ster*MeV/n)	Y_syst_tot(#/SP*ster*MeV/n)	X_tot(MeV/n)
45.107515	46.362167	47.616818	0.000163682343601	0.000000405312797	0.000345715439477	0.122046406231769
47.663617	49.139000	50.614384	0.000192645883453	0.000000642564168	0.000457437320254	0.227620066916831
50.614416	52.089800	53.565183	0.000188749415720	0.000000527826507	0.000375954984366	0.248556246921476
53.489792	55.107867	56.725941	0.000197400398845	0.000000604439098	0.000404815482241	0.047155096113676
56.801335	58.553200	60.305065	0.000219188162373	0.000000814762463	0.000488566898453	0.232728430426968
60.234225	62.104400	63.974575	0.000213242103162	0.000000786690056	0.000435901609645	0.104729290092749
64.045380	66.079500	68.113620	0.000215143526088	0.000000854086418	0.000441127601297	0.171562197111601
68.053247	70.290667	72.528087	0.000228465788518	0.000001091294779	0.000512249729967	0.083231406928575
72.529775	74.930000	77.330225	0.000227260225715	0.000001108367756	0.000477250582257	0.105391225458384
77.380935	80.006000	82.631065	0.000232846998365	0.000001336258341	0.000534275149582	0.089885094326089
82.639053	85.557333	88.475613	0.000231112717802	0.000001298158241	0.000467252304060	0.093622584072488
88.459060	91.668700	94.878340	0.000225297506050	0.000001385532170	0.000452942031066	0.091109406734651
94.847987	98.430267	102.012547	0.000244654333450	0.000001655989154	0.000485324945681	0.069217120197968
101.982680	105.966000	109.949320	0.000261244394202	0.000001998086675	0.000534700489888	0.056094197712330
109.941685	114.367000	118.792315	0.000296530890873	0.000002529805838	0.000598538098147	0.048786856072403
118.786622	123.810667	128.834712	0.000249321379217	0.000002305641540	0.000483571423644	0.014308303556481
128.800180	134.484000	140.167820	0.000316530661646	0.000002847268567	0.000528272744675	0.039015076893555
140.132142	146.629667	153.127192	0.000420403918292	0.000012915885891	0.002045615338812	0.078229203505277
153.114965	160.594000	168.073035	0.000525050631246	0.000013176257449	0.001899647576685	0.089506956860626
168.025345	176.738000	185.450655	0.000712317408355	0.000012213782136	0.001455396163412	0.132069064901551
185.373553	195.606333	205.839113	0.001127459330613	0.000024170548848	0.002457163962885	0.244699454801191
205.751493	217.957333	230.163173	0.001703583819473	0.000043247070160	0.003692726384570	0.327213917801490
230.033945	244.785000	259.536055	0.000779725189069	0.000029320355092	0.002208615310977	0.434010065404018
259.347083	277.522333	295.697583	0.000099634976845	0.000003390944356	0.000202129875257	0.607572849627927
295.413500	318.330000	341.246500	0.000034915287985	0.000001566776213	0.000075417582114	0.850884235936946
340.776150	370.537000	400.297850	0.000008315494061	0.000000437211269	0.000016467564938	1.219876480119606

Table A.I.4. Deuteron Yields from Helium 400 MeV/n on 20 g/cm^2 Aluminium at 32.7 deg

KE_left(MeV/n)	KE_mid(MeV/n)	KE_right(MeV/n)	Norm_Cts(#/SP*ster*MeV/n)	Y_stat(#/SP*ster*MeV/n)	Y_syst_tot(#/SP*ster*MeV/n)	X_tot(MeV/n)
44.263166	45.461400	46.659634	0.000094899323114	0.000000258461792	0.000223996866281	0.127270252502500
46.678225	48.140833	49.603441	0.000061830979703	0.000000156038877	0.000112110591308	0.244610761358142
49.603425	51.066033	52.528641	0.000077553523316	0.000000222617345	0.000159872867365	0.238926219448201
52.472926	54.006833	55.540740	0.000085425882837	0.000000244421172	0.000171123050996	0.070026690887261
55.596460	57.346900	59.097340	0.000086143382735	0.000000308934135	0.000185361973194	0.278911935554935
59.077597	60.847767	62.617937	0.000100401347834	0.000000330509715	0.000196825951265	0.164595402237708
62.637692	64.681067	66.724442	0.000101797779867	0.000000423214968	0.000217495280349	0.255691788590170
66.661073	68.795133	70.929193	0.000093795681692	0.000000361080635	0.000177828285307	0.136987785161488
70.992573	73.334433	75.676293	0.000115448883996	0.000000532109467	0.000238625279669	0.211690717812567
75.625480	78.220700	80.815920	0.000106680236209	0.000000510039035	0.000207549692999	0.129180309808926
80.788348	83.613533	86.438718	0.000098209119732	0.000000555765772	0.000203827845698	0.162510624782043
86.430675	89.541100	92.651525	0.000098818276607	0.000000589954052	0.000199895538295	0.142671911706439
92.650570	96.093500	99.536430	0.000098116644829	0.000000560399974	0.000170927070195	0.114435251879349
99.550507	103.367667	107.184827	0.000091325726167	0.000000559124252	0.000154833197891	0.113165317450445
107.162212	111.458667	115.755122	0.000103427306747	0.000000822536523	0.000203759558053	0.075383154650691
115.760083	120.564333	125.368583	0.000085854343435	0.000000671668533	0.000147142279462	0.082171355228206
125.356588	130.821333	136.286078	0.000089168679000	0.000000885988709	0.000170465767779	0.030137651430740
136.251545	142.467000	148.682455	0.000103517983177	0.000003619771702	0.000591614825900	0.019157013107541
148.650128	155.810333	162.970538	0.000134465451692	0.000007189046049	0.001064234637214	0.070577017136246
162.901895	171.188000	179.474105	0.000154830247971	0.000002699916796	0.000346211987206	0.136837511487932
179.432787	189.142667	198.852547	0.000114450385180	0.000001989850584	0.000216413269297	0.201447276892094
199.059595	202.676000	206.292405	0.000068958214035	0.000000765038000	0.000074046600000	0.184575000000000

Table A.I.5. Deuteron Yields from Helium 400 MeV/n on 20 g/cm^2 Aluminium at 30.0 deg

KE_left(MeV/n)	KE_mid(MeV/n)	KE_right(MeV/n)	Norm_Cts(#/SP*ster*MeV/n)	Y_stat(#/SP*ster*MeV/n)	Y_syst_tot(#/SP*ster*MeV/n)	X_tot(MeV/n)
44.320186	45.554800	46.789414	0.000128683847025	0.000000314156253	0.000267307584025	0.269121436643386
46.714777	48.079300	49.443822	0.000105153473702	0.000000286731918	0.000217616786459	0.150142561584382
49.518430	51.034900	52.551370	0.000091193753089	0.000000294555918	0.000203979065200	0.179108298023849
52.551430	54.067900	55.584370	0.000119677154452	0.000000343867287	0.000238204661250	0.169915890610325
55.533883	57.281533	59.029183	0.000096574590145	0.000000290743164	0.000175631919787	0.179511823891910
59.079670	60.883000	62.686330	0.000136804712174	0.000000518291124	0.000301808832238	0.196027925663054
62.627267	64.643067	66.658867	0.000115751870428	0.000000439210105	0.000230379236432	0.205334174638375
66.708295	68.813400	70.918505	0.000115837569661	0.000000488285992	0.000243795345202	0.164915117292442
70.928145	73.321500	75.714855	0.000099599938821	0.000000448001870	0.000196605092208	0.198636312334477
75.641527	78.220167	80.798807	0.000100205077771	0.000000426962655	0.000173365727426	0.126384249520816
80.797378	83.615533	86.433688	0.000103863658038	0.000000533224640	0.000201642527637	0.172849239093263
86.438843	89.549533	92.660223	0.000118117351368	0.000000718547842	0.000242112117921	0.153511426054545
92.652302	96.101267	99.550232	0.000126783657134	0.000000821608975	0.000252178665704	0.127885382204770
99.541468	103.369333	107.197198	0.000108915184161	0.000000723798915	0.000197978975162	0.114542319313475
107.186965	111.466000	115.745035	0.000115464364916	0.000000853589028	0.000210571368210	0.081242488280517
115.747015	120.572000	125.396985	0.000101729506731	0.000000816286412	0.000179557458575	0.096493031422689
125.369585	130.833000	136.296415	0.000075348156687	0.000000702474387	0.000135049888383	0.044715359969254
136.276035	142.487000	148.697965	0.000030656577662	0.000000343366700	0.000059393972143	0.032049745582298
148.831360	151.113000	153.394640	0.000006651827002	0.000000034543900	0.000005304040000	0.005948840000000

Table A.I.6. Deuteron Yields from Helium 400 MeV/n on 20 g/cm^2 Aluminium at 27.2 deg

KE_left(MeV/n)	KE_mid(MeV/n)	KE_right(MeV/n)	Norm_Cts(#/SP*ster*MeV/n)	Y_stat(#/SP*ster*MeV/n)	Y_syst_tot(#/SP*ster*MeV/n)	X_tot(MeV/n)
44.291980	45.567700	46.843420	0.000122263046004	0.000000329815529	0.000271522448143	0.291684021225024
46.834977	48.119100	49.403223	0.000103405548636	0.000000276669028	0.000225247278603	0.235455095293965
49.411640	50.968400	52.525160	0.000129486437893	0.000000354941375	0.000239562894899	0.073258234084436
52.525140	54.081900	55.638660	0.000126294223368	0.000000451735992	0.000304686035934	0.197155724918781
55.560443	57.256433	58.952423	0.000124943063240	0.000000402951177	0.000253568289360	0.123649005703402
59.030652	60.873567	62.716482	0.000121233038742	0.000000464712478	0.000264804478129	0.173066766536617
62.637537	64.620067	66.602597	0.000131557775832	0.000000512024010	0.000268494026185	0.149352928440021
66.681552	68.816067	70.950582	0.000120792899346	0.000000511920667	0.000251875334602	0.156221712442477
70.900893	73.282933	75.664973	0.000118041258981	0.000000570340292	0.000251570631460	0.156511212939159
75.635973	78.202833	80.769693	0.000118064439203	0.000000580419506	0.000240492033988	0.109530721106450
80.788078	83.601233	86.414388	0.000099466178959	0.000000463160756	0.000174396608947	0.156800066592875
86.417700	89.528600	92.639500	0.000128227413542	0.000000661675480	0.000224379194949	0.126654397959605
92.630105	96.083400	99.536695	0.000125610283134	0.000000776241055	0.000236613816446	0.105664526067976
99.516107	103.351667	107.187227	0.000114776887836	0.000000845165494	0.000230962992071	0.085329768898140
107.193692	111.458667	115.723642	0.000125298904118	0.000000914335818	0.000225878928877	0.058833537731637
115.717080	120.557000	125.396920	0.000100665893235	0.000000832237668	0.000180258957016	0.064570927741903
125.348015	130.809000	136.269985	0.000159029416358	0.000001500745172	0.000284756495634	0.022394609875146
136.253910	142.468000	148.682090	0.000211107251344	0.000008295332335	0.001361619745299	0.041567529835450
148.640795	155.801000	162.961205	0.000235058109622	0.000009720071186	0.001432998728533	0.086743772755282
162.907205	171.200000	179.492795	0.000218864040459	0.000003404144428	0.000432867897084	0.116026997601420
179.456560	189.166000	198.875440	0.000161289462706	0.000002914714112	0.000319124401320	0.160070121049151
199.105995	202.733000	206.360005	0.000014494971999	0.000000120809000	0.000011668500000	0.127291000000000

Table A.I.7. Proton Yields from Helium 400 MeV/n on 20 g/cm^2 Aluminium at 12.7 deg

KE_left(MeV/n)	KE_mid(MeV/n)	KE_right(MeV/n)	Norm_Cts(#/SP*ster*MeV/n)	Y_stat(#/SP*ster*MeV/n)	Y_syst_tot(#/SP*ster*MeV/n)	X_tot(MeV/n)
46.580420	48.257000	49.933580	0.000296544401333	0.000001221406979	0.000765132261840	0.292910677775666
49.933520	51.610100	53.286680	0.000347909281122	0.000001254958717	0.000786420752128	0.125746068589559
53.276110	55.264100	57.252090	0.000338177921754	0.000001524471494	0.000806918216320	0.291773016111731
57.262700	59.261300	61.259900	0.000365774357615	0.000001698010209	0.000892392914912	0.271969971779974
61.191563	63.425233	65.658903	0.000359296625483	0.000001822806075	0.000864700360299	0.129480104434780
65.727258	68.055933	70.384608	0.000409749661176	0.000002227731958	0.001004768334333	0.298018458731150
70.360050	73.000600	75.641150	0.000399214709350	0.000002490135388	0.000989386227269	0.178409131738148
75.575060	78.397800	81.220540	0.000384949712349	0.000002482890865	0.000918833324518	0.206846920725255
81.246545	84.331600	87.416655	0.000397986548443	0.000003003181458	0.001023546406296	0.195175574520097
87.425507	90.836867	94.248227	0.000462005363091	0.000003845152608	0.001181831414836	0.175412367112385
94.236825	98.027800	101.818775	0.000522110445291	0.000004913550099	0.001358192701943	0.164960325216580
101.796430	106.013000	110.229570	0.000526689168679	0.000005119968246	0.001270966191764	0.190180406725193
110.235348	114.918333	119.601318	0.000477357566340	0.000005176732643	0.001166196324294	0.149321155574353
119.589197	124.923667	130.258137	0.000362653259247	0.000004344248798	0.000855309215887	0.137333606825824
130.201480	136.228000	142.254520	0.000223425338209	0.000002996053869	0.000524421485245	0.102285953136978
142.240653	149.116333	155.992013	0.000133272672283	0.000001858184811	0.000287063338577	0.074609085296966
155.965995	163.935000	171.904005	0.000085101490311	0.000001367130929	0.000182502102139	0.060864855642727
171.848398	181.109333	190.370268	0.000040543472007	0.000000722567197	0.000084357427864	0.014432054259671
190.303953	201.246333	212.188713	0.000011474685445	0.000000216597552	0.000021419741877	0.068901198214980
212.077642	225.164667	238.251692	0.000001695290199	0.000000033532973	0.000002708658950	0.154814018239499
238.107710	254.010000	269.912290	0.000001681814909	0.000000059479613	0.000003785612647	0.248482554759887
269.696300	289.414000	309.131700	0.000002270033990	0.000000086800941	0.000004606665231	0.422423967942161
308.796883	333.892333	358.987783	0.000002820431240	0.000000105286619	0.000004435644926	0.648494740155231
358.410867	391.392667	424.374467	0.000000944691016	0.000000059170792	0.000001905845237	0.994981501332562

Table A.I.8. Proton Yields from Helium 400 MeV/n on 20 g/cm^2 Aluminium at 10.0 deg

KE_left(MeV/n)	KE_mid(MeV/n)	KE_right(MeV/n)	Norm_Cts(#/SP*ster*MeV/n)	Y_stat(#/SP*ster*MeV/n)	Y_syst_tot(#/SP*ster*MeV/n)	X_tot(MeV/n)
44.260342	45.950467	47.640592	0.000337449942616	0.000001309734193	0.000813084718425	0.177871728206284
47.660858	49.371233	51.081608	0.000335302308237	0.000001276344682	0.000783948070526	0.255350233307119
51.070332	52.791967	54.513602	0.000350594850482	0.000001374117667	0.000837007723930	0.105491436551512
54.524863	56.557333	58.589803	0.000360669338428	0.000001788561538	0.000924267065276	0.292023080690277
58.589830	60.622300	62.654770	0.000412698576150	0.000001943434805	0.001004328124922	0.213441757988356
62.603610	64.914800	67.225990	0.000380308144991	0.000001987440647	0.000902489225255	0.235481191865104
67.242830	69.639500	72.036170	0.000402947721814	0.000002305589083	0.001011173803168	0.213376010006959
72.070463	74.768933	77.467403	0.000459829908562	0.000002987703281	0.001162791499915	0.250288788870856
77.391212	80.317167	83.243122	0.000472290726552	0.000003411976763	0.001232346596401	0.159957885733152
83.228558	86.425333	89.622108	0.000476249274900	0.000003630154606	0.001197827379691	0.185916298467886
89.626380	93.156400	96.686420	0.000528460824957	0.000004631313295	0.001377467323214	0.179160040033736
96.675308	100.590833	104.506358	0.000531575261851	0.000004950984611	0.001334509679667	0.170813463934229
104.522367	108.868667	113.214967	0.000598623103916	0.000006073332621	0.001469325236665	0.161306512396896
113.194915	118.115000	123.035085	0.000614176280699	0.000007140997304	0.001525460588255	0.135095854319850
123.005347	128.531667	134.057987	0.000665881021815	0.000008437937428	0.001597160766244	0.132202477695768
134.036628	140.337333	146.638038	0.000763244949288	0.000011573129376	0.001917865366521	0.109683348927811
146.615475	153.836000	161.056525	0.000837428716062	0.000016038766305	0.002326992529532	0.080745665331397
160.999252	169.364667	177.730082	0.000916128374517	0.000017314577583	0.002177168678835	0.036110459407575
177.686818	187.465333	197.243848	0.001193740229089	0.000025356413385	0.002688590560796	0.014731634779918
197.161658	208.760333	220.359008	0.001491799046375	0.000039124520926	0.003536699279922	0.079132278358518
220.240348	234.176333	248.112318	0.001567142158898	0.000049646694240	0.003714584241083	0.159611952231905
247.960017	265.001667	282.043317	0.001624152670403	0.000062246752427	0.003857924474909	0.259323518322192
281.798467	303.106667	324.414867	0.000882590983708	0.000043766237674	0.002238663405955	0.436703159256949
324.011933	351.400333	378.788733	0.000121283684586	0.000008353742133	0.000345240365669	0.665388276440906

Table A.I.9. Proton Yields from Helium 400 MeV/n on 20 g/cm^2 Aluminium at 7.20 deg

KE_left(MeV/n)	KE_mid(MeV/n)	KE_right(MeV/n)	Norm_Cts(#/SP*ster*MeV/n)	Y_stat(#/SP*ster*MeV/n)	Y_syst_tot(#/SP*ster*MeV/n)	X_tot(MeV/n)
46.483020	48.210300	49.937580	0.000319775223855	0.000001265125922	0.000769385210933	0.216865057824561
49.937587	51.664867	53.392147	0.000346328222425	0.000001342330605	0.000816400431495	0.187100647149495
53.310397	55.221967	57.133537	0.000414384790951	0.000001841150678	0.001013571394520	0.195211661494799
57.215262	59.264667	61.314072	0.000414466659211	0.000002068948670	0.001060248425090	0.269935398992055
61.232010	63.417700	65.603390	0.000448189321405	0.000002387895819	0.001147683439799	0.101805646729895
65.685450	68.064600	70.443750	0.000398192074604	0.000002322911277	0.001025361588480	0.298422227158099
70.371847	72.983167	75.594487	0.000437585292592	0.000002705582280	0.001078734012080	0.144040793028225
75.597888	78.404733	81.211578	0.000478762381985	0.000003229371732	0.001199643205088	0.228318786587963
81.258407	84.337267	87.416127	0.000568457517032	0.000004184860259	0.001428145154071	0.203562024907914
87.430453	90.842933	94.255413	0.000489277749991	0.000004127351298	0.001270023611427	0.184622644846075
94.224110	98.021900	101.819690	0.000547481128029	0.000004999237054	0.001379310871541	0.154374458433544
101.781378	106.009333	110.237288	0.000587466346230	0.000006038523623	0.001499013284700	0.176796768785207
110.219208	114.917333	119.615458	0.000672787402950	0.000007907651113	0.001757606778413	0.149722208865085
119.593453	124.918333	130.243213	0.000697665785027	0.000008585327014	0.001694495140845	0.133450043633564
130.207023	136.233333	142.259643	0.000823874453859	0.000011171106798	0.001942646129948	0.108344925694977
142.244415	149.127000	156.009585	0.000926288122637	0.000016515433660	0.002518221635619	0.093301970083220
155.966403	163.931333	171.896263	0.001035267577829	0.000018410828792	0.002425050627183	0.055670738791667
171.843920	181.110000	190.376080	0.001368361082878	0.000027847945871	0.003122793618381	0.008273366785130
190.316033	201.259333	212.202633	0.001942078845231	0.000048006458045	0.004563715485873	0.052890424725941
212.095875	225.184000	238.272125	0.001930846949368	0.000057263267184	0.004597996257089	0.120791085614502
238.131847	254.038667	269.945487	0.001858558610921	0.000067317108976	0.004468479444319	0.199594553287809
269.732267	289.454667	309.177067	0.000851017026091	0.000038890676589	0.002141242884447	0.351350206500580
308.843067	333.953667	359.064267	0.000152136611470	0.000009581353700	0.000429739993537	0.540892992202709
358.482950	391.483000	424.483050	0.000014366823981	0.000000975007519	0.000033488899768	0.838184418204610

Table A.I.10. Proton Yields from Helium 400 MeV/n on 20 g/cm^2 Aluminium at 32.7 deg

KE_left(MeV/n)	KE_mid(MeV/n)	KE_right(MeV/n)	Norm_Cts(#/SP*ster*MeV/n)	Y_stat(#/SP*ster*MeV/n)	Y_syst_tot(#/SP*ster*MeV/n)	X_tot(MeV/n)
45.358290	46.911767	48.465244	0.000279753470826	0.000000976002556	0.000654043976031	0.158533621554861
48.520838	50.347433	52.174028	0.000265595892205	0.000001130932712	0.000650169869921	0.156351337948641
52.174038	54.000633	55.827228	0.000299223204357	0.000001302477006	0.000748738077412	0.395166953055288
55.738195	57.718300	59.698405	0.000301012390682	0.000001427019624	0.000752977424478	0.197791743296049
59.787430	61.954600	64.121770	0.000290788290473	0.000001376330621	0.000666951306104	0.251541405587629
64.039242	66.338267	68.637292	0.000311923831741	0.000001634352648	0.000751692878514	0.244454232372851
68.719850	71.234000	73.748150	0.000310973038150	0.000001866085572	0.000779330399670	0.248386828187406
73.676580	76.446100	79.215620	0.000378008950288	0.000002427866926	0.000928579303690	0.255598405890960
79.205032	82.198667	85.192302	0.000347652441961	0.000002553283731	0.000908416513739	0.195517659295139
85.210650	88.505400	91.800150	0.000381598199536	0.000002897938879	0.000923658851822	0.238930157847518
91.799707	95.457467	99.115227	0.000381085683339	0.000003245488615	0.000930078367662	0.230840852731920
99.099320	103.172000	107.244680	0.000370876577605	0.000003434012641	0.000890977966040	0.213947779490791
107.221435	111.754000	116.286565	0.000445494528124	0.000004806185084	0.001113530895524	0.197507821395407
116.255452	121.360667	126.465882	0.000450613766590	0.000005349412397	0.001103966631240	0.155382772918911
126.473142	132.241667	138.010192	0.000441320001474	0.000006004531831	0.001087555275629	0.140788289924979
137.979312	144.579667	151.180022	0.000448846787072	0.000007801155163	0.001235005545926	0.123977735159383
151.155403	158.733333	166.311263	0.000463100073465	0.000008355204671	0.001163182393812	0.084894938265188
166.267982	175.078667	183.889352	0.000475268659028	0.000008615423038	0.001027177400033	0.018749673602802
183.814660	194.177000	204.539340	0.000488870522234	0.000010984521573	0.001108889159318	0.078263358876680
204.450398	216.761333	229.072268	0.000376590016302	0.000010206854543	0.000879696699357	0.170042603914578
228.951188	243.859333	258.767478	0.000235898136537	0.000007470332895	0.000530756706107	0.301481162671899
258.567050	276.916000	295.264950	0.000122667716044	0.000004885936418	0.000286686548000	0.497414846118409
294.986517	318.121667	341.256817	0.000049267673037	0.000002288476868	0.000106794189459	0.751582632630638
340.776300	370.850000	400.923700	0.000013529911970	0.000000763386262	0.000027657250737	1.153317346845178

Table A.I.11. Proton Yields from Helium 400 MeV/n on 20 g/cm^2 Aluminium at 30.0 deg

KE_left(MeV/n)	KE_mid(MeV/n)	KE_right(MeV/n)	Norm_Cts(#/SP*ster*MeV/n)	Y_stat(#/SP*ster*MeV/n)	Y_syst_tot(#/SP*ster*MeV/n)	X_tot(MeV/n)
44.400872	45.997967	47.595062	0.000277189160275	0.000001002891482	0.000659438992933	0.381405675902968
47.595038	49.192133	50.789228	0.000275679587470	0.000001009436560	0.000663731345044	0.157244089826148
50.761818	52.662933	54.564048	0.000258573790055	0.000001104860321	0.000607476705451	0.191114241505807
54.591480	56.520000	58.448520	0.000282748670377	0.000001336916748	0.000727879736092	0.433199596686100
58.360065	60.440600	62.521135	0.000327981044380	0.000001568743524	0.000772474886288	0.103064148098392
62.609570	64.878200	67.146830	0.000270102238660	0.000001353308023	0.000626445008378	0.332047061944538
67.054225	69.506500	71.958775	0.000340855784715	0.000002091023538	0.000894120976287	0.178790454236489
72.051403	74.666233	77.281063	0.000367474923440	0.000002316552949	0.000930181220680	0.261394991698387
77.273288	80.232133	83.190978	0.000350100173277	0.000002368438428	0.000839948129453	0.213616593482342
83.121078	86.331133	89.541188	0.000376773505705	0.000002803353169	0.000918376237390	0.227280782447615
89.526902	93.059067	96.591232	0.000404384696377	0.000003207997952	0.000952395030303	0.208304129203456
96.594513	100.506733	104.418953	0.000454946723986	0.000004299275847	0.001149638286199	0.216213495665835
104.435005	108.778000	113.120995	0.000460851518880	0.000004821977107	0.001165775798406	0.181488835133625
113.108963	118.046333	122.983703	0.000424535258477	0.000004565233753	0.000969022993974	0.183318274984411
122.929848	128.463333	133.996818	0.000345905654001	0.000004248730995	0.000813052749591	0.160104630352311
133.980257	140.286667	146.593077	0.000240811097073	0.000003322539077	0.000553940609844	0.132579931166674
146.571108	153.802333	161.033558	0.000141352557684	0.000002026214397	0.000299033166164	0.109392755684003
160.969720	169.348000	177.726280	0.000067284147547	0.000001072075081	0.000137062035875	0.024922820128517
177.690663	187.479333	197.268003	0.000029413309466	0.000000543032126	0.000059029814000	0.018394885384989
197.192208	208.815333	220.438458	0.000019904155798	0.000000438801546	0.000039757005004	0.089909555027427
220.316177	234.284667	248.253157	0.000005618392667	0.000000140847120	0.000011030827183	0.184915867051073
248.091817	265.182667	282.273517	0.000001473706933	0.000000042959897	0.000002724347594	0.314605863349684
282.021250	303.393000	324.764750	0.000000646101287	0.000000032879053	0.000001661684058	0.502448171870493
325.481300	333.840000	342.198700	0.000000311583802	0.000000009732000	0.000000407441000	0.379661000000000

Table A.I.12. Proton Yields from Helium 400 MeV/n on 20 g/cm^2 Aluminium at 27.2 deg

KE_left(MeV/n)	KE_mid(MeV/n)	KE_right(MeV/n)	Norm_Cts(#/SP*ster*MeV/n)	Y_stat(#/SP*ster*MeV/n)	Y_syst_tot(#/SP*ster*MeV/n)	X_tot(MeV/n)
46.480030	48.153100	49.826170	0.000409860000975	0.000001720753976	0.001079857470577	0.270885923065411
49.826130	51.499200	53.172270	0.000391234613435	0.000001505649241	0.000945045885284	0.135864563076080
53.156920	55.146500	57.136080	0.000386942897917	0.000001817773336	0.000958268902919	0.308546194251363
57.151455	59.156400	61.161345	0.000429125855063	0.000001904397265	0.000997522748218	0.274311567816598
61.083535	63.307900	65.532265	0.000458515095536	0.000002386747625	0.001131603272281	0.137589103351610
65.610077	67.954667	70.299257	0.000439303313748	0.000002365973157	0.001059635361626	0.334408736454358
70.241543	72.873833	75.506123	0.000454891219095	0.000002871039382	0.001150043352426	0.178594426475241
75.483860	78.297000	81.110140	0.000494238471532	0.000003346731308	0.001251698975311	0.241401090759528
81.153087	84.231567	87.310047	0.000426722789963	0.000003020304208	0.001031457958768	0.223776232976717
87.334892	90.745467	94.156042	0.000500031928158	0.000004184281176	0.001287522421104	0.205037994957032
94.131570	97.929400	101.727230	0.000508758189668	0.000004708317415	0.001298841872514	0.188037725061116
101.687988	105.920333	110.152678	0.000508859990988	0.000005273607160	0.001316240191650	0.205805458717596
110.127077	114.835667	119.544257	0.000477570305589	0.000005269145592	0.001180862743005	0.197907584030123
119.516332	124.842667	130.169002	0.000498752172356	0.000006237872886	0.001225907432164	0.155856910659746
130.142800	136.176000	142.209200	0.000661037427763	0.000009190078661	0.001577211892570	0.144766398963434
142.193547	149.093667	155.993787	0.000730825218083	0.000004951633053	0.000788365925049	0.124164473993208
155.930600	163.902000	171.873400	0.000640709595598	0.000003720185510	0.000467426434150	0.042835672283409
171.823317	181.113667	190.404017	0.000678121042800	0.000013793341965	0.001543773305812	0.017053466926405
190.351813	201.316333	212.280853	0.000708325344522	0.000017002170658	0.001634294215850	0.038044062563876
212.182940	225.297000	238.411060	0.000498257204112	0.000014481611732	0.001173697986738	0.090587524619839
238.265557	254.214667	270.163777	0.000255756165566	0.000008705873733	0.000583355707154	0.207574054481768
269.954717	289.750667	309.546617	0.000124480314264	0.000005179718309	0.000282823774634	0.326915631408166
309.200783	334.398333	359.595883	0.000050285435524	0.000002607221012	0.000114323381099	0.521067796522679
359.023200	392.169000	425.314800	0.000014681002022	0.000000944028312	0.000031690579573	0.801290814005752

Table A.I.13. Triton Yields from Helium 400 MeV/n on 20 g/cm^2 Aluminium at 12.7 deg

KE_left(MeV/n)	KE_mid(MeV/n)	KE_right(MeV/n)	Norm_Cts(#/SP*ster*MeV/n)	Y_stat(#/SP*ster*MeV/n)	Y_syst_tot(#/SP*ster*MeV/n)	X_tot(MeV/n)
43.833975	45.048500	46.263024	0.000023763833438	0.000000061987700	0.000053616734838	38.806289034897425
46.263009	47.477533	48.692058	0.000034952108629	0.000000095094043	0.000082230333300	0.209735853468118
48.623747	49.967167	51.310587	0.000036133942232	0.000000081959721	0.000061473203916	0.091141404005040
51.378905	52.843833	54.308762	0.000024062855365	0.000000053467285	0.000038383676394	0.125360023256459
54.275096	55.773700	57.272304	0.000024372196842	0.000000046155862	0.000032699700425	0.098092640357827
57.305963	59.027333	60.748703	0.000032202662175	0.000000080307764	0.000049058678874	0.116759326058949
60.701943	62.476033	64.250123	0.000023814942848	0.000000062857506	0.000037454236341	0.080670708821604
64.296870	66.281100	68.265330	0.000023988346600	0.000000061773397	0.000032743554658	0.149226399533662
68.198332	70.341067	72.483802	0.000037533967419	0.000000146666937	0.000073143833297	0.104736254538522
72.500682	74.812667	77.124652	0.000024255285699	0.000000080461752	0.000037056527932	0.092035115848735
77.171062	79.705067	82.239072	0.000029923292389	0.000000132581340	0.000054877664165	0.104740796131450
82.242738	85.056633	87.870528	0.000029928732954	0.000000122510731	0.000045749924171	0.077855983234752
87.853042	90.950667	94.048292	0.000021727811701	0.000000102238784	0.000034633706663	0.058142953092588

Table A.I.14. Triton Yields from Helium 400 MeV/n on 20 g/cm^2 Aluminium at 10.0 deg

KE_left(MeV/n)	KE_mid(MeV/n)	KE_right(MeV/n)	Norm_Cts(#/SP*ster*MeV/n)	Y_stat(#/SP*ster*MeV/n)	Y_syst_tot(#/SP*ster*MeV/n)	X_tot(MeV/n)
44.622528	45.849400	47.076273	0.000030514346696	0.000000055631466	0.000047705375537	31.965438608288814
47.076261	48.303133	49.530006	0.000036876252543	0.000000079889189	0.000068428362038	0.208160445478962
49.478865	50.885767	52.292669	0.000048523215680	0.000000114831884	0.000087392590869	0.063181668921235
52.343795	53.820800	55.297805	0.000039691512823	0.000000115930319	0.000082460297006	0.116717904936689
55.237992	56.809067	58.380142	0.000042967332067	0.000000087366861	0.000059497409711	0.116255615601226
58.439965	60.173200	61.906435	0.000041440242223	0.000000152093922	0.000092144962907	0.114783094488213
61.837258	63.690533	65.543808	0.000034945169953	0.000000109057906	0.000061949277205	0.095344982254454
65.612970	67.608900	69.604830	0.000041772639877	0.000000142504404	0.000075016937407	0.124639551445197
69.566797	71.794167	74.021537	0.000034456053872	0.000000102656888	0.000048181809966	0.134962540223167
73.983505	76.384900	78.786295	0.000034364924861	0.000000149805862	0.000065638986973	0.081552743639009
78.802217	81.429867	84.057517	0.000042486606960	0.000000143768233	0.000057701616060	0.082769706058799
84.060717	86.959867	89.859017	0.000049402439463	0.000000304483455	0.000112381944812	0.084028795581568
89.851147	93.062167	96.273187	0.000054900644358	0.000000300615563	0.000096932436237	0.068824605743658
96.255580	99.815300	103.375020	0.000059504109268	0.000000220591700	0.000063911965187	0.068730065595051
103.387267	107.335667	111.284067	0.000073724973894	0.000002208270103	0.000582472110375	0.029955070124139
111.276348	115.752333	120.228318	0.000094265054095	0.000001656090053	0.000398383017476	0.024260018367780
120.179518	125.206333	130.233148	0.000072815018038	0.000000661602052	0.000140482586107	0.027681013060040

Table A.I.15. Triton Yields from Helium 400 MeV/n on 20 g/cm^2 Aluminium at 7.20 deg

KE_left(MeV/n)	KE_mid(MeV/n)	KE_right(MeV/n)	Norm_Cts(#/SP*ster*MeV/n)	Y_stat(#/SP*ster*MeV/n)	Y_syst_tot(#/SP*ster*MeV/n)	X_tot(MeV/n)
45.432726	46.665767	47.898807	0.000031616726045	0.000000073002250	0.000062232919585	22.813443878627730
47.898793	49.131833	50.364874	0.000054169166912	0.000000114993394	0.000098026446423	0.176883029590433
50.362257	51.842700	53.323144	0.000015973438536	0.000000045423663	0.000032214049833	0.079935630336566
53.325762	54.808800	56.291838	0.000045099892164	0.000000134886323	0.000095553188639	0.127591315245709
56.233696	57.883767	59.533838	0.000038590063300	0.000000109057906	0.000071790576006	0.109269615348733
59.591973	61.331133	63.070293	0.000035052395295	0.000000068456912	0.000041432956744	0.118336555397941
63.019415	64.956100	66.892785	0.000035762396510	0.000000117942054	0.000062986680504	0.113002991006074
66.900237	68.945467	70.990697	0.000027845368910	0.000000073669482	0.000037787336629	0.093760535231514
71.034120	73.305300	75.576480	0.000033980583972	0.000000062970282	0.000029155651628	0.136690980742476
75.527310	78.019500	80.511690	0.000034256535352	0.000000144981960	0.000061805631550	0.107055025001772
80.492927	83.214667	85.936407	0.000038631165653	0.000000165529902	0.000062854870015	0.074016878712764
85.930258	88.926633	91.923008	0.000038937366099	0.000000230230592	0.000079454264764	0.076005293784423
91.927840	95.239100	98.550360	0.000039243570279	0.000000234413675	0.000075171883366	0.083168942211922
98.554122	102.228167	105.902212	0.000029011747847	0.000000176663117	0.000051528345544	0.045108229797969
105.965465	108.659500	111.353535	0.000004771558944	0.000000024822130	0.000006456034706	0.026726333352894

Table A.I.16. Helium-4 Yields from Helium 400 MeV/n on 20 g/cm^2 Aluminium at 12.7 deg

KE_left(MeV/n)	KE_mid(MeV/n)	KE_right(MeV/n)	Norm_Cts(#/SP*ster*MeV/n)	Y_stat(#/SP*ster*MeV/n)	Y_syst_tot(#/SP*ster*MeV/n)	X_tot(MeV/n)
46.383135	48.080100	49.777065	0.000015143345901	0.000000076940990	0.000047613477204	0.329607987796109
49.777035	51.474000	53.170965	0.000023677423486	0.000000081421143	0.000050423231754	0.172832852443770
53.111680	55.061800	57.011920	0.000016008604000	0.000000056063963	0.000029862493456	0.195240467314054
57.071250	59.091600	61.111950	0.000014291507633	0.000000047760862	0.000024859824572	0.334846222879996
61.027370	63.235700	65.444030	0.000021474746232	0.000000101278745	0.000049246715368	0.099807613058574
65.528587	67.880167	70.231747	0.000012985770476	0.000000055801473	0.000024944863089	0.314624857222057
70.172792	72.797567	75.422342	0.000016508307052	0.000000089984894	0.000035579804908	0.149625811945299
75.401653	78.215233	81.028813	0.000021877892411	0.000000115284583	0.000041211585952	0.208250498448383
81.059667	84.141067	87.222467	0.000044219109938	0.000000270768924	0.000093083438372	0.192548104038160
87.240823	90.653333	94.065843	0.000029000515555	0.000000205753396	0.000063628010166	0.181733124147058
94.037510	97.834000	101.630490	0.000021428882587	0.000000143036461	0.000039137663525	0.165145950378476
101.606143	105.832333	110.058523	0.000025847301951	0.000000203735909	0.000050279346193	0.187140700285881
110.051778	114.748333	119.444888	0.000033964364151	0.000000240427715	0.000053105365191	0.163560884697809
119.427283	124.765333	130.103383	0.000031118683247	0.000000326713502	0.000063672716680	0.147559806449487
130.057115	136.096000	142.134885	0.000040306879565	0.000000477355042	0.000083790328635	0.114014615679614
142.119455	149.016000	155.912545	0.000045576585907	0.000000517000662	0.000079619449096	0.078649870634096
155.880077	163.872667	171.865257	0.000070206807645	0.000001015421236	0.000130947927666	0.061279055178829
171.812018	181.110333	190.408648	0.000118933350328	0.000001905300567	0.000214761357129	0.012384269892816
190.344538	201.338333	212.332128	0.000189600728855	0.000003818124137	0.000360692154084	0.063449437620597
212.221387	225.383667	238.545947	0.000292163635455	0.000007002381437	0.000551141798181	0.148120700164460
238.399482	254.412667	270.425852	0.000226763579350	0.000006783410313	0.000457173109522	0.237014837776035
270.200533	290.090333	309.980133	0.000034413273777	0.000001329951021	0.000074736520473	0.412553442689550
309.640033	334.987333	360.334633	0.000002073803095	0.000000089845974	0.000004013267415	0.642393317618576

Table A.I.17. Helium-4 Yields from Helium 400 MeV/n on 20 g/cm^2 Aluminium at 10.0 deg

KE_left(MeV/n)	KE_mid(MeV/n)	KE_right(MeV/n)	Norm_Cts(#/SP*ster*MeV/n)	Y_stat(#/SP*ster*MeV/n)	Y_syst_tot(#/SP*ster*MeV/n)	X_tot(MeV/n)
48.617075	49.194000	49.770925	0.000007959735151	0.000000021729900	0.000013182100000	0.171803000000000
49.770958	51.501733	53.232508	0.000015126422641	0.000000048137652	0.000029242613057	0.203956462264009
53.145208	55.045333	56.945458	0.000013600446033	0.000000059268783	0.000033018235324	0.128401999362576
57.032743	59.086933	61.141123	0.000024384322099	0.000000110482591	0.000056501117786	0.321897512082650
61.063375	63.240400	65.417425	0.000028948625890	0.000000155603694	0.000070932619661	0.100851445831405
65.495157	67.880367	70.265577	0.000047211304515	0.000000121222271	0.000053438739172	0.311934646951890
70.189187	72.794967	75.400747	0.000043610578174	0.000000166914748	0.000067064868245	0.131523432747477
75.412050	78.215400	81.018750	0.000040657619567	0.000000310152575	0.000118707821359	0.222100932442977
81.072073	84.149633	87.227193	0.000038102105594	0.000000300615563	0.000102438520968	0.205470085175434
87.238953	90.654033	94.069113	0.000034407194670	0.000000275916137	0.000084874640036	0.180904672316665
94.036770	97.836400	101.636030	0.000029793625669	0.000000208948227	0.000058051025981	0.161542401964004
101.593712	105.827667	110.061622	0.000033122524935	0.000000232606469	0.000058463816398	0.176266795792628
110.038548	114.745333	119.452118	0.000034339894498	0.000000253727988	0.000057019990885	0.162554938032685
119.428090	124.760000	130.091910	0.000033655694107	0.000000276442595	0.000054379658049	0.144607573341440
130.059393	136.098333	142.137273	0.000047729910990	0.000000507937040	0.000088205768723	0.117744322987183
142.122018	149.023333	155.924648	0.000049762417504	0.000000532109467	0.000080980364718	0.091402695408287
155.879930	163.870000	171.860070	0.000072415118393	0.000001019731405	0.000131956004300	0.057589629469407
171.808747	181.110667	190.412587	0.000112295019748	0.000001739100254	0.000196919499139	0.008199491088903
190.352723	201.347333	212.341943	0.000202057920432	0.000004321955367	0.000402538382551	0.051567855552913
212.233765	225.397000	238.560235	0.000327123636287	0.000008189664831	0.000645773710207	0.123990037097623
238.416928	254.433333	270.449738	0.000420523645924	0.000012773066842	0.000830217293926	0.202317307785592
270.226133	290.119333	310.012533	0.000348396363519	0.000012978633484	0.000706469331966	0.362090378520336
309.671300	335.029000	360.386700	0.000049172549970	0.000002777437394	0.000124379070917	0.570505669940273
359.797983	393.219333	426.640683	0.000001212374761	0.000000062542020	0.000002062481659	0.872372042452072

Table A.I.18. Helium-4 Yields from Helium 400 MeV/n on 20 g/cm^2 Aluminium at 7.20 deg

KE_left(MeV/n)	KE_mid(MeV/n)	KE_right(MeV/n)	Norm_Cts(#/SP*ster*MeV/n)	Y_stat(#/SP*ster*MeV/n)	Y_syst_tot(#/SP*ster*MeV/n)	X_tot(MeV/n)
47.430140	48.012700	48.595260	0.000008265601203	0.000000023827300	0.000014313500000	0.122949000000000
49.760420	51.508100	53.255780	0.000024966235214	0.000000075240880	0.000045302325804	0.210778437132454
54.367050	55.660600	56.954150	0.000045186322657	0.000000129348665	0.000071440632186	0.098766301335830
57.008005	59.079100	61.150195	0.000017768689277	0.000000093178098	0.000047244075230	0.307001333725116
61.083147	63.245167	65.407187	0.000020861560733	0.000000116997036	0.000058838726748	0.111514104963677
65.474257	67.876267	70.278277	0.000021671501487	0.000000198072152	0.000086657154525	0.304635805782905
70.193332	72.790067	75.386802	0.000022504809602	0.000000225900985	0.000088964405010	0.126544978972380
75.413802	78.212367	81.010932	0.000023666470665	0.000000287603504	0.000108614458258	0.227415536140256
81.068835	84.151200	87.233565	0.000025155468806	0.000000234413675	0.000079938229995	0.209121826911970
87.227125	90.652200	94.077275	0.000020889573072	0.000000174610322	0.000053659235112	0.178675532798982
94.049332	97.835667	101.622002	0.000047171586432	0.000000315269051	0.000087329958962	0.158837262450629
101.585717	105.823667	110.061617	0.000047275579020	0.000000365847862	0.000090663756957	0.169148277520760
110.031005	114.743000	119.454995	0.000053240087182	0.000000489799301	0.000109321964705	0.160903576809871
119.428005	124.757000	130.085995	0.000068383671375	0.000000688010909	0.000136189269855	0.142581368862695
130.059910	136.099000	142.138090	0.000077339680727	0.000000814038521	0.000142366839228	0.119199198936025
142.122877	149.026667	155.930457	0.000115312944314	0.000001378818303	0.000209514954686	0.097272739012583
155.879413	163.868333	171.857253	0.000172385575001	0.000002550609456	0.000330043626088	0.055483250110246
171.807170	181.111000	190.414830	0.000343914887307	0.000006091646336	0.000675273748441	0.006078143949538
190.357223	201.352333	212.347443	0.000794066564163	0.000017134985161	0.001597006699786	0.046428908276263
212.240503	225.404333	238.568163	0.001375380336260	0.000035321054957	0.002788319313386	0.111343172702820
238.425502	254.443667	270.461832	0.001768920661075	0.000055548834739	0.003650053187256	0.183908466147184
270.239183	290.134333	310.029483	0.000439238840469	0.000020395948680	0.001148962673291	0.335346686713914
309.687517	335.050667	360.413817	0.000012145477320	0.000000786341349	0.000035451737261	0.532469925305646
361.322400	371.399000	381.475600	0.000000619911431	0.000000009732000	0.000000339128000	0.400095000000000

Table A.II.1. Deuteron Yields from Helium 400 MeV/n on 40 g/cm^2 Aluminium at 12.7 deg

KE_left(MeV/n)	KE_mid(MeV/n)	KE_right(MeV/n)	Norm_Cts(#/SP*ster*MeV/n)	Y_stat(#/SP*ster*MeV/n)	Y_syst_tot(#/SP*ster*MeV/n)	X_tot(MeV/n)
44.124919	45.392100	46.659281	0.000277186269733	0.000000830089122	0.000690360750821	0.231593858478587
46.659219	47.926400	49.193581	0.000357363130693	0.000001162803676	0.000966361528647	0.111573120719150
49.136906	50.681600	52.226295	0.000261946519465	0.000001024786700	0.000687586767534	0.216029945114676
52.282970	53.885900	55.488830	0.000252315545840	0.000001070586019	0.000703249598201	0.260077514897001
55.488870	57.091800	58.694730	0.000339546050480	0.000001376236471	0.000904283216699	0.115305603993822
58.679217	60.603767	62.528317	0.000268849753611	0.000001335137401	0.000727499722483	0.259160844390525
62.543827	64.483867	66.423907	0.000306557602622	0.000001764740820	0.000956683639721	0.217462283786614
66.361427	68.567067	70.772707	0.000316265087987	0.000001891659973	0.000896958757627	0.133752102466204
70.817417	73.114967	75.412517	0.000326137851005	0.000002056404445	0.000941432532488	0.230152088245230
75.430245	78.053400	80.676555	0.000241062979883	0.000001607875000	0.000645254010674	0.145750975122844
80.594417	83.434667	86.274917	0.000298645208418	0.000002164821378	0.000798675025005	0.110405715843583
86.269022	89.386567	92.504112	0.000310689367695	0.000002347557375	0.000780987106313	0.107168350261120
92.507917	95.964867	99.421817	0.000365027114972	0.000003477322594	0.001075344810418	0.063726691358017
99.410178	103.258333	107.106488	0.000378949294786	0.000003385236256	0.000917771492833	0.063922405519035
107.117840	111.402000	115.686160	0.000369343027928	0.000003629886570	0.000905230043519	0.011863637679127
115.664282	120.523667	125.383052	0.000266676491869	0.000003035730829	0.000664520489485	0.080814546174064
125.358585	130.832000	136.305415	0.000114453492500	0.000001466913989	0.000288734666632	0.110437217091386
136.283153	142.538333	148.793513	0.000032951425531	0.000000463758760	0.000078865995479	0.188991034396053
148.770737	155.952667	163.134597	0.000021841333327	0.000000385053110	0.000056579947684	0.257576931005088
163.078690	171.415000	179.751310	0.000012406958015	0.000000207038406	0.000026332437767	0.403950595000181
179.704848	189.468333	199.231818	0.000007336552104	0.000000136579715	0.000014495788121	0.542979294114426
199.146278	210.742333	222.338388	0.000004157885746	0.000000099892818	0.000009132455938	0.732316176416307
222.220323	236.174333	250.128343	0.000003639525801	0.000000106516464	0.000007929864943	0.993566969630634
249.977467	267.063667	284.149867	0.000002935510251	0.000000115642012	0.000007492507035	1.340222418847334
283.900150	305.310000	326.719850	0.000001841434105	0.000000113888789	0.000005322699578	1.828120562639128
327.030900	344.557500	362.084100	0.000001031545637	0.000000045234184	0.000001865252732	1.969041021131861

Table A.II.2. Deuteron Yields from Helium 400 MeV/n on 40 g/cm^2 Aluminium at 10.0 deg

KE_left(MeV/n)	KE_mid(MeV/n)	KE_right(MeV/n)	Norm_Cts(#/SP*ster*MeV/n)	Y_stat(#/SP*ster*MeV/n)	Y_syst_tot(#/SP*ster*MeV/n)	X_tot(MeV/n)
45.816088	47.110900	48.405712	0.000307285371813	0.000001025157548	0.000833860688118	0.198114376171948
48.343444	49.713267	51.083090	0.000334506687133	0.000001349033061	0.001007592234044	0.161172399874203
51.145342	52.775167	54.404992	0.000318352895800	0.000001396686287	0.000902231623497	0.191030823917215
54.405008	56.034833	57.664658	0.000337427068360	0.000001438204924	0.000929179057200	0.195563287369179
57.579207	59.353167	61.127127	0.000322124089829	0.000001668508739	0.000992150478632	0.098848154194097
61.212553	63.178933	65.145313	0.000359069246309	0.000001966679809	0.001052334473453	0.275897122784925
65.073483	67.142333	69.211183	0.000358854065969	0.000002026603679	0.001018312401556	0.095263319175200
69.283005	71.588700	73.894395	0.000331218681281	0.000001914920732	0.000874366408072	0.250317341602395
73.810815	76.323100	78.835385	0.000372096015852	0.000002569939736	0.001095340187712	0.065034845656168
78.857660	81.574500	84.291340	0.000382490308606	0.000002713065417	0.001046267703989	0.164620917643050
84.351590	87.348900	90.346210	0.000366505391341	0.000002862944883	0.001004823419376	0.112325496273464
90.347235	93.696000	97.044765	0.000375319334896	0.000003244063213	0.001019221664734	0.060463359584049
97.010472	100.730967	104.451462	0.000408493669526	0.000003678788080	0.001041535967751	0.040755621834908
104.412657	108.579667	112.746677	0.000503595945118	0.000005520421961	0.001409916770870	0.040698799924936
112.720613	117.363333	122.006053	0.000442629265255	0.000005308620692	0.001218877118915	0.057242999454369
121.980753	127.248333	132.515913	0.000572032482037	0.000007707481557	0.001550479095584	0.116598841752294
132.485855	138.464000	144.442145	0.000617127715100	0.000010910504639	0.001890597136797	0.161094575653093
144.427220	151.270000	158.112780	0.000887717641826	0.000049085927772	0.007435589656732	0.235377956372299
158.067167	165.999667	173.932167	0.001160708516761	0.000041459739582	0.005632379766910	0.351869349278962
173.882155	183.127000	192.371845	0.001539840571068	0.000039757417724	0.004479187731397	0.500738018970000
192.312087	203.248667	214.185247	0.002051125104172	0.000062235767468	0.005903450422888	0.642484930901107
214.077473	227.179333	240.281193	0.002514846874194	0.000095731378970	0.007844144207044	0.878634054605784
240.138187	256.085667	272.033147	0.000624078639206	0.000029563988419	0.002045110353752	1.166144544197674
271.811900	291.621000	311.430100	0.000122070817575	0.000005812122811	0.000316973774877	1.587896447539323
311.090983	336.337333	361.583683	0.000043053318797	0.000002612813545	0.000113589553995	2.198707810032975
361.001750	394.255000	427.508250	0.000008657859687	0.000000602093609	0.000020559912586	3.146870741991161

Table A.II.3. Deuteron Yields from Helium 400 MeV/n on 40 g/cm^2 Aluminium at 7.20 deg

KE_left(MeV/n)	KE_mid(MeV/n)	KE_right(MeV/n)	Norm_Cts(#/SP*ster*MeV/n)	Y_stat(#/SP*ster*MeV/n)	Y_syst_tot(#/SP*ster*MeV/n)	X_tot(MeV/n)
44.932137	46.245333	47.558529	0.000328220366987	0.000001189027371	0.000953037734941	0.203166238930094
47.558504	48.871700	50.184896	0.000430265227133	0.000001528237093	0.001225157472778	0.239814644896845
50.116032	51.668633	53.221234	0.000321314645537	0.000001564169258	0.001063274787209	0.129367143394333
53.290098	54.937833	56.585568	0.000427932531907	0.000002206988010	0.001408846458337	0.205076522542196
56.585565	58.233300	59.881035	0.000395907048773	0.000001644867813	0.001051444190200	0.090363905032003
59.870730	61.844300	63.817870	0.000325887535987	0.000001743542607	0.000929006227048	0.227230709047193
63.828185	65.812100	67.796015	0.000393243609469	0.000002164187919	0.001147779619520	0.162704379888803
67.752867	70.032667	72.312467	0.000355224819774	0.000002181192354	0.001011056310029	0.213243517915668
72.295520	74.684500	77.073480	0.000347814068678	0.000002011920834	0.000891075995766	0.129471806281715
77.133615	79.799400	82.465185	0.000408237937136	0.000002936348076	0.001158930735763	0.172719896787284
82.403452	85.347167	88.290882	0.000495884499151	0.000004065796190	0.001457477933962	0.091295254034150
88.268487	91.499167	94.729847	0.000427126793154	0.000003788203344	0.001241404785695	0.084618284892628
94.725847	98.303767	101.881687	0.000418454443867	0.000003919027722	0.001132571147173	0.049876323951350
101.892250	105.868000	109.843750	0.000579442227457	0.000005566256313	0.001466315255005	0.028565214955237
109.818692	114.302667	118.786642	0.000590032907107	0.000006489343409	0.001518675659503	0.074272635499913
118.786485	123.820000	128.853515	0.000621251247356	0.000007657394350	0.001598607270369	0.093323085321001
128.835270	134.567000	140.298730	0.000817166934499	0.000012032328678	0.002190707872196	0.142799431683463
140.272078	146.801333	153.330588	0.001184556284887	0.000056350753616	0.008951396835338	0.211357088118662
153.292952	160.854667	168.416382	0.001541302867050	0.000051424207569	0.007307916750627	0.300533124007987
168.338652	177.114667	185.890682	0.001964303172263	0.000048483450078	0.005767697143176	0.456185310553727
185.845347	196.176667	206.507987	0.003180837348434	0.000094776983460	0.009465478587863	0.576543962857994
206.418748	218.723333	231.027918	0.003587579148841	0.000129508451690	0.011336515099694	0.776086575126126
230.909080	245.825000	260.740920	0.001045217167678	0.000044045874607	0.003224716379473	1.027845178986116
260.540350	278.928000	297.315650	0.000162992299268	0.000007708663545	0.000458303188579	1.392600617843465
297.025233	320.243333	343.461433	0.000042940342626	0.000002601949951	0.000125177759839	1.899205954029473
342.978233	373.188333	403.398433	0.000007071906380	0.000000385595629	0.000014350414985	2.689048988285635

Table A.II.4. Deuteron Yields from Helium 400 MeV/n on 40 g/cm^2 Aluminium at 32.7 deg

KE_left(MeV/n)	KE_mid(MeV/n)	KE_right(MeV/n)	Norm_Cts(#/SP*ster*MeV/n)	Y_stat(#/SP*ster*MeV/n)	Y_syst_tot(#/SP*ster*MeV/n)	X_tot(MeV/n)
43.626032	45.042667	46.459301	0.000143419643520	0.000000554714861	0.000411972133031	0.141666321933090
46.459299	47.875933	49.292568	0.000123547139539	0.000000375949777	0.000279766662050	0.450964789815125
49.292566	50.709200	52.125835	0.000127708581893	0.000000452854029	0.000336499831272	0.551055941360766
52.042952	53.590733	55.138515	0.000133568313303	0.000000593031547	0.000396202555071	0.086326906034272
55.221392	56.990867	58.760342	0.000097267538843	0.000000358055955	0.000213356846018	0.208918018218271
58.760358	60.529833	62.299308	0.000133062532772	0.000000657745087	0.000390962964806	0.392039860862387
62.233898	64.278733	66.323568	0.000157020664588	0.000000865649556	0.000445806841206	0.148081216296497
66.388970	68.512100	70.635230	0.000105415105901	0.000000579156452	0.000287027152935	0.243976480583683
70.570587	72.974367	75.378147	0.000120339502834	0.000000780804839	0.000340945335522	0.209564947672553
75.380387	77.926967	80.473547	0.000130604254521	0.000000777638451	0.000323345266495	0.178569936404452
80.535965	83.374400	86.212835	0.000165293647424	0.000001143520569	0.000423799465798	0.232742980502635
86.161182	89.311467	92.461752	0.000145732964234	0.000001269414874	0.000424100312074	0.196592052774902
92.438885	95.908200	99.377515	0.000125002348895	0.000000866561577	0.000261291453151	0.158609243473765
99.378595	103.227000	107.075405	0.000133187709586	0.000001276816883	0.000345732136027	0.118205471788154
107.060025	111.382000	115.703975	0.000144845525657	0.000001591303942	0.000388854607319	0.058804097492459
115.694233	120.567333	125.440433	0.000123969655440	0.000001143520569	0.000247861412188	0.033152019053897
125.392658	130.900333	136.408008	0.000134833922630	0.000001843747433	0.000347127305161	0.068815246666273
136.391243	142.671333	148.951423	0.000214903042481	0.000010605803698	0.001714664571131	0.131393729659600
148.936973	156.143333	163.349693	0.000278683579252	0.000015749466846	0.002311984896923	0.223700032317834
163.316835	171.704000	180.091165	0.000224129719446	0.000004592467411	0.000590441944745	0.363352907219689
180.024000	189.855000	199.686000	0.000173143580826	0.000004141120788	0.000438801183947	0.532035593453107
199.800390	207.334500	214.868610	0.000097426897864	0.000002066618860	0.000193059460400	0.600785618502973

Table A.II.5. Deuteron Yields from Helium 400 MeV/n on 40 g/cm^2 Aluminium at 30.0 deg

KE_left(MeV/n)	KE_mid(MeV/n)	KE_right(MeV/n)	Norm_Cts(#/SP*ster*MeV/n)	Y_stat(#/SP*ster*MeV/n)	Y_syst_tot(#/SP*ster*MeV/n)	X_tot(MeV/n)
44.022609	45.181200	46.339791	0.000163973881200	0.000000470208370	0.000427254850164	0.218362543081202
46.304389	47.777100	49.249810	0.000128396755335	0.000000496811411	0.000349068744778	0.339337491148520
49.285240	50.793400	52.301560	0.000128775295493	0.000000470208370	0.000328271502073	0.676868025295183
52.301540	53.809700	55.317860	0.000189733903480	0.000000798209443	0.000556864039397	0.394739909698779
55.235807	56.963667	58.691527	0.000158565471899	0.000000725534149	0.000482856698115	0.168818658455190
58.773600	60.631200	62.488800	0.000161300324259	0.000000731931573	0.000414728213434	0.568937367000973
62.422422	64.362167	66.301912	0.000147826950187	0.000000791450818	0.000435619956459	0.292509268699233
66.368272	68.576767	70.785262	0.000134240842691	0.000000595888680	0.000284528908299	0.365292938761482
70.702793	73.040833	75.378873	0.000158069336666	0.000000851587675	0.000389876099738	0.352501454208348
75.461365	78.023500	80.585635	0.000143086672095	0.000000834085544	0.000342763388465	0.329621809621269
80.531100	83.396100	86.261100	0.000143082327892	0.000000786889044	0.000290523057732	0.261752708156000
86.224192	89.351867	92.479542	0.000131415417769	0.000001050594375	0.000360635678186	0.247140192570937
92.470777	95.930367	99.389957	0.000148242506225	0.000001097597056	0.000336114132619	0.191794116910921
99.391328	103.239333	107.087338	0.000147241174806	0.000001246135656	0.000347277586351	0.146829838684274
107.106227	111.390667	115.675107	0.000172210058984	0.000001614110272	0.000397218482613	0.056528479109295
115.657458	120.529333	125.401208	0.000128257475676	0.000001243589962	0.000267096244328	0.065842999347994
125.366817	130.845667	136.324517	0.000110412207197	0.000001437871358	0.000273554587403	0.168592498470750
136.306050	142.568000	148.829950	0.000056112443621	0.000000719941263	0.000123716471453	0.307653161657734
148.910180	153.585000	158.259820	0.000005536580336	0.000000090748137	0.000013814458026	0.348705003545977

Table A.II.6. Deuteron Yields from Helium 400 MeV/n on 40 g/cm^2 Aluminium at 27.2 deg

KE_left(MeV/n)	KE_mid(MeV/n)	KE_right(MeV/n)	Norm_Cts(#/SP*ster*MeV/n)	Y_stat(#/SP*ster*MeV/n)	Y_syst_tot(#/SP*ster*MeV/n)	X_tot(MeV/n)
44.080455	45.327400	46.574346	0.000170817886027	0.000000572103506	0.000482743859011	0.441703495446889
46.574354	47.821300	49.068246	0.000199015793347	0.000000625343420	0.000527986849860	0.337838879309354
49.058290	50.642300	52.226310	0.000178499694563	0.000000940435627	0.000622483345193	0.411005444661017
52.236255	53.830200	55.424145	0.000154967373820	0.000000646679619	0.000427133004415	0.422346416125436
55.424155	57.018100	58.612045	0.000151709860125	0.000000534086702	0.000353123423699	0.259211958717745
58.606933	60.543233	62.479533	0.000170236761408	0.000000768735390	0.000417889939857	0.437197756089850
62.484628	64.426033	66.367438	0.000206192234365	0.000000979844017	0.000531158945412	0.385942966607762
66.299893	68.504533	70.709173	0.000187174504135	0.000001048522855	0.000491679686677	0.261235487220936
70.776700	73.067500	75.358300	0.000164976803185	0.000000899547357	0.000413370459586	0.399033292327846
75.354565	77.994200	80.633835	0.000160221939509	0.000001014126071	0.000404423942162	0.287612281820509
80.543538	83.380133	86.216728	0.000177451003362	0.000001049630853	0.000382637088053	0.255419712893289
86.231885	89.347900	92.463915	0.000182543279594	0.000001570311190	0.000535758242297	0.239866149387528
92.468945	95.929300	99.389655	0.000173629273743	0.000001461098520	0.000445336893650	0.175492791117841
99.378635	103.237000	107.095365	0.000187728757329	0.000001588080445	0.000435872107803	0.128892007844940
107.080222	111.382667	115.685112	0.000163372641907	0.000001489589079	0.000364085972533	0.064303039264408
115.658537	120.505667	125.352797	0.000163629327451	0.000001603830328	0.000349037406371	0.111842423189638
125.373497	130.845667	136.317837	0.000198152396323	0.000002296883780	0.000437621120626	0.169509397422562
136.295360	142.564000	148.832640	0.000221869724894	0.000013242296820	0.002153478599117	0.310363446708855
148.781898	155.994333	163.206768	0.000248156635785	0.000020414646265	0.002986755649078	0.485766756246246
163.133505	171.481000	179.828495	0.000277131681091	0.000005542235260	0.000698091976061	0.749026788458864
179.786243	189.564333	199.342423	0.000243120886192	0.000005830367911	0.000630257675826	1.035622644195752
199.599715	203.248000	206.896285	0.000197631115640	0.000003001260000	0.000288351000000	0.725533000000000

Table A.II.7. Proton Yields from Helium 400 MeV/n on 40 g/cm^2 Aluminium at 12.7 deg

KE_left(MeV/n)	KE_mid(MeV/n)	KE_right(MeV/n)	Norm_Cts(#/SP*ster*MeV/n)	Y_stat(#/SP*ster*MeV/n)	Y_syst_tot(#/SP*ster*MeV/n)	X_tot(MeV/n)
46.121355	47.823300	49.525245	0.000595863501398	0.000003203044176	0.001979979636688	0.257527113855998
49.525255	51.227200	52.929145	0.000636254425037	0.000003642214579	0.002250796820273	0.337823797592769
52.824907	54.705367	56.585827	0.000632229727128	0.000003657453802	0.002066611989925	0.248831334941964
56.690040	58.794600	60.899160	0.000638096344398	0.000004366466928	0.002182318010144	0.295710494859415
60.899173	63.003733	65.108293	0.000705097346810	0.000004600412151	0.002299590340756	0.226608644220405
65.063250	67.530100	69.996950	0.000701814190775	0.000005609275804	0.002395217363957	0.330627246129898
70.042000	72.553900	75.065800	0.000830268582189	0.000006938161175	0.002904631231757	0.270008974590550
75.048250	77.953100	80.857950	0.000652447432517	0.000005784365335	0.002097553608683	0.333556485030647
80.771707	83.867467	86.963227	0.000709031121065	0.000006703243132	0.002302392062030	0.210855490580634
87.004195	90.403200	93.802205	0.000890624480334	0.000009531520131	0.002931236857455	0.305051920223837
93.832375	97.618700	101.405025	0.000954851392272	0.000011172388517	0.003111918602310	0.261509606731760
101.373243	105.613333	109.853423	0.001124386188544	0.000014821123412	0.003674839846211	0.231592549783019
109.821225	114.570000	119.318775	0.000954002522541	0.000014325127392	0.003169400959582	0.247665701268868
119.311470	124.616000	129.920530	0.000799194276924	0.000013153726191	0.002621161819995	0.210041513011119
129.904748	135.982333	142.059918	0.000482456932687	0.000008522028260	0.001483126177954	0.184664937976894
142.008192	148.932667	155.857142	0.000371537992538	0.000007262758836	0.001110089428189	0.127069459341299
155.804698	163.814333	171.823968	0.000191680009231	0.000003802260299	0.000504587494274	0.060474873597718
171.774785	181.108000	190.441215	0.000085059585469	0.000002086008601	0.000241021430846	0.027818680149755
190.378578	201.381333	212.384088	0.000011887321768	0.000000365810420	0.000036981567529	0.120821022069878
212.290755	225.483000	238.675245	0.000007167897706	0.000000187589335	0.000015128931171	0.243057834839776
238.524583	254.558333	270.592083	0.000004781200471	0.000000146838766	0.000009692158127	0.433896676158046
270.372700	290.284000	310.195300	0.000003960675337	0.000000133569116	0.000007216309417	0.711040415630504
309.847267	335.197667	360.548067	0.000003837440705	0.000000158528097	0.000006807909835	1.114067160688708
359.970250	393.359000	426.747750	0.000001860648256	0.000000129672870	0.000004155797544	1.723958640564500

Table A.II.8. Proton Yields from Helium 400 MeV/n on 40 g/cm^2 Aluminium at 10.0 deg

KE_left(MeV/n)	KE_mid(MeV/n)	KE_right(MeV/n)	Norm_Cts(#/SP*ster*MeV/n)	Y_stat(#/SP*ster*MeV/n)	Y_syst_tot(#/SP*ster*MeV/n)	X_tot(MeV/n)
43.706083	45.408533	47.110983	0.000517128131231	0.000002584897910	0.001587133466025	0.186115063591728
47.161880	48.915200	50.668520	0.000520449372807	0.000002647840931	0.001589720589705	0.260580115233223
50.668513	52.421833	54.175153	0.000704466611577	0.000003848701935	0.002309535547637	0.406340692558597
54.076355	55.992000	57.907645	0.000713293549239	0.000003982082056	0.002201372556452	0.280086782879950
58.006485	60.162300	62.318115	0.000797155429013	0.000005509356131	0.002688100420092	0.253211368862064
62.318085	64.473900	66.629715	0.000842714111327	0.000006015776330	0.002934632329765	0.231791101060847
66.610445	69.153800	71.697155	0.000831233616740	0.000006828434829	0.002823037225915	0.299175915029937
71.682440	74.279100	76.875760	0.000899198550899	0.000007445009245	0.003012122179942	0.215100463504847
76.909775	79.882400	82.855025	0.000900987308356	0.000009067915500	0.003207465246094	0.339092028717869
82.752067	85.966967	89.181867	0.001070538042190	0.000011397248960	0.003718543123335	0.226441892165496
89.190220	92.720900	96.251580	0.001013146065244	0.000010983058145	0.003245628379836	0.258184254329907
96.257670	100.185300	104.112930	0.001120233413501	0.000013813546032	0.003692659781309	0.258813605189159
104.099138	108.488333	112.877528	0.001307657498424	0.000018004036323	0.004330597081997	0.239611470731265
112.872555	117.777000	122.681445	0.001437739975210	0.000022130351887	0.004766454198185	0.223376003234457
122.650703	128.223333	133.795963	0.001536459189218	0.000027020522415	0.005088929664409	0.167766621651776
133.770560	140.094000	146.417440	0.001909202560396	0.000036525921278	0.006072193262891	0.154210377994511
146.392272	153.659667	160.927062	0.002104199481820	0.000050517051251	0.007260648438404	0.112790075683546
160.880677	169.284667	177.688657	0.002370621466246	0.000059917146272	0.007484686892088	0.030327980963790
177.639410	187.496000	197.352590	0.003103509172795	0.000091242855419	0.009625819636062	0.056862811420646
197.261775	208.936000	220.610225	0.003779277473013	0.000131738585847	0.011848203492627	0.171625808562145
220.505718	234.547333	248.588948	0.003853348893454	0.000163453360327	0.012207859873041	0.300097926925529
248.421767	265.618667	282.815567	0.002731581296071	0.000140150024854	0.008708603956025	0.526765522847690
282.562350	304.077000	325.591650	0.000885176757820	0.000061452896034	0.003179878435372	0.818749519978485
325.184317	352.866667	380.549017	0.000080115860423	0.000006746604358	0.000274779627819	1.259010254400257

Table A.II.9. Proton Yields from Helium 400 MeV/n on 40 g/cm^2 Aluminium at 7.20 deg

KE_left(MeV/n)	KE_mid(MeV/n)	KE_right(MeV/n)	Norm_Cts(#/SP*ster*MeV/n)	Y_stat(#/SP*ster*MeV/n)	Y_syst_tot(#/SP*ster*MeV/n)	X_tot(MeV/n)
45.882457	47.670067	49.457677	0.000534335071373	0.000002822093473	0.001661595412610	0.142374418186097
49.457657	51.245267	53.032877	0.000711348436318	0.000003877380983	0.002282478023640	0.371676813481821
53.032890	54.820500	56.608110	0.000773248941692	0.000004709338589	0.002770439867332	0.462868799666817
56.540655	58.662400	60.784145	0.000758819279451	0.000005351382876	0.002653926971979	0.119033064458116
60.851597	63.041567	65.231537	0.000854267039604	0.000005770449943	0.002772100428087	0.277374080861929
65.126140	67.496800	69.867460	0.000765455208520	0.000005713236547	0.002523715897501	0.241628471097675
69.972827	72.569267	75.165707	0.000851364205573	0.000007327611541	0.002967858493898	0.276834876738824
75.067603	77.915833	80.764063	0.000926086927721	0.000008440003937	0.003104037203466	0.253644560420305
80.802572	83.868267	86.933962	0.001179337070197	0.000011146652188	0.003830502506004	0.229284985229387
86.993562	90.412767	93.831972	0.001076844544800	0.000011411723593	0.003510608408467	0.303067877378979
93.800112	97.604567	101.409022	0.001201929443057	0.000014844185906	0.004093917637594	0.251184523597773
101.392708	105.602333	109.811958	0.001364438034113	0.000018225026877	0.004550655511605	0.223776394093211
109.778262	114.541667	119.305072	0.001596288465272	0.000025959901109	0.005714031240534	0.201594489681638
119.266472	124.597667	129.928862	0.001778432381870	0.000031038740357	0.006118123393640	0.180932409231320
129.895513	135.960333	142.025153	0.001884925966922	0.000035545073005	0.006163092392890	0.150077554023145
141.997595	148.925000	155.852405	0.002305387715620	0.000057312917115	0.008648096725240	0.116221935788946
155.811890	163.806000	171.800110	0.002780654535899	0.000068308163498	0.008955540124979	0.039094951652355
171.773115	181.109000	190.444885	0.003872530934820	0.000107588325514	0.011993959260586	0.026619144288651
190.360435	201.372000	212.383565	0.005712462894971	0.000189719546037	0.017982650982589	0.140057306369750
212.284685	225.477000	238.669315	0.005388377039939	0.000214050342508	0.017139029940837	0.252121675599303
238.517573	254.550333	270.583093	0.003355085666795	0.000161181239161	0.010755025146414	0.447370913928253
270.368383	290.288333	310.208283	0.001068456195390	0.000066534059378	0.003693688505872	0.703707489729930
309.859050	335.222000	360.584950	0.000105301670989	0.000008473956889	0.000376495571495	1.072845993380224
360.003850	393.405000	426.806150	0.000010236798581	0.000000950917205	0.000032516254786	1.643985847315603

Table A.II.10. Proton Yields from Helium 400 MeV/n on 40 g/cm^2 Aluminium at 32.7 deg

KE_left(MeV/n)	KE_mid(MeV/n)	KE_right(MeV/n)	Norm_Cts(#/SP*ster*MeV/n)	Y_stat(#/SP*ster*MeV/n)	Y_syst_tot(#/SP*ster*MeV/n)	X_tot(MeV/n)
44.908720	46.414300	47.919880	0.000422310053610	0.000002047088047	0.001429632445146	0.298601851337194
47.823103	49.596733	51.370363	0.000372284398250	0.000001987473832	0.001186540693716	0.305085725862421
51.467165	53.391500	55.315835	0.000414088478645	0.000002472324747	0.001351145492874	0.419197332446188
55.315832	57.240167	59.164502	0.000463742230285	0.000002790989049	0.001525238816424	0.318625887204728
59.050317	61.200767	63.351217	0.000497369529115	0.000003294789179	0.001625895467965	0.189763553552441
63.465397	65.816167	68.166937	0.000472989948384	0.000003475732119	0.001554713188250	0.526682928366774
68.078087	70.552367	73.026647	0.000541847688157	0.000004348689860	0.001848797564067	0.193648052815565
73.115493	75.895233	78.674973	0.000549066703124	0.000004690482307	0.001774434670542	0.458260558749059
78.563350	81.583400	84.603450	0.000564915755426	0.000005275292898	0.001837537285309	0.237859718105021
84.645363	87.926133	91.206903	0.000553576326088	0.000005679152501	0.001813902880511	0.370232438083550
91.276607	94.921967	98.567327	0.000531896409960	0.000005813142934	0.001676920226458	0.332528678518109
98.563328	102.648433	106.733538	0.000594215300989	0.000007331789926	0.001886968349019	0.290279060838015
106.671987	111.262667	115.853347	0.000593215689840	0.000008710606252	0.001998656029836	0.281606939349868
115.810032	120.957667	126.105302	0.000652638821174	0.000010058824842	0.002067700777796	0.293382312708179
126.069113	131.870333	137.671553	0.000642625273156	0.000010759551999	0.001944724190882	0.210698057169234
137.667163	144.300333	150.933503	0.000629240387730	0.000014608208463	0.002303430347569	0.194635746102919
150.883125	158.540000	166.196875	0.000639827702812	0.000015018963098	0.002063645422208	0.109276066810395
166.143933	175.023333	183.902733	0.000666716448256	0.000016559355676	0.001961768795985	0.016171229730914
183.832982	194.285667	204.738352	0.000674545602309	0.000019394128332	0.001939963705099	0.124373199524737
204.656313	217.099333	229.542353	0.000507269103599	0.000017541721061	0.001489840516445	0.285727812975916
229.426902	244.483667	259.540432	0.000320188317537	0.000013407966917	0.000954286343131	0.516044776446773
259.340133	277.931333	296.522533	0.000136674281058	0.000007232793268	0.000418867982479	0.841919242118863
296.224167	319.686667	343.149167	0.000047403612559	0.000002907636993	0.000137415937835	1.310812837312025
342.657100	373.215000	403.772900	0.000011458482039	0.000000958524540	0.000035317383211	2.019413612858941

Table A.II.11. Proton Yields from Helium 400 MeV/n on 40 g/cm^2 Aluminium at 30.0 deg

KE_left(MeV/n)	KE_mid(MeV/n)	KE_right(MeV/n)	Norm_Cts(#/SP*ster*MeV/n)	Y_stat(#/SP*ster*MeV/n)	Y_syst_tot(#/SP*ster*MeV/n)	X_tot(MeV/n)
43.836407	45.516467	47.196527	0.000409314615928	0.000001988246569	0.001245091360967	0.544623346908669
47.196540	48.876600	50.556660	0.000455890638398	0.000002562175818	0.001603251957882	0.977215053584931
50.556673	52.236733	53.916793	0.000523457010932	0.000002716897833	0.001700788560771	0.655686800168343
53.863905	55.910200	57.956495	0.000494425714631	0.000003364212822	0.001722726034586	0.323034084238243
58.009395	60.108600	62.207805	0.000500617779884	0.000002789851919	0.001398796425821	0.634348123044437
62.131425	64.318700	66.505975	0.000512924999745	0.000003251133966	0.001570611325134	0.610822485953161
66.582387	69.104967	71.627547	0.000542753997642	0.000004371678005	0.001822049897506	0.554787751304046
71.549423	74.164433	76.779443	0.000552882401185	0.000004606026165	0.001857148427536	0.534788737026127
76.857615	79.806000	82.754385	0.000517213143002	0.000004434475117	0.001581966835448	0.618891898319892
82.656073	85.881033	89.105993	0.000602599349079	0.000006025120734	0.001979595429450	0.573289589554005
89.104882	92.636067	96.167252	0.000617626110262	0.000006446586415	0.001917493573966	0.512545771608741
96.178652	100.106067	104.033482	0.000706365972486	0.000008350515985	0.002230565945965	0.551136547644955
104.022772	108.416667	112.810562	0.000786472634153	0.000010777706634	0.002585689186175	0.516046783468321
112.789463	117.707333	122.625203	0.000702277489910	0.000010706379618	0.002306633540813	0.468746373411038
122.593627	128.156667	133.719707	0.000585032460845	0.000009920544324	0.001875463346643	0.381707979976840
133.732707	140.054667	146.376627	0.000389742655658	0.000007026389940	0.001179124654423	0.343018326374845
146.337555	153.621000	160.904445	0.000209234886725	0.000004142662273	0.000599923252816	0.232305307318279
160.873123	169.285333	177.697543	0.000112675138604	0.000002247147101	0.000285319919776	0.115819332136824
177.648618	187.508333	197.368048	0.000049081571114	0.000001069789113	0.000115401204875	0.092010769021131
197.277523	208.964333	220.651143	0.000018417964425	0.000000459255346	0.000042967963986	0.373919906886488
220.531173	234.599333	248.667493	0.000003023897420	0.000000115979537	0.000008437605860	0.720263558067462
248.500450	265.712000	282.923550	0.000002421925500	0.000000097805980	0.000005766437034	1.205656484777069
283.161300	296.946500	310.731700	0.000001859770487	0.000000075649530	0.000003929460055	1.452768359331934
326.467200	334.898000	343.328800	0.000000521793320	0.000000020311900	0.000000844373000	1.482850000000000

Table A.II.12. Proton Yields from Helium 400 MeV/n on 40 g/cm^2 Aluminium at 27.2 deg

KE_left(MeV/n)	KE_mid(MeV/n)	KE_right(MeV/n)	Norm_Cts(#/SP*ster*MeV/n)	Y_stat(#/SP*ster*MeV/n)	Y_syst_tot(#/SP*ster*MeV/n)	X_tot(MeV/n)
45.745552	47.464200	49.182849	0.000404096604609	0.000001936244594	0.001207636180959	0.381475835716877
49.269695	51.113000	52.956305	0.000464742684057	0.000002506156277	0.001430320088444	0.862577975970868
52.956295	54.799600	56.642905	0.000472167801575	0.000002669019719	0.001522860195477	0.643385945629060
56.540322	58.551867	60.563412	0.000524569755365	0.000003430110906	0.001756340970316	0.275419959594888
60.666022	62.927767	65.189512	0.000491936306429	0.000003377969013	0.001570668202581	0.744082145622377
65.166437	67.451267	69.736097	0.000583355673309	0.000004083245681	0.001881924699399	0.576741706354760
69.759180	72.442500	75.125820	0.000576740554767	0.000004937039777	0.001934427802556	0.536704215084995
75.042580	77.834200	80.625820	0.000599622238264	0.000005105719946	0.001922934295835	0.596565511729433
80.709058	83.816533	86.924008	0.000635907078280	0.000006229832502	0.002107663147042	0.569015307640313
86.849475	90.303000	93.756525	0.000700921091588	0.000007525780259	0.002275502162205	0.547813329270108
93.727373	97.525133	101.322893	0.000700263859303	0.000008156691005	0.002241893090091	0.543609681838909
101.318738	105.541333	109.763928	0.000714014885329	0.000009079023932	0.002265417553432	0.519792928237774
109.780275	114.492000	119.203725	0.000685354906858	0.000010338665016	0.002289286556877	0.485931301858606
119.178992	124.542667	129.906342	0.000729579387602	0.000011552394380	0.002263815706214	0.429714964540450
129.885962	135.932667	141.979372	0.000926407305490	0.000018061040968	0.003086155046543	0.384271029463581
141.955592	148.901667	155.847742	0.001047150030626	0.000020262952152	0.003033693112182	0.286581630232993
155.805050	163.826000	171.846950	0.000857489313777	0.000022758090300	0.002965052918280	0.195722889436187
171.765423	181.113333	190.461243	0.000865302027838	0.000023896392242	0.002656916702552	0.045805018693807
190.410297	201.442667	212.475037	0.000944251456758	0.000030457609942	0.002912077189190	0.192351744906694
212.364377	225.567667	238.770957	0.000682369306076	0.000025253474075	0.002032622014911	0.505422762389072
238.640617	254.714667	270.788717	0.000349362152665	0.000016027998888	0.001071439608072	0.879344649175737
270.562333	290.517333	310.472333	0.000154783764729	0.000008655428865	0.000471185167232	1.456027017412108
310.123733	335.538333	360.952933	0.000055246260409	0.000003803625893	0.000163555963994	2.313747073558387
360.373433	393.864333	427.355233	0.000011555446338	0.000000897237793	0.000028902949592	3.583993620111509

Table A.II.13. Triton Yields from Helium 400 MeV/n on 40 g/cm^2 Aluminium at 12.7 deg

KE_left(MeV/n)	KE_mid(MeV/n)	KE_right(MeV/n)	Norm_Cts(#/SP*ster*MeV/n)	Y_stat(#/SP*ster*MeV/n)	Y_syst_tot(#/SP*ster*MeV/n)	X_tot(MeV/n)
46.035801	47.183800	48.331799	0.000035748997243	0.000000087878740	0.000080596676095	23.025581500755056
48.334913	49.779933	51.224954	0.000049838283864	0.000000250446671	0.000182184497569	0.227634739709562
51.224946	52.669967	54.114987	0.000029349694906	0.000000079613959	0.000058155484691	0.279746394798932
54.074136	55.560033	57.045930	0.000058552507154	0.000000175527927	0.000126897754369	0.080015028357104
57.086785	58.834000	60.581215	0.000042995524288	0.000000154429909	0.000093194844664	0.197842582826853
60.581185	62.328400	64.075615	0.000037576704277	0.000000135147624	0.000081662548272	0.192789445263194
64.054477	66.086267	68.118057	0.000051351578309	0.000000168436683	0.000087698072852	0.135848522424243
68.090075	70.192200	72.294325	0.000055548031624	0.000000248455396	0.000121360806332	0.155349897830800
72.343480	74.706700	77.069920	0.000053094016194	0.000000271203041	0.000120895284469	0.092786095127988
77.001865	79.581500	82.161135	0.000055770326155	0.000000274342644	0.000117784073685	0.061739741731413
82.147147	84.964867	87.782587	0.000051130023008	0.000000322517869	0.000118395927481	0.050545056556329
87.790437	90.903667	94.016897	0.000015388115016	0.000000087878740	0.000029284832259	0.045495033261445

Table A.II.14. Triton Yields from Helium 400 MeV/n on 40 g/cm^2 Aluminium at 10.0 deg

KE_left(MeV/n)	KE_mid(MeV/n)	KE_right(MeV/n)	Norm_Cts(#/SP*ster*MeV/n)	Y_stat(#/SP*ster*MeV/n)	Y_syst_tot(#/SP*ster*MeV/n)	X_tot(MeV/n)
44.508576	45.672333	46.836090	0.000070517788722	0.000000207836552	0.000187993570194	39.267673799322516
46.794158	47.999833	49.205509	0.000077298815283	0.000000145517659	0.000125997669626	0.081516302679725
49.247418	50.710700	52.173981	0.000067232326151	0.000000320442955	0.000230243730818	0.258517709566695
52.173985	53.637267	55.100548	0.000068885810125	0.000000255422009	0.000183799508059	0.193194511544609
55.034637	56.595033	58.155429	0.000069097852692	0.000000291820468	0.000193198137526	0.037229636253125
58.221350	59.986400	61.751450	0.000046114855760	0.000000291294994	0.000173442976052	0.236823778720064
61.705015	63.516500	65.327985	0.000036449592374	0.000000192751683	0.000113932402130	0.145998415691575
65.374438	67.444933	69.515428	0.000070181681673	0.000000338301364	0.000172013119522	0.175707277317959
69.439353	71.634733	73.830113	0.000060098997960	0.000000307667314	0.000139654867256	0.078356228511130
73.906170	76.286700	78.667230	0.000064816834445	0.000000272161291	0.000120658063740	0.113720904711711
78.650433	81.329433	84.008433	0.000064453518493	0.000000357656222	0.000140357197326	0.058968688018388
83.971715	85.888450	87.805185	0.000066615918739	0.000000261488937	0.000095882911721	0.018683792893575

Table A.II.15. Triton Yields from Helium 400 MeV/n on 40 g/cm^2 Aluminium at 7.20 deg

KE_left(MeV/n)	KE_mid(MeV/n)	KE_right(MeV/n)	Norm_Cts(#/SP*ster*MeV/n)	Y_stat(#/SP*ster*MeV/n)	Y_syst_tot(#/SP*ster*MeV/n)	X_tot(MeV/n)
45.285502	46.461800	47.638099	0.000044923151182	0.000000121944169	0.000109224217751	32.345039171598110
47.570952	48.849000	50.127047	0.000094003691220	0.000000261862901	0.000227599563352	0.045166798847051
50.194161	51.669600	53.145039	0.000062796710706	0.000000253080737	0.000180548617866	0.262951101792710
53.145061	54.620500	56.095939	0.000083365894200	0.000000344127905	0.000245528022942	0.131378066128445
56.018072	57.662000	59.305928	0.000048874239947	0.000000178218706	0.000113058190953	0.069934815557443
59.383755	61.160700	62.937645	0.000039371254636	0.000000124726258	0.000074161820578	0.250653707197799
62.861872	64.764467	66.667062	0.000050312347038	0.000000154429909	0.000087149033761	0.068706187794300
66.742820	68.825000	70.907180	0.000065472486794	0.000000230473935	0.000116840276068	0.190050391117303
70.839465	73.131600	75.423735	0.000041377605135	0.000000179345201	0.000082979908689	0.037599205466069
75.432037	77.897267	80.362497	0.000055166256263	0.000000333536626	0.000138272130779	0.119200075183743
80.421900	83.129100	85.836300	0.000084378036546	0.000000434778895	0.000169186516742	0.059464668300008
85.836087	88.863867	91.891647	0.000045302833465	0.000000224761099	0.000078309462274	0.018361863185159
91.868480	95.200000	98.531520	0.000048055993656	0.000000335126527	0.000105977395577	0.022832619385870

Table A.II.16. Helium-4 Yields from Helium 400 MeV/n on 40 g/cm^2 Aluminium at 12.7 deg

KE_left(MeV/n)	KE_mid(MeV/n)	KE_right(MeV/n)	Norm_Cts(#/SP*ster*MeV/n)	Y_stat(#/SP*ster*MeV/n)	Y_syst_tot(#/SP*ster*MeV/n)	X_tot(MeV/n)
46.453440	47.611650	48.769860	0.000007464447294	0.000000044246823	0.000026760200486	0.170729145230830
50.507190	51.665400	52.823610	0.000030748232646	0.000000103033033	0.000062524510454	0.240126753746849
52.757850	54.560900	56.363950	0.000037924159799	0.000000158007183	0.000093181122447	0.204841986023764
56.429745	58.571100	60.712455	0.000052850819292	0.000000250203878	0.000123288428140	0.316246455064717
60.712445	62.853800	64.995155	0.000059010430144	0.000000368224081	0.000181018329252	0.271152114472228
64.906432	67.326167	69.745902	0.000044011874296	0.000000239575372	0.000101623876709	0.265847163938531
69.834632	72.384467	74.934302	0.000055006467023	0.000000358239677	0.000148041409526	0.339840878237154
74.860380	77.737300	80.614220	0.000041712401132	0.000000361777886	0.000131153871634	0.267143057218170
80.602293	83.682933	86.763573	0.000101978095960	0.000000768735390	0.000267224820805	0.260365623141766
86.832207	90.225867	93.619527	0.000056967987870	0.000000451867050	0.000139815645788	0.300572125382578
93.636737	97.432067	101.227397	0.000068982486362	0.000000794172184	0.000220086440423	0.254783369357185
101.189995	105.433000	109.676005	0.000091527780798	0.000000905919965	0.000224131839160	0.220925614153271
109.626173	114.390333	119.154493	0.000092452831022	0.000001269978993	0.000276023637406	0.229365448012555
119.128863	124.454333	129.779803	0.000120945498441	0.000001643423701	0.000323304921096	0.205310916294385
129.756612	135.840667	141.924722	0.000149919416401	0.000002632822643	0.000449461190259	0.171821058823999
141.879232	148.822667	155.766102	0.000188082026569	0.000003275640225	0.000496731149772	0.111939214878478
155.719925	163.749000	171.778075	0.000231754232643	0.000004675941642	0.000611315721490	0.049499815723723
171.738513	181.109333	190.480153	0.000373229469130	0.000008039144649	0.000895826176372	0.027386083544757
190.410638	201.465333	212.520028	0.000494154442748	0.000013738520579	0.001299591702764	0.135025707743192
212.424168	225.693333	238.962498	0.000314548863187	0.000010058433949	0.000820138538228	0.266249074789003
238.807917	254.953667	271.099417	0.000059319264019	0.000002377862719	0.000164638327789	0.459662651336825
271.333450	284.188500	297.043550	0.000002282442126	0.000000092527511	0.000005171374984	0.563126722571394
362.824200	373.006000	383.187800	0.000000730889389	0.000000040417300	0.000001389900000	0.897878000000000

Table A.II.17. Helium-4 Yields from Helium 400 MeV/n on 40 g/cm^2 Aluminium at 10.0 deg

KE_left(MeV/n)	KE_mid(MeV/n)	KE_right(MeV/n)	Norm_Cts(#/SP*ster*MeV/n)	Y_stat(#/SP*ster*MeV/n)	Y_syst_tot(#/SP*ster*MeV/n)	X_tot(MeV/n)
50.482770	51.675250	52.867730	0.000027286942843	0.000000089121255	0.000052564550070	0.253897653484628
52.867680	54.656400	56.445120	0.000055767789276	0.000000168436683	0.000099800316584	0.366120324060274
56.373700	58.486500	60.599300	0.000037562828202	0.000000168436683	0.000085181310909	0.177296408151688
60.670750	62.863300	65.055850	0.000064102795961	0.000000374619736	0.000179898089679	0.277538052212665
64.953480	67.317100	69.680720	0.000060020902756	0.000000348874319	0.000162594244342	0.219219844557672
69.783077	72.383567	74.984057	0.000040614910305	0.000000308938386	0.000125036475678	0.328204372783179
74.882503	77.726533	80.570563	0.000063434680911	0.000000453030901	0.000168846268547	0.220223140153005
80.620363	83.683733	86.747103	0.000115571248622	0.000000944013274	0.000320127988701	0.273456222494223
86.798842	90.225067	93.651292	0.000107768219638	0.000000924606225	0.000284214027852	0.297554976750516
93.612370	97.418200	101.224030	0.000094795907744	0.000000994236891	0.000274661725566	0.243734769054909
101.208555	105.422000	109.635445	0.000148945703382	0.000001690932168	0.000420140977633	0.207045915002953
109.604170	114.370000	119.135830	0.000133487184423	0.000001700685699	0.000376102999240	0.197393784219286
119.101603	124.443333	129.785063	0.000190556447446	0.000002678254978	0.000522482870778	0.190612532130524
129.748503	135.825333	141.902163	0.000220865093932	0.000003627556156	0.000617910865137	0.152075146118884
141.876470	148.822000	155.767530	0.000277887282525	0.000005196889730	0.000783839609064	0.110718836046492
155.725477	163.745667	171.765857	0.000336873603537	0.000006699362460	0.000870995179004	0.033572864952220
171.737240	181.110000	190.482760	0.000581571917269	0.000013778647797	0.001519900449770	0.026296702520356
190.399450	201.460000	212.520550	0.000930517801538	0.000026594076854	0.002492382100682	0.147574660440368
212.422317	225.691667	238.961017	0.001244370387397	0.000041651111687	0.003284878258003	0.269224903203623
238.805683	254.951333	271.096983	0.000677641688014	0.000028694172481	0.001944724419917	0.463674323184927
270.875917	290.958667	311.041417	0.000098916544776	0.000005753693372	0.000322693282718	0.739550702403155
310.682567	336.299667	361.916767	0.000003044243948	0.000000146154552	0.000006417580013	1.139083621986112
383.181100	394.401000	405.620900	0.000000666045931	0.000000040417300	0.000001261300000	0.994623000000000

Table A.II.18. Helium-4 Yields from Helium 400 MeV/n on 40 g/cm^2 Aluminium at 7.20 deg

KE_left(MeV/n)	KE_mid(MeV/n)	KE_right(MeV/n)	Norm_Cts(#/SP*ster*MeV/n)	Y_stat(#/SP*ster*MeV/n)	Y_syst_tot(#/SP*ster*MeV/n)	X_tot(MeV/n)
48.011935	48.619600	49.227265	0.000042661538931	0.000000161669000	0.000093227900000	0.006474630000000
49.227272	51.050267	52.873262	0.000070919294732	0.000000298176387	0.000172636410266	0.253381785079354
52.873238	54.696233	56.519228	0.000093864597133	0.000000444014050	0.000256566949442	0.436838339733362
56.416710	58.470300	60.523890	0.000096545949066	0.000000531954218	0.000266791121670	0.171810392378954
60.626422	62.853067	65.079712	0.000082677892482	0.000000565943221	0.000267424068709	0.258147621974327
65.000513	67.328933	69.657353	0.000100340832008	0.000000548540619	0.000250735478523	0.227041971384147
69.736542	72.370767	75.004992	0.000094533858884	0.000000726357119	0.000290139113168	0.303179880970027
74.896265	77.719800	80.543335	0.000096135535526	0.000000714666395	0.000268314753336	0.200670426434116
80.644260	83.697100	86.749940	0.000137305927177	0.000001038656725	0.000358181980971	0.279646091746264
86.757758	90.217133	93.676508	0.000147419801375	0.000001392508174	0.000423692267842	0.287186544082413
93.604787	97.406867	101.208947	0.000168361954115	0.000001712776797	0.000470310331973	0.235135533596456
101.205125	105.420000	109.634875	0.000226068249985	0.000002477552829	0.000611964496351	0.204982081736941
109.615532	114.362667	119.109802	0.000273654953345	0.000003658803620	0.000814142677099	0.185346897111551
119.092140	124.445000	129.797860	0.000408050018903	0.000006137839680	0.001202341326566	0.189239114891214
129.746192	135.818667	141.891142	0.000521680749840	0.000008822911785	0.001522100063785	0.143073258843887
141.872720	148.820000	155.767280	0.000733404526378	0.000013316724199	0.002000908550484	0.109458746817146
155.731658	163.746333	171.761008	0.001332100020021	0.000028836305554	0.003732403735249	0.034271742840276
171.735928	181.110333	190.484738	0.002407930292846	0.000058850658540	0.006521235841978	0.025285767950086
190.394455	201.462000	212.529545	0.003944621878014	0.000114154226256	0.010739196292200	0.145238331962365
212.424223	225.691333	238.958443	0.003663782695955	0.000126258186983	0.010177146746422	0.268832687233156
238.806000	254.952000	271.098000	0.000702253295264	0.000033878376827	0.002345087068401	0.462283376950762
270.878900	290.966000	311.053100	0.000021019800027	0.000001234500442	0.000069619351464	0.727106577615001
310.696567	336.316667	361.936767	0.000001452725118	0.000000074065085	0.000003245982252	1.109608057305371

Table A.III.1. Deuteron Yields from Helium 400 MeV/n on 60 g/cm^2 Aluminium at 12.7 deg

KE_left(MeV/n)	KE_mid(MeV/n)	KE_right(MeV/n)	Norm_Cts(#/SP*ster*MeV/n)	Y_stat(#/SP*ster*MeV/n)	Y_syst_tot(#/SP*ster*MeV/n)	X_tot(MeV/n)
43.807814	45.143500	46.479185	0.000251189940760	0.000000863140298	0.000684337228802	22.158447836663044
46.479181	47.814867	49.150552	0.000277890004400	0.000001025792052	0.000812160629695	0.576991752310204
49.150548	50.486233	51.821919	0.000342188388960	0.000001366769534	0.001080877974288	0.293697331131371
51.796897	53.492167	55.187437	0.000387188593560	0.000001590553448	0.000989069863123	0.354863395723044
55.212462	56.932767	58.653072	0.000376026914827	0.000001701933965	0.001047187571048	0.774732808749571
58.650972	60.373367	62.095762	0.000336061220472	0.000001338334339	0.000824085449507	0.421115928828393
62.097835	64.200700	66.303565	0.000308152542859	0.000001660149009	0.000835196867351	0.379210765147879
66.303535	68.406400	70.509265	0.000448353977130	0.000002399283045	0.001206978430413	0.589121377485149
70.445252	72.866467	75.287682	0.000346719800984	0.000002283255883	0.001005957956698	0.321781572477356
75.304805	77.837400	80.369995	0.000452234621051	0.000002838762412	0.001182166179270	0.429933288799553
80.416930	83.287300	86.157670	0.000383779887701	0.000002633841386	0.000970622732191	0.361327710768217
86.078895	89.229900	92.380905	0.000490549824235	0.000004099555715	0.001373285208881	0.331955711332099
92.357245	95.829900	99.302555	0.000482823976735	0.000004450057506	0.001356452801765	0.257860818291884
99.299982	103.162667	107.025352	0.000632371218167	0.000005546113601	0.001512721436576	0.194501254389374
107.040355	111.349000	115.657645	0.000521998437479	0.000005640825956	0.001400905206743	0.107161110978797
115.627452	120.503667	125.379882	0.000385323600244	0.000004392470881	0.000960585674686	0.087967072321977
125.391312	130.884667	136.378022	0.000179516897079	0.000002268167001	0.000446158187288	0.191604021238178
136.365072	142.655667	148.946262	0.000061420361502	0.000000808490199	0.000136131017409	0.382945558220748
148.886205	156.129000	163.371795	0.000024868447483	0.000000373159065	0.000054936502681	0.649180440602611
163.339633	171.715333	180.091033	0.000020227719477	0.000000337633388	0.000042630073914	0.954719410443718
180.025143	189.868333	199.711523	0.000016168928616	0.000000372749821	0.000038775586417	1.428011797322767
199.614927	211.282667	222.950407	0.000008929299460	0.000000179138497	0.000016730555409	2.006213034076890
222.839492	236.890667	250.941842	0.000004486028169	0.000000150255457	0.000011476894820	2.807854083690960
250.789417	268.004667	285.219917	0.000002880722940	0.000000106050238	0.000006542434244	3.907622870211505
284.971533	306.544333	328.117133	0.000001766651059	0.000000112501586	0.000005857864045	5.525661636311076
328.429650	346.113000	363.796350	0.000001285102359	0.000000085453213	0.000003476971390	6.074225613598824

Table A.III.2. Deuteron Yields from Helium 400 MeV/n on 60 g/cm^2 Aluminium at 10.0 deg

KE_left(MeV/n)	KE_mid(MeV/n)	KE_right(MeV/n)	Norm_Cts(#/SP*ster*MeV/n)	Y_stat(#/SP*ster*MeV/n)	Y_syst_tot(#/SP*ster*MeV/n)	X_tot(MeV/n)
45.519690	46.897033	48.274377	0.000327335883627	0.000001344793941	0.001031647137555	0.608515990778385
48.274390	49.651733	51.029077	0.000285962705262	0.000001297778197	0.000998411344171	0.494611786671123
50.955923	52.424967	53.894011	0.000313568439529	0.000001747934194	0.001266475413312	0.193942594660688
53.967145	55.727800	57.488455	0.000340048788649	0.000002471527983	0.001482269011816	0.640528328995682
57.488445	59.249100	61.009755	0.000375119801967	0.000002418643654	0.001451442642039	0.603965544344212
60.914240	62.834200	64.754160	0.000420008732627	0.000001767640169	0.000982498011140	0.249228331848207
64.849697	66.991967	69.134237	0.000448147991931	0.000002364721433	0.001166018754690	0.594952654991134
69.052737	71.312067	73.571397	0.000461456700334	0.000002927600600	0.001341865526351	0.376951405389342
73.652923	76.177333	78.701743	0.000469714431996	0.000003236755896	0.001354893884586	0.456358136823482
78.612567	81.381767	84.150967	0.000497507001560	0.000003528649581	0.001365890494813	0.339417909623225
84.162602	87.174667	90.186732	0.000534484395149	0.000003943743242	0.001399029025787	0.338783740933652
90.220492	93.560167	96.899842	0.000526142903012	0.000004377306184	0.001379787602378	0.267883969524121
96.897252	100.630867	104.364482	0.000545627679765	0.000004962632898	0.001401200452718	0.223100533619375
104.333527	108.515667	112.697807	0.000659800723660	0.000007305434602	0.001841287057052	0.156490128924383
112.665685	117.343000	122.020315	0.000697940625397	0.000007623069322	0.001729306767568	0.088492673090884
121.985982	127.268667	132.551352	0.000842866333109	0.000011056260184	0.002191251189549	0.156721602256294
132.557035	138.563000	144.568965	0.001335936592609	0.000025915190685	0.004464591039334	0.315204308528611
144.529805	151.434000	158.338195	0.001890587250802	0.000096417536953	0.014619219499074	0.542220158793455
158.317762	166.273667	174.229572	0.002451078823943	0.000087803808891	0.011880777207250	0.807023397958200
174.187675	183.513000	192.838325	0.003080031963828	0.000079774852323	0.008981554827183	1.226784002705448
192.747278	203.748333	214.749388	0.003748310321214	0.000119669538354	0.011408085752386	1.771331450039772
214.649865	227.849000	241.048135	0.002835055826767	0.000106582683757	0.008790193871781	2.452749886474363
240.898102	256.966667	273.035232	0.000600937062977	0.000027274713594	0.001881872759920	3.414342342574921
272.814183	292.776333	312.738483	0.000093760946920	0.000004847210437	0.000269860418600	4.808969970409463
312.393667	337.865667	363.337667	0.000020370016113	0.000001341057083	0.000059161326735	6.876549051908232
362.738083	396.307333	429.876583	0.000004924543304	0.000000351222560	0.000011985828187	10.113217446085098

Table A.III.3. Deuteron Yields from Helium 400 MeV/n on 60 g/cm^2 Aluminium at 7.20 deg

KE_left(MeV/n)	KE_mid(MeV/n)	KE_right(MeV/n)	Norm_Cts(#/SP*ster*MeV/n)	Y_stat(#/SP*ster*MeV/n)	Y_syst_tot(#/SP*ster*MeV/n)	X_tot(MeV/n)
44.502466	45.912100	47.321734	0.000411784043627	0.000001629755669	0.001222391680808	0.526460272302669
47.321733	48.731367	50.141001	0.000390160647795	0.000001757696235	0.001320225981312	0.535935055906963
50.140999	51.550633	52.960267	0.000404075037779	0.000002154913868	0.001617460385737	0.405902535489740
52.871225	54.523533	56.175841	0.000418347165281	0.000002837034245	0.001796072336588	0.375647868379417
56.264873	58.056833	59.848793	0.000431903817747	0.000003487099113	0.002054218510470	0.662772707418614
59.848807	61.640767	63.432727	0.000474366124264	0.000002478461197	0.001462044086582	0.418431021830361
63.391590	65.523300	67.655010	0.000460558569298	0.000002563878976	0.001271470106168	0.410388236737897
67.696163	69.869033	72.041903	0.000477052654683	0.000003050003958	0.001481852913445	0.560644495702937
71.977560	74.466200	76.954840	0.000463072827397	0.000003195026332	0.001340411203031	0.331708282125861
76.952410	79.579300	82.206190	0.000498356176057	0.000003409607471	0.001371984172167	0.417354310199380
82.272962	85.211267	88.149572	0.000650799150966	0.000004870393929	0.001751545256455	0.362956139678061
88.087528	91.350833	94.614138	0.000611915817648	0.000005323833684	0.001721522926847	0.275098802487397
94.593482	98.192467	101.791452	0.000727895781323	0.000007050967185	0.002048136017773	0.245417780156614
101.792950	105.793000	109.793050	0.000827614018299	0.000008385215215	0.002195471912596	0.169185657898446
109.778820	114.272000	118.765180	0.000977904907681	0.000011161137382	0.002619903575707	0.085312135382489
118.758622	123.845667	128.932712	0.001117873621449	0.000015070124627	0.003088812110974	0.071853505907088
128.879892	134.637667	140.395442	0.001567424624996	0.000022965014271	0.004148916362787	0.243471937836786
140.378448	146.960333	153.542218	0.002516707963514	0.000120273277635	0.018887981052627	0.424002647929232
153.521742	161.092667	168.663592	0.003495320376954	0.000125227574055	0.017823442585696	0.690987773760144
168.647297	177.483667	186.320037	0.004711798288854	0.000119587501094	0.014120177121626	1.052999476167961
186.225487	196.641667	207.057847	0.006511611029881	0.000195772844158	0.019708339903198	1.539940485528256
206.968953	219.358333	231.747713	0.003638205458636	0.000124705017171	0.010840011059409	2.139373502243122
231.620115	246.652000	261.683885	0.001115302326292	0.000047631821076	0.003497485274580	2.987369552951225
261.478467	280.012667	298.546867	0.000132464280737	0.000006321534429	0.000380915076677	4.192135425651228
298.260000	321.677000	345.094000	0.000022863347164	0.000001414574698	0.000068601478727	5.947925468715963
344.600283	375.107333	405.614383	0.000004915694941	0.000000350648417	0.000012668599833	8.655057412923382

Table A.III.4. Deuteron Yields from Helium 400 MeV/n on 60 g/cm^2 Aluminium at 32.7 deg

KE_left(MeV/n)	KE_mid(MeV/n)	KE_right(MeV/n)	Norm_Cts(#/SP*ster*MeV/n)	Y_stat(#/SP*ster*MeV/n)	Y_syst_tot(#/SP*ster*MeV/n)	X_tot(MeV/n)
46.259290	47.576933	48.894577	0.000121008101900	0.000000429601401	0.000344675869012	0.853457188650374
48.893751	50.212233	51.530716	0.000104802772374	0.000000380674169	0.000304726160515	0.369895812036041
51.531600	53.255700	54.979800	0.000113161238135	0.000000493141383	0.000302362564278	0.153112121105679
54.979800	56.703900	58.428000	0.000119096610391	0.000000552146409	0.000338214603092	0.413867486079784
58.428000	60.152100	61.876200	0.000137776584696	0.000000616385680	0.000377562043760	0.479389379099079
61.850597	63.951667	66.052737	0.000109043355757	0.000000477891832	0.000240712392008	0.275655842535235
66.078327	68.204967	70.331607	0.000145759487683	0.000000726828097	0.000361254340689	0.345386247127763
70.246598	72.653633	75.060668	0.000136930351311	0.000000723620307	0.000314595633566	0.342152356228917
75.145677	77.673867	80.202057	0.000127276230913	0.000000741675163	0.000310140035374	0.304068692280215
80.184495	83.097600	86.010705	0.000128919701150	0.000000772485328	0.000280469359678	0.348411510230360
85.921492	89.071667	92.221842	0.000124706333351	0.000000955698030	0.000314821277941	0.227526513271509
92.234383	95.716533	99.198683	0.000119366100926	0.000000887253203	0.000266780782556	0.224279819313598
99.199160	103.086000	106.972840	0.000144671349569	0.000001376247150	0.000381122777252	0.176103185852187
106.955407	111.305667	115.655927	0.000132668734970	0.000001171050425	0.000285431798800	0.092246617522866
115.676815	120.540000	125.403185	0.000125066587336	0.000001360707294	0.000303465740691	0.044503228852972
125.390563	130.971333	136.552103	0.000101653026551	0.000001506120072	0.000279858932923	0.111875604303530
136.486182	142.820667	149.155152	0.000110871617340	0.000008858536568	0.001433043463274	0.292098521001049
149.138745	156.410000	163.681255	0.000119820881826	0.000012207427801	0.001793661460446	0.478324336626310
163.644355	172.117000	180.589645	0.000122262233441	0.000003413050276	0.000434902840186	0.731833009500118
180.532802	190.447667	200.362532	0.000128867488900	0.000002851100294	0.000302397259358	1.078123529035054
200.474345	208.112500	215.750655	0.000079842724586	0.000001782585877	0.000166280867232	1.192175314993982

Table A.III.5. Deuteron Yields from Helium 400 MeV/n on 60 g/cm^2 Aluminium at 30.0 deg

KE_left(MeV/n)	KE_mid(MeV/n)	KE_right(MeV/n)	Norm_Cts(#/SP*ster*MeV/n)	Y_stat(#/SP*ster*MeV/n)	Y_syst_tot(#/SP*ster*MeV/n)	X_tot(MeV/n)
46.146584	47.604467	49.062350	0.000081035454292	0.000000280941343	0.000203984123870	0.905666685208195
49.062350	50.520233	51.978116	0.000113922419773	0.000000417956046	0.000302943603275	0.828689688030447
51.978117	53.436000	54.893883	0.000180254967907	0.000000679725239	0.000492588959000	0.413009563418331
54.830107	56.624767	58.419427	0.000124167850794	0.000000577366409	0.000335385380828	0.318943999667982
58.483193	60.341633	62.200073	0.000156855658121	0.000000742194271	0.000421773249055	0.809376108929588
62.148840	64.058500	65.968160	0.000127734582667	0.000000573904470	0.000322388144833	0.481735854119247
66.019387	68.275867	70.532347	0.000166972941634	0.000000805642032	0.000377990640743	0.477114618411551
70.495373	72.788833	75.082293	0.000130903517526	0.000000630820404	0.000291103798204	0.592890244042690
75.119277	77.773767	80.428257	0.000132157213081	0.000001073094490	0.000426111310086	0.464869680230922
80.319933	83.166233	86.012533	0.000144754041318	0.000000868740187	0.000327410115642	0.458965466838193
86.058835	89.175000	92.291165	0.000151677253244	0.000001060157871	0.000360602889654	0.390291412800743
92.338983	95.809733	99.280483	0.000141190135316	0.000001211711618	0.000369203160230	0.374009303801389
99.265325	103.157000	107.048675	0.000140627522262	0.000001176715713	0.000319336115890	0.297703126029943
107.000517	111.367667	115.734817	0.000166314541708	0.000001588472640	0.000383827384945	0.208791326586834
115.698417	120.587667	125.476917	0.000108816947480	0.000001192349135	0.000256009112363	0.109160954624078
125.439273	130.980333	136.521393	0.000049987643068	0.000000598256017	0.000118192432915	0.095495345088543
136.672950	138.661000	140.649050	0.000006577780997	0.000000074052400	0.000013060200000	0.121302000000000

Table A.III.6. Deuteron Yields from Helium 400 MeV/n on 60 g/cm^2 Aluminium at 27.2 deg

KE_left(MeV/n)	KE_mid(MeV/n)	KE_right(MeV/n)	Norm_Cts(#/SP*ster*MeV/n)	Y_stat(#/SP*ster*MeV/n)	Y_syst_tot(#/SP*ster*MeV/n)	X_tot(MeV/n)
46.054188	47.364333	48.674478	0.000168063883606	0.000000551308797	0.000459943067808	0.488392029141549
48.760693	50.347033	51.933373	0.000149600656213	0.000000578700879	0.000385684186562	0.523489178448800
51.933360	53.519700	55.106040	0.000174792875733	0.000000700105118	0.000466390741466	0.539610567222326
55.106027	56.692367	58.278707	0.000178810089520	0.000000677842040	0.000452042030268	0.404051923241308
58.231577	60.167567	62.103557	0.000189363678602	0.000000780806276	0.000424420422889	0.543120187470508
62.150662	64.133767	66.116872	0.000181068083115	0.000000885695670	0.000471703008323	0.582322811015505
66.015460	68.171000	70.326540	0.000200860585424	0.000001013556280	0.000511249796074	0.298743619982770
70.427973	72.806433	75.184893	0.000212731213464	0.000001301493773	0.000577588862404	0.607325054448604
75.082917	77.683667	80.284417	0.000198840078727	0.000001265060791	0.000522719156088	0.318482738599755
80.364660	83.160900	85.957140	0.000187396047341	0.000001165718808	0.000440516943233	0.462587913703979
85.978860	89.151600	92.324340	0.000190269720893	0.000001473472154	0.000490147596861	0.345181171957568
92.253447	95.748667	99.243887	0.000202880251823	0.000001689324768	0.000511917117540	0.259485156463718
99.234603	103.108333	106.982063	0.000178108155179	0.000001534770599	0.000415648540811	0.203140146037163
106.989268	111.306333	115.623398	0.000175695825775	0.000001423047214	0.000351493623905	0.110076741868980
115.609758	120.533333	125.456908	0.000141350947832	0.000001605286531	0.000346101784678	0.071083768474174
125.422997	130.939667	136.456337	0.000215313448215	0.000002951744058	0.000559719305765	0.169879398825785
136.447095	142.763000	149.078905	0.000219721086214	0.000016697120380	0.002753447345347	0.392294673309491
149.025630	156.311000	163.596370	0.000215890584274	0.000018789263088	0.002748302002292	0.656752814414982
163.552447	171.978667	180.404887	0.000219504884475	0.000005597321205	0.000709559875549	0.971075326688924
180.341038	190.244333	200.147628	0.000290566218151	0.000007353952815	0.000788761148081	1.433774655723137
200.372960	204.055000	207.737040	0.000107466515162	0.000001529800000	0.000146157000000	1.034000000000000

Table A.III.7. Proton Yields from Helium 400 MeV/n on 60 g/cm^2 Aluminium at 12.7 deg

KE_left(MeV/n)	KE_mid(MeV/n)	KE_right(MeV/n)	Norm_Cts(#/SP*ster*MeV/n)	Y_stat(#/SP*ster*MeV/n)	Y_syst_tot(#/SP*ster*MeV/n)	X_tot(MeV/n)
45.553250	47.134233	48.715216	0.000820875959210	0.000003993118325	0.002682552192763	0.146870924607073
48.809110	50.716900	52.624690	0.000721857211105	0.000004520061912	0.002501669973118	0.546086803959773
52.624677	54.532467	56.440257	0.000833985447522	0.000005114713813	0.002831469919053	1.096452535817670
56.440277	58.348067	60.255857	0.000940156642537	0.000005598569658	0.003100483114677	0.770172266795553
60.183707	62.483967	64.784227	0.001015902218825	0.000007737145391	0.003568534886939	0.438557082560526
64.856370	67.228800	69.601230	0.001043643545779	0.000008048023805	0.003580770943107	0.841461727502802
69.480148	72.060833	74.641518	0.001215582398260	0.000010304880543	0.004243584859526	0.658594227237075
74.762607	77.600367	80.438127	0.001070245989726	0.000010105555634	0.003757924449600	0.716003211680646
80.329722	83.463667	86.597612	0.001200869398707	0.000011854761699	0.003997611226333	0.699549405110175
86.623822	90.018367	93.412912	0.001346401903052	0.000014858800865	0.004581017761994	0.642109632453836
93.492327	97.266767	101.041207	0.001578945199773	0.000019694951338	0.005504450851302	0.704783790693288
101.043315	105.286000	109.528685	0.001677454546502	0.000022351913999	0.005559509056437	0.668111382934014
109.464487	114.244667	119.024847	0.001459639103761	0.000021753122007	0.004790813761742	0.607269702772994
118.975515	124.350000	129.724485	0.001192600138242	0.000019480927735	0.003833492119269	0.572470588389482
129.686355	135.754000	141.821645	0.000813439936385	0.000015274483175	0.002683862826208	0.478071943140360
141.814160	148.775000	155.735840	0.000474944067579	0.000010326224615	0.001581713725536	0.354108448617087
155.683288	163.741333	171.799378	0.000280595566795	0.000005862793594	0.000775665650603	0.223398627936722
171.725473	181.107333	190.489193	0.000138989349483	0.000003444367630	0.000394858565933	0.076660808230021
190.425298	201.498333	212.571368	0.000067438253425	0.000002058749374	0.000202573334497	0.366737488360544
212.491170	225.757000	239.022830	0.000020390707057	0.000000713742840	0.000059128633711	0.759219065517983
238.863950	255.011000	271.158050	0.000007469083822	0.000000358876542	0.000024614445732	1.386275451548501
270.937883	290.989333	311.040783	0.000003658651436	0.000000199341512	0.000011292135615	2.272745210290850
310.690667	336.238667	361.786667	0.000001595163547	0.000000067874995	0.000003064878273	3.634632280245142
372.730700	395.237500	417.744300	0.000000946471179	0.000000076599267	0.000002628782435	4.734605681078414

Table A.III.8. Proton Yields from Helium 400 MeV/n on 60 g/cm^2 Aluminium at 10.0 deg

KE_left(MeV/n)	KE_mid(MeV/n)	KE_right(MeV/n)	Norm_Cts(#/SP*ster*MeV/n)	Y_stat(#/SP*ster*MeV/n)	Y_syst_tot(#/SP*ster*MeV/n)	X_tot(MeV/n)
43.780758	45.308133	46.835508	0.000936134602173	0.000004324966433	0.002993161898812	0.734682681589814
46.835492	48.362867	49.890242	0.001159152451167	0.000005438605906	0.003762881023378	0.336280805241691
49.856033	51.807633	53.759233	0.000867023362520	0.000005547465461	0.002996214300914	0.471119509790679
53.793443	55.779233	57.765023	0.000949074245988	0.000006197442684	0.003294967487563	1.076792693770718
57.765010	59.750800	61.736590	0.001153372887368	0.000007445671800	0.003958817380027	0.720539158290512
61.642068	63.962633	66.283198	0.001173961674322	0.000008934064524	0.004103822426044	0.422332472759318
66.377685	68.827200	71.276715	0.001396961554410	0.000011132556124	0.004797416346848	0.903869487511333
71.155615	73.813700	76.471785	0.001451356166953	0.000012454871563	0.004984870683879	0.568147266614916
76.592927	79.506767	82.420607	0.001481452581550	0.000013990017765	0.005067599806259	0.748510812450963
82.324335	85.569800	88.815265	0.001656858113524	0.000017742315205	0.005760183814029	0.654269267888994
88.809573	92.338833	95.868093	0.001636790633019	0.000018858281016	0.005628845209082	0.673392881942629
95.891473	99.817133	103.742793	0.001818370679728	0.000022740567169	0.006100009892721	0.613302288003233
103.738590	108.145000	112.551410	0.002157792592137	0.000031097433780	0.007419340513051	0.620177659037312
112.526125	117.480000	122.433875	0.002439367370455	0.000037799143850	0.008007468665808	0.603918065050219
122.424540	127.981000	133.537460	0.002558233550734	0.000044038000723	0.008331773076465	0.538117869425463
133.514628	139.893333	146.272038	0.002971216019489	0.000064672294564	0.010618422935808	0.423764513856458
146.216067	153.510667	160.805267	0.003405929743404	0.000095597485062	0.013801944193895	0.288037281882051
160.759040	169.214000	177.668960	0.003924812256842	0.000103178876579	0.012842915577317	0.092460634662866
177.629097	187.536667	197.444237	0.005210754748497	0.000153626869933	0.016224891038688	0.153258375773855
197.361308	209.096333	220.831358	0.005788275933337	0.000204483127250	0.018424566813904	0.498202562384017
220.721983	234.865333	249.008683	0.004502964331868	0.000191655110044	0.014407960962846	0.964514302270319
248.840367	266.153667	283.466967	0.002483884521612	0.000127890408103	0.007962855560287	1.643070508077483
283.198950	304.874000	326.549050	0.000748491396798	0.000050596521964	0.002604963413279	2.682712609449622
326.135650	354.038000	381.940350	0.000058789173008	0.000005054216580	0.000207326895298	4.214076301456821

Table A.III.9. Proton Yields from Helium 400 MeV/n on 60 g/cm^2 Aluminium at 7.20 deg

KE_left(MeV/n)	KE_mid(MeV/n)	KE_right(MeV/n)	Norm_Cts(#/SP*ster*MeV/n)	Y_stat(#/SP*ster*MeV/n)	Y_syst_tot(#/SP*ster*MeV/n)	X_tot(MeV/n)
45.859908	47.447133	49.034358	0.001093493182738	0.000005736445966	0.003815678550782	0.634119554179651
48.992350	50.621600	52.250850	0.001122508045223	0.000005782976857	0.003743932784733	0.373134790879918
52.292892	54.339267	56.385642	0.000995580177413	0.000006751235051	0.003482815015659	0.798368448435307
56.385658	58.432033	60.478408	0.001153974082917	0.000007670258219	0.003957962248241	0.889498917785739
60.454232	62.524767	64.595302	0.001486568242635	0.000009709768644	0.004942911736679	0.514727988636717
64.619450	67.128800	69.638150	0.001349758699600	0.000010905813605	0.004588183476857	0.694497623037689
69.638150	72.147500	74.656850	0.001619402275433	0.000013875010064	0.005833297049885	0.811517960414309
74.595897	77.507867	80.419837	0.001613242925542	0.000015587890202	0.005633171885679	0.577268712380985
80.400212	83.460067	86.519922	0.002002549866642	0.000020181269330	0.006956177146034	0.713856555676979
86.600523	90.038133	93.475743	0.002002853464000	0.000022945103881	0.007041549371310	0.673356712776371
93.397857	97.224067	101.050277	0.002217529463513	0.000028377498269	0.007819470078113	0.626801449450302
101.029960	105.266000	109.502040	0.002453279832281	0.000034116824324	0.008505418439842	0.629656871050416
109.508067	114.235667	118.963267	0.003095389906881	0.000048785264427	0.010838601160800	0.586040124843001
118.932572	124.306667	129.680762	0.003614609672299	0.000061447763983	0.012032543707916	0.506524482096374
129.674363	135.740333	141.806303	0.003892931594334	0.000077019976969	0.013312148669681	0.456508886141332
141.787325	148.757000	155.726675	0.004870423765024	0.000124087130850	0.018671483027773	0.318905099120412
155.658602	163.709667	171.760732	0.005654659830849	0.000143370710900	0.018770658764412	0.167118607528246
171.732330	181.110000	190.487670	0.007619351046313	0.000217141073954	0.024143280791144	0.082859489454860
190.396152	201.489667	212.583182	0.010022353611935	0.000336029600589	0.031792728205519	0.388298691103897
212.487200	225.740000	238.992800	0.006996043004097	0.000283934944813	0.023067748732237	0.788221492265975
238.850467	255.009667	271.168867	0.002768779772696	0.000134530999975	0.008990796097399	1.389641969268703
270.933867	290.991667	311.049467	0.000817397314151	0.000051430896291	0.002852614450784	2.268918008236525
310.694317	336.255667	361.817017	0.000078495899044	0.000006414812237	0.000285969164501	3.605641891536096
361.236067	394.921667	428.607267	0.000006120313277	0.000000482484637	0.000016565355145	5.662385298308478

Table A.III.10. Proton Yields from Helium 400 MeV/n on 60 g/cm^2 Aluminium at 32.7 deg

KE_left(MeV/n)	KE_mid(MeV/n)	KE_right(MeV/n)	Norm_Cts(#/SP*ster*MeV/n)	Y_stat(#/SP*ster*MeV/n)	Y_syst_tot(#/SP*ster*MeV/n)	X_tot(MeV/n)
43.867467	45.677367	47.487267	0.000412531132342	0.000002206500336	0.001286692553787	0.231018444566379
47.487300	49.297200	51.107100	0.000390066080640	0.000002043186166	0.001191637452864	0.851047840872650
51.107100	52.917000	54.726900	0.000410384114610	0.000002112402204	0.001232301965407	0.929335918477813
54.710225	56.536800	58.363375	0.000414234715054	0.000002149882702	0.001238926239551	0.362269672871040
58.380050	60.680000	62.979950	0.000432183015614	0.000003060678189	0.001403427325321	0.318740896692109
62.979850	65.279800	67.579750	0.000516275535990	0.000003596679651	0.001649335601097	0.761408113383355
67.462162	69.951667	72.441172	0.000534447064414	0.000003621408870	0.001532865838635	0.409468337579354
72.558780	75.348600	78.138420	0.000560539723737	0.000004721639650	0.001785063457152	0.520929657202390
78.012593	81.016733	84.020873	0.000545873404175	0.000005175952392	0.001821013038733	0.500549325114918
84.146678	87.425933	90.705188	0.000543328623380	0.000005590158659	0.001796886007517	0.496445927127014
90.662980	94.390100	98.117220	0.000613443071989	0.000006859207644	0.001937939461929	0.514610450001746
98.051153	102.151633	106.252113	0.000549551041573	0.000006989065494	0.001811026472568	0.490247733255341
106.245097	110.819667	115.394237	0.000655174419864	0.000009072701951	0.002120817690915	0.478155810598386
115.411817	120.537667	125.663517	0.000674965145644	0.000010622812955	0.002182534101841	0.424258516903315
125.641503	131.525333	137.409163	0.000609486334228	0.000011652554742	0.002071007878836	0.363127777242392
137.351850	144.022000	150.692150	0.000590818444922	0.000012661906910	0.001986378207492	0.291236077167648
150.658075	158.361000	166.063925	0.000549245186984	0.000013780075034	0.001892989463838	0.187515621044781
166.043488	174.976333	183.909178	0.000514896660696	0.000013390525440	0.001585429023397	0.067843690875202
183.854778	194.406333	204.957888	0.000474435309347	0.000013540736404	0.001360886562786	0.200338366960126
204.838007	217.399667	229.961327	0.000287187091297	0.000009576446233	0.000822603597136	0.510865715930322
229.829752	245.044667	260.259582	0.000149173468143	0.000005889317064	0.000414555466583	0.943798821879430
260.065483	278.850333	297.635183	0.000070637061930	0.000003417716632	0.000197707258007	1.573750142689112
297.335800	321.076000	344.816200	0.000022997833604	0.000001329244345	0.000063000111418	2.503182580755946
344.311000	375.284000	406.257000	0.000004878067399	0.000000436011876	0.000016316938524	3.939057464940059

Table A.III.11. Proton Yields from Helium 400 MeV/n on 60 g/cm^2 Aluminium at 30.0 deg

KE_left(MeV/n)	KE_mid(MeV/n)	KE_right(MeV/n)	Norm_Cts(#/SP*ster*MeV/n)	Y_stat(#/SP*ster*MeV/n)	Y_syst_tot(#/SP*ster*MeV/n)	X_tot(MeV/n)
43.534138	45.126433	46.718728	0.000395225967172	0.000001774066566	0.001176517939378	0.856578686773726
46.718738	48.311033	49.903328	0.000478724278332	0.000002206307958	0.001462616250503	0.951451569439559
49.804460	51.532500	53.260540	0.000563276471464	0.000003215152458	0.001980959551682	0.739586534304810
53.359380	55.434300	57.509220	0.000472318096303	0.000003208059278	0.001629817890294	0.709732186933917
57.509247	59.584167	61.659087	0.000562202614083	0.000003666215203	0.001863176663819	0.782460011929683
61.577292	63.735767	65.894242	0.000574301166563	0.000004011979008	0.001936589937484	0.599843903309019
65.976015	68.536200	71.096385	0.000597414423349	0.000004547772162	0.001873983757106	0.907459807736409
71.096382	73.656567	76.216752	0.000538904096540	0.000004083671356	0.001682734796561	0.712957721862243
76.198430	79.225100	82.251770	0.000637013668828	0.000005817484522	0.002025891640957	0.829444865088693
82.172180	85.349100	88.526020	0.000655432157590	0.000006432784609	0.002135326897175	0.703871054110055
88.623908	92.153933	95.683958	0.000707887613180	0.000007913656410	0.002362714535656	0.836859449053424
95.643455	99.619500	103.595545	0.000753781876433	0.000008949714143	0.002369886863840	0.721697242872661
103.548122	107.952667	112.357212	0.000796299134129	0.000010901523442	0.002609304321424	0.683301459472318
112.358972	117.285667	122.212362	0.000729300759525	0.000011102952048	0.002372979223950	0.649945134129028
122.194172	127.832667	133.471162	0.000526259620927	0.000008681237338	0.001642196228905	0.618400417869361
133.424015	139.780000	146.135985	0.000343711669604	0.000005757108198	0.000963461026389	0.510924693779817
146.115053	153.441333	160.767613	0.000202761982003	0.000003841829871	0.000559806667730	0.373163671282455
160.717370	169.216000	177.714630	0.000088275043673	0.000001857711008	0.000235031327045	0.205257366617352
177.618932	187.562667	197.506402	0.000037330917621	0.000000898443268	0.000096440882013	0.151929307341309
197.452380	209.248000	221.043620	0.000009654872445	0.000000215947601	0.000020066868784	0.461012188255365
220.932080	235.123000	249.313920	0.000003464307863	0.000000102891920	0.000007642604661	0.970188423990928
284.480900	291.187000	297.893100	0.000001303923675	0.000000019588000	0.000001043270000	1.370580000000000
328.041600	336.585000	345.128400	0.000001022580619	0.000000038310500	0.000001576600000	2.158520000000000

Table A.III.12. Proton Yields from Helium 400 MeV/n on 60 g/cm^2 Aluminium at 27.2 deg

KE_left(MeV/n)	KE_mid(MeV/n)	KE_right(MeV/n)	Norm_Cts(#/SP*ster*MeV/n)	Y_stat(#/SP*ster*MeV/n)	Y_syst_tot(#/SP*ster*MeV/n)	X_tot(MeV/n)
45.092002	46.927867	48.763732	0.000453072350708	0.000002500663558	0.001437232190308	0.443347462950720
48.763735	50.599600	52.435465	0.000490086001855	0.000002744206852	0.001576890831339	1.175399142232544
52.435435	54.271300	56.107165	0.000517180549643	0.000002732008628	0.001570974868973	1.004202950016081
56.016472	57.963767	59.911062	0.000541147805165	0.000003278430949	0.001786753343073	0.400438677485629
60.001725	62.319300	64.636875	0.000515081937650	0.000003668627691	0.001669312300222	0.657751669561545
64.636858	66.954433	69.272008	0.000722829323355	0.000005489055244	0.002496004168126	0.996951440361064
69.163492	71.797967	74.432442	0.000601192340814	0.000005128009024	0.002056585772707	0.556388447388153
74.540958	77.340333	80.139708	0.000634929459267	0.000005578936190	0.002101147268803	0.801377626724131
80.045683	83.205333	86.364983	0.000666881022170	0.000006598039271	0.002215519052164	0.694618637360818
86.365683	89.765933	93.166183	0.000734622301384	0.000007798226640	0.002387304101136	0.705439891243046
93.249595	97.023400	100.797205	0.000793424366097	0.000009714807176	0.002712010453391	0.703683958144564
100.807052	105.055667	109.304282	0.000730458055980	0.000009448106457	0.002343969193164	0.693341359041850
109.247310	114.031000	118.814690	0.000707591761295	0.000010305645917	0.002267846263418	0.640789862779523
118.761422	124.154667	129.547912	0.000719992590407	0.000011353718033	0.002211102644406	0.591310167689513
129.522223	135.594333	141.666443	0.000831093887332	0.000015824140087	0.002728527150479	0.502729913808598
141.661275	148.640000	155.618725	0.000819749157284	0.000018326299793	0.002754564320705	0.354536332999877
155.557057	163.653667	171.750277	0.000781022057559	0.000021975114958	0.002855419182992	0.207461790203329
171.697257	181.109667	190.522077	0.000755725150233	0.000019320521118	0.002157356127671	0.093822234155023
190.436285	201.576000	212.715715	0.000747351356832	0.000023014528960	0.002194015824761	0.394980885847657
212.617528	225.937333	239.257138	0.000429874349240	0.000016382563076	0.001321589984281	0.810130083165043
239.116300	255.360000	271.603700	0.000207555231156	0.000008877738940	0.000585139897123	1.437282909975973
271.367100	291.549000	311.730900	0.000087863830848	0.000004792047356	0.000256629408892	2.365704330659264
311.376450	337.121000	362.865550	0.000032685867928	0.000002187800659	0.000094190673217	3.720641858940470
362.270900	396.230000	430.189100	0.000006471698632	0.000000715186759	0.000024499136774	5.828599712400913

Table A.III.13. Triton Yields from Helium 400 MeV/n on 60 g/cm^2 Aluminium at 12.7 deg

KE_left(MeV/n)	KE_mid(MeV/n)	KE_right(MeV/n)	Norm_Cts(#/SP*ster*MeV/n)	Y_stat(#/SP*ster*MeV/n)	Y_syst_tot(#/SP*ster*MeV/n)	X_tot(MeV/n)
45.912716	47.166367	48.420017	0.000059284692440	0.000000191854547	0.000162115814509	23.024421250375024
48.420016	49.673667	50.927317	0.000066923677429	0.000000204886383	0.000172969378723	0.321840708736480
50.853693	52.341067	53.828440	0.000061906814424	0.000000146307946	0.000103229889387	0.365454480789332
53.902077	55.496667	57.091257	0.000087547252110	0.000000399070409	0.000264211971478	0.465960805670391
57.091243	58.685833	60.280423	0.000069976266342	0.000000275340963	0.000182735790614	0.295107204908725
60.238895	62.132400	64.025905	0.000081039167084	0.000000380396390	0.000211443046821	0.349762618194112
64.067418	66.002433	67.937448	0.000083573199079	0.000000368682135	0.000201471482779	0.387846377543996
67.870505	70.060800	72.251095	0.000092920682102	0.000000485683625	0.000232415109912	0.199615724843661
72.303050	74.595200	76.887350	0.000054769665599	0.000000279182831	0.000129023360829	0.312338962982270
76.902337	79.524667	82.146997	0.000037731016456	0.000000148263275	0.000060362605826	0.197028500298840
82.146990	83.021100	83.895210	0.000026715584960	0.000000098791700	0.000039738800000	0.116609000000000

Table A.III.14. Triton Yields from Helium 400 MeV/n on 60 g/cm^2 Aluminium at 10.0 deg

KE_left(MeV/n)	KE_mid(MeV/n)	KE_right(MeV/n)	Norm_Cts(#/SP*ster*MeV/n)	Y_stat(#/SP*ster*MeV/n)	Y_syst_tot(#/SP*ster*MeV/n)	X_tot(MeV/n)
44.157519	45.439333	46.721148	0.000071379340259	0.000000293047714	0.000241363991633	39.057402857973031
46.721152	48.002967	49.284781	0.000094982563772	0.000000320277883	0.000264243566815	0.418116948392432
49.284752	50.566567	51.848381	0.000073239211043	0.000000299145547	0.000246301648966	0.370061833931844
51.783042	53.322100	54.861158	0.000061966404312	0.000000170656627	0.000121345666565	0.353123761038534
54.926500	56.548300	58.170100	0.000049138285897	0.000000198857473	0.000129866773420	0.422193350896245
58.162230	59.791900	61.421570	0.000040677750348	0.000000149217413	0.000097532512420	0.235928049893797
61.429480	62.737200	64.044920	0.000034994772159	0.000000155148728	0.000083564342365	0.294658822920679

Table A.III.15. Triton Yields from Helium 400 MeV/n on 60 g/cm^2 Aluminium at 7.20 deg

KE_left(MeV/n)	KE_mid(MeV/n)	KE_right(MeV/n)	Norm_Cts(#/SP*ster*MeV/n)	Y_stat(#/SP*ster*MeV/n)	Y_syst_tot(#/SP*ster*MeV/n)	X_tot(MeV/n)
44.950644	46.254300	47.557956	0.000065788509469	0.000000262414724	0.000213039205954	32.131973040478485
47.557944	48.861600	50.165256	0.000086243686120	0.000000216265191	0.000176607401424	0.409022237749979
50.165244	51.468900	52.772556	0.000129237792916	0.000000468026719	0.000379260656175	0.418754668273680
52.735805	54.342000	55.948195	0.000085852587639	0.000000324848407	0.000213430501543	0.319823062614315

Table A.III.16. Helium-4 Yields from Helium 400 MeV/n on 60 g/cm^2 Aluminium at 12.7 deg

KE_left(MeV/n)	KE_mid(MeV/n)	KE_right(MeV/n)	Norm_Cts(#/SP*ster*MeV/n)	Y_stat(#/SP*ster*MeV/n)	Y_syst_tot(#/SP*ster*MeV/n)	X_tot(MeV/n)
45.619006	47.117800	48.616594	0.000068012453116	0.000000258254299	0.000182939678141	0.450868809300444
48.537232	50.410567	52.283902	0.000073796139532	0.000000400404919	0.000234787713397	0.262454875675591
52.363302	54.321567	56.279832	0.000079663452438	0.000000484843861	0.000261553180531	0.811928572679888
56.279835	58.238100	60.196365	0.000072234134589	0.000000378470555	0.000204645372980	1.013719689079284
60.071662	62.276767	64.481872	0.000078182928717	0.000000464246765	0.000220190149763	0.451957945296905
64.606593	67.030533	69.454473	0.000091183578462	0.000000619967931	0.000270521887227	0.728880616206797
69.369108	71.893633	74.418158	0.000138045067547	0.000000996680908	0.000415474266962	0.747378858168332
74.503500	77.393700	80.283900	0.000185241047012	0.000001637874707	0.000598439641101	0.693802684090369
80.161145	83.263900	86.366655	0.000227934217139	0.000001688124207	0.000586686468324	0.682200426235575
86.466738	89.846733	93.226728	0.000201430884820	0.000002019871303	0.000632356978286	0.668750619837470
93.249380	97.075700	100.902020	0.000171915924622	0.000001867286808	0.000515748522376	0.722711875282259
100.848035	105.092000	109.335965	0.000227502953047	0.000002564377645	0.000634133691850	0.654241151085745
109.318890	114.068000	118.817110	0.000271384219687	0.000003430245403	0.000757190107903	0.593105418525240
118.785835	124.184000	129.582165	0.000283931210020	0.000003781799553	0.000741829218568	0.562104415312671
129.548843	135.619333	141.689823	0.000275303687949	0.000004361244529	0.000758073984124	0.486263506281317
141.678652	148.658667	155.638682	0.000292564043692	0.000004968963258	0.000754585898994	0.356194096293018
155.574207	163.665667	171.757127	0.000354427187276	0.000006745611974	0.000872431320540	0.205911806882194
171.691935	181.109000	190.526065	0.000214102212367	0.000005038965835	0.000580731737635	0.087421676639264
190.629595	197.837500	205.045405	0.000028508966227	0.000000650777667	0.000065392153366	0.247258771237746

Table A.III.17. Helium-4 Yields from Helium 400 MeV/n on 60 g/cm^2 Aluminium at 10.0 deg

KE_left(MeV/n)	KE_mid(MeV/n)	KE_right(MeV/n)	Norm_Cts(#/SP*ster*MeV/n)	Y_stat(#/SP*ster*MeV/n)	Y_syst_tot(#/SP*ster*MeV/n)	X_tot(MeV/n)
45.702835	47.278300	48.853765	0.000129427038549	0.000002541756895	0.001705935305528	0.699111727103043
48.779635	50.429200	52.078765	0.000153921095571	0.000002689371449	0.001722648083981	0.282711003835748
52.152888	54.189033	56.225178	0.000177692443573	0.000001943069866	0.001010961751637	0.612743165048783
56.225188	58.261333	60.297478	0.000201825146085	0.000001244738661	0.000646801123293	1.048086449905255
60.254238	62.333633	64.413028	0.000208294131392	0.000001144434203	0.000579468665267	0.577636038075015
64.456273	66.957133	69.457993	0.000209741437136	0.000001535127403	0.000648906178603	0.616762021574772
69.458007	71.958867	74.459727	0.000298777795778	0.000002023511815	0.000856014478338	0.855722747774652
74.411122	77.328667	80.246212	0.000305560609297	0.000002368231586	0.000858792420585	0.590864498066181
80.210852	83.273367	86.335882	0.000403500116133	0.000003385823120	0.001183699990372	0.703155581341000
86.419823	89.852333	93.284843	0.000372090580953	0.000003878969097	0.001193180030910	0.673629543759773
93.213653	97.043333	100.873013	0.000410731710595	0.000004393571888	0.001213030836298	0.667899351181748
100.848140	105.088000	109.327860	0.000477607024563	0.000005601556248	0.001402298016821	0.641939600683740
109.332788	114.065333	118.797878	0.000525623746014	0.000007032306703	0.001568828880837	0.587775659616830
118.768965	124.155000	129.541035	0.000640168190000	0.000009929885331	0.001939078252521	0.517147866429902
129.532978	135.608333	141.683688	0.000672711365761	0.000011656480703	0.002019794476228	0.467332582084750
141.666140	148.654000	155.641860	0.000825390771526	0.000015525278871	0.002343764978448	0.343717715814882
155.570863	163.651333	171.731803	0.000893786501591	0.000019371377615	0.002520184799752	0.176333545921359
171.695088	181.110333	190.525578	0.001111499983589	0.000025468293905	0.002843892650312	0.091284481050231
190.435332	201.576667	212.718002	0.000565170408001	0.000015823058861	0.001553443879304	0.380280571136628
213.011085	217.169000	221.326915	0.000059017642294	0.000000777834000	0.000066120200000	0.345440000000000

Table A.III.18. Helium-4 Yields from Helium 400 MeV/n on 60 g/cm^2 Aluminium at 7.20 deg

KE_left(MeV/n)	KE_mid(MeV/n)	KE_right(MeV/n)	Norm_Cts(#/SP*ster*MeV/n)	Y_stat(#/SP*ster*MeV/n)	Y_syst_tot(#/SP*ster*MeV/n)	X_tot(MeV/n)
45.682937	47.318567	48.954197	0.000337630035733	0.000003645179510	0.002355583373137	0.762043754177541
48.954170	50.589800	52.225430	0.000355960675983	0.000002807203582	0.001813835748542	0.515856050226223
52.125990	54.077900	56.029810	0.000308386967168	0.000001919555162	0.001051999249060	0.425229063693911
56.129293	58.225933	60.322573	0.000290587497877	0.000001627548657	0.000821965458282	0.986037767583981
60.322560	62.419200	64.515840	0.000449528993172	0.000002823571152	0.001422734597523	0.702393770875710
64.428763	66.882733	69.336703	0.000439325962715	0.000003211388629	0.001381272400461	0.497228082250993
69.423807	71.984367	74.544927	0.000611286170502	0.000004537133427	0.001872693093756	0.896195756381941
74.440120	77.305700	80.171280	0.000567071673798	0.000004872314172	0.001790920984298	0.544375167285393
80.266727	83.301167	86.335607	0.000800650345575	0.000007182709525	0.002497731685630	0.750159103082140
86.344962	89.835867	93.326772	0.000760563853454	0.000008332804045	0.002518587815543	0.646576469168961
93.227460	97.044400	100.861340	0.001015852419131	0.000011522710452	0.003183747124208	0.667568055866216
100.844685	105.083000	109.321315	0.001237956390581	0.000015266303932	0.003794178134076	0.630190738629187
109.329730	114.069000	118.808270	0.001498087587754	0.000021391653765	0.004728512811614	0.590980332512851
118.780900	124.141000	129.501100	0.001925595413073	0.000029700599578	0.005830588239938	0.494107197740531
129.504330	135.602000	141.699670	0.002182858128253	0.000038401837171	0.006619353401202	0.456451697166305
141.663597	148.648667	155.633737	0.002917868786759	0.000057496606083	0.008664707381216	0.332625324849146
155.585297	163.650667	171.716037	0.003839598450298	0.000085206596135	0.011057622874719	0.167278615862518
171.696503	181.111333	190.526163	0.002857759207629	0.000068939904159	0.007952245989939	0.093358452921254
190.430515	201.582000	212.733485	0.000286564880448	0.000009724870160	0.000973191680757	0.370163437250358

Table A.III.19. Helium-3 Yields from Helium 400 MeV/n on 60 g/cm^2 Aluminium at 12.7 deg

KE_left(MeV/n)	KE_mid(MeV/n)	KE_right(MeV/n)	Norm_Cts(#/SP*ster*MeV/n)	Y_stat(#/SP*ster*MeV/n)	Y_syst_tot(#/SP*ster*MeV/n)	X_tot(MeV/n)
66.666913	69.284233	71.901553	0.000011805880227	0.000000133696678	0.000053916016674	0.940081513468912
71.774447	74.679967	77.585487	0.000025855916626	0.000000126770565	0.000045819556978	0.743853440955945
77.712580	79.792250	81.871920	0.000011393974888	0.000000101661281	0.000034398910679	0.691679848491338
83.863573	87.391233	90.918893	0.000020103775116	0.000000172741920	0.000051818609871	0.819181863206211
90.881418	94.712833	98.544248	0.000018101369074	0.000000155688271	0.000043740017393	0.822039906090939
98.569013	102.831333	107.093653	0.000013773081256	0.000000134037066	0.000032367564128	0.798682421821089
107.088253	111.875333	116.662413	0.000022152025035	0.000000293457278	0.000062359072595	0.835533978723187
116.632975	122.018000	127.403025	0.000029222964602	0.000000360899806	0.000072132624360	0.799512409018146
127.392762	133.475667	139.558572	0.000032362298323	0.000000485623755	0.000084043535060	0.758012036643218
139.557497	146.531667	153.505837	0.000034085798443	0.000000502541132	0.000076267541915	0.651371617302289
153.454373	161.520333	169.586293	0.000047447203348	0.000000824180162	0.000106992106902	0.557962770422006
169.545378	178.934333	188.323288	0.000058325325901	0.000001080472327	0.000122935717616	0.448836797307217
188.246638	199.322333	210.398028	0.000088800756223	0.000002310948109	0.000218718835334	0.218557833026959
210.278695	223.530000	236.781305	0.000060201529785	0.000001585028246	0.000131934003181	0.164908829765298
236.945000	247.312000	257.679000	0.000003423256247	0.000000064987116	0.000004604604549	0.426353324411808

Table A.III.20. Helium-3 Yields from Helium 400 MeV/n on 60 g/cm^2 Aluminium at 10.0 deg

KE_left(MeV/n)	KE_mid(MeV/n)	KE_right(MeV/n)	Norm_Cts(#/SP*ster*MeV/n)	Y_stat(#/SP*ster*MeV/n)	Y_syst_tot(#/SP*ster*MeV/n)	X_tot(MeV/n)
64.725860	65.631900	66.537940	0.000004037146302	0.000000018722400	0.000007279590000	0.253758000000000
68.349980	71.068100	73.786220	0.000021622797531	0.000000180039659	0.000069972139186	1.010936377417491
73.649633	76.626733	79.603833	0.000021386890183	0.000000167996576	0.000059976725569	0.655369136092020
79.740385	82.960000	86.179615	0.000019564065565	0.000000145768601	0.000048063673829	0.897498689285951
86.099683	89.742833	93.385983	0.000020535056163	0.000000186388706	0.000055376618390	0.754924140746605
93.325538	97.302033	101.278528	0.000019123021499	0.000000170453824	0.000046198486729	0.800018536420876
101.295938	105.724333	110.152728	0.000021620560834	0.000000183683021	0.000045229250997	0.817764895168532
110.141717	115.110667	120.079617	0.000022285972819	0.000000222568398	0.000048524132314	0.793100408597802
120.094630	125.674000	131.253370	0.000036831858237	0.000000510381951	0.000096060910483	0.770459587151721
131.225203	137.628333	144.031463	0.000037882339111	0.000000550495435	0.000090165015039	0.694997395022456
143.974067	151.285667	158.597267	0.000046129161434	0.000000787878730	0.000113844710091	0.626857050143013
158.577397	167.031667	175.485937	0.000061818314285	0.000001223965258	0.000154664733669	0.515427382925083
175.423512	185.334667	195.245822	0.000078686740513	0.000001856287986	0.000194963580314	0.325319640921049
195.170802	206.905667	218.640532	0.000112513230343	0.000002655956614	0.000234962611724	0.120200255481800
218.513917	232.623667	246.733417	0.000169698236880	0.000005427590369	0.000406546075849	0.321615606839904
246.581600	263.856000	281.130400	0.000082036859123	0.000003486897974	0.000226645580171	0.816176855945450
281.646900	288.291000	294.935100	0.000000744845237	0.000000018722400	0.000000992694000	0.727759000000000

Table A.III.21. Helium-3 Yields from Helium 400 MeV/n on 60 g/cm^2 Aluminium at 7.20 deg

KE_left(MeV/n)	KE_mid(MeV/n)	KE_right(MeV/n)	Norm_Cts(#/SP*ster*MeV/n)	Y_stat(#/SP*ster*MeV/n)	Y_syst_tot(#/SP*ster*MeV/n)	X_tot(MeV/n)
50.182450	52.110700	54.038950	0.000009987801626	0.000000061565824	0.000031412333722	0.447968085768395
55.663180	57.195600	58.728020	0.000037729107874	0.000000173204962	0.000080069157285	0.889570408098201
58.728070	61.026700	63.325330	0.000028666259860	0.000000185277435	0.000085286304751	0.911491760182724
63.216773	65.675133	68.133493	0.000036316559075	0.000000286866811	0.000128508094134	0.526110269752454
68.242065	71.038500	73.834935	0.000020511625941	0.000000166713726	0.000063076095089	0.966340305175149
73.741277	76.651667	79.562057	0.000058187825085	0.000000519874931	0.000193123889208	0.709770160220194
79.655673	82.953033	86.250393	0.000037261058547	0.000000231631709	0.000075064024325	0.891506142241320
86.130203	89.737533	93.344863	0.000054570926234	0.000000568851313	0.000170250840560	0.745558266681418
93.355143	97.316733	101.278323	0.000066633267848	0.000000657249507	0.000172299015972	0.827397557419648
101.290810	105.719000	110.147190	0.000058907037771	0.000000742728912	0.000180457749484	0.804664876365932
110.132405	115.112000	120.091595	0.000068051715359	0.000000823650998	0.000177611896585	0.790416244363690
120.065988	125.664333	131.262678	0.000104218211071	0.000001498445167	0.000281304302459	0.757501866105952
131.218255	137.602000	143.985745	0.000116321143119	0.000001825942656	0.000301866438739	0.653107570206471
143.968397	151.278667	158.588937	0.000169303540877	0.000003154334791	0.000448566729874	0.616465612611928
158.563488	167.029333	175.495178	0.000208442450230	0.000004327838788	0.000539040646179	0.511413416982777
175.403718	185.311333	195.218948	0.000364087186404	0.000009485809372	0.000991677150285	0.286407429537015
195.169165	206.896000	218.622835	0.000263788814167	0.000007876213233	0.000737971081715	0.099242050450603
218.786280	227.882000	236.977720	0.000010535750090	0.000000277486334	0.000022207076794	0.184438906022591

Table A.IV.1. Deuteron Yields from Iron 400 MeV/n on 20 g/cm^2 Aluminium at 12.7 deg

KE_left(MeV/n)	KE_mid(MeV/n)	KE_right(MeV/n)	Norm_Cts(#/SP*ster*MeV/n)	Y_stat(#/SP*ster*MeV/n)	Y_syst_tot(#/SP*ster*MeV/n)	X_tot(MeV/n)
45.844164	47.246233	48.648303	0.001429730231293	0.000000259048796	0.000202494723077	0.143113046878403
48.693916	50.142367	51.590818	0.001552386820533	0.000000278791451	0.000211335777097	0.330177799735234
51.569303	53.039267	54.509231	0.001752212559908	0.000000296478613	0.000222975329328	0.130974603719996
54.530762	56.256167	57.981572	0.001737439406933	0.000000328488605	0.000211462029469	0.106247790085347
57.981562	59.706967	61.432372	0.001871265062347	0.000000335806888	0.000216935060592	0.224136518180349
61.412190	63.400100	65.388010	0.002009564024780	0.000000362296338	0.000205774489075	0.089363605252250
65.358832	67.418667	69.478502	0.001955362457275	0.000000368036629	0.000201474195859	0.144215310491393
69.527835	71.824500	74.121165	0.002017790540407	0.000000394187429	0.000195425802559	0.115665823225964
74.060212	76.567167	79.074122	0.001988492177787	0.000000404199000	0.000185674350059	0.108180049869234
79.055737	81.784967	84.514197	0.002303438887961	0.000000456882648	0.000194527492365	0.092401210235527
84.522162	87.526667	90.531172	0.002321486810796	0.000000475018326	0.000185080089445	0.081783910660044
90.526080	93.851600	97.177120	0.002860916008354	0.000000549654062	0.000200279373960	0.100804574935161
97.167972	100.855167	104.542362	0.002782801459705	0.000000607039155	0.000202672411428	0.075376118288620
104.547758	108.650333	112.752908	0.002517808802655	0.000000612556296	0.000187988632194	0.030726603599513
112.748772	117.389667	122.030562	0.002189498535777	0.000000547846434	0.000143461352395	0.021161088745452
121.983073	127.207333	132.431593	0.001656227375799	0.000000498802297	0.000113854917841	0.032800315404644
132.416792	138.351667	144.286542	0.001037559398153	0.000000436147615	0.000084946288613	0.051035682287886
144.259020	151.051000	157.842980	0.000834789504389	0.000000543341831	0.000095813877519	0.116818592098689
157.837525	165.693000	173.548475	0.000589035788609	0.000000417898308	0.000062907674407	0.124559624063097
173.481120	182.671000	191.860880	0.000158474676135	0.000000195718915	0.000023841560844	0.202909476704786
191.769282	202.601667	213.434052	0.000032802160531	0.000000091899106	0.000009103240731	0.320279085058641
213.339760	226.304000	239.268240	0.000028060197849	0.000000095256959	0.000007734426113	0.426168666788163
239.131922	254.901667	270.671412	0.000019719427989	0.000000084925757	0.000005715382223	0.568004917550016
270.458300	290.022000	309.585700	0.000014337598817	0.000000081455198	0.000004450980590	0.804505150883448
309.257000	334.151000	359.045000	0.000010419731874	0.000000069726306	0.000003006173891	1.134334969266574
358.479583	391.199333	423.919083	0.000003619549641	0.000000055383888	0.000001872373498	1.625701778569797

Table A.IV.2. Deuteron Yields from Iron 400 MeV/n on 20 g/cm^2 Aluminium at 10.0 deg

KE_left(MeV/n)	KE_mid(MeV/n)	KE_right(MeV/n)	Norm_Cts(#/SP*ster*MeV/n)	Y_stat(#/SP*ster*MeV/n)	Y_syst_tot(#/SP*ster*MeV/n)	X_tot(MeV/n)
44.343166	45.538567	46.733968	0.001547529893875	0.000000261873108	0.000239789737456	0.107609504650839
46.721542	48.175500	49.629458	0.001700256799998	0.000000310175849	0.000236612963003	0.152458011605065
49.641890	51.108300	52.574711	0.001852114128325	0.000000340904262	0.000259501656920	0.314465361763422
52.520145	54.057967	55.595789	0.002006763564002	0.000000383875010	0.000283960272258	0.067559729223647
55.650355	57.393400	59.136445	0.002156698362775	0.000000364422165	0.000236054561587	0.154316134969549
59.095755	60.879500	62.663245	0.002407842754228	0.000000387589939	0.000246579657419	0.203812685611102
62.703965	64.729400	66.754835	0.002302913202443	0.000000396414778	0.000222847439496	0.136549823472057
66.682508	68.828633	70.974758	0.002543883341138	0.000000427279008	0.000230736870998	0.114388194335124
71.047045	73.360900	75.674755	0.002534626845227	0.000000441452045	0.000221781907042	0.112139344765073
75.665617	78.265067	80.864517	0.002703644377388	0.000000484384402	0.000219122175311	0.100176950826625
80.812620	83.639700	86.466780	0.002841133616738	0.000000510264501	0.000214176384508	0.098785843505130
86.456708	89.563733	92.670758	0.003041385608892	0.000000551817364	0.000214608296790	0.096668492549744
92.673460	96.105700	99.537940	0.002889515553100	0.000000573378360	0.000203168461571	0.069103184610245
99.534687	103.349667	107.164647	0.003374732335321	0.000000735820225	0.000252006311171	0.058290175109533
107.159668	111.460333	115.760998	0.003648012556539	0.000000710746674	0.000213085598021	0.035782752616392
115.724358	120.528333	125.332308	0.004331740182139	0.000000790373571	0.000220807070281	0.032364352567910
125.329777	130.772667	136.215557	0.005099605779480	0.000000917588329	0.000240560957111	0.038472248278857
136.179427	142.396667	148.613907	0.004181003873554	0.000000895965009	0.000203902561259	0.068381959556377
148.599440	155.715000	162.830560	0.003069123990634	0.000000817105538	0.000157816568190	0.098677961952049
162.804447	171.076667	179.348887	0.002590945806178	0.000000809157684	0.000133260213699	0.121200138780572
179.264635	188.961000	198.657365	0.001859421370156	0.000000739503158	0.000103089193947	0.226306261962766
198.584007	210.060667	221.537327	0.001349954015712	0.000000684355004	0.000075870239497	0.312552758010548
221.426545	235.252000	249.077455	0.001088853158349	0.000000672692983	0.000064182705404	0.418524379363974
248.913450	265.820000	282.726550	0.000322667020176	0.000000402692719	0.000027624518920	0.572145541710324
282.481067	303.627667	324.774267	0.000162489786713	0.000000314213924	0.000016690805549	0.809951846042714
324.374583	351.548333	378.722083	0.000066754896728	0.000000220644407	0.000008974471469	1.150786074839716

Table A.IV.3. Deuteron Yields from Iron 400 MeV/n on 20 g/cm^2 Aluminium at 7.20 deg

KE_left(MeV/n)	KE_mid(MeV/n)	KE_right(MeV/n)	Norm_Cts(#/SP*ster*MeV/n)	Y_stat(#/SP*ster*MeV/n)	Y_syst_tot(#/SP*ster*MeV/n)	X_tot(MeV/n)
45.883771	47.228700	48.573630	0.002236459091313	0.000000322355283	0.000267675185690	0.120359031286864
48.647216	50.122600	51.597983	0.002367768066100	0.000000354563394	0.000271747109782	0.300344228554504
51.597983	53.073367	54.548750	0.002502082309000	0.000000383877149	0.000295720582315	0.153338423727812
54.507098	56.217333	57.927568	0.002637486363521	0.000000389199752	0.000258742503692	0.084061207015186
57.969235	59.721100	61.472965	0.002775501505890	0.000000399275781	0.000260829043009	0.244488165498864
61.418273	63.382533	65.346793	0.002499532096232	0.000000403314818	0.000236115618444	0.069001227214385
65.390400	67.435600	69.480800	0.002898281973728	0.000000451047993	0.000255680689574	0.161978578275802
69.491850	71.814300	74.136750	0.002776066982957	0.000000467616483	0.000235550593092	0.100644302994804
74.064460	76.562900	79.061340	0.003016868083422	0.000000512356405	0.000243373318155	0.098200565137783
79.064040	81.789500	84.514960	0.003396456345564	0.000000542644716	0.000240207372988	0.091999774445593
84.521653	87.526033	90.530413	0.003518637978259	0.000000583285106	0.000238429259190	0.078508164480263
90.524320	93.852600	97.180880	0.003465854202370	0.000000608736435	0.000227594093392	0.095342958453889
97.163777	100.856067	104.548357	0.003905945164490	0.000000742968173	0.000265343865105	0.077232756974356
104.564640	108.658000	112.751360	0.004530058650799	0.000000801259638	0.000264539723991	0.041400472692350
112.741632	117.392667	122.043702	0.004953362006695	0.000000828969927	0.000245099204366	0.033887326495599
121.991183	127.214333	132.437483	0.006793145234742	0.000001039047749	0.000300620217958	0.027574149748531
132.422728	138.360333	144.297938	0.006841420226177	0.000001426395922	0.000459801371937	0.034819145034449
144.276233	151.065333	157.854433	0.006730035764254	0.000001707784121	0.000557134065561	0.092150748002716
157.844615	165.708000	173.571385	0.006448838909934	0.000001257752093	0.000270358913500	0.098439356731391
173.502843	182.693333	191.883823	0.002810834090645	0.000000891755603	0.000138935523177	0.163660139242059
191.790845	202.628000	213.465155	0.002018257055603	0.000000818114497	0.000102263295168	0.273866161080554
213.372230	226.342000	239.311770	0.001915680180445	0.000000870377732	0.000099033806969	0.359640596910304
239.174637	254.952667	270.730697	0.000470503725163	0.000000462067737	0.000035349862377	0.480181054862642
270.518600	290.093000	309.667400	0.000188249285542	0.000000323620746	0.000018895441834	0.681759275821019
309.337417	334.249667	359.161917	0.000058046203145	0.000000196651056	0.000008708212779	0.962766768580532
358.595083	391.341333	424.087583	0.000019520435260	0.000000120856842	0.000004089894004	1.378615161357222

Table A.IV.4. Deuteron Yields from Iron 400 MeV/n on 20 g/cm^2 Aluminium at 32.7 deg

KE_left(MeV/n)	KE_mid(MeV/n)	KE_right(MeV/n)	Norm_Cts(#/SP*ster*MeV/n)	Y_stat(#/SP*ster*MeV/n)	Y_syst_tot(#/SP*ster*MeV/n)	X_tot(MeV/n)
44.999103	46.291667	47.584230	0.000390964543246	0.000000123529524	0.000101921492981	0.114128298363114
47.653292	49.115900	50.578508	0.000346053744213	0.000000117639176	0.000085311950009	0.283421770360006
50.578492	52.041100	53.503708	0.000361782214013	0.000000135888758	0.000098313860136	0.176324876923394
53.431549	55.061400	56.691251	0.000359843497134	0.000000131132430	0.000085819470854	0.123401050702091
56.763427	58.513867	60.264307	0.000352274017893	0.000000143719841	0.000087036804591	0.288496172234572
60.192618	62.060433	63.928248	0.000400336965295	0.000000156004360	0.000089770171379	0.094645840628275
63.999958	66.043333	68.086708	0.000417042781951	0.000000163301632	0.000084997623961	0.283363257544093
68.017445	70.251000	72.484555	0.000349970348850	0.000000149913233	0.000070959197214	0.115664313059171
72.503357	74.895667	77.287977	0.000393817523765	0.000000173526880	0.000077589588823	0.185954792674160
77.338442	79.984667	82.630892	0.000368700975316	0.000000165972548	0.000066889457136	0.184615814211134
82.602795	85.531500	88.460205	0.000355024362877	0.000000162951360	0.000059395329848	0.132091110314586
88.433858	91.649933	94.866008	0.000337228933715	0.000000171965538	0.000057400134340	0.126616754076544
94.873997	98.424767	101.975537	0.000342770452897	0.000000183243510	0.000055187469919	0.105255695397921
101.958850	105.963000	109.967150	0.000373955573171	0.000000199138366	0.000053473985277	0.103642187720493
109.938097	114.384667	118.831237	0.000382437107502	0.000000215988939	0.000052104685401	0.101281097926958
118.808913	123.839333	128.869753	0.000317459951361	0.000000203502831	0.000043459570334	0.048488478045923
128.841107	134.535667	140.230227	0.000419418000810	0.000000288312529	0.000054817033635	0.020255987176902
140.216378	146.713333	153.210288	0.000485540133204	0.000000536949753	0.000096742653372	0.028668138699303
153.173037	160.683667	168.194297	0.000471134767362	0.000000379098942	0.000057526548325	0.091881111918446
168.140160	176.860000	185.579840	0.000355555122335	0.000000301454800	0.000038051278275	0.156299686774126
185.522883	195.791333	206.059783	0.000174376606808	0.000000215449134	0.000022653393102	0.254626599415693
205.972337	218.199667	230.426997	0.000187035619919	0.000000254697175	0.000023013825278	0.365170137585208
230.297290	245.086000	259.874710	0.000036122662322	0.000000109250970	0.000008102536986	0.540615086991660
271.345250	283.936500	296.527750	0.000003588638622	0.000000031412541	0.000001750227621	0.638196980582014
295.884650	318.891000	341.897350	0.000002901011958	0.000000038071341	0.000001796768167	1.065553241806809
351.648650	371.628500	391.608350	0.000001113902140	0.000000026870295	0.000000984219748	1.254781338366968

Table A.IV.5. Deuteron Yields from Iron 400 MeV/n on 20 g/cm^2 Aluminium at 30.0 deg

KE_left(MeV/n)	KE_mid(MeV/n)	KE_right(MeV/n)	Norm_Cts(#/SP*ster*MeV/n)	Y_stat(#/SP*ster*MeV/n)	Y_syst_tot(#/SP*ster*MeV/n)	X_tot(MeV/n)
45.143253	46.377867	47.612481	0.000528749189867	0.000000145376265	0.000124950335651	0.247819148545870
47.561825	49.020300	50.478775	0.000412513550079	0.000000129292014	0.000094605988086	0.128619600349713
50.529430	52.045900	53.562370	0.000373779408533	0.000000133983765	0.000093630676280	0.176515601763697
53.522457	55.078867	56.635277	0.000427872643485	0.000000142423135	0.000096903543467	0.139857133307172
56.675203	58.478533	60.281863	0.000376424339720	0.000000150021195	0.000088313698252	0.225314061782659
60.264180	62.085200	63.906220	0.000486827855545	0.000000165972758	0.000096909448895	0.138292631509501
63.923900	66.019400	68.114900	0.000475853395197	0.000000178168056	0.000090633052271	0.247255266478512
68.045510	70.249900	72.454290	0.000472995556637	0.000000184524884	0.000089449182081	0.106679443021699
72.523712	74.917067	77.310422	0.000522615844868	0.000000199077554	0.000089002191272	0.205783503830142
77.293093	79.973033	82.652973	0.000456704414197	0.000000190034765	0.000075968232225	0.185190009137453
82.607222	85.528767	88.450312	0.000479822861909	0.000000201748144	0.000074211365992	0.126656570023509
88.442283	91.658533	94.874783	0.000465744760418	0.000000211202071	0.000070562833021	0.137373958603150
94.879893	98.436633	101.993373	0.000451107992957	0.000000212184573	0.000063911863455	0.124953991537165
101.978237	105.957667	109.937097	0.000506468922973	0.000000233810238	0.000063331118614	0.092488310721193
109.929858	114.394333	118.858808	0.000454101862190	0.000000238553128	0.000057799332125	0.110542407745354
118.818525	123.843000	128.867475	0.000393701474519	0.000000233390824	0.000049995969240	0.060103555281614
128.852078	134.549333	140.246588	0.000293663204388	0.000000217402206	0.000041474692412	0.041385175958911
140.232873	146.739333	153.245793	0.000127889558084	0.000000147967118	0.000024279385244	0.029753258141346
153.190315	160.700000	168.209685	0.000068285849416	0.000000101377231	0.000014344029412	0.063664962855090
168.159740	176.888000	185.616260	0.000025488536280	0.000000066849904	0.000008027617185	0.107932509574317
185.571623	195.845333	206.119043	0.000008680660894	0.000000048676282	0.000005052311478	0.159605695504296
213.891030	222.302500	230.713970	0.000007010257671	0.000000037754619	0.000003148532046	0.208831379787617
230.655615	240.195000	249.734385	0.000002281028250	0.000000021509926	0.000001580257922	0.288388316984236
326.286750	334.601000	342.915250	0.000000935591550	0.000000016187500	0.000000680932000	0.489654000000000

Table A.IV.6. Deuteron Yields from Iron 400 MeV/n on 20 g/cm^2 Aluminium at 27.2 deg

KE_left(MeV/n)	KE_mid(MeV/n)	KE_right(MeV/n)	Norm_Cts(#/SP*ster*MeV/n)	Y_stat(#/SP*ster*MeV/n)	Y_syst_tot(#/SP*ster*MeV/n)	X_tot(MeV/n)
45.992913	47.268633	48.544353	0.000580771478747	0.000000152477058	0.000127173033164	0.297184973457609
48.484717	49.956200	51.427683	0.000562844551226	0.000000163939287	0.000120917881816	0.045971453838877
51.487307	53.044067	54.600827	0.000633969004520	0.000000177571779	0.000121780395547	0.155896332500960
54.556962	56.157567	57.758172	0.000556532924264	0.000000163301632	0.000109876629407	0.170733852917575
57.802018	59.644933	61.487848	0.000499788723698	0.000000173012472	0.000100043346249	0.167699794759445
61.445470	63.330800	65.216130	0.000632667555974	0.000000181138032	0.000102953956234	0.093485159068432
65.258518	67.393033	69.527548	0.000583187710380	0.000000188182124	0.000094514288142	0.201778781095164
69.445067	71.727967	74.010867	0.000594974890045	0.000000195477879	0.000093024641363	0.106852614375582
74.059625	76.525300	78.990975	0.000629692687009	0.000000226170029	0.000098470689496	0.158134858921425
79.024743	81.760233	84.495723	0.000647285585661	0.000000231695098	0.000091215029215	0.167716379358249
84.470068	87.489833	90.509598	0.000522169882121	0.000000209274501	0.000074396067838	0.124925558372136
90.495253	93.817133	97.139013	0.000660764408219	0.000000262043746	0.000085341353850	0.105847373809131
97.121978	100.831233	104.540488	0.000723127851947	0.000000275541933	0.000080993188702	0.074431604614505
104.518100	108.660000	112.801900	0.000638980372488	0.000000280253194	0.000073795298329	0.074790493983794
112.781263	117.400333	122.019403	0.000651359633059	0.000000283861215	0.000067200253593	0.055354280250944
122.020687	127.248667	132.476647	0.000775234903995	0.000000431596666	0.000093786974708	0.042395032377037
132.453700	138.409000	144.364300	0.000789544629512	0.000000667707660	0.000138150070028	0.041635063107314
144.321235	151.157000	157.992765	0.000756140118771	0.000000427361896	0.000071563822417	0.060978696932052
157.923617	165.807667	173.691717	0.000741509376068	0.000000413589189	0.000058853386817	0.106053824224353
173.653322	182.852667	192.052012	0.000471550337782	0.000000344655588	0.000041974336141	0.148514195386333
192.003957	202.874667	213.745377	0.000369927580488	0.000000340926865	0.000034882311361	0.216534689859246
213.642628	226.665333	239.688038	0.000057351381356	0.000000135889172	0.000011276778176	0.307585340531697
239.545925	255.390000	271.234075	0.000012422883847	0.000000068469699	0.000004754280092	0.421269271562738
271.014817	290.699667	310.384517	0.000004486863039	0.000000048704013	0.000002668125703	0.585386158635477
310.035283	335.089333	360.143383	0.000002321766086	0.000000034029974	0.000001460774557	0.828948419233067

Table A.IV.7. Proton Yields from Iron 400 MeV/n on 20 g/cm^2 Aluminium at 12.7 deg

KE_left(MeV/n)	KE_mid(MeV/n)	KE_right(MeV/n)	Norm_Cts(#/SP*ster*MeV/n)	Y_stat(#/SP*ster*MeV/n)	Y_syst_tot(#/SP*ster*MeV/n)	X_tot(MeV/n)
45.462687	47.139267	48.815847	0.002503177879533	0.000000400532130	0.000272238125016	0.295685340947095
48.815820	50.492400	52.168980	0.002921778338433	0.000000435753062	0.000299609997462	0.209018647219070
52.093883	53.974533	55.855183	0.002652085495306	0.000000435829222	0.000270793644765	0.160303232242449
55.930300	57.928900	59.927500	0.002976037873767	0.000000482860686	0.000283198454590	0.350396098320172
59.849155	61.972800	64.096445	0.003325290295757	0.000000519957363	0.000293462284713	0.107059393616075
64.174792	66.503467	68.832142	0.003620641354067	0.000000572401782	0.000298253743088	0.315938363694566
68.749208	71.277633	73.806058	0.003531690890320	0.000000587723979	0.000283551412659	0.128037008564126
73.845360	76.554000	79.262640	0.003877272225797	0.000000634857741	0.000293612997137	0.239094469388901
79.306250	82.313600	85.320950	0.004318478986800	0.000000697467271	0.000299013014797	0.198049228522002
85.282585	88.599800	91.917015	0.004487886435901	0.000000745963265	0.000297356088009	0.171381146351225
91.895227	95.542767	99.190307	0.005378356107699	0.000000863056397	0.000329728586528	0.171240547159719
99.187367	103.242667	107.297967	0.005712722887536	0.000000926378534	0.000327783040013	0.154000290131935
107.279067	111.837667	116.396267	0.004824784577302	0.000000905075079	0.000281275228079	0.174877369746260
116.373527	121.452667	126.531807	0.004291740949353	0.000000880878324	0.000245729391563	0.147302153155309
126.528353	132.298333	138.068313	0.002953884884703	0.000000780641731	0.000182067703902	0.108048642305306
138.029132	144.623667	151.218202	0.001933304892955	0.000000659612328	0.000126886614359	0.090154334748641
151.184460	158.765000	166.345540	0.001315523914826	0.000000576508687	0.000093417412470	0.073067298299171
166.287930	175.085000	183.882070	0.000769770171281	0.000000484325944	0.000065708571924	0.017210529999512
183.818260	194.162000	204.505740	0.000400119659565	0.000000358238675	0.000039294295773	0.039962647274048
204.421193	216.710333	228.999473	0.000102819727242	0.000000195959492	0.000017816879061	0.117903425234469
228.877283	243.758333	258.639383	0.000046057889352	0.000000130282591	0.000009254545874	0.218481619126186
258.439650	276.750000	295.060350	0.000038386137737	0.000000133456823	0.000007677428595	0.356543776683874
294.778983	317.858333	340.937683	0.000021135985607	0.000000108583527	0.000005092172227	0.556854096643816
340.461217	370.441667	400.422117	0.000009045797154	0.000000085442487	0.000003061919722	0.862886439363257

Table A.IV.8. Proton Yields from Iron 400 MeV/n on 20 g/cm^2 Aluminium at 10.0 deg

KE_left(MeV/n)	KE_mid(MeV/n)	KE_right(MeV/n)	Norm_Cts(#/SP*ster*MeV/n)	Y_stat(#/SP*ster*MeV/n)	Y_syst_tot(#/SP*ster*MeV/n)	X_tot(MeV/n)
46.520592	48.230967	49.941342	0.003156841385817	0.000000456775940	0.000310785007830	0.249647018436031
49.941358	51.651733	53.362108	0.003945226157400	0.000000509763804	0.000354749697724	0.169861616050390
53.294268	55.230633	57.166998	0.003529094321991	0.000000508224123	0.000315470277505	0.227319871666099
57.234830	59.267300	61.299770	0.003935653584287	0.000000558134424	0.000332436421524	0.276102271357915
61.209432	63.410667	65.611902	0.004228176161332	0.000000590728096	0.000331740513385	0.111142285028561
65.702265	68.064600	70.426935	0.004263084642093	0.000000625883355	0.000329028377541	0.302126418472467
70.363673	72.984433	75.605193	0.004600568831658	0.000000683337292	0.000333650922124	0.153968744552036
75.592603	78.404533	81.216463	0.005114765443390	0.000000741836206	0.000348094374561	0.222093673307503
81.252078	84.332833	87.413588	0.005470919998478	0.000000801169373	0.000350723639849	0.198634393972947
87.430420	90.842400	94.254380	0.005393250042106	0.000000845157493	0.000338571510099	0.182789549865412
94.225180	98.020600	101.816020	0.005852951484856	0.000000925446271	0.000345954449045	0.154331510823616
101.787582	106.011667	110.235752	0.006887281970833	0.000001045502907	0.000374253383542	0.182398274418811
110.225657	114.918667	119.611677	0.007267592939724	0.000001132226487	0.000380326653302	0.150382789012107
119.593030	124.921000	130.248970	0.007466712832401	0.000001206847546	0.000368918636272	0.135240703993472
130.205367	136.231667	142.257967	0.008275917482899	0.000001337098662	0.000386329531697	0.106458352772622
142.242785	149.123000	156.003215	0.009612345149748	0.000001528484144	0.000421780974893	0.086395252947196
155.966457	163.932667	171.898877	0.010038352813107	0.000001658242124	0.000421770516557	0.057615390723834
171.845372	181.109667	190.373962	0.011004580982899	0.000001851170430	0.000434033422367	0.010388288784251
190.311752	201.254667	212.197582	0.011747525507937	0.000002089393886	0.000458970478626	0.057818926192035
212.089648	225.177333	238.265018	0.009042445100196	0.000002015223219	0.000361758373560	0.132545399718474
238.123447	254.028667	269.933887	0.006758638311019	0.000001909190488	0.000270130099012	0.216632772984606
269.720300	289.441000	309.161700	0.004024031242770	0.000001647024262	0.000171137658158	0.376108387135942
308.826933	333.932333	359.037733	0.000836569117800	0.000000831435675	0.000051088459204	0.578245046546877
358.457917	391.451667	424.445417	0.000090767821782	0.000000301634757	0.000010662173526	0.892452087624316

Table A.IV.9. Proton Yields from Iron 400 MeV/n on 20 g/cm^2 Aluminium at 7.20 deg

KE_left(MeV/n)	KE_mid(MeV/n)	KE_right(MeV/n)	Norm_Cts(#/SP*ster*MeV/n)	Y_stat(#/SP*ster*MeV/n)	Y_syst_tot(#/SP*ster*MeV/n)	X_tot(MeV/n)
45.331487	47.058767	48.786047	0.003347224007350	0.000000472554506	0.000320279283116	0.162753927981508
48.786053	50.513333	52.240613	0.004064237962117	0.000000525222245	0.000362905883055	0.230820847292873
52.179205	53.983400	55.787595	0.004371636812754	0.000000555799600	0.000373150105107	0.106820932430493
55.848995	57.898400	59.947805	0.004317270121683	0.000000588493356	0.000353278314237	0.291994045386203
59.921425	61.997200	64.072975	0.005384804816000	0.000000656585749	0.000399549876994	0.160104728479992
64.099350	66.478500	68.857650	0.005170326879847	0.000000678378807	0.000367691452963	0.284192421092541
68.780285	71.279600	73.778915	0.005652507985274	0.000000740405068	0.000389944427710	0.132221726827326
73.856335	76.571500	79.286665	0.005860564267733	0.000000790781299	0.000390056077006	0.259615097236274
79.264365	82.299200	85.334035	0.006290114651030	0.000000859537601	0.000390442849027	0.188172697172039
85.286203	88.597033	91.907863	0.006902474929284	0.000000928818048	0.000404818682358	0.163836085016610
91.901723	95.550233	99.198743	0.007538884981205	0.000001020541283	0.000422233949632	0.184082974347466
99.207707	103.245667	107.283627	0.008099894220149	0.000001106324712	0.000427329625607	0.153894937164710
107.266552	111.826667	116.386782	0.008604418780246	0.000001201634431	0.000435061646495	0.154598326405689
116.375472	121.453667	126.531862	0.010031045566695	0.000001368629279	0.000476362473516	0.154339109876402
126.518992	132.303667	138.088342	0.010624131737526	0.000001524542795	0.000497591902708	0.113274238931233
138.052165	144.630000	151.207835	0.011627257849359	0.000001905932485	0.000644744508677	0.098419535211918
151.170970	158.764000	166.357030	0.012299029243415	0.000001948240107	0.000585726868994	0.071840353634709
166.282590	175.082000	183.881410	0.016719713712149	0.000002233849736	0.000642371593757	0.011297319899644
183.832842	194.174667	204.516492	0.019914127738537	0.000002629408364	0.000744819163936	0.016397010725641
204.425750	216.723000	229.020250	0.016366145372218	0.000002626789045	0.000627638490695	0.096515928094900
228.904228	243.785333	258.666438	0.008597189709305	0.000002091797795	0.000350115894691	0.172624964052596
258.468683	276.785333	295.101983	0.004110613650217	0.000001599988675	0.000176547644235	0.295722855775471
294.822667	317.911667	341.000667	0.001083952748806	0.000000898499801	0.000061775335456	0.463327468230624
340.523333	370.522333	400.521333	0.000106120252088	0.000000311446833	0.000012082429773	0.722932528149758

Table A.IV.10. Proton Yields from Iron 400 MeV/n on 20 g/cm^2 Aluminium at 32.7 deg

KE_left(MeV/n)	KE_mid(MeV/n)	KE_right(MeV/n)	Norm_Cts(#/SP*ster*MeV/n)	Y_stat(#/SP*ster*MeV/n)	Y_syst_tot(#/SP*ster*MeV/n)	X_tot(MeV/n)
45.358290	46.911767	48.465244	0.000891889354970	0.000000222924903	0.000155116867281	0.158533621554861
48.520838	50.347433	52.174028	0.000751319859822	0.000000210401354	0.000124130605038	0.156351337948641
52.174038	54.000633	55.827228	0.000980012991190	0.000000258445617	0.000152986652101	0.395166953055288
55.738195	57.718300	59.698405	0.000936229880005	0.000000255950812	0.000140345815486	0.197791743296049
59.787430	61.954600	64.121770	0.001090074198721	0.000000295799427	0.000148741767837	0.251541405587629
64.039242	66.338267	68.637292	0.001051576284524	0.000000290877117	0.000139925290144	0.244454232372851
68.719850	71.234000	73.748150	0.001070559170437	0.000000308712972	0.000134725899158	0.248386828187406
73.676580	76.446100	79.215620	0.001212996190344	0.000000355809704	0.000142639606369	0.255598405890960
79.205032	82.198667	85.192302	0.001069301342355	0.000000343403030	0.000126170443140	0.195517659295139
85.210650	88.505400	91.800150	0.001071531856296	0.000000353328433	0.000119103797785	0.238930157847518
91.799707	95.457467	99.115227	0.001070309588054	0.000000369804288	0.000112826058789	0.230840852731920
99.099320	103.172000	107.244680	0.001209130916452	0.000000425570384	0.000117648719595	0.213947779490791
107.221435	111.754000	116.286565	0.001221930135667	0.000000436318469	0.000109558804322	0.197507821395407
116.255452	121.360667	126.465882	0.001259298231333	0.000000471757536	0.000106337464160	0.155382772918911
126.473142	132.241667	138.010192	0.001225688735717	0.000000513575172	0.000102808727987	0.140788289924979
137.979312	144.579667	151.180022	0.001336022485957	0.000000548956086	0.000097940098469	0.123977735159383
151.155403	158.733333	166.311263	0.001277193727445	0.000000567411713	0.000088922262180	0.084894938265188
166.267982	175.078667	183.889352	0.001216408536655	0.000000579487355	0.000078761125917	0.018749673602802
183.814660	194.177000	204.539340	0.000955048666759	0.000000564220009	0.000064978210315	0.078263358876680
204.450398	216.761333	229.072268	0.000550198183764	0.000000463711090	0.000043613245305	0.170042603914578
228.951188	243.859333	258.767478	0.000286570936146	0.000000365639990	0.000027737762557	0.301481162671899
258.567050	276.916000	295.264950	0.000055474828760	0.000000165258356	0.000009901390529	0.497414846118409
294.986517	318.121667	341.256817	0.000004146984854	0.000000050801077	0.000002426071940	0.751582632630638
341.600350	360.699000	379.797650	0.000000732880467	0.000000022181626	0.000000817250160	0.872250453966635

Table A.IV.11. Proton Yields from Iron 400 MeV/n on 20 g/cm^2 Aluminium at 30.0 deg

KE_left(MeV/n)	KE_mid(MeV/n)	KE_right(MeV/n)	Norm_Cts(#/SP*ster*MeV/n)	Y_stat(#/SP*ster*MeV/n)	Y_syst_tot(#/SP*ster*MeV/n)	X_tot(MeV/n)
45.465605	47.062700	48.659795	0.000877906728073	0.000000219583388	0.000148023294322	0.307504948530914
48.595268	50.275433	51.955598	0.000811041110169	0.000000216343704	0.000138342041584	0.104856717459320
52.020080	53.948600	55.877120	0.000876468641160	0.000000242407150	0.000135966351668	0.340906408250490
55.877180	57.805700	59.734220	0.000987390335210	0.000000269199224	0.000151124229037	0.335824017780146
59.671495	61.865400	64.059305	0.001081421291001	0.000000286443499	0.000142591039752	0.127010959587145
64.122003	66.390633	68.659263	0.001154045838140	0.000000307460799	0.000148412890781	0.342736958831405
68.612125	71.179800	73.747475	0.001168862055294	0.000000338260324	0.000144561667263	0.178104552513657
73.719052	76.443367	79.167682	0.001264418961972	0.000000360766305	0.000147115526189	0.240660010350702
79.238052	82.209867	85.181682	0.001214856612096	0.000000353985856	0.000132332791220	0.214189011683606
85.186915	88.510900	91.834885	0.001276293468520	0.000000386677964	0.000130411682496	0.226189495815367
91.800977	95.454167	99.107357	0.001318353602431	0.000000419555104	0.000129398603610	0.213765776390890
99.085375	103.156000	107.226625	0.001434347988356	0.000000444680325	0.000124987260821	0.196274584050508
107.197643	111.757333	116.317023	0.001389062012641	0.000000474506511	0.000119531109946	0.196362628171070
116.299595	121.381000	126.462405	0.001398073332536	0.000000498807807	0.000113805132723	0.193073238466676
126.457097	132.240667	138.024237	0.001085954354442	0.000000463647903	0.000091987047252	0.137603304041327
137.988740	144.582000	151.175260	0.000800642795835	0.000000415458953	0.000071411658083	0.121142931963363
151.134650	158.736000	166.337350	0.000389977536143	0.000000295327246	0.000042959308247	0.093722432410496
166.260593	175.074333	183.888073	0.000172409380180	0.000000200585177	0.000025014167087	0.008912909625840
183.843123	194.200333	204.557543	0.000080285647454	0.000000147967081	0.000015242086579	0.033305577315773
204.458018	216.784333	229.110648	0.000013307700687	0.000000057701715	0.000005008647030	0.132027218834678
228.999798	243.907333	258.814868	0.000004158805139	0.000000043727594	0.000003120261000	0.219582100628102
259.015600	270.805000	282.594400	0.000005745696203	0.000000045993225	0.000002706925280	0.273561839672495
295.613450	310.413500	325.213550	0.000002319587063	0.000000026920456	0.000001262573535	0.434316978705645

Table A.IV.12. Proton Yields from Iron 400 MeV/n on 20 g/cm^2 Aluminium at 27.2 deg

KE_left(MeV/n)	KE_mid(MeV/n)	KE_right(MeV/n)	Norm_Cts(#/SP*ster*MeV/n)	Y_stat(#/SP*ster*MeV/n)	Y_syst_tot(#/SP*ster*MeV/n)	X_tot(MeV/n)
45.364630	47.037700	48.710770	0.001062360902562	0.000000256522875	0.000165790746450	0.258282692124347
48.710763	50.383833	52.056903	0.001159162912517	0.000000260157596	0.000168931136663	0.212431362690658
51.978045	53.857000	55.735955	0.001176385523497	0.000000284596129	0.000165336832323	0.203418953925744
55.814822	57.819767	59.824712	0.001157415867067	0.000000290876975	0.000158407172788	0.339887278048179
59.751583	61.862733	63.973883	0.001266243104516	0.000000304577730	0.000159752379776	0.120771497184145
64.047010	66.391600	68.736190	0.001176520316647	0.000000321252474	0.000150120964750	0.346029269545222
68.640287	71.157367	73.674447	0.001394968956255	0.000000355895716	0.000158105177820	0.137698949055612
73.764545	76.460600	79.156655	0.001284821607451	0.000000356806169	0.000146659598661	0.277280919693368
79.162458	82.203933	85.245408	0.001380991224600	0.000000389763141	0.000143384204925	0.211209540219873
85.178447	88.494867	91.811287	0.001506655162326	0.000000425933130	0.000145153017413	0.196026880606334
91.801672	95.454067	99.106462	0.001456498919286	0.000000442794558	0.000137566505051	0.210322627315750
99.113370	103.157000	107.200630	0.001552422447554	0.000000467416650	0.000132783383251	0.192269023147672
107.179880	111.739000	116.298120	0.001603232281268	0.000000515975522	0.000131160106543	0.169728252502640
116.285312	121.378667	126.472022	0.001641798800798	0.000000535312063	0.000123671214378	0.199774840831772
126.453057	132.243667	138.034277	0.001591468497994	0.000000595288243	0.000123207204726	0.143042810137525
138.001323	144.586333	151.171343	0.001622903472922	0.000000660401202	0.000122915997461	0.123934916759604
151.124118	158.726333	166.328548	0.001614410198210	0.000000636418011	0.000102183884803	0.083543605178683
166.261288	175.078333	183.895378	0.001677642166414	0.000000700914307	0.000098111921492	0.017547351155374
183.856078	194.210333	204.564588	0.001459645399649	0.000000696093344	0.000083503401715	0.013966874883241
204.476182	216.814667	229.153152	0.000864970044044	0.000000589753870	0.000057186378097	0.077906314839427
229.030992	243.938667	258.846342	0.000414706092500	0.000000444368193	0.000034311165635	0.166794922228616
258.667683	277.038333	295.408983	0.000096669929372	0.000000227404522	0.000013933004352	0.282204084270586
295.114700	318.295000	341.475300	0.000005943612432	0.000000051010457	0.000002403653337	0.450696660846295
340.989167	371.115667	401.242167	0.000002514048558	0.000000037790345	0.000001353624818	0.691378159034547

Table A.IV.13. Triton Yields from Iron 400 MeV/n on 20 g/cm^2 Aluminium at 12.7 deg

KE_left(MeV/n)	KE_mid(MeV/n)	KE_right(MeV/n)	Norm_Cts(#/SP*ster*MeV/n)	Y_stat(#/SP*ster*MeV/n)	Y_syst_tot(#/SP*ster*MeV/n)	X_tot(MeV/n)
43.833975	45.048500	46.263024	0.000820917838666	0.000000164908580	0.000145216108094	38.806289034897425
46.263009	47.477533	48.692058	0.000824000064604	0.000000217546355	0.000193974673878	0.209735853468118
48.623747	49.967167	51.310587	0.000827146124447	0.000000248608120	0.000202841639261	0.091141404005040
51.378905	52.843833	54.308762	0.000830164516479	0.000000272964290	0.000203956702489	0.125360023256459
54.275096	55.773700	57.272304	0.000833269829570	0.000000263791550	0.000194044658770	0.098092640357827
57.305963	59.027333	60.748703	0.000868563124624	0.000000261108861	0.000166165031958	0.116759326058949
60.701943	62.476033	64.250123	0.000936385021615	0.000000237091626	0.000146512314635	0.080670708821604
64.296870	66.281100	68.265330	0.001154547394501	0.000000242196857	0.000133074905845	0.149226399533662
68.198332	70.341067	72.483802	0.001348108494876	0.000000243304680	0.000123355912885	0.104736254538522
72.500682	74.812667	77.124652	0.001474718734830	0.000000304632838	0.000145682757131	0.092035115848735
77.171062	79.705067	82.239072	0.001666258800294	0.000000330029584	0.000145073387501	0.104740796131450
82.242738	85.056633	87.870528	0.001933477033445	0.000000378747727	0.000152682133140	0.077855983234752
87.853042	90.950667	94.048292	0.002076183103525	0.000000419232238	0.000155176147206	0.058142953092588
94.014340	97.469500	100.924660	0.002182379347131	0.000000504051442	0.000172713709102	0.058372610696884
100.898902	104.733667	108.568432	0.001955300960691	0.000000619753632	0.000203990188308	0.031414360462540
108.557478	112.825333	117.093188	0.001710467480009	0.000000472812341	0.000131662103861	0.027710985117307
117.091167	121.917667	126.744167	0.000793247742521	0.000000318908318	0.000074788592130	0.044994564613212
126.721518	132.186333	137.651148	0.000219573395492	0.000000165295911	0.000032743682003	0.057940332283738
137.613127	143.852667	150.092207	0.000126908193293	0.000000133115153	0.000022701187993	0.122233764448372
150.077157	157.246667	164.416177	0.000159586664186	0.000000165336496	0.000024607019699	0.110385334210030
164.378025	172.701000	181.023975	0.000106966439982	0.000000152521698	0.000019800689654	0.192098399550855
180.950790	190.724000	200.497210	0.000042306378293	0.000000095828532	0.000010422270601	0.282551726209556
200.411767	212.008667	223.605567	0.000037647477143	0.000000101377231	0.000009263901373	0.381583710148900
223.485187	237.455667	251.426147	0.000041394914441	0.000000117844891	0.000008928529895	0.525932127181826
251.260800	268.389000	285.517200	0.000027885963047	0.000000102974066	0.000006335632365	0.699798635352342
285.270433	306.727333	328.184233	0.000017896401986	0.000000086901493	0.000004367611597	0.960073919742641
327.773500	355.417000	383.060500	0.000005841509016	0.000000062334536	0.000002458900333	1.366565289278928

Table A.IV.14. Triton Yields from Iron 400 MeV/n on 20 g/cm^2 Aluminium at 10.0 deg

KE_left(MeV/n)	KE_mid(MeV/n)	KE_right(MeV/n)	Norm_Cts(#/SP*ster*MeV/n)	Y_stat(#/SP*ster*MeV/n)	Y_syst_tot(#/SP*ster*MeV/n)	X_tot(MeV/n)
44.622528	45.849400	47.076273	0.001129582116368	0.000000274236805	0.000244682545420	31.965438608288814
47.076261	48.303133	49.530006	0.001142622809807	0.000000320377191	0.000291197028216	0.208160445478962
49.478865	50.885767	52.292669	0.001155880100122	0.000000344438424	0.000278285470729	0.063181668921235
52.343795	53.820800	55.297805	0.001168704196686	0.000000300346439	0.000224976572658	0.116717904936689
55.237992	56.809067	58.380142	0.001181981205096	0.000000284782469	0.000200015975977	0.116255615601226
58.439965	60.173200	61.906435	0.001286939809793	0.000000267699855	0.000168898956346	0.114783094488213
61.837258	63.690533	65.543808	0.001372282722584	0.000000273725563	0.000162214991275	0.095344982254454
65.612970	67.608900	69.604830	0.001651352129238	0.000000295691792	0.000163726244448	0.124639551445197
69.566797	71.794167	74.021537	0.001936500360012	0.000000311796922	0.000154833860892	0.134962540223167
73.983505	76.384900	78.786295	0.002222048220578	0.000000351222474	0.000163474818908	0.081552743639009
78.802217	81.429867	84.057517	0.002710284897034	0.000000395012640	0.000171073654757	0.082769706058799
84.060717	86.959867	89.859017	0.003118876951594	0.000000465777439	0.000187088452185	0.084028795581568
89.851147	93.062167	96.273187	0.003436508449505	0.000000528231830	0.000194887050493	0.068824605743658
96.255580	99.815300	103.375020	0.003756671458886	0.000000781392781	0.000292542609734	0.068730065595051
103.387267	107.335667	111.284067	0.003899564738147	0.000000733882840	0.000251260484872	0.029955070124139
111.276348	115.752333	120.228318	0.002999958818535	0.000000619551794	0.000171600137029	0.024260018367780
120.179518	125.206333	130.233148	0.002312868606598	0.000000574854987	0.000142341775583	0.027681013060040
130.219300	135.926000	141.632700	0.001596502110920	0.000000511140533	0.000106009050379	0.048422259106634
141.616647	148.129667	154.642687	0.003345537353701	0.000000796758020	0.000167151702612	0.085469054481374
154.627883	162.168333	169.708783	0.002772915798875	0.000000784664170	0.000141090342896	0.097745424095760
169.649872	178.425667	187.201462	0.002286329231709	0.000000764062924	0.000116633308813	0.172381422303710
187.124983	197.454333	207.783683	0.003355905493517	0.000001017455372	0.000147678005034	0.248978433278869
207.696558	220.015333	232.334108	0.001530815655550	0.000000745840791	0.000084422733266	0.350424625233444
232.208295	247.142000	262.075705	0.000499397534817	0.000000459183881	0.000036133750649	0.464992428207170
261.883300	280.304000	298.724700	0.000282378525965	0.000000392261527	0.000024530008750	0.642341502328785
298.435100	321.724000	345.012900	0.000111165955639	0.000000263755779	0.000012785318445	0.889778744017860
344.515000	374.843000	405.171000	0.000027512200998	0.000000142478522	0.000005161832581	1.309065447510169

Table A.IV.15. Triton Yields from Iron 400 MeV/n on 20 g/cm^2 Aluminium at 7.20 deg

KE_left(MeV/n)	KE_mid(MeV/n)	KE_right(MeV/n)	Norm_Cts(#/SP*ster*MeV/n)	Y_stat(#/SP*ster*MeV/n)	Y_syst_tot(#/SP*ster*MeV/n)	X_tot(MeV/n)
43.788660	45.021700	46.254741	0.001297321654676	0.000000330559013	0.000299011247056	38.760092721638323
46.254759	47.487800	48.720841	0.001357420797424	0.000000414875537	0.000385856914321	0.226906356766398
48.666122	49.979900	51.293679	0.001418751067181	0.000000455575744	0.000406373613106	0.117223833909424
51.348362	52.831400	54.314438	0.001477619082919	0.000000427023247	0.000333123588162	0.104070642827889
54.314462	55.797500	57.280538	0.001537718225667	0.000000366763259	0.000279937371978	0.139362135492751
57.276822	59.012267	60.747712	0.001660272959979	0.000000335113329	0.000215227897778	0.092245649156424
60.728962	62.490567	64.252172	0.001879164156521	0.000000304538919	0.000191490650135	0.099417766996040
64.274620	66.276400	68.278180	0.001809935697770	0.000000329072721	0.000182452906951	0.141360057725299
68.203870	70.338900	72.473930	0.002024492847825	0.000000346397398	0.000181890755775	0.103236952783826
72.511450	74.819400	77.127350	0.002455222673657	0.000000399882385	0.000197036624588	0.099228612057763
77.164127	79.711667	82.259207	0.003007425492663	0.000000451235875	0.000206393150693	0.109547218870266
82.244442	85.060667	87.876892	0.003717171932302	0.000000524228195	0.000222916265788	0.088690241616426
87.863235	90.956500	94.049765	0.004203909202874	0.000000594157000	0.000237240493361	0.074828178913939
94.029388	97.479733	100.930078	0.004690812897207	0.000000782502087	0.000307865266105	0.063020639499266
100.906083	104.746333	108.586583	0.004827912756730	0.000000872511229	0.000321940182130	0.050069186686924
108.576975	112.842000	117.107025	0.003945009914498	0.000000686550097	0.000207433811914	0.028380049122096
117.102145	121.937000	126.771855	0.005630351182741	0.000000897186829	0.000264911637602	0.018393846469102
126.740608	132.207333	137.674058	0.016745986610212	0.000001560235481	0.000564472311393	0.020666755230033
137.643193	143.881333	150.119473	0.010576023967452	0.000001238921864	0.000327942299615	0.073323490021479
150.103370	157.280000	164.456630	0.006764564653959	0.000001204209579	0.000284828039239	0.055636223442376
164.417193	172.741333	181.065473	0.004261509090093	0.000001032485284	0.000187196139378	0.122531722980010
180.994057	190.775667	200.557277	0.005659422141934	0.000001291396813	0.000225353925233	0.193230515130737
200.470853	212.074333	223.677813	0.002812236489049	0.000000977035303	0.000137007869780	0.267735481970545
223.557518	237.539333	251.521148	0.000559341013849	0.000000471648598	0.000040159085855	0.381064798878091
251.354967	268.497667	285.640367	0.000316723404476	0.000000384721875	0.000026015426389	0.511237896939380
285.393383	306.871333	328.349283	0.000108955865631	0.000000256490365	0.000013411732876	0.710217987948771
327.937717	355.612667	383.287617	0.000022952727940	0.000000123474811	0.000004847696159	1.027279986999163

Table A.IV.16. Triton Yields from Iron 400 MeV/n on 20 g/cm^2 Aluminium at 32.7 deg

KE_left(MeV/n)	KE_mid(MeV/n)	KE_right(MeV/n)	Norm_Cts(#/SP*ster*MeV/n)	Y_stat(#/SP*ster*MeV/n)	Y_syst_tot(#/SP*ster*MeV/n)	X_tot(MeV/n)
45.291996	46.578033	47.864070	0.000098427514425	0.000000050002634	0.000040935302379	22.742686788886651
47.864030	49.150067	50.436104	0.000133216125495	0.000000057701684	0.000047272651525	0.292722420829017
50.372492	51.762567	53.152642	0.000094785525310	0.000000057725083	0.000043183272566	0.072098679835140
53.216278	54.763033	56.309788	0.000127017069210	0.000000066849883	0.000045575757597	0.140665641754659
56.279968	57.856533	59.433098	0.000117424353263	0.000000062119869	0.000041493188559	0.197146610618823
59.462905	61.276000	63.089095	0.000116871872293	0.000000076895158	0.000044629973322	0.114348001122057
63.035673	64.918233	66.800793	0.000122199090582	0.000000078288942	0.000044337464971	0.104284667180224
66.854193	68.939733	71.025273	0.000123645335264	0.000000077672495	0.000039234019535	0.102048322775095
70.966517	73.247667	75.528817	0.000086945074842	0.000000075738438	0.000034230430939	0.087751101853823
75.520372	77.991167	80.461962	0.000130463280491	0.000000073861920	0.000031810413790	0.070565062133183
80.475623	83.188833	85.902043	0.000103437151901	0.000000077724635	0.000030347799513	0.071261182911175
85.902762	88.903967	91.905172	0.000101211844338	0.000000077724635	0.000027274593706	0.088307059025879
91.894687	95.224467	98.554247	0.000094070741650	0.000000073096206	0.000023570357022	0.064456027877479
98.533833	102.229133	105.924433	0.000028286314344	0.000000038071295	0.000010847061491	0.054964327658218

Table A.IV.17. Triton Yields from Iron 400 MeV/n on 20 g/cm^2 Aluminium at 30.0 deg

KE_left(MeV/n)	KE_mid(MeV/n)	KE_right(MeV/n)	Norm_Cts(#/SP*ster*MeV/n)	Y_stat(#/SP*ster*MeV/n)	Y_syst_tot(#/SP*ster*MeV/n)	X_tot(MeV/n)
45.208406	46.494600	47.780794	0.000116933884960	0.000000057283867	0.000047409343291	22.634223609773855
47.817391	49.140233	50.463076	0.000095660327367	0.000000052251868	0.000041550780281	0.274717953008172
50.450865	51.785900	53.120934	0.000147199871841	0.000000073916724	0.000058152357580	0.129606523908328
53.133163	54.715933	56.298703	0.000133510153801	0.000000080761454	0.000053705622659	0.108085146751392
56.298730	57.881500	59.464270	0.000137525867665	0.000000071486772	0.000047588592544	0.214769303767461
59.422098	61.228433	63.034768	0.000181182378138	0.000000086701762	0.000050687961797	0.094129329130192
63.066238	64.925433	66.784628	0.000199113957552	0.000000089627923	0.000050829214753	0.119362569358489
66.795343	68.915833	71.036323	0.000189972930421	0.000000096732141	0.000048181572057	0.062457230711664
70.961277	73.227967	75.494657	0.000190030528839	0.000000101616614	0.000046829503296	0.065548099250093
75.516613	77.979833	80.443053	0.000127991326831	0.000000077103729	0.000032746648387	0.053071060785299
80.469600	83.180500	85.891400	0.000152741767907	0.000000100525709	0.000039101215831	0.057170429591004
85.891560	88.894600	91.897640	0.000231263688528	0.000000128454493	0.000045302667891	0.065167151414037
91.870287	95.205267	98.540247	0.000064078149577	0.000000070980590	0.000022641630869	0.058237130324304

Table A.IV.18. Triton Yields from Iron 400 MeV/n on 20 g/cm^2 Aluminium at 27.2 deg

KE_left(MeV/n)	KE_mid(MeV/n)	KE_right(MeV/n)	Norm_Cts(#/SP*ster*MeV/n)	Y_stat(#/SP*ster*MeV/n)	Y_syst_tot(#/SP*ster*MeV/n)	X_tot(MeV/n)
46.004199	47.314867	48.625535	0.000214906770727	0.000000085633032	0.000068980470898	0.115890266623259
48.665261	50.015633	51.366005	0.000132632564357	0.000000064173907	0.000050083629173	0.245955907587112
51.333390	52.716367	54.099344	0.000181145111540	0.000000071037653	0.000054486638039	0.120241225561406
54.131927	55.741667	57.351407	0.000168372919945	0.000000088093138	0.000057665398850	0.168512288226853
57.351427	58.961167	60.570907	0.000201894854571	0.000000086701762	0.000056850987476	0.153091190878280
60.565043	62.434233	64.303423	0.000172284189423	0.000000092982889	0.000052405710539	0.086079896270035
64.259598	66.193133	68.126668	0.000254237434507	0.000000108610277	0.000059399546236	0.110301420349060
68.176372	70.323067	72.469762	0.000181354984977	0.000000095647469	0.000047048631997	0.083430318267941
72.413705	74.763300	77.112895	0.000203039217669	0.000000112860424	0.000050361932391	0.038834966930576
77.094468	79.647833	82.201198	0.000194445953193	0.000000107621848	0.000044618578282	0.045843350406388
82.210887	85.018067	87.825247	0.000206797203483	0.000000110745726	0.000041438847457	0.042880241473784
87.822647	90.927367	94.032087	0.000212159377572	0.000000128482533	0.000043918913022	0.038388297683799
94.018780	97.460300	100.901820	0.000157316456838	0.000000099404045	0.000030731929905	0.043520063951470
100.982370	102.185000	103.387630	0.000038545937846	0.000000033950600	0.000009889300000	0.020288800000000

Table A.IV.19. Helium-4 Yields from Iron 400 MeV/n on 20 g/cm^2 Aluminium at 12.7 deg

KE_left(MeV/n)	KE_mid(MeV/n)	KE_right(MeV/n)	Norm_Cts(#/SP*ster*MeV/n)	Y_stat(#/SP*ster*MeV/n)	Y_syst_tot(#/SP*ster*MeV/n)	X_tot(MeV/n)
45.251835	46.948800	48.645765	0.000719323246738	0.000000261986871	0.000168758033720	0.331575574279831
48.645735	50.342700	52.039665	0.000725844803232	0.000000262043662	0.000169055449601	0.255334889872673
51.955308	53.797633	55.639958	0.000732493552481	0.000000221879501	0.000131795433940	0.090278391631497
55.724350	57.744700	59.765050	0.000738887916219	0.000000232097931	0.000124671243024	0.349992845945456
59.702380	61.800300	63.898220	0.000832527244823	0.000000241529514	0.000124928739788	0.152654728457424
63.960853	66.312433	68.664013	0.000827189733188	0.000000255642658	0.000118816500890	0.302386949157929
68.572973	71.085233	73.597493	0.000924356886480	0.000000273780000	0.000119746692753	0.145775223180381
73.678587	76.377667	79.076747	0.001003223788449	0.000000305260590	0.000125331334899	0.232976511528523
79.086708	82.119333	85.151958	0.001065661771336	0.000000327907453	0.000120653647999	0.186002286171434
85.090520	88.404900	91.719280	0.001262478132599	0.000000378273794	0.000129606377485	0.181341602765857
91.711817	95.361367	99.010917	0.001237001741532	0.000000393658090	0.000122952946049	0.181353616435543
99.015275	103.057000	107.098725	0.001038036912454	0.000000368960260	0.000103111621687	0.158766789968494
107.086987	111.658667	116.230347	0.001125658076920	0.000000404612538	0.000101469577951	0.161538963535520
116.210633	121.292333	126.374033	0.001214222537777	0.000000445007380	0.000101269900215	0.169967386533417
126.365438	132.158333	137.951228	0.001011510384867	0.000000429263860	0.000085414780164	0.114152241472912
137.907405	144.510000	151.112595	0.001039676796947	0.000000452489657	0.000079617485708	0.093132581943432
151.078643	158.687333	166.296023	0.001168472861264	0.000000506649978	0.000079434564592	0.077163186704348
166.231862	175.061667	183.891472	0.001253140006312	0.000000559536802	0.000077175124822	0.012623264324575
183.831600	194.221000	204.610400	0.000687699362626	0.000000432357781	0.000049464322039	0.037023116117096
204.731365	212.723000	220.714635	0.000126625574947	0.000000154291470	0.000014129724099	0.083430618104926

Table A.IV.20. Helium-4 Yields from Iron 400 MeV/n on 20 g/cm^2 Aluminium at 10.0 deg

KE_left(MeV/n)	KE_mid(MeV/n)	KE_right(MeV/n)	Norm_Cts(#/SP*ster*MeV/n)	Y_stat(#/SP*ster*MeV/n)	Y_syst_tot(#/SP*ster*MeV/n)	X_tot(MeV/n)
45.155592	46.886367	48.617142	0.001528994824337	0.000000374948272	0.000245058266559	0.225486511691941
48.617092	50.347867	52.078642	0.001596070621356	0.000000382070823	0.000250047334675	0.256874087945826
52.022213	53.814533	55.606853	0.001663914171888	0.000000388017888	0.000245470116847	0.077941812460045
55.663277	57.717467	59.771657	0.001730222215394	0.000000378720559	0.000208758031707	0.306126995617832
59.759148	61.825833	63.892518	0.001977769593050	0.000000381387909	0.000209494313357	0.185005374392299
63.905023	66.290233	68.675443	0.001968063158320	0.000000407625716	0.000195975242646	0.280207504605516
68.601917	71.095267	73.588617	0.002200309243105	0.000000440563952	0.000205842967276	0.160106332244168
73.662133	76.384633	79.107133	0.002281821274740	0.000000478777560	0.000205997232649	0.245331786904999
79.073557	82.105767	85.137977	0.002348859322615	0.000000494552094	0.000193686112280	0.173697674046143
85.097847	88.408267	91.718687	0.002436943081400	0.000000540426949	0.000195746492451	0.185217085726452
91.712908	95.363333	99.013758	0.002337166612523	0.000000556048455	0.000183619725700	0.183224947371503
99.023322	103.065667	107.108012	0.002618243311484	0.000000603656370	0.000184033567107	0.164089630271294
107.087965	111.649000	116.210035	0.002681050488308	0.000000642616206	0.000177588710193	0.147073298831739
116.201860	121.291000	126.380140	0.002675523461378	0.000000667475891	0.000167456162116	0.173287721051695
126.365697	132.160667	137.955637	0.002681239950385	0.000000708047526	0.000158819401127	0.117814768219056
137.922280	144.514000	151.105720	0.002815582589173	0.000000760890727	0.000153009358036	0.098231118069887
151.069183	158.686333	166.303483	0.003003881437854	0.000000838313587	0.000152255752814	0.075754726919117
166.228440	175.060000	183.891560	0.002778706795761	0.000000849323700	0.000132816980069	0.008422146812334
183.841003	194.229333	204.617663	0.001747738847037	0.000000720041852	0.000094939422769	0.020824413326387
204.859180	208.730000	212.600820	0.000478617772475	0.000000219634000	0.000021564600000	0.047801100000000

Table A.IV.21. Helium-4 Yields from Iron 400 MeV/n on 20 g/cm^2 Aluminium at 7.20 deg

KE_left(MeV/n)	KE_mid(MeV/n)	KE_right(MeV/n)	Norm_Cts(#/SP*ster*MeV/n)	Y_stat(#/SP*ster*MeV/n)	Y_syst_tot(#/SP*ster*MeV/n)	X_tot(MeV/n)
46.265053	48.012733	49.760413	0.003256529342346	0.000000506644598	0.000345669636656	0.217909241924729
49.760420	51.508100	53.255780	0.003429823202726	0.000000528684598	0.000362304698703	0.210778437132454
53.177090	55.053200	56.929310	0.003606436332698	0.000000532534420	0.000342085552621	0.115215423722521
57.008005	59.079100	61.150195	0.003927964385933	0.000000556655175	0.000324987113581	0.307001333725116
61.083147	63.245167	65.407187	0.004116545601454	0.000000575681634	0.000326059244135	0.111514104963677
65.474257	67.876267	70.278277	0.004224421682880	0.000000618748391	0.000319224173911	0.304635805782905
70.193332	72.790067	75.386802	0.004634397223237	0.000000671419185	0.000329494057139	0.126544978972380
75.413802	78.212367	81.010932	0.004735756002622	0.000000700915466	0.000323152823316	0.227415536140256
81.068835	84.151200	87.233565	0.005106720310230	0.000000753176716	0.000323464459677	0.209121826911970
87.227125	90.652200	94.077275	0.005229264889028	0.000000803289074	0.000318053925983	0.178675532798982
94.049332	97.835667	101.622002	0.005523337182613	0.000000865992597	0.000318345526433	0.158837262450629
101.585717	105.823667	110.061617	0.005924594572873	0.000000935047304	0.000317634921230	0.169148277520760
110.031005	114.743000	119.454995	0.006472899109588	0.000001038592241	0.000331450206713	0.160903576809871
119.428005	124.757000	130.085995	0.006821772868478	0.000001102378178	0.000322864346192	0.142581368862695
130.059910	136.099000	142.138090	0.007079361331680	0.000001181823767	0.000317790206087	0.119199198936025
142.122877	149.026667	155.930457	0.007491409179374	0.000001276553323	0.000315942062160	0.097272739012583
155.879413	163.868333	171.857253	0.007608276499866	0.000001354757457	0.000299939905811	0.055483250110246
171.807170	181.111000	190.414830	0.005047782640503	0.000001166535977	0.000212483625772	0.006078143949538
190.539570	197.662000	204.784430	0.001079915406330	0.000000469245128	0.000055303503131	0.011215195394000

Table A.IV.22. Helium-3 Yields from Iron 400 MeV/n on 20 g/cm^2 Aluminium at 12.7 deg

KE_left(MeV/n)	KE_mid(MeV/n)	KE_right(MeV/n)	Norm_Cts(#/SP*ster*MeV/n)	Y_stat(#/SP*ster*MeV/n)	Y_syst_tot(#/SP*ster*MeV/n)	X_tot(MeV/n)
50.021293	52.045933	54.070573	0.000171371637360	0.000000108548107	0.000056729259990	0.438060535406923
54.070593	56.095233	58.119873	0.000355609095228	0.000000158355475	0.000083432883112	0.233038945192880
58.106535	60.464100	62.821665	0.000350232796146	0.000000174226840	0.000078986114903	0.194268202217739
62.834982	65.205867	67.576752	0.000466638211302	0.000000207625268	0.000094318154965	0.331471263649279
67.572965	70.296100	73.019235	0.000568978635203	0.000000253618380	0.000101347119692	0.200585331782785
72.933452	75.807967	78.682482	0.000672661123157	0.000000325843650	0.000125666856791	0.237622371004836
78.737528	81.862033	84.986538	0.000791983872656	0.000000383874364	0.000138297571148	0.227232774955551
85.021020	88.480500	91.939980	0.000905695422466	0.000000407930593	0.000134888224289	0.230398786355310
91.927392	95.757867	99.588342	0.000922924246394	0.000000374281450	0.000111042542248	0.224144463601045
99.538820	103.818000	108.097180	0.000545826403775	0.000000278246756	0.000071348418377	0.205449012603346
108.062287	112.826667	117.591047	0.000648249032690	0.000000327036299	0.000076268535391	0.214720419525019
117.561140	122.897000	128.232860	0.000644469588193	0.000000330273106	0.000069361339241	0.193831019945209
128.235463	134.286333	140.337203	0.000585556844521	0.000000336438874	0.000062202851954	0.174627520573477
140.297662	147.232667	154.167672	0.000587865742406	0.000000359017758	0.000058097806400	0.144962291127658
154.141147	162.106667	170.072187	0.000702269225230	0.000000410111628	0.000059390849106	0.138416186348201
170.030348	179.324333	188.618318	0.000751164243993	0.000000449659252	0.000056721249308	0.098420995946851
188.531678	199.480333	210.428988	0.000742641948000	0.000000487414198	0.000052041344482	0.030154363289806
210.323855	223.415000	236.506145	0.000785596315196	0.000000520179185	0.000048527582624	0.055774630772960
236.360185	252.251000	268.141815	0.000189313607204	0.000000272699146	0.000019802927299	0.146545030069839

Table A.IV.23. Helium-3 Yields from Iron 400 MeV/n on 20 g/cm^2 Aluminium at 10.0 deg

KE_left(MeV/n)	KE_mid(MeV/n)	KE_right(MeV/n)	Norm_Cts(#/SP*ster*MeV/n)	Y_stat(#/SP*ster*MeV/n)	Y_syst_tot(#/SP*ster*MeV/n)	X_tot(MeV/n)
46.292450	48.083600	49.874750	0.000432805686588	0.000000384446840	0.000245816650341	0.091548583285871
49.927250	51.995300	54.063350	0.000505772433902	0.000000311901384	0.000167885484123	0.361265172208725
54.063350	56.131400	58.199450	0.000581267358146	0.000000209772710	0.000109350003619	0.278553698914590
58.124582	60.430267	62.735952	0.000753305673887	0.000000235364754	0.000111586840156	0.136842313727443
62.810843	65.225633	67.640423	0.000807017698320	0.000000278544940	0.000126623603341	0.350824526158021
67.574342	70.265467	72.956592	0.000855547708986	0.000000357101496	0.000148824074157	0.157311239243037
72.953845	75.810100	78.666355	0.000903608985161	0.000000408903672	0.000164060472874	0.257606363068073
78.735197	81.868967	85.002737	0.000973004250293	0.000000451293175	0.000166086667541	0.237400742345090
84.985080	88.470500	91.955920	0.001033419853001	0.000000482437198	0.000163584241570	0.212831817771686
91.920303	95.745533	99.570763	0.001083262166530	0.000000493672602	0.000153027582586	0.201838182965488
99.560740	103.814000	108.067260	0.001142118526891	0.000000411447326	0.000111423289932	0.193929741710497
108.043737	112.820667	117.597597	0.001144302044686	0.000000438551742	0.000106033681540	0.203303968913546
117.573382	122.899667	128.225952	0.001198018003267	0.000000460118465	0.000100843364745	0.197911292601003
128.222793	134.277333	140.331873	0.001186385900733	0.000000491537530	0.000095719320035	0.160110208840317
140.289100	147.225000	154.160900	0.001166375038451	0.000000504578133	0.000086838985720	0.129682381453843
154.127193	162.103333	170.079473	0.001353379042847	0.000000584713940	0.000090121819417	0.132356842526898
170.035428	179.318333	188.601238	0.001381012703509	0.000000630854017	0.000084974348978	0.087454689491073
188.520483	199.479333	210.438183	0.001991056978653	0.000000809908382	0.000099297539162	0.031581073224695
210.324295	223.413000	236.501705	0.001845007641013	0.000000818594296	0.000088947345661	0.059774616641514
236.358940	252.250000	268.141060	0.000506171429255	0.000000475026121	0.000036813998325	0.147938123145118
268.603500	274.687000	280.770500	0.000040365585742	0.000000074616600	0.000004347370000	0.117750000000000

Table A.IV.24. Helium-3 Yields from Iron 400 MeV/n on 20 g/cm^2 Aluminium at 7.20 deg

KE_left(MeV/n)	KE_mid(MeV/n)	KE_right(MeV/n)	Norm_Cts(#/SP*ster*MeV/n)	Y_stat(#/SP*ster*MeV/n)	Y_syst_tot(#/SP*ster*MeV/n)	X_tot(MeV/n)
46.367070	48.126300	49.885530	0.000851934034233	0.000000397282343	0.000256461347665	0.120732148454337
49.877760	51.959800	54.041840	0.000942116255442	0.000000351380651	0.000190740645902	0.310740161433053
54.049585	56.139400	58.229215	0.000945190674058	0.000000264050806	0.000138758632089	0.288282650771773
58.138698	60.419633	62.700568	0.000850484415371	0.000000254020002	0.000121975683987	0.117778823459270
62.791050	65.227800	67.664550	0.000801038177444	0.000000264661690	0.000118600633536	0.350015690382588
67.586083	70.262033	72.937983	0.000979896584496	0.000000301801905	0.000124858226103	0.143355545614985
72.961480	75.809200	78.656920	0.001067717793696	0.000000378068148	0.000149297704628	0.265615181984841
78.711893	81.867533	85.023173	0.001182310699555	0.000000455726772	0.000167575850025	0.236787986667398
84.979930	88.461500	91.943070	0.001287058544109	0.000000552248427	0.000191935840593	0.200290133197444
91.919545	95.744500	99.569455	0.001378839435256	0.000000583898146	0.000186859212184	0.198408753962848
99.570902	103.809667	108.048432	0.001524711525823	0.000000500468990	0.000139217801254	0.186459564153143
108.031958	112.815333	117.598708	0.001599195264995	0.000000519144705	0.000129328014996	0.194733918127891
117.577255	122.899000	128.220745	0.001889930597049	0.000000593385438	0.000136469440378	0.197601476642357
128.213250	134.278000	140.342750	0.001952935733739	0.000000637087401	0.000131483013709	0.160856334001400
140.292670	147.221000	154.149330	0.002205377987566	0.000000709703602	0.000132529606599	0.122505485954303
154.119435	162.101000	170.082565	0.002417764397835	0.000000791403550	0.000133219858144	0.128061707306009
170.031910	179.315000	188.598090	0.002620276650443	0.000000868225953	0.000130635506145	0.081144802568618
188.520157	199.478667	210.437177	0.003931415552265	0.000001131266573	0.000164744385575	0.033231517760044
210.324683	223.412333	236.499983	0.004490158931428	0.000001303152218	0.000182452550058	0.062000496432287
236.675285	246.901000	257.126715	0.001197536357109	0.000000590828098	0.000052246506111	0.103685448943861

Table A.V.1. Deuteron Yields from Iron 400 MeV/n on 40 g/cm^2 Aluminium at 12.7 deg

KE_left(MeV/n)	KE_mid(MeV/n)	KE_right(MeV/n)	Norm_Cts(#/SP*ster*MeV/n)	Y_stat(#/SP*ster*MeV/n)	Y_syst_tot(#/SP*ster*MeV/n)	X_tot(MeV/n)
45.814453	47.081633	48.348814	0.001069979669627	0.000000189781426	0.000179290813577	0.151099460053867
48.256322	49.689100	51.121878	0.001147083034463	0.000000222144291	0.000191268237802	0.157040319793007
51.214370	52.817300	54.420230	0.001181968671000	0.000000230472472	0.000176089563388	0.262631059522670
54.420237	56.023167	57.626097	0.001217786913600	0.000000251055386	0.000198991596762	0.185582495267442
57.546020	59.358200	61.170380	0.001283264423538	0.000000272248983	0.000195633626194	0.142725392736892
61.250460	63.190500	65.130540	0.001446384579072	0.000000278570240	0.000187480425360	0.300496900158720
65.042010	67.134400	69.226790	0.001594159715985	0.000000304200842	0.000194207569711	0.086793108221909
69.315310	71.595100	73.874890	0.001565240534440	0.000000316634827	0.000187358679225	0.260885611782252
73.804473	76.330933	78.857393	0.001559270929213	0.000000333534290	0.000182389388434	0.085684000828043
78.855465	81.579800	84.304135	0.001706570404403	0.000000354233594	0.000183270016192	0.151232985013998
84.347415	87.347400	90.347385	0.001960605974989	0.000000393212967	0.000194307046771	0.108783210935971
90.362400	93.700000	97.037600	0.002267633726146	0.000000448379649	0.000212275860674	0.071314929433044
97.006380	100.733300	104.460220	0.002194389397083	0.000000500177739	0.000225609915033	0.060950043918688
104.426060	108.587000	112.747940	0.001941669287107	0.000000508288206	0.000209074782092	0.048617085352168
112.733558	117.368333	122.003108	0.001636480357783	0.000000443736255	0.000152529684437	0.040703854314937
121.983343	127.255333	132.527323	0.001141772851209	0.000000375509473	0.000105259043266	0.100742066382470
132.486852	138.464667	144.442482	0.000483916553429	0.000000258295722	0.000056453677882	0.158835715221514
144.427185	151.266000	158.104815	0.000180136282610	0.000000164721818	0.000028628873261	0.241607675892137
158.069105	166.003000	173.936895	0.000128003450519	0.000000150824436	0.000022033341904	0.346578855559597
173.884868	183.126333	192.367798	0.000054991368316	0.000000099218963	0.000012008003861	0.502020382090210
192.305308	203.240333	214.175358	0.000027381111881	0.000000071762152	0.000007146227749	0.657410423380250
214.065563	227.165333	240.265103	0.000016162829744	0.000000060387368	0.000004840825466	0.903763533553440
240.119965	256.063000	272.006035	0.000011498492878	0.000000054395594	0.000003726173265	1.205374333392328
271.783217	291.586667	311.390117	0.000003917715619	0.000000037340741	0.000002040759026	1.647524628192246
311.051950	336.286000	361.520050	0.000003386752633	0.000000039071837	0.000001733575222	2.287752542518530

Table A.V.2. Deuteron Yields from Iron 400 MeV/n on 40 g/cm^2 Aluminium at 10.0 deg

KE_left(MeV/n)	KE_mid(MeV/n)	KE_right(MeV/n)	Norm_Cts(#/SP*ster*MeV/n)	Y_stat(#/SP*ster*MeV/n)	Y_syst_tot(#/SP*ster*MeV/n)	X_tot(MeV/n)
44.089655	45.384467	46.679279	0.001329246447233	0.000000214217676	0.000201566497301	0.216103044650000
46.679288	47.974100	49.268912	0.001436721546300	0.000000265765345	0.000262051422959	0.189120551884241
49.182206	50.663700	52.145194	0.001536291266876	0.000000282098783	0.000249841307207	0.154369635186781
52.231908	53.861733	55.491558	0.001630980093300	0.000000298538521	0.000243000028883	0.219355779271940
55.491542	57.121367	58.751192	0.001728109366800	0.000000287122988	0.000235253392688	0.135069444387137
58.687055	60.573200	62.459345	0.001908570291865	0.000000320217497	0.000236799117319	0.213011307136898
62.523487	64.489867	66.456247	0.002045466517215	0.000000330660076	0.000231435032566	0.220880134736015
66.377312	68.559267	70.741222	0.002015600976949	0.000000346271236	0.000225827681091	0.101862736170624
70.820138	73.125833	75.431528	0.002224742607927	0.000000378636055	0.000240305271598	0.231167052532233
75.409432	78.036067	80.662702	0.002156771530356	0.000000397883500	0.000227454491978	0.132080897404135
80.591658	83.424333	86.257008	0.002379072715881	0.000000422820492	0.000228522667357	0.122383296345539
86.271452	89.386267	92.501082	0.002315668399179	0.000000433885813	0.000218559991410	0.109451129082938
92.503602	95.961467	99.419332	0.002625704370596	0.000000491328688	0.000234930648790	0.056193619880107
99.406762	103.258667	107.110572	0.003013059201771	0.000000607465981	0.000294717227988	0.048562875191961
107.108467	111.398667	115.688867	0.003260300252118	0.000000609277631	0.000266468406947	0.019426744282378
115.661652	120.513667	125.365682	0.003368565208284	0.000000631228826	0.000254651364579	0.101551409896909
125.360470	130.832000	136.303530	0.003469751106097	0.000000689356551	0.000260140509281	0.110692901357433
136.280580	142.538000	148.795420	0.002243055363838	0.000000583619637	0.000175841497449	0.188452013739015
148.765590	155.953000	163.140410	0.002277050160403	0.000000645887201	0.000175839842234	0.257551124437460
163.075360	171.412000	179.748640	0.002188689055550	0.000000684904509	0.000167158596402	0.408763910629351
179.710050	189.472000	199.233950	0.001699877261790	0.000000643833680	0.000132374492656	0.536328127402433
199.152507	210.752667	222.352827	0.001344854296532	0.000000619502336	0.000103365230341	0.713970156839906
222.232157	236.190667	250.149177	0.000706749840696	0.000000486317486	0.000063622785589	0.964486523821354
249.997100	267.090000	284.182900	0.000165093625256	0.000000252035661	0.000019148051379	1.294326316622667
283.933400	305.349000	326.764600	0.000080628125607	0.000000196959559	0.000011198924338	1.760349138927844
326.350300	353.913000	381.475700	0.000032052429847	0.000000142227086	0.000005927368661	2.464676921099396

Table A.V.3. Deuteron Yields from Iron 400 MeV/n on 40 g/cm^2 Aluminium at 7.20 deg

KE_left(MeV/n)	KE_mid(MeV/n)	KE_right(MeV/n)	Norm_Cts(#/SP*ster*MeV/n)	Y_stat(#/SP*ster*MeV/n)	Y_syst_tot(#/SP*ster*MeV/n)	X_tot(MeV/n)
45.807571	47.120767	48.433963	0.001839344816500	0.000000268432835	0.000262507924107	0.215381155522019
48.417592	49.747167	51.076742	0.001881883142284	0.000000299727148	0.000299246619032	0.221748149872237
51.093165	52.740900	54.388635	0.001924073544400	0.000000337400536	0.000286185374127	0.136271980088535
54.388565	56.036300	57.684035	0.001966437908350	0.000000341908777	0.000290186196421	0.194210978139265
57.612817	59.362267	61.111717	0.002057823515516	0.000000350622997	0.000282557359014	0.070178841468871
61.182985	63.166900	65.150815	0.002333432642017	0.000000362547803	0.000260199701952	0.252905936001906
65.089830	67.143600	69.197370	0.002391166373338	0.000000375625998	0.000264957353002	0.117043489158347
69.258340	71.581300	73.904260	0.002688303888967	0.000000418439645	0.000276749013169	0.239491254154906
73.812012	76.315267	78.818522	0.002741939713847	0.000000444250776	0.000277882152210	0.065579965836069
78.864455	81.576600	84.288745	0.003277652950772	0.000000495928035	0.000303115360683	0.169027817535576
84.335093	87.348233	90.361373	0.003504757750897	0.000000533860424	0.000307780077206	0.114626416487126
90.343960	93.692100	97.040240	0.003409495191644	0.000000555513082	0.000295677749953	0.056111266222212
97.021613	100.728833	104.436053	0.003995504360761	0.000000671522684	0.000365714941495	0.029529174949131
104.402820	108.574000	112.745180	0.004231288362334	0.000000699594759	0.000352478649545	0.040361930701002
112.711522	117.359667	122.007812	0.004820567016625	0.000000742993944	0.000351869092387	0.068286345744247
121.979478	127.244333	132.509188	0.005450189073163	0.000000851994662	0.000387585430463	0.126852599998860
132.485455	138.464000	144.442545	0.004253842843075	0.000000800339860	0.000307216860066	0.161959390099741
144.428082	151.273667	158.119252	0.003550514263943	0.000000786228557	0.000262126025961	0.229665246029956
158.067548	165.999333	173.931118	0.003308016343039	0.000000811347483	0.000241538110976	0.352957209679870
173.882023	183.129333	192.376643	0.002913267422116	0.000000823002250	0.000212115584274	0.496712620074224
192.319105	203.257000	214.194895	0.002361844445213	0.000000807491285	0.000171058527473	0.628552730813414
214.088390	227.192000	240.295610	0.001294585594965	0.000000650954058	0.000106936988518	0.856836803384985
240.153453	256.104333	272.055213	0.000201918720989	0.000000280945749	0.000023817426016	1.133640473249346
271.834833	291.648333	311.461833	0.000078856414930	0.000000188921582	0.000011352066991	1.540103284163111
311.122033	336.377333	361.632633	0.000025680945732	0.000000113778051	0.000005225691863	2.128869145767301
361.049483	394.315333	427.581183	0.000005606095090	0.000000053209210	0.000001760853999	3.040763411480742

Table A.V.4. Deuteron Yields from Iron 400 MeV/n on 40 g/cm^2 Aluminium at 32.7 deg

KE_left(MeV/n)	KE_mid(MeV/n)	KE_right(MeV/n)	Norm_Cts(#/SP*ster*MeV/n)	Y_stat(#/SP*ster*MeV/n)	Y_syst_tot(#/SP*ster*MeV/n)	X_tot(MeV/n)
44.570465	45.987100	47.403734	0.000204745304693	0.000000090519575	0.000068705135436	0.170829265306182
47.403732	48.820367	50.237001	0.000161406842329	0.000000069371250	0.000052885657847	0.594511227730814
50.236999	51.653633	53.070268	0.000170402682573	0.000000076926958	0.000058328177828	0.366810506518502
52.996372	54.661767	56.327162	0.000182998743432	0.000000086504167	0.000056017158735	0.076384125113403
56.401058	58.170533	59.940008	0.000181982451320	0.000000089336583	0.000054633530124	0.295377276851148
59.900402	61.709467	63.518532	0.000153050202394	0.000000074422625	0.000044455166339	0.327106061884964
63.558137	65.681267	67.804397	0.000181742789734	0.000000091561434	0.000046950262373	0.202176802583679
67.761063	69.927533	72.094003	0.000239570162747	0.000000104159622	0.000053203753611	0.233851168179678
72.137338	74.616433	77.095528	0.000180526583761	0.000000099858780	0.000044051718117	0.226545358453887
76.998240	79.664600	82.330960	0.000186435433100	0.000000104458426	0.000043350522645	0.200494502975742
82.364678	85.272633	88.180588	0.000210269508072	0.000000117039488	0.000044183481476	0.156489253044738
88.222265	91.446100	94.669935	0.000177353355987	0.000000111523550	0.000038046757312	0.196763054583832
94.662512	98.261967	101.861422	0.000197310737748	0.000000126181686	0.000038715128076	0.158736933101311
101.821033	105.846333	109.871633	0.000193035136704	0.000000129816777	0.000035803213205	0.114694296688469
109.841200	114.336000	118.830800	0.000155446888443	0.000000118208889	0.000029297826415	0.067496139384857
118.803298	123.859333	128.915368	0.000214819570564	0.000000155050934	0.000034441194244	0.029409245189735
128.923285	134.661000	140.398715	0.000258081632201	0.000000286263286	0.000064480898671	0.091975349862341
140.364630	146.950000	153.535370	0.000300549015857	0.000000393671207	0.000085199892025	0.169115275160495
153.504985	161.082000	168.659015	0.000265356804087	0.000000219498758	0.000034722018578	0.259132922420136
168.612585	177.436000	186.259415	0.000163359419391	0.000000184847839	0.000024126244105	0.416060726727481
186.183517	196.584667	206.985817	0.000085616693867	0.000000137923418	0.000014883071072	0.618136350082245
206.896553	219.281333	231.666113	0.000116433300596	0.000000184401371	0.000017358907825	0.853234472550776
231.535635	246.559000	261.582365	0.000017972545749	0.000000071929867	0.000005417800789	1.190730936580972
261.382000	279.919000	298.456000	0.000004913037393	0.000000040567284	0.000002382244785	1.643374366833376
313.022200	329.276000	345.529800	0.000001140274408	0.000000022310540	0.000000952858598	1.969513515668273
345.841050	355.079000	364.316950	0.000000694298726	0.000000013420300	0.000000508512000	1.646910000000000

Table A.V.5. Deuteron Yields from Iron 400 MeV/n on 40 g/cm^2 Aluminium at 30.0 deg

KE_left(MeV/n)	KE_mid(MeV/n)	KE_right(MeV/n)	Norm_Cts(#/SP*ster*MeV/n)	Y_stat(#/SP*ster*MeV/n)	Y_syst_tot(#/SP*ster*MeV/n)	X_tot(MeV/n)
44.729169	45.968833	47.208498	0.000211221340537	0.000000085529992	0.000077488906433	0.112333805943990
47.274373	48.782533	50.290693	0.000248869838680	0.000000097186945	0.000070047604247	0.556255973589498
50.290673	51.798833	53.306993	0.000272892377107	0.000000099858780	0.000072342750287	0.584495427443192
53.306973	54.815133	56.323293	0.000224882116600	0.000000094119511	0.000067518526348	0.287973424614772
56.310060	58.154400	59.998740	0.000237296124338	0.000000098904376	0.000058946374566	0.302019493833180
60.012000	61.869600	63.727200	0.000280554598709	0.000000107517680	0.000063734859946	0.561220150302891
63.637590	65.694300	67.751010	0.000266073844501	0.000000107807168	0.000057724797330	0.220053850906909
67.840605	70.049100	72.257595	0.000252484123463	0.000000117668887	0.000058679139106	0.448844181085151
72.182913	74.638833	77.094753	0.000226843668791	0.000000120987714	0.000054721310360	0.269157134794900
77.108197	79.734967	82.361737	0.000272950949001	0.000000129612080	0.000054968884077	0.301451016362526
82.422920	85.342400	88.261880	0.000253574841984	0.000000133032187	0.000050523531441	0.259895429036372
88.228945	91.477200	94.725455	0.000245175397129	0.000000134584971	0.000046243950477	0.233230191321793
94.695652	98.277467	101.859282	0.000262664704184	0.000000145539933	0.000045667633087	0.181238722443219
101.861210	105.846000	109.830790	0.000297741943460	0.000000162909623	0.000046345062517	0.116563270366141
109.812337	114.319667	118.826997	0.000219392065088	0.000000141256595	0.000035418192682	0.053340554581388
118.812068	123.832333	128.852598	0.000171928779828	0.000000133274640	0.000029818601466	0.078320595106843
128.842575	134.587000	140.331425	0.000094244901868	0.000000106092277	0.000020058877188	0.215728707907895
140.292203	146.834333	153.376463	0.000078646639092	0.000000108289829	0.000017964349820	0.361711601399513
153.335240	160.904000	168.472760	0.000038694566200	0.000000069648930	0.000010010714638	0.569608425172065
168.519860	174.223000	179.926140	0.000008418674884	0.000000028393462	0.000003488913362	0.664208052652932
185.920345	196.260000	206.599655	0.000006293505154	0.000000036829222	0.000003842737406	1.180314400359921
206.500898	218.822333	231.143768	0.000002608501346	0.000000026754563	0.000002327915092	1.651284019173261
231.031787	245.955667	260.879547	0.000001547485012	0.000000021227160	0.000001493453660	2.240140375088133
261.298000	266.992000	272.686000	0.000002099221548	0.000000017693000	0.000001088870000	1.587180000000000

Table A.V.6. Deuteron Yields from Iron 400 MeV/n on 40 g/cm^2 Aluminium at 27.2 deg

KE_left(MeV/n)	KE_mid(MeV/n)	KE_right(MeV/n)	Norm_Cts(#/SP*ster*MeV/n)	Y_stat(#/SP*ster*MeV/n)	Y_syst_tot(#/SP*ster*MeV/n)	X_tot(MeV/n)
45.743055	46.990000	48.236946	0.000306435334413	0.000000091746423	0.000080457911696	0.372442788805207
48.156523	49.624867	51.093210	0.000360715943970	0.000000121083034	0.000090133857564	0.376130934081471
51.173622	52.767567	54.361512	0.000337512257293	0.000000115759901	0.000080132934169	0.419452778202744
54.361522	55.955467	57.549412	0.000404926334493	0.000000126181727	0.000088202782543	0.348993578665855
57.470487	59.290967	61.111447	0.000377653094799	0.000000137923418	0.000084389496081	0.314059388833211
61.190362	63.131767	65.073172	0.000380823805509	0.000000136721273	0.000078411079981	0.466197928285830
64.985425	67.073600	69.161775	0.000314387249994	0.000000129487427	0.000069760693542	0.215041003493659
69.249500	71.540300	73.831100	0.000314544521042	0.000000133594653	0.000064947206236	0.446368249303196
73.751503	76.273633	78.795763	0.000369546868167	0.000000153810845	0.000069332299894	0.223888842754613
78.810912	81.528667	84.246422	0.000339139011571	0.000000142559358	0.000059595974955	0.305221879095339
84.310865	87.310700	90.310535	0.000365695794773	0.000000164887957	0.000062279587662	0.247270069056083
90.306302	93.663067	97.019832	0.000316951189334	0.000000160163885	0.000054085042459	0.185603610542037
96.994243	100.706033	104.417823	0.000353120817171	0.000000171432239	0.000053147551428	0.138935766470625
104.379693	108.556333	112.732973	0.000310609451579	0.000000167782476	0.000046180983442	0.093754825139883
112.697167	117.356667	122.016167	0.000365159279457	0.000000194264920	0.000048601997936	0.067059983198104
121.979875	127.247000	132.514125	0.000330739710076	0.000000198288233	0.000044345516635	0.161772206142464
132.497368	138.483333	144.469298	0.000241248957263	0.000000180551679	0.000034957143360	0.261134531935169
144.453767	151.316667	158.179567	0.000200474830400	0.000000173275234	0.000029262803633	0.401580556437933
158.115818	166.053333	173.990848	0.000167008893377	0.000000172139022	0.000024685533115	0.671276226980369
173.941572	183.210667	192.479762	0.000158782810555	0.000000181958960	0.000022483836275	0.939723624759429
192.425395	203.380000	214.334605	0.000227269034277	0.000000230053664	0.000026051631478	1.263068096000370
214.235808	227.357333	240.478858	0.000041019273921	0.000000096901277	0.000008496248486	1.725341582298705
240.333460	256.313000	272.292540	0.000005637698576	0.000000037402470	0.000002523269471	2.370919818699063
278.846750	292.106000	305.365250	0.000003179961414	0.000000028393462	0.000001492854513	2.648301454234393
312.429450	320.161000	327.892550	0.000000834112737	0.000000013420300	0.000000607590000	2.308690000000000

Table A.V.7. Proton Yields from Iron 400 MeV/n on 40 g/cm^2 Aluminium at 12.7 deg

KE_left(MeV/n)	KE_mid(MeV/n)	KE_right(MeV/n)	Norm_Cts(#/SP*ster*MeV/n)	Y_stat(#/SP*ster*MeV/n)	Y_syst_tot(#/SP*ster*MeV/n)	X_tot(MeV/n)
44.986722	46.688667	48.390612	0.002101870032183	0.000000336228835	0.000273538304113	0.186006640309318
48.390622	50.092567	51.794512	0.002191635389417	0.000000342448235	0.000281757499295	0.344803931788778
51.750212	53.496467	55.242722	0.002368834064891	0.000000367246536	0.000298527279480	0.268656915669409
55.287007	57.391567	59.496127	0.002418085258633	0.000000407604445	0.000289719778155	0.271103400681364
59.496107	61.600667	63.705227	0.002816555252673	0.000000427280461	0.000315530382919	0.284862152470278
63.599730	65.930800	68.261870	0.002709089717425	0.000000443845320	0.000301846252940	0.243593803305523
68.367400	70.879300	73.391200	0.002781360047333	0.000000469187112	0.000302242371346	0.351643303185202
73.294113	76.062133	78.830153	0.002961422534583	0.000000508839595	0.000312015525064	0.225860552906965
78.891803	81.849633	84.807463	0.003557631476534	0.000000577718936	0.000354026911329	0.312011861550166
84.842887	88.179067	91.515247	0.003742270565800	0.000000624308995	0.000360494269167	0.315961004992705
91.443405	95.120800	98.798195	0.004384448536556	0.000000716415811	0.000407874617036	0.230776460994725
98.787122	102.854667	106.922212	0.004905251697128	0.000000782741324	0.000433324710972	0.241725315442963
106.929063	111.456333	115.983603	0.004031106710404	0.000000749553344	0.000360499742595	0.226847979018990
115.969408	121.128333	126.287258	0.003526760084450	0.000000734634420	0.000309996780609	0.234181445355946
126.248927	132.029667	137.810407	0.002368679945100	0.000000631356793	0.000215435565330	0.182757642625445
137.797952	144.417667	151.037382	0.001473822720983	0.000000524365146	0.000136009310118	0.160154483859803
150.983113	158.619333	166.255553	0.001013016627569	0.000000460245316	0.000097336126819	0.091173433972512
166.193435	175.045000	183.896565	0.000550494661196	0.000000357043490	0.000059394992994	0.014490817837320
183.833235	194.240000	204.646765	0.000234584988912	0.000000245831190	0.000030598947196	0.092008957646579
204.582267	216.966667	229.351067	0.000047535246915	0.000000113403415	0.000010353562476	0.188506859786826
229.224692	244.224667	259.224642	0.000030627181464	0.000000101086366	0.000007313104169	0.362116255422206
259.028967	277.502667	295.976367	0.000018900856271	0.000000081274307	0.000004874281251	0.607888139755992
295.671617	318.994667	342.317717	0.000009490959881	0.000000069648930	0.000003194710462	0.964893104390326
341.834983	372.158333	402.481683	0.000003395853688	0.000000047904674	0.000001759140807	1.484326710128872

Table A.V.8. Proton Yields from Iron 400 MeV/n on 40 g/cm^2 Aluminium at 10.0 deg

KE_left(MeV/n)	KE_mid(MeV/n)	KE_right(MeV/n)	Norm_Cts(#/SP*ster*MeV/n)	Y_stat(#/SP*ster*MeV/n)	Y_syst_tot(#/SP*ster*MeV/n)	X_tot(MeV/n)
45.992980	47.746300	49.499620	0.002691973862983	0.000000388251960	0.000326269789769	0.159983046566544
49.499647	51.252967	53.006287	0.003286991041167	0.000000427280461	0.000378611165928	0.381781585263093
52.978120	54.759600	56.541080	0.003461959430385	0.000000446680546	0.000394683601105	0.370762217778511
56.569285	58.725100	60.880915	0.003270792485720	0.000000477495532	0.000360564959419	0.187516522440024
60.880885	63.036700	65.192515	0.003860762093737	0.000000512744271	0.000405244979944	0.270872431027966
65.095688	67.503433	69.911178	0.004013365714158	0.000000551017094	0.000411367997333	0.256555487530476
70.008022	72.570667	75.133312	0.004319890749837	0.000000593328093	0.000432156081817	0.283741678611021
75.053520	77.923500	80.793480	0.004410931257248	0.000000635210824	0.000433245719962	0.284709558743643
80.792528	83.869633	86.946738	0.004846196622054	0.000000682768186	0.000454744476946	0.221626089221215
87.021905	90.413500	93.805095	0.005132443097907	0.000000741722789	0.000472663657539	0.308930955647051
93.810502	97.613767	101.417032	0.005135259651700	0.000000776772854	0.000462274798856	0.258372471706817
101.378747	105.609667	109.840587	0.006134623260779	0.000000891781556	0.000528094431210	0.228634265784921
109.794355	114.555000	119.315645	0.006337579511166	0.000000959945684	0.000538847315748	0.222438516372502
119.285645	124.606000	129.926355	0.006589201876582	0.000001022795806	0.000537318990565	0.193062008436771
129.901022	135.970667	142.040312	0.007978290635536	0.000001201210317	0.000629903958226	0.164721968179141
141.999652	148.925667	155.851682	0.009073611116798	0.000001353553161	0.000697245645807	0.117320836939991
155.808592	163.808667	171.808742	0.008353533911974	0.000001379166097	0.000626446357440	0.043141818914598
171.774052	181.108667	190.443282	0.008587108304913	0.000001487856558	0.000616692423817	0.027260351023785
190.368115	201.373000	212.377885	0.009009142720096	0.000001657850065	0.000647390678513	0.137120101684691
212.283662	225.478667	238.673672	0.006609748736373	0.000001567380813	0.000485271127476	0.249916069523350
238.519448	254.552333	270.585218	0.003968683696385	0.000001333671079	0.000295356127739	0.444472981361072
270.368233	290.284333	310.200433	0.002148785092080	0.000001081577057	0.000168626202820	0.710135906106711
309.851883	335.209333	360.566783	0.000354275326309	0.000000487039327	0.000036791617147	1.094138315125195
359.987117	393.382667	426.778217	0.000039030107357	0.000000176905257	0.000006589718401	1.682723555489730

Table A.V.9. Proton Yields from Iron 400 MeV/n on 40 g/cm^2 Aluminium at 7.20 deg

KE_left(MeV/n)	KE_mid(MeV/n)	KE_right(MeV/n)	Norm_Cts(#/SP*ster*MeV/n)	Y_stat(#/SP*ster*MeV/n)	Y_syst_tot(#/SP*ster*MeV/n)	X_tot(MeV/n)
44.752458	46.478333	48.204208	0.003071822389201	0.000000413460144	0.000362371111836	0.235784571784966
48.265923	50.053533	51.841143	0.003654976001650	0.000000460895318	0.000411903991742	0.290233470912660
51.841157	53.628767	55.416377	0.004287887676650	0.000000495093461	0.000465812474050	0.499088486823729
55.304975	57.292600	59.280225	0.004361446229760	0.000000534233205	0.000467573048209	0.172615699686587
59.391630	61.581600	63.771570	0.004567586592753	0.000000562748904	0.000464016432305	0.251134517750946
63.726330	65.961500	68.196670	0.005083572786731	0.000000600866897	0.000506087974844	0.256209346734267
68.241893	70.838333	73.434773	0.005231547617297	0.000000656843637	0.000507532938100	0.279079232545168
73.350820	76.062500	78.774180	0.005803141311436	0.000000712222663	0.000554555122344	0.191936376926861
78.858143	81.864233	84.870323	0.006168549236910	0.000000768972615	0.000569307852162	0.311037057235951
84.798362	88.139467	91.480572	0.006763224629622	0.000000848399024	0.000606409544195	0.275171171854248
91.449198	95.114633	98.780068	0.007038225256451	0.000000908181616	0.000623442746902	0.217927924534787
98.773522	102.842667	106.911812	0.007418698716789	0.000000969355776	0.000631088427690	0.235352902674601
106.925003	111.461333	115.997663	0.008026660683666	0.000001062658323	0.000673645511269	0.239769454495355
115.965145	121.092000	126.218855	0.009052970799087	0.000001191885008	0.000732726651838	0.172444700417989
126.229863	132.016333	137.802803	0.010864056382320	0.000001385221298	0.000858790289648	0.164824654778829
137.785598	144.408333	151.031068	0.014795717146158	0.000001700450804	0.001112598063948	0.140321547617926
150.968865	158.601000	166.233135	0.012957938888837	0.000001699381793	0.000973201973325	0.058455330124378
166.198847	175.047667	183.896487	0.013817705126350	0.000001848444552	0.000991996651496	0.021189829574822
183.818130	194.237000	204.655870	0.015036435977847	0.000002093500002	0.001064787212916	0.102304660692414
204.564638	216.954333	229.344028	0.010689393107173	0.000001935670208	0.000791456358818	0.209220206950500
229.228832	244.219667	259.210502	0.004786315083158	0.000001417331917	0.000361433349117	0.371061363677223
259.016817	277.503667	295.990517	0.002035245598097	0.000001013600774	0.000160892890693	0.605363657221839
295.686567	319.012667	342.338767	0.000474886674345	0.000000536281325	0.000046602009455	0.932040041176880
341.855517	372.194667	402.533817	0.000037687933428	0.000000161760931	0.000006470145314	1.420277471774442

Table A.V.10. Proton Yields from Iron 400 MeV/n on 40 g/cm^2 Aluminium at 32.7 deg

KE_left(MeV/n)	KE_mid(MeV/n)	KE_right(MeV/n)	Norm_Cts(#/SP*ster*MeV/n)	Y_stat(#/SP*ster*MeV/n)	Y_syst_tot(#/SP*ster*MeV/n)	X_tot(MeV/n)
44.908720	46.414300	47.919880	0.000675454149622	0.000000168628109	0.000128933965310	0.298601851337194
47.823103	49.596733	51.370363	0.000601819654167	0.000000174696919	0.000116067100768	0.305085725862421
51.467165	53.391500	55.315835	0.000589243559118	0.000000179461467	0.000108139770391	0.419197332446188
55.315832	57.240167	59.164502	0.000762868492798	0.000000206750978	0.000127572149521	0.318625887204728
59.050317	61.200767	63.351217	0.000677289343802	0.000000213158919	0.000117551995659	0.189763553552441
63.465397	65.816167	68.166937	0.000713875364986	0.000000219058991	0.000111896913459	0.526682928366774
68.078087	70.552367	73.026647	0.000721844778701	0.000000226245850	0.000111146856519	0.193648052815565
73.115493	75.895233	78.674973	0.000710935981261	0.000000234319943	0.000103574634824	0.458260558749059
78.563350	81.583400	84.603450	0.000787623757705	0.000000264448077	0.000109379560612	0.237859718105021
84.645363	87.926133	91.206903	0.000824169563204	0.000000281638894	0.000108720133520	0.370232438083550
91.276607	94.921967	98.567327	0.000755622924960	0.000000285893331	0.000099431992838	0.332528678518109
98.563328	102.648433	106.733538	0.000844339616103	0.000000321374018	0.000102739580735	0.290279060838015
106.671987	111.262667	115.853347	0.000771843782663	0.000000320005939	0.000091722316445	0.281606939349868
115.810032	120.957667	126.105302	0.000843529844136	0.000000345709158	0.000091994339914	0.293382312708179
126.069113	131.870333	137.671553	0.000777865038194	0.000000363514508	0.000085981055591	0.210698057169234
137.667163	144.300333	150.933503	0.000693540962447	0.000000375041888	0.000080139348229	0.194635746102919
150.883125	158.540000	166.196875	0.000727027522303	0.000000386396560	0.000071748302172	0.109276066810395
166.143933	175.023333	183.902733	0.000786346988277	0.000000427067439	0.000071615820617	0.016171229730914
183.832982	194.285667	204.738352	0.000559345175526	0.000000383731239	0.000053036002516	0.124373199524737
204.656313	217.099333	229.542353	0.000336215817718	0.000000324487844	0.000035406012064	0.285727812975916
229.426902	244.483667	259.540432	0.000190513444467	0.000000270953535	0.000023302530439	0.516044776446773
259.340133	277.931333	296.522533	0.000041046110412	0.000000133744052	0.000008386669060	0.841919242118863
296.224167	319.686667	343.149167	0.000005298900411	0.000000052714102	0.000002482157368	1.310812837312025
362.444000	372.584000	382.724000	0.000000517280351	0.000000011728200	0.000000404864000	1.141290000000000

Table A.V.11. Proton Yields from Iron 400 MeV/n on 40 g/cm^2 Aluminium at 30.0 deg

KE_left(MeV/n)	KE_mid(MeV/n)	KE_right(MeV/n)	Norm_Cts(#/SP*ster*MeV/n)	Y_stat(#/SP*ster*MeV/n)	Y_syst_tot(#/SP*ster*MeV/n)	X_tot(MeV/n)
44.956473	46.636533	48.316593	0.000585784339385	0.000000161700236	0.000110821936038	0.691424351993043
48.316573	49.996633	51.676693	0.000645824468017	0.000000174696492	0.000120214908467	0.991981447950515
51.601202	53.368067	55.134932	0.000794537858589	0.000000210693847	0.000140026391455	0.423273263350805
55.210462	57.309667	59.408872	0.000744967030678	0.000000217909651	0.000123505919319	0.437891949150701
59.408895	61.508100	63.607305	0.000721654358192	0.000000210693731	0.000118721288119	0.684490235121729
63.495500	65.823900	68.152300	0.000789491262954	0.000000232010511	0.000119872191922	0.547757988651010
68.264120	70.786700	73.309280	0.000832573004563	0.000000243693201	0.000119618241804	0.583925402890643
73.198155	75.955100	78.712045	0.000903046511469	0.000000273418389	0.000124439252042	0.558598221108875
78.823182	81.771567	84.719952	0.000931687478492	0.000000286014003	0.000123201467264	0.552540278501034
84.710833	88.078633	91.446433	0.000932763015873	0.000000299141336	0.000115920068543	0.614699578059071
91.363042	95.038167	98.713292	0.000934535480107	0.000000316575038	0.000113999548657	0.541614414714934
98.700032	102.772667	106.845302	0.000975771184527	0.000000336778650	0.000111425249128	0.508532367568673
106.854445	111.395000	115.935555	0.000924515840408	0.000000350024717	0.000104856903190	0.507659405709182
115.907473	121.035333	126.163193	0.000925003052834	0.000000368538881	0.000099918180631	0.422839506859281
126.162742	131.965667	137.768592	0.000694930268490	0.000000332937118	0.000077207834173	0.377327129916469
137.741303	144.372333	151.003363	0.000491454158485	0.000000298402774	0.000058200603425	0.314093701097300
150.963263	158.582333	166.201403	0.000290157576473	0.000000234959717	0.000037992278200	0.173281757789013
166.178332	175.045667	183.913002	0.000122663344243	0.000000158653263	0.000020684940625	0.066587693708447
183.835123	194.263333	204.691543	0.000032982402331	0.000000085901339	0.000009222628900	0.163911269032547
204.579567	216.990667	229.401767	0.000007464070896	0.000000038463479	0.000003302281621	0.473206089527597
229.274075	244.281000	259.287925	0.000003358397270	0.000000033523789	0.000002340286553	0.869287581507984
265.395450	277.748500	290.101550	0.000002275387015	0.000000025947078	0.000001537331704	1.173970525684525
296.684500	303.840000	310.995500	0.000000826078010	0.000000013247300	0.000000648041000	1.093740000000000
342.854700	362.130500	381.406300	0.000000578533755	0.000000017692983	0.000000641029690	2.608898741787423

Table A.V.12. Proton Yields from Iron 400 MeV/n on 40 g/cm^2 Aluminium at 27.2 deg

KE_left(MeV/n)	KE_mid(MeV/n)	KE_right(MeV/n)	Norm_Cts(#/SP*ster*MeV/n)	Y_stat(#/SP*ster*MeV/n)	Y_syst_tot(#/SP*ster*MeV/n)	X_tot(MeV/n)
44.781017	46.363733	47.946449	0.000826890163089	0.000000196959390	0.000147574985320	0.217933173619552
48.040828	49.884133	51.727438	0.000794888592878	0.000000210656422	0.000135028961505	0.805162198495434
51.727428	53.570733	55.414038	0.000933949923582	0.000000228401095	0.000149441133276	0.731763001639875
55.385268	57.257333	59.129398	0.000921737097118	0.000000228366972	0.000146842955618	0.372277414505970
59.158188	61.419933	63.681678	0.000858443730034	0.000000244948124	0.000131238665951	0.559806717853582
63.681688	65.943433	68.205178	0.000968194227453	0.000000256218812	0.000139715441269	0.756877531381399
68.119187	70.685067	73.250947	0.001042246152577	0.000000282484893	0.000141667024860	0.422187449340930
73.336947	76.020267	78.703587	0.000969875513377	0.000000277661921	0.000131449471355	0.667707608084557
78.670477	81.744867	84.819257	0.001012690193985	0.000000307927756	0.000129339590655	0.509679476914659
84.737008	88.048133	91.359258	0.001077930147177	0.000000333463439	0.000132461064488	0.553168409551739
91.386902	95.041067	98.695232	0.001076354476368	0.000000343599022	0.000127023018292	0.538286243061255
98.697037	102.774667	106.852297	0.001136252080196	0.000000371158441	0.000125596396278	0.511624336335753
106.834432	111.399667	115.964902	0.001112684373148	0.000000380153655	0.000118654973703	0.519269741156752
115.960103	121.066333	126.172563	0.001125318006165	0.000000408860812	0.000115290682517	0.479408968488284
126.145898	131.971333	137.796768	0.001291389000396	0.000000460420039	0.000122035442419	0.384512296257220
137.753702	144.380667	151.007632	0.001282932361381	0.000000493931840	0.000117591674871	0.329936683401528
150.990333	158.612333	166.234333	0.001090677956763	0.000000473389144	0.000097163846587	0.225598095218023
166.171813	175.047333	183.922853	0.001144320286128	0.000000519852446	0.000095386793487	0.071684161796732
183.877942	194.286667	204.695392	0.000996381806516	0.000000524246367	0.000082356686629	0.117756685627356
204.613105	217.041000	229.468895	0.000554089829522	0.000000427142741	0.000051391041350	0.388621953210315
229.325437	244.351667	259.377897	0.000239205559769	0.000000298486981	0.000026315915617	0.743547580057255
259.198100	277.707000	296.215900	0.000065836853470	0.000000173295821	0.000011349998098	1.237287526471919
295.909200	319.294000	342.678800	0.000006409796251	0.000000056155929	0.000002761874776	1.997824399414523
343.030000	362.335000	381.640000	0.000001154257771	0.000000022102787	0.000000816551321	2.318457752666630

Table A.V.13. Triton Yields from Iron 400 MeV/n on 40 g/cm^2 Aluminium at 12.7 deg

KE_left(MeV/n)	KE_mid(MeV/n)	KE_right(MeV/n)	Norm_Cts(#/SP*ster*MeV/n)	Y_stat(#/SP*ster*MeV/n)	Y_syst_tot(#/SP*ster*MeV/n)	X_tot(MeV/n)
46.035801	47.183800	48.331799	0.000683710772501	0.000000157825844	0.000157153077416	23.025581500755056
48.334913	49.779933	51.224954	0.000726708021107	0.000000173559237	0.000140167722847	0.227634739709562
51.224946	52.669967	54.114987	0.000769743900804	0.000000184848111	0.000150526183471	0.279746394798932
54.074136	55.560033	57.045930	0.000813174414436	0.000000205676695	0.000165091932207	0.080015028357104
57.086785	58.834000	60.581215	0.000855815660199	0.000000210040129	0.000145379017761	0.197842582826853
60.581185	62.328400	64.075615	0.001002655804586	0.000000196790732	0.000134715439359	0.192789445263194
64.054477	66.086267	68.118057	0.001050828432368	0.000000192037042	0.000112382837034	0.135848522424243
68.090075	70.192200	72.294325	0.001097329260453	0.000000209701053	0.000121209214243	0.155349897830800
72.343480	74.706700	77.069920	0.001131948894923	0.000000215210813	0.000109579486440	0.092786095127988
77.001865	79.581500	82.161135	0.001213993313734	0.000000247743066	0.000120339126715	0.061739741731413
82.147147	84.964867	87.782587	0.001341269220490	0.000000282384037	0.000130164770292	0.050545056556329
87.790437	90.903667	94.016897	0.001378464816098	0.000000311702005	0.000134982512008	0.045495033261445
94.010510	97.467900	100.925290	0.001415661452243	0.000000463107283	0.000225349694318	0.035018239570424
100.916487	104.760667	108.604847	0.001363733383646	0.000000550757690	0.000256722143028	0.089035878232879
108.599253	112.899333	117.199413	0.001312920025385	0.000000397571018	0.000140857702279	0.142534717710072
117.199562	122.062667	126.925772	0.000617077401592	0.000000256498363	0.000069242769886	0.171528678943901
126.891298	132.400333	137.909368	0.000124936299527	0.000000119508774	0.000024151679575	0.238656541337127
137.887878	144.161333	150.434788	0.000094437664189	0.000000107700128	0.000019134093901	0.336026977763691
150.395837	157.640667	164.885497	0.000084879914047	0.000000113259642	0.000017261926575	0.442360409599458
164.815730	173.214000	181.612270	0.000027768195387	0.000000059320890	0.000007827789784	0.609521231385749
181.581722	191.434667	201.287612	0.000012486057357	0.000000046093810	0.000004961526912	0.736283596222271
201.203213	212.921333	224.639453	0.000006619031291	0.000000039612649	0.000003551694713	0.959064825549347
224.527875	238.644000	252.760125	0.000011014478169	0.000000053339097	0.000004096790258	1.251620525995000
252.590300	269.938000	287.285700	0.000006453638405	0.000000041376157	0.000002546784109	1.669861240634383
287.030167	308.779667	330.529167	0.000005465994636	0.000000047458421	0.000002349347584	2.253182017325720
330.109833	358.186333	386.262833	0.000001327418549	0.000000028474624	0.000001081382062	3.177163036436752
387.315100	398.583000	409.850900	0.000001765773896	0.000000013420300	0.000000421341000	2.330430000000000

Table A.V.14. Triton Yields from Iron 400 MeV/n on 40 g/cm^2 Aluminium at 10.0 deg

KE_left(MeV/n)	KE_mid(MeV/n)	KE_right(MeV/n)	Norm_Cts(#/SP*ster*MeV/n)	Y_stat(#/SP*ster*MeV/n)	Y_syst_tot(#/SP*ster*MeV/n)	X_tot(MeV/n)
44.508576	45.672333	46.836090	0.000799990852060	0.000000198183392	0.000200821343669	39.267673799322516
46.794158	47.999833	49.205509	0.000842256990571	0.000000245971116	0.000253888963336	0.081516302679725
49.247418	50.710700	52.173981	0.000883554689750	0.000000264561647	0.000228676398828	0.258517709566695
52.173985	53.637267	55.100548	0.000925336608594	0.000000257179708	0.000222468645989	0.193194511544609
55.034637	56.595033	58.155429	0.000967985322398	0.000000239244285	0.000193730754975	0.037229636253125
58.221350	59.986400	61.751450	0.001048274350297	0.000000218351753	0.000152181407572	0.236823778720064
61.705015	63.516500	65.327985	0.001172419116448	0.000000227923289	0.000157526217805	0.145998415691575
65.374438	67.444933	69.515428	0.001263455608353	0.000000244947757	0.000148519601793	0.175707277317959
69.439353	71.634733	73.830113	0.001379090570624	0.000000256102123	0.000148995590193	0.078356228511130
73.906170	76.286700	78.667230	0.001491152673347	0.000000294945409	0.000164513846213	0.113720904711711
78.650433	81.329433	84.008433	0.001734575722911	0.000000319576033	0.000162457519061	0.058968688018388
83.958095	86.880400	89.802705	0.001924281754313	0.000000354745466	0.000172079928474	0.025442004054909
89.793078	93.015433	96.237788	0.002051710616036	0.000000348376733	0.000153135980985	0.026613089287980
96.242072	99.812667	103.383262	0.002215885593321	0.000000614485367	0.000329303435187	0.025998585595492
103.373447	107.361667	111.349887	0.002611328572892	0.000000541029883	0.000245449044351	0.131756963765563
111.346748	115.847333	120.347918	0.002324595853916	0.000000492168747	0.000182949742908	0.121524421823558
120.301160	125.360000	130.418840	0.001019135973208	0.000000346414091	0.000097722028956	0.202664425449954
130.404570	136.154000	141.903430	0.000884445211556	0.000000346423281	0.000083694138445	0.260486038685378
141.888335	148.468000	155.047665	0.001553071970667	0.000000496804010	0.000128623961176	0.329135023806340
154.985307	162.582667	170.180027	0.000446146136390	0.000000275070614	0.000049512733105	0.488364816670898
170.134078	178.983333	187.832588	0.000266666070064	0.000000227054343	0.000031608474662	0.618020890221358
187.785567	198.216667	208.647767	0.000260275717277	0.000000245676117	0.000029816695572	0.760378317279629
208.558960	221.007000	233.455040	0.000191819993575	0.000000230362285	0.000022937241010	0.982074577891618
233.322602	248.413667	263.504732	0.000170242950933	0.000000240121472	0.000019974760228	1.307453494771420
263.319300	281.987000	300.654700	0.000086172488510	0.000000188525259	0.000012221716862	1.730540340727427
300.348050	323.970000	347.591950	0.000036599694801	0.000000138115777	0.000006719222561	2.361628347157952
347.075117	377.902667	408.730217	0.000011604494751	0.000000081243667	0.000003016032965	3.383329152964577

Table A.V.15. Triton Yields from Iron 400 MeV/n on 40 g/cm^2 Aluminium at 7.20 deg

KE_left(MeV/n)	KE_mid(MeV/n)	KE_right(MeV/n)	Norm_Cts(#/SP*ster*MeV/n)	Y_stat(#/SP*ster*MeV/n)	Y_syst_tot(#/SP*ster*MeV/n)	X_tot(MeV/n)
46.069702	47.246000	48.422299	0.000937965538779	0.000000297092043	0.000336034361009	23.066819955252782
48.356506	49.734267	51.112028	0.001028369834260	0.000000345708974	0.000356310952464	0.147579120634492
51.177794	52.653233	54.128672	0.001114599895673	0.000000334616675	0.000317880822687	0.244962142122002
54.128661	55.604100	57.079539	0.001202917074119	0.000000295332336	0.000261844920583	0.078442199952153
57.047037	58.791467	60.535897	0.001291782976802	0.000000268539055	0.000202343463576	0.165987743973373
60.568388	62.345333	64.122278	0.001597256405640	0.000000260469657	0.000186065824291	0.202976206415333
64.062427	66.066767	68.071107	0.001677828700596	0.000000273418822	0.000174977756658	0.117278749406982
68.127588	70.213133	72.298678	0.001947126275788	0.000000289855619	0.000183318298097	0.161408348158742
72.302035	74.694100	77.086165	0.002219660459125	0.000000354260069	0.000207410962550	0.090584492023889
77.005492	79.575767	82.146042	0.002603728460375	0.000000400276299	0.000234710092357	0.088380440947418
82.155487	84.969367	87.783247	0.003097138495918	0.000000439747589	0.000246968498319	0.056296080053028
87.789710	90.903300	94.016890	0.003401130314297	0.000000487184756	0.000262031045722	0.023872804842406
94.009273	97.470333	100.931393	0.003689204747519	0.000000676018290	0.000402902961127	0.021058555650851
100.911818	104.762333	108.612848	0.003705288960200	0.000000742382708	0.000429954947237	0.091333955230383
108.621253	112.912333	117.203413	0.003740587939105	0.000000614607267	0.000273593619995	0.116557584169628
117.197800	122.073000	126.948200	0.002771663930481	0.000000569368413	0.000217219339230	0.153329041209583
126.897785	132.407000	137.916215	0.001470488565023	0.000000436543298	0.000123517573471	0.228129331093132
137.900657	144.178667	150.456677	0.002535728669854	0.000000626674023	0.000190641164161	0.306085188125790
150.413548	157.657333	164.901118	0.001174212442067	0.000000454928239	0.000102987736260	0.412990938818275
164.845910	173.249000	181.652090	0.000452921457587	0.000000304327937	0.000047797365240	0.549120416802180
181.614067	191.470667	201.327267	0.000358417962843	0.000000282613890	0.000037529728038	0.673411740614908
201.246875	212.975000	224.703125	0.000264856424490	0.000000263845519	0.000029227271343	0.865832437782277
224.586333	238.714333	252.842333	0.000164789739537	0.000000226393258	0.000019903749918	1.129058029769064
252.672583	270.034333	287.396083	0.000092416865860	0.000000185666462	0.000012892292077	1.502727395570467
287.142567	308.913667	330.684767	0.000031521936232	0.000000117167755	0.000006209900887	2.020609101558240
330.263900	358.375000	386.486100	0.000006026312062	0.000000049319443	0.000001941904607	2.849050792720270

Table A.V.16. Triton Yields from Iron 400 MeV/n on 40 g/cm^2 Aluminium at 32.7 deg

KE_left(MeV/n)	KE_mid(MeV/n)	KE_right(MeV/n)	Norm_Cts(#/SP*ster*MeV/n)	Y_stat(#/SP*ster*MeV/n)	Y_syst_tot(#/SP*ster*MeV/n)	X_tot(MeV/n)
44.999196	46.182200	47.365204	0.000040756725447	0.000000028393451	0.000024176232693	32.248778172863226
47.433878	48.830433	50.226989	0.000042174529218	0.000000034977933	0.000026466622813	0.082053975017058
50.227011	51.623567	53.020122	0.000054831095099	0.000000039071865	0.000029596771981	0.264104057585263
52.967208	54.417400	55.867592	0.000051417439583	0.000000033523789	0.000024766506921	0.193597366277648
56.491070	57.632200	58.773330	0.000047942773285	0.000000031405299	0.000019430923191	0.114489735563063
59.343905	61.055600	62.767295	0.000038600240378	0.000000031405331	0.000019409909293	0.148391353924749
62.712102	64.681667	66.651232	0.000021705215626	0.000000029133249	0.000015746829524	0.147122640901176
66.706443	68.735733	70.765023	0.000044517001022	0.000000038583242	0.000020127533813	0.132074807149906
70.747727	73.081067	75.414407	0.000035646921839	0.000000039198160	0.000017729557394	0.162200029815195
75.350505	77.836000	80.321495	0.000056170508833	0.000000048832128	0.000021237743615	0.052565019661748
80.362647	83.079167	85.795687	0.000039754475432	0.000000043498185	0.000017000609619	0.133235590989983
85.833168	88.843233	91.853298	0.000026782081920	0.000000033592528	0.000011812455164	0.061733999476788
91.844390	95.200000	98.555610	0.000019516345356	0.000000036829209	0.000011600766373	0.022651986586325
98.508577	102.254667	106.000757	0.000006947975027	0.000000025113689	0.000007086667223	0.101375543473710
106.058855	107.404000	108.749145	0.000005007489094	0.000000013247300	0.000003447260000	0.046485500000000

Table A.V.17. Triton Yields from Iron 400 MeV/n on 40 g/cm^2 Aluminium at 30.0 deg

KE_left(MeV/n)	KE_mid(MeV/n)	KE_right(MeV/n)	Norm_Cts(#/SP*ster*MeV/n)	Y_stat(#/SP*ster*MeV/n)	Y_syst_tot(#/SP*ster*MeV/n)	X_tot(MeV/n)
45.249458	46.394767	47.540075	0.000052246521489	0.000000036820222	0.000033960370073	32.565757905946604
47.465059	48.800800	50.136541	0.000097581837649	0.000000054268236	0.000045553871565	0.062752018215302
50.211577	51.668400	53.125223	0.000054704338929	0.000000036891794	0.000026898565472	0.350203591530698
53.125177	54.582000	56.038823	0.000071143348118	0.000000044941680	0.000032765400817	0.449935546890885
55.969760	57.636167	59.302573	0.000051887825982	0.000000038894335	0.000025053381770	0.155569153173661
59.371643	61.141133	62.910623	0.000064593085661	0.000000049841619	0.000029869508324	0.300046310080627
62.829775	64.736500	66.643225	0.000069335708507	0.000000050273302	0.000028679200284	0.225820449515185
66.724055	68.809100	70.894145	0.000076109162015	0.000000052888857	0.000027007561478	0.231184491837147
70.821142	73.113367	75.405592	0.000063188241225	0.000000044941680	0.000020782831328	0.195896471280751
75.424112	77.883967	80.343822	0.000076620612456	0.000000058183972	0.000025136752369	0.138264284545249
80.398268	83.127233	85.856198	0.000072717992703	0.000000057076372	0.000022292905547	0.161217008027565
85.828690	88.859800	91.890910	0.000054947483935	0.000000051533769	0.000018199141139	0.084962563007266
91.862433	95.200233	98.538033	0.000010120239831	0.000000028555490	0.000009025694403	0.064603417998508

Table A.V.18. Triton Yields from Iron 400 MeV/n on 40 g/cm^2 Aluminium at 27.2 deg

KE_left(MeV/n)	KE_mid(MeV/n)	KE_right(MeV/n)	Norm_Cts(#/SP*ster*MeV/n)	Y_stat(#/SP*ster*MeV/n)	Y_syst_tot(#/SP*ster*MeV/n)	X_tot(MeV/n)
46.057279	47.262267	48.467254	0.000043551505085	0.000000025113724	0.000022064520071	23.253135087921304
48.817318	49.720650	50.623982	0.000018138294270	0.000000022310540	0.000018151055222	0.065135641687310
51.077240	51.582100	52.086960	0.000011292740289	0.000000013420300	0.000009304790000	0.129130000000000
55.116130	56.125850	57.135570	0.000022512720721	0.000000023145242	0.000016088815742	0.346902009237479
57.055117	58.743467	60.431817	0.000030130246244	0.000000029777281	0.000018363612353	0.125983966186314
60.512243	62.338133	64.164023	0.000059216796274	0.000000045369124	0.000026364883879	0.350639353542925
64.084037	66.045067	68.006097	0.000125385759306	0.000000069549509	0.000037845744371	0.231411062962102
68.086063	70.226533	72.367003	0.000139163284175	0.000000075247204	0.000037896493101	0.238975220483212
72.301165	74.669200	77.037235	0.000301586683221	0.000000124995800	0.000057899305085	0.195919211796189
77.036268	79.588033	82.139798	0.000451590808023	0.000000153779878	0.000068717689607	0.162131094399717
82.184098	84.989733	87.795368	0.000494609391926	0.000000171144869	0.000069358563477	0.136156145296678
87.813830	90.930300	94.046770	0.000520220941160	0.000000172572939	0.000064502000808	0.100133980171768
94.022737	97.498367	100.973997	0.000274923576307	0.000000138150277	0.000044416343799	0.085695130707059
100.934183	104.811333	108.688483	0.000398223751854	0.000000180410276	0.000053973005630	0.074294002960291
108.697460	111.517500	114.337540	0.000247179432523	0.000000121996648	0.000033106029826	0.127053679038625
117.262805	122.135000	127.007195	0.000010568969396	0.000000028555490	0.000006234965147	0.275991199274542
127.134585	128.874000	130.613415	0.000007237620797	0.000000017822900	0.000003590590000	0.202622000000000

Table A.V.19. Helium-4 Yields from Iron 400 MeV/n on 40 g/cm^2 Aluminium at 12.7 deg

KE_left(MeV/n)	KE_mid(MeV/n)	KE_right(MeV/n)	Norm_Cts(#/SP*ster*MeV/n)	Y_stat(#/SP*ster*MeV/n)	Y_syst_tot(#/SP*ster*MeV/n)	X_tot(MeV/n)
44.716085	46.453400	48.190715	0.000435388861422	0.000000184848111	0.000125455333995	0.133075845322170
48.190785	49.928100	51.665415	0.000449608842239	0.000000201965136	0.000138857840625	0.309343886504970
51.665385	53.402700	55.140015	0.000463828823055	0.000000204760520	0.000140205683384	0.246207581623718
55.072157	57.144567	59.216977	0.000478206494125	0.000000188056478	0.000108527803449	0.260491419855165
59.284878	61.426233	63.567588	0.000504384096860	0.000000170425085	0.000092996422703	0.322220577978812
63.474825	65.758400	68.041975	0.000486415204759	0.000000175978022	0.000091790662774	0.143393701936033
68.134765	70.684600	73.234435	0.000424500631394	0.000000172425043	0.000078826084055	0.403360337248223
73.125347	75.865067	78.604787	0.000468706466364	0.000000189096951	0.000082279991697	0.176434162598603
78.713865	81.675300	84.636735	0.000482880485105	0.000000198248810	0.000079886431602	0.341300558455447
84.617580	87.974900	91.332220	0.000484826006156	0.000000209579620	0.000075391479159	0.280047620973648
91.263990	94.936900	98.609810	0.000555536379727	0.000000239541309	0.000080741161413	0.228227185992379
98.601065	102.672100	106.743135	0.000511180975096	0.000000234784670	0.000071791075527	0.251034556202926
106.754260	111.289000	115.823740	0.000496042582485	0.000000248737099	0.000068236950065	0.228390159153147
115.800350	120.953000	126.105650	0.000501822501071	0.000000255676029	0.000063390217459	0.198569979348944
126.097925	131.884000	137.670075	0.000443287286407	0.000000255558710	0.000055888421275	0.191220861745679
137.658227	144.295667	150.933107	0.000415339687275	0.000000262379418	0.000050020763493	0.137219576433685
150.868680	158.534000	166.199320	0.000527618507035	0.000000306464741	0.000054159141695	0.077596682275291
166.141098	175.024333	183.907568	0.000488430981359	0.000000317851851	0.000048913377396	0.012140602499069
183.837223	194.293333	204.749443	0.000220041390931	0.000000222202174	0.000027004686809	0.101259854369735
205.026780	208.920000	212.813220	0.000008485099318	0.000000022206900	0.000002016790000	0.093021900000000

Table A.V.20. Helium-4 Yields from Iron 400 MeV/n on 40 g/cm^2 Aluminium at 10.0 deg

KE_left(MeV/n)	KE_mid(MeV/n)	KE_right(MeV/n)	Norm_Cts(#/SP*ster*MeV/n)	Y_stat(#/SP*ster*MeV/n)	Y_syst_tot(#/SP*ster*MeV/n)	X_tot(MeV/n)
44.599343	46.314633	48.029923	0.000845353178557	0.000000277559008	0.000209551959795	0.158620037392524
48.097780	49.886500	51.675220	0.000856318285294	0.000000282384375	0.000209197159154	0.245774561449797
51.675213	53.463933	55.252653	0.000867442125853	0.000000298538521	0.000221558562285	0.351489257306678
55.144643	57.122833	59.101023	0.000878818281268	0.000000277946912	0.000187275548006	0.239996855378336
59.209050	61.401600	63.594150	0.000911526613180	0.000000242867128	0.000139665305175	0.278260840338701
63.559060	65.786700	68.014340	0.001045772510123	0.000000256921341	0.000147228585770	0.191298084739210
68.049410	70.649900	73.250390	0.001047016055260	0.000000277559333	0.000140056444215	0.343759003364276
73.169210	75.876200	78.583190	0.001129859123947	0.000000298538521	0.000147433254801	0.174146009540414
78.664357	81.675967	84.687577	0.001244958297203	0.000000327560693	0.000149966776553	0.335082236455471
84.612720	87.952500	91.292280	0.001275497875845	0.000000353506640	0.000148618562505	0.254798969860182
91.261157	94.927467	98.593777	0.001226010934265	0.000000363764864	0.000140668620718	0.221044438451299
98.587683	102.660133	106.732583	0.001327014728308	0.000000384513991	0.000139922881423	0.241296348489591
106.746083	111.288333	115.830583	0.001425786719169	0.000000425596949	0.000143924845808	0.226978246347530
115.798725	120.931000	126.063275	0.001363786106902	0.000000435142906	0.000131572080972	0.165063467777155
126.073843	131.873333	137.672823	0.001368923104028	0.000000455086906	0.000126440747202	0.180232637335306
137.655347	144.293667	150.931987	0.001322147672368	0.000000477833181	0.000117181801740	0.129372694864450
150.869777	158.524667	166.179557	0.001495541993940	0.000000535328765	0.000123461466008	0.055629096743790
166.144055	175.026000	183.907945	0.001339523624939	0.000000533404274	0.000104877338987	0.015502559907773
183.827325	194.291000	204.754675	0.000583836483190	0.000000371100195	0.000056275110676	0.109731244732984
204.886455	212.937000	220.987545	0.000051057900203	0.000000082664692	0.000007908374682	0.161378578020752

Table A.V.21. Helium-4 Yields from Iron 400 MeV/n on 40 g/cm^2 Aluminium at 7.20 deg

KE_left(MeV/n)	KE_mid(MeV/n)	KE_right(MeV/n)	Norm_Cts(#/SP*ster*MeV/n)	Y_stat(#/SP*ster*MeV/n)	Y_syst_tot(#/SP*ster*MeV/n)	X_tot(MeV/n)
45.667965	47.412800	49.157635	0.002072470290572	0.000000375752256	0.000313813576752	0.196040609020292
49.227272	51.050267	52.873262	0.002196072778621	0.000000387577268	0.000311242298163	0.253381785079354
52.873238	54.696233	56.519228	0.002321548836120	0.000000375039253	0.000302195198276	0.436838339733362
56.416710	58.470300	60.523890	0.002191054319930	0.000000376461028	0.000267290339874	0.171810392378954
60.626422	62.853067	65.079712	0.002392835328520	0.000000405969806	0.000271532784534	0.258147621974327
65.000513	67.328933	69.657353	0.002660340098745	0.000000436363710	0.000290556123992	0.227041971384147
69.736542	72.370767	75.004992	0.002618639925580	0.000000459615270	0.000278930594855	0.303179880970027
74.896265	77.719800	80.543335	0.002889617598106	0.000000502765888	0.000299677383519	0.200670426434116
80.644260	83.697100	86.749940	0.003251562222512	0.000000536654090	0.000311252932123	0.279646091746264
86.757758	90.217133	93.676508	0.003226767766977	0.000000582647121	0.000305231445960	0.287186544082413
93.604787	97.406867	101.208947	0.003188121222943	0.000000597443414	0.000295867423090	0.235135533596456
101.205125	105.420000	109.634875	0.003423047494230	0.000000639485308	0.000297745568815	0.204982081736941
109.615532	114.362667	119.109802	0.003585663691848	0.000000695497119	0.000305156522909	0.185346897111551
119.092140	124.445000	129.797860	0.003919195608090	0.000000757671432	0.000311768849825	0.189239114891214
129.746192	135.818667	141.891142	0.003924107192598	0.000000806098545	0.000307867526800	0.143073258843887
141.872720	148.820000	155.767280	0.004331033771908	0.000000886248475	0.000317881786048	0.109458746817146
155.731658	163.746333	171.761008	0.004252524387535	0.000000921145033	0.000295830505947	0.034271742840276
171.735928	181.110333	190.484738	0.002634413293697	0.000000769882226	0.000194158447236	0.025285767950086
190.567970	197.739500	204.911030	0.000288415568762	0.000000209606090	0.000028005531529	0.098825110408286

Table A.V.22. Helium-3 Yields from Iron 400 MeV/n on 40 g/cm^2 Aluminium at 12.7 deg

KE_left(MeV/n)	KE_mid(MeV/n)	KE_right(MeV/n)	Norm_Cts(#/SP*ster*MeV/n)	Y_stat(#/SP*ster*MeV/n)	Y_syst_tot(#/SP*ster*MeV/n)	X_tot(MeV/n)
45.834377	47.565467	49.296557	0.000216477795711	0.000000269214287	0.000196922637231	0.385904120592149
49.229468	51.309733	53.389998	0.000255068385813	0.000000253673579	0.000155637518135	0.219839571758794
53.457093	55.604433	57.751773	0.000280086925811	0.000000142380179	0.000074666823983	0.323285045844994
57.751793	59.899133	62.046473	0.000273521766029	0.000000136839282	0.000071909892542	0.224715439162088
62.024447	64.584567	67.144687	0.000284295752080	0.000000149732533	0.000067156589605	0.382176877246649
67.166688	69.748833	72.330978	0.000289738184452	0.000000188724370	0.000087121788950	0.312519533002803
72.260560	75.213400	78.166240	0.000295239642139	0.000000241407973	0.000102520452548	0.353584675650063
78.157452	81.269867	84.382282	0.000307665309773	0.000000279696967	0.000117244249007	0.288881419614087
84.461535	87.930000	91.398465	0.000316557124274	0.000000316575322	0.000123824217877	0.376543151053103
91.340135	95.199400	99.058665	0.000322229870252	0.000000282888253	0.000097434651458	0.286298246395415
99.030232	103.291667	107.553102	0.000328110573795	0.000000191864413	0.000053750901636	0.286960096607525
107.559945	112.301000	117.042055	0.000377467142233	0.000000223345147	0.000057139018977	0.286085710391134
117.022305	122.425000	127.827695	0.000296095911734	0.000000202028897	0.000045056544087	0.295757108584054
127.802133	133.858333	139.914533	0.000271225953776	0.000000201032086	0.000040132651902	0.273413494228065
139.901433	146.854333	153.807233	0.000245689388983	0.000000202067518	0.000034988432161	0.222698200536623
153.740768	161.782333	169.823898	0.000328660348487	0.000000258949687	0.000040929959058	0.175980500457323
169.757975	179.096000	188.434025	0.000273014724897	0.000000248297385	0.000033469794824	0.124233765623763
188.362505	199.374000	210.385495	0.000267824368899	0.000000259930398	0.000029996204065	0.044643953322187
210.302767	223.471667	236.640567	0.000212900973773	0.000000240896713	0.000023699944496	0.068159394262567
236.796545	247.104000	257.411455	0.000048849846997	0.000000096603012	0.000007314981587	0.174161092055602

Table A.V.23. Helium-3 Yields from Iron 400 MeV/n on 40 g/cm^2 Aluminium at 10.0 deg

KE_left(MeV/n)	KE_mid(MeV/n)	KE_right(MeV/n)	Norm_Cts(#/SP*ster*MeV/n)	Y_stat(#/SP*ster*MeV/n)	Y_syst_tot(#/SP*ster*MeV/n)	X_tot(MeV/n)
45.881492	47.674967	49.468442	0.000385776252885	0.000000303623519	0.000228227742930	0.573273211121887
49.377233	51.304333	53.231433	0.000429845002983	0.000000295555819	0.000206814993095	0.261886480557960
53.322630	55.536300	57.749970	0.000471922624967	0.000000276420969	0.000161209085042	0.219508561540296
57.749963	59.963633	62.177303	0.000520192294507	0.000000201070923	0.000108115861683	0.321779289672285
62.069063	64.538133	67.007203	0.000553571231527	0.000000202708821	0.000098656198309	0.281231364182589
67.115485	69.764200	72.412915	0.000565898215677	0.000000245681992	0.000117656109840	0.325504498406704
72.300527	75.199867	78.099207	0.000578683733547	0.000000304933583	0.000139427273606	0.289157983407496
78.211577	81.301067	84.390557	0.000604536612010	0.000000342393327	0.000151544469664	0.320047362999932
84.384395	87.912600	91.440805	0.000624220853140	0.000000376209445	0.000153058256581	0.355557053302279
91.351555	95.198100	99.044645	0.000637369342169	0.000000367010123	0.000139240649507	0.277540072077889
99.031270	103.292000	107.552730	0.000656479825858	0.000000281251811	0.000086387854227	0.292664002996610
107.562670	112.312000	117.061330	0.000777800541157	0.000000325294922	0.000093531453468	0.304284761565544
117.027438	122.401333	127.775228	0.000707435757183	0.000000321374469	0.000082022628514	0.256877935952078
127.780365	133.851000	139.921635	0.000698732097382	0.000000343088458	0.000078384039718	0.265231826088047
139.902010	146.858000	153.813990	0.000647057080297	0.000000344850411	0.000069237548296	0.225335109354934
153.747717	161.776667	169.805617	0.000739748056752	0.000000394585589	0.000072580206062	0.164062358279893
169.768875	179.106000	188.443125	0.000681171000561	0.000000393443495	0.000063339289522	0.141126935507330
188.356793	199.379333	210.401873	0.000980499719687	0.000000511689656	0.000078578727873	0.062693502798376
210.315068	223.476333	236.637598	0.000567626540890	0.000000411783859	0.000050364879506	0.059567867850461
236.976225	241.964000	246.951775	0.000120774569970	0.000000111035000	0.000008856550000	0.104478000000000

Table A.V.24. Helium-3 Yields from Iron 400 MeV/n on 40 g/cm^2 Aluminium at 7.20 deg

KE_left(MeV/n)	KE_mid(MeV/n)	KE_right(MeV/n)	Norm_Cts(#/SP*ster*MeV/n)	Y_stat(#/SP*ster*MeV/n)	Y_syst_tot(#/SP*ster*MeV/n)	X_tot(MeV/n)
45.868647	47.704467	49.540287	0.000506247081057	0.000000346762941	0.000263499376071	0.626589164129895
49.540280	51.376100	53.211920	0.000547704957664	0.000000313763610	0.000234562053890	0.389539413449833
53.207195	55.460400	57.713605	0.000589191936169	0.000000225470665	0.000122846556386	0.141068169846142
57.718350	59.976300	62.234250	0.000692181152798	0.000000218387421	0.000116917054152	0.343911504804652
62.134392	64.546867	66.959342	0.000645399107156	0.000000227499629	0.000114218137127	0.308879277582683
67.059215	69.752300	72.445385	0.000713496217216	0.000000270217426	0.000127186559804	0.303383488149899
72.338708	75.205033	78.071358	0.000784172688499	0.000000344467903	0.000169300762628	0.276579800970714
78.178065	81.311700	84.445335	0.000872130389776	0.000000405982370	0.000195184306331	0.326071988470338
84.377440	87.887800	91.398160	0.000953886483506	0.000000452702805	0.000204637912406	0.327331854187520
91.353703	95.193033	99.032363	0.001026216984514	0.000000473280338	0.000202782166191	0.270432532297133
99.021467	103.282667	107.543867	0.001119337939285	0.000000379564001	0.000130127745650	0.287805401389272
107.555748	112.311333	117.066918	0.001113566789686	0.000000393659494	0.000121698284616	0.307212254828807
117.050255	122.406000	127.761745	0.001167321145570	0.000000422528565	0.000120015274794	0.261490888952177
127.763323	133.851333	139.939343	0.001234654442915	0.000000457388415	0.000120149778832	0.265354912846927
139.902147	146.856667	153.811187	0.001326208650868	0.000000498619550	0.000119859619473	0.223129216376968
153.760995	161.779000	169.797005	0.001399719342706	0.000000538076037	0.000119054858125	0.167646589207774
169.773652	179.110667	188.447682	0.001390912170925	0.000000578348406	0.000112655570561	0.149604941101589
188.354715	199.385000	210.415285	0.001845795465906	0.000000716965418	0.000135819540734	0.072960603836739
210.320947	223.479667	236.638387	0.001390647150844	0.000000656929942	0.000110648432628	0.054203653556656
236.811385	247.131000	257.450615	0.000193712624838	0.000000212945993	0.000019080289189	0.136107907347663

Table A.VI.1. Deuteron Yields from Iron 400 MeV/n on 60 g/cm^2 Aluminium at 12.7 deg

KE_left(MeV/n)	KE_mid(MeV/n)	KE_right(MeV/n)	Norm_Cts(#/SP*ster*MeV/n)	Y_stat(#/SP*ster*MeV/n)	Y_syst_tot(#/SP*ster*MeV/n)	X_tot(MeV/n)
45.588748	46.924433	48.260119	0.000736871309800	0.000000138278461	0.000141709128520	0.658732332807492
48.260081	49.595767	50.931452	0.000885585789457	0.000000152885961	0.000164656757555	0.404415523344493
50.837670	52.404733	53.971797	0.000907913285611	0.000000169106480	0.000164256918375	0.177226427328940
54.065595	55.785900	57.506205	0.000929055321080	0.000000170323942	0.000149219185107	0.730857009416343
57.506195	59.226500	60.946805	0.000971239306621	0.000000191550174	0.000177339620080	0.571556368366236
60.862465	62.839900	64.817335	0.001035289344734	0.000000203073628	0.000165957934567	0.254812098019384
64.901635	67.004500	69.107365	0.001057926916326	0.000000206450676	0.000160557837091	0.611972913261690
69.001223	71.294833	73.588443	0.001081482347188	0.000000221290523	0.000164506420245	0.339539300678139
73.694620	76.180300	78.665980	0.001125848489850	0.000000230225909	0.000163678749047	0.457615038514907
78.596112	81.385167	84.174222	0.001203092675132	0.000000243549989	0.000161264636138	0.344805613888463
84.150515	87.172300	90.194085	0.001456213551678	0.000000288552325	0.000186164580093	0.332402505035687
90.216135	93.558300	96.900465	0.001652492422583	0.000000322289940	0.000205433900778	0.266869909360647
96.900770	100.631500	104.362230	0.001637999838869	0.000000350354733	0.000215604144383	0.229896625071009
104.345935	108.521000	112.696065	0.001419311421092	0.000000359394795	0.000199231617157	0.162327880003313
112.676787	117.343667	122.010547	0.001166436377139	0.000000312869663	0.000145905703805	0.082438196464564
121.977875	127.269000	132.560125	0.000861682009769	0.000000279407237	0.000102709490941	0.151642708004869
132.550257	138.556667	144.563077	0.000398609490573	0.000000196661812	0.000054095694377	0.328479691014528
144.533643	151.432333	158.331023	0.000153713022392	0.000000130073623	0.000025225440882	0.543659840923532
158.300273	166.258333	174.216393	0.000084649741221	0.000000101304235	0.000016081399161	0.833358652839220
174.176398	183.496333	192.816268	0.000045452518717	0.000000077296807	0.000009920864198	1.255912589358432
192.730682	203.728667	214.726652	0.000015361731705	0.000000046933289	0.000004823614668	1.805439564007613
214.627650	227.816000	241.004350	0.000005173009287	0.000000025666143	0.000002193649222	2.510007568394964
240.860518	256.922333	272.984148	0.000006405197627	0.000000033073755	0.000002217194920	3.491903548510468
279.572100	292.883500	306.194900	0.000003381689345	0.000000020748286	0.000001123140878	4.034677887973214
312.320850	337.773000	363.225150	0.000002448669072	0.000000025235320	0.000001063074131	7.037526369925729
364.136550	374.246000	384.355450	0.000000459692242	0.000000009721770	0.000000337296000	5.157720000000000

Table A.VI.2. Deuteron Yields from Iron 400 MeV/n on 60 g/cm^2 Aluminium at 10.0 deg

KE_left(MeV/n)	KE_mid(MeV/n)	KE_right(MeV/n)	Norm_Cts(#/SP*ster*MeV/n)	Y_stat(#/SP*ster*MeV/n)	Y_syst_tot(#/SP*ster*MeV/n)	X_tot(MeV/n)
43.683256	45.060600	46.437944	0.001118509582627	0.000000179469960	0.000194644477225	22.045173283770509
46.437923	47.815267	49.192610	0.001213622532844	0.000000185008301	0.000199539522551	0.574426164437171
49.192623	50.569967	51.947310	0.001250331555378	0.000000202987642	0.000235242177551	0.418642362502889
51.850085	53.446900	55.043715	0.001288019679358	0.000000224638524	0.000243606324341	0.248187658618877
55.140912	56.901567	58.662222	0.001323749600444	0.000000220186695	0.000210280365843	0.720242010184771
58.662212	60.422867	62.183522	0.001418797679208	0.000000242394811	0.000244384746416	0.492925066307243
62.109435	64.156600	66.203765	0.001487239975749	0.000000245606567	0.000216618161771	0.307745439317693
66.277863	68.420133	70.562403	0.001584669878073	0.000000259300795	0.000223678666457	0.608944724805134
70.474057	72.860767	75.247477	0.001671873966446	0.000000278532872	0.000230483479204	0.309365148736893
75.335857	77.860267	80.384677	0.001825424274263	0.000000303190663	0.000246737574822	0.463992407901250
80.373340	83.270600	86.167860	0.001869495390945	0.000000320069600	0.000233204966073	0.333863090802203
86.084563	89.225733	92.366903	0.001899184437383	0.000000337938264	0.000235007451867	0.326508477637258
92.359997	95.830067	99.300137	0.002090370971817	0.000000375218712	0.000252888720935	0.255924420415481
99.298490	103.164000	107.029510	0.002314659086979	0.000000452931209	0.000322719065947	0.194118456299884
107.032658	111.348333	115.664008	0.002380691025377	0.000000437617582	0.000274215626610	0.114417094568644
115.643688	120.506333	125.368978	0.002700753303389	0.000000481763333	0.000286023473362	0.077379361189532
125.373443	130.882333	136.391223	0.002948082152470	0.000000532912325	0.000307919751067	0.195463236985091
136.371482	142.661667	148.951852	0.002132466265399	0.000000482789047	0.000227016613447	0.370035715836999
148.900158	156.134333	163.368508	0.001902037010212	0.000000492442634	0.000204320560566	0.638734055375944
163.353028	171.729333	180.105638	0.002057334201634	0.000000556555810	0.000217597412418	0.930605030482857
180.037972	189.888667	199.739362	0.001621611052836	0.000000539053544	0.000177303086681	1.392354179923341
199.631687	211.304667	222.977647	0.001441097803326	0.000000554674017	0.000151909978736	1.967101558486496
222.868723	236.926333	250.983943	0.000743938370196	0.000000431649321	0.000091086532613	2.745086125807349
250.829400	268.055000	285.280600	0.000125623813623	0.000000190883814	0.000017979492010	3.819929747560811
285.028867	306.614667	328.200467	0.000054115411319	0.000000140253194	0.000009005219140	5.402817061848384
327.784283	355.596333	383.408383	0.000020495362123	0.000000090638548	0.000004190627488	7.785235153840891

Table A.VI.3. Deuteron Yields from Iron 400 MeV/n on 60 g/cm^2 Aluminium at 7.20 deg

KE_left(MeV/n)	KE_mid(MeV/n)	KE_right(MeV/n)	Norm_Cts(#/SP*ster*MeV/n)	Y_stat(#/SP*ster*MeV/n)	Y_syst_tot(#/SP*ster*MeV/n)	X_tot(MeV/n)
45.442233	46.851867	48.261501	0.001351465634711	0.000000204281376	0.000229463095022	0.529618340612370
48.261499	49.671133	51.080767	0.001443254858444	0.000000217893182	0.000256185440685	0.526433418677994
51.080733	52.490367	53.900001	0.001535044082178	0.000000249235152	0.000316613163545	0.302114526755997
53.887817	55.667567	57.447317	0.001627043213000	0.000000256893425	0.000268819400829	0.549901536825458
57.459507	59.251467	61.043427	0.001755959539335	0.000000267353766	0.000277449808639	0.605025499857651
60.972530	62.850300	64.728070	0.001927828979316	0.000000280762600	0.000289952787814	0.285961299147000
64.799030	66.971900	69.144770	0.002031186146697	0.000000293141072	0.000275277263671	0.566081329504869
69.083380	71.317600	73.551820	0.002221465421156	0.000000316738710	0.000297889542732	0.403906908868727
73.613200	76.167700	78.722200	0.002241890087470	0.000000340294755	0.000295454357825	0.445053283552655
78.618375	81.373200	84.128025	0.002447765886459	0.000000363183614	0.000303483815445	0.333820821437190
84.166515	87.171800	90.177085	0.002663204078787	0.000000392132117	0.000318721757679	0.340494820592032
90.229375	93.567700	96.906025	0.002852575759449	0.000000427236012	0.000336686553591	0.275647985145910
96.898917	100.635267	104.371617	0.003272521567859	0.000000505928813	0.000415995144482	0.221319028725141
104.321940	108.510000	112.698060	0.003438449417723	0.000000533000835	0.000403523850607	0.153079688572554
112.664897	117.350667	122.036437	0.003671988902418	0.000000555914932	0.000384484333964	0.085309772012003
122.005937	127.282667	132.559397	0.004438579135821	0.000000646722533	0.000454831902386	0.130309527633784
132.563542	138.569667	144.575792	0.003290388276366	0.000000590388481	0.000341350709772	0.302761851695355
144.535393	151.444333	158.353273	0.002917374918837	0.000000599484457	0.000308984086328	0.522710794481040
158.329282	166.289667	174.250052	0.002987437562125	0.000000657874101	0.000312409747686	0.780386959033786
174.206087	183.530667	192.855247	0.002800880495745	0.000000686443987	0.000295093343547	1.195825139395389
192.766785	203.773000	214.779215	0.002319193756202	0.000000676076328	0.000240514182985	1.728983968028622
214.675710	227.882000	241.088290	0.001244738045919	0.000000544179779	0.000146427040107	2.394791767252426
240.936303	257.011333	273.086363	0.000195948717265	0.000000230990623	0.000026595173715	3.336990602009541
272.866217	292.837667	312.809117	0.000044997674378	0.000000114304651	0.000007693852598	4.702100102613724
312.464517	337.953667	363.442817	0.000013050541559	0.000000067420164	0.000003228761605	6.723271892865854
362.840883	396.435333	430.029783	0.000002781378395	0.000000037806415	0.000001258046065	9.890350987427089

Table A.VI.4. Deuteron Yields from Iron 400 MeV/n on 60 g/cm^2 Aluminium at 32.7 deg

KE_left(MeV/n)	KE_mid(MeV/n)	KE_right(MeV/n)	Norm_Cts(#/SP*ster*MeV/n)	Y_stat(#/SP*ster*MeV/n)	Y_syst_tot(#/SP*ster*MeV/n)	X_tot(MeV/n)
44.502456	45.820100	47.137743	0.000116438863825	0.000000049785976	0.000041820813949	0.752504607472273
47.137723	48.455367	49.773010	0.000103976871077	0.000000048043033	0.000039951655705	0.771414782624108
49.682432	51.136400	52.590368	0.000106356342456	0.000000051465904	0.000040626667516	0.183653064313783
52.681000	54.405100	56.129200	0.000106451165127	0.000000055868622	0.000035859861874	0.259433719671210
56.129200	57.853300	59.577400	0.000121888881393	0.000000056662755	0.000037001880782	0.455588035438816
59.496457	61.329167	63.161877	0.000100228516632	0.000000051705938	0.000030605623910	0.396397123762030
63.242793	65.369433	67.496073	0.000098428187817	0.000000060594247	0.000031657673747	0.337239362752927
67.483398	69.622733	71.762068	0.000117090235628	0.000000064375669	0.000033794974806	0.312653243034516
71.774743	74.302933	76.831123	0.000090665317711	0.000000060594237	0.000026830449219	0.378688375028862
76.747558	79.392333	82.037108	0.000121417120686	0.000000070047029	0.000030616973321	0.239951862589145
82.120682	85.051367	87.982052	0.000089042534237	0.000000062120064	0.000023867974270	0.351685832250888
87.931662	91.216767	94.501872	0.000096409695527	0.000000068024333	0.000023527009779	0.265206927197406
94.465230	98.083400	101.701570	0.000090375741535	0.000000071943608	0.000022787638915	0.180946924633551
101.698825	105.723000	109.747175	0.000107646489513	0.000000081812625	0.000023246759095	0.132519628706279
109.752725	114.252000	118.751275	0.000086707488931	0.000000072732492	0.000018605575806	0.046588343880202
118.740882	123.875667	129.010452	0.000107556272756	0.000000088819986	0.000020338202271	0.040139163193196
128.953327	134.740667	140.528007	0.000104093020536	0.000000139297637	0.000031271800267	0.208547297142687
140.508592	147.141667	153.774742	0.000146098712079	0.000000263707745	0.000067104536058	0.348710344621435
153.753200	161.399000	169.044800	0.000155121183162	0.000000182830715	0.000036455277821	0.541412991714273
168.986977	177.901667	186.816357	0.000088538359312	0.000000108052290	0.000015094347287	0.842645839210638
186.756065	197.256000	207.755935	0.000057275058661	0.000000094131540	0.000010676054898	1.206416079323796
207.650112	220.181667	232.713222	0.000065062113418	0.000000114975154	0.000011457282290	1.745230221803416
232.594142	247.781667	262.969192	0.000011438728353	0.000000048697632	0.000003679236955	2.421546102328015
262.781983	281.554333	300.326683	0.000001510888675	0.000000018918473	0.000001091064233	3.387115337791141
308.131850	324.006000	339.880150	0.000001980329386	0.000000018392690	0.000000838634159	3.917607001946469
366.579850	388.215000	409.850150	0.000000546474446	0.000000014364214	0.000000477842581	5.956180417146546

Table A.VI.5. Deuteron Yields from Iron 400 MeV/n on 60 g/cm^2 Aluminium at 30.0 deg

KE_left(MeV/n)	KE_mid(MeV/n)	KE_right(MeV/n)	Norm_Cts(#/SP*ster*MeV/n)	Y_stat(#/SP*ster*MeV/n)	Y_syst_tot(#/SP*ster*MeV/n)	X_tot(MeV/n)
44.202717	45.660600	47.118483	0.000122626284208	0.000000052496937	0.000040003078923	0.517366054337739
47.118517	48.576400	50.034283	0.000120035207243	0.000000055884581	0.000042322957492	0.965413128203672
50.034284	51.492167	52.950050	0.000137249372040	0.000000056662755	0.000043353622335	0.703755925528873
52.882278	54.409900	55.937522	0.000126978883003	0.000000058291502	0.000042803868422	0.272084918371471
56.005293	57.863733	59.722173	0.000133402165733	0.000000058291502	0.000035934397145	0.499017788037661
59.722127	61.580567	63.439007	0.000153327985532	0.000000067979863	0.000041581720120	0.807466772282922
63.333493	65.375833	67.418173	0.000138308066698	0.000000065133095	0.000036611899518	0.355489763707761
67.523720	69.780200	72.036680	0.000138254558864	0.000000068749223	0.000034863935197	0.591818532246161
71.935903	74.362033	76.788163	0.000163489144687	0.000000076391672	0.000037409273949	0.497658242653530
76.888943	79.543433	82.197923	0.000149605636400	0.000000083555168	0.000036165125637	0.496675128575007
82.128657	85.108167	88.087677	0.000141538180886	0.000000082187827	0.000032249495417	0.441763593813478
88.046867	91.297167	94.547467	0.000136448215902	0.000000081982133	0.000029178513235	0.381196472053454
94.562520	98.168600	101.774680	0.000136751031184	0.000000088407526	0.000028487519650	0.326123834923178
101.768585	105.797000	109.825415	0.000168372731754	0.000000102510919	0.000030272095065	0.269396662371678
109.819873	114.325333	118.830793	0.000137647153317	0.000000096609088	0.000025593910200	0.192983252148703
118.803252	123.893667	128.984082	0.000104675821839	0.000000089336262	0.000020502716374	0.028017073177796
129.004277	134.769667	140.535057	0.000091321441409	0.000000088315870	0.000017938001915	0.153314074244898
140.514645	147.134000	153.753355	0.000036650691334	0.000000054250924	0.000009353952991	0.359755868890280
153.694388	161.344333	168.994278	0.000017469406110	0.000000043912348	0.000006238945022	0.642410345701250
168.911563	177.796333	186.681103	0.000004013462736	0.000000021215770	0.000002515053279	1.025482347096234
186.641770	197.090000	207.538230	0.000002576434948	0.000000018392708	0.000001897251596	1.493723766731989
207.457862	219.954667	232.451472	0.000000954865458	0.000000014444528	0.000001206467772	2.141151694345826
232.599710	242.335000	252.070290	0.000000840737030	0.000000012217412	0.000000874100311	2.333951645107499
286.941150	293.639000	300.336850	0.000000541799411	0.000000007554190	0.000000395286000	2.737630000000000

Table A.VI.6. Deuteron Yields from Iron 400 MeV/n on 60 g/cm^2 Aluminium at 27.2 deg

KE_left(MeV/n)	KE_mid(MeV/n)	KE_right(MeV/n)	Norm_Cts(#/SP*ster*MeV/n)	Y_stat(#/SP*ster*MeV/n)	Y_syst_tot(#/SP*ster*MeV/n)	X_tot(MeV/n)
45.350287	46.535467	47.720647	0.000199809902360	0.000000069945272	0.000065733290607	0.564988990772387
47.711882	49.289467	50.867052	0.000169120470217	0.000000063873720	0.000046470968342	0.472534408906907
50.875793	52.462133	54.048473	0.000213620880387	0.000000079959382	0.000057690063511	0.540537213495056
54.048493	55.634833	57.221173	0.000206175367613	0.000000081129606	0.000058036423533	0.484476895972347
57.117265	58.921000	60.724735	0.000201974203890	0.000000077618974	0.000051607720959	0.385155524383333
60.828595	62.811700	64.794805	0.000206104743203	0.000000087424537	0.000050732561291	0.651308015949443
64.754145	66.777900	68.801655	0.000182227677347	0.000000080749420	0.000045614899910	0.372530031902678
68.842307	71.220767	73.599227	0.000198802384011	0.000000083116494	0.000041930784708	0.558108995864607
73.525137	75.993867	78.462597	0.000185797651760	0.000000091040971	0.000043135518032	0.392651482459955
78.536680	81.311200	84.085720	0.000201906181553	0.000000098654853	0.000042072303002	0.478930389914860
84.004480	87.066200	90.127920	0.000185593319062	0.000000093208891	0.000036442174747	0.307742917868145
90.101698	93.463133	96.824568	0.000196848497813	0.000000105070292	0.000037893129980	0.307002744166889
96.832155	100.570800	104.309445	0.000199356588991	0.000000104637400	0.000034642087054	0.233284893278583
104.297992	108.475667	112.653342	0.000168450934756	0.000000098654853	0.000028876738098	0.150977245177046
112.673730	117.342000	122.010270	0.000214615051487	0.000000122624047	0.000033064314191	0.032746837705800
121.990707	127.323667	132.656627	0.000190214061829	0.000000123445232	0.000029485000259	0.136147818037639
132.603573	138.641333	144.679093	0.000103322464209	0.000000094433350	0.000018656838221	0.319280844816910
144.662145	151.592000	158.521855	0.000090870549392	0.000000095839970	0.000016583631013	0.535745424098050
158.478225	166.486000	174.493775	0.000082168636595	0.000000099893503	0.000014899402867	0.875111759633591
174.457165	183.833000	193.208835	0.000090990408351	0.000000113870111	0.000015127161658	1.253720750059199
193.127243	204.201333	215.275423	0.000158851165643	0.000000170439186	0.000021507825636	1.807652622007060
215.175772	228.461667	241.747562	0.000026123862903	0.000000073832300	0.000006581344157	2.538141020944266
241.604617	257.803667	274.002717	0.000002985524298	0.000000024972384	0.000001646392523	3.498231699716301
280.650700	294.090500	307.530300	0.000002879783375	0.000000017344856	0.000000994193900	4.001857662661180
322.505500	339.684000	356.862500	0.000000535741495	0.000000013579349	0.000000560282822	5.661104013052578
366.096650	376.329000	386.561350	0.000000352908491	0.000000007554190	0.000000258744000	5.018340000000000

Table A.VI.7. Proton Yields from Iron 400 MeV/n on 60 g/cm^2 Aluminium at 12.7 deg

KE_left(MeV/n)	KE_mid(MeV/n)	KE_right(MeV/n)	Norm_Cts(#/SP*ster*MeV/n)	Y_stat(#/SP*ster*MeV/n)	Y_syst_tot(#/SP*ster*MeV/n)	X_tot(MeV/n)
44.679506	46.130933	47.582360	0.001787572719900	0.000000239056716	0.000291542984318	0.312167288470397
47.559808	49.445033	51.330258	0.001569686935127	0.000000260643894	0.000252333539429	0.350840759608938
51.352843	53.260633	55.168423	0.001650152426300	0.000000267436235	0.000261948621804	0.929674397843137
55.168410	57.076200	58.983990	0.001858015963683	0.000000280559497	0.000288698497275	1.014553402364804
58.856687	61.002067	63.147447	0.001966938535424	0.000000307761287	0.000295902136501	0.396383197272538
63.274770	65.647200	68.019630	0.002187585185180	0.000000342783870	0.000318171763499	0.741181794547060
67.966492	70.392067	72.817642	0.002256976900957	0.000000347085698	0.000325120217127	0.772118513890841
72.870773	75.708533	78.546293	0.002203183304590	0.000000376898189	0.000314008631797	0.664287499211749
78.447587	81.426167	84.404747	0.002633097009851	0.000000411177261	0.000363408405288	0.706847169132055
84.503445	87.807300	91.111155	0.002893040393400	0.000000456045856	0.000390057844354	0.694722503244281
91.045938	94.752333	98.458728	0.003305470437339	0.000000521591934	0.000437310695612	0.693106104896646
98.420440	102.508400	106.596360	0.003436427246679	0.000000551946351	0.000442551740462	0.669841826231387
106.594968	111.153333	115.711698	0.002934568824484	0.000000538504804	0.000376875900491	0.637539829395780
115.710738	120.830333	125.949928	0.002718122879872	0.000000540970120	0.000341024295466	0.561362413429150
125.941238	131.796333	137.651428	0.001746582223378	0.000000460245116	0.000223315333397	0.509137440550192
137.581287	144.231667	150.882047	0.001040992053769	0.000000366411598	0.000133540749151	0.394012133800471
150.862787	158.517667	166.172547	0.000648630633180	0.000000309773057	0.000085134772006	0.274501475659057
166.105437	175.007667	183.909897	0.000370894578121	0.000000244101554	0.000051013068972	0.055908575918637
183.848428	194.318333	204.788238	0.000138004304518	0.000000159357620	0.000022831275790	0.265161342603404
204.712212	217.181667	229.651122	0.000028930033490	0.000000075911601	0.000007288550936	0.605628308596948
229.522157	244.609667	259.697177	0.000013722321992	0.000000054183557	0.000004074868423	1.156836232785782
259.513250	278.116000	296.718750	0.000008160210146	0.000000045701201	0.000002775995121	1.934470033311708
296.416400	319.914000	343.411600	0.000004124182693	0.000000038244803	0.000001785814031	3.124466669705408
342.923900	373.499000	404.074100	0.000002121899723	0.000000032767749	0.000001177011950	4.914512911225282

Table A.VI.8. Proton Yields from Iron 400 MeV/n on 60 g/cm^2 Aluminium at 10.0 deg

KE_left(MeV/n)	KE_mid(MeV/n)	KE_right(MeV/n)	Norm_Cts(#/SP*ster*MeV/n)	Y_stat(#/SP*ster*MeV/n)	Y_syst_tot(#/SP*ster*MeV/n)	X_tot(MeV/n)
45.817258	47.344633	48.872008	0.002534136501300	0.000000293140748	0.000388720298083	0.467663749312473
48.758705	50.557500	52.356295	0.002334258872102	0.000000306359042	0.000359828750584	0.269794843053773
52.469577	54.455367	56.441157	0.002416247548150	0.000000331245106	0.000362321531924	0.976817052683357
56.441143	58.426933	60.412723	0.002880644310233	0.000000365384352	0.000424824807104	0.887858295079795
60.301143	62.467133	64.633123	0.002989286143242	0.000000379604143	0.000430344551713	0.401761756780060
64.744685	67.194200	69.643715	0.003021190539433	0.000000408938228	0.000423860130052	0.791551962356231
69.589923	72.093233	74.596543	0.003423838993652	0.000000442707094	0.000476086079903	0.734680966467759
74.650360	77.564200	80.478040	0.003426279397963	0.000000475991934	0.000470358002833	0.660658138868356
80.367502	83.457867	86.548232	0.003680932027577	0.000000500194881	0.000491395470904	0.694529761199619
86.658760	90.037900	93.417040	0.003930564980200	0.000000544301840	0.000518434553340	0.672277482938407
93.411410	97.252100	101.092790	0.004154670662247	0.000000603478488	0.000544191109936	0.674359210324883
101.021130	105.260000	109.498870	0.004457430390471	0.000000641136189	0.000561171266661	0.626072032780574
109.503247	114.230667	118.958087	0.004632407653079	0.000000698401919	0.000580626205779	0.582511217057663
118.934025	124.330000	129.725975	0.004686279993165	0.000000734705989	0.000566178348030	0.541771438913127
129.696802	135.749667	141.802532	0.005436452059584	0.000000839816559	0.000651483312657	0.470696222705260
141.793598	148.758333	155.723068	0.006847625373825	0.000000987799030	0.000786316106517	0.324619422291705
155.653088	163.720333	171.787578	0.005826552324381	0.000000970561248	0.000660749108780	0.189485178309809
171.729737	181.108667	190.487597	0.005951866824781	0.000001044081556	0.000645956735113	0.080596061200284
190.406602	201.490667	212.574732	0.005872857170186	0.000001131176046	0.000643761564771	0.384913829994455
212.489680	225.745000	239.000320	0.004126827617982	0.000001045031338	0.000464769529785	0.779640911266847
238.850300	255.006000	271.161700	0.002286956468151	0.000000852744809	0.000258305658502	1.395501370647123
270.931183	290.985333	311.039483	0.001162143028558	0.000000675555449	0.000134525653562	2.279726712503058
310.684650	336.239000	361.793350	0.000304780858877	0.000000382886461	0.000041179572786	3.633423357400016
361.211983	394.890333	428.568683	0.000030017539564	0.000000130315341	0.000005762671563	5.717415339766738

Table A.VI.9. Proton Yields from Iron 400 MeV/n on 60 g/cm^2 Aluminium at 7.20 deg

KE_left(MeV/n)	KE_mid(MeV/n)	KE_right(MeV/n)	Norm_Cts(#/SP*ster*MeV/n)	Y_stat(#/SP*ster*MeV/n)	Y_syst_tot(#/SP*ster*MeV/n)	X_tot(MeV/n)
44.801742	46.388967	47.976192	0.002884379012183	0.000000319986283	0.000433902369360	0.701725018198012
47.976208	49.563433	51.150658	0.003417287155417	0.000000354167914	0.000506564511980	0.482919930581665
51.062683	52.998033	54.933383	0.003045716265892	0.000000372040645	0.000448611326640	0.520189075657111
55.021392	57.067767	59.114142	0.003312896830883	0.000000395552502	0.000479787265834	0.981917510839378
59.114158	61.160533	63.206908	0.003985826103207	0.000000430479360	0.000560280205817	0.667620651848039
63.112048	65.491233	67.870418	0.003728057028676	0.000000448278574	0.000519807032300	0.495524701771768
67.965250	70.474600	72.983950	0.004222356816407	0.000000493345897	0.000577362381810	0.899731178825098
72.860622	75.618067	78.375512	0.004488855662321	0.000000535103123	0.000609647680027	0.516073454800768
78.498842	81.471767	84.444692	0.004786582876600	0.000000567897438	0.000633729925651	0.786715481456289
84.376755	87.746400	91.116045	0.005076396887625	0.000000619545988	0.000660118088087	0.596898375344581
91.054483	94.725133	98.395783	0.005323963825199	0.000000661424527	0.000688572564382	0.640226768129856
98.414688	102.494233	106.573778	0.005568423814168	0.000000705079982	0.000703659208215	0.641768490363932
106.566383	111.136333	115.706283	0.006027628403934	0.000000779092216	0.000748803310997	0.608411345487574
115.705093	120.830333	125.955573	0.006659958890070	0.000000860738665	0.000805629897892	0.561612068149359
125.917347	131.750667	137.583987	0.007541171417034	0.000000975147868	0.000897992005688	0.434881756079742
137.579645	144.220000	150.860355	0.010524705415609	0.000001211884045	0.001213344647131	0.375956789353511
150.817123	158.485333	166.153543	0.008474959218665	0.000001155149758	0.000973381981905	0.230138994340572
166.123378	175.011333	183.899288	0.008687113300899	0.000001232514164	0.000948126279037	0.061848668163914
183.838408	194.321333	204.804258	0.009070589864208	0.000001364695104	0.000985620654644	0.256939078806942
204.688763	217.161333	229.633903	0.006391975957817	0.000001258370517	0.000727664329887	0.635063856195580
229.509343	244.601333	259.693323	0.002557140037244	0.000000868792981	0.000302785549417	1.168876303341376
259.515550	278.118000	296.720450	0.000994215594949	0.000000595812243	0.000117999223290	1.928956377180158
296.416767	319.925667	343.434567	0.000265841477235	0.000000340568210	0.000037037778998	3.101614438256309
342.935500	373.529000	404.122500	0.000028806552984	0.000000120848871	0.000005631891673	4.859905822019599

Table A.VI.10. Proton Yields from Iron 400 MeV/n on 60 g/cm^2 Aluminium at 32.7 deg

KE_left(MeV/n)	KE_mid(MeV/n)	KE_right(MeV/n)	Norm_Cts(#/SP*ster*MeV/n)	Y_stat(#/SP*ster*MeV/n)	Y_syst_tot(#/SP*ster*MeV/n)	X_tot(MeV/n)
43.867467	45.677367	47.487267	0.000391521254425	0.000000121347167	0.000083658143365	0.231018444566379
47.487300	49.297200	51.107100	0.000425200175903	0.000000133612963	0.000091364783603	0.851047840872650
51.107100	52.917000	54.726900	0.000393545525650	0.000000120037221	0.000082897547229	0.929335918477813
54.710225	56.536800	58.363375	0.000555639772106	0.000000148339267	0.000106364282188	0.362269672871040
58.380050	60.680000	62.979950	0.000444704394459	0.000000143363202	0.000082148522188	0.318740896692109
62.979850	65.279800	67.579750	0.000503166737406	0.000000155801723	0.000090459854228	0.761408113383355
67.462162	69.951667	72.441172	0.000473320714875	0.000000156756837	0.000085685856140	0.409468337579354
72.558780	75.348600	78.138420	0.000487883948689	0.000000172457255	0.000084492775622	0.520929657202390
78.012593	81.016733	84.020873	0.000524792613642	0.000000180737928	0.000085362987189	0.500549325114918
84.146678	87.425933	90.705188	0.000529229714960	0.000000187332648	0.000082862171054	0.496445927127014
90.662980	94.390100	98.117220	0.000511820347677	0.000000197307461	0.000078368745918	0.514610450001746
98.051153	102.151633	106.252113	0.000563110917179	0.000000222557870	0.000082607308627	0.490247733255341
106.245097	110.819667	115.394237	0.000518533459359	0.000000224305434	0.000075314626928	0.478155810598386
115.411817	120.537667	125.663517	0.000507718321932	0.000000230063267	0.000070357695097	0.424258516903315
125.641503	131.525333	137.409163	0.000502982977908	0.000000240604210	0.000066161813313	0.363127777242392
137.351850	144.022000	150.692150	0.000502326803681	0.000000260853864	0.000066622363056	0.291236077167648
150.658075	158.361000	166.063925	0.000450262305058	0.000000255230980	0.000056433636813	0.187515621044781
166.043488	174.976333	183.909178	0.000439735669971	0.000000271412799	0.000052585043968	0.067843690875202
183.854778	194.406333	204.957888	0.000313604415096	0.000000249604382	0.000038535294728	0.200338366960126
204.838007	217.399667	229.961327	0.000194960207415	0.000000210576571	0.000025736910357	0.510865715930322
229.829752	245.044667	260.259582	0.000109684190665	0.000000170129739	0.000015841493938	0.943798821879430
260.065483	278.850333	297.635183	0.000038620836860	0.000000107631498	0.000007441098006	1.573750142689112
297.335800	321.076000	344.816200	0.000005969759818	0.000000044880114	0.000002236331480	2.503182580755946
344.311000	375.284000	406.257000	0.000000773719168	0.000000018329676	0.000000622071880	3.939057464940059

Table A.VI.11. Proton Yields from Iron 400 MeV/n on 60 g/cm^2 Aluminium at 30.0 deg

KE_left(MeV/n)	KE_mid(MeV/n)	KE_right(MeV/n)	Norm_Cts(#/SP*ster*MeV/n)	Y_stat(#/SP*ster*MeV/n)	Y_syst_tot(#/SP*ster*MeV/n)	X_tot(MeV/n)
44.595672	46.187967	47.780262	0.000492235809280	0.000000130153591	0.000102465487334	0.888202449455641
47.780272	49.372567	50.964862	0.000534948803907	0.000000132729529	0.000106735747999	0.957767108258057
50.849218	52.738133	54.627048	0.000470266443734	0.000000135819496	0.000092988272598	0.615968904101498
54.742680	56.817600	58.892520	0.000459368688562	0.000000143180866	0.000089400982905	0.758758474239333
58.892513	60.967433	63.042353	0.000566858145795	0.000000151532850	0.000099448950987	0.760925332426908
62.908437	65.228667	67.548897	0.000565399355427	0.000000163930571	0.000096662260886	0.689244032750375
67.682815	70.243000	72.803185	0.000594905036025	0.000000176337236	0.000097968348038	0.886609578780311
72.701510	75.405000	78.108490	0.000613198654993	0.000000181404020	0.000098105210429	0.616878259687436
78.210145	81.255100	84.300055	0.000562973799223	0.000000188315376	0.000089276632628	0.910378570033917
84.182323	87.520933	90.859543	0.000605662260037	0.000000204366750	0.000092152280102	0.666434082606074
90.882622	94.534367	98.186112	0.000547309463207	0.000000205278952	0.000083805251179	0.777919143072080
98.218485	102.297200	106.375915	0.000639397091529	0.000000235672281	0.000090851429751	0.740322764113734
106.354842	110.945667	115.536492	0.000614769637324	0.000000245222044	0.000085479375787	0.687536009807486
115.507158	120.677333	125.847508	0.000556293428162	0.000000240303053	0.000075081820068	0.662834773147124
125.842303	131.647333	137.452363	0.000492580162705	0.000000238127010	0.000066069553821	0.572654997723760
137.436265	144.130000	150.823735	0.000333446571432	0.000000207364367	0.000046578192975	0.473380325502655
150.769423	158.440333	166.111243	0.000197369503381	0.000000166345143	0.000030100835373	0.306528912667305
166.053658	175.009333	183.965008	0.000082060084804	0.000000112451196	0.000015279903681	0.139470547839642
183.877760	194.383000	204.888240	0.000034539723275	0.000000077116644	0.000008636394249	0.239906483141265
204.817730	217.346000	229.874270	0.000008783356371	0.000000033073697	0.000003028127104	0.613679843420003
229.743653	244.909333	260.075013	0.000001441817068	0.000000017278021	0.000001228025762	1.186933032435276
259.879433	278.591333	297.303233	0.000000913529331	0.000000019324215	0.000001113019968	2.029604293809264
296.998267	320.646667	344.295067	0.000001055136288	0.000000020803939	0.000000951709307	3.256083891379336
384.151800	395.405000	406.658200	0.000000386156411	0.000000009721770	0.000000302781000	3.395850000000000

Table A.VI.12. Proton Yields from Iron 400 MeV/n on 60 g/cm^2 Aluminium at 27.2 deg

KE_left(MeV/n)	KE_mid(MeV/n)	KE_right(MeV/n)	Norm_Cts(#/SP*ster*MeV/n)	Y_stat(#/SP*ster*MeV/n)	Y_syst_tot(#/SP*ster*MeV/n)	X_tot(MeV/n)
44.043503	45.742933	47.442364	0.000541613868883	0.000000140455764	0.000109457737492	0.214036792869357
47.539835	49.375700	51.211565	0.000547409317892	0.000000145535985	0.000103973219881	0.988979905682618
51.211535	53.047400	54.883265	0.000615973703215	0.000000151616829	0.000111679464517	1.150220167542284
54.883235	56.719100	58.554965	0.000653025015222	0.000000161417707	0.000118614024605	0.625987491435731
58.505832	60.774267	63.042702	0.000651748029190	0.000000177305980	0.000109882002599	0.469147888192455
63.091792	65.409367	67.726942	0.000711487809975	0.000000181839368	0.000114206966272	0.985910907677768
67.621325	70.095200	72.569075	0.000677011844476	0.000000184096032	0.000108730046288	0.650317126235347
72.674692	75.474067	78.273442	0.000685934198914	0.000000200954977	0.000107049466728	0.737536831382677
78.153378	81.152433	84.151488	0.000777847854670	0.000000220108209	0.000115356257902	0.734052316156008
84.271573	87.552733	90.833893	0.000758985903220	0.000000226544577	0.000109402659707	0.715740698019192
90.792043	94.514133	98.236223	0.000738832535912	0.000000238044375	0.000104285433257	0.728859951190899
98.173632	102.270567	106.367502	0.000690009101622	0.000000242313176	0.000095902751672	0.694349356892480
106.362120	110.931000	115.499880	0.000743659868372	0.000000262656778	0.000098629224817	0.667131629321381
115.516727	120.633667	125.750607	0.000760854351492	0.000000283903814	0.000097291476652	0.589510608876549
125.734923	131.617333	137.499743	0.000783228619228	0.000000306117772	0.000096386463808	0.520540268130142
137.420447	144.084667	150.748887	0.000771683521922	0.000000321329394	0.000091719349319	0.401348903804408
150.727928	158.414333	166.100738	0.000655874427263	0.000000312300545	0.000076444652827	0.272607060674077
166.060497	174.983667	183.906837	0.000653780203046	0.000000330503950	0.000072237827260	0.082770635342554
183.853142	194.376667	204.900192	0.000590387054813	0.000000342136141	0.000064432370508	0.257607553138180
204.788835	217.319000	229.849165	0.000361144865548	0.000000289259281	0.000042118087376	0.651673275021310
229.723800	244.895000	260.066200	0.000146389582140	0.000000198438002	0.000020038032127	1.206456692196201
259.882550	278.600000	297.317450	0.000044487950887	0.000000117173719	0.000008147358766	2.012084019145324
297.011383	320.672333	344.333283	0.000006149719629	0.000000046933283	0.000002265235919	3.207103961536014
343.831700	374.667000	405.502300	0.000001307358684	0.000000022912969	0.000000823619210	5.014003641781685

Table A.VI.13. Triton Yields from Iron 400 MeV/n on 60 g/cm^2 Aluminium at 12.7 deg

KE_left(MeV/n)	KE_mid(MeV/n)	KE_right(MeV/n)	Norm_Cts(#/SP*ster*MeV/n)	Y_stat(#/SP*ster*MeV/n)	Y_syst_tot(#/SP*ster*MeV/n)	X_tot(MeV/n)
45.912716	47.166367	48.420017	0.000370284428968	0.000000093819219	0.000090615694568	23.024421250375024
48.420016	49.673667	50.927317	0.000388815140186	0.000000105688572	0.000107442990297	0.321840708736480
50.853693	52.341067	53.828440	0.000407791110109	0.000000117878478	0.000103609226068	0.365454480789332
53.902077	55.496667	57.091257	0.000425876562621	0.000000130073592	0.000107104209586	0.465960805670391
57.091243	58.685833	60.280423	0.000444407273839	0.000000116440188	0.000095982743598	0.295107204908725
60.238895	62.132400	64.025905	0.000516551631595	0.000000130413854	0.000092951196686	0.349762618194112
64.067418	66.002433	67.937448	0.000537071320033	0.000000134466669	0.000093662932855	0.387846377543996
67.870505	70.060800	72.251095	0.000561307808628	0.000000141247014	0.000090769757458	0.199615724843661
72.303050	74.595200	76.887350	0.000607023205549	0.000000146944348	0.000091473122931	0.312338962982270
76.902337	79.524667	82.146997	0.000682701743022	0.000000168224165	0.000095623179197	0.197028500298840
82.065775	84.910100	87.754425	0.000789742161590	0.000000185105619	0.000101150996556	0.136942385055942
87.744203	90.872133	94.000063	0.000844694910651	0.000000211024944	0.000113141875160	0.075697607182526
94.002560	97.475200	100.947840	0.000899647018726	0.000000305433965	0.000182745260850	0.037954308716139
100.935963	104.804333	108.672703	0.000880887138832	0.000000368508013	0.000226205378351	0.159965780841591
108.695367	113.003667	117.311967	0.000838276804423	0.000000259368462	0.000116857625327	0.283997887439326
117.297767	122.209667	127.121567	0.000439372936639	0.000000179901397	0.000058114961316	0.447420816469238
127.067273	132.602333	138.137393	0.000117522304100	0.000000095840027	0.000021732816987	0.660025763396400
138.122012	144.446667	150.771322	0.000079330570423	0.000000087331893	0.000016426195703	0.938069112789138
150.756720	158.015000	165.273280	0.000048309769540	0.000000072811988	0.000011533962141	1.274714755923850
165.253633	173.711333	182.169033	0.000020986181203	0.000000050040967	0.000006721795364	1.698050159953174
182.083075	192.023000	201.962925	0.000006799147892	0.000000028656875	0.000003122636220	2.290152563345945
201.868037	213.658667	225.449297	0.000007708923597	0.000000033497168	0.000003124011622	3.043569006216222
225.344710	239.575000	253.805290	0.000006508098899	0.000000033600661	0.000002617245158	4.059202717295602
253.627600	271.107000	288.586400	0.000004492612529	0.000000027043202	0.000001689369559	5.518748153431175
288.321217	310.257667	332.194117	0.000003241411668	0.000000030261029	0.000001537368239	7.604236321932664
332.527900	350.543500	368.559100	0.000001008913549	0.000000018392690	0.000000717163108	8.234996991043772

Table A.VI.14. Triton Yields from Iron 400 MeV/n on 60 g/cm^2 Aluminium at 10.0 deg

KE_left(MeV/n)	KE_mid(MeV/n)	KE_right(MeV/n)	Norm_Cts(#/SP*ster*MeV/n)	Y_stat(#/SP*ster*MeV/n)	Y_syst_tot(#/SP*ster*MeV/n)	X_tot(MeV/n)
44.157519	45.439333	46.721148	0.000494370020511	0.000000127668220	0.000135922044923	39.057402857973031
46.721152	48.002967	49.284781	0.000534223309653	0.000000158164627	0.000177197061272	0.418116948392432
49.284752	50.566567	51.848381	0.000574076598794	0.000000161830728	0.000186179152367	0.370061833931844
51.783042	53.322100	54.861158	0.000614644078228	0.000000169447560	0.000163970128007	0.353123761038534
54.926500	56.548300	58.170100	0.000653783177076	0.000000164590401	0.000149763143315	0.422193350896245
58.162230	59.791900	61.421570	0.000721176476889	0.000000156167575	0.000135095226538	0.235928049893797
61.429487	63.391067	65.352647	0.000749511432542	0.000000155370443	0.000114205420787	0.394123356290895
65.352620	67.314200	69.275780	0.000804126747857	0.000000175826063	0.000133694843604	0.301137896771579
69.253865	71.535200	73.816535	0.000902298535040	0.000000195215748	0.000132832563035	0.292274905080748
73.769932	76.163767	78.557602	0.001001078609492	0.000000222724018	0.000156111193062	0.210609151006147
78.626100	81.274200	83.922300	0.001185872501749	0.000000231604378	0.000152629565600	0.219164214474649
83.878897	86.832567	89.786237	0.001338033734466	0.000000238662845	0.000144418096340	0.088640714207560
89.754622	92.998267	96.241912	0.001448179245279	0.000000265011002	0.000152742057456	0.046531382695231
96.238452	99.832167	103.425882	0.001557254702495	0.000000445250023	0.000345253302966	0.054186219326412
103.437198	107.431333	111.425468	0.001791948637376	0.000000434781983	0.000304299333271	0.205000507844469
111.411130	115.950000	120.488870	0.001769988390240	0.000000367221184	0.000187901913692	0.340984614780491
120.468350	125.537000	130.605650	0.001000421007669	0.000000291089407	0.000116384582665	0.491290875562533
130.599747	136.384667	142.169587	0.000905327077944	0.000000293983303	0.000102210831862	0.739757880102673
142.123283	148.759333	155.395383	0.001333650909330	0.000000393463627	0.000146989613963	1.045979773260458
155.366307	163.006667	170.647027	0.000435610003187	0.000000239678709	0.000057966130089	1.368968902280837
170.605352	179.511667	188.417982	0.000196767268658	0.000000169327468	0.000027839063569	1.847435127845089
188.338767	198.848667	209.358567	0.000172199351935	0.000000171659504	0.000024196885101	2.478019221717217
209.253508	221.801333	234.349158	0.000149837166189	0.000000175115912	0.000020791454642	3.284323552103234
234.214043	249.422333	264.630623	0.000106398879526	0.000000165088684	0.000015622744383	4.415092751879625
264.437950	283.255000	302.072050	0.000057799537958	0.000000129465264	0.000009502790453	6.008802529872321
301.763500	325.593000	349.422500	0.000020760698212	0.000000084583113	0.000004346479772	8.333382538213400
348.899800	380.028000	411.156200	0.000006665552401	0.000000050424743	0.000001818546836	11.993078153505879

Table A.VI.15. Triton Yields from Iron 400 MeV/n on 60 g/cm^2 Aluminium at 7.20 deg

KE_left(MeV/n)	KE_mid(MeV/n)	KE_right(MeV/n)	Norm_Cts(#/SP*ster*MeV/n)	Y_stat(#/SP*ster*MeV/n)	Y_syst_tot(#/SP*ster*MeV/n)	X_tot(MeV/n)
45.819744	47.123400	48.427056	0.000831403914991	0.000000208986839	0.000262260829959	22.947568699041735
48.427044	49.730700	51.034356	0.000872267774560	0.000000230777994	0.000315658926878	0.418213294798240
50.971191	52.351200	53.731209	0.000913885271308	0.000000249981697	0.000325423407265	0.373087898523927
53.794365	55.437300	57.080235	0.000953995493698	0.000000222570406	0.000230609462080	0.364945311661898
57.080232	58.723167	60.366102	0.000994859353267	0.000000198088069	0.000189543338733	0.345649310964162
60.277127	62.105567	63.934007	0.001172799438771	0.000000186712262	0.000160272303315	0.274021335855440
64.022995	66.005200	67.987405	0.001338109332698	0.000000200980750	0.000159732527496	0.385927803967271
67.893357	70.043867	72.194377	0.001524107665367	0.000000214347717	0.000168767989538	0.171485046312919
72.288385	74.611900	76.935415	0.001703659672565	0.000000243469451	0.000185049129404	0.323443634352262
76.881073	79.494833	82.108593	0.001966367951671	0.000000263882383	0.000191054448391	0.165737690437269
82.069458	84.901833	87.734208	0.002317662817665	0.000000290726817	0.000205646465649	0.154797580487863
87.752562	90.876967	94.001372	0.002521683879045	0.000000328202687	0.000228112256052	0.093268488064847
94.001620	97.477100	100.952580	0.002725871995038	0.000000494794378	0.000433475018978	0.043388651335257
100.938103	104.814333	108.690563	0.002881684948026	0.000000537297884	0.000450365092570	0.133163547311793
108.690775	113.011000	117.331225	0.002808195398620	0.000000449654573	0.000286863323126	0.270567904798407
117.307912	122.208667	127.109422	0.002270786176129	0.000000433274486	0.000238749218039	0.451947893034142
127.084917	132.618667	138.152417	0.001419385295487	0.000000364303135	0.000152475812498	0.632486737236442
138.126548	144.457333	150.788118	0.002119143241887	0.000000479054522	0.000220830255445	0.920616280393194
150.773978	158.044333	165.314688	0.001150466213248	0.000000381926623	0.000131068263136	1.224527195896441
165.280265	173.742000	182.203735	0.000400844468221	0.000000235247674	0.000050113478012	1.645138774745158
182.130637	192.072667	202.014697	0.000269274634874	0.000000208703074	0.000034677374564	2.203737387485178
201.915570	213.719000	225.522430	0.000190110980540	0.000000190286009	0.000025424035694	2.938897276683893
225.421328	239.661333	253.901338	0.000106814461346	0.000000158164580	0.000015804428019	3.908980380022392
253.724567	271.227667	288.730767	0.000053614238907	0.000000121186071	0.000009318293798	5.308908520684831
288.467083	310.432333	332.397583	0.000012507719851	0.000000060608991	0.000003237918990	7.300412037227762
331.968983	360.352333	388.735683	0.000003500100970	0.000000030836099	0.000001242009509	10.367642826505936

Table A.VI.16. Triton Yields from Iron 400 MeV/n on 60 g/cm^2 Aluminium at 32.7 deg

KE_left(MeV/n)	KE_mid(MeV/n)	KE_right(MeV/n)	Norm_Cts(#/SP*ster*MeV/n)	Y_stat(#/SP*ster*MeV/n)	Y_syst_tot(#/SP*ster*MeV/n)	X_tot(MeV/n)
44.778104	45.503100	46.228096	0.000011252931147	0.000000013579349	0.000013149534676	31.894782646226012
47.194490	48.137500	49.080510	0.000038805965175	0.000000023753703	0.000017983998408	0.114407129550741
50.023552	51.438067	52.852582	0.000021261170607	0.000000020692438	0.000015532012617	0.625582395156705
52.852585	54.267100	55.681615	0.000047854686292	0.000000027043202	0.000020596375423	0.431175572418302
55.641742	57.374167	59.106592	0.000029132682667	0.000000025877432	0.000016055490174	0.167411718768102
59.146420	60.918700	62.690980	0.000014478307671	0.000000020748271	0.000012363041864	0.394385261669348
62.607663	64.510833	66.414003	0.000024349487074	0.000000024078127	0.000013405955952	0.307437389204696
66.497300	68.626700	70.756100	0.000037336268297	0.000000034630487	0.000017371829199	0.302040560695083
70.665832	72.946567	75.227302	0.000024308657039	0.000000030222786	0.000014454877569	0.260017688792513
75.317565	77.805600	80.293635	0.000017186783598	0.000000022862430	0.000009767588011	0.265350921351331
80.240530	83.037000	85.833470	0.000022179309939	0.000000025235320	0.000009671654620	0.251611822097055
85.790770	88.840000	91.889230	0.000008969221769	0.000000021215770	0.000007177906855	0.155690288513767
91.890668	95.265533	98.640398	0.000026841253290	0.000000034597066	0.000010928346999	0.146778603127840
99.916540	102.431350	104.946160	0.000004015057473	0.000000013748659	0.000003846379467	0.096153783354011
106.253120	107.573000	108.892880	0.000003745164708	0.000000009721770	0.000002581480000	0.042734200000000

Table A.VI.17. Triton Yields from Iron 400 MeV/n on 60 g/cm^2 Aluminium at 30.0 deg

KE_left(MeV/n)	KE_mid(MeV/n)	KE_right(MeV/n)	Norm_Cts(#/SP*ster*MeV/n)	Y_stat(#/SP*ster*MeV/n)	Y_syst_tot(#/SP*ster*MeV/n)	X_tot(MeV/n)
45.042489	46.191733	47.340978	0.000033400360069	0.000000024126113	0.000022294841944	32.327681047306811
47.261368	48.530433	49.799499	0.000031444616480	0.000000021324490	0.000018350212835	0.086907555066685
49.879115	51.385100	52.891085	0.000040719842399	0.000000029421230	0.000021031192512	0.556991774956327
52.891115	54.397100	55.903085	0.000031040641164	0.000000022132985	0.000015746017347	0.624075699621448
55.844497	57.409067	58.973637	0.000032323128442	0.000000027643300	0.000018450941559	0.258470444727366
59.032223	60.892133	62.752043	0.000027335215935	0.000000028466360	0.000016245838353	0.372525997753298
62.752023	64.611933	66.471843	0.000033359797559	0.000000025966702	0.000014957861473	0.480208554605184
66.412463	68.566433	70.720403	0.000035002834420	0.000000030042139	0.000015142109806	0.209864035681700
70.779132	72.993867	75.208602	0.000038666591484	0.000000033796531	0.000016466396485	0.346147887844199
75.209242	77.779567	80.349892	0.000028739465643	0.000000031857091	0.000013292095409	0.217397910648217
80.251337	83.005367	85.759397	0.000033998093555	0.000000033073694	0.000013049636430	0.172589441385648
85.786077	88.810367	91.834657	0.000022233695029	0.000000025966702	0.000009177363878	0.101310558425911
91.906580	93.004400	94.102220	0.000016685262557	0.000000012311700	0.000003993570000	0.079272500000000

Table A.VI.18. Triton Yields from Iron 400 MeV/n on 60 g/cm^2 Aluminium at 27.2 deg

KE_left(MeV/n)	KE_mid(MeV/n)	KE_right(MeV/n)	Norm_Cts(#/SP*ster*MeV/n)	Y_stat(#/SP*ster*MeV/n)	Y_syst_tot(#/SP*ster*MeV/n)	X_tot(MeV/n)
45.814780	47.053000	48.291220	0.000044962557455	0.000000026591084	0.000023040022154	23.074204997294991
48.291247	49.529467	50.767687	0.000035740983334	0.000000022912969	0.000019817727743	0.306103901432177
50.703338	52.219667	53.735996	0.000029614379723	0.000000023386624	0.000016850398844	0.403006794193349
53.800367	55.391867	56.983367	0.000052085656416	0.000000038567316	0.000026026092008	0.486543192016906
56.983400	58.574900	60.166400	0.000028183666124	0.000000023337118	0.000015640257839	0.292968479370751
60.125117	62.026967	63.928817	0.000057941699954	0.000000040641030	0.000023356399114	0.350329943463030
63.970085	65.913200	67.856315	0.000050882878001	0.000000033038709	0.000018427905770	0.421393255838296
67.782008	69.972333	72.162658	0.000041402461910	0.000000030042139	0.000014829135256	0.184529457605283
72.236958	74.532633	76.828308	0.000041509394081	0.000000032767749	0.000015435537363	0.330864514704977
76.818230	79.458900	82.099570	0.000038560022697	0.000000033038709	0.000013645509320	0.175329066253745
82.015860	84.863500	87.711140	0.000050083145896	0.000000041787675	0.000015880707117	0.164409742648501
87.722602	90.858067	93.993532	0.000061129558994	0.000000048887308	0.000017186991467	0.069700638887388
93.996760	97.483800	100.970840	0.000050888262022	0.000000048876576	0.000015157226525	0.040745924081066
100.957948	104.849333	108.740718	0.000213887474230	0.000000114463769	0.000035502256093	0.154938803769262
108.739865	113.081000	117.422135	0.000145889331368	0.000000096662663	0.000027773595954	0.290130155257946
117.395593	122.316333	127.237073	0.000066742460979	0.000000063046165	0.000014716580653	0.500893823210069
127.355990	129.112000	130.868010	0.000019597409628	0.000000020370900	0.000004163970000	0.339992000000000

Table A.VI.19. Helium-4 Yields from Iron 400 MeV/n on 60 g/cm^2 Aluminium at 12.7 deg

KE_left(MeV/n)	KE_mid(MeV/n)	KE_right(MeV/n)	Norm_Cts(#/SP*ster*MeV/n)	Y_stat(#/SP*ster*MeV/n)	Y_syst_tot(#/SP*ster*MeV/n)	X_tot(MeV/n)
44.619806	46.118600	47.617394	0.000113151525905	0.000000117878478	0.000102701315102	0.660984978177265
47.492555	49.212733	50.932911	0.000126036770902	0.000000135216010	0.000107512885305	0.163200792267961
51.057768	53.016033	54.974298	0.000138179230717	0.000000134087970	0.000089801245309	0.620693598921400
54.974335	56.932600	58.890865	0.000150693083123	0.000000131746897	0.000090941708035	1.062514304778529
58.808553	60.858433	62.908313	0.000167535810199	0.000000104467206	0.000065361669344	0.602990825798370
62.990627	65.414567	67.838507	0.000214299937765	0.000000109353841	0.000056304922075	0.619327227822256
67.838493	70.262433	72.686373	0.000231762239520	0.000000101304235	0.000052770035381	0.824050736004768
72.631535	75.466900	78.302265	0.000208893033835	0.000000107561845	0.000047546073306	0.632189628628942
78.300260	81.247300	84.194340	0.000234495553173	0.000000116563190	0.000050256229136	0.679560701410109
84.251155	87.608500	90.965845	0.000259924651394	0.000000128852381	0.000050939438464	0.725414005387958
90.869188	94.561833	98.254478	0.000245608132014	0.000000133557384	0.000048119144350	0.689386930297493
98.228435	102.315200	106.401965	0.000194756942664	0.000000115769558	0.000037377402158	0.653751004733453
106.403128	110.970333	115.537538	0.000219610157616	0.000000136332339	0.000040102825730	0.624139372237484
115.560618	120.676333	125.792048	0.000177544102867	0.000000123822567	0.000032311757044	0.585268133427748
125.771770	131.642000	137.512230	0.000163496873493	0.000000125508254	0.000028690811253	0.509452072506335
137.444312	144.106667	150.769022	0.000144466022143	0.000000128852381	0.000025280865067	0.392110896142915
150.749975	158.432000	166.114025	0.000158059892483	0.000000136315363	0.000024484982163	0.273128161556512
166.051657	174.981667	183.911677	0.000133230430258	0.000000135848018	0.000020408486115	0.073332601308422
183.853690	194.373000	204.892310	0.000073400614855	0.000000106395538	0.000013087837019	0.256213513320453
205.035155	213.126000	221.216845	0.000017763873800	0.000000038761202	0.000003662720541	0.428618592663687

Table A.VI.20. Helium-4 Yields from Iron 400 MeV/n on 60 g/cm^2 Aluminium at 10.0 deg

KE_left(MeV/n)	KE_mid(MeV/n)	KE_right(MeV/n)	Norm_Cts(#/SP*ster*MeV/n)	Y_stat(#/SP*ster*MeV/n)	Y_syst_tot(#/SP*ster*MeV/n)	X_tot(MeV/n)
44.652535	46.228000	47.803465	0.000533359621048	0.000000174350233	0.000165680943984	0.832111688764195
47.803435	49.378900	50.954365	0.000536045787258	0.000000181839368	0.000176569983786	0.427767271577665
50.876682	52.833367	54.790052	0.000538768314757	0.000000185696360	0.000146984834131	0.364849470929884
54.867755	56.903900	58.940045	0.000541418119679	0.000000170034455	0.000120658363182	1.018180756712186
58.940055	60.976200	63.012345	0.000503470198970	0.000000141200814	0.000096591723940	0.783949807027848
62.923495	65.312700	67.701905	0.000522297553761	0.000000156167542	0.000094711386931	0.456473539349216
67.790773	70.291633	72.792493	0.000535506579538	0.000000166001800	0.000096382024903	0.878860090429643
72.672878	75.435333	78.197788	0.000583545504105	0.000000176422652	0.000098958765707	0.582790387603468
78.317370	81.283500	84.249630	0.000599220909926	0.000000187916188	0.000098318153690	0.741818225677288
84.190565	87.564000	90.937435	0.000597689501912	0.000000201251600	0.000094770477624	0.650315904226554
90.868707	94.542267	98.215827	0.000608456722153	0.000000211990463	0.000094603273015	0.651070915097580
98.230833	102.313633	106.396433	0.000620063115708	0.000000222557574	0.000091625826214	0.646416541295936
106.389003	110.963333	115.537663	0.000599546438528	0.000000233604882	0.000086724211909	0.611838895349094
115.539695	120.671000	125.802305	0.000631892629392	0.000000248555565	0.000085869729056	0.579411508914002
125.765498	131.612333	137.459168	0.000607918253779	0.000000255900578	0.000080154567482	0.460518497598088
137.448357	144.105667	150.762977	0.000538260263232	0.000000249163410	0.000068830556260	0.386997036646277
150.722010	158.412000	166.101990	0.000495781605078	0.000000262649201	0.000061764906786	0.246864720192578
166.065445	174.988000	183.910555	0.000445800226155	0.000000253453547	0.000052895544428	0.086104817161643
183.848542	194.375667	204.902792	0.000197628371878	0.000000178391471	0.000027599443190	0.250267647576769
205.022840	213.107500	221.192160	0.000027173649926	0.000000052166293	0.000005161499771	0.453820510774910

Table A.VI.21. Helium-4 Yields from Iron 400 MeV/n on 60 g/cm^2 Aluminium at 7.20 deg

KE_left(MeV/n)	KE_mid(MeV/n)	KE_right(MeV/n)	Norm_Cts(#/SP*ster*MeV/n)	Y_stat(#/SP*ster*MeV/n)	Y_syst_tot(#/SP*ster*MeV/n)	X_tot(MeV/n)
45.682937	47.318567	48.954197	0.001111794200146	0.000000260533350	0.000301832397832	0.762043754177541
48.954170	50.589800	52.225430	0.001142307936737	0.000000271751258	0.000319499898772	0.515856050226223
52.125990	54.077900	56.029810	0.001173575849682	0.000000259732703	0.000251281928928	0.425229063693911
56.129293	58.225933	60.322573	0.001276646947917	0.000000248643679	0.000216792108653	0.986037767583981
60.322560	62.419200	64.515840	0.001552678788360	0.000000265492468	0.000234400751545	0.702393770875710
64.428763	66.882733	69.336703	0.001484947116977	0.000000281957486	0.000221751361928	0.497228082250993
69.423807	71.984367	74.544927	0.001597318736440	0.000000295519173	0.000233042793978	0.896195756381941
74.440120	77.305700	80.171280	0.001616391316787	0.000000320069600	0.000232855265334	0.544375167285393
80.266727	83.301167	86.335607	0.001845265420194	0.000000336890877	0.000248941227457	0.750159103082140
86.344962	89.835867	93.326772	0.001699010643787	0.000000355189916	0.000228882054476	0.646576469168961
93.227460	97.044400	100.861340	0.001723970023387	0.000000370847731	0.000230235679307	0.667568055866216
100.844685	105.083000	109.321315	0.001838218934379	0.000000391152247	0.000230254104070	0.630190738629187
109.329730	114.069000	118.808270	0.001886930075402	0.000000421861726	0.000234160780907	0.590980332512851
118.780900	124.141000	129.501100	0.001983067344405	0.000000455266788	0.000232551728856	0.494107197740531
129.504330	135.602000	141.699670	0.001901108597199	0.000000475586340	0.000221268949701	0.456451697166305
141.663597	148.648667	155.633737	0.001904022972027	0.000000490086050	0.000209646441620	0.332625324849146
155.585297	163.650667	171.716037	0.001685698362740	0.000000488726146	0.000177570688443	0.167278615862518
171.696503	181.111333	190.526163	0.001112608909816	0.000000419414751	0.000121170297993	0.093358452921254
190.430515	201.582000	212.733485	0.000167203784370	0.000000171099599	0.000026363323538	0.370163437250358

Table A.VI.22. Helium-3 Yields from Iron 400 MeV/n on 60 g/cm^2 Aluminium at 12.7 deg

KE_left(MeV/n)	KE_mid(MeV/n)	KE_right(MeV/n)	Norm_Cts(#/SP*ster*MeV/n)	Y_stat(#/SP*ster*MeV/n)	Y_syst_tot(#/SP*ster*MeV/n)	X_tot(MeV/n)
45.107243	46.901033	48.694823	0.000227676814715	0.000000191951996	0.000162675940261	0.232992425937089
48.794670	50.914500	53.034330	0.000274539958591	0.000000204366901	0.000154541222581	0.630304919045536
53.034337	55.154167	57.273997	0.000322682628950	0.000000218575948	0.000170182815791	1.162366137530253
57.273970	59.393800	61.513630	0.000347117682092	0.000000206810608	0.000160699855138	0.876467586137673
61.472960	64.049600	66.626240	0.000320048037252	0.000000170656541	0.000098118272304	0.577226802477155
66.666913	69.284233	71.901553	0.000286475438849	0.000000170412109	0.000096127046840	0.940081513468912
71.774447	74.679967	77.585487	0.000252077076715	0.000000182275928	0.000097666791376	0.743853440955945
77.712595	80.832100	83.951605	0.000223828070771	0.000000194168907	0.000097654237595	0.836632024484480
83.863573	87.391233	90.918893	0.000191227962319	0.000000213043687	0.000099566676816	0.819181863206211
90.881418	94.712833	98.544248	0.000156130555306	0.000000170864712	0.000070668548290	0.822039906090939
98.569013	102.831333	107.093653	0.000151703050065	0.000000111445759	0.000033178985527	0.798682421821089
107.088253	111.875333	116.662413	0.000101035690518	0.000000093208944	0.000023791285104	0.835533978723187
116.632975	122.018000	127.403025	0.000113546279835	0.000000101304279	0.000023723718757	0.799512409018146
127.392762	133.475667	139.558572	0.000085236632891	0.000000095979987	0.000019288802650	0.758012036643218
139.557497	146.531667	153.505837	0.000063406571034	0.000000085014155	0.000014641059191	0.651371617302289
153.454373	161.520333	169.586293	0.000067955159927	0.000000091624810	0.000013863611730	0.557962770422006
169.545378	178.934333	188.323288	0.000066254324505	0.000000094192953	0.000012678174845	0.448836797307217
188.246638	199.322333	210.398028	0.000052110393091	0.000000092728750	0.000010098198220	0.218557833026959
210.278695	223.530000	236.781305	0.000044567316345	0.000000094735785	0.000008948144050	0.164908829765298
236.945000	247.312000	257.679000	0.000003505841042	0.000000018392691	0.000001307936959	0.426353324411808

Table A.VI.23. Helium-3 Yields from Iron 400 MeV/n on 60 g/cm^2 Aluminium at 10.0 deg

KE_left(MeV/n)	KE_mid(MeV/n)	KE_right(MeV/n)	Norm_Cts(#/SP*ster*MeV/n)	Y_stat(#/SP*ster*MeV/n)	Y_syst_tot(#/SP*ster*MeV/n)	X_tot(MeV/n)
45.408898	47.149633	48.890368	0.000181339271352	0.000000217893403	0.000212428674708	0.633737969127620
48.759425	50.733100	52.706775	0.000205030667872	0.000000209227246	0.000176441582935	0.313924042226476
52.837715	55.058000	57.278285	0.000227476497024	0.000000174845229	0.000118968985281	1.012937159241875
57.278315	59.498600	61.718885	0.000252289176504	0.000000116897471	0.000067136799927	1.032930541590285
61.600518	64.010033	66.419548	0.000274934989532	0.000000115872824	0.000062245275858	0.496504284010722
66.537880	69.256000	71.974120	0.000291182794305	0.000000146096851	0.000074317340583	0.902960276496148
71.887798	74.697733	77.507668	0.000307993486896	0.000000191201240	0.000107098922944	0.802641425122078
77.593985	80.813600	84.033215	0.000331885040077	0.000000219462605	0.000116705081466	0.810370636275155
83.894670	87.370000	90.845330	0.000352985810805	0.000000244684647	0.000125211416136	0.790255451085280
90.899388	94.707333	98.515278	0.000370033738793	0.000000257559374	0.000125740193928	0.806308998276715
98.569403	102.828333	107.087263	0.000383575806551	0.000000181403909	0.000066123487910	0.792173755458359
107.056620	111.855000	116.653380	0.000319427494176	0.000000175115912	0.000053822690827	0.800146999001433
116.604132	122.011667	127.419202	0.000300231167112	0.000000176252006	0.000048970636989	0.785958837984535
127.401617	133.475667	139.549717	0.000275493392933	0.000000175649403	0.000043719008535	0.760453483158569
139.529633	146.529333	153.529033	0.000256496726900	0.000000179385654	0.000038818290242	0.645480131970768
153.480113	161.516333	169.552553	0.000250562205915	0.000000185949536	0.000036075653360	0.546227372582151
169.503515	178.913000	188.322485	0.000220366488858	0.000000190180630	0.000031328268604	0.414109208838683
188.245560	199.302000	210.358440	0.000242115761169	0.000000209619293	0.000030733383494	0.182166910666811
210.262463	223.519333	236.776203	0.000110915698388	0.000000142829847	0.000017085978938	0.185516512672053

Table A.VI.24. Helium-3 Yields from Iron 400 MeV/n on 60 g/cm^2 Aluminium at 7.20 deg

KE_left(MeV/n)	KE_mid(MeV/n)	KE_right(MeV/n)	Norm_Cts(#/SP*ster*MeV/n)	Y_stat(#/SP*ster*MeV/n)	Y_syst_tot(#/SP*ster*MeV/n)	X_tot(MeV/n)
45.436347	47.250567	49.064787	0.000327539226819	0.000000248184205	0.000245567414096	0.796734622782894
49.064780	50.879000	52.693220	0.000358674785400	0.000000262656599	0.000268542828551	0.536196745162631
52.645810	54.897000	57.148190	0.000390029053626	0.000000243498156	0.000193680359919	0.767807308319607
57.195637	59.494267	61.792897	0.000421616424984	0.000000171321320	0.000110566274309	1.016795463967066
61.792903	64.091533	66.390163	0.000433322467166	0.000000149447287	0.000092192835075	0.647014120163540
66.383970	69.174200	71.964430	0.000433302168846	0.000000192229392	0.000110314381161	0.782433376290915
71.970632	74.767067	77.563502	0.000433281900597	0.000000255893094	0.000168244504644	0.904708152422095
77.510460	80.754800	83.999140	0.000443277868383	0.000000297738912	0.000180789577172	0.723112066782183
83.948843	87.388533	90.828223	0.000448023422747	0.000000317955324	0.000193865809600	0.828587878936809
90.931520	94.731800	98.532080	0.000448002736700	0.000000331331987	0.000189781703715	0.848615245293767
98.524977	102.823367	107.121757	0.000459058827060	0.000000251629339	0.000104743808871	0.781778917111481
107.082100	111.849000	116.615900	0.000514611477900	0.000000220706708	0.000077990537619	0.784170782171205
116.567218	121.989333	127.411448	0.000541620653666	0.000000247627727	0.000078981254341	0.748685998449283
127.362668	133.462333	139.561998	0.000573366452662	0.000000266234157	0.000079843218561	0.741788696199261
139.526805	146.517000	153.507195	0.000619656808714	0.000000279737006	0.000079393425157	0.625458170355940
153.470473	161.512333	169.554193	0.000527335661728	0.000000280769782	0.000067386305692	0.538444278384495
169.492688	178.892333	188.291978	0.000471747347866	0.000000274627337	0.000057327281977	0.380283721001833
188.221137	199.284667	210.348197	0.000463324588229	0.000000291125937	0.000052584811799	0.151098816744672
210.279403	223.521333	236.763263	0.000519414655168	0.000000332103060	0.000060172415918	0.184438906022591
236.612233	252.736333	268.860433	0.000097565672674	0.000000154940339	0.000015129834729	0.623014329894586
269.315700	275.488000	281.660300	0.000002390742076	0.000000013664300	0.000000784964000	0.582639000000000

Table A.VII.1. Deuteron Yields from Iron 800 MeV/n on 20 g/cm^2 Aluminium at 12.7 deg

KE_left(MeV/n)	KE_mid(MeV/n)	KE_right(MeV/n)	Norm_Cts(#/SP*ster*MeV/n)	Y_stat(#/SP*ster*MeV/n)	Y_syst_tot(#/SP*ster*MeV/n)	X_tot(MeV/n)
45.030051	46.341667	47.653282	0.001410929675860	0.000000455276159	0.000369562595787	0.136827427549669
47.728282	49.176733	50.625184	0.001016241379320	0.000000429438624	0.000313692829787	0.270401814885200
50.625182	52.073633	53.522084	0.001680266521067	0.000000562909584	0.000413172723075	0.233702029403598
53.467733	55.122333	56.776933	0.001308326076043	0.000000541771399	0.000350762120670	0.067361990595439
56.831295	58.556700	60.282105	0.001655187639867	0.000000594077851	0.000367308433373	0.231483585718923
60.212533	62.106233	63.999933	0.001628406216508	0.000000593545384	0.000335304555248	0.079937318130207
64.069465	66.077500	68.085535	0.001690254370017	0.000000612900242	0.000326555541300	0.165609224881466
68.041145	70.293400	72.545655	0.001918617702711	0.000000728715208	0.000348347518094	0.099480349236314
72.519978	74.928633	77.337288	0.001548011053231	0.000000660069726	0.000293083522754	0.105427700529368
77.370192	79.998967	82.627742	0.002093526626518	0.000000803799255	0.000328714431957	0.083794778608395
82.656037	85.557867	88.459697	0.002539860010883	0.000000893739000	0.000335452284945	0.101751163008046
88.448987	91.669567	94.890147	0.002583241266754	0.000000967231435	0.000327496245626	0.097665108637724
94.852783	98.432733	102.012683	0.002737300174424	0.000001033620572	0.000316903545761	0.073417248459064
101.986730	105.963000	109.939270	0.002722371643787	0.000001057548884	0.000292252146752	0.057289308068536
109.928585	114.360000	118.791415	0.002905272373487	0.000001174603167	0.000293597348227	0.031163260514473
118.790330	123.803000	128.815670	0.001818609445462	0.000000962828950	0.000210353616465	0.024906223460896
128.794115	134.477000	140.159885	0.001593633363193	0.000000965741278	0.000185801177254	0.051997630923533
140.116873	146.619333	153.121793	0.000955738203057	0.000000757376846	0.000127066403738	0.098211001825508
153.108678	160.579333	168.049988	0.000387505151464	0.000000503962669	0.000072136036549	0.114793980995042
168.003665	176.719000	185.434335	0.000136057093112	0.000000319712813	0.000038221574437	0.165386703572264
185.353287	195.582667	205.812047	0.000086443531439	0.000000292827488	0.000030751077907	0.286115906322945
205.724425	217.922000	230.119575	0.000058811158222	0.000000222272542	0.000018823815654	0.388627002926971
229.993865	244.739000	259.484135	0.000052081612771	0.000000243746690	0.000017491345472	0.513467087094197
259.294100	277.459000	295.623900	0.000062185084641	0.000000309670268	0.000017867029414	0.716826745207655
295.339783	318.241333	341.142883	0.000056278896707	0.000000367535586	0.000016868162854	1.005126714681288
340.673767	370.411667	400.149567	0.000060065465952	0.000000380630718	0.000013542597216	1.437758240709821
399.323267	439.513667	479.704067	0.000044829641538	0.000000422182188	0.000011242356804	2.129104927498877
478.044950	535.479000	592.913050	0.000030900459536	0.000000381551503	0.000007273227995	3.389980287627053
589.049983	678.486333	767.922683	0.000009606889510	0.000000263076573	0.000003192083818	6.026509132076380

Table A.VII.2. Deuteron Yields from Iron 800 MeV/n on 20 g/cm^2 Aluminium at 10.0 deg

KE_left(MeV/n)	KE_mid(MeV/n)	KE_right(MeV/n)	Norm_Cts(#/SP*ster*MeV/n)	Y_stat(#/SP*ster*MeV/n)	Y_syst_tot(#/SP*ster*MeV/n)	X_tot(MeV/n)
44.343166	45.538567	46.733968	0.001829269373200	0.000000497299154	0.000442556629878	0.107609504650839
46.721542	48.175500	49.629458	0.001288396823960	0.000000448438010	0.000328332411685	0.152458011605065
49.641890	51.108300	52.574711	0.001596859147600	0.000000519774276	0.000377289055337	0.314465361763422
52.520145	54.057967	55.595789	0.001856771853776	0.000000588436023	0.000412076841366	0.067559729223647
55.650355	57.393400	59.136445	0.001727590825467	0.000000593959209	0.000364268186919	0.154316134969549
59.095755	60.879500	62.663245	0.002019099473944	0.000000665579276	0.000400460427890	0.203812685611102
62.703965	64.729400	66.754835	0.001758134900390	0.000000636921937	0.000336485770866	0.136549823472057
66.682508	68.828633	70.974758	0.001679389767616	0.000000646225974	0.000326642630783	0.114388194335124
71.047045	73.360900	75.674755	0.001949653842217	0.000000733278633	0.000340579124484	0.112139344765073
75.665617	78.265067	80.864517	0.002058401905556	0.000000781225463	0.000324262111054	0.100176950826625
80.812620	83.639700	86.466780	0.002335795411685	0.000000854984463	0.000326796550406	0.098785843505130
86.456708	89.563733	92.670758	0.002314862746466	0.000000893227392	0.000312164220546	0.096668492549744
92.673460	96.105700	99.537940	0.002370284038567	0.000000943506349	0.000300500700680	0.069103184610245
99.534687	103.349667	107.164647	0.002927136081725	0.000001060135471	0.000305769714617	0.058290175109533
107.159668	111.460333	115.760998	0.002977460594292	0.000001198001060	0.000310328763581	0.035782752616392
115.724358	120.528333	125.332308	0.003349657849165	0.000001319127883	0.000306789397563	0.032364352567910
125.329777	130.772667	136.215557	0.004049960556149	0.000001551783901	0.000325386653807	0.038472248278857
136.179427	142.396667	148.613907	0.004112176709664	0.000001771425044	0.000335060807499	0.068381959556377
148.599440	155.715000	162.830560	0.005041925516273	0.000003171624885	0.000618615398148	0.098677961952049
162.804447	171.076667	179.348887	0.007266167359448	0.000003044932119	0.000515773513196	0.121200138780572
179.264635	188.961000	198.657365	0.007509182648895	0.000002922784721	0.000398009654982	0.226306261962766
198.584007	210.060667	221.537327	0.010067439564970	0.000003707856685	0.000476462929661	0.312552758010548
221.426545	235.252000	249.077455	0.014482695103909	0.000005054715256	0.000635736084574	0.418524379363974
248.913450	265.820000	282.726550	0.008929450501099	0.000004172613860	0.000443383535539	0.572145541710324
282.481067	303.627667	324.774267	0.002696300743906	0.000002562242437	0.000156995909042	0.809951846042714
324.374583	351.548333	378.722083	0.001953934715533	0.000002443706686	0.000116029530163	1.150786074839716
378.042917	414.222667	450.402417	0.001064632004949	0.000002065665603	0.000069744357396	1.665588975465736
449.102750	499.739000	550.375250	0.000560916438682	0.000001769041866	0.000042575240226	2.599697596336928
547.527467	623.809667	700.091867	0.000164591669763	0.000001140291407	0.000017668501512	4.426226982001714
704.597650	739.576000	774.554350	0.000047509122000	0.000000406245000	0.000004155740000	3.821330000000000

Table A.VII.3. Deuteron Yields from Iron 800 MeV/n on 20 g/cm^2 Aluminium at 7.20 deg

KE_left(MeV/n)	KE_mid(MeV/n)	KE_right(MeV/n)	Norm_Cts(#/SP*ster*MeV/n)	Y_stat(#/SP*ster*MeV/n)	Y_syst_tot(#/SP*ster*MeV/n)	X_tot(MeV/n)
44.351284	45.555833	46.760383	0.001464190347467	0.000000448986007	0.000395369720167	0.104898386094020
46.720193	48.155400	49.590608	0.001640520456972	0.000000541771399	0.000403616742212	0.156493343255304
49.630817	51.106200	52.581584	0.001667323359000	0.000000547765647	0.000395542051739	0.309526541133390
52.533986	54.059900	55.585814	0.001694677361260	0.000000613416207	0.000431097969844	0.085782542151011
55.633402	57.385267	59.137132	0.001721434073100	0.000000636424749	0.000388964761763	0.146442989078651
59.112910	60.889000	62.665090	0.001823962110074	0.000000636921937	0.000382249545728	0.209436897199705
62.689280	64.723400	66.757520	0.002061364193391	0.000000686279944	0.000362086236894	0.132818330589009
66.689790	68.831100	70.972410	0.002008294000814	0.000000708807963	0.000356846574871	0.119020988313238
71.040150	73.362600	75.685050	0.002209746938043	0.000000777440632	0.000360990691161	0.114672002687055
75.664612	78.261267	80.857922	0.002203592762253	0.000000822348257	0.000342178639681	0.093727402676378
80.814078	83.639933	86.465788	0.002491787212902	0.000000893738406	0.000344743025486	0.097580974352637
86.456157	89.563167	92.670177	0.002733613926195	0.000000962828950	0.000340232020332	0.095853152997124
92.673248	96.106433	99.539618	0.002726577558839	0.000001033620572	0.000329865842721	0.068412282048986
99.542588	103.353333	107.164078	0.003329211895487	0.000001271223143	0.000368219619122	0.056227796045195
107.157077	111.460667	115.764257	0.003704640916451	0.000001315129713	0.000344059544501	0.038608298233273
115.728792	120.531667	125.334542	0.004455021624780	0.000001531134429	0.000362666999606	0.034714803234707
125.331770	130.775000	136.218230	0.006254665027742	0.000001903843233	0.000417334124091	0.035990364470230
136.181623	142.400333	148.619043	0.008360793621566	0.000002946629301	0.000633836515541	0.060997462040482
148.602343	155.720333	162.838323	0.009153419636475	0.000002930998394	0.000571475431057	0.089504661916238
162.811912	171.082667	179.353422	0.010265291664299	0.000003111005738	0.000515657739941	0.111068394840702
179.270095	188.969000	198.667905	0.011412746033957	0.000003557943933	0.000533900810311	0.212895983629189
198.594088	210.071333	221.548578	0.011580524093845	0.000003918190095	0.000517661174726	0.294025019625882
221.438537	235.266667	249.094797	0.006747036856578	0.000003269469901	0.000337117346157	0.392810695868888
248.929850	265.840000	282.750150	0.003123668900400	0.000002432087283	0.000186916419010	0.537868343006911
282.504833	303.655333	324.805833	0.001588643973558	0.000001951279775	0.000110904216755	0.762648103023275
324.405817	351.586667	378.767517	0.000844913558036	0.000001619643318	0.000068976439538	1.084188150436076
378.087450	414.278000	450.468550	0.000727393828226	0.000001714161187	0.000055918238150	1.569085890383315
449.168050	499.823000	550.477950	0.000273567688163	0.000001206209493	0.000027635531317	2.453256029137603
547.626983	623.945333	700.263683	0.000061018594297	0.000000712957082	0.000010638473137	4.188161611662091
704.773450	739.772000	774.770550	0.000015807486000	0.000000206721000	0.000002086010000	3.625270000000000

Table A.VII.4. Deuteron Yields from Iron 800 MeV/n on 20 g/cm^2 Aluminium at 32.7 deg

KE_left(MeV/n)	KE_mid(MeV/n)	KE_right(MeV/n)	Norm_Cts(#/SP*ster*MeV/n)	Y_stat(#/SP*ster*MeV/n)	Y_syst_tot(#/SP*ster*MeV/n)	X_tot(MeV/n)
44.263166	45.461400	46.659634	0.000987580713442	0.000000359029972	0.000316538497657	0.127270252502500
46.678225	48.140833	49.603441	0.000992037721813	0.000000402380013	0.000290751283158	0.244610761358142
49.603425	51.066033	52.528641	0.001175168742187	0.000000422182188	0.000305675548585	0.238926219448201
52.472926	54.006833	55.540740	0.000960245236095	0.000000401943742	0.000277505498738	0.070026690887261
55.596460	57.346900	59.097340	0.001185413267000	0.000000497299154	0.000301007732309	0.278911935554935
59.077597	60.847767	62.617937	0.001291952132828	0.000000497299154	0.000298121416044	0.164595402237708
62.637692	64.681067	66.724442	0.001139908161942	0.000000497793365	0.000258415408225	0.255691788590170
66.661073	68.795133	70.929193	0.001100997906398	0.000000497298836	0.000248439493531	0.136987785161488
70.992573	73.334433	75.676293	0.001105587586074	0.000000562909584	0.000254837827380	0.211690717812567
75.625480	78.220700	80.815920	0.001007044563190	0.000000542225077	0.000222383731017	0.129180309808926
80.788348	83.613533	86.438718	0.001020228229841	0.000000541771399	0.000204642719008	0.162510624782043
86.430675	89.541100	92.651525	0.000869731639246	0.000000520247137	0.000177214373094	0.142671911706439
92.650570	96.093500	99.536430	0.001104262310843	0.000000613416207	0.000189727072960	0.114435251879349
99.550507	103.367667	107.184827	0.001114289454271	0.000000659590257	0.000184567465557	0.113165317450445
107.162212	111.458667	115.755122	0.001001954345682	0.000000708807750	0.000177705527756	0.075383154650691
115.760083	120.564333	125.368583	0.000996697157282	0.000000707815660	0.000157330376957	0.082171355228206
125.356588	130.821333	136.286078	0.001046996114610	0.000000776943534	0.000152071060050	0.030137651430740
136.251545	142.467000	148.682455	0.001403942295492	0.000001323658487	0.000235047894687	0.019157013107541
148.650128	155.810333	162.970538	0.002064892263522	0.000002101966665	0.000348717509482	0.070577017136246
162.901895	171.188000	179.474105	0.001782646148486	0.000001279427825	0.000172043828373	0.136837511487932
179.432787	189.142667	198.852547	0.001378722655024	0.000001211118340	0.000135584579048	0.201447276892094
198.763647	210.281667	221.799687	0.001625834276535	0.000001442427596	0.000139095905104	0.339275671195269
221.696392	235.547667	249.398942	0.000659439004596	0.000000991203373	0.000081316884439	0.473382067444469
249.232433	266.208333	283.184233	0.000098622476772	0.000000381551503	0.000024076722730	0.676269900242499
282.938833	304.165333	325.391833	0.000033617729557	0.000000222272542	0.000011294218560	0.943174530237644
324.995950	352.287000	379.578050	0.000020134701329	0.000000222272202	0.000008630684034	1.355523300814117
378.882617	415.253667	451.624717	0.000009128324427	0.000000172049072	0.000004854453935	2.005346304164196
450.315083	501.266333	552.217583	0.000001635099803	0.000000099685565	0.000002085208361	3.111096254087938
549.323350	626.214000	703.104650	0.000001804547146	0.000000099332693	0.000001389781208	5.252859683534293
707.668700	742.983000	778.297300	0.000000789157140	0.000000057756500	0.000000572002000	4.467810000000000

Table A.VII.5. Deuteron Yields from Iron 800 MeV/n on 20 g/cm^2 Aluminium at 30.0 deg

KE_left(MeV/n)	KE_mid(MeV/n)	KE_right(MeV/n)	Norm_Cts(#/SP*ster*MeV/n)	Y_stat(#/SP*ster*MeV/n)	Y_syst_tot(#/SP*ster*MeV/n)	X_tot(MeV/n)
45.930363	47.200933	48.471504	0.001018909624471	0.000000358541172	0.000299189990618	0.195586977725410
48.507463	50.023933	51.540403	0.000868173753520	0.000000381091389	0.000265546350336	0.162339213760447
51.540430	53.056900	54.573370	0.001103049643160	0.000000437137437	0.000304985900195	0.173922967853616
54.496303	56.148333	57.800363	0.001026980786101	0.000000429847093	0.000274552477807	0.156090150678670
57.877437	59.680767	61.484097	0.001229490950503	0.000000497299154	0.000292509545843	0.226524320093892
61.413257	63.331667	65.250077	0.001027080997771	0.000000455276256	0.000250101758302	0.098830849030971
65.320900	67.416400	69.511900	0.001212535284906	0.000000541771399	0.000274237964815	0.250110459385628
69.448925	71.752600	74.056275	0.001185215845507	0.000000541771399	0.000249413000062	0.142065261089156
74.057527	76.534867	79.012207	0.001217071958156	0.000000594077851	0.000254424216872	0.163517653122989
79.056435	81.771200	84.485965	0.001178239261491	0.000000588436023	0.000230249481539	0.189135098001006
84.503508	87.510933	90.518358	0.001212096965601	0.000000618319472	0.000218977441420	0.148862901017849
90.498972	93.837867	97.176762	0.001361040863374	0.000000682433066	0.000218497812927	0.132709246778889
97.136165	100.854000	104.571835	0.001246237904393	0.000000729245183	0.000209431643397	0.109493331719653
104.542948	108.674333	112.805718	0.001290474071676	0.000000687201306	0.000176647772004	0.106255867925729
112.780330	117.409000	122.037670	0.001225755058847	0.000000784902616	0.000182259459888	0.079892532248890
122.048993	127.271333	132.493673	0.001068307435381	0.000000776445468	0.000159127780206	0.066308296593865
132.469337	138.429667	144.389997	0.000679503453754	0.000000618319175	0.000111335008721	0.038192039606442
144.353088	151.181333	158.009578	0.000396613328095	0.000000520247137	0.000080886706993	0.030388479716425
157.935870	165.821000	173.706130	0.000234110883256	0.000000401943742	0.000054308064512	0.084203243762102
173.679138	182.873333	192.067528	0.000066107302384	0.000000222745627	0.000025556249080	0.112157993429626
192.018532	202.888667	213.758802	0.000040652892995	0.000000198488201	0.000019268834698	0.192447640963068
222.029315	230.965000	239.900685	0.000027594867912	0.000000140227789	0.000010896025988	0.249528801530004
239.547380	255.391000	271.234620	0.000006908567439	0.000000114597429	0.000007495171840	0.419791539655101
271.691400	277.769000	283.846600	0.000008999919464	0.000000057145300	0.000003291050000	0.302383000000000
310.993200	318.646000	326.298800	0.000003594232448	0.000000057756500	0.000002639540000	0.438321000000000
359.549200	392.498000	425.446800	0.000003346853813	0.000000099332693	0.000003194111096	1.252460930472484
425.955250	454.385500	482.815750	0.000003900215868	0.000000081248991	0.000002011094709	1.439896292204407
535.823750	580.381000	624.938250	0.000001869744250	0.000000081248991	0.000001316166223	2.625670059718090

Table A.VII.6. Deuteron Yields from Iron 800 MeV/n on 20 g/cm^2 Aluminium at 27.2 deg

KE_left(MeV/n)	KE_mid(MeV/n)	KE_right(MeV/n)	Norm_Cts(#/SP*ster*MeV/n)	Y_stat(#/SP*ster*MeV/n)	Y_syst_tot(#/SP*ster*MeV/n)	X_tot(MeV/n)
44.291980	45.567700	46.843420	0.000856492498827	0.000000334473831	0.000276713761674	0.291684021225024
46.834977	48.119100	49.403223	0.001095532478647	0.000000402380013	0.000330872189605	0.235455095293965
49.411640	50.968400	52.525160	0.001076644036920	0.000000456739470	0.000310256823941	0.073258234084436
52.525140	54.081900	55.638660	0.001275694276227	0.000000473758676	0.000322479765452	0.197155724918781
55.560443	57.256433	58.952423	0.001222771132651	0.000000473239366	0.000300585415290	0.123649005703402
59.030652	60.873567	62.716482	0.001162388281527	0.000000498286769	0.000286385449889	0.173066766536617
62.637537	64.620067	66.602597	0.001114038459237	0.000000497299154	0.000270818618655	0.149352928440021
66.681552	68.816067	70.950582	0.001301872037499	0.000000568804658	0.000282997214322	0.156221712442477
70.900893	73.282933	75.664973	0.001047583026585	0.000000527087018	0.000234705523849	0.156511212939159
75.635973	78.202833	80.769693	0.001397576140706	0.000000637418458	0.000264735183325	0.109530721106450
80.788078	83.601233	86.414388	0.001360399323444	0.000000636921937	0.000240484583400	0.156800066592875
86.417700	89.528600	92.639500	0.001303178629263	0.000000659590257	0.000226704209941	0.126654397959605
92.630105	96.083400	99.536695	0.001255513654720	0.000000707816563	0.000219041810561	0.105664526067976
99.516107	103.351667	107.187227	0.001300386713922	0.000000732751760	0.000204896234143	0.085329768898140
107.193692	111.458667	115.723642	0.001230439950322	0.000000803887484	0.000203169001829	0.058833537731637
115.717080	120.557000	125.396920	0.001223069083285	0.000000752958638	0.000167516206678	0.064570927741903
125.348015	130.809000	136.269985	0.001689913239767	0.000000988400524	0.000195399734636	0.022394609875146
136.253910	142.468000	148.682090	0.002111459525077	0.000001599937024	0.000289071084970	0.041567529835450
148.640795	155.801000	162.961205	0.002542619542514	0.000001873333145	0.000308690243918	0.086743772755282
162.907205	171.200000	179.492795	0.002123466247518	0.000001386928266	0.000187520483188	0.116026997601420
179.456560	189.166000	198.875440	0.001945236256631	0.000001416152452	0.000162480763433	0.160070121049151
198.800080	210.336000	221.871920	0.001541837528445	0.000001405363039	0.000134059224479	0.244314805893953
221.750913	235.621333	249.491753	0.001342081804506	0.000001433268619	0.000120778655523	0.343775145032331
249.332417	266.324667	283.316917	0.000138885983782	0.000000456201134	0.000029128773211	0.474710400268416
283.067733	304.329333	325.590933	0.000052974673063	0.000000292827488	0.000014985237934	0.658535125803476
325.193533	352.533333	379.873133	0.000019088244175	0.000000214637911	0.000008413546240	0.925305691603591
379.178367	415.632667	452.086967	0.000014400861492	0.000000236805374	0.000007180624636	1.344340343342414
450.767317	501.861667	552.956017	0.000005408147058	0.000000151424628	0.000003057159109	2.070880620557351
553.658900	601.038000	648.417100	0.000003516766459	0.000000114903438	0.000001711534313	2.548579328115960

Table A.VII.7. Proton Yields from Iron 800 MeV/n on 20 g/cm^2 Aluminium at 12.7 deg

KE_left(MeV/n)	KE_mid(MeV/n)	KE_right(MeV/n)	Norm_Cts(#/SP*ster*MeV/n)	Y_stat(#/SP*ster*MeV/n)	Y_syst_tot(#/SP*ster*MeV/n)	X_tot(MeV/n)
45.462687	47.139267	48.815847	0.002368487998283	0.000000728715208	0.000466884139685	0.295685340947095
48.815820	50.492400	52.168980	0.002180678868850	0.000000681969320	0.000436804057404	0.209018647219070
52.093883	53.974533	55.855183	0.002558913485328	0.000000800209217	0.000461906638491	0.160303232242449
55.930300	57.928900	59.927500	0.002481100943917	0.000000844364376	0.000455542442768	0.350396098320172
59.849155	61.972800	64.096445	0.002785279730585	0.000000872969057	0.000450253491692	0.107059393616075
64.174792	66.503467	68.832142	0.002800100723767	0.000000940524608	0.000439288069926	0.315938363694566
68.749208	71.277633	73.806058	0.003108488564922	0.000001034130940	0.000447872114881	0.128037008564126
73.845360	76.554000	79.262640	0.003260213994970	0.000001080947640	0.000439735785502	0.239094469388901
79.306250	82.313600	85.320950	0.004023167343400	0.000001246579512	0.000464245079763	0.198049228522002
85.282585	88.599800	91.917015	0.004563418617173	0.000001479061942	0.000502363851547	0.171381146351225
91.895227	95.542767	99.190307	0.004761892767821	0.000001573680412	0.000491794775245	0.171240547159719
99.187367	103.242667	107.297967	0.004417875090381	0.000001526862614	0.000431278748591	0.154000290131935
107.279067	111.837667	116.396267	0.004743213489031	0.000001714677755	0.000437478643177	0.174877369746260
116.373527	121.452667	126.531807	0.003807740465779	0.000001600373097	0.000364791202084	0.147302153155309
126.528353	132.298333	138.068313	0.002536562672330	0.000001362470861	0.000265938242993	0.108048642305306
138.029132	144.623667	151.218202	0.001957694383346	0.000001246635673	0.000210536008780	0.090154334748641
151.184460	158.765000	166.345540	0.001509219797369	0.000001176931766	0.000172662027975	0.073067298299171
166.287930	175.085000	183.882070	0.000343080389438	0.000000548342858	0.000067592531490	0.017210529999512
183.818260	194.162000	204.505740	0.000062582910347	0.000000244178482	0.000025193689123	0.039962647274048
204.421193	216.710333	228.999473	0.000078764545221	0.000000293066814	0.000024800523705	0.117903425234469
228.877283	243.758333	258.639383	0.000059769174533	0.000000303080105	0.000021953770120	0.218481619126186
258.439650	276.750000	295.060350	0.000062437169504	0.000000334997980	0.000019624918871	0.356543776683874
294.778983	317.858333	340.937683	0.000063315616780	0.000000402380013	0.000018694686258	0.556854096643816
340.461217	370.441667	400.422117	0.000053073515965	0.000000402380013	0.000014326233086	0.862886439363257
399.570133	440.099333	480.628533	0.000039353916360	0.000000381091389	0.000010203695337	1.343761610695141
478.948633	536.922333	594.896033	0.000016839444241	0.000000292827488	0.000005635904582	2.182234613555564
580.865250	681.418000	781.970750	0.000008193587127	0.000000309670268	0.000003554939247	3.907921575953131

Table A.VII.8. Proton Yields from Iron 800 MeV/n on 20 g/cm^2 Aluminium at 10.0 deg

KE_left(MeV/n)	KE_mid(MeV/n)	KE_right(MeV/n)	Norm_Cts(#/SP*ster*MeV/n)	Y_stat(#/SP*ster*MeV/n)	Y_syst_tot(#/SP*ster*MeV/n)	X_tot(MeV/n)
44.260342	45.950467	47.640592	0.002225963079628	0.000000728715208	0.000461905563801	0.177871728206284
47.660858	49.371233	51.081608	0.002321429358867	0.000000728715208	0.000457651488765	0.255350233307119
51.070332	52.791967	54.513602	0.002901942190656	0.000000833333641	0.000522312328756	0.105491436551512
54.524863	56.557333	58.589803	0.002791513608233	0.000000869139337	0.000464002970496	0.292023080690277
58.589830	60.622300	62.654770	0.002925934396243	0.000000893227392	0.000476895365969	0.213441757988356
62.603610	64.914800	67.225990	0.003137364234692	0.000000991309424	0.000468016470964	0.235481191865104
67.242830	69.639500	72.036170	0.003531847753920	0.000001080947079	0.000494837372523	0.213376010006959
72.070463	74.768933	77.467403	0.003584123909797	0.000001150209867	0.000471051363988	0.250288788870856
77.391212	80.317167	83.243122	0.004073461868623	0.000001269121878	0.000484237387300	0.159957885733152
83.228558	86.425333	89.622108	0.004173219791391	0.000001363939179	0.000477899871393	0.185916298467886
89.626380	93.156400	96.686420	0.004200141158510	0.000001409592153	0.000451462426722	0.179160040033736
96.675308	100.590833	104.506358	0.004599901667789	0.000001550108250	0.000453549043676	0.170813463934229
104.522367	108.868667	113.214967	0.005074709123232	0.000001714676982	0.000458547268131	0.161306512396896
113.194915	118.115000	123.035085	0.005519251557683	0.000001901372735	0.000457943644991	0.135095854319850
123.005347	128.531667	134.057987	0.006273889091229	0.000002136312299	0.000469513460230	0.132202477695768
134.036628	140.337333	146.638038	0.006335341275702	0.000002350130742	0.000464099782820	0.109683348927811
146.615475	153.836000	161.056525	0.006771000988783	0.000002944496561	0.000557926465019	0.080745665331397
160.999252	169.364667	177.730082	0.009030809769942	0.000003303281412	0.000556609664240	0.036110459407575
177.686818	187.465333	197.243848	0.012790518301840	0.000003913765813	0.000609955804099	0.014731634779918
197.161658	208.760333	220.359008	0.014048325277187	0.000004554217296	0.000643537208109	0.079132278358518
220.240348	234.176333	248.112318	0.013133994698298	0.000004598953654	0.000548717611338	0.159611952231905
247.960017	265.001667	282.043317	0.011459424699216	0.000004949104223	0.000507316305128	0.259323518322192
281.798467	303.106667	324.414867	0.009650224632163	0.000005113960162	0.000422487304378	0.436703159256949
324.011933	351.400333	378.788733	0.003866018077187	0.000003667020822	0.000210726997618	0.665388276440906
378.085733	414.559333	451.032933	0.000788136373120	0.000001863504995	0.000062283677304	1.042846797519175
449.721950	500.803000	551.884050	0.000358691230847	0.000001483021635	0.000033989089175	1.648768300546199
548.981317	626.052667	703.124017	0.000147112654924	0.000001131667619	0.000017081126990	2.849900010210885
697.758800	743.100000	788.441200	0.000048187136000	0.000000487494000	0.000003881280000	2.453920000000000

Table A.VII.9. Proton Yields from Iron 800 MeV/n on 20 g/cm^2 Aluminium at 7.20 deg

KE_left(MeV/n)	KE_mid(MeV/n)	KE_right(MeV/n)	Norm_Cts(#/SP*ster*MeV/n)	Y_stat(#/SP*ster*MeV/n)	Y_syst_tot(#/SP*ster*MeV/n)	X_tot(MeV/n)
46.483020	48.210300	49.937580	0.002662518188500	0.000000776445468	0.000484932490548	0.216865057824561
49.937587	51.664867	53.392147	0.002967902430583	0.000000848305256	0.000530429383456	0.187100647149495
53.310397	55.221967	57.133537	0.003001229359137	0.000000869664505	0.000496908505044	0.195211661494799
57.215262	59.264667	61.314072	0.002805325800007	0.000000893738406	0.000472471271085	0.269935398992055
61.232010	63.417700	65.603390	0.003250812536446	0.000000988400524	0.000498319225591	0.101805646729895
65.685450	68.064600	70.443750	0.003330021120520	0.000001057548884	0.000486346263839	0.298422227158099
70.371847	72.983167	75.594487	0.003406564143710	0.000001103372395	0.000468114992546	0.144040793028225
75.597888	78.404733	81.211578	0.003684582799163	0.000001174603167	0.000466920778697	0.228318786587963
81.258407	84.337267	87.416127	0.004634129746385	0.000001386446838	0.000507865899958	0.203562024907914
87.430453	90.842933	94.255413	0.004325291294416	0.000001431431666	0.000473370106396	0.184622644846075
94.224110	98.021900	101.819690	0.004623840123156	0.000001551739163	0.000466411295169	0.154374458433544
101.781378	106.009333	110.237288	0.004681377187351	0.000001644695873	0.000447417677874	0.176796768785207
110.219208	114.917333	119.615458	0.005583308850202	0.000001854681532	0.000467784787775	0.149722208865085
119.593453	124.918333	130.243213	0.006518862249337	0.000002162901547	0.000491386210459	0.133450043633564
130.207023	136.233333	142.259643	0.008417265826454	0.000002584927476	0.000548019347116	0.108344925694977
142.244415	149.127000	156.009585	0.011786616290819	0.000003221680082	0.000658326539558	0.093301970083220
155.966403	163.931333	171.896263	0.013382816759544	0.000003559301203	0.000651572078135	0.055670738791667
171.843920	181.110000	190.376080	0.016937587540382	0.000004403086312	0.000769290794583	0.008273366785130
190.316033	201.259333	212.202633	0.020892815063885	0.000005348367869	0.000893508024216	0.052890424725941
212.095875	225.184000	238.272125	0.017532764310950	0.000005397711366	0.000754216441222	0.120791085614502
238.131847	254.038667	269.945487	0.011921493994519	0.000004890499967	0.000538739873164	0.199594553287809
269.732267	289.454667	309.177067	0.005908917507183	0.000003827908625	0.000295482673238	0.351350206500580
308.843067	333.953667	359.064267	0.002839432816626	0.000002937395146	0.000164664893693	0.540892992202709
358.482950	391.483000	424.483050	0.000668652014081	0.000001635779505	0.000059267718003	0.838184418204610
423.434517	468.792667	514.150817	0.000318478981984	0.000001314622410	0.000032920468962	1.318128583443209
511.964017	578.479667	644.995317	0.000171153947594	0.000001152587750	0.000019721874540	2.206776642345120
635.810100	710.845000	785.879900	0.000056230817251	0.000000694797876	0.000007358921410	2.962500544624422

Table A.VII.10. Proton Yields from Iron 800 MeV/n on 20 g/cm^2 Aluminium at 32.7 deg

KE_left(MeV/n)	KE_mid(MeV/n)	KE_right(MeV/n)	Norm_Cts(#/SP*ster*MeV/n)	Y_stat(#/SP*ster*MeV/n)	Y_syst_tot(#/SP*ster*MeV/n)	X_tot(MeV/n)
46.320611	47.984067	49.647523	0.001868607252535	0.000000588436023	0.000378440414700	0.091048810299421
49.738572	51.565167	53.391762	0.002278297212817	0.000000703636980	0.000413188297582	0.235269166763709
53.391772	55.218367	57.044962	0.002266608397750	0.000000757793137	0.000443549533164	0.398633704539644
56.982570	59.076200	61.169830	0.002310034615311	0.000000803318575	0.000412303405601	0.150608875406099
61.232197	63.399367	65.566537	0.002480186985470	0.000000844364376	0.000418777816809	0.260468261715319
65.494848	67.909533	70.324218	0.002324565586041	0.000000844364376	0.000378743853348	0.238923557819232
70.375600	72.910100	75.444600	0.002385530347841	0.000000893739000	0.000380738154912	0.216718854717350
75.464920	78.331600	81.198280	0.002486426958747	0.000000988400524	0.000372899149007	0.279168242658437
81.121235	84.234200	87.347165	0.002839536439228	0.000001083478368	0.000381932805267	0.237661111956184
87.326355	90.742300	94.158245	0.002562971638959	0.000001080947079	0.000344659230879	0.220141811498952
94.156243	97.937133	101.718023	0.002654225163416	0.000001150728813	0.000334521732080	0.207066198192752
101.730877	105.928667	110.126457	0.003000797719091	0.000001316650585	0.000346406493106	0.221628081605288
110.098675	114.818000	119.537325	0.002994014056589	0.000001361491344	0.000320078713411	0.162438420080103
119.544775	124.851000	130.157225	0.003081083693217	0.000001433245307	0.000301783052649	0.158237793346501
130.139513	136.177333	142.215153	0.003192160190797	0.000001526862942	0.000285409818538	0.149478701372604
142.176457	149.072667	155.968877	0.003684840773506	0.000001738320630	0.000288595097668	0.090960940240798
155.943415	163.914000	171.884585	0.004118726158996	0.000002054337243	0.000309022342770	0.059915740102748
171.832433	181.109333	190.386233	0.003877429402676	0.000002084021851	0.000265454590770	0.021852730364227
190.312152	201.271667	212.231182	0.003789217363710	0.000002262367710	0.000245566656821	0.109909028995165
212.120000	225.231000	238.342000	0.003439206190927	0.000002352873669	0.000216223898892	0.205771842142311
238.196260	254.130000	270.063740	0.002614158777220	0.000002230995157	0.000169731349246	0.354560566118118
269.848850	289.609000	309.369150	0.001389492878534	0.000001798037535	0.000107933808985	0.573482314546839
309.033400	334.198000	359.362600	0.000196378227329	0.000000759529576	0.000033848923298	0.870917136495201
358.780017	391.862667	424.945317	0.000024843687195	0.000000263476689	0.000008582795587	1.335764756132606
423.893600	469.390000	514.886400	0.000005071316660	0.000000128329207	0.000003006851032	2.083266962777455
512.681700	579.456000	646.230300	0.000003080500397	0.000000128329207	0.000002062474864	3.436384162255437
637.986600	712.390500	786.794400	0.000001038568977	0.000000099685572	0.000000929730310	4.514593443545055

Table A.VII.11. Proton Yields from Iron 800 MeV/n on 20 g/cm^2 Aluminium at 30.0 deg

KE_left(MeV/n)	KE_mid(MeV/n)	KE_right(MeV/n)	Norm_Cts(#/SP*ster*MeV/n)	Y_stat(#/SP*ster*MeV/n)	Y_syst_tot(#/SP*ster*MeV/n)	X_tot(MeV/n)
44.400872	45.997967	47.595062	0.001736573638650	0.000000613416207	0.000408260785107	0.381405675902968
47.595038	49.192133	50.789228	0.002105419916950	0.000000660069726	0.000440808787241	0.157244089826148
50.761818	52.662933	54.564048	0.002022541518230	0.000000728715208	0.000409169294910	0.191114241505807
54.591480	56.520000	58.448520	0.002483740691233	0.000000800209217	0.000445338842960	0.433199596686100
58.360065	60.440600	62.521135	0.002548616871013	0.000000822348257	0.000428018487701	0.103064148098392
62.609570	64.878200	67.146830	0.002235092620773	0.000000825841448	0.000390741985516	0.332047061944538
67.054225	69.506500	71.958775	0.002605658465810	0.000000920315169	0.000404562209641	0.178790454236489
72.051403	74.666233	77.281063	0.002476084103153	0.000000940039028	0.000387971811252	0.261394991698387
77.273288	80.232133	83.190978	0.002701427983115	0.000001033620572	0.000379301599125	0.213616593482342
83.121078	86.331133	89.541188	0.002913397004233	0.000001106327495	0.000376664380203	0.227280782447615
89.526902	93.059067	96.591232	0.003125383320014	0.000001198001060	0.000372577458890	0.208304129203456
96.594513	100.506733	104.418953	0.002878298102877	0.000001220950645	0.000343071412089	0.216213495665835
104.435005	108.778000	113.120995	0.003412194628184	0.000001407273961	0.000360486978085	0.181488835133625
113.108963	118.046333	122.983703	0.003473406289715	0.000001526862614	0.000346170049318	0.183318274984411
122.929848	128.463333	133.996818	0.003279068641565	0.000001526862942	0.000310414024147	0.160104630352311
133.980257	140.286667	146.593077	0.002848830868407	0.000001504238208	0.000267639319783	0.132579931166674
146.571108	153.802333	161.033558	0.002258728455210	0.000001433245307	0.000221495173026	0.109392755684003
160.969720	169.348000	177.726280	0.000983617639345	0.000000965741278	0.000125772003491	0.024922820128517
177.690663	187.479333	197.268003	0.000428259668285	0.000000666054434	0.000073109350571	0.018394885384989
197.192208	208.815333	220.438458	0.000285312407946	0.000000593545075	0.000054530305656	0.089909555027427
220.316177	234.284667	248.253157	0.000074468261235	0.000000319163073	0.000024426548173	0.184915867051073
248.091817	265.182667	282.273517	0.000041696265642	0.000000263076573	0.000016444853323	0.314605863349684
282.021250	303.393000	324.764750	0.000007146178700	0.000000139977153	0.000006906743500	0.502448171870493
333.764500	352.111500	370.458500	0.000006988107677	0.000000099332700	0.000003719496604	0.633349549934315
379.736200	402.866500	425.996800	0.000006674543752	0.000000099685572	0.000003081381847	0.894639103725072
450.538250	501.879000	553.219750	0.000002003263312	0.000000099685565	0.000002070040963	1.880803202703568
599.700000	625.250000	650.800000	0.000001000998400	0.000000057145300	0.000000782234000	1.795850000000000

Table A.VII.12. Proton Yields from Iron 800 MeV/n on 20 g/cm^2 Aluminium at 27.2 deg

KE_left(MeV/n)	KE_mid(MeV/n)	KE_right(MeV/n)	Norm_Cts(#/SP*ster*MeV/n)	Y_stat(#/SP*ster*MeV/n)	Y_syst_tot(#/SP*ster*MeV/n)	X_tot(MeV/n)
46.480030	48.153100	49.826170	0.002184988945050	0.000000681969320	0.000435600295943	0.270885923065411
49.826130	51.499200	53.172270	0.002197350773633	0.000000708262483	0.000451861651559	0.135864563076080
53.156920	55.146500	57.136080	0.002145319374372	0.000000753984133	0.000406051373229	0.308546194251363
57.151455	59.156400	61.161345	0.002499119192723	0.000000822348257	0.000440409064090	0.274311567816598
61.083535	63.307900	65.532265	0.002659056443890	0.000000917180640	0.000446865481534	0.137589103351610
65.610077	67.954667	70.299257	0.002392876216450	0.000000851156428	0.000391051589402	0.334408736454358
70.241543	72.873833	75.506123	0.002723319611433	0.000000988400524	0.000405865631749	0.178594426475241
75.483860	78.297000	81.110140	0.003140689747093	0.000001087101462	0.000419781471412	0.241401090759528
81.153087	84.231567	87.310047	0.002799890492551	0.000001057548311	0.000374233077897	0.223776232976717
87.334892	90.745467	94.156042	0.002943199138702	0.000001150209867	0.000369231361276	0.205037994957032
94.131570	97.929400	101.727230	0.003270246088937	0.000001269177041	0.000369010780955	0.188037725061116
101.687988	105.920333	110.152678	0.003038310537622	0.000001291324988	0.000338004205997	0.205805458717596
110.127077	114.835667	119.544257	0.003432392992479	0.000001480817248	0.000350585366657	0.197907584030123
119.516332	124.842667	130.169002	0.003583011684055	0.000001551263692	0.000328617851025	0.155856910659746
130.142800	136.176000	142.209200	0.003826178337023	0.000001716064668	0.000323854659750	0.144766398963434
142.193547	149.093667	155.993787	0.003978935581757	0.000002090538309	0.000355683074268	0.124164473993208
155.930600	163.902000	171.873400	0.003707568525006	0.000001973046051	0.000289382495625	0.042835672283409
171.823317	181.113667	190.404017	0.004314294250580	0.000002185216867	0.000279696531371	0.017053466926405
190.351813	201.316333	212.280853	0.005155188974050	0.000002640995014	0.000298023850524	0.038044062563876
212.182940	225.297000	238.411060	0.004220399730473	0.000002601406192	0.000249132116972	0.090587524619839
238.265557	254.214667	270.163777	0.002984108820994	0.000002410156303	0.000187967236318	0.207574054481768
269.954717	289.750667	309.546617	0.001621936798785	0.000002000206578	0.000119431920204	0.326915631408166
309.200783	334.398333	359.595883	0.000354757506013	0.000001025623691	0.000046996850731	0.521067796522679
359.023200	392.169000	425.314800	0.000030261548995	0.000000320042131	0.000010605897129	0.801290814005752
424.259083	469.868333	515.477583	0.000009592767878	0.000000190637709	0.000004313297386	1.248736962564575
513.254883	580.240333	647.225783	0.000004602097201	0.000000140727396	0.000002252816301	2.063450901258375
639.751550	713.645500	787.539450	0.000001737957472	0.000000114903438	0.000001147987168	2.730371393437164

Table A.VII.13. Triton Yields from Iron 800 MeV/n on 20 g/cm^2 Aluminium at 12.7 deg

KE_left(MeV/n)	KE_mid(MeV/n)	KE_right(MeV/n)	Norm_Cts(#/SP*ster*MeV/n)	Y_stat(#/SP*ster*MeV/n)	Y_syst_tot(#/SP*ster*MeV/n)	X_tot(MeV/n)
45.453342	46.667867	47.882391	0.000482077227584	0.000000243746690	0.000211276072545	22.827899042499315
47.839415	49.099367	50.359319	0.000794104808177	0.000000319712573	0.000266559873134	0.138012526914770
50.402272	51.867200	53.332129	0.000632921848516	0.000000334998209	0.000241227179457	0.112076255970567
53.332172	54.797100	56.262029	0.000749279298140	0.000000309103173	0.000223053571576	0.107178303544934
56.216235	57.885800	59.555365	0.000774701312309	0.000000359029972	0.000227999752829	0.108065435937815
59.601130	61.322500	63.043870	0.000694724495203	0.000000344098143	0.000211031092218	0.104915497366881
63.008970	64.958300	66.907630	0.000614372360625	0.000000334997980	0.000182076001083	0.127459551773612
66.889658	68.942533	70.995408	0.000544091246520	0.000000309670268	0.000160619959077	0.079354807222046
71.048257	73.302067	75.555877	0.000736788706793	0.000000402380013	0.000188848334670	0.137440831888671
75.521875	78.018200	80.514525	0.000535913367232	0.000000430010938	0.000181919756398	0.105899400645754
80.486678	83.209733	85.932788	0.000484164218046	0.000000462545462	0.000180834557127	0.066914001788564
85.925935	88.921400	91.916865	0.000369584518373	0.000000636424749	0.000227442721293	0.060395101366062
91.921045	95.229600	98.538155	0.000255115991753	0.000000494146727	0.000162698082259	0.063522311566646
99.766745	102.212050	104.657355	0.000099136449204	0.000000140976420	0.000041270385475	0.029269367770938
111.351110	112.798000	114.244890	0.000141647469097	0.000000128875000	0.000031243600000	0.015354400000000
114.132438	118.759333	123.386228	0.000062744756547	0.000000128602540	0.000028993058370	0.045087140805140
123.385885	128.620000	133.854115	0.000071342715403	0.000000190084138	0.000038755354988	0.053478196884899
133.821913	139.792333	145.762753	0.000033500190645	0.000000114597429	0.000019986304104	0.108852858565451
145.748167	152.574667	159.401167	0.000133358391649	0.000000275209775	0.000041925143403	0.099271824750480
159.486965	164.632500	169.778035	0.000044206364269	0.000000140227789	0.000018956991155	0.122402777917047
175.135210	184.395000	193.654790	0.000015361177524	0.000000128329207	0.000014597458270	0.253881721486601
193.566148	204.498333	215.430518	0.000020805592767	0.000000128329207	0.000012230090353	0.350156840461528
223.745340	232.752000	241.758660	0.000024994151174	0.000000114903438	0.000008959652860	0.414448882465618
241.408030	257.369000	273.329970	0.000014185332343	0.000000114597429	0.000007454401110	0.627000658572222
273.112367	292.970667	312.828967	0.000022894637738	0.000000191005541	0.000009893265435	0.864388476578673
312.473867	337.789667	363.105467	0.000062744237772	0.000000389115177	0.000015852955766	1.210634622026811
362.523983	395.890333	429.256683	0.000050407667877	0.000000381551503	0.000012366297621	1.770199910054229
428.174250	474.201000	520.227750	0.000028527742663	0.000000320042131	0.000007812319342	2.725732719710427
517.943583	585.739333	653.535083	0.000010516347729	0.000000243747000	0.000004034780087	4.619685751152344
654.203200	720.995000	787.786800	0.000003827699779	0.000000140227203	0.000001573543000	6.532216486124751

Table A.VII.14. Triton Yields from Iron 800 MeV/n on 20 g/cm^2 Aluminium at 10.0 deg

KE_left(MeV/n)	KE_mid(MeV/n)	KE_right(MeV/n)	Norm_Cts(#/SP*ster*MeV/n)	Y_stat(#/SP*ster*MeV/n)	Y_syst_tot(#/SP*ster*MeV/n)	X_tot(MeV/n)
44.622528	45.849400	47.076273	0.000496378505190	0.000000243314130	0.000208897186274	31.965438608288814
47.076261	48.303133	49.530006	0.000834880414962	0.000000319163073	0.000274602405754	0.208160445478962
49.478865	50.885767	52.292669	0.001058666463472	0.000000402380013	0.000306625194741	0.063181668921235
52.343795	53.820800	55.297805	0.000627043307384	0.000000292467528	0.000209307730688	0.116717904936689
55.237992	56.809067	58.380142	0.000746335954753	0.000000335521310	0.000226148657644	0.116255615601226
58.439965	60.173200	61.906435	0.000540291819871	0.000000319163073	0.000194078219711	0.114783094488213
61.837258	63.690533	65.543808	0.000793117964445	0.000000358541172	0.000207190554251	0.095344982254454
65.612970	67.608900	69.604830	0.000722136482816	0.000000358541172	0.000189960987458	0.124639551445197
69.566797	71.794167	74.021537	0.000696513440360	0.000000401943742	0.000191204658009	0.134962540223167
73.983505	76.384900	78.786295	0.000851462768098	0.000000401943742	0.000177692128588	0.081552743639009
78.802217	81.429867	84.057517	0.001218078888617	0.000000599549667	0.000244843431035	0.082769706058799
84.060717	86.959867	89.859017	0.001562317315764	0.000000562909584	0.000206989077927	0.084028795581568
89.851147	93.062167	96.273187	0.001868278101108	0.000000612900242	0.000204973095478	0.068824605743658
96.255580	99.815300	103.375020	0.002141350840962	0.000000803799990	0.000242717511140	0.068730065595051
103.387267	107.335667	111.284067	0.002406256823620	0.000001295451127	0.000365835887419	0.029955070124139
111.276348	115.752333	120.228318	0.002152780739988	0.000000991309424	0.000243059389588	0.024260018367780
120.179518	125.206333	130.233148	0.001544674108522	0.000000852146078	0.000186158364490	0.027681013060040
130.219300	135.926000	141.632700	0.000166227343083	0.000000304005672	0.000055050524643	0.048422259106634
141.616647	148.129667	154.642687	0.000996625950228	0.000000807938699	0.000135704328855	0.085469054481374
154.627883	162.168333	169.708783	0.000517693090132	0.000000623578146	0.000089728020027	0.097745424095760
169.649872	178.425667	187.201462	0.000175389090461	0.000000358540958	0.000043339308494	0.172381422303710
187.124983	197.454333	207.783683	0.000184406578310	0.000000418044216	0.000042669837143	0.248978433278869
207.696558	220.015333	232.334108	0.000310800285464	0.000000562909584	0.000049090433333	0.350424625233444
232.208295	247.142000	262.075705	0.000445985186108	0.000000803799255	0.000057788649178	0.464992428207170
261.883300	280.304000	298.724700	0.000706191899436	0.000001157785637	0.000069514142580	0.642341502328785
298.435100	321.724000	345.012900	0.001045297204760	0.000001647172779	0.000080965287123	0.889778744017860
344.515000	374.843000	405.171000	0.001169657240118	0.000001951278129	0.000076905023781	1.309065447510169
404.298633	445.438333	486.578033	0.000776333776956	0.000001832541757	0.000053691839329	1.980630607325859
484.824117	543.928667	603.033217	0.000269220295024	0.000001279427825	0.000025518786492	3.282777961635541
598.879900	691.743000	784.606100	0.000039902455002	0.000000591026080	0.000007547703826	6.361869791767197

Table A.VII.15. Triton Yields from Iron 800 MeV/n on 20 g/cm^2 Aluminium at 7.20 deg

KE_left(MeV/n)	KE_mid(MeV/n)	KE_right(MeV/n)	Norm_Cts(#/SP*ster*MeV/n)	Y_stat(#/SP*ster*MeV/n)	Y_syst_tot(#/SP*ster*MeV/n)	X_tot(MeV/n)
45.432726	46.665767	47.898807	0.000613709569204	0.000000263476689	0.000225276538064	22.813443878627730
47.898793	49.131833	50.364874	0.000731629904824	0.000000292467255	0.000250300985458	0.176883029590433
50.362257	51.842700	53.323144	0.000709156174007	0.000000334997980	0.000238836325769	0.079935630336566
53.325762	54.808800	56.291838	0.000870735263389	0.000000344302108	0.000245623056859	0.127591315245709
56.233696	57.883767	59.533838	0.000650180958511	0.000000334473831	0.000217570324459	0.109269615348733
59.591973	61.331133	63.070293	0.000829418970784	0.000000358541172	0.000217994661812	0.118336555397941
63.019415	64.956100	66.892785	0.000871717198041	0.000000410586696	0.000228843310019	0.113002991006074
66.900237	68.945467	70.990697	0.000584061832994	0.000000358541172	0.000183763797502	0.093760535231514
71.034120	73.305300	75.576480	0.000769550170859	0.000000455276159	0.000212671464550	0.136690980742476
75.527310	78.019500	80.511690	0.001011548664589	0.000000520247137	0.000221866720143	0.107055025001772
80.492927	83.214667	85.936407	0.001401498042300	0.000000613416207	0.000240229024237	0.074016878712764
85.930258	88.926633	91.923008	0.001670023775664	0.000000636921937	0.000228528749931	0.076005293784423
91.927840	95.239100	98.550360	0.001938552784182	0.000000776445468	0.000253117892171	0.083168942211922
98.554122	102.228167	105.902212	0.002218168898979	0.000001129819196	0.000337159715141	0.045108229797969
105.895768	110.042333	114.188898	0.002495324764926	0.000001140013951	0.000307978567827	0.036822213388796
114.153488	118.779333	123.405178	0.002400664182423	0.000001058047137	0.000251790975519	0.018205514869472
123.403677	128.639667	133.875657	0.000933344196751	0.000000693634264	0.000148791745554	0.019114673953769
133.843320	139.818000	145.792680	0.000945732064838	0.000000738336955	0.000132934565420	0.066346781872583
145.774260	152.607000	159.439740	0.000753993463424	0.000000721718577	0.000115656108057	0.045237433908877
159.409132	167.327667	175.246202	0.000262846316686	0.000000429438728	0.000058023939214	0.100377538248206
175.180262	184.443667	193.707072	0.000245712568487	0.000000463455753	0.000052221070465	0.169650035181046
193.618493	204.558333	215.498173	0.000342970678476	0.000000624085411	0.000060085635298	0.245928454199590
215.402253	228.515333	241.628413	0.000351536406779	0.000000681969320	0.000055664748649	0.343301880602190
241.494865	257.469000	273.443135	0.000289362204564	0.000000660069726	0.000044291685720	0.453982115561836
273.224733	293.101333	312.977933	0.000442502886170	0.000000931465237	0.000050520869684	0.637755954430063
312.622567	337.965667	363.308767	0.000612335636567	0.000001293389463	0.000056933370524	0.905319169111645
362.725983	396.134333	429.542683	0.000713339115746	0.000001595782580	0.000055217122945	1.345740936714047
428.456033	474.555333	520.654633	0.000437251923873	0.000001489612715	0.000038115544987	2.108619571425818
518.360067	586.287667	654.215267	0.000069698785729	0.000000634574976	0.000010968201843	3.663286190567153
651.502100	721.838500	792.174900	0.000006480080825	0.000000206890510	0.000002182712780	5.334535164726164

Table A.VII.16. Triton Yields from Iron 800 MeV/n on 20 g/cm^2 Aluminium at 32.7 deg

KE_left(MeV/n)	KE_mid(MeV/n)	KE_right(MeV/n)	Norm_Cts(#/SP*ster*MeV/n)	Y_stat(#/SP*ster*MeV/n)	Y_syst_tot(#/SP*ster*MeV/n)	X_tot(MeV/n)
45.291996	46.578033	47.864070	0.000190184474281	0.000000128602540	0.000105080496274	22.742686788886651
47.864030	49.150067	50.436104	0.000209061294025	0.000000152349068	0.000124471086658	0.292722420829017
50.372492	51.762567	53.152642	0.000334435850527	0.000000199546815	0.000156331535722	0.072098679835140
53.216278	54.763033	56.309788	0.000251962008359	0.000000172049072	0.000116981058540	0.140665641754659
56.279968	57.856533	59.433098	0.000201167414190	0.000000172049072	0.000113433586608	0.197146610618823
59.462905	61.276000	63.089095	0.000239933431654	0.000000172049072	0.000099843407286	0.114348001122057
63.035673	64.918233	66.800793	0.000217002565689	0.000000172660261	0.000097922697734	0.104284667180224
66.854193	68.939733	71.025273	0.000273513692486	0.000000214637528	0.000108314547831	0.102048322775095
70.966517	73.247667	75.528817	0.000202446846727	0.000000198488201	0.000092771767410	0.087751101853823
75.520372	77.991167	80.461962	0.000162604271093	0.000000206550499	0.000090124900558	0.070565062133183
80.475623	83.188833	85.902043	0.000260459001323	0.000000244178482	0.000095263232780	0.071261182911175
85.902762	88.903967	91.905172	0.000339312451377	0.000000288052231	0.000100750272050	0.088307059025879
91.894687	95.224467	98.554247	0.000418443027739	0.000000286462138	0.000090297105932	0.064456027877479
98.533833	102.229133	105.924433	0.000483260920610	0.000000389115177	0.000110045271799	0.054964327658218
105.927758	110.038333	114.148908	0.000572071396061	0.000000777439983	0.000203042494523	0.032361676450099
114.144497	118.798667	123.452837	0.000617734097867	0.000000634187116	0.000147335453061	0.071903849442572
123.410038	128.660333	133.910628	0.000208094763128	0.000000304005921	0.000062792661770	0.126638196667119

Table A.VII.17. Triton Yields from Iron 800 MeV/n on 20 g/cm^2 Aluminium at 30.0 deg

KE_left(MeV/n)	KE_mid(MeV/n)	KE_right(MeV/n)	Norm_Cts(#/SP*ster*MeV/n)	Y_stat(#/SP*ster*MeV/n)	Y_syst_tot(#/SP*ster*MeV/n)	X_tot(MeV/n)
46.053658	47.376500	48.699343	0.000312766738041	0.000000189899752	0.000150927740336	0.155286567249843
48.699258	50.022100	51.344943	0.000332296130526	0.000000172660261	0.000137361961680	0.261573228045226
51.283156	52.704833	54.126510	0.000275225159987	0.000000199546815	0.000146342437733	0.085869556793371
54.188330	55.771100	57.353870	0.000246720083059	0.000000214801062	0.000142667555108	0.192049192333579
57.308925	58.938100	60.567275	0.000284236750581	0.000000198488201	0.000130221725296	0.150290156190783
60.612257	62.460767	64.309277	0.000265105729273	0.000000199018212	0.000113213713283	0.106164843752393
64.245278	66.195133	68.144988	0.000349138185331	0.000000263476689	0.000144554404711	0.092634585405776
68.209010	70.329500	72.449990	0.000321316183560	0.000000222745627	0.000110590156051	0.084525998742754
72.410493	74.770033	77.129573	0.000334426117339	0.000000222272542	0.000098418294427	0.048278325094912
77.095337	79.653667	82.211997	0.000316931836208	0.000000243746690	0.000101694359571	0.050803546344393
82.211947	85.020267	87.828587	0.000347294021415	0.000000281454792	0.000105818818951	0.064672714489652
87.827047	90.929867	94.032687	0.000376351179605	0.000000293066814	0.000099568087388	0.059693856078243
94.025488	97.462633	100.899778	0.000405409286720	0.000000320042131	0.000096685960481	0.048449599604744
100.917787	104.725667	108.533547	0.000416662948231	0.000000500852320	0.000138508218720	0.037436533029783
108.522318	112.838333	117.154348	0.000515245238938	0.000000708262483	0.000174845315525	0.076607979479501
117.114432	121.939667	126.764902	0.000583829382690	0.000000623578146	0.000140037942048	0.109284874965432
126.754990	132.231000	137.707010	0.000482954615777	0.000000473759011	0.000092847728134	0.147016550508166
137.832565	139.810000	141.787435	0.000101884567773	0.000000128875000	0.000022845600000	0.105268000000000

Table A.VII.18. Triton Yields from Iron 800 MeV/n on 20 g/cm^2 Aluminium at 27.2 deg

KE_left(MeV/n)	KE_mid(MeV/n)	KE_right(MeV/n)	Norm_Cts(#/SP*ster*MeV/n)	Y_stat(#/SP*ster*MeV/n)	Y_syst_tot(#/SP*ster*MeV/n)	X_tot(MeV/n)
44.538867	45.680200	46.821533	0.000213613977022	0.000000152118165	0.000143688957659	31.858088226300744
46.864761	48.215133	49.565505	0.000234863816867	0.000000172660261	0.000134356523785	0.187832484157453
49.565495	50.915867	52.266239	0.000271396631389	0.000000172660261	0.000134442088085	0.201094344902312
52.197734	53.667167	55.136600	0.000265397277197	0.000000172049072	0.000127453289625	0.092266369890816
55.205093	56.814833	58.424573	0.000288475787990	0.000000199546815	0.000130376921063	0.217692729450113
58.367580	60.059900	61.752220	0.000324408020132	0.000000222745967	0.000143124950762	0.068319582557126
61.809222	63.684267	65.559312	0.000275795939120	0.000000199018212	0.000111638502615	0.125738622652747
65.488248	67.512333	69.536418	0.000215065726989	0.000000172049072	0.000088024237017	0.056072908656766
69.590125	71.754200	73.918275	0.000251609041311	0.000000199018212	0.000097156813025	0.085301557799843
73.935658	76.360633	78.785608	0.000238670595315	0.000000263476689	0.000114321252393	0.052686763350380
78.733357	81.381767	84.030177	0.000345215688213	0.000000263076573	0.000105225559950	0.035904931066539
84.017412	86.921967	89.826522	0.000445030481765	0.000000319712324	0.000116295749705	0.035070280366858
89.825968	93.030433	96.234898	0.000533452451542	0.000000335521310	0.000111372109668	0.034655238170441
96.244973	99.788633	103.332293	0.000612583364750	0.000000429847093	0.000127704557865	0.048016990449007
103.321323	107.325333	111.329343	0.000681199020632	0.000000585474786	0.000154766826933	0.069587529086772
111.315802	115.755667	120.195532	0.000793511244430	0.000000872445878	0.000211538525425	0.075433194469402
120.185660	125.235000	130.284340	0.000643342860138	0.000000547765601	0.000115616043117	0.114939621711967
130.310860	134.039000	137.767140	0.000316405090956	0.000000320151643	0.000060671819665	0.126241496976707

Table A.VII.19. Helium-4 Yields from Iron 800 MeV/n on 20 g/cm^2 Aluminium at 12.7 deg

KE_left(MeV/n)	KE_mid(MeV/n)	KE_right(MeV/n)	Norm_Cts(#/SP*ster*MeV/n)	Y_stat(#/SP*ster*MeV/n)	Y_syst_tot(#/SP*ster*MeV/n)	X_tot(MeV/n)
46.383140	47.514450	48.645760	0.000057093770338	0.000000081680026	0.000050530422399	0.269925066820405
48.645735	50.342700	52.039665	0.000189372761856	0.000000172660261	0.000107072496635	0.255334889872673
51.955308	53.797633	55.639958	0.000174060349739	0.000000214637911	0.000126083943256	0.090278391631497
55.724350	57.744700	59.765050	0.000338873159637	0.000000275210050	0.000143761662324	0.349992845945456
59.702380	61.800300	63.898220	0.000486614395029	0.000000334473831	0.000170857637450	0.152654728457424
63.960853	66.312433	68.664013	0.000414494223752	0.000000389115177	0.000175108353734	0.302386949157929
68.572973	71.085233	73.597493	0.000554894980043	0.000000430010938	0.000180624248575	0.145775223180381
73.678587	76.377667	79.076747	0.000691335445171	0.000000613416207	0.000241922274958	0.232976511528523
79.086708	82.119333	85.151958	0.000864542469264	0.000000568680744	0.000200271662863	0.186002286171434
85.090520	88.404900	91.719280	0.000872571190734	0.000000562909584	0.000181560605931	0.181341602765857
91.711817	95.361367	99.010917	0.000817327903364	0.000000588436023	0.000171982279183	0.181353616435543
99.015275	103.057000	107.098725	0.000822661375048	0.000000636921657	0.000168186114241	0.158766789968494
107.086987	111.658667	116.230347	0.000604975327063	0.000000568248187	0.000131753936719	0.161538963535520
116.210633	121.292333	126.374033	0.000655444116646	0.000000574517189	0.000119773103091	0.169967386533417
126.365438	132.158333	137.951228	0.000999149824514	0.000000785393581	0.000146105720087	0.114152241472912
137.907405	144.510000	151.112595	0.000832835759012	0.000000757376002	0.000122814806179	0.093132581943432
151.078643	158.687333	166.296023	0.000871155917600	0.000000848305256	0.000120298096727	0.077163186704348
166.231862	175.061667	183.891472	0.001821619903294	0.000001267003296	0.000159359382378	0.012623264324575
183.831600	194.221000	204.610400	0.001712554773455	0.000001348442780	0.000148106087469	0.037023116117096
204.525550	216.882000	229.238450	0.000247740304423	0.000000526086056	0.000047833436819	0.110232908667829

Table A.VII.20. Helium-4 Yields from Iron 800 MeV/n on 20 g/cm^2 Aluminium at 10.0 deg

KE_left(MeV/n)	KE_mid(MeV/n)	KE_right(MeV/n)	Norm_Cts(#/SP*ster*MeV/n)	Y_stat(#/SP*ster*MeV/n)	Y_syst_tot(#/SP*ster*MeV/n)	X_tot(MeV/n)
48.617075	49.194000	49.770925	0.000037319197962	0.000000057756500	0.000035015400000	0.171803000000000
50.924800	52.078650	53.232500	0.000111562374304	0.000000114903438	0.000069741658986	0.133655358662681
53.145208	55.045333	56.945458	0.000225301412164	0.000000236508057	0.000126677398593	0.128401999362576
57.032743	59.086933	61.141123	0.000423987651255	0.000000293426039	0.000150902323049	0.321897512082650
61.063375	63.240400	65.417425	0.000509945072628	0.000000334997980	0.000165923773285	0.100851445831405
65.495157	67.880367	70.265577	0.000481217585649	0.000000409558914	0.000181688789710	0.311934646951890
70.189187	72.794967	75.400747	0.000587707872050	0.000000473759011	0.000193129202013	0.131523432747477
75.412050	78.215400	81.018750	0.000703003014236	0.000000588973420	0.000223538642997	0.222100932442977
81.072073	84.149633	87.227193	0.000829931422795	0.000000612900242	0.000213065313275	0.205470085175434
87.238953	90.654033	94.069113	0.000939207186953	0.000000753472229	0.000237406344376	0.180904672316665
94.036770	97.836400	101.636030	0.001070362842842	0.000000664047133	0.000187149641074	0.161542401964004
101.593712	105.827667	110.061622	0.001060695615662	0.000000733709468	0.000185714130270	0.176266795792628
110.038548	114.745333	119.452118	0.001175716562328	0.000000800209217	0.000183452432952	0.162554938032685
119.428090	124.760000	130.091910	0.001152090907503	0.000000825842163	0.000168266696905	0.144607573341440
130.059393	136.098333	142.137273	0.001483514725383	0.000001034130353	0.000187594636040	0.117744322987183
142.122018	149.023333	155.924648	0.001855020141407	0.000001182468640	0.000190870500766	0.091402695408287
155.879930	163.870000	171.860070	0.002137587522383	0.000001355533385	0.000189281008870	0.057589629469407
171.808747	181.110667	190.412587	0.003734610536296	0.000001916415886	0.000243373363888	0.008199491088903
190.352723	201.347333	212.341943	0.002129746418366	0.000001556874979	0.000166817443047	0.051567855552913
212.612390	216.734000	220.855610	0.000480869971820	0.000000448281000	0.000038965700000	0.051583100000000

Table A.VII.21. Helium-4 Yields from Iron 800 MeV/n on 20 g/cm^2 Aluminium at 7.20 deg

KE_left(MeV/n)	KE_mid(MeV/n)	KE_right(MeV/n)	Norm_Cts(#/SP*ster*MeV/n)	Y_stat(#/SP*ster*MeV/n)	Y_syst_tot(#/SP*ster*MeV/n)	X_tot(MeV/n)
46.265053	48.012733	49.760413	0.000639062572492	0.000000728715208	0.000447785434839	0.217909241924729
49.760420	51.508100	53.255780	0.000709714935862	0.000000660069726	0.000405047672792	0.210778437132454
53.177090	55.053200	56.929310	0.000633992823302	0.000000462393491	0.000269780476102	0.115215423722521
57.008005	59.079100	61.150195	0.000389664867199	0.000000309670268	0.000157855613748	0.307001333725116
61.083147	63.245167	65.407187	0.000415916711288	0.000000497299154	0.000242682332938	0.111514104963677
65.474257	67.876267	70.278277	0.000539049284291	0.000000526620299	0.000233590303534	0.304635805782905
70.193332	72.790067	75.386802	0.000665734318649	0.000000613416207	0.000252230019704	0.126544978972380
75.413802	78.212367	81.010932	0.000801888833395	0.000000682433066	0.000262180413008	0.227415536140256
81.068835	84.151200	87.233565	0.000952297438259	0.000000707815660	0.000247111065212	0.209121826911970
87.227125	90.652200	94.077275	0.000979786569523	0.000000613416207	0.000191669851633	0.178675532798982
94.049332	97.835667	101.622002	0.001017666571878	0.000000659590257	0.000186822204154	0.158837262450629
101.585717	105.823667	110.061617	0.001305236646298	0.000000803799255	0.000205279012578	0.169148277520760
110.031005	114.743000	119.454995	0.001581202647387	0.000000962828950	0.000221999664130	0.160903576809871
119.428005	124.757000	130.085995	0.001636304232477	0.000001036843011	0.000213498189430	0.142581368862695
130.059910	136.099000	142.138090	0.002186895704616	0.000001251443451	0.000231251798672	0.119199198936025
142.122877	149.026667	155.930457	0.003181490870223	0.000001557654580	0.000258508591720	0.097272739012583
155.879413	163.868333	171.857253	0.006087562844898	0.000002312815983	0.000360479860195	0.055483250110246
171.807170	181.111000	190.414830	0.003824439892419	0.000001937078257	0.000251972356240	0.006078143949538
190.357223	201.352333	212.347443	0.000665396483030	0.000000864642897	0.000090643036982	0.046428908276263

Table A.VII.22. Helium-4 Yields from Iron 800 MeV/n on 20 g/cm^2 Aluminium at 32.7 deg

KE_left(MeV/n)	KE_mid(MeV/n)	KE_right(MeV/n)	Norm_Cts(#/SP*ster*MeV/n)	Y_stat(#/SP*ster*MeV/n)	Y_syst_tot(#/SP*ster*MeV/n)	X_tot(MeV/n)
63.953075	64.683700	65.414325	0.000030550989491	0.000000057756500	0.000027647300000	0.144196000000000
65.326017	67.717067	70.108117	0.000150490958817	0.000000237693433	0.000101583166274	0.237609136722475
70.196442	72.736467	75.276492	0.000145939839240	0.000000243746690	0.000100941334469	0.232330652580778
75.256058	78.129333	81.002608	0.000143285091905	0.000000320590201	0.000117506248669	0.267098013833873
80.934208	84.040333	87.146458	0.000142400220913	0.000000303427475	0.000101480684351	0.224509000268675
87.140782	90.555667	93.970552	0.000137583558320	0.000000275210050	0.000085823654837	0.221939186141722
93.968062	97.752967	101.537872	0.000167142136295	0.000000243746690	0.000068073470569	0.224297181445086
101.539918	105.746333	109.952748	0.000144240635731	0.000000244178482	0.000060834446333	0.222149116390883
109.938497	114.652667	119.366837	0.000185592867434	0.000000304928852	0.000068386697626	0.170376278399107
119.369110	124.695000	130.020890	0.000167520817648	0.000000281454792	0.000055767178530	0.159029786938454
129.991652	136.040667	142.089682	0.000098479187931	0.000000257068412	0.000044871558907	0.150372713784682
142.062387	148.969667	155.876947	0.000167744576968	0.000000319493207	0.000048887542770	0.094363366415628
155.849883	163.852333	171.854783	0.000105186814579	0.000000275210050	0.000035942485197	0.052848622596715
171.799328	181.110333	190.421338	0.000071794528270	0.000000222272542	0.000025721710098	0.020760163263915
190.349932	201.363667	212.377402	0.000093034802986	0.000000275846557	0.000026461014841	0.111566429070890
212.263357	225.449667	238.635977	0.000077507466026	0.000000292827488	0.000023201426160	0.206856360586181
238.488765	254.534000	270.579235	0.000069470610958	0.000000293426039	0.000019124560798	0.355381466779009
270.356383	290.287333	310.218283	0.000051904194689	0.000000275846832	0.000015208274234	0.577601009352477
310.873450	318.634000	326.394550	0.000011492448707	0.000000081249000	0.000003664940000	0.429649000000000

Table A.VII.23. Helium-4 Yields from Iron 800 MeV/n on 20 g/cm^2 Aluminium at 30.0 deg

KE_left(MeV/n)	KE_mid(MeV/n)	KE_right(MeV/n)	Norm_Cts(#/SP*ster*MeV/n)	Y_stat(#/SP*ster*MeV/n)	Y_syst_tot(#/SP*ster*MeV/n)	X_tot(MeV/n)
49.527740	51.270500	53.013260	0.000049416595955	0.000000100037192	0.000060854821323	0.077438519641390
53.091480	55.043400	56.995320	0.000120516597917	0.000000162065013	0.000087221028393	0.360294775069262
56.995347	58.947267	60.899187	0.000178492100422	0.000000172660261	0.000093028050414	0.291618018196819
60.882360	63.158800	65.435240	0.000177013021781	0.000000222272542	0.000103192764070	0.169050769685471
65.428950	67.745300	70.061650	0.000131667460979	0.000000243314130	0.000110207265770	0.310347627184034
70.084700	72.725300	75.365900	0.000147354595813	0.000000263476689	0.000105113334421	0.211079077578902
75.272202	78.102267	80.932332	0.000165819624926	0.000000275592277	0.000101107841720	0.215149033291461
80.955478	84.041233	87.126988	0.000186551629584	0.000000304352329	0.000105451545426	0.212550763273153
87.138368	90.549733	93.961098	0.000163021970467	0.000000263476689	0.000081100249833	0.207648663704922
93.953430	97.747700	101.541970	0.000141841756964	0.000000214309812	0.000060214591895	0.216268752832234
101.520712	105.746667	109.972622	0.000177855289822	0.000000256658592	0.000063846577033	0.221167262069344
109.969858	114.670333	119.370808	0.000118915880228	0.000000244178482	0.000054457247012	0.200883803735916
119.352290	124.697000	130.041710	0.000229089447082	0.000000334997980	0.000065960251621	0.163960690988450
129.995620	136.042000	142.088380	0.000159426553480	0.000000292467528	0.000050327610434	0.148843710476661
142.072412	148.983667	155.894922	0.000187216640272	0.000000334998209	0.000050512294440	0.117608810087212
155.844888	163.846333	171.847778	0.000144625883241	0.000000334998209	0.000043593264008	0.047009877000584
171.790972	181.111667	190.432362	0.000163039903570	0.000000309103173	0.000034859276115	0.009225894668578
190.373745	201.389000	212.404255	0.000119676055644	0.000000334997980	0.000031885068511	0.075808377949736
212.299047	225.487667	238.676287	0.000104021664999	0.000000319163323	0.000025227215961	0.141416677944647
238.534937	254.589667	270.644397	0.000073018542017	0.000000309670268	0.000020678436660	0.258120765427735
270.426850	290.371000	310.315150	0.000023721777050	0.000000140727396	0.000007473704973	0.431591592935961
318.661150	335.659000	352.656850	0.000019269539749	0.000000140227203	0.000006183761528	0.544865380350963

Table A.VII.24. Helium-4 Yields from Iron 800 MeV/n on 20 g/cm^2 Aluminium at 27.2 deg

KE_left(MeV/n)	KE_mid(MeV/n)	KE_right(MeV/n)	Norm_Cts(#/SP*ster*MeV/n)	Y_stat(#/SP*ster*MeV/n)	Y_syst_tot(#/SP*ster*MeV/n)	X_tot(MeV/n)
46.280285	47.975300	49.670315	0.004018179460160	0.000000963303043	0.000614645357898	0.292468148022994
49.670285	51.365300	53.060315	0.004396827609387	0.000000988471816	0.000633255705492	0.173692497081883
52.996310	54.943700	56.891090	0.004287734440162	0.000001057548311	0.000594683880344	0.230735856166852
56.955130	58.983400	61.011670	0.004433502838873	0.000001083477541	0.000583873713585	0.329936913534997
60.917722	63.114067	65.310412	0.004650557026935	0.000001174603167	0.000586956338503	0.109992081028136
65.404300	67.773400	70.142500	0.004824418097235	0.000001317663448	0.000615717692341	0.341498072561179
70.070293	72.685133	75.299973	0.005003608652724	0.000001268651362	0.000535519102965	0.146988369625899
75.304007	78.106967	80.909927	0.005180072575572	0.000001361491344	0.000539435627332	0.241790810946157
80.972212	84.046467	87.120722	0.005581494249249	0.000001504775087	0.000547180527382	0.220593607475375
87.126623	90.553133	93.979643	0.005765760886221	0.000001433759726	0.000469179869921	0.200301521911342
93.951733	97.740133	101.528533	0.006049797859837	0.000001526862942	0.000452720976067	0.192732399852749
101.487427	105.729667	109.971907	0.006436228071882	0.000001880075972	0.000511191864453	0.190836742743660
109.936405	114.659000	119.381595	0.006630144564302	0.000002066647588	0.000513764498054	0.190300982556686
119.346813	124.676333	130.005853	0.004262298619239	0.000001662493244	0.000367027562084	0.139374752372444
129.988450	136.034000	142.079550	0.003451802266486	0.000001567070643	0.000292519702465	0.134471685624930
142.063710	148.985000	155.906290	0.008342709729795	0.000002581641430	0.000462903693847	0.118206957448282
155.843388	163.838333	171.833278	0.008902064207508	0.000002822222857	0.000447099550237	0.026742987643164
171.783895	181.112000	190.440105	0.004791048066857	0.000002187112943	0.000284130889004	0.023693913708166
190.384103	201.400333	212.416563	0.001036979444480	0.000001098412311	0.000113770680670	0.050457643874739
212.317310	225.507000	238.696690	0.000090626282740	0.000000339526579	0.000028324595849	0.106223034712439
239.053800	244.043000	249.032200	0.000017504153326	0.000000057145300	0.000004014220000	0.104834000000000

Table A.VII.25. Helium-3 Yields from Iron 800 MeV/n on 20 g/cm^2 Aluminium at 12.7 deg

KE_left(MeV/n)	KE_mid(MeV/n)	KE_right(MeV/n)	Norm_Cts(#/SP*ster*MeV/n)	Y_stat(#/SP*ster*MeV/n)	Y_syst_tot(#/SP*ster*MeV/n)	X_tot(MeV/n)
58.106530	59.673800	61.241070	0.000193427228801	0.000000181678287	0.000081048035099	0.085362423301547
61.254415	63.625300	65.996185	0.000137106578071	0.000000172049072	0.000076344636916	0.367274690108099
65.915763	68.520233	71.124703	0.000216810498161	0.000000250635933	0.000098064664424	0.150145134498791
71.178497	73.931967	76.685437	0.000260310604015	0.000000281454792	0.000107811028692	0.265400119272769
76.711985	79.802000	82.892015	0.000397106670533	0.000000334998209	0.000114978227661	0.222739862408955
82.821452	86.192267	89.563082	0.000312849900725	0.000000334998209	0.000104466533867	0.224959941611835
89.547373	93.248633	96.949893	0.000418425521423	0.000000409987377	0.000119615702553	0.236162389984095
96.953005	101.046500	105.139995	0.000431640874817	0.000000473758676	0.000123332494882	0.215626489367610
105.129392	109.695667	114.261942	0.000331379501232	0.000000389746336	0.000091030365047	0.190147379620888
114.258685	119.415000	124.571315	0.000438820282644	0.000000473758676	0.000098444670291	0.203086836611830
124.516950	130.324000	136.131050	0.000497254034343	0.000000594491913	0.000109574383137	0.172233411478842
136.114102	142.728667	149.343232	0.000493436628283	0.000000594078151	0.000095703689214	0.170702904962071
149.326712	156.906667	164.486622	0.000580555590346	0.000000733278633	0.000102800315524	0.125977966111777
164.468400	173.291000	182.113600	0.000858662834068	0.000000872968989	0.000107512945986	0.118362750314531
182.022188	192.388333	202.754478	0.000821997732869	0.000000940525173	0.000098523306454	0.050924514577657
202.659640	214.957000	227.254360	0.000840447809156	0.000001040426687	0.000091963189933	0.037736969979234
227.136520	242.007000	256.877480	0.000426952586659	0.000000757376002	0.000055949753128	0.109990694417392
256.689767	274.974667	293.259567	0.000071825921455	0.000000367822763	0.000022559893945	0.232126602829146

Table A.VII.26. Helium-3 Yields from Iron 800 MeV/n on 20 g/cm^2 Aluminium at 10.0 deg

KE_left(MeV/n)	KE_mid(MeV/n)	KE_right(MeV/n)	Norm_Cts(#/SP*ster*MeV/n)	Y_stat(#/SP*ster*MeV/n)	Y_syst_tot(#/SP*ster*MeV/n)	X_tot(MeV/n)
54.063350	55.442050	56.820750	0.000106826448105	0.000000140227203	0.000071270183118	0.254939445943542
56.741562	58.931667	61.121772	0.000145690651414	0.000000181484940	0.000086837952680	0.113564450385145
61.200977	63.615767	66.030557	0.000287782094091	0.000000298586338	0.000130309823528	0.355568783192507
65.938468	68.510933	71.083398	0.000253084731503	0.000000263076573	0.000109473184463	0.144986706829212
71.175497	73.946267	76.717037	0.000344496695509	0.000000309103173	0.000117938724509	0.288451654730910
76.681545	79.779800	82.878055	0.000275715050639	0.000000319712813	0.000108250275405	0.195480054954873
82.825580	86.187900	89.550220	0.000447181001834	0.000000422182188	0.000133416139539	0.216658417683228
89.537005	93.237100	96.937195	0.000418880640575	0.000000402380013	0.000114957638851	0.218636062539577
96.941788	101.039733	105.137678	0.000472225707714	0.000000474277418	0.000123609741404	0.203371615473276
105.157390	109.704000	114.250610	0.000614583679652	0.000000562909584	0.000132211463267	0.197756780980299
114.237578	119.407333	124.577088	0.000747158780309	0.000000664523386	0.000138397458296	0.190113205711755
124.515875	130.318000	136.120125	0.000806418279726	0.000000728715208	0.000135011441062	0.164070156259114
136.102587	142.719667	149.336747	0.001030314405513	0.000000872445878	0.000143112253462	0.157076312171823
149.321443	156.908333	164.495223	0.000917785276480	0.000000872968381	0.000124486186994	0.127318688096799
164.461285	173.284000	182.106715	0.001355540382509	0.000001152587750	0.000145492717326	0.106109543552972
182.027945	192.389000	202.750055	0.001550523380884	0.000001303961496	0.000141306798793	0.049522960396265
202.649380	214.951000	227.252620	0.001749459096409	0.000001483021635	0.000137035317587	0.045281232914460
227.140628	242.007333	256.874038	0.000615141736593	0.000000938937213	0.000070953813362	0.110441720163623
257.069100	268.817500	280.565900	0.000104317562583	0.000000329662022	0.000020226764512	0.158355561809493

Table A.VII.27. Helium-3 Yields from Iron 800 MeV/n on 20 g/cm^2 Aluminium at 7.20 deg

KE_left(MeV/n)	KE_mid(MeV/n)	KE_right(MeV/n)	Norm_Cts(#/SP*ster*MeV/n)	Y_stat(#/SP*ster*MeV/n)	Y_syst_tot(#/SP*ster*MeV/n)	X_tot(MeV/n)
51.263195	51.959800	52.656405	0.000090980450608	0.000000081249000	0.000040842300000	0.207641000000000
52.656385	54.746200	56.836015	0.000232147469448	0.000000236805402	0.000119295635002	0.339649774208669
56.772277	58.937567	61.102857	0.000186865727386	0.000000198488201	0.000096016086408	0.142177245969424
61.166550	63.603300	66.040050	0.000311678857720	0.000000281454792	0.000121834428624	0.338858663623936
65.960305	68.517600	71.074895	0.000390232278466	0.000000358541172	0.000151251757966	0.157365885790314
71.154685	73.947400	76.740115	0.000396411770556	0.000000381091389	0.000144071563377	0.291924070480665
76.677763	79.767433	82.857103	0.000505224711419	0.000000422182188	0.000145019966536	0.180741774996374
82.822967	86.181467	89.539967	0.000494587492039	0.000000430010938	0.000136569040512	0.210095281375499
89.536393	93.236233	96.936073	0.000606722759358	0.000000520247137	0.000149186122833	0.216491890088497
96.933293	101.033733	105.134173	0.000594530231040	0.000000542225077	0.000141055205339	0.194341762237791
105.154397	109.705667	114.256937	0.000720697176652	0.000000641645325	0.000150024787554	0.199038592063173
114.238838	119.401333	124.563828	0.000888017848968	0.000000733278817	0.000152546417612	0.181238938202253
124.520443	130.320333	136.120223	0.001304285907461	0.000000965741278	0.000180882739145	0.167918645692996
136.096162	142.714667	149.333172	0.001667524877427	0.000001153044935	0.000191844474565	0.150072671362044
149.317193	156.908333	164.499473	0.002284597725426	0.000001386928266	0.000208960127943	0.126701538443896
164.457735	173.280000	182.102265	0.002919825034856	0.000001700417221	0.000226348025211	0.098995809415803
182.030653	192.389333	202.748013	0.003780362323987	0.000002095258255	0.000243711665923	0.048652337370881
202.644090	214.948000	227.251910	0.001878691377003	0.000001552009699	0.000149861690245	0.049729640760075
227.426685	237.007500	246.588315	0.000202606319035	0.000000410244020	0.000031139894640	0.067897700451856

Table A.VIII.1. Deuteron Yields from Iron 800 MeV/n on 40 g/cm^2 Aluminium at 12.7 deg

KE_left(MeV)	KE_mid(MeV)	KE_right(MeV)	Norm_Cts(#/SP*ster*MeV)	Y_stat(#/SP*ster*MeV)	Y_syst_tot(#/SP*ster*MeV)	X_tot(MeV)
44.969686	46.236867	47.504047	0.001700348886133	0.000000533475372	0.000462228395997	0.191206926446612
47.450339	48.771200	50.092062	0.001742773847463	0.000000535292848	0.000450098480213	0.073569705729329
50.145770	51.748700	53.351630	0.001781941364933	0.000000633279844	0.000438735730805	0.263546199253565
53.351603	54.954533	56.557463	0.001893398120667	0.000000621411105	0.000435908646931	0.235849613633349
56.487723	58.187533	59.887343	0.002183916748196	0.000000683433945	0.000461927664061	0.051234551843361
59.957093	61.897133	63.837173	0.002309928259577	0.000000731859552	0.000432532390631	0.308708078757262
63.798093	65.777233	67.756373	0.002137776772582	0.000000733564077	0.000422519375617	0.145817805880421
67.795443	70.075233	72.355023	0.002418488239237	0.000000835649896	0.000426108085318	0.239255813256523
72.272795	74.684800	77.096805	0.002530850399439	0.000000884350897	0.000430705777763	0.112037105597431
77.179045	79.802200	82.425355	0.002636221152290	0.000000959911550	0.000429807013490	0.169836094500580
82.410635	85.366800	88.322965	0.003355419427935	0.000001113996837	0.000459897890489	0.098496562755936
88.268995	91.504100	94.739205	0.003276433084507	0.000001159187900	0.000440611657841	0.082470731603218
94.732900	98.309200	101.885500	0.003267712594798	0.000001261571413	0.000448780228108	0.057145376686920
101.894943	105.864333	109.833723	0.003223926370648	0.000001247366342	0.000399323693543	0.056855384732671
109.818433	114.320333	118.822233	0.002999190722303	0.000001311875952	0.000381224504127	0.040779274111877
118.808838	123.826333	128.843828	0.002420170096328	0.000001160981857	0.000289741295498	0.070815232820347
128.833365	134.568000	140.302635	0.001870716054450	0.000001089016394	0.000233392657273	0.141178585290192
140.259013	146.798333	153.337653	0.000969991152221	0.000000833821437	0.000148884941275	0.217564243962559
153.303692	160.856667	168.409642	0.000458907131026	0.000000558766520	0.000083783875466	0.296327508917076
168.343052	177.115667	185.888282	0.000195783037601	0.000000393876782	0.000049353650328	0.454822148129354
185.830727	196.161667	206.492607	0.000091776180312	0.000000302293095	0.000031366838279	0.603108700664316
206.408655	218.704000	230.999345	0.000065030744802	0.000000261793567	0.000022904722487	0.810188598150455
230.875507	245.787667	260.699827	0.000057266906930	0.000000261793567	0.000019313762749	1.092532981994137
260.497467	278.874667	297.251867	0.000054506308053	0.000000312868301	0.000018322467528	1.485420974143357
296.959850	320.162000	343.364150	0.000049523689520	0.000000302293095	0.000014134678607	2.040845370281639
342.882817	373.067667	403.252517	0.000046203292788	0.000000333335976	0.000011878609002	2.900038591381156
402.397417	443.295667	484.193917	0.000051825478720	0.000000491044867	0.000013474901181	4.314167108933079
482.471617	541.140667	599.809717	0.000022362890065	0.000000386249401	0.000007424359595	6.911072482140525
589.593117	687.654667	785.716217	0.000009372075965	0.000000260199118	0.000003163503835	9.606280046662183

Table A.VIII.2. Deuteron Yields from Iron 800 MeV/n on 40 g/cm^2 Aluminium at 10.0 deg

KE_left(MeV)	KE_mid(MeV)	KE_right(MeV)	Norm_Cts(#/SP*ster*MeV)	Y_stat(#/SP*ster*MeV)	Y_syst_tot(#/SP*ster*MeV)	X_tot(MeV)
44.089655	45.384467	46.679279	0.002049108675333	0.000000609033169	0.000519879782094	0.216103044650000
46.679288	47.974100	49.268912	0.002421373202400	0.000000662915649	0.000571409797474	0.189120551884241
49.182206	50.663700	52.145194	0.002439841562176	0.000000683433440	0.000528848664494	0.154369635186781
52.231908	53.861733	55.491558	0.002439729565600	0.000000708942001	0.000496245242700	0.219355779271940
55.491542	57.121367	58.751192	0.003008743490000	0.000000838210455	0.000593143732755	0.135069444387137
58.687055	60.573200	62.459345	0.002757971553324	0.000000809259858	0.000501595052902	0.213011307136898
62.523487	64.489867	66.456247	0.002850158597623	0.000000833821351	0.000493686727503	0.220880134736015
66.377312	68.559267	70.741222	0.002929858181254	0.000000885047969	0.000479885031436	0.101862736170624
70.820138	73.125833	75.431528	0.003071113192107	0.000000961788424	0.000495374221070	0.231167052532233
75.409432	78.036067	80.662702	0.003181714814671	0.000001040782914	0.000479681659868	0.132080897404135
80.591658	83.424333	86.257008	0.003260776023245	0.000001061490273	0.000454946048030	0.122383296345539
86.271452	89.386267	92.501082	0.003137494762170	0.000001110698662	0.000432720596463	0.109451129082938
92.503602	95.961467	99.419332	0.003792315226683	0.000001286052647	0.000472863759095	0.056193619880107
99.406762	103.258667	107.110572	0.004539796546111	0.000001436966538	0.000490599914935	0.048562875191961
107.108467	111.398667	115.688867	0.004296620931588	0.000001590232635	0.000509615435539	0.019426744282378
115.661652	120.513667	125.365682	0.004490816194287	0.000001613807573	0.000451978200096	0.101551409896909
125.360470	130.832000	136.303530	0.005879598334067	0.000001941533366	0.000527321579711	0.110692901357433
136.280580	142.538000	148.795420	0.004948803885597	0.000001939640285	0.000456449987286	0.188452013739015
148.765590	155.953000	163.140410	0.004292987956680	0.000001921835579	0.000400282984487	0.257551124437460
163.075360	171.412000	179.748640	0.004814632770907	0.000002184595393	0.000420970321672	0.408763910629351
179.710050	189.472000	199.233950	0.004094729118317	0.000002176110812	0.000353505781783	0.536328127402433
199.152507	210.752667	222.352827	0.005123284910540	0.000002687125775	0.000409843978404	0.713970156839906
222.232157	236.190667	250.149177	0.008938781723743	0.000003931029782	0.000656040744054	0.964486523821354
249.997100	267.090000	284.182900	0.003803559021190	0.000002839888572	0.000323087177503	1.294326316622667
283.933400	305.349000	326.764600	0.001641941852439	0.000002016710146	0.000146127013510	1.760349138927844
326.350300	353.913000	381.475700	0.001173817858144	0.000001964907718	0.000107575163617	2.464676921099396
380.773267	417.556667	454.340067	0.000828495275887	0.000001915852190	0.000077105560559	3.590815446566420
452.987483	504.640333	556.293183	0.000481264540192	0.000001690140459	0.000047895681544	5.588108534432738
553.299250	631.511000	709.722750	0.000138642150868	0.000001097743165	0.000018550572728	9.703635915062971
708.478700	750.444000	792.409300	0.000035494428000	0.000000396685000	0.000003558610000	2.951730000000000

Table A.VIII.3. Deuteron Yields from Iron 800 MeV/n on 40 g/cm^2 Aluminium at 7.20 deg

KE_left(MeV)	KE_mid(MeV)	KE_right(MeV)	Norm_Cts(#/SP*ster*MeV)	Y_stat(#/SP*ster*MeV)	Y_syst_tot(#/SP*ster*MeV)	X_tot(MeV)
44.056671	45.369867	46.683063	0.002643012583733	0.000000683433945	0.000586146609454	0.190953069752754
46.683037	47.996233	49.309429	0.003147180350185	0.000000710701492	0.000609685533682	0.227597538183083
49.229645	50.670733	52.111821	0.003112041424354	0.000000835649811	0.000681012934504	0.179509922497365
52.191632	53.839367	55.487102	0.003078669643538	0.000000788595151	0.000547136221641	0.183847254877521
55.487065	57.134800	58.782535	0.003044414290215	0.000000788595151	0.000552362308378	0.148522465957242
58.704423	60.565933	62.427443	0.003258555032741	0.000000910918008	0.000571165409150	0.174965156727569
62.505585	64.489500	66.473415	0.003015217374510	0.000000882623334	0.000519187987893	0.217448537842865
66.383682	68.550467	70.717252	0.003415220113072	0.000000986271809	0.000544770927846	0.096847393011118
70.806973	73.129933	75.452893	0.003829200464577	0.000001083723534	0.000568223030331	0.229250781826998
75.404670	78.022200	80.639730	0.004042409930842	0.000001184445611	0.000564587802657	0.126117617725558
80.595370	83.423300	86.251230	0.004496844247419	0.000001236605616	0.000558196951821	0.127228115456451
86.271313	89.384533	92.497753	0.004457597776095	0.000001287885707	0.000534409486557	0.112183883023231
92.499488	95.958133	99.416778	0.004381691546323	0.000001390249488	0.000520601626641	0.054271607882022
99.403440	103.258000	107.112560	0.005662950242794	0.000001667474873	0.000602643322583	0.039026494671907
107.101635	111.396000	115.690365	0.006003258016955	0.000001764820481	0.000589911997717	0.029413327401629
115.659670	120.507000	125.354330	0.006335553409055	0.000001919966652	0.000579553861939	0.115404453042073
125.362525	130.833000	136.303475	0.008247277437447	0.000002318527455	0.000689590116807	0.110984391520884
136.279253	142.538333	148.797413	0.005425578609722	0.000002001166319	0.000493264976987	0.187252708686523
148.763113	155.954333	163.145553	0.005557416239360	0.000002186402502	0.000490237050303	0.255633535004702
163.074925	171.412000	179.749075	0.006513242684210	0.000002559712431	0.000534389080482	0.409286489613327
179.715128	189.476333	199.237538	0.007747537519730	0.000003042573419	0.000599820468798	0.528479109835952
199.159168	210.762333	222.365498	0.012218823965132	0.000004148051466	0.000873156405736	0.697434704890716
222.243130	236.205000	250.166870	0.006304642058768	0.000003311891802	0.000511999756178	0.939643668243446
250.013867	267.111667	284.209467	0.001917478681429	0.000001976562751	0.000180181269710	1.256902054077803
283.959467	305.379667	326.799867	0.000889421902046	0.000001512835039	0.000095114776367	1.706400647207449
326.385917	353.958667	381.531417	0.000622163882536	0.000001412502921	0.000067437173179	2.384553468765169
380.828083	417.626333	454.424583	0.000559028747145	0.000001536744397	0.000057146160286	3.468808916472627
453.071150	504.751000	556.430850	0.000206342520293	0.000001092182067	0.000027249558748	5.395133744014137
553.432517	631.697667	709.962817	0.000042669758461	0.000000581240668	0.000009064330484	9.376563699410355
708.877200	750.719000	792.560800	0.000009210161400	0.000000174529000	0.000001498070000	2.676560000000000

Table A.VIII.4. Deuteron Yields from Iron 800 MeV/n on 40 g/cm^2 Aluminium at 32.7 deg

KE_left(MeV)	KE_mid(MeV)	KE_right(MeV)	Norm_Cts(#/SP*ster*MeV)	Y_stat(#/SP*ster*MeV)	Y_syst_tot(#/SP*ster*MeV)	X_tot(MeV)
43.626032	45.042667	46.459301	0.000526066479240	0.000000283504596	0.000213474349515	0.141666321933090
46.459299	47.875933	49.292568	0.000794939049853	0.000000359801701	0.000272821684376	0.450964789815125
49.292566	50.709200	52.125835	0.000759247849880	0.000000331248406	0.000251692508657	0.551055941360766
52.042952	53.590733	55.138515	0.000822759056088	0.000000386249401	0.000271209201794	0.086326906034272
55.221392	56.990867	58.760342	0.000664011067053	0.000000369858045	0.000225342103348	0.208918018218271
58.760358	60.529833	62.299308	0.000949067396025	0.000000420491786	0.000258133841590	0.392039860862387
62.233898	64.278733	66.323568	0.000795066808384	0.000000431134503	0.000229833174685	0.148081216296497
66.388970	68.512100	70.635230	0.000898979177532	0.000000488495145	0.000249703170268	0.243976480583683
70.570587	72.974367	75.378147	0.000783221363989	0.000000480926071	0.000216791843283	0.209564947672553
75.380387	77.926967	80.473547	0.000902830923661	0.000000560501993	0.000240246869653	0.178569936404452
80.535965	83.374400	86.212835	0.000780630787578	0.000000508836302	0.000194775346153	0.232742980502635
86.161182	89.311467	92.461752	0.000897544464230	0.000000558766520	0.000194672316358	0.196592052774902
92.438885	95.908200	99.377515	0.000750099240427	0.000000540308503	0.000172444131452	0.158609243473765
99.378595	103.227000	107.075405	0.000958092292188	0.000000610625477	0.000175279264673	0.118205471788154
107.060025	111.382000	115.703975	0.000763547166084	0.000000558766520	0.000143650011162	0.058804097492459
115.694233	120.567333	125.440433	0.000775756182404	0.000000637525299	0.000143823665895	0.033152019053897
125.392658	130.900333	136.408008	0.000920700522938	0.000000715845518	0.000146272673728	0.068815246666273
136.391243	142.671333	148.951423	0.001428496535311	0.000001355249906	0.000279596653001	0.131393729659600
148.936973	156.143333	163.349693	0.002060547424248	0.000002050475142	0.000421465824104	0.223700032317834
163.316835	171.704000	180.091165	0.001610303280607	0.000001255545260	0.000189738426837	0.363352907219689
180.024000	189.855000	199.686000	0.000985497311357	0.000001061490273	0.000127583370718	0.532035593453107
199.589730	211.261000	222.932270	0.001209822835403	0.000001278744789	0.000135017113191	0.770220986590212
222.817190	236.874000	250.930810	0.000812806133490	0.000001150135849	0.000109777929013	1.073299850108533
250.775217	268.006667	285.238117	0.000116150765185	0.000000431134503	0.000027307467879	1.475833079468678
284.981233	306.593333	328.205433	0.000066926501023	0.000000409307426	0.000020788300198	2.044417121161922
327.787067	355.629667	383.472267	0.000017095886802	0.000000207013040	0.000007998511212	2.888936179790063
382.751633	419.993333	457.235033	0.000005628837247	0.000000124530146	0.000003562285620	4.210196722054683
455.844300	508.256000	560.667700	0.000001714307396	0.000000107524189	0.000002193771579	6.494676967309460
605.855650	662.941500	720.027350	0.000001023947509	0.000000085660047	0.000001060845106	9.752012084744358
720.382900	758.635000	796.887100	0.000000764048040	0.000000060570800	0.000000554272000	3.886540000000000

Table A.VIII.5. Deuteron Yields from Iron 800 MeV/n on 40 g/cm^2 Aluminium at 30.0 deg

KE_left(MeV)	KE_mid(MeV)	KE_right(MeV)	Norm_Cts(#/SP*ster*MeV)	Y_stat(#/SP*ster*MeV)	Y_syst_tot(#/SP*ster*MeV)	X_tot(MeV)
45.477946	46.834133	48.190321	0.000883717677664	0.000000394580539	0.000301725209669	0.153078224701824
48.279807	49.787967	51.296127	0.000714913306653	0.000000359801701	0.000256032874379	0.662502137694664
51.296107	52.804267	54.312427	0.000985391503467	0.000000409307941	0.000294038517460	0.489364616805302
54.239187	55.850567	57.461947	0.001008809621376	0.000000461460634	0.000307073349306	0.185688668266564
57.535200	59.392800	61.250400	0.001078403664942	0.000000459955014	0.000271130212099	0.475985527714867
61.250400	63.108000	64.965600	0.000864727964027	0.000000409307941	0.000238852020056	0.444688553990318
64.930758	67.104433	69.278108	0.001046196788078	0.000000535292432	0.000268441551592	0.266632635067353
69.301273	71.521433	73.741593	0.001216862135287	0.000000582961852	0.000287929253191	0.423155018788623
73.753265	76.315400	78.877535	0.001052630210386	0.000000557025639	0.000239596949826	0.298023594050874
78.779948	81.525833	84.271718	0.001066700503985	0.000000581293437	0.000232498907597	0.278306770729711
84.299838	87.306933	90.314028	0.001130123646701	0.000000611080079	0.000224236411798	0.241641744591037
90.327335	93.664700	97.002065	0.001001563673805	0.000000617054590	0.000205482138026	0.207000394242716
96.991395	100.715400	104.439405	0.001065537350506	0.000000631304609	0.000189724054682	0.176064950166267
104.417773	108.576333	112.734893	0.001144044872661	0.000000689184048	0.000185990915131	0.120036174841462
112.732163	117.367333	122.002503	0.001102717964760	0.000000708942488	0.000174279161557	0.042298921382111
121.984238	127.266333	132.548428	0.001014766327020	0.000000755735337	0.000161729146868	0.120680408308474
132.501868	138.487333	144.472798	0.000694430289431	0.000000635562716	0.000120067279711	0.248973540387327
144.457723	151.308333	158.158943	0.000344654855223	0.000000506923540	0.000081015904922	0.414963290842696
158.111328	166.053333	173.995338	0.000096492974602	0.000000260199118	0.000035234354238	0.673703199745259
173.939098	183.197333	192.455568	0.000041682030161	0.000000151146894	0.000017359333684	0.962641785476820
192.396053	203.345333	214.294613	0.000040587727198	0.000000183988750	0.000017822157576	1.324142785658707
222.603430	231.618000	240.632570	0.000013078397475	0.000000107524149	0.000008471081317	1.568002311541664
240.775380	245.737000	250.698620	0.000059257467126	0.000000174529000	0.000012468500000	1.285340000000000
272.424650	285.133000	297.841350	0.000004740361343	0.000000088840472	0.000004904373810	2.654793748015088
311.305633	336.587333	361.869033	0.000005963709761	0.000000108806912	0.000004568420088	4.811135008976572
362.250700	383.328000	404.405300	0.000002853738990	0.000000088840472	0.000002960885010	5.252617778232107
455.285150	487.577000	519.868850	0.000001843747249	0.000000087264750	0.000001897820217	9.011153401701693
559.368200	581.629000	603.889800	0.000002625822600	0.000000060570800	0.000000955594000	9.400680000000000
646.360900	718.238000	790.115100	0.000001234948484	0.000000106225937	0.000001015271296	17.710353189307096

Table A.VIII.6. Deuteron Yields from Iron 800 MeV/n on 40 g/cm^2 Aluminium at 27.2 deg

KE_left(MeV)	KE_mid(MeV)	KE_right(MeV)	Norm_Cts(#/SP*ster*MeV)	Y_stat(#/SP*ster*MeV)	Y_syst_tot(#/SP*ster*MeV)	X_tot(MeV)
44.080455	45.327400	46.574346	0.000765404787440	0.000000312868301	0.000269146115619	0.441703495446889
46.574354	47.821300	49.068246	0.001269399554827	0.000000432740484	0.000375961573485	0.337838879309354
49.058290	50.642300	52.226310	0.000994869338953	0.000000431134503	0.000294979542221	0.411005444661017
52.236255	53.830200	55.424145	0.001336458801600	0.000000506923540	0.000347786031367	0.422346416125436
55.424155	57.018100	58.612045	0.001017099565227	0.000000459955014	0.000311823141189	0.259211958717745
58.606933	60.543233	62.479533	0.001039985072234	0.000000516533733	0.000289391140243	0.437197756089850
62.484628	64.426033	66.367438	0.001153199724688	0.000000533475372	0.000299316443058	0.385942966607762
66.299893	68.504533	70.709173	0.001125319965907	0.000000560501993	0.000278143321309	0.261235487220936
70.776700	73.067500	75.358300	0.001123062960422	0.000000533475372	0.000256550495351	0.399033292327846
75.354565	77.994200	80.633835	0.001024189438153	0.000000558766520	0.000233241176429	0.287612281820509
80.543538	83.380133	86.216728	0.001178382639827	0.000000612667385	0.000242094319196	0.255419712893289
86.231885	89.347900	92.463915	0.001044894586457	0.000000631304609	0.000222510743383	0.239866149387528
92.468945	95.929300	99.389655	0.001156281121302	0.000000683433945	0.000219416833780	0.175492791117841
99.378635	103.237000	107.095365	0.001307593756227	0.000000731859552	0.000213689625263	0.128892007844940
107.080222	111.382667	115.685112	0.001312613189878	0.000000760938561	0.000202864470266	0.064303039264408
115.658537	120.505667	125.352797	0.001245235254974	0.000000783929198	0.000184601097535	0.111842423189638
125.373497	130.845667	136.317837	0.001243767747451	0.000000862268493	0.000180172705944	0.169509397422562
136.295360	142.564000	148.832640	0.001600127269006	0.000001796256117	0.000407406495773	0.310363446708855
148.781898	155.994333	163.206768	0.002012519680057	0.000002246690013	0.000482322504046	0.485766756246246
163.133505	171.481000	179.828495	0.002035746224594	0.000001416959976	0.000216388935015	0.749026788458864
179.786243	189.564333	199.342423	0.002102348710360	0.000001568162442	0.000209462746034	1.035622644195752
199.286213	210.899333	222.512453	0.001730019695461	0.000001512864334	0.000174263944926	1.400191027515175
222.394855	236.386000	250.377145	0.001199602555001	0.000001378713999	0.000131629420612	1.921992485807372
250.202667	267.343667	284.484667	0.000178447977483	0.000000547563741	0.000036543615657	2.625989684880731
284.231450	305.692000	327.152550	0.000051005631633	0.000000342954917	0.000017680083739	3.611810549807395
326.746483	354.380333	382.014183	0.000026631848429	0.000000260199118	0.000010080792543	5.061912215773798
381.296683	418.191333	455.085983	0.000013711208546	0.000000186237397	0.000005229443180	7.349062325841304
453.734350	505.563000	557.391650	0.000005701870361	0.000000161977594	0.000003575010220	11.191006465733992
554.380633	632.937333	711.494033	0.000001129942028	0.000000106225978	0.000001448597113	18.581990595261853
711.364100	752.426000	793.487900	0.000002188155600	0.000000087264700	0.000000746818000	10.095599999999999

Table A.VIII.7. Proton Yields from Iron 800 MeV/n on 40 g/cm^2 Aluminium at 12.7 deg

KE_left(MeV)	KE_mid(MeV)	KE_right(MeV)	Norm_Cts(#/SP*ster*MeV)	Y_stat(#/SP*ster*MeV)	Y_syst_tot(#/SP*ster*MeV)	X_tot(MeV)
44.986722	46.688667	48.390612	0.003903101788067	0.000000982608012	0.000690792340318	0.186006640309318
48.390622	50.092567	51.794512	0.003699168231167	0.000000959911550	0.000670272846184	0.344803931788778
51.750212	53.496467	55.242722	0.004188487345196	0.000001013787259	0.000708719162646	0.268656915669409
55.287007	57.391567	59.496127	0.004222483316450	0.000001160981981	0.000681050040881	0.271103400681364
59.496107	61.600667	63.705227	0.005075398007940	0.000001237888368	0.000747698515736	0.284862152470278
63.599730	65.930800	68.261870	0.004958451947287	0.000001311875975	0.000726409566667	0.243593803305523
68.367400	70.879300	73.391200	0.005684469992023	0.000001515818454	0.000789016671542	0.351643303185202
73.294113	76.062133	78.830153	0.005962119500292	0.000001587923782	0.000782488950842	0.225860552906965
78.891803	81.849633	84.807463	0.006927006080762	0.000001738915009	0.000834220988989	0.312011861550166
84.842887	88.179067	91.515247	0.006721649347800	0.000001814285875	0.000787265614045	0.315961004992705
91.443405	95.120800	98.798195	0.007707993819831	0.000002042799693	0.000852663745704	0.230776460994725
98.787122	102.854667	106.922212	0.007039262359076	0.000002040965747	0.000761716841448	0.241725315442963
106.929063	111.456333	115.983603	0.007403636911815	0.000002192016887	0.000769854798983	0.226847979018990
115.969408	121.128333	126.287258	0.006033207754436	0.000002094294626	0.000634585946441	0.234181445355946
126.248927	132.029667	137.810407	0.003997421376105	0.000001788830072	0.000447048035784	0.182757642625445
137.797952	144.417667	151.037382	0.003259432329578	0.000001719793097	0.000361952903913	0.160154483859803
150.983113	158.619333	166.255553	0.002316282282203	0.000001516498959	0.000266891158224	0.091173433972512
166.193435	175.045000	183.896565	0.000908246221538	0.000001019171232	0.000137484341977	0.014490817837320
183.833235	194.240000	204.646765	0.000441671381121	0.000000736855468	0.000081162304948	0.092008957646579
204.582267	216.966667	229.351067	0.000141764525975	0.000000449994096	0.000040923953359	0.188506859786826
229.224692	244.224667	259.224642	0.000082017549505	0.000000331248406	0.000024009509928	0.362116255422206
259.028967	277.502667	295.976367	0.000076924266471	0.000000386249401	0.000022966821536	0.607888139755992
295.671617	318.994667	342.317717	0.000063693058025	0.000000409307426	0.000019421888545	0.964893104390326
341.834983	372.158333	402.481683	0.000054395524222	0.000000439561879	0.000015763431297	1.484326710128872
401.613700	442.697000	483.780300	0.000029572148359	0.000000326514961	0.000009088767630	2.342669129988270
482.040100	540.976000	599.911900	0.000016440399499	0.000000333335976	0.000006141876428	3.881738535282870
590.223117	688.215667	786.208217	0.000006199045680	0.000000239853314	0.000002994144843	43.799451647713582

Table A.VIII.8. Proton Yields from Iron 800 MeV/n on 40 g/cm^2 Aluminium at 10.0 deg

KE_left(MeV)	KE_mid(MeV)	KE_right(MeV)	Norm_Cts(#/SP*ster*MeV)	Y_stat(#/SP*ster*MeV)	Y_syst_tot(#/SP*ster*MeV)	X_tot(MeV)
43.706083	45.408533	47.110983	0.004309263469335	0.000001065201750	0.000750435832143	0.186115063591728
47.161880	48.915200	50.668520	0.004365838682617	0.000001089016262	0.000751026105392	0.260580115233223
50.668513	52.421833	54.175153	0.004940571303150	0.000001160981981	0.000811589893523	0.406340692558597
54.076355	55.992000	57.907645	0.005543197475598	0.000001239568523	0.000826849494576	0.280086782879950
58.006485	60.162300	62.318115	0.005279561924593	0.000001314881311	0.000777777377856	0.253211368862064
62.318085	64.473900	66.629715	0.006363631389307	0.000001410635076	0.000864806722617	0.231791101060847
66.610445	69.153800	71.697155	0.005946690277019	0.000001512152034	0.000794854129811	0.299175915029937
71.682440	74.279100	76.875760	0.006346810249310	0.000001563475921	0.000821214128863	0.215100463504847
76.909775	79.882400	82.855025	0.006833536800963	0.000001764823774	0.000837527306471	0.339092028717869
82.752067	85.966967	89.181867	0.007791854122173	0.000001941429247	0.000893153930002	0.226441892165496
89.190220	92.720900	96.251580	0.008033909400591	0.000002065090509	0.000893078588447	0.258184254329907
96.257670	100.185300	104.112930	0.009103318724107	0.000002291995879	0.000947693692258	0.258813605189159
104.099138	108.488333	112.877528	0.009174725696645	0.000002419868049	0.000921285537723	0.239611470731265
112.872555	117.777000	122.681445	0.010080867390057	0.000002672356360	0.000965465821910	0.223376003234457
122.650703	128.223333	133.795963	0.010619328856545	0.000002924391434	0.000973308766631	0.167766621651776
133.770560	140.094000	146.417440	0.010834983333994	0.000003113434522	0.000952606251677	0.154210377994511
146.392272	153.659667	160.927062	0.014761760315799	0.000003866708959	0.001236613678086	0.112790075683546
160.880677	169.284667	177.688657	0.014575466891991	0.000004068838606	0.001163205646933	0.030327980963790
177.639410	187.496000	197.352590	0.016140758683910	0.000004594279738	0.001218087519577	0.056862811420646
197.261775	208.936000	220.610225	0.016843034298433	0.000005141086187	0.001263869333779	0.171625808562145
220.505718	234.547333	248.588948	0.016189069839881	0.000005542054658	0.001211928636859	0.300097926925529
248.421767	265.618667	282.815567	0.014794652900408	0.000005892967393	0.001103914849223	0.526765522847690
282.562350	304.077000	325.591650	0.008761336689978	0.000005038134142	0.000691086986207	0.818749519978485
325.184317	352.866667	380.549017	0.001861388305382	0.000002608214208	0.000180332577364	1.259010254400257
379.838433	416.777333	453.716233	0.000563867375137	0.000001614273510	0.000061643870045	1.961689231839743
452.365167	504.228667	556.092167	0.000303851923686	0.000001388551546	0.000036532205540	3.144164391440117
553.079600	631.646000	710.212400	0.000114226310243	0.000001046087062	0.000017058307155	5.528029705871704
709.437000	751.140000	792.843000	0.000044324992000	0.000000436324000	0.000004066510000	43.319499999999998

Table A.VIII.9. Proton Yields from Iron 800 MeV/n on 40 g/cm^2 Aluminium at 7.20 deg

KE_left(MeV)	KE_mid(MeV)	KE_right(MeV)	Norm_Cts(#/SP*ster*MeV)	Y_stat(#/SP*ster*MeV)	Y_syst_tot(#/SP*ster*MeV)	X_tot(MeV)
45.882457	47.670067	49.457677	0.005014264539667	0.000001136844161	0.000793226019518	0.142374418186097
49.457657	51.245267	53.032877	0.005174954362783	0.000001184445611	0.000822334157396	0.371676813481821
53.032890	54.820500	56.608110	0.005892460001000	0.000001234696402	0.000880564048201	0.462868799666817
56.540655	58.662400	60.784145	0.005990310583884	0.000001388552272	0.000852847318994	0.119033064458116
60.851597	63.041567	65.231537	0.006440013083160	0.000001488231156	0.000889613516986	0.277374080861929
65.126140	67.496800	69.867460	0.007534523537215	0.000001613807573	0.000948906568931	0.241628471097675
69.972827	72.569267	75.165707	0.007487631228997	0.000001714481860	0.000930180354532	0.276834876738824
75.067603	77.915833	80.764063	0.007718356071432	0.000001817696953	0.000925428396116	0.253644560420305
80.802572	83.868267	86.933962	0.008333409628945	0.000001941533366	0.000944600864766	0.229284985229387
86.993562	90.412767	93.831972	0.009076837589800	0.000002146519822	0.000983781365705	0.303067877378979
93.800112	97.604567	101.409022	0.008990549372335	0.000002243462668	0.000947281407259	0.251184523597773
101.392708	105.602333	109.811958	0.010690672591411	0.000002572107281	0.001053583343322	0.223776394093211
109.778262	114.541667	119.305072	0.011385560258491	0.000002847541546	0.001088326202792	0.201594489681638
119.266472	124.597667	129.928862	0.012791252046089	0.000003152714088	0.001148012422296	0.180932409231320
129.895513	135.960333	142.025153	0.015243207703612	0.000003608127919	0.001296231338520	0.150077554023145
141.997595	148.925000	155.852405	0.017856772609295	0.000004174535940	0.001480347673273	0.116221935788946
155.811890	163.806000	171.800110	0.017183654734247	0.000004330163193	0.001375662553537	0.039094951652355
171.773115	181.109000	190.444885	0.021925396702903	0.000005231949639	0.001642032821030	0.026619144288651
190.360435	201.372000	212.383565	0.023736255126196	0.000005913953272	0.001755489850146	0.140057306369750
212.284685	225.477000	238.669315	0.019988889349118	0.000005950582800	0.001483600115693	0.252121675599303
238.517573	254.550333	270.583093	0.011634854834200	0.000005002197782	0.000903652167147	0.447370913928253
270.368383	290.288333	310.208283	0.006416278701548	0.000004132026931	0.000508272095611	0.703707489729930
309.859050	335.222000	360.584950	0.001810717479534	0.000002451645653	0.000177509149939	1.072845993380224
360.003850	393.405000	426.806150	0.000460923552330	0.000001391934204	0.000055603999962	1.643985847315603
425.727250	471.736000	517.744750	0.000252518690805	0.000001212435000	0.000033423811977	2.593430294629104
515.481517	583.183667	650.885817	0.000147831751678	0.000001090727765	0.000020740471328	4.387267620205086
646.153400	718.175000	790.196600	0.000042938915445	0.000000623417084	0.000006996957412	43.334334856789951

Table A.VIII.10. Proton Yields from Iron 800 MeV/n on 40 g/cm^2 Aluminium at 32.7 deg

KE_left(MeV)	KE_mid(MeV)	KE_right(MeV)	Norm_Cts(#/SP*ster*MeV)	Y_stat(#/SP*ster*MeV)	Y_syst_tot(#/SP*ster*MeV)	X_tot(MeV)
45.912420	47.418000	48.923580	0.002505594451383	0.000000738923907	0.000551491477195	0.247569957844242
48.912485	50.825700	52.738915	0.002250107230772	0.000000731859552	0.000437844578477	0.365475153208806
52.750065	54.674400	56.598735	0.002147132806517	0.000000760573983	0.000447366008580	0.421308770306292
56.598698	58.523033	60.447368	0.002591056706650	0.000000838540354	0.000501296173752	0.226948566481240
60.389205	62.681800	64.974395	0.002509976338567	0.000000884350897	0.000448872019037	0.377678162580205
65.032563	67.383333	69.734103	0.002960102384207	0.000001010161957	0.000503610385450	0.439923746567516
69.632297	72.249567	74.866837	0.002709595857722	0.000000986271809	0.000449142697037	0.210616154884330
74.968627	77.748367	80.528107	0.002536677762520	0.000001010161957	0.000427023643699	0.446042343484338
80.480870	83.644700	86.808530	0.002884442516165	0.000001162773294	0.000440791537578	0.297779186650108
86.736037	90.161567	93.587097	0.002775998688425	0.000001159187900	0.000410444759261	0.331667536682881
93.609902	97.400167	101.190432	0.002968355040549	0.000001288902906	0.000417275319622	0.328225216650092
101.188222	105.421667	109.655112	0.003268694200087	0.000001410635076	0.000423178062633	0.308747352055042
109.633187	114.372667	119.112147	0.003196277946513	0.000001486458472	0.000402349698817	0.282613820399852
119.118792	124.439667	129.760542	0.003288087127957	0.000001542912569	0.000379863997533	0.251784549285694
129.755107	135.839667	141.924227	0.003711327476184	0.000001790614862	0.000401802450907	0.225503077741502
141.880110	148.827000	155.773890	0.004295109000361	0.000001891873053	0.000378911202274	0.154465775401705
155.715780	163.752000	171.788220	0.004694263390126	0.000002070449641	0.000376597350019	0.073167919282565
171.743715	181.109000	190.474285	0.004266983085119	0.000002265146181	0.000376899970886	0.029897999364840
190.400347	201.450667	212.500987	0.004125906368733	0.000002478629005	0.000352600631883	0.172225657763325
212.407195	225.658000	238.908805	0.003494080856093	0.000002495629609	0.000299584171394	0.345370459844208
238.753217	254.860667	270.968117	0.002647535178017	0.000002370441881	0.000233912614346	0.624368703938626
270.757950	290.790000	310.822050	0.001210487093934	0.000001752162459	0.000125322435572	0.979170699768432
310.467983	335.997333	361.526683	0.000178970215165	0.000000702761564	0.000033865016832	1.514980128597732
360.932683	394.578333	428.223983	0.000021264545448	0.000000275452361	0.000009154657442	2.338117839481150
428.742550	457.844500	486.946450	0.000005761964541	0.000000152971982	0.000003846659238	2.753204336659377
517.654983	586.120333	654.585683	0.000002009133941	0.000000123410957	0.000001864934782	6.144864704816534
658.444650	689.232000	720.019350	0.000001793715200	0.000000087264700	0.000000993255000	5.102150000000000

Table A.VIII.11. Proton Yields from Iron 800 MeV/n on 40 g/cm^2 Aluminium at 30.0 deg

KE_left(MeV)	KE_mid(MeV)	KE_right(MeV)	Norm_Cts(#/SP*ster*MeV)	Y_stat(#/SP*ster*MeV)	Y_syst_tot(#/SP*ster*MeV)	X_tot(MeV)
43.836407	45.516467	47.196527	0.002162831805750	0.000000733564077	0.000488215811920	0.544623346908669
47.196540	48.876600	50.556660	0.002138418501967	0.000000733564077	0.000487487853946	0.977215053584931
50.556673	52.236733	53.916793	0.002923330105350	0.000000833821351	0.000568320433131	0.655686800168343
53.863905	55.910200	57.956495	0.002634729707964	0.000000882623334	0.000499109103581	0.323034084238243
58.009395	60.108600	62.207805	0.002858937987317	0.000000934737972	0.000516271979430	0.634348123044437
62.131425	64.318700	66.505975	0.003037187298540	0.000000988098613	0.000529610242623	0.610822485953161
66.582387	69.104967	71.627547	0.003176326073947	0.000001083723534	0.000511453884405	0.554787751304046
71.549423	74.164433	76.779443	0.003315270516950	0.000001114246265	0.000512012693582	0.534788737026127
76.857615	79.806000	82.754385	0.003341559668523	0.000001186201492	0.000491218318675	0.618891898319892
82.656073	85.881033	89.105993	0.003309106504251	0.000001211798249	0.000463981081707	0.573289589554005
89.104882	92.636067	96.167252	0.003762438320545	0.000001360321527	0.000492305712773	0.512545771608741
96.178652	100.106067	104.033482	0.003322016425420	0.000001335435320	0.000431071018694	0.551136547644955
104.022772	108.416667	112.810562	0.003941240117223	0.000001563475814	0.000467980908074	0.516046783468321
112.789463	117.707333	122.625203	0.004149484625691	0.000001688246010	0.000464738388537	0.468746373411038
122.593627	128.156667	133.719707	0.003915425809761	0.000001738911667	0.000427278009847	0.381707979976840
133.732707	140.054667	146.376627	0.003180824461999	0.000001637963354	0.000350101590950	0.343018326374845
146.337555	153.621000	160.904445	0.002186859492637	0.000001461019924	0.000257499209560	0.232305307318279
160.873123	169.285333	177.697543	0.001028796231260	0.000001037043711	0.000145416351838	0.115819332136824
177.648618	187.508333	197.368048	0.000447677057281	0.000000708942001	0.000080853714133	0.092010769021131
197.277523	208.964333	220.651143	0.000152296640079	0.000000439561805	0.000041539879657	0.373919906886488
220.531173	234.599333	248.667493	0.000058050911377	0.000000261793982	0.000019950961409	0.720263558067462
248.500450	265.712000	282.923550	0.000038198353009	0.000000275955132	0.000018264347303	1.205656484777069
282.662750	304.208000	325.753250	0.000015266637889	0.000000151146894	0.000007475830796	1.929061333492536
343.312350	352.513000	361.713650	0.000014997325991	0.000000087264700	0.000003362250000	1.701800000000000
553.497067	632.169667	710.842267	0.000001046517814	0.000000106225978	0.000001446388431	12.835207635176769
710.440350	751.826000	793.211650	0.000000679344640	0.000000062819700	0.000000531326000	42.633600000000001

Table A.VIII.12. Proton Yields from Iron 800 MeV/n on 40 g/cm^2 Aluminium at 27.2 deg

KE_left(MeV)	KE_mid(MeV)	KE_right(MeV)	Norm_Cts(#/SP*ster*MeV)	Y_stat(#/SP*ster*MeV)	Y_syst_tot(#/SP*ster*MeV)	X_tot(MeV)
45.745552	47.464200	49.182849	0.002909743059463	0.000000861947434	0.000572108167846	0.381475835716877
49.269695	51.113000	52.956305	0.003118988734400	0.000000882623334	0.000558284854394	0.862577975970868
52.956295	54.799600	56.642905	0.003267686363300	0.000000915240058	0.000580202045865	0.643385945629060
56.540322	58.551867	60.563412	0.002838129798065	0.000000906881018	0.000527228371806	0.275419959594888
60.666022	62.927767	65.189512	0.002837990573213	0.000000984441610	0.000505048630691	0.744082145622377
65.166437	67.451267	69.736097	0.003275819151480	0.000001008375124	0.000526162075325	0.576741706354760
69.759180	72.442500	75.125820	0.002963126692220	0.000001061490273	0.000472688811164	0.536704215084995
75.042580	77.834200	80.625820	0.003338423203612	0.000001186201492	0.000513898811169	0.596565511729433
80.709058	83.816533	86.924008	0.003407212293200	0.000001234696402	0.000487741969674	0.569015307640313
86.849475	90.303000	93.756525	0.003453296725241	0.000001286052623	0.000469703092637	0.547813329270108
93.727373	97.525133	101.322893	0.003605780901863	0.000001414368299	0.000473731053344	0.543609681838909
101.318738	105.541333	109.763928	0.003828282427970	0.000001511468941	0.000466886653728	0.519792928237774
109.780275	114.492000	119.203725	0.003884895134932	0.000001615612530	0.000455717262232	0.485931301858606
119.178992	124.542667	129.906342	0.004004933045121	0.000001717056596	0.000435602563596	0.429714964540450
129.885962	135.932667	141.979372	0.004437635403920	0.000001914039323	0.000453283105356	0.384271029463581
141.955592	148.901667	155.847742	0.004442138425989	0.000002146408819	0.000461873412452	0.286581630232993
155.805050	163.826000	171.846950	0.004291412423446	0.000002292150056	0.000446059028001	0.195722889436187
171.765423	181.113333	190.461243	0.004434900451526	0.000002295623326	0.000381570753347	0.045805018693807
190.410297	201.442667	212.475037	0.005469266080100	0.000002813497639	0.000440012457142	0.192351744906694
212.364377	225.567667	238.770957	0.004686838892667	0.000002902576025	0.000390332281281	0.505422762389072
238.640617	254.714667	270.788717	0.003030970548043	0.000002535336525	0.000262561190586	0.879344649175737
270.562333	290.517333	310.472333	0.001548860234987	0.000002006958148	0.000150727673365	1.456027017412108
310.123733	335.538333	360.952933	0.000367867488349	0.000001065592833	0.000054682527570	2.313747073558387
360.373433	393.864333	427.355233	0.000028789293765	0.000000294754580	0.000009978522344	3.583993620111509
426.264000	472.409000	518.554000	0.000008333589933	0.000000172932224	0.000003863203963	5.682662091036208
516.276117	584.212667	652.149217	0.000003650519177	0.000000137473916	0.000002189247649	9.484550403413964
648.351050	719.726500	791.101950	0.000001153507974	0.000000106225937	0.000001021218038	42.220322313560089

Table A.VIII.13. Triton Yields from Iron 800 MeV/n on 40 g/cm^2 Aluminium at 12.7 deg

KE_left(MeV)	KE_mid(MeV)	KE_right(MeV)	Norm_Cts(#/SP*ster*MeV)	Y_stat(#/SP*ster*MeV)	Y_syst_tot(#/SP*ster*MeV)	X_tot(MeV)
45.275625	46.420533	47.565441	0.001013017370826	0.000000344167117	0.000322720036358	32.301353576796068
47.499792	48.847867	50.195941	0.000977087778895	0.000000417178651	0.000330313414208	0.125166859894303
50.261613	51.706633	53.151654	0.000942840431662	0.000000462061696	0.000348663171736	0.328197871330696
53.151646	54.596667	56.041687	0.000907751962080	0.000000453440509	0.000342506535805	0.112270178218341
55.988173	57.675533	59.362893	0.000872248599737	0.000000488495145	0.000314992234019	0.115295709622735
59.416385	61.163600	62.910815	0.000901609923809	0.000000489062982	0.000304761950896	0.259161572068469
62.835825	64.765700	66.695575	0.000894473070347	0.000000492455509	0.000283349638881	0.066863990403954
66.770607	68.823567	70.876527	0.000886148868849	0.000000453440509	0.000239785119791	0.191195779487937
70.823935	73.132900	75.441865	0.001089845231199	0.000000469935184	0.000227132437237	0.066721356267165
75.422305	77.896800	80.371295	0.001323320630645	0.000000581293437	0.000261567126134	0.092401974315388
80.411367	83.122067	85.832767	0.001737321730347	0.000000508835864	0.000205571406168	0.054319613348058
85.860275	88.864500	91.868725	0.001995979089137	0.000000814121155	0.000314700149541	0.038288689751805
91.853695	95.200000	98.546305	0.002255905562144	0.000001230907388	0.000469618904656	0.049436380657164
98.504683	102.235633	105.966583	0.002413429426476	0.000001417154853	0.000495012701972	0.088324878447194
105.937772	110.091667	114.245562	0.002376962713083	0.000001365908641	0.000429957830269	0.105310771235852
114.223053	118.879333	123.535613	0.001780209045304	0.000000939311930	0.000241438824916	0.165769872371309
123.547417	128.809667	134.071917	0.000425978901435	0.000000471473759	0.000102398275247	0.214915719171493
134.047357	140.064667	146.081977	0.000056436833557	0.000000138479495	0.000024322328965	0.310562096157918
146.039307	152.944667	159.850027	0.000194698726184	0.000000384449259	0.000059437297428	0.381959363672368
159.774623	167.756333	175.738043	0.000057261796966	0.000000173732689	0.000023391002382	0.561861156665061
194.301850	205.344000	216.386150	0.000013774775997	0.000000123410957	0.000011631576377	0.874010252354628
224.946940	229.352000	233.757060	0.000013756314240	0.000000087264700	0.000006944800000	0.645980000000000
242.611467	258.775667	274.939867	0.000007465310608	0.000000122281526	0.000007843477110	1.526101517936798
274.729233	294.838333	314.947433	0.000030479909474	0.000000204992230	0.000010560502123	2.025575611054794
314.595767	340.292667	365.989567	0.000061661214705	0.000000395634487	0.000016824009967	2.819942441345213
365.370200	399.327000	433.283800	0.000045943226103	0.000000386249401	0.000012581868890	4.087014631414965
432.153800	479.128000	526.102200	0.000020795929615	0.000000282032530	0.000006404671863	6.312219814272948
523.711067	593.258667	662.806267	0.000011451553207	0.000000261793982	0.000004215002419	10.819174078967396
666.451850	732.399000	798.346150	0.000003242977941	0.000000123410922	0.000001324247564	15.645257210634155

Table A.VIII.14. Triton Yields from Iron 800 MeV/n on 40 g/cm^2 Aluminium at 10.0 deg

KE_left(MeV)	KE_mid(MeV)	KE_right(MeV)	Norm_Cts(#/SP*ster*MeV)	Y_stat(#/SP*ster*MeV)	Y_syst_tot(#/SP*ster*MeV)	X_tot(MeV)
44.508576	45.672333	46.836090	0.000832879090063	0.000000302293095	0.000281123984003	39.267673799322516
46.794158	47.999833	49.205509	0.000885062228227	0.000000462061696	0.000420991679183	0.081516302679725
49.247418	50.710700	52.173981	0.000936049699947	0.000000582961852	0.000443275606464	0.258517709566695
52.173985	53.637267	55.100548	0.000987635004889	0.000000531651263	0.000402066052685	0.193194511544609
55.034637	56.595033	58.155429	0.001040290482850	0.000000482941349	0.000346628144463	0.037229636253125
58.221350	59.986400	61.751450	0.001133458264493	0.000000480926071	0.000297769057538	0.236823778720064
61.705015	63.516500	65.327985	0.001032920296230	0.000000432740484	0.000259479533815	0.145998415691575
65.374438	67.444933	69.515428	0.001192497290592	0.000000515995957	0.000271695849608	0.175707277317959
69.439353	71.634733	73.830113	0.001362185235632	0.000000535292432	0.000268644639783	0.078356228511130
73.906170	76.286700	78.667230	0.001526630205859	0.000000604587923	0.000283181103587	0.113720904711711
78.650433	81.329433	84.008433	0.001831152608308	0.000000736855338	0.000310804173436	0.058968688018388
83.958095	86.880400	89.802705	0.002083684086430	0.000000787009635	0.000309880001415	0.025442004054909
89.793078	93.015433	96.237788	0.002270678930030	0.000000885047969	0.000322722767592	0.026613089287980
96.242072	99.812667	103.383262	0.002421985989043	0.000001124326762	0.000388092391100	0.025998585595492
103.373447	107.361667	111.349887	0.002949945758679	0.000001690138652	0.000592806946233	0.131756963765563
111.346748	115.847333	120.347918	0.003264576412559	0.000001266340067	0.000356831415425	0.121524421823558
120.301160	125.360000	130.418840	0.002582089083629	0.000001189523595	0.000295210316088	0.202664425449954
130.404570	136.154000	141.903430	0.000689341713863	0.000000651492717	0.000135246711018	0.260486038685378
141.888335	148.468000	155.047665	0.001424434432224	0.000001015898849	0.000187766149086	0.329135023806340
154.985307	162.582667	170.180027	0.000478042583924	0.000000594249459	0.000089523806863	0.488364816670898
170.134078	178.983333	187.832588	0.000134681218621	0.000000331248406	0.000039948631137	0.618020890221358
187.785567	198.216667	208.647767	0.000198719404447	0.000000439561326	0.000045361696353	0.760378317279629
208.558960	221.007000	233.455040	0.000321753666086	0.000000631304609	0.000056930576430	0.982074577891618
233.322602	248.413667	263.504732	0.000422075528761	0.000000818954248	0.000062290576424	1.307453494771420
263.319300	281.987000	300.654700	0.000764978419763	0.000001240848095	0.000084436266243	1.730540340727427
300.348050	323.970000	347.591950	0.001041850156363	0.000001646150593	0.000098012129433	2.361628347157952
347.075117	377.902667	408.730217	0.000986755006331	0.000001869328856	0.000088783499425	3.383329152964577
407.828233	449.758333	491.688433	0.000654570468303	0.000001790618108	0.000062454032399	5.095582791222218
489.864217	550.380667	610.897117	0.000208653310627	0.000001178495453	0.000026366469772	8.401535228998327
609.810200	702.225000	794.639800	0.000030795635885	0.000000536645282	0.000007049610029	17.346829682178239

Table A.VIII.15. Triton Yields from Iron 800 MeV/n on 40 g/cm^2 Aluminium at 7.20 deg

KE_left(MeV)	KE_mid(MeV)	KE_right(MeV)	Norm_Cts(#/SP*ster*MeV)	Y_stat(#/SP*ster*MeV)	Y_syst_tot(#/SP*ster*MeV)	X_tot(MeV)
45.285502	46.461800	47.638099	0.001000840156309	0.000000490479779	0.000460760827958	32.345039171598110
47.570952	48.849000	50.127047	0.001105279237982	0.000000683433945	0.000603696376187	0.045166798847051
50.194161	51.669600	53.145039	0.001204423775893	0.000000742191231	0.000573485802759	0.262951101792710
53.145061	54.620500	56.095939	0.001306215585685	0.000000731859552	0.000562953193148	0.131378066128445
56.018072	57.662000	59.305928	0.001410081752437	0.000000611080079	0.000425545778314	0.069934815557443
59.383755	61.160700	62.937645	0.001627345251499	0.000000582961852	0.000362278282220	0.250653707197799
62.861872	64.764467	66.667062	0.001577157008376	0.000000582961852	0.000344611474234	0.068706187794300
66.742820	68.825000	70.907180	0.001687482759227	0.000000604587923	0.000324767848935	0.190050391117303
70.839465	73.131600	75.423735	0.001951617889260	0.000000683433945	0.000334624824722	0.037599205466069
75.432037	77.897267	80.362497	0.002210761640907	0.000000818276924	0.000377168720495	0.119200075183743
80.421900	83.129100	85.836300	0.002761600503091	0.000000838540354	0.000360159401174	0.059464668300008
85.836087	88.863867	91.891647	0.003052869525515	0.000000961788424	0.000376940293813	0.018361863185159
91.868480	95.200000	98.531520	0.003344803881422	0.000001085642331	0.000398161574983	0.022832619385870
98.500758	102.233133	105.965508	0.003529540834785	0.000001703439769	0.000659388713165	0.091455925609638
105.936197	110.098667	114.261137	0.003715632114484	0.000001758429756	0.000628744857415	0.087232291911023
114.242538	118.893333	123.544128	0.003789083256663	0.000001385706675	0.000390304597342	0.140971483815770
123.544852	128.816667	134.088482	0.000907730547944	0.000000719410318	0.000165236637042	0.204922659912075
134.066292	140.078667	146.091042	0.001716161740316	0.000001072585596	0.000218005529198	0.285119131925587
146.046267	152.959667	159.873067	0.000770653144817	0.000000736436918	0.000125048963217	0.356251288383635
159.802265	167.787000	175.771735	0.000368296798345	0.000000533475372	0.000074421179688	0.508602623513682
175.733793	185.064333	194.394873	0.000307310007180	0.000000540822645	0.000063194897407	0.630473512240602
194.347495	205.392000	216.436505	0.000400089859201	0.000000662497199	0.000068180542131	0.790824488210248
216.335260	229.594000	242.852740	0.000335797776009	0.000000683433945	0.000058643452761	1.032520091836474
242.684917	258.863667	275.042417	0.000310233358886	0.000000731859552	0.000051346174070	1.373517176688373
274.827800	294.958000	315.088200	0.000389339775708	0.000000897019944	0.000052530976188	1.817414673569024
314.734833	340.460333	366.185833	0.000602160738332	0.000001316673682	0.000065762811587	2.528735534491498
365.565167	399.568667	433.572167	0.000608630947031	0.000001539800835	0.000061223582883	3.666385306606494
432.438850	479.491000	526.543150	0.000314335108552	0.000001275860042	0.000036405786965	5.679544810334716
524.141817	593.839667	663.537517	0.000055344338155	0.000000600854043	0.000010609647151	9.803561046731948
667.745150	733.318000	798.890850	0.000004688459379	0.000000164527324	0.000001806992933	16.015588563412209

Table A.VIII.16. Helium-4 Yields from Iron 800 MeV/n on 40 g/cm^2 Aluminium at 12.7 deg

KE_left(MeV)	KE_mid(MeV)	KE_right(MeV)	Norm_Cts(#/SP*ster*MeV)	Y_stat(#/SP*ster*MeV)	Y_syst_tot(#/SP*ster*MeV)	X_tot(MeV)
44.716085	46.453400	48.190715	0.000117935072373	0.000000122281526	0.000074481568269	0.133075845322170
48.190785	49.928100	51.665415	0.000342257100693	0.000000238111537	0.000147374670004	0.309343886504970
51.665385	53.402700	55.140015	0.000595467366837	0.000000359801115	0.000223169623345	0.246207581623718
55.072157	57.144567	59.216977	0.000725569854634	0.000000431134503	0.000227189616466	0.260491419855165
59.284878	61.426233	63.567588	0.000781667121012	0.000000510741028	0.000262379052727	0.322220577978812
63.474825	65.758400	68.041975	0.000850256901920	0.000000609033169	0.000302526431723	0.143393701936033
68.134765	70.684600	73.234435	0.000907416923469	0.000000633279844	0.000280895074825	0.403360337248223
73.125347	75.865067	78.604787	0.000966709557332	0.000000809259858	0.000341402761215	0.176434162598603
78.713865	81.675300	84.636735	0.001053169117075	0.000000811143685	0.000316367185179	0.341300558455447
84.617580	87.974900	91.332220	0.001149410393126	0.000000738923440	0.000251055976886	0.280047620973648
91.263990	94.936900	98.609810	0.000885479998296	0.000000656935661	0.000200853417820	0.228227185992379
98.601065	102.672100	106.743135	0.001077307391685	0.000000731859552	0.000206211218194	0.251034556202926
106.754260	111.289000	115.823740	0.000947978003190	0.000000736855468	0.000186349549768	0.228390159153147
115.800350	120.953000	126.105650	0.000959825122436	0.000000765744423	0.000169655260289	0.198569979348944
126.097925	131.884000	137.670075	0.001157335306377	0.000000898719994	0.000182220496193	0.191220861745679
137.658227	144.295667	150.933107	0.001005461611503	0.000000897019939	0.000157469426160	0.137219576433685
150.868680	158.534000	166.199320	0.001013541320829	0.000000940640260	0.000145977304267	0.077596682275291
166.141098	175.024333	183.907568	0.001492562472102	0.000001215456711	0.000169884521820	0.012140602499069
183.837223	194.293333	204.749443	0.001102967874774	0.000001113996837	0.000131487365845	0.101259854369735
204.678903	217.129333	229.579763	0.000390050446255	0.000000694886277	0.000065156472486	0.212395216275249
229.451812	244.549667	259.647522	0.000097526908253	0.000000368730885	0.000027215914366	0.383661964999138

Table A.VIII.17. Helium-4 Yields from Iron 800 MeV/n on 40 g/cm^2 Aluminium at 10.0 deg

KE_left(MeV)	KE_mid(MeV)	KE_right(MeV)	Norm_Cts(#/SP*ster*MeV)	Y_stat(#/SP*ster*MeV)	Y_syst_tot(#/SP*ster*MeV)	X_tot(MeV)
44.610390	45.133200	45.656010	0.000172754775328	0.000000121142000	0.000081443700000	0.138849000000000
45.712847	47.501567	49.290287	0.000204315836160	0.000000211797868	0.000125483132097	0.111484818326289
49.290280	51.079000	52.867720	0.000634007761675	0.000000373590745	0.000225820292093	0.298094924614627
52.867680	54.656400	56.445120	0.000796704534507	0.000000432740484	0.000262335618100	0.366120324060274
56.373700	58.486500	60.599300	0.001081160595883	0.000000551099864	0.000285977930914	0.177296408151688
60.670750	62.863300	65.055850	0.001294694963755	0.000000611080079	0.000310416524927	0.277538052212665
64.953480	67.317100	69.680720	0.001474098051006	0.000000783929198	0.000378921137233	0.219219844557672
69.783077	72.383567	74.984057	0.001646749852272	0.000000833821437	0.000374415031584	0.328204372783179
74.882503	77.726533	80.570563	0.001825604599215	0.000000909240924	0.000374641962413	0.220223140153005
80.620363	83.683733	86.747103	0.002084275749680	0.000000958031000	0.000373070579254	0.273456222494223
86.798842	90.225067	93.651292	0.002266706022904	0.000001058028432	0.000375922675481	0.297554976750516
93.612370	97.418200	101.224030	0.001579703335473	0.000000882623334	0.000272250862214	0.243734769054909
101.208555	105.422000	109.635445	0.001790370348033	0.000000986271804	0.000278439807422	0.207045915002953
109.604170	114.370000	119.135830	0.001577083646736	0.000000993684021	0.000246917731840	0.197393784219286
119.101603	124.443333	129.785063	0.001504355476402	0.000001008375124	0.000225011213396	0.190612532130524
129.748503	135.825333	141.902163	0.001693577247708	0.000001114246265	0.000229296388140	0.152075146118884
141.876470	148.822000	155.767530	0.002105600837567	0.000001305291502	0.000245824211593	0.110718836046492
155.725477	163.745667	171.765857	0.001838991115723	0.000001264695526	0.000202000681991	0.033572864952220
171.737240	181.110000	190.482760	0.003049216696867	0.000001790618108	0.000273124482579	0.026296702520356
190.399450	201.460000	212.520550	0.001742861608520	0.000001463737909	0.000182927309267	0.147574660440368
212.668705	221.229500	229.790295	0.000329437947522	0.000000531594286	0.000048823313958	0.198012639051147

Table A.VIII.18. Helium-4 Yields from Iron 800 MeV/n on 40 g/cm^2 Aluminium at 7.20 deg

KE_left(MeV)	KE_mid(MeV)	KE_right(MeV)	Norm_Cts(#/SP*ster*MeV)	Y_stat(#/SP*ster*MeV)	Y_syst_tot(#/SP*ster*MeV)	X_tot(MeV)
45.667965	47.412800	49.157635	0.000965750446307	0.000000760573983	0.000509242493208	0.196040609020292
49.227272	51.050267	52.873262	0.001094589432683	0.000000506923540	0.000305810428051	0.253381785079354
52.873238	54.696233	56.519228	0.000794567981931	0.000000409307941	0.000244853071651	0.436838339733362
56.416710	58.470300	60.523890	0.001004568816251	0.000000535292848	0.000284844051679	0.171810392378954
60.626422	62.853067	65.079712	0.001202258473091	0.000000685258935	0.000344812221892	0.258147621974327
65.000513	67.328933	69.657353	0.001369025132663	0.000000794708612	0.000391595600384	0.227041971384147
69.736542	72.370767	75.004992	0.001531002010111	0.000000909240924	0.000410393388861	0.303179880970027
74.896265	77.719800	80.543335	0.001698030997098	0.000001046293441	0.000443620633589	0.200670426434116
80.644260	83.697100	86.749940	0.001938454922809	0.000001061752035	0.000421497198143	0.279646091746264
86.757758	90.217133	93.676508	0.002181486474848	0.000001035303275	0.000357515614227	0.287186544082413
93.604787	97.406867	101.208947	0.001979364769223	0.000001037043711	0.000324116078893	0.235135533596456
101.205125	105.420000	109.634875	0.002459949149818	0.000001184445611	0.000346406191727	0.204982081736941
109.615532	114.362667	119.109802	0.002353068300218	0.000001210487850	0.000318793940847	0.185346897111551
119.092140	124.445000	129.797860	0.002495118467696	0.000001316462399	0.000313482339696	0.189239114891214
129.746192	135.818667	141.891142	0.002847401550414	0.000001503134469	0.000330654667026	0.143073258843887
141.872720	148.820000	155.767280	0.003554966281962	0.000001725580367	0.000352978892647	0.109458746817146
155.731658	163.746333	171.761008	0.006889862382752	0.000002543684292	0.000546109114588	0.034271742840276
171.735928	181.110333	190.484738	0.003933428123387	0.000002053819552	0.000341092411620	0.025285767950086
190.394455	201.462000	212.529545	0.000941958497608	0.000001066691109	0.000128133566479	0.145238331962365

Table A.VIII.19. Helium-3 Yields from Iron 800 MeV/n on 40 g/cm^2 Aluminium at 12.7 deg

KE_left(MeV)	KE_mid(MeV)	KE_right(MeV)	Norm_Cts(#/SP*ster*MeV)	Y_stat(#/SP*ster*MeV)	Y_syst_tot(#/SP*ster*MeV)	X_tot(MeV)
44.680310	46.411400	48.142490	0.000320128546685	0.000000462061696	0.000291045456226	0.424875132085887
48.027618	49.969133	51.910648	0.000367421940814	0.000000453440509	0.000256566364619	0.240499968879603
52.025527	54.172867	56.320207	0.000412514552177	0.000000432740484	0.000218971089966	0.303503732291713
56.320227	58.467567	60.614907	0.000458707554923	0.000000386249401	0.000194320443821	0.292620979476865
60.510948	62.926133	65.341318	0.000520721092940	0.000000386249947	0.000175031239600	0.296393104121553
65.445255	68.027400	70.609545	0.000527241447317	0.000000409307941	0.000171978452761	0.388775424044525
70.488057	73.293867	76.099677	0.000496718098192	0.000000416512771	0.000163174706142	0.206886847957646
76.221165	79.244400	82.267635	0.000490126701792	0.000000439561805	0.000157930062248	0.416430431707386
82.208432	85.617667	89.026902	0.000651101762359	0.000000535292432	0.000172811219037	0.315259408827477
88.966907	92.676467	96.386027	0.000682758557437	0.000000582961852	0.000173488205717	0.277221610314005
96.390668	100.501033	104.611398	0.000498214318878	0.000000489063049	0.000130233290618	0.310017897138214
104.602828	109.191333	113.779838	0.000541309580069	0.000000535292848	0.000129041150508	0.306689726409282
113.797288	118.926333	124.055378	0.000580207292027	0.000000610625477	0.000132620558515	0.301243621188898
124.029367	129.880667	135.731967	0.000590462777921	0.000000656935661	0.000125435100658	0.261332308507769
135.683625	142.322000	148.960375	0.000587933636285	0.000000686965422	0.000117490672290	0.235181338905216
148.939872	156.579667	164.219462	0.000638923257016	0.000000758930124	0.000113294997454	0.213211245868974
164.157970	173.019000	181.880030	0.000825498164982	0.000000892920905	0.000119153933650	0.129736873880405
181.822738	192.238333	202.653928	0.000651411156701	0.000000868273444	0.000096556155501	0.078184104020383
202.568663	214.954333	227.340003	0.000721383497357	0.000000965659985	0.000093115402216	0.047226587689284
227.213428	242.181333	257.149238	0.000208686562119	0.000000521729815	0.000040512121113	0.180962686585495
257.580850	263.287000	268.993150	0.000005593131628	0.000000062819700	0.000003854420000	0.161942000000000

Table A.VIII.20. Helium-3 Yields from Iron 800 MeV/n on 40 g/cm^2 Aluminium at 10.0 deg

KE_left(MeV)	KE_mid(MeV)	KE_right(MeV)	Norm_Cts(#/SP*ster*MeV)	Y_stat(#/SP*ster*MeV)	Y_syst_tot(#/SP*ster*MeV)	X_tot(MeV)
44.685825	46.479300	48.272775	0.000847430357169	0.000000631304609	0.000396307469439	0.542465290235237
48.272792	50.066267	51.859742	0.000977889843108	0.000000609033169	0.000379988121172	0.430306611210251
51.853303	54.060533	56.267763	0.001108476208906	0.000000685258935	0.000348784995018	0.134060124083468
56.274197	58.487867	60.701537	0.001238808814987	0.000000662915649	0.000334791257576	0.322770966803088
60.616378	62.940433	65.264488	0.001147225874909	0.000000567499232	0.000276695076040	0.278807123653611
65.349652	67.998367	70.647082	0.001091415106666	0.000000609032850	0.000257938950804	0.336828698513057
70.563552	73.315967	76.068382	0.001138080255700	0.000000687078575	0.000279121634916	0.205817666212816
76.151910	79.241400	82.330890	0.001066113700187	0.000000683433440	0.000247910695501	0.399469049151496
82.229980	85.609900	88.989820	0.001362781157673	0.000000783929198	0.000267051715293	0.280760175869389
88.986650	92.683600	96.380550	0.001264884911505	0.000000781979813	0.000243566311277	0.288350708036238
96.392022	100.501767	104.611512	0.001395497867018	0.000000882623334	0.000250369731983	0.316232003328253
104.599822	109.196667	113.793512	0.001419435932416	0.000000906881018	0.000234645796165	0.315481825692067
113.775983	118.920333	124.064683	0.001459413515406	0.000000959911550	0.000225165753091	0.288478832551021
124.025275	129.858000	135.690725	0.001217332991871	0.000000988161255	0.000198666649252	0.227763289937163
135.692462	142.327667	148.962872	0.001384471033403	0.000001087359017	0.000198534410000	0.242354386673730
148.920957	156.568667	164.216377	0.001258413395783	0.000001089016597	0.000173032177595	0.197901915160920
164.177735	173.033000	181.888265	0.001531886202975	0.000001290946328	0.000185496127608	0.153219838125649
181.826975	192.250000	202.673025	0.001603556461077	0.000001353768016	0.000172933303204	0.095045313507453
202.567203	214.955333	227.343463	0.001441351699066	0.000001388352404	0.000146090997808	0.035791799573785
227.220722	242.191667	257.162612	0.000407299853584	0.000000798540611	0.000063386149599	0.160020316211286
257.376050	269.211500	281.046950	0.000071359187943	0.000000275955116	0.000017348031504	0.246449918129424

Table A.VIII.21. Helium-3 Yields from Iron 800 MeV/n on 40 g/cm^2 Aluminium at 7.20 deg

KE_left(MeV)	KE_mid(MeV)	KE_right(MeV)	Norm_Cts(#/SP*ster*MeV)	Y_stat(#/SP*ster*MeV)	Y_syst_tot(#/SP*ster*MeV)	X_tot(MeV)
44.644780	46.480600	48.316420	0.002087577260081	0.000000787009862	0.000491506796655	0.548396998504733
48.316380	50.152200	51.988020	0.002179761146221	0.000000857679845	0.000548730485235	0.557349815439101
51.892672	54.005167	56.117662	0.002273991774028	0.000000938655253	0.000527305529542	0.064203697553801
56.213050	58.471000	60.728950	0.002364128918500	0.000000835649896	0.000432506685230	0.297701969279681
60.719470	62.986900	65.254330	0.002511699523453	0.000000909240969	0.000466927653721	0.360978999074738
65.263815	67.956900	70.649985	0.002466692856330	0.000000959911550	0.000425332133440	0.271742788513329
70.623625	73.343100	76.062575	0.002642272076571	0.000001015838383	0.000449622611393	0.251420463323891
76.088965	79.222600	82.356235	0.002611363209307	0.000001065201770	0.000416828472580	0.364235570252275
82.234807	85.596967	88.959127	0.002803314635423	0.000001184445611	0.000435078071527	0.256954862045535
88.993528	92.683333	96.373138	0.002925984026474	0.000001234696402	0.000421397641389	0.292659400343881
96.381863	100.492133	104.602403	0.002892792463496	0.000001262828958	0.000392076577323	0.310053642405375
104.588527	109.191667	113.794807	0.003241255877647	0.000001410635076	0.000406597251133	0.311216212437591
113.762870	118.918000	124.073130	0.003243183517561	0.000001488924257	0.000390185629919	0.284661214409340
124.044795	129.866000	135.687205	0.003485599715254	0.000001639912347	0.000392045752005	0.238790625781248
135.693623	142.327333	148.961043	0.003534547059629	0.000001740750978	0.000373165418849	0.242314380986767
148.913540	156.567000	164.220460	0.003590389145559	0.000001871545373	0.000363840235502	0.194885047299684
164.188030	173.040000	181.891970	0.003640707431012	0.000002012376802	0.000349778112333	0.165627722738586
181.827933	192.256333	202.684733	0.004063613883941	0.000002253250649	0.000347251615412	0.105321115037679
202.568775	214.959000	227.349225	0.002170696974606	0.000001751905925	0.000209892225893	0.026520274887934
227.510740	237.157000	246.803260	0.000416353992739	0.000000620964009	0.000050124043070	0.103354331864707

Table A.IX.1. Deuteron Yields from Iron 800 MeV/n on 60 g/cm^2 Aluminium at12.7 deg

KE_left(MeV)	KE_mid(MeV)	KE_right(MeV)	Norm_Cts(#/SP*ster*MeV)	Y_stat(#/SP*ster*MeV)	Y_syst_tot(#/SP*ster*MeV)	X_tot(MeV)
44.698281	46.033967	47.369652	0.001544997606533	0.000000480731129	0.000423826975128	0.740581149529206
47.369648	48.705333	50.041019	0.001558720432533	0.000000480731129	0.000424248667880	0.495412986186273
49.963876	51.402733	52.841590	0.001864518229222	0.000000556593227	0.000477892771761	0.176298114648966
52.918728	54.639033	56.359338	0.001772581693867	0.000000598977900	0.000427175139563	0.571129695131500
56.359328	58.079633	59.799938	0.001869689670133	0.000000592475705	0.000430291585427	0.709906834729741
59.714218	61.564133	63.414048	0.002208793141155	0.000000673036305	0.000457827860669	0.287509442302405
63.499735	65.602600	67.705465	0.002296043963913	0.000000729648535	0.000453556344573	0.518158577986508
67.642295	69.808300	71.974305	0.002185071155602	0.000000719389153	0.000430987414799	0.478831445686267
72.037487	74.523167	77.008847	0.002398022401207	0.000000812049503	0.000442630383400	0.408641761431697
76.907708	79.568533	82.229358	0.002727169663529	0.000000906976302	0.000473576615493	0.385460414404644
82.308302	85.200867	88.093432	0.002750040496969	0.000000947995588	0.000454578248975	0.343808065167180
88.115637	91.373667	94.631697	0.003035680554553	0.000001018951283	0.000464200977502	0.315136976944947
94.585188	98.188333	101.791478	0.003472090421695	0.000001154758312	0.000497791436935	0.246418834980527
101.787360	105.782000	109.776640	0.003375985349084	0.000001217865863	0.000480451156178	0.164053343542428
109.749987	114.277667	118.805347	0.003073327398113	0.000001244520454	0.000447053683017	0.090438090461321
118.770422	123.833667	128.896912	0.002244055984195	0.000001044084522	0.000314874003990	0.100067053369478
128.869793	134.634333	140.398873	0.001634013815460	0.000000949276589	0.000235890025853	0.247364567731516
140.367157	146.943667	153.520177	0.000945970831281	0.000000789679736	0.000162549378017	0.450127128684775
153.484470	161.064000	168.643530	0.000398011189075	0.000000538386474	0.000086353652711	0.740381604950447
168.623068	177.453333	186.283598	0.000110791436652	0.000000256811484	0.000032789063639	1.105476723524290
186.200245	196.599000	206.997755	0.000060777169835	0.000000227056742	0.000023783634733	1.613671125994389
206.915637	219.303667	231.691697	0.000065390473861	0.000000255805929	0.000022611026002	2.234683208533147
231.556517	246.569667	261.582817	0.000046574970208	0.000000249230245	0.000018130822079	3.130461909271538
261.386767	279.902667	298.418567	0.000032167200141	0.000000209480112	0.000012570084382	4.383238896136052
298.129317	321.517667	344.906017	0.000032180828089	0.000000259377150	0.000011922389165	6.224678699868773
344.415300	374.874000	405.332700	0.000036809495228	0.000000279274413	0.000010426428697	9.061170960267774
404.451650	445.759000	487.066350	0.000033686630693	0.000000343502233	0.000009626666144	13.740015908116701
485.310667	544.660667	604.010667	0.000014278053959	0.000000263197530	0.000005082509236	22.325059610446733
597.169700	693.094000	789.018300	0.000005479574163	0.000000197476622	0.000002382830938	29.337249689820958

Table A.IX.2. Deuteron Yields from Iron 800 MeV/n on 60 g/cm^2 Aluminium at10.0 deg

KE_left(MeV)	KE_mid(MeV)	KE_right(MeV)	Norm_Cts(#/SP*ster*MeV)	Y_stat(#/SP*ster*MeV)	Y_syst_tot(#/SP*ster*MeV)	X_tot(MeV)
43.683256	45.060600	46.437944	0.001780252401733	0.000000532571477	0.000462053852662	22.045173283770509
46.437923	47.815267	49.192610	0.001842269945200	0.000000556593130	0.000481396243583	0.574426164437171
49.192623	50.569967	51.947310	0.002228335079467	0.000000606745521	0.000538207688813	0.418642362502889
51.850085	53.446900	55.043715	0.002202883156746	0.000000660263559	0.000519398482440	0.248187658618877
55.140912	56.901567	58.662222	0.002508151094533	0.000000714230923	0.000526551489530	0.720242010184771
58.662212	60.422867	62.183522	0.003084875747793	0.000000819104895	0.000611370572557	0.492925066307243
62.109435	64.156600	66.203765	0.002560201129122	0.000000783555523	0.000501257255390	0.307745439317693
66.277863	68.420133	70.562403	0.002784481110473	0.000000799030337	0.000507648389238	0.608944724805134
70.474057	72.860767	75.247477	0.002349789082725	0.000000808773935	0.000447690566879	0.309365148736893
75.335857	77.860267	80.384677	0.003046820601000	0.000000966590976	0.000535276938093	0.463992407901250
80.373340	83.270600	86.167860	0.002863487036573	0.000000948359347	0.000462503952174	0.333863090802203
86.084563	89.225733	92.366903	0.003309090024992	0.000001020143723	0.000494413162611	0.326508477637258
92.359997	95.830067	99.300137	0.003296797969358	0.000001127669199	0.000492605067830	0.255924420415481
99.298490	103.164000	107.029510	0.003262223327020	0.000001241785904	0.000505790158408	0.194118456299884
107.032658	111.348333	115.664008	0.003583964898442	0.000001367148517	0.000536446230018	0.114417094568644
115.643688	120.506333	125.368978	0.004004864202411	0.000001391506529	0.000488382689589	0.077379361189532
125.373443	130.882333	136.391223	0.005360470101943	0.000001750536768	0.000623702293231	0.195463236985091
136.371482	142.661667	148.951852	0.004344983468305	0.000001689340392	0.000529149215731	0.370035715836999
148.900158	156.134333	163.368508	0.002689815591441	0.000001403111454	0.000340265029690	0.638734055375944
163.353028	171.729333	180.105638	0.003085022866824	0.000001634669444	0.000372022396936	0.930605030482857
180.037972	189.888667	199.739362	0.003669344389789	0.000001934858647	0.000420659415400	1.392354179923341
199.631687	211.304667	222.977647	0.004465412272974	0.000002366359685	0.000492529639129	1.967101558486496
222.868723	236.926333	250.983943	0.007487162715882	0.000003400188175	0.000798949964226	2.745086125807349
250.829400	268.055000	285.280600	0.003020572922853	0.000002386515442	0.000360562011263	3.819929747560811
285.028867	306.614667	328.200467	0.001348936120419	0.000001723546669	0.000160013147013	5.402817061848384
327.784283	355.596333	383.408383	0.000990513477412	0.000001691802725	0.000118568971481	7.785235153840891
382.683700	419.832000	456.980300	0.000800091856011	0.000001767342251	0.000094622108830	11.618387590836345
455.605767	507.848667	560.091567	0.000381619653936	0.000001426002741	0.000050460598653	18.367911400276295
557.022550	636.330000	715.637450	0.000110908442494	0.000000944355127	0.000018071530105	32.085106377414427
718.098600	757.041000	795.983400	0.000035252652000	0.000000367792000	0.000003873490000	3.874480000000000

Table A.IX.3. Deuteron Yields from Iron 800 MeV/n on 60 g/cm^2 Aluminium at7.20 deg

KE_left(MeV)	KE_mid(MeV)	KE_right(MeV)	Norm_Cts(#/SP*ster*MeV)	Y_stat(#/SP*ster*MeV)	Y_syst_tot(#/SP*ster*MeV)	X_tot(MeV)
46.381999	47.791633	49.201267	0.001927152251286	0.000000599323200	0.000529571124128	0.532776986712076
49.201233	50.610867	52.020501	0.002092028553143	0.000000719472072	0.000650257048858	0.483484729815741
51.939601	53.464467	54.989333	0.002261058012505	0.000000778822201	0.000689576839800	0.245518916853671
55.070240	56.862200	58.654160	0.002421781156857	0.000000841858295	0.000627828804205	0.653220654948234
58.654173	60.446133	62.238093	0.002698254755680	0.000000799347279	0.000590082062995	0.527203460229540
62.139727	64.144467	66.149207	0.003235380309275	0.000000894413047	0.000604458108069	0.274246695239596
66.247597	68.420467	70.593337	0.003144124960900	0.000000893410686	0.000565309281751	0.608212168116522
70.488070	72.849500	75.210930	0.003511793726872	0.000000945556473	0.000593467879456	0.304727900573430
75.316200	77.870700	80.425200	0.003902448695970	0.000001088312383	0.000636494299282	0.480253666728324
80.369640	83.252400	86.135160	0.003827327359075	0.000001100581099	0.000576860859567	0.306644115066636
86.084005	89.218300	92.352595	0.004083783013589	0.000001177452638	0.000592462661116	0.320353896548801
92.368045	95.836700	99.305355	0.004052221005918	0.000001228524405	0.000571349220959	0.263142612843302
99.301800	103.170000	107.038200	0.005002008546487	0.000001527922047	0.000699986827406	0.198443452380873
107.025107	111.346667	115.668227	0.005504978210286	0.000001621670646	0.000695274444517	0.121981216540581
115.666927	120.519667	125.372407	0.006185579536677	0.000001758691734	0.000719551603412	0.052004689449510
125.371063	130.892333	136.413603	0.007566695192276	0.000002077573924	0.000843507517044	0.176082119580297
136.378292	142.668667	148.959042	0.005222678319692	0.000001818301092	0.000616734519816	0.357205067067924
148.919855	156.148000	163.376145	0.004505667884686	0.000001854020886	0.000530796969236	0.613895096724188
163.360917	171.744667	180.128417	0.005451537426997	0.000002196160106	0.000610336777701	0.904967108363061
180.058588	189.909333	199.760078	0.006587519927820	0.000002611537325	0.000717160478222	1.355654923859682
199.653498	211.331333	223.009168	0.010980000079885	0.000003767839784	0.001146130932432	1.920486410808470
222.899087	236.962667	251.026247	0.004910695757021	0.000002738465587	0.000582633050918	2.681742526157200
250.869817	268.104667	285.339517	0.001406938468490	0.000001590026756	0.000175222878926	3.733320339831555
285.085300	306.683000	328.280700	0.000716097252055	0.000001256563344	0.000095155066688	5.283656699020102
327.866450	355.696000	383.525550	0.000529861540567	0.000001235687448	0.000070707512783	7.611852144051407
382.799783	419.978333	457.156883	0.000476580520338	0.000001335926232	0.000062348466260	11.363500875073669
455.779383	508.075333	560.371283	0.000165299012188	0.000000903119888	0.000025916129392	17.971700838217846
557.294917	636.707667	716.120417	0.000034930008145	0.000000503994005	0.000008184959415	31.423620738068998
718.898800	757.593000	796.287200	0.000004150005000	0.000000098470600	0.000000921172000	4.426300000000000

Table A.IX.4. Deuteron Yields from Iron 800 MeV/n on 60 g/cm^2 Aluminium at32.7 deg

KE_left(MeV)	KE_mid(MeV)	KE_right(MeV)	Norm_Cts(#/SP*ster*MeV)	Y_stat(#/SP*ster*MeV)	Y_syst_tot(#/SP*ster*MeV)	X_tot(MeV)
46.259290	47.576933	48.894577	0.002896938570800	0.000000691482817	0.000632787211845	0.853457188650374
48.893751	50.212233	51.530716	0.003446954307812	0.000000741281589	0.000696710883327	0.369895812036041
51.531600	53.255700	54.979800	0.002475027414933	0.000000714231000	0.000509346419363	0.153112121105679
54.979800	56.703900	58.428000	0.002686795991600	0.000000715484615	0.000522671656450	0.413867486079784
58.428000	60.152100	61.876200	0.003716917501593	0.000000835528369	0.000636297556821	0.479389379099079
61.850597	63.951667	66.052737	0.003039575487809	0.000000861281320	0.000529898843027	0.275655842535235
66.078327	68.204967	70.331607	0.003605124563773	0.000000945239926	0.000591261569907	0.345386247127763
70.246598	72.653633	75.060668	0.003675190429089	0.000001025781070	0.000587709117863	0.342152356228917
75.145677	77.673867	80.202057	0.004046537181280	0.000001110785708	0.000615346899986	0.304068692280215
80.184495	83.097600	86.010705	0.003880158534650	0.000001116531412	0.000542324345923	0.348411510230360
85.921492	89.071667	92.221842	0.004065083693511	0.000001189443083	0.000553690734827	0.227526513271509
92.234383	95.716533	99.198683	0.003276644067633	0.000001125088567	0.000457070896529	0.224279819313598
99.199160	103.086000	106.972840	0.004357275860372	0.000001324141277	0.000519265279505	0.176103185852187
106.955407	111.305667	115.655927	0.004451884318357	0.000001409772041	0.000514531302144	0.092246617522866
115.676815	120.540000	125.403185	0.004344069462761	0.000001481555273	0.000491874588803	0.044503228852972
125.390563	130.971333	136.552103	0.004614263226985	0.000001624034315	0.000496193202866	0.111875604303530
136.486182	142.820667	149.155152	0.005186084818299	0.000001070517497	0.000274042831896	0.292098521001049
149.138745	156.410000	163.681255	0.005534289443681	0.000001147217886	0.000243246534320	0.478324336626310
163.644355	172.117000	180.589645	0.005270879665484	0.000002175407425	0.000533073978274	0.731833009500118
180.532802	190.447667	200.362532	0.004278315167629	0.000002137772125	0.000435738825650	1.078123529035054
200.282823	212.083333	223.883843	0.001502037262819	0.000001339481348	0.000181187453133	1.546458716512342
223.760948	237.984333	252.207718	0.000642690725732	0.000000968873137	0.000098680203031	2.168042794365462
252.026633	269.486333	286.946033	0.000100784996580	0.000000389500610	0.000025470364054	3.029551361736586
286.681683	308.583333	330.484983	0.000042903303688	0.000000264436069	0.000013586001421	4.250957922186481
330.062167	358.332667	386.603167	0.000016115000007	0.000000194449647	0.000007589538901	6.078924317714442
385.855667	423.737667	461.619667	0.000005512438522	0.000000132590741	0.000003743183626	9.000720999319999
462.203300	495.564500	528.925700	0.000004021291958	0.000000112265416	0.000002460274977	10.475634773936136
615.931900	642.831000	669.730100	0.000000967170240	0.000000053917200	0.000000702503000	13.543600000000000

Table A.IX.5. Deuteron Yields from Iron 800 MeV/n on 60 g/cm^2 Aluminium at30.0 deg

KE_left(MeV)	KE_mid(MeV)	KE_right(MeV)	Norm_Cts(#/SP*ster*MeV)	Y_stat(#/SP*ster*MeV)	Y_syst_tot(#/SP*ster*MeV)	X_tot(MeV)
45.174650	46.632533	48.090416	0.002478379414267	0.000000628264972	0.000525117632966	0.761297464872306
48.090417	49.548300	51.006183	0.002958956114267	0.000000708631906	0.000601867309769	0.917353771730405
51.006217	52.464100	53.921983	0.002920802583733	0.000000723133215	0.000607713092967	0.557358733874333
53.811692	55.472833	57.133974	0.003353064227158	0.000000831051767	0.000649877972603	0.217735564344023
57.244227	59.102667	60.961107	0.003296127349630	0.000000835528369	0.000584864548467	0.688404256915223
60.961093	62.819533	64.677973	0.003817799026213	0.000000890434465	0.000632913223791	0.684899004236391
64.606613	66.781633	68.956653	0.003870359861521	0.000000985003458	0.000615108700125	0.363159673390370
69.028020	71.284500	73.540980	0.004095023837410	0.000001058747579	0.000642625832318	0.649821057388878
73.464900	76.023700	78.582500	0.004397257978280	0.000001129980228	0.000640618304519	0.421373095669384
78.600010	81.313100	84.026190	0.004532639363652	0.000001196752363	0.000634588518372	0.477209149200851
84.084780	87.138900	90.193020	0.004709345044477	0.000001266516961	0.000620103397794	0.434112401134775
90.124298	93.508733	96.893168	0.004480664316123	0.000001261491058	0.000575213099020	0.384154994347334
96.876290	100.617700	104.359110	0.004789427093907	0.000001369273107	0.000578260635476	0.315756896691110
104.363178	108.528333	112.693488	0.005189872127773	0.000001488142030	0.000583850939944	0.229015241145650
112.669650	117.375000	122.080350	0.005166667826711	0.000001590488467	0.000568685652824	0.112886664960437
122.070688	127.381333	132.691978	0.004661570650734	0.000001565927133	0.000504592011637	0.047497944623531
132.656683	138.706333	144.755983	0.003455168849301	0.000001462771621	0.000394469616353	0.199453441703973
144.727538	151.649333	158.571128	0.002231619012003	0.000001264397360	0.000275542054057	0.432929866954222
158.519410	166.546000	174.572590	0.001275801635895	0.000001032526153	0.000175546943060	0.775605795009939
174.507640	183.878000	193.248360	0.000563493316457	0.000000722249130	0.000095315839196	1.176269311025753
193.198333	204.277333	215.356333	0.000108705110395	0.000000312038930	0.000033281829247	1.677215734023504
215.261592	228.535667	241.809742	0.000027656380515	0.000000182414127	0.000014532696811	2.409557025450944
241.663850	257.857000	274.050150	0.000016398461733	0.000000139093367	0.000009157846899	3.406373806410565
280.681150	294.133000	307.584850	0.000005743144634	0.000000076250435	0.000004019973003	3.942497734393769
322.555400	339.719500	356.883600	0.000006260467736	0.000000112469953	0.000004442999072	5.611585985984711
364.578350	398.523000	432.467650	0.000003173766453	0.000000112265428	0.000003410211494	10.015606073987735
461.527800	477.060000	492.592200	0.000001688167800	0.000000054341800	0.000001226190000	8.687049999999999
527.419550	547.344000	567.268450	0.000001316016300	0.000000054341800	0.000000955887000	11.935000000000000

Table A.IX.6. Deuteron Yields from Iron 800 MeV/n on 60 g/cm^2 Aluminium at27.2 deg

KE_left(MeV)	KE_mid(MeV)	KE_right(MeV)	Norm_Cts(#/SP*ster*MeV)	Y_stat(#/SP*ster*MeV)	Y_syst_tot(#/SP*ster*MeV)	X_tot(MeV)
46.054188	47.364333	48.674478	0.003899128139811	0.000000795701630	0.000786079387253	0.488392029141549
48.760693	50.347033	51.933373	0.003382689572533	0.000000787620084	0.000635634077886	0.523489178448800
51.933360	53.519700	55.106040	0.003563634570800	0.000000819105336	0.000664671143166	0.539610567222326
55.106027	56.692367	58.278707	0.004395152637467	0.000000904095663	0.000762882209114	0.404051923241308
58.231577	60.167567	62.103557	0.003830356385645	0.000000914592718	0.000632933457695	0.543120187470508
62.150662	64.133767	66.116872	0.004164145796433	0.000000988891002	0.000671728980861	0.582322811015505
66.015460	68.171000	70.326540	0.004644956266400	0.000001050478947	0.000675695303152	0.298743619982770
70.427973	72.806433	75.184893	0.004683815711410	0.000001138014386	0.000682896424584	0.607325054448604
75.082917	77.683667	80.284417	0.004587966559534	0.000001152537215	0.000657845700646	0.318482738599755
80.364660	83.160900	85.957140	0.004854591628274	0.000001239405187	0.000658874042947	0.462587913703979
85.978860	89.151600	92.324340	0.004941150161634	0.000001338794990	0.000642872013668	0.345181171957568
92.253447	95.748667	99.243887	0.005058067126337	0.000001367589949	0.000608567968285	0.259485156463718
99.234603	103.108333	106.982063	0.005615572782573	0.000001485505832	0.000635795218312	0.203140146037163
106.989268	111.306333	115.623398	0.005741123763904	0.000001566128978	0.000620652317142	0.110076741868980
115.609758	120.533333	125.456908	0.005919489471891	0.000001674794496	0.000592514855080	0.071083768474174
125.422997	130.939667	136.456337	0.006072174615050	0.000001934809195	0.000663040259089	0.169879398825785
136.447095	142.763000	149.078905	0.006136564225484	0.000001510226112	0.000427355798493	0.392294673309491
149.025630	156.311000	163.596370	0.006227376946253	0.000001107010738	0.000234179989304	0.656752814414982
163.552447	171.978667	180.404887	0.006378578821586	0.000002394630845	0.000629425688596	0.971075326688924
180.341038	190.244333	200.147628	0.006338041853200	0.000002632081431	0.000615976536444	1.433774655723137
200.058893	211.809333	223.559773	0.003329559906355	0.000002042006716	0.000358518728968	2.022474813909929
223.444875	237.607000	251.769125	0.001139739089057	0.000001286266284	0.000147196884743	2.824240153333282
251.616333	268.982333	286.348333	0.000154807750691	0.000000503993844	0.000034571690562	3.906967944915853
286.092733	307.886333	329.679933	0.000039898240229	0.000000253204124	0.000012621832123	5.461988187702350
329.247483	357.356333	385.465183	0.000020792320022	0.000000215712663	0.000008325611241	7.777364193234106
384.730583	422.350333	459.970083	0.000008499180521	0.000000158911987	0.000004560508766	11.414255793581113
458.550467	511.593667	564.636867	0.000002950535004	0.000000108259860	0.000002189647079	17.692306640483597
565.346050	614.875000	664.403950	0.000003159883804	0.000000120752651	0.000001810519699	21.893275444757005

Table A.IX.7. Proton Yields from Iron 800 MeV/n on 60 g/cm^2 Aluminium at12.7 deg

KE_left(MeV)	KE_mid(MeV)	KE_right(MeV)	Norm_Cts(#/SP*ster*MeV)	Y_stat(#/SP*ster*MeV)	Y_syst_tot(#/SP*ster*MeV)	X_tot(MeV)
44.679506	46.130933	47.582360	0.004571188008883	0.000000911422465	0.000891068536953	0.312167288470397
47.559808	49.445033	51.330258	0.003445608848443	0.000000901155384	0.000674911338976	0.350840759608938
51.352843	53.260633	55.168423	0.004408956880200	0.000001040747690	0.000816519660204	0.929674397843137
55.168410	57.076200	58.983990	0.004405152435917	0.000001040460107	0.000814810009772	1.014553402364804
58.856687	61.002067	63.147447	0.005026504025462	0.000001189443170	0.000871018172083	0.396383197272538
63.274770	65.647200	68.019630	0.004977699242557	0.000001220692029	0.000834364723183	0.741181794547060
67.966492	70.392067	72.817642	0.005717398494163	0.000001379077760	0.000942382394826	0.772118513890841
72.870773	75.708533	78.546293	0.005753333915483	0.000001444866895	0.000908928910469	0.664287499211749
78.447587	81.426167	84.404747	0.006893241842572	0.000001621996710	0.001040863677382	0.706847169132055
84.503445	87.807300	91.111155	0.007411414837400	0.000001780055107	0.001082031098182	0.694722503244281
91.045938	94.752333	98.458728	0.007776196819243	0.000001948143712	0.001114492996103	0.693106104896646
98.420440	102.508400	106.596360	0.007731762403723	0.000002050443222	0.001080617274595	0.669841826231387
106.594968	111.153333	115.711698	0.008178716138088	0.000002205068193	0.001110650040567	0.637539829395780
115.710738	120.830333	125.949928	0.006110514817308	0.000001984435369	0.000833724882135	0.561362413429150
125.941238	131.796333	137.651428	0.003769005656184	0.000001635169251	0.000532456385889	0.509137440550192
137.581287	144.231667	150.882047	0.002508440993919	0.000001423584194	0.000364158621952	0.394012133800471
150.862787	158.517667	166.172547	0.002236542290856	0.000001401859402	0.000317771851524	0.274501475659057
166.105437	175.007667	183.909897	0.000794623582261	0.000000876407265	0.000135514125369	0.055908575918637
183.848428	194.318333	204.788238	0.000292807893354	0.000000572127392	0.000067490578095	0.265161342603404
204.712212	217.181667	229.651122	0.000109423803382	0.000000354493939	0.000032249658756	0.605628308596948
229.522157	244.609667	259.697177	0.000073393530159	0.000000326631636	0.000023939008897	1.156836232785782
259.513250	278.116000	296.718750	0.000057196032351	0.000000314109777	0.000018691177790	1.934470033311708
296.416400	319.914000	343.411600	0.000047689461250	0.000000313377876	0.000014750824641	3.124466669705408
342.923900	373.499000	404.074100	0.000038972833126	0.000000336452847	0.000012070243093	4.914512911225282
403.188750	444.648000	486.107250	0.000031868001992	0.000000338729508	0.000009672092324	7.903782246222374
484.346517	543.911667	603.476817	0.000012616038119	0.000000248194133	0.000004588853813	13.278650458333482
604.189600	661.107000	718.024400	0.000006508935246	0.000000156255334	0.000001994182541	17.552875081023050

Table A.IX.8. Proton Yields from Iron 800 MeV/n on 60 g/cm^2 Aluminium at10.0 deg

KE_left(MeV)	KE_mid(MeV)	KE_right(MeV)	Norm_Cts(#/SP*ster*MeV)	Y_stat(#/SP*ster*MeV)	Y_syst_tot(#/SP*ster*MeV)	X_tot(MeV)
43.780758	45.308133	46.835508	0.004978141498117	0.000000975218239	0.000936967657489	0.734682681589814
46.835492	48.362867	49.890242	0.005199378127917	0.000001023909548	0.000979908623459	0.336280805241691
49.856033	51.807633	53.759233	0.004557902196946	0.000001096515547	0.000839338376566	0.471119509790679
53.793443	55.779233	57.765023	0.005749523088833	0.000001216918672	0.000991211991998	1.076792693770718
57.765010	59.750800	61.736590	0.006044486573697	0.000001250801859	0.001027181823487	0.720539158290512
61.642068	63.962633	66.283198	0.006341642813736	0.000001409462148	0.001035725531818	0.422332472759318
66.377685	68.827200	71.276715	0.006301059746500	0.000001450427681	0.001016771748473	0.903869487511333
71.155615	73.813700	76.471785	0.006964173253773	0.000001588963215	0.001093235186200	0.568147266614916
76.592927	79.506767	82.420607	0.007090186807560	0.000001662467708	0.001078826868543	0.748510812450963
82.324335	85.569800	88.815265	0.007417586887912	0.000001799031926	0.001092738355549	0.654269267888994
88.809573	92.338833	95.868093	0.007640795659206	0.000001916628275	0.001111107534507	0.673392881942629
95.891473	99.817133	103.742793	0.008821099783958	0.000002132724136	0.001228870159738	0.613302288003233
103.738590	108.145000	112.551410	0.009552982005327	0.000002330323043	0.001280205262964	0.620177659037312
112.526125	117.480000	122.433875	0.009384008607595	0.000002423711394	0.001238242795184	0.603918065050219
122.424540	127.981000	133.537460	0.010443946989577	0.000002696606790	0.001322706413294	0.538117869425463
133.514628	139.893333	146.272038	0.012052083405025	0.000003093625288	0.001478463098364	0.423764513856458
146.216067	153.510667	160.805267	0.015233052722842	0.000003724662360	0.001824589894817	0.288037281882051
160.759040	169.214000	177.668960	0.014100695908563	0.000003770481533	0.001609099494029	0.092460634662866
177.629097	187.536667	197.444237	0.016232733538996	0.000004351227730	0.001785756159669	0.153258375773855
197.361308	209.096333	220.831358	0.016437204210809	0.000004827172333	0.001825118511056	0.498202562384017
220.721983	234.865333	249.008683	0.014315421408212	0.000004961586461	0.001601794520253	0.964514302270319
248.840367	266.153667	283.466967	0.011582091777746	0.000004908282699	0.001298391897375	1.643070508077483
283.198950	304.874000	326.549050	0.007396194584979	0.000004356566428	0.000882797714947	2.682712609449622
326.135650	354.038000	381.940350	0.001443533843280	0.000002144830449	0.000190608242301	4.214076301456821
381.224600	418.491000	455.757400	0.000540688517979	0.000001508514307	0.000073481558906	6.688791129307298
454.379867	506.770667	559.161467	0.000275578539038	0.000001274067129	0.000039705986870	10.987286243390585
556.079617	635.609667	715.139717	0.000095033422221	0.000000896672439	0.000016809781288	19.530234101835543

Table A.IX.9. Proton Yields from Iron 800 MeV/n on 60 g/cm^2 Aluminium at7.20 deg

KE_left(MeV)	KE_mid(MeV)	KE_right(MeV)	Norm_Cts(#/SP*ster*MeV)	Y_stat(#/SP*ster*MeV)	Y_syst_tot(#/SP*ster*MeV)	X_tot(MeV)
45.859908	47.447133	49.034358	0.005997994099800	0.000001122808923	0.001082389504969	0.634119554179651
48.992350	50.621600	52.250850	0.005674481305912	0.000001080270070	0.001024137225897	0.373134790879918
52.292892	54.339267	56.385642	0.006041272704750	0.000001293618492	0.001034496432611	0.798368448435307
56.385658	58.432033	60.478408	0.006201959040750	0.000001323937890	0.001061329993339	0.889498917785739
60.454232	62.524767	64.595302	0.007096868978233	0.000001395391307	0.001151179948344	0.514727988636717
64.619450	67.128800	69.638150	0.006462387229173	0.000001473296307	0.001031289332404	0.694497623037689
69.638150	72.147500	74.656850	0.008179298354913	0.000001642823806	0.001251608248163	0.811517960414309
74.595897	77.507867	80.419837	0.008196832895397	0.000001780055354	0.001226976171315	0.577268712380985
80.400212	83.460067	86.519922	0.009020236443637	0.000001902836449	0.001298023565406	0.713856555676979
86.600523	90.038133	93.475743	0.009516187545200	0.000002105859196	0.001349670693916	0.673356712776371
93.397857	97.224067	101.050277	0.009280091017575	0.000002170272262	0.001299136082655	0.626801449450302
101.029960	105.266000	109.502040	0.010289479732994	0.000002388539446	0.001378254069603	0.629656871050416
109.508067	114.235667	118.963267	0.011337157066547	0.000002643146754	0.001491984820520	0.586040124843001
118.932572	124.306667	129.680762	0.012744326026267	0.000002960156540	0.001597606358053	0.506524482096374
129.674363	135.740333	141.806303	0.015506032099484	0.000003463623542	0.001907129930865	0.456508886141332
141.787325	148.757000	155.726675	0.019065973725984	0.000004076172772	0.002257944617102	0.318905099120412
155.658602	163.709667	171.760732	0.017229718526750	0.000004078785391	0.001974339704053	0.167118607528246
171.732330	181.110000	190.487670	0.021810728371223	0.000004919703005	0.002394176677253	0.082859489454860
190.396152	201.489667	212.583182	0.024391921120886	0.000005664136200	0.002691108557955	0.388298691103897
212.487200	225.740000	238.992800	0.018524827826489	0.000005467278169	0.002075557903143	0.788221492265975
238.850467	255.009667	271.168867	0.010296230348156	0.000004484712579	0.001173696215613	1.389641969268703
270.933867	290.991667	311.049467	0.005766595845742	0.000003694589321	0.000681401401187	2.268918008236525
310.694317	336.255667	361.817017	0.001396355623730	0.000002012898299	0.000193884967120	3.605641891536096
361.236067	394.921667	428.607267	0.000400278231984	0.000001216941544	0.000058423392859	5.662385298308478
427.510233	473.972333	520.434433	0.000207958783173	0.000001018951535	0.000032640033269	9.155093939272279
518.121217	586.608667	655.096117	0.000097310126438	0.000000849493770	0.000017708592621	15.734636031840711
658.947800	689.736000	720.524200	0.000048197376000	0.000000387735000	0.000005319340000	13.350199999999999

Table A.IX.10. Proton Yields from Iron 800 MeV/n on 60 g/cm^2 Aluminium at32.7 deg

KE_left(MeV)	KE_mid(MeV)	KE_right(MeV)	Norm_Cts(#/SP*ster*MeV)	Y_stat(#/SP*ster*MeV)	Y_syst_tot(#/SP*ster*MeV)	X_tot(MeV)
45.074100	46.884000	48.693900	0.002353200478817	0.000000741281589	0.000506869640564	0.367873013919027
48.693900	50.503800	52.313700	0.002219727601283	0.000000714231000	0.000485200502331	1.007928101892690
52.313700	54.123600	55.933500	0.002409566232617	0.000000715484615	0.000497889759056	0.755077916839050
55.819042	57.808967	59.798892	0.002909777328839	0.000000835528369	0.000560871610062	0.159140314261283
59.913317	62.213267	64.513217	0.002524698779477	0.000000861281320	0.000484169508869	0.475598060234690
64.513150	66.813100	69.113050	0.003032130364510	0.000000955332781	0.000550392582350	0.755662106887066
69.012972	71.665767	74.318562	0.003039645188439	0.000001025781070	0.000534010723137	0.331940093904006
74.418680	77.208500	79.998320	0.003356089652270	0.000001110785708	0.000559250000101	0.573023854072411
79.906582	83.073867	86.241152	0.003120304578058	0.000001138447693	0.000505668564051	0.467815597714527
86.237990	89.638400	93.038810	0.003284990961178	0.000001189443083	0.000512429443739	0.484969793725341
93.130390	96.903000	100.675610	0.002627568959191	0.000001125088567	0.000423035576156	0.495991780829078
100.678875	104.940000	109.201125	0.003282867633600	0.000001324141277	0.000474363190572	0.493803519601673
109.146358	113.924333	118.702308	0.003356329815126	0.000001409772041	0.000468616741217	0.459349338548560
118.650682	124.055667	129.460652	0.003327967461530	0.000001481555273	0.000444835964979	0.422067024506772
129.442078	135.514333	141.586588	0.003496207671983	0.000001624034315	0.000454962961599	0.364753144898026
141.575117	148.582667	155.590217	0.004069769016566	0.000001052167611	0.000240944425191	0.252942918730689
155.515247	163.612667	171.710087	0.004529891526807	0.000001076051064	0.000204814924942	0.136895504691060
171.683017	181.110667	190.538317	0.004450006825816	0.000002175407425	0.000480287201884	0.079327750169849
190.451513	201.626333	212.801153	0.003527074228591	0.000002137772125	0.000386521176937	0.302164778907139
212.671163	226.031333	239.391503	0.000920849901431	0.000001142456984	0.000138514970384	0.644343735530966
239.258967	255.540667	271.822367	0.000124702771906	0.000000442964248	0.000031980576117	1.122590908242624
271.595450	291.846000	312.096550	0.000058397611411	0.000000336111333	0.000018288017145	1.846253219963340
311.739883	337.588333	363.436783	0.000039735695744	0.000000305635197	0.000013679048421	2.905470298006847
362.826617	396.941667	431.056717	0.000008509751121	0.000000132590741	0.000004202111115	4.586469237757951
429.924833	477.111333	524.297833	0.000004770797675	0.000000136049961	0.000003160029968	7.380691654641860
521.895450	591.715000	661.534550	0.000002081863943	0.000000120943241	0.000001918107054	12.540240018556263
665.506650	697.004000	728.501350	0.000000766120960	0.000000053917200	0.000000599945000	70.676000000000002

Table A.IX.11. Proton Yields from Iron 800 MeV/n on 60 g/cm^2 Aluminium at30.0 deg

KE_left(MeV)	KE_mid(MeV)	KE_right(MeV)	Norm_Cts(#/SP*ster*MeV)	Y_stat(#/SP*ster*MeV)	Y_syst_tot(#/SP*ster*MeV)	X_tot(MeV)
43.534138	45.126433	46.718728	0.002575504166317	0.000000708631906	0.000552474856266	0.856578686773726
46.718738	48.311033	49.903328	0.002505263175300	0.000000723133215	0.000555639648194	0.951451569439559
49.804460	51.532500	53.260540	0.003046040028873	0.000000831051767	0.000616941351081	0.739586534304810
53.359380	55.434300	57.509220	0.002749145140733	0.000000835528369	0.000525775880084	0.709732186933917
57.509247	59.584167	61.659087	0.003062317409577	0.000000890434465	0.000567544217210	0.782460011929683
61.577292	63.735767	65.894242	0.003555483054840	0.000000985003458	0.000625010136454	0.599843903309019
65.976015	68.536200	71.096385	0.003297470393040	0.000001058747579	0.000567498181866	0.907459807736409
71.096382	73.656567	76.216752	0.004011787579327	0.000001129980228	0.000643950990042	0.712957721862243
76.198430	79.225100	82.251770	0.003546532740385	0.000001196752363	0.000569038570715	0.829444865088693
82.172180	85.349100	88.526020	0.003933328417515	0.000001266516961	0.000598235406613	0.703871054110055
88.623908	92.153933	95.683958	0.003738125234400	0.000001261491058	0.000550792910596	0.836859449053424
95.643455	99.619500	103.595545	0.003752960019154	0.000001369273107	0.000541182289086	0.721697242872661
103.548122	107.952667	112.357212	0.004057254166195	0.000001488142030	0.000553168171155	0.683301459472318
112.358972	117.285667	122.212362	0.004093141198806	0.000001590488467	0.000542509774839	0.649945134129028
122.194172	127.832667	133.471162	0.003638033760950	0.000001534791840	0.000467352277181	0.618400417869361
133.424015	139.780000	146.135985	0.002706198070337	0.000001423898414	0.000360955703112	0.510924693779817
146.115053	153.441333	160.767613	0.001888564954685	0.000001264397360	0.000261758545589	0.373163671282455
160.717370	169.216000	177.714630	0.001072968477030	0.000000991678268	0.000159624810050	0.205257366617352
177.618932	187.562667	197.506402	0.000478282523405	0.000000722249130	0.000088792361835	0.151929307341309
197.452380	209.248000	221.043620	0.000096313491529	0.000000325713800	0.000032453849970	0.461012188255365
221.187630	230.345000	239.502370	0.000021218973896	0.000000146030014	0.000011459553361	0.694808741226677
255.079600	266.702500	278.325400	0.000006199672980	0.000000076551262	0.000004662265523	1.406847685630538
283.702900	305.514000	327.325100	0.000005509334679	0.000000120943241	0.000005881644440	2.796670029463612
326.903983	354.996333	383.088683	0.000002583575228	0.000000093878256	0.000003540449527	4.407000967381332
383.521700	407.229500	430.937300	0.000003066976127	0.000000093878287	0.000002837147423	5.229212903879512
490.040500	507.527000	525.013500	0.000002759923200	0.000000053917200	0.000001088240000	6.446390000000000
586.584000	640.574000	694.564000	0.000002374771101	0.000000112469991	0.000001503881790	74.439731207580948

Table A.IX.12. Proton Yields from Iron 800 MeV/n on 60 g/cm^2 Aluminium at27.2 deg

KE_left(MeV)	KE_mid(MeV)	KE_right(MeV)	Norm_Cts(#/SP*ster*MeV)	Y_stat(#/SP*ster*MeV)	Y_syst_tot(#/SP*ster*MeV)	X_tot(MeV)
45.092002	46.927867	48.763732	0.002751879040200	0.000000787620084	0.000549240583420	0.443347462950720
48.763735	50.599600	52.435465	0.002931388831967	0.000000819105336	0.000576378136047	1.175399142232544
52.435435	54.271300	56.107165	0.003563191603867	0.000000904095663	0.000658195749878	1.004202950016081
56.016472	57.963767	59.911062	0.003433921916188	0.000000914592718	0.000638753814551	0.400438677485629
60.001725	62.319300	64.636875	0.003239739793037	0.000000988891002	0.000574785788234	0.657751669561545
64.636858	66.954433	69.272008	0.003623649537215	0.000001050478947	0.000623209998604	0.996951440361064
69.163492	71.797967	74.432442	0.003656155495557	0.000001138014386	0.000616741055848	0.556388447388153
74.540958	77.340333	80.139708	0.003882752826293	0.000001152537215	0.000610021395385	0.801377626724131
80.045683	83.205333	86.364983	0.003707123412737	0.000001239405187	0.000584947774984	0.694618637360818
86.365683	89.765933	93.166183	0.003662544794195	0.000001338794990	0.000601835223112	0.705439891243046
93.249595	97.023400	100.797205	0.003777706984411	0.000001367589949	0.000564435855308	0.703683958144564
100.807052	105.055667	109.304282	0.004011644027388	0.000001507842568	0.000586652773829	0.693341359041850
109.247310	114.031000	118.814690	0.004132056923893	0.000001566128978	0.000560614457471	0.640789862779523
118.761422	124.154667	129.547912	0.004396064671702	0.000001674794496	0.000543301703914	0.591310167689513
129.522223	135.594333	141.666443	0.004520069887566	0.000001934809195	0.000601297959886	0.502729913808598
141.661275	148.640000	155.618725	0.004811808266035	0.000001417674712	0.000367507484938	0.354536332999877
155.557057	163.653667	171.750277	0.005077036147499	0.000001003994442	0.000194041745284	0.207461790203329
171.697257	181.109667	190.522077	0.005357956341462	0.000002394630845	0.000563998160539	0.093822234155023
190.436285	201.576000	212.715715	0.005185036402412	0.000002596813889	0.000542102897632	0.394980885847657
212.617528	225.937333	239.257138	0.002071434188715	0.000001768425906	0.000267665833442	0.810130083165043
239.116300	255.360000	271.603700	0.000181714872729	0.000000512456504	0.000040327056968	1.437282909975973
271.367100	291.549000	311.730900	0.000045839596497	0.000000270132220	0.000014924675592	2.365704330659264
311.376450	337.121000	362.865550	0.000020733994890	0.000000218129138	0.000009116694482	3.720641858940470
362.270900	396.230000	430.189100	0.000012909425161	0.000000211251522	0.000006823884375	5.828599712400913
429.069817	475.994667	522.919517	0.000005158626906	0.000000132590741	0.000003043226881	9.329526791831405
520.548667	589.883667	659.218667	0.000004581670492	0.000000155665613	0.000002590335912	15.744221870279903
663.146450	694.385000	725.623550	0.000000772467200	0.000000053917200	0.000000604915000	73.294799999999995

Table A.IX.13. Triton Yields from Iron 800 MeV/n on 60 g/cm^2 Aluminium at12.7 deg

KE_left(MeV)	KE_mid(MeV)	KE_right(MeV)	Norm_Cts(#/SP*ster*MeV)	Y_stat(#/SP*ster*MeV)	Y_syst_tot(#/SP*ster*MeV)	X_tot(MeV)
45.076950	46.330600	47.584251	0.000837936932352	0.000000305484206	0.000274587213833	32.263588751921581
47.584249	48.837900	50.091550	0.000762423497411	0.000000270132220	0.000242452836638	0.370068745640590
50.013640	51.387367	52.761094	0.000788546245087	0.000000314667458	0.000264856450118	0.281133978787695
52.839010	54.433600	56.028190	0.000939241428701	0.000000374742036	0.000269110192702	0.476388344614979
56.028177	57.622767	59.217357	0.000881529261201	0.000000383789285	0.000271717529541	0.385947542064981
59.127870	60.907900	62.687930	0.000761627618438	0.000000333017981	0.000210929967947	0.216666053511020
62.777385	64.712400	66.647415	0.000838503593605	0.000000388754948	0.000227296811159	0.454478671986926
66.562378	68.638633	70.714888	0.000658402703709	0.000000327558762	0.000181888609531	0.186630561012552
70.799965	73.077100	75.354235	0.000778467559426	0.000000408014709	0.000203969651019	0.354563567347239
75.282520	77.804800	80.327080	0.001125366580989	0.000000494326595	0.000231491624954	0.147704870961827
80.324780	83.052700	85.780620	0.001471047762395	0.000000512797322	0.000222068626204	0.185848665418937
85.816202	88.826167	91.836132	0.001681359570723	0.000000589815133	0.000246308311112	0.096260445956841
91.847050	95.200000	98.552950	0.001893183510724	0.000000641903645	0.000241051878559	0.046456349838531
98.519022	102.265867	106.012712	0.002047074394316	0.000001112970429	0.000461873282845	0.152643494993956
105.987837	110.172667	114.357497	0.002224154283434	0.000001389177845	0.000557902222567	0.221619085460278
114.357178	119.019333	123.681488	0.001785825739620	0.000000885575444	0.000270738547750	0.374176531328463
123.670222	128.999667	134.329112	0.000433629591081	0.000000452519067	0.000101453927533	0.581969854156553
134.276663	140.320333	146.364003	0.000031820383397	0.000000135880958	0.000023902397344	0.838395912116704
146.339143	153.269333	160.199523	0.000159234482437	0.000000307569822	0.000048545435797	1.171672325390081
160.185438	168.218333	176.251228	0.000033979405972	0.000000124725973	0.000016807577873	1.534787393441189
179.374150	185.648000	191.921850	0.000008523490618	0.000000076250435	0.000008565427141	1.695540699865385
194.904208	206.025333	217.146458	0.000009972993319	0.000000112265451	0.000010720903209	2.763093983363577
217.044425	230.387000	243.729575	0.000022250211703	0.000000165435065	0.000013463955147	3.688611686271679
243.576583	259.861333	276.146083	0.000018048568387	0.000000171039930	0.000011289155930	4.977661607833541
275.925433	296.200333	316.475233	0.000016010999074	0.000000135880922	0.000007161719409	6.819588182133875
316.121567	342.047667	367.973767	0.000047714408294	0.000000321649379	0.000013645460071	9.561248716088292
367.344683	401.638333	435.931983	0.000029090417082	0.000000282548909	0.000009578613575	13.964419197907946
434.783417	482.290667	529.797917	0.000012683851399	0.000000206962304	0.000004867264741	21.587299489746279
527.351750	597.851000	668.350250	0.000006256979020	0.000000176128299	0.000002826093360	36.666563791279920
675.956150	739.081000	802.205850	0.000002130422190	0.000000108259887	0.000001211787931	29.035103689327510

Table A.IX.14. Triton Yields from Iron 800 MeV/n on 60 g/cm^2 Aluminium at10.0 deg

KE_left(MeV)	KE_mid(MeV)	KE_right(MeV)	Norm_Cts(#/SP*ster*MeV)	Y_stat(#/SP*ster*MeV)	Y_syst_tot(#/SP*ster*MeV)	X_tot(MeV)
44.157519	45.439333	46.721148	0.000994309771433	0.000000369587396	0.000322815321968	39.057402857973031
46.721152	48.002967	49.284781	0.001342649884524	0.000000400975211	0.000363453504096	0.418116948392432
49.284752	50.566567	51.848381	0.001492188387980	0.000000425724455	0.000387911765965	0.370061833931844
51.783042	53.322100	54.861158	0.001585424970548	0.000000480730934	0.000376453022336	0.353123761038534
54.926500	56.548300	58.170100	0.001109489892840	0.000000431561403	0.000306523380867	0.422193350896245
58.162230	59.791900	61.421570	0.001277374057674	0.000000432233187	0.000315255115426	0.235928049893797
61.429487	63.391067	65.352647	0.000978590383970	0.000000374434935	0.000224505895150	0.394123356290895
65.352620	67.314200	69.275780	0.001124218121120	0.000000425701715	0.000255268142867	0.301137896771579
69.253865	71.535200	73.816535	0.001156711701864	0.000000492556181	0.000256918999122	0.292274905080748
73.769932	76.163767	78.557602	0.001310289714549	0.000000463516725	0.000229414253903	0.210609151006147
78.626100	81.274200	83.922300	0.001604892162258	0.000000586553960	0.000276122273214	0.219164214474649
83.878897	86.832567	89.786237	0.001860270592200	0.000000749421629	0.000325898040698	0.088640714207560
89.754622	92.998267	96.241912	0.002059456757573	0.000000766721816	0.000315423243433	0.046531382695231
96.238452	99.832167	103.425882	0.002224721795416	0.000001031103673	0.000443922106133	0.054186219326412
103.437198	107.431333	111.425468	0.002508790222390	0.000001569328135	0.000728148616277	0.205000507844469
111.411130	115.950000	120.488870	0.002948935508957	0.000001299400612	0.000471881157333	0.340984614780491
120.468350	125.537000	130.605650	0.002419052403730	0.000001082153998	0.000325746686224	0.491290875562533
130.599747	136.384667	142.169587	0.000414901746925	0.000000453473341	0.000093607214550	0.739757880102673
142.123283	148.759333	155.395383	0.001355431238592	0.000000943293471	0.000204246553103	1.045979773260458
155.366307	163.006667	170.647027	0.000492422448397	0.000000567454184	0.000097007963982	1.368968902280837
170.605352	179.511667	188.417982	0.000161086482584	0.000000349041514	0.000044015330491	1.847435127845089
188.338767	198.848667	209.358567	0.000241757909513	0.000000471572926	0.000052373243283	2.478019221717217
209.253508	221.801333	234.349158	0.000407661584769	0.000000681748038	0.000069553220782	3.284323552103234
234.214043	249.422333	264.630623	0.000558988014795	0.000000929207019	0.000083797908363	4.415092751879625
264.437950	283.255000	302.072050	0.000813138266052	0.000001235323904	0.000104647941504	6.008802529872321
301.763500	325.593000	349.422500	0.000951422915666	0.000001518875184	0.000113676379111	8.333382538213400
348.899800	380.028000	411.156200	0.000851855375621	0.000001632281634	0.000100224041961	11.993078153505879
410.235100	452.630000	495.024900	0.000505458199585	0.000001460146646	0.000062974315643	18.133369156681834
493.155700	554.467000	615.778300	0.000143343241810	0.000000923805494	0.000022669308975	29.688537308025126
618.620967	708.552667	798.484367	0.000017863506211	0.000000358378899	0.000004849121790	38.188822038654195

Table A.IX.15. Triton Yields from Iron 800 MeV/n on 60 g/cm^2 Aluminium at7.20 deg

KE_left(MeV)	KE_mid(MeV)	KE_right(MeV)	Norm_Cts(#/SP*ster*MeV)	Y_stat(#/SP*ster*MeV)	Y_syst_tot(#/SP*ster*MeV)	X_tot(MeV)
44.950644	46.254300	47.557956	0.001311159695950	0.000000480024123	0.000430798191604	32.131973040478485
47.557944	48.861600	50.165256	0.001319506697860	0.000000579619825	0.000536887100991	0.409022237749979
50.165244	51.468900	52.772556	0.001327853699770	0.000000618703985	0.000582896637042	0.418754668273680
52.735805	54.342000	55.948195	0.001336264344606	0.000000564763756	0.000422749603569	0.319823062614315
55.984965	57.627900	59.270835	0.001344547703590	0.000000503417814	0.000363192385804	0.388718748471179
59.208950	60.924300	62.639650	0.001459486670679	0.000000488646239	0.000340240289332	0.217700966238095
62.701495	64.683700	66.665905	0.001347617891620	0.000000454526975	0.000271919674636	0.402195522518588
66.611393	68.648133	70.684873	0.001578590247001	0.000000513423872	0.000300463214090	0.225145178047286
70.739385	73.062900	75.386415	0.002155948190375	0.000000548300958	0.000281156089925	0.333101487552968
75.291710	77.790600	80.289490	0.002722842920179	0.000000631530235	0.000319206326532	0.134529219129080
80.336223	83.052333	85.768443	0.003664829126688	0.000000719582400	0.000348568620312	0.206278701392573
85.816413	88.833333	91.850253	0.004285775777128	0.000000850355504	0.000381148245449	0.103458340534681
91.839875	95.200000	98.560125	0.004911043686158	0.000000939132413	0.000396773973340	0.003979667675196
98.530662	102.270767	106.010872	0.005382370884399	0.000001642774730	0.000841412475930	0.126515479083391
105.975220	110.172000	114.368780	0.005522115278475	0.000001614766343	0.000755116091669	0.219223888192528
114.348192	119.025667	123.703142	0.003778836331794	0.000001331860468	0.000467254970223	0.366496034503786
123.683052	129.006667	134.330282	0.001685604189007	0.000000887646288	0.000264928539536	0.570384634358255
134.290650	140.337000	146.383350	0.001676577218376	0.000000988299166	0.000237942877225	0.809697586774840
146.367207	153.290667	160.214127	0.000766613227040	0.000000702306814	0.000135237455629	1.133774988376882
160.196558	168.246333	176.296108	0.000426375096747	0.000000552229721	0.000084391501573	1.486617074263241
176.229865	185.634000	195.038135	0.000340793701965	0.000000518434845	0.000066365921294	1.998442110470053
194.951983	206.083333	217.214683	0.000473269661064	0.000000690337806	0.000079942599646	2.662770683442342
217.108515	230.464000	243.819485	0.000322911118500	0.000000610464431	0.000058219362504	3.554266673422241
243.663567	259.967667	276.271767	0.000363989242438	0.000000741622639	0.000059440688934	4.792998467201925
276.054900	296.356000	316.657100	0.000478791098684	0.000000948673860	0.000067619163198	6.548807971318139
316.300317	342.267667	368.235017	0.000554718038197	0.000001178100510	0.000072375901185	9.178020822622925
367.601917	401.960667	436.319417	0.000480739251923	0.000001302611344	0.000062032427703	13.402367941647476
435.163433	482.782333	530.401233	0.000217628233989	0.000000980322221	0.000033031917837	20.729011952575068
527.940950	598.649000	669.357050	0.000032877332407	0.000000457562915	0.000008428956950	35.269997294726295
677.746550	740.354500	802.962450	0.000002996449206	0.000000132243531	0.000001478131071	29.317243985238449

Table A.IX.16. Helium-4 Yields from Iron 800 MeV/n on 60 g/cm^2 Aluminium at12.7 deg

KE_left(MeV)	KE_mid(MeV)	KE_right(MeV)	Norm_Cts(#/SP*ster*MeV)	Y_stat(#/SP*ster*MeV)	Y_syst_tot(#/SP*ster*MeV)	X_tot(MeV)
49.752245	50.405000	51.057755	0.000123649248832	0.000000076551300	0.000042022400000	0.119524000000000
51.057768	53.016033	54.974298	0.000234244630528	0.000000194803835	0.000108930912095	0.620693598921400
54.974335	56.932600	58.890865	0.000396379900853	0.000000299753675	0.000169784657373	1.062514304778529
58.808553	60.858433	62.908313	0.000623040026964	0.000000362601856	0.000206522061818	0.602990825798370
62.990627	65.414567	67.838507	0.000485037660551	0.000000382120152	0.000182400812381	0.619327227822256
67.838493	70.262433	72.686373	0.000508708219935	0.000000374741593	0.000179306521920	0.824050736004768
72.631535	75.466900	78.302265	0.000532531372856	0.000000538002144	0.000228283478000	0.632189628628942
78.300260	81.247300	84.194340	0.000572127796315	0.000000574862858	0.000236515228438	0.679560701410109
84.251155	87.608500	90.965845	0.000604209645979	0.000000616998478	0.000225637760612	0.725414005387958
90.869188	94.561833	98.254478	0.000629177840442	0.000000512797322	0.000166847349453	0.689386930297493
98.228435	102.315200	106.401965	0.000589977576532	0.000000518124888	0.000149392524355	0.653751004733453
106.403128	110.970333	115.537538	0.000623502037045	0.000000529418560	0.000142510985779	0.624139372237484
115.560618	120.676333	125.792048	0.000680752165901	0.000000589464878	0.000141689493705	0.585268133427748
125.771770	131.642000	137.512230	0.000693994585098	0.000000653218781	0.000138928527206	0.509452072506335
137.444312	144.106667	150.769022	0.000832694830443	0.000000751578458	0.000146734423384	0.392110896142915
150.749975	158.432000	166.114025	0.000586617314245	0.000000648752912	0.000106571380604	0.273128161556512
166.051657	174.981667	183.911677	0.000832325334248	0.000000819178130	0.000124681417704	0.073332601308422
183.853690	194.373000	204.892310	0.000643543031391	0.000000760564762	0.000103442979145	0.256213513320453
205.149555	209.071000	212.992445	0.000085083909220	0.000000165157000	0.000015440800000	0.269421000000000

Table A.IX.17. Helium-4 Yields from Iron 800 MeV/n on 60 g/cm^2 Aluminium at10.0 deg

KE_left(MeV)	KE_mid(MeV)	KE_right(MeV)	Norm_Cts(#/SP*ster*MeV)	Y_stat(#/SP*ster*MeV)	Y_syst_tot(#/SP*ster*MeV)	X_tot(MeV)
49.829940	50.954350	52.078760	0.000089657952728	0.000000108259887	0.000068422661619	0.143746182449540
52.152888	54.189033	56.225178	0.000420314833653	0.000000313743989	0.000171079141638	0.612743165048783
56.225188	58.261333	60.297478	0.000632946948395	0.000000374741593	0.000209991086387	1.048086449905255
60.254238	62.333633	64.413028	0.000828221499373	0.000000418707960	0.000230732223404	0.577636038075015
64.456273	66.957133	69.457993	0.000921805478501	0.000000489239071	0.000228178619636	0.616762021574772
69.458007	71.958867	74.459727	0.000972661105678	0.000000637199157	0.000315413760228	0.855722747774652
74.411122	77.328667	80.246212	0.001023799027346	0.000000727142092	0.000327266272605	0.590864498066181
80.210852	83.273367	86.335882	0.001120314314039	0.000000790983445	0.000344212946436	0.703155581341000
86.419823	89.852333	93.284843	0.001172762235763	0.000000719389153	0.000279905087280	0.673629543759773
93.213653	97.043333	100.873013	0.001148825953702	0.000000704517269	0.000237910727505	0.667899351181748
100.848140	105.088000	109.327860	0.001177245932411	0.000000737492562	0.000226162692538	0.641939600683740
109.332788	114.065333	118.797878	0.001121594584919	0.000000762877303	0.000212055981597	0.587775659616830
118.768965	124.155000	129.541035	0.001120418762289	0.000000762877303	0.000191880542265	0.517147866429902
129.532978	135.608333	141.683688	0.001131697939765	0.000000831051733	0.000189784282796	0.467332582084750
141.666140	148.654000	155.641860	0.001327541833928	0.000000977950231	0.000200618829476	0.343717715814882
155.570863	163.651333	171.731803	0.001379213935698	0.000001037388193	0.000191317369595	0.176333545921359
171.695088	181.110333	190.525578	0.002003530052790	0.000001311542788	0.000240029149465	0.091284481050231
190.435332	201.576667	212.718002	0.001113247846297	0.000001085449191	0.000153000435368	0.380280571136628
212.858110	221.469500	230.080890	0.000183415644349	0.000000347906111	0.000033901180499	0.548372079414151

Table A.IX.18. Helium-4 Yields from Iron 800 MeV/n on 60 g/cm^2 Aluminium at7.20 deg

KE_left(MeV)	KE_mid(MeV)	KE_right(MeV)	Norm_Cts(#/SP*ster*MeV)	Y_stat(#/SP*ster*MeV)	Y_syst_tot(#/SP*ster*MeV)	X_tot(MeV)
45.682937	47.318567	48.954197	0.001032492840009	0.000000736276331	0.000589366849280	0.762043754177541
48.954170	50.589800	52.225430	0.001129967796722	0.000000492229484	0.000354508586291	0.515856050226223
52.125990	54.077900	56.029810	0.000806766239062	0.000000408296228	0.000247365543433	0.425229063693911
56.129293	58.225933	60.322573	0.000854751305715	0.000000498423228	0.000282911828956	0.986037767583981
60.322560	62.419200	64.515840	0.001063142664086	0.000000579620159	0.000343674819952	0.702393770875710
64.428763	66.882733	69.336703	0.001217899865436	0.000000736276764	0.000392118241394	0.497228082250993
69.423807	71.984367	74.544927	0.001368239695134	0.000000900823745	0.000483419669737	0.896195756381941
74.440120	77.305700	80.171280	0.001523536012456	0.000000942794056	0.000463112583648	0.544375167285393
80.266727	83.301167	86.335607	0.001744188289362	0.000000975572060	0.000476197878022	0.750159103082140
86.344962	89.835867	93.326772	0.001903018128461	0.000000882933969	0.000352622303190	0.646576469168961
93.227460	97.044400	100.861340	0.001875485366701	0.000000935345100	0.000341291725931	0.667568055866216
100.844685	105.083000	109.321315	0.002026701739394	0.000000975217777	0.000334619601442	0.630190738629187
109.329730	114.069000	118.808270	0.002181133214238	0.000001102907281	0.000348378053455	0.590980332512851
118.780900	124.141000	129.501100	0.002231735276722	0.000001157324075	0.000332211481784	0.494107197740531
129.504330	135.602000	141.699670	0.002640667840625	0.000001338471413	0.000369775163937	0.456451697166305
141.663597	148.648667	155.633737	0.002962700654452	0.000001471840677	0.000375766909719	0.332625324849146
155.585297	163.650667	171.716037	0.005100590285661	0.000002073477803	0.000572797582200	0.167278615862518
171.696503	181.111333	190.526163	0.002882230433440	0.000001652300944	0.000345435804970	0.093358452921254
190.430515	201.582000	212.733485	0.000246581032476	0.000000496760468	0.000058671888603	0.370163437250358

Table A.IX.19. Helium-3 Yields from Iron 800 MeV/n on 60 g/cm^2 Aluminium at12.7 deg

KE_left(MeV)	KE_mid(MeV)	KE_right(MeV)	Norm_Cts(#/SP*ster*MeV)	Y_stat(#/SP*ster*MeV)	Y_syst_tot(#/SP*ster*MeV)	X_tot(MeV)
50.207890	50.914500	51.621110	0.000084026167727	0.000000053917200	0.000027423400000	0.342228000000000
51.621103	53.740933	55.860763	0.000046828248241	0.000000093878256	0.000046981347460	1.013133525613480
55.860770	57.980600	60.100430	0.000270483877224	0.000000235353013	0.000122624175004	1.115576848356939
59.976290	62.387100	64.797910	0.000256914163090	0.000000263197530	0.000121718534415	0.502103944264532
64.922047	67.539367	70.156687	0.000421902972653	0.000000341770424	0.000147183690124	0.851417362245450
70.060608	72.798733	75.536858	0.000370842384628	0.000000341434154	0.000139299556646	0.839513419672968
75.632928	78.752433	81.871938	0.000404967092668	0.000000389500610	0.000140518471653	0.811895027271999
81.735910	85.095500	88.455090	0.000324362717056	0.000000333017981	0.000110930619249	0.804898737226615
88.552135	92.214800	95.877465	0.000375098511215	0.000000362412184	0.000114260510320	0.792358017341908
95.916402	100.046367	104.176332	0.000405504775695	0.000000432233225	0.000120414294134	0.876014276739255
104.139117	108.740667	113.342217	0.000423246682353	0.000000444571065	0.000113418412853	0.832657545229730
113.294608	118.485333	123.676058	0.000494231907110	0.000000504103930	0.000118715126077	0.779077853294522
123.635585	129.505000	135.374415	0.000441445963653	0.000000509522371	0.000104528963294	0.775759240982020
135.309502	141.972667	148.635832	0.000402817750013	0.000000527284552	0.000093782341909	0.677026972190916
148.612957	156.285667	163.958377	0.000331144488935	0.000000512797377	0.000078422710379	0.599149081528963
163.940183	172.835333	181.730483	0.000399421241459	0.000000574862786	0.000079356267377	0.497884236510858
181.685943	192.146333	202.606723	0.000369621308899	0.000000577520824	0.000069356347842	0.296732769171185
202.500512	214.968667	227.436822	0.000349017126658	0.000000616327718	0.000060866563665	0.109278333753768
227.292822	242.358667	257.424512	0.000148888275916	0.000000435181695	0.000034102254273	0.448945101455623
257.631700	269.544000	281.456300	0.000058429642798	0.000000226429374	0.000014172610167	0.728438334258295
294.905400	302.090000	309.274600	0.000015421265960	0.000000076551300	0.000003817940000	0.918487000000000

Table A.IX.20. Helium-3 Yields from Iron 800 MeV/n on 60 g/cm^2 Aluminium at10.0 deg

KE_left(MeV)	KE_mid(MeV)	KE_right(MeV)	Norm_Cts(#/SP*ster*MeV)	Y_stat(#/SP*ster*MeV)	Y_syst_tot(#/SP*ster*MeV)	X_tot(MeV)
55.798115	58.018400	60.238685	0.000273772244610	0.000000257794080	0.000127913144644	1.168875626724247
60.215430	62.459000	64.702570	0.000584901984136	0.000000391701020	0.000199162233848	0.638949855389294
64.725813	67.443933	70.162053	0.000633070244936	0.000000435983560	0.000186666459714	0.707867213319702
70.162047	72.880167	75.598287	0.000640801794510	0.000000428147936	0.000184303758956	0.973789121874957
75.522935	78.667200	81.811465	0.000610236815874	0.000000448608766	0.000168288551932	0.679761819520632
81.801557	85.109067	88.416577	0.000769135306948	0.000000532873142	0.000193879054377	0.837537020119111
88.501792	92.224867	95.947942	0.000751990510483	0.000000566837918	0.000184650487852	0.806562251500775
95.864022	100.009067	104.154112	0.000692986399944	0.000000562160014	0.000164525428133	0.810358363436819
104.135473	108.733333	113.331193	0.000728558058451	0.000000584787506	0.000159274432511	0.815679633637496
113.340480	118.480000	123.619520	0.000856121640977	0.000000709942035	0.000175551458657	0.768644590097400
123.596335	129.484000	135.371665	0.000845566246193	0.000000754108892	0.000165775471564	0.742974714003781
135.331530	141.980000	148.628470	0.000870061366510	0.000000779913176	0.000155652290146	0.689048937862181
148.600263	156.278333	163.956403	0.000938637894461	0.000000862306754	0.000154736850305	0.581689721529442
163.908462	172.823667	181.738872	0.000982292464544	0.000000932551951	0.000151012029694	0.479752112688417
181.659645	192.121000	202.582355	0.001146649770758	0.000001105540165	0.000159171087799	0.253386476620202
202.495240	214.958000	227.420760	0.000971153817245	0.000001088104792	0.000128700958245	0.119415518563920
227.286528	242.349333	257.412138	0.000417231035997	0.000000756655396	0.000068540748322	0.461515173481869
257.623900	269.536500	281.449100	0.000070983166447	0.000000239460588	0.000015392430948	0.738455225023833

Table A.IX.21. Helium-3 Yields from Iron 800 MeV/n on 60 g/cm^2 Aluminium at7.20 deg

KE_left(MeV)	KE_mid(MeV)	KE_right(MeV)	Norm_Cts(#/SP*ster*MeV)	Y_stat(#/SP*ster*MeV)	Y_syst_tot(#/SP*ster*MeV)	X_tot(MeV)
44.226880	46.041100	47.855320	0.001197135762015	0.000000627936098	0.000431214737588	0.843633235171541
47.855280	49.669500	51.483720	0.001285828956956	0.000000700673965	0.000485628932162	0.625318047986782
51.360313	53.450033	55.539753	0.001376806555260	0.000000728419053	0.000440312079554	0.524240079858456
55.663203	57.961833	60.260463	0.001463215346839	0.000000687352612	0.000376389177481	1.067453395370496
60.260470	62.559100	64.857730	0.001528942006211	0.000000652902037	0.000359219809462	0.795090367974610
64.745072	67.369367	69.993662	0.001570707224178	0.000000700673965	0.000349397663870	0.574065501536192
70.106365	72.902800	75.699235	0.001825174537167	0.000000807681634	0.000383349861243	1.007145942557979
75.570202	78.647567	81.724932	0.001718413041886	0.000000775347662	0.000344490511083	0.638795763472176
81.853907	85.151267	88.448627	0.001910335111860	0.000000872003548	0.000363734763016	0.904824175964590
88.423330	92.198300	95.973270	0.002068430133644	0.000000962627550	0.000369164317867	0.765963491086227
95.883810	100.013800	104.143790	0.001897960777474	0.000000975524542	0.000341791865866	0.820058124735070
104.130122	108.727667	113.325212	0.002174293046740	0.000001104440319	0.000362216999020	0.802264444450831
113.338577	118.488667	123.638757	0.002238047215127	0.000001160246648	0.000353746513685	0.778381845365114
123.597497	129.453667	135.309837	0.002422345804059	0.000001292010037	0.000359333560816	0.696031998972748
135.328265	141.974000	148.619735	0.002744262134116	0.000001454130428	0.000379850653955	0.680786050838294
148.593493	156.270333	163.947173	0.002695685635177	0.000001511398676	0.000359964712623	0.566960921867636
163.878090	172.810000	181.741910	0.002808464745171	0.000001663247281	0.000352495154083	0.457155882887883
181.635585	192.099000	202.562415	0.002836875904132	0.000001769882193	0.000331841334023	0.215644733871801
202.498727	214.958667	227.418607	0.001270266104195	0.000001216768540	0.000171793213074	0.103091423750038
227.290428	242.352333	257.414238	0.000106081392603	0.000000374398617	0.000029770107633	0.454959595710432

Table A.X.1. Deuteron Yields from Hydrogen 400 MeV/n on 20 g/cm^2 Aluminium at12.7 deg

KE_left(MeV)	KE_mid(MeV)	KE_right(MeV)	Norm_Cts(#/SP*ster*MeV)	Y_stat(#/SP*ster*MeV)	Y_syst_tot(#/SP*ster*MeV)	X_tot(MeV)
44.276238	45.497400	46.718562	0.000043761952540	0.000000019773426	0.000017119393950	0.141179851673707
46.762649	48.211100	49.659551	0.000047286673115	0.000000022942085	0.000016738853923	0.163807235297529
49.659549	51.108000	52.556451	0.000044392730972	0.000000023020001	0.000016784028981	0.317316039665504
52.487751	54.050033	55.612315	0.000044399070176	0.000000024367736	0.000016359626602	0.057630784782527
55.681028	57.406433	59.131838	0.000052641834657	0.000000026468066	0.000016241376715	0.168327974570420
59.075710	60.875200	62.674690	0.000041610411433	0.000000026804699	0.000015719104144	0.182364960268825
62.730765	64.738800	66.746835	0.000041658995607	0.000000026735491	0.000014060805912	0.143426585530159
66.667922	68.823967	70.980012	0.000032792113658	0.000000025308649	0.000012466265109	0.108725444271426
71.045278	73.355633	75.665988	0.000036072532349	0.000000027102229	0.000012397349141	0.105848529299466
75.679668	78.271233	80.862798	0.000044415637188	0.000000030288697	0.000012372834025	0.112382267981875
80.808248	83.637933	86.467618	0.000035829081171	0.000000028407426	0.000010649538495	0.102154002970907
86.456720	89.563900	92.671080	0.000039471616625	0.000000030114500	0.000010414630952	0.098921607541376
92.673107	96.103567	99.534027	0.000047523212954	0.000000034811766	0.000010768883883	0.071534607096065
99.525370	103.349000	107.172630	0.000043838726393	0.000000034240556	0.000009565342348	0.056075962935304
107.164458	111.459333	115.754208	0.000033136511555	0.000000035225401	0.000008686610829	0.030908642381426
115.715352	120.521667	125.327982	0.000034846947298	0.000000037658904	0.000008326810279	0.031943571845991
125.326357	130.768667	136.210977	0.000020636450969	0.000000027684191	0.000005387318209	0.044646859311872
136.178630	142.393000	148.607370	0.000010447573836	0.000000020921985	0.000003621255582	0.074707273603177
148.722700	150.983000	153.243300	0.000001027362305	0.000000004827650	0.000000747045000	0.069362200000000

Table A.X.2. Deuteron Yields from Hydrogen 400 MeV/n on 20 g/cm^2 Aluminium at10.0 deg

KE_left(MeV)	KE_mid(MeV)	KE_right(MeV)	Norm_Cts(#/SP*ster*MeV)	Y_stat(#/SP*ster*MeV)	Y_syst_tot(#/SP*ster*MeV)	X_tot(MeV)
44.343166	45.538567	46.733968	0.000345332601373	0.000000061296185	0.000055581437025	0.107609504650839
46.721542	48.175500	49.629458	0.000176118609930	0.000000049085468	0.000036293270813	0.152458011605065
49.641890	51.108300	52.574711	0.000149275456720	0.000000040755908	0.000029786665268	0.314465361763422
52.520145	54.057967	55.595789	0.000097096679175	0.000000036862741	0.000025474496183	0.067559729223647
55.650355	57.393400	59.136445	0.000095286747988	0.000000036624276	0.000022379977314	0.154316134969549
59.095755	60.879500	62.663245	0.000088504297555	0.000000034274374	0.000020307225600	0.203812685611102
62.703965	64.729400	66.754835	0.000081179147587	0.000000034184050	0.000017974569388	0.136549823472057
66.682508	68.828633	70.974758	0.000061777523821	0.000000034335883	0.000017104216346	0.114388194335124
71.047045	73.360900	75.674755	0.000071230141334	0.000000038867231	0.000017829283355	0.112139344765073
75.665617	78.265067	80.864517	0.000051804505196	0.000000033925642	0.000013831878274	0.100176950826625
80.812620	83.639700	86.466780	0.000055347390651	0.000000038725514	0.000014465301904	0.098785843505130
86.456708	89.563733	92.670758	0.000053484427399	0.000000035826963	0.000012279102994	0.096668492549744
92.673460	96.105700	99.537940	0.000055374404818	0.000000038491227	0.000011983104258	0.069103184610245
99.534687	103.349667	107.164647	0.000052398389697	0.000000039438071	0.000010943557530	0.058290175109533
107.159668	111.460333	115.760998	0.000070494100028	0.000000047440421	0.000011817880999	0.035782752616392
115.724358	120.528333	125.332308	0.000051423680533	0.000000043081612	0.000009523508220	0.032364352567910
125.329777	130.772667	136.215557	0.000070279565523	0.000000054627626	0.000010739224033	0.038472248278857
136.179427	142.396667	148.613907	0.000031327368053	0.000000040419497	0.000006956414942	0.068381959556377
148.690520	153.318000	157.945480	0.000003706572905	0.000000012614863	0.000001945114516	0.081132167165989

Table A.X.3. Deuteron Yields from Hydrogen 400 MeV/n on 20 g/cm^2 Aluminium at7.20 deg

KE_left(MeV)	KE_mid(MeV)	KE_right(MeV)	Norm_Cts(#/SP*ster*MeV)	Y_stat(#/SP*ster*MeV)	Y_syst_tot(#/SP*ster*MeV)	X_tot(MeV)
44.351284	45.555833	46.760383	0.000350911735733	0.000000061296147	0.000055193791695	0.104898386094020
46.720193	48.155400	49.590608	0.000220688514147	0.000000055881828	0.000041846646937	0.156493343255304
49.630817	51.106200	52.581584	0.000148528016427	0.000000044395040	0.000032119992102	0.309526541133390
52.533986	54.059900	55.585814	0.000124682902877	0.000000042477219	0.000029603571196	0.085782542151011
55.633402	57.385267	59.137132	0.000107403244053	0.000000039678754	0.000024156132582	0.146442989078651
59.112910	60.889000	62.665090	0.000093185662865	0.000000038437856	0.000022990514772	0.209436897199705
62.689280	64.723400	66.757520	0.000090190737273	0.000000043810235	0.000022851067269	0.132818330589009
66.689790	68.831100	70.972410	0.000077054441861	0.000000038637867	0.000019172861477	0.119020988313238
71.040150	73.362600	75.685050	0.000078678437361	0.000000040793076	0.000018664781593	0.114672002687055
75.664612	78.261267	80.857922	0.000068169331059	0.000000039359677	0.000016056949498	0.093727402676378
80.814078	83.639933	86.465788	0.000075027534884	0.000000043373388	0.000016366094609	0.097580974352637
86.456157	89.563167	92.670177	0.000076333531316	0.000000041644196	0.000014426284249	0.095853152997124
92.673248	96.106433	99.539618	0.000068251593965	0.000000045378353	0.000014133976108	0.068412282048986
99.542588	103.353333	107.164078	0.000076758360561	0.000000046854334	0.000013111939622	0.056227796045195
107.157077	111.460667	115.764257	0.000075494491969	0.000000049152646	0.000012241672003	0.038608298233273
115.728792	120.531667	125.334542	0.000058859453186	0.000000047431631	0.000010540923322	0.034714803234707
125.331770	130.775000	136.218230	0.000065880260670	0.000000052214805	0.000010316641999	0.035990364470230
136.181623	142.400333	148.619043	0.000021848133822	0.000000029031269	0.000005049207405	0.060997462040482
148.740640	151.000000	153.259360	0.000006805133450	0.000000008940540	0.000001389410000	0.052667500000000

Table A.X.4. Proton Yields from Hydrogen 400 MeV/n on 20 g/cm^2 Aluminium at12.7 deg

KE_left(MeV)	KE_mid(MeV)	KE_right(MeV)	Norm_Cts(#/SP*ster*MeV)	Y_stat(#/SP*ster*MeV)	Y_syst_tot(#/SP*ster*MeV)	X_tot(MeV)
45.462687	47.139267	48.815847	0.000088386725659	0.000000038162225	0.000024170311989	0.295685340947095
48.815820	50.492400	52.168980	0.000095815609264	0.000000042430343	0.000026877565093	0.209018647219070
52.093883	53.974533	55.855183	0.000105166903707	0.000000044413514	0.000025542340694	0.160303232242449
55.930300	57.928900	59.927500	0.000114517957468	0.000000046456374	0.000024863103959	0.350396098320172
59.849155	61.972800	64.096445	0.000130128501395	0.000000053751640	0.000027409271531	0.107059393616075
64.174792	66.503467	68.832142	0.000112396293167	0.000000051896002	0.000023835796820	0.315938363694566
68.749208	71.277633	73.806058	0.000127121907442	0.000000059530934	0.000025434105875	0.128037008564126
73.845360	76.554000	79.262640	0.000108224290328	0.000000056082159	0.000022157924644	0.239094469388901
79.306250	82.313600	85.320950	0.000153333491220	0.000000064007231	0.000023189947898	0.198049228522002
85.282585	88.599800	91.917015	0.000166501773500	0.000000076129784	0.000024963387109	0.171381146351225
91.895227	95.542767	99.190307	0.000127314683171	0.000000072320009	0.000021431263279	0.171240547159719
99.187367	103.242667	107.297967	0.000147292392935	0.000000075127709	0.000020283023448	0.154000290131935
107.279067	111.837667	116.396267	0.000113907438930	0.000000072397052	0.000017320092790	0.174877369746260
116.373527	121.452667	126.531807	0.000084061296531	0.000000065892650	0.000014050329108	0.147302153155309
126.528353	132.298333	138.068313	0.000064296542816	0.000000058647374	0.000011028914971	0.108048642305306
138.029132	144.623667	151.218202	0.000040457785986	0.000000050867374	0.000008210961376	0.090154334748641
151.184460	158.765000	166.345540	0.000014360731346	0.000000031284652	0.000004364943369	0.073067298299171
166.287930	175.085000	183.882070	0.000010512387660	0.000000026606770	0.000003270722230	0.017210529999512
183.818260	194.162000	204.505740	0.000003159649006	0.000000016510311	0.000001675890297	0.039962647274048
204.421193	216.710333	228.999473	0.000001798465142	0.000000013534134	0.000001152883010	0.117903425234469
229.315740	233.961000	238.606260	0.000001697057238	0.000000008940540	0.000000673840000	0.115630000000000

Table A.X.5. Proton Yields from Hydrogen 400 MeV/n on 20 g/cm^2 Aluminium at10.0 deg

KE_left(MeV)	KE_mid(MeV)	KE_right(MeV)	Norm_Cts(#/SP*ster*MeV)	Y_stat(#/SP*ster*MeV)	Y_syst_tot(#/SP*ster*MeV)	X_tot(MeV)
45.380358	47.090733	48.801108	0.000085467764911	0.000000040467182	0.000025092863296	0.213698542245847
48.801092	50.511467	52.221842	0.000116690500894	0.000000046748452	0.000029142240935	0.230643850434496
52.146533	53.975533	55.804533	0.000127461053665	0.000000046946596	0.000027942499704	0.110505876763598
55.879830	57.912300	59.944770	0.000104939754635	0.000000047300765	0.000024824665816	0.317326847310466
59.888553	61.979833	64.071113	0.000142989388833	0.000000052152147	0.000026930341423	0.147274934167767
64.127365	66.489700	68.852035	0.000163679204651	0.000000064756693	0.000029563893345	0.298307038915025
68.765918	71.274633	73.783348	0.000230406554591	0.000000079492057	0.000034634147967	0.126561141030452
73.869430	76.567900	79.266370	0.000273521068370	0.000000085723060	0.000035197774569	0.255298559504377
79.265820	82.305800	85.345780	0.000262323340285	0.000000092455462	0.000033612310522	0.192824552099078
85.282405	88.595200	91.907995	0.000289005927360	0.000000099954875	0.000033728480737	0.162595708934769
91.901040	95.549100	99.197160	0.000265486961865	0.000000102874623	0.000031596474911	0.180841857494027
99.205703	103.241333	107.276963	0.000175321448063	0.000000087878066	0.000023891092884	0.149890565033861
107.263858	111.831333	116.398808	0.000148767218788	0.000000081676728	0.000019686134014	0.162302674293740
116.381678	121.454333	126.526988	0.000156860288372	0.000000092995120	0.000020173050385	0.152709586939393
126.516853	132.302333	138.087813	0.000140325151457	0.000000094000833	0.000017855149123	0.111792853219291
138.044038	144.627333	151.210628	0.000156896899006	0.000000100765901	0.000017038391195	0.094723489452247
151.175518	158.764333	166.353148	0.000162934804607	0.000000110301896	0.000016466561823	0.072537878407216
166.284440	175.083000	183.881560	0.000159000199530	0.000000113121875	0.000014681230358	0.013367555670956
183.827943	194.170333	204.512723	0.000106754491993	0.000000104252486	0.000011306482314	0.024344285249087
204.423858	216.718333	229.012808	0.000046375890948	0.000000069372554	0.000006297458879	0.103960404902299
229.334820	233.979000	238.623180	0.000008202264472	0.000000016134800	0.000001226130000	0.097939800000000

Table A.X.6. Proton Yields from Hydrogen 400 MeV/n on 20 g/cm^2 Aluminium at7.20 deg

KE_left(MeV)	KE_mid(MeV)	KE_right(MeV)	Norm_Cts(#/SP*ster*MeV)	Y_stat(#/SP*ster*MeV)	Y_syst_tot(#/SP*ster*MeV)	X_tot(MeV)
45.331487	47.058767	48.786047	0.000134310831668	0.000000048042776	0.000029731231947	0.162753927981508
48.786053	50.513333	52.240613	0.000109393639527	0.000000043284572	0.000026702859160	0.230820847292873
52.179205	53.983400	55.787595	0.000121674692432	0.000000045378353	0.000026966272263	0.106820932430493
55.848995	57.898400	59.947805	0.000109281982051	0.000000047808116	0.000024911241653	0.291994045386203
59.921425	61.997200	64.072975	0.000161493464476	0.000000059138146	0.000030644001959	0.160104728479992
64.099350	66.478500	68.857650	0.000139318475270	0.000000057333580	0.000025928265444	0.284192421092541
68.780285	71.279600	73.778915	0.000208401741309	0.000000074174185	0.000032311254687	0.132221726827326
73.856335	76.571500	79.286665	0.000267375344823	0.000000090053924	0.000036557229188	0.259615097236274
79.264365	82.299200	85.334035	0.000272277115898	0.000000092294728	0.000033741390855	0.188172697172039
85.286203	88.597033	91.907863	0.000279976806047	0.000000096876324	0.000032707408925	0.163836085016610
91.901723	95.550233	99.198743	0.000243051378913	0.000000101074394	0.000030833627426	0.184082974347466
99.207707	103.245667	107.283627	0.000218700207975	0.000000097047520	0.000026693593943	0.153894937164710
107.266552	111.826667	116.386782	0.000185895189906	0.000000097052893	0.000023475751790	0.154598326405689
116.375472	121.453667	126.531862	0.000171423250891	0.000000095220427	0.000020801197678	0.154339109876402
126.518992	132.303667	138.088342	0.000182026804124	0.000000104401901	0.000020095300038	0.113274238931233
138.052165	144.630000	151.207835	0.000171765550209	0.000000104967458	0.000017948518252	0.098419535211918
151.170970	158.764000	166.357030	0.000194694967842	0.000000119622532	0.000018065234519	0.071840353634709
166.282590	175.082000	183.881410	0.000161195877891	0.000000116596847	0.000015060544716	0.011297319899644
183.832842	194.174667	204.516492	0.000086620404982	0.000000095097828	0.000010353958869	0.016397010725641
204.425750	216.723000	229.020250	0.000024438661381	0.000000051213266	0.000004519680113	0.096515928094900
229.344315	233.988000	238.631685	0.000008809121909	0.000000018469600	0.000001402150000	0.088636000000000

Table A.X.7. Proton Yields from Hydrogen 400 MeV/n on 20 g/cm^2 Aluminium at32.7 deg

KE_left(MeV)	KE_mid(MeV)	KE_right(MeV)	Norm_Cts(#/SP*ster*MeV)	Y_stat(#/SP*ster*MeV)	Y_syst_tot(#/SP*ster*MeV)	X_tot(MeV)
45.358290	46.911767	48.465244	0.000120567128284	0.000000049374110	0.000027501611221	0.158533621554861
48.520838	50.347433	52.174028	0.000127239984281	0.000000051238136	0.000025695536297	0.156351337948641
52.174038	54.000633	55.827228	0.000141148945403	0.000000058204583	0.000027903648103	0.395166953055288
55.738195	57.718300	59.698405	0.000132930036823	0.000000058267586	0.000025208088110	0.197791743296049
59.787430	61.954600	64.121770	0.000130892781811	0.000000058563838	0.000023404919935	0.251541405587629
64.039242	66.338267	68.637292	0.000163685420836	0.000000070109032	0.000025745200067	0.244454232372851
68.719850	71.234000	73.748150	0.000183933479162	0.000000078502623	0.000026286268475	0.248386828187406
73.676580	76.446100	79.215620	0.000195550186394	0.000000083907324	0.000025516652654	0.255598405890960
79.205032	82.198667	85.192302	0.000192321691173	0.000000088013485	0.000024078522172	0.195517659295139
85.210650	88.505400	91.800150	0.000213901650849	0.000000096181990	0.000024057363734	0.238930157847518
91.799707	95.457467	99.115227	0.000195336851512	0.000000104155724	0.000022792892361	0.230840852731920
99.099320	103.172000	107.244680	0.000216339049317	0.000000111029663	0.000021745607602	0.213947779490791
107.221435	111.754000	116.286565	0.000243211460925	0.000000127575988	0.000022114649341	0.197507821395407
116.255452	121.360667	126.465882	0.000269684176134	0.000000146244384	0.000022022048647	0.155382772918911
126.473142	132.241667	138.010192	0.000351827420710	0.000000181391262	0.000024186585495	0.140788289924979
137.979312	144.579667	151.180022	0.000520348668457	0.000000218434886	0.000029234068136	0.123977735159383
151.155403	158.733333	166.311263	0.000342443931459	0.000000182865680	0.000023314242681	0.084894938265188
166.267982	175.078667	183.889352	0.000179363239240	0.000000148775672	0.000013272587732	0.018749673602802
183.814660	194.177000	204.539340	0.000133330188026	0.000000120909051	0.000011069298569	0.078263358876680
204.450398	216.761333	229.072268	0.000092708828568	0.000000104130745	0.000009236762398	0.170042603914578
228.951188	243.859333	258.767478	0.000043181097575	0.000000073772773	0.000005425018422	0.301481162671899

Table A.X.8. Proton Yields from Hydrogen 400 MeV/n on 20 g/cm^2 Aluminium at30.0 deg

KE_left(MeV)	KE_mid(MeV)	KE_right(MeV)	Norm_Cts(#/SP*ster*MeV)	Y_stat(#/SP*ster*MeV)	Y_syst_tot(#/SP*ster*MeV)	X_tot(MeV)
45.465605	47.062700	48.659795	0.000162502426360	0.000000055747075	0.000031358915369	0.307504948530914
48.595268	50.275433	51.955598	0.000157964106587	0.000000059226349	0.000030548557664	0.104856717459320
52.020080	53.948600	55.877120	0.000126286453151	0.000000054074416	0.000025578427673	0.340906408250490
55.877180	57.805700	59.734220	0.000164532102616	0.000000064206781	0.000028348173093	0.335824017780146
59.671495	61.865400	64.059305	0.000124612856447	0.000000062083895	0.000024967533460	0.127010959587145
64.122003	66.390633	68.659263	0.000165152418900	0.000000068211269	0.000025543009676	0.342736958831405
68.612125	71.179800	73.747475	0.000145198731855	0.000000068975769	0.000023147271229	0.178104552513657
73.719052	76.443367	79.167682	0.000168576598561	0.000000077855301	0.000023974761064	0.240660010350702
79.238052	82.209867	85.181682	0.000199635609237	0.000000089608680	0.000025033768571	0.214189011683606
85.186915	88.510900	91.834885	0.000197084698141	0.000000092047718	0.000023162496235	0.226189495815367
91.800977	95.454167	99.107357	0.000157148617282	0.000000089581482	0.000020322106254	0.213765776390890
99.085375	103.156000	107.226625	0.000105646680167	0.000000076155648	0.000014985105139	0.196274584050508
107.197643	111.757333	116.317023	0.000056530424270	0.000000056968135	0.000010181148774	0.196362628171070
116.299595	121.381000	126.462405	0.000023228337097	0.000000042408446	0.000006328013770	0.193073238466676
126.457097	132.240667	138.024237	0.000015794736357	0.000000035335498	0.000004613148811	0.137603304041327
137.988740	144.582000	151.175260	0.000041060335646	0.000000050613125	0.000007502263987	0.121142931963363
151.134650	158.736000	166.337350	0.000024505738852	0.000000040907233	0.000005661245473	0.093722432410496
166.260593	175.074333	183.888073	0.000011533043371	0.000000028757999	0.000002900206291	0.008912909625840
183.843123	194.200333	204.557543	0.000005640908526	0.000000019849186	0.000001718854831	0.033305577315773
204.458018	216.784333	229.110648	0.000002585422297	0.000000016902087	0.000001332478611	0.132027218834678
229.285915	238.892000	248.498085	0.000001316653953	0.000000009472011	0.000000690586674	0.155162913697990

Table A.X.9. Proton Yields from Hydrogen 400 MeV/n on 20 g/cm^2 Aluminium at27.2 deg

KE_left(MeV)	KE_mid(MeV)	KE_right(MeV)	Norm_Cts(#/SP*ster*MeV)	Y_stat(#/SP*ster*MeV)	Y_syst_tot(#/SP*ster*MeV)	X_tot(MeV)
45.364630	47.037700	48.710770	0.000149241493564	0.000000054252710	0.000031423973428	0.258282692124347
48.710763	50.383833	52.056903	0.000179324939712	0.000000054562304	0.000031273480121	0.212431362690658
51.978045	53.857000	55.735955	0.000156371672956	0.000000059324444	0.000030106907653	0.203418953925744
55.814822	57.819767	59.824712	0.000158826918215	0.000000061067205	0.000029522648696	0.339887278048179
59.751583	61.862733	63.973883	0.000145989595320	0.000000064323129	0.000028512144669	0.120771497184145
64.047010	66.391600	68.736190	0.000192096018407	0.000000069096087	0.000028163019484	0.346029269545222
68.640287	71.157367	73.674447	0.000206143852289	0.000000080225507	0.000029835784854	0.137698949055612
73.764545	76.460600	79.156655	0.000224384815010	0.000000089168109	0.000030431527643	0.277280919693368
79.162458	82.203933	85.245408	0.000249871565202	0.000000091232937	0.000028238610953	0.211209540219873
85.178447	88.494867	91.811287	0.000293474249335	0.000000109291485	0.000030255181780	0.196026880606334
91.801672	95.454067	99.106462	0.000293109634881	0.000000113982115	0.000028558663465	0.210322627315750
99.113370	103.157000	107.200630	0.000335508236100	0.000000128984458	0.000029232593661	0.192269023147672
107.179880	111.739000	116.298120	0.000539253512477	0.000000182544532	0.000034719025285	0.169728252502640
116.285312	121.378667	126.472022	0.000370425744114	0.000000165146861	0.000028734349346	0.199774840831772
126.453057	132.243667	138.034277	0.000203248148139	0.000000118015636	0.000019295781468	0.143042810137525
138.001323	144.586333	151.171343	0.000569212695673	0.000000201523855	0.000035484604203	0.123934916759604
151.124118	158.726333	166.328548	0.000618545785506	0.000000220781515	0.000036055836448	0.083543605178683
166.261288	175.078333	183.895378	0.000548115496849	0.000000222384154	0.000031285669455	0.017547351155374
183.856078	194.210333	204.564588	0.000297215485600	0.000000176256970	0.000020216886987	0.013966874883241
204.476182	216.814667	229.153152	0.000093682121113	0.000000107358368	0.000009890069460	0.077906314839427
229.030992	243.938667	258.846342	0.000014863493908	0.000000044653666	0.000003282417587	0.166794922228616

Table A.XI.1. Deuteron Yields from Hydrogen 400 MeV/n on 40 g/cm^2 Aluminium at12.7 deg

KE_left(MeV)	KE_mid(MeV)	KE_right(MeV)	Norm_Cts(#/SP*ster*MeV)	Y_stat(#/SP*ster*MeV)	Y_syst_tot(#/SP*ster*MeV)	X_tot(MeV)
44.124919	45.392100	46.659281	0.000044505810021	0.000000019949093	0.000016907789823	0.231593858478587
46.659219	47.926400	49.193581	0.000046041359064	0.000000022709061	0.000019184952426	0.111573120719150
49.136906	50.681600	52.226295	0.000036791180778	0.000000023919478	0.000016655611625	0.216029945114676
52.282970	53.885900	55.488830	0.000047448865436	0.000000027095019	0.000018135552571	0.260077514897001
55.488870	57.091800	58.694730	0.000043760147584	0.000000026251410	0.000017549507926	0.115305603993822
58.679217	60.603767	62.528317	0.000058254973200	0.000000032680842	0.000018386305963	0.259160844390525
62.543827	64.483867	66.423907	0.000043105279690	0.000000028020065	0.000015510205440	0.217462283786614
66.361427	68.567067	70.772707	0.000062562510065	0.000000034545010	0.000017090121581	0.133752102466204
70.817417	73.114967	75.412517	0.000046708038816	0.000000030593759	0.000014421344132	0.230152088245230
75.430245	78.053400	80.676555	0.000059662824456	0.000000038248920	0.000015956597583	0.145750975122844
80.594417	83.434667	86.274917	0.000065425251992	0.000000036467311	0.000014122534481	0.110405715843583
86.269022	89.386567	92.504112	0.000065672814077	0.000000041297898	0.000014742636018	0.107168350261120
92.507917	95.964867	99.421817	0.000053201536995	0.000000040240287	0.000012843476590	0.063726691358017
99.410178	103.258333	107.106488	0.000055779627097	0.000000036976130	0.000010701348846	0.063922405519035
107.117840	111.402000	115.686160	0.000035662504084	0.000000035407569	0.000009103192848	0.011863637679127
115.664282	120.523667	125.383052	0.000020765895354	0.000000024967639	0.000005682457369	0.080814546174064
125.358585	130.832000	136.305415	0.000008429977360	0.000000015831270	0.000003081736513	0.110437217091386
136.369385	140.449500	144.529615	0.000003350001891	0.000000010483796	0.000001817822940	0.135288025549529

Table A.XI.2. Deuteron Yields from Hydrogen 400 MeV/n on 40 g/cm^2 Aluminium at10.0 deg

KE_left(MeV)	KE_mid(MeV)	KE_right(MeV)	Norm_Cts(#/SP*ster*MeV)	Y_stat(#/SP*ster*MeV)	Y_syst_tot(#/SP*ster*MeV)	X_tot(MeV)
44.089655	45.384467	46.679279	0.000464180423040	0.000000087115642	0.000079742220203	0.216103044650000
46.679288	47.974100	49.268912	0.000523521552453	0.000000088807926	0.000083285128972	0.189120551884241
49.182206	50.663700	52.145194	0.000380028753970	0.000000084195309	0.000068855510508	0.154369635186781
52.231908	53.861733	55.491558	0.000188753489973	0.000000060417011	0.000041785869244	0.219355779271940
55.491542	57.121367	58.751192	0.000145205648027	0.000000051868751	0.000035344900068	0.135069444387137
58.687055	60.573200	62.459345	0.000102848151321	0.000000043911188	0.000026177251611	0.213011307136898
62.523487	64.489867	66.456247	0.000127164462924	0.000000050001532	0.000028340515588	0.220880134736015
66.377312	68.559267	70.741222	0.000089415508229	0.000000044827724	0.000022967775054	0.101862736170624
70.820138	73.125833	75.431528	0.000120027115216	0.000000052369245	0.000025500545529	0.231167052532233
75.409432	78.036067	80.662702	0.000096688553485	0.000000046340577	0.000019912313903	0.132080897404135
80.591658	83.424333	86.257008	0.000106718572248	0.000000053815966	0.000021515889935	0.122383296345539
86.271452	89.386267	92.501082	0.000082137446305	0.000000052733202	0.000018867491463	0.109451129082938
92.503602	95.961467	99.419332	0.000056907628169	0.000000048087621	0.000015137751696	0.056193619880107
99.406762	103.258667	107.110572	0.000082597730084	0.000000046861269	0.000013968719779	0.048562875191961
107.108467	111.398667	115.688867	0.000054779656755	0.000000044845740	0.000011620008276	0.019426744282378
115.661652	120.513667	125.365682	0.000053866733920	0.000000044594841	0.000010365506388	0.101551409896909
125.360470	130.832000	136.303530	0.000019073166630	0.000000025682950	0.000005111530418	0.110692901357433
136.360055	140.445000	144.529945	0.000011604819720	0.000000017072400	0.000003014559948	0.142323514944966

Table A.XI.3. Deuteron Yields from Hydrogen 400 MeV/n on 40 g/cm^2 Aluminium at7.20 deg

KE_left(MeV)	KE_mid(MeV)	KE_right(MeV)	Norm_Cts(#/SP*ster*MeV)	Y_stat(#/SP*ster*MeV)	Y_syst_tot(#/SP*ster*MeV)	X_tot(MeV)
44.056671	45.369867	46.683063	0.000640402620920	0.000000104738304	0.000098264872547	0.190953069752754
46.683037	47.996233	49.309429	0.000645604331267	0.000000097536746	0.000093490036049	0.227597538183083
49.229645	50.670733	52.111821	0.000616005088652	0.000000101281104	0.000090630823679	0.179509922497365
52.191632	53.839367	55.487102	0.000385010643427	0.000000085680334	0.000063026354737	0.183847254877521
55.487065	57.134800	58.782535	0.000214557588267	0.000000061387371	0.000042694779393	0.148522465957242
58.704423	60.565933	62.427443	0.000149095144145	0.000000049139205	0.000030190352964	0.174965156727569
62.505585	64.489500	66.473415	0.000123654136216	0.000000050510699	0.000028280635208	0.217448537842865
66.383682	68.550467	70.717252	0.000144476629921	0.000000052404086	0.000027332164748	0.096847393011118
70.806973	73.129933	75.452893	0.000112781191764	0.000000053167417	0.000025463224448	0.229250781826998
75.404670	78.022200	80.639730	0.000112202336492	0.000000055825665	0.000023850751506	0.126117617725558
80.595370	83.423300	86.251230	0.000121490498612	0.000000055484226	0.000022265963476	0.127228115456451
86.271313	89.384533	92.497753	0.000098940789625	0.000000054224203	0.000019724663674	0.112183883023231
92.499488	95.958133	99.416778	0.000086320304823	0.000000054167909	0.000017592518142	0.054271607882022
99.403440	103.258000	107.112560	0.000102490137545	0.000000057834909	0.000017254306298	0.039026494671907
107.101635	111.396000	115.690365	0.000090875869767	0.000000056534281	0.000015152691265	0.029413327401629
115.659670	120.507000	125.354330	0.000039885907149	0.000000041612246	0.000009485055426	0.115404453042073
125.362525	130.833000	136.303475	0.000021404864532	0.000000030230452	0.000005997058372	0.110984391520884
136.353750	140.442000	144.530250	0.000006509727373	0.000000013393330	0.000002353591819	0.146110767455516

Table A.XI.4. Proton Yields from Hydrogen 400 MeV/n on 40 g/cm^2 Aluminium at12.7 deg

KE_left(MeV)	KE_mid(MeV)	KE_right(MeV)	Norm_Cts(#/SP*ster*MeV)	Y_stat(#/SP*ster*MeV)	Y_syst_tot(#/SP*ster*MeV)	X_tot(MeV)
44.986722	46.688667	48.390612	0.000122844076191	0.000000048342513	0.000031637875763	0.186006640309318
48.390622	50.092567	51.794512	0.000150396203428	0.000000049663874	0.000033187954046	0.344803931788778
51.750212	53.496467	55.242722	0.000122352348231	0.000000053190861	0.000033611335119	0.268656915669409
55.287007	57.391567	59.496127	0.000153791295086	0.000000057199578	0.000031516188232	0.271103400681364
59.496107	61.600667	63.705227	0.000155609963875	0.000000056600444	0.000031008435096	0.284862152470278
63.599730	65.930800	68.261870	0.000169456418837	0.000000066438968	0.000033569689597	0.243593803305523
68.367400	70.879300	73.391200	0.000177490330689	0.000000071628546	0.000033427012595	0.351643303185202
73.294113	76.062133	78.830153	0.000185608622130	0.000000073849131	0.000032204821507	0.225860552906965
78.891803	81.849633	84.807463	0.000185943286149	0.000000078173247	0.000031620266009	0.312011861550166
84.842887	88.179067	91.515247	0.000190382160720	0.000000085349257	0.000030938835528	0.315961004992705
91.443405	95.120800	98.798195	0.000200371567645	0.000000093821282	0.000031330780761	0.230776460994725
98.787122	102.854667	106.922212	0.000197341021087	0.000000091303499	0.000028234592789	0.241725315442963
106.929063	111.456333	115.983603	0.000193803827234	0.000000098260735	0.000027335599096	0.226847979018990
115.969408	121.128333	126.287258	0.000153988241576	0.000000093386398	0.000022458982388	0.234181445355946
126.248927	132.029667	137.810407	0.000099505860980	0.000000077349371	0.000016025832031	0.182757642625445
137.797952	144.417667	151.037382	0.000069820043813	0.000000062529396	0.000011298140142	0.160154483859803
150.983113	158.619333	166.255553	0.000042442615621	0.000000054984232	0.000008146359676	0.091173433972512
166.193435	175.045000	183.896565	0.000021127396400	0.000000041226725	0.000005081536945	0.014490817837320
183.833235	194.240000	204.646765	0.000020004722280	0.000000044433546	0.000004669290822	0.092008957646579
204.582267	216.966667	229.351067	0.000005418279600	0.000000028508721	0.000002577474353	0.188506859786826

Table A.XI.5. Proton Yields from Hydrogen 400 MeV/n on 40 g/cm^2 Aluminium at10.0 deg

KE_left(MeV)	KE_mid(MeV)	KE_right(MeV)	Norm_Cts(#/SP*ster*MeV)	Y_stat(#/SP*ster*MeV)	Y_syst_tot(#/SP*ster*MeV)	X_tot(MeV)
44.824080	46.577400	48.330720	0.000136094143132	0.000000053416239	0.000033999428775	0.110535404123353
48.330780	50.084100	51.837420	0.000159716220143	0.000000054224194	0.000035185216187	0.334364253285246
51.837380	53.590700	55.344020	0.000163589011913	0.000000056443910	0.000036532773450	0.430902870054262
55.264023	57.313833	59.363643	0.000144605998869	0.000000060854813	0.000034257207105	0.139965728158860
59.443685	61.599500	63.755315	0.000143669429676	0.000000062012325	0.000032538214475	0.279410752273423
63.671332	65.943467	68.215602	0.000201886710863	0.000000074176732	0.000038572269680	0.224154777461914
68.299588	70.862233	73.424878	0.000208916617583	0.000000079765858	0.000037112833808	0.318742814107236
73.322413	76.055733	78.789053	0.000311448564627	0.000000106818269	0.000048352275632	0.196409746611516
78.891542	81.864167	84.836792	0.000375195800353	0.000000115359093	0.000050967128356	0.318342149111612
84.803472	88.156167	91.508862	0.000377555806606	0.000000122962648	0.000049043368841	0.293616247560468
91.451268	95.121033	98.790798	0.000357613589421	0.000000131110820	0.000047255409272	0.224680648441048
98.782502	102.850667	106.918832	0.000377478782227	0.000000134184340	0.000045584495835	0.240352914868969
106.930367	111.461667	115.992967	0.000226436792384	0.000000111061140	0.000031463090000	0.237288379409949
115.967237	121.107667	126.248097	0.000229699232905	0.000000116508515	0.000029533787070	0.197821045507398
126.249515	132.023000	137.796485	0.000231710062177	0.000000122674089	0.000028445611195	0.173153637200638
137.785800	144.410000	151.034200	0.000189965466892	0.000000117699367	0.000023219542294	0.146146031506333
150.966542	158.607667	166.248792	0.000228011961481	0.000000140258614	0.000025619580934	0.069394083654877
166.197305	175.047000	183.896695	0.000271953818131	0.000000164057960	0.000027280938854	0.018789658615845
183.821822	194.235667	204.649512	0.000353480729347	0.000000199851246	0.000031656877842	0.103979701089492
204.571307	216.958667	229.346027	0.000191366877978	0.000000157916667	0.000022485540349	0.202140789482504

Table A.XI.6. Proton Yields from Hydrogen 400 MeV/n on 40 g/cm^2 Aluminium at7.20 deg

KE_left(MeV)	KE_mid(MeV)	KE_right(MeV)	Norm_Cts(#/SP*ster*MeV)	Y_stat(#/SP*ster*MeV)	Y_syst_tot(#/SP*ster*MeV)	X_tot(MeV)
44.752458	46.478333	48.204208	0.000165250505321	0.000000058105222	0.000038125346871	0.235784571784966
48.265923	50.053533	51.841143	0.000161284376508	0.000000058921772	0.000037331805079	0.290233470912660
51.841157	53.628767	55.416377	0.000181045517947	0.000000064026876	0.000040624648382	0.499088486823729
55.304975	57.292600	59.280225	0.000211833987544	0.000000068791748	0.000040531888940	0.172615699686587
59.391630	61.581600	63.771570	0.000178293707296	0.000000066992459	0.000035334011349	0.251134517750946
63.726330	65.961500	68.196670	0.000204833950033	0.000000073968557	0.000038562923894	0.256209346734267
68.241893	70.838333	73.434773	0.000205833901725	0.000000077157758	0.000035515638776	0.279079232545168
73.350820	76.062500	78.774180	0.000267193770447	0.000000095443867	0.000042807679398	0.191936376926861
78.858143	81.864233	84.870323	0.000444272856693	0.000000132060628	0.000058605096186	0.311037057235951
84.798362	88.139467	91.480572	0.000455319471117	0.000000140630101	0.000057478201068	0.275171171854248
91.449198	95.114633	98.780068	0.000427088429390	0.000000136462777	0.000052029370312	0.217927924534787
98.773522	102.842667	106.911812	0.000481603341600	0.000000151098547	0.000054424874987	0.235352902674601
106.925003	111.461333	115.997663	0.000373143142461	0.000000137434474	0.000043678159386	0.239769454495355
115.965145	121.092000	126.218855	0.000254351097146	0.000000123630318	0.000032050366184	0.172444700417989
126.229863	132.016333	137.802803	0.000273612607701	0.000000135080458	0.000032085553558	0.164824654778829
137.785598	144.408333	151.031068	0.000271780453376	0.000000138548625	0.000029616065622	0.140321547617926
150.968865	158.601000	166.233135	0.000288832539554	0.000000155836465	0.000030082806045	0.058455330124378
166.198847	175.047667	183.896487	0.000318754409206	0.000000176275208	0.000030456078802	0.021189829574822
183.818130	194.237000	204.655870	0.000426414784199	0.000000226513431	0.000037194364618	0.102304660692414
204.564638	216.954333	229.344028	0.000219394510018	0.000000177276458	0.000027853355919	0.209220206950500

Table A.XI.7. Proton Yields from Hydrogen 400 MeV/n on 40 g/cm^2 Aluminium at32.7 deg

KE_left(MeV)	KE_mid(MeV)	KE_right(MeV)	Norm_Cts(#/SP*ster*MeV)	Y_stat(#/SP*ster*MeV)	Y_syst_tot(#/SP*ster*MeV)	X_tot(MeV)
44.908720	46.414300	47.919880	0.000100462254990	0.000000047059198	0.000027093730384	0.298601851337194
47.823103	49.596733	51.370363	0.000120773753285	0.000000053333462	0.000030573980253	0.305085725862421
51.467165	53.391500	55.315835	0.000123406795695	0.000000053585238	0.000029685413396	0.419197332446188
55.315832	57.240167	59.164502	0.000106102823119	0.000000051084281	0.000024449304038	0.318625887204728
59.050317	61.200767	63.351217	0.000100040216884	0.000000053404833	0.000024999225647	0.189763553552441
63.465397	65.816167	68.166937	0.000110934735403	0.000000063721547	0.000025698233478	0.526682928366774
68.078087	70.552367	73.026647	0.000124852535003	0.000000068661976	0.000026784791333	0.193648052815565
73.115493	75.895233	78.674973	0.000135047518110	0.000000075634118	0.000026791038098	0.458260558749059
78.563350	81.583400	84.603450	0.000163821193686	0.000000083153072	0.000027196102703	0.237859718105021
84.645363	87.926133	91.206903	0.000170663011293	0.000000097361024	0.000028814848965	0.370232438083550
91.276607	94.921967	98.567327	0.000175059349641	0.000000099912725	0.000027234874326	0.332528678518109
98.563328	102.648433	106.733538	0.000182260177041	0.000000107624252	0.000026404821386	0.290279060838015
106.671987	111.262667	115.853347	0.000209514690746	0.000000121031392	0.000027068311998	0.281606939349868
115.810032	120.957667	126.105302	0.000217653626447	0.000000135078797	0.000027016230786	0.293382312708179
126.069113	131.870333	137.671553	0.000052149830057	0.000000091878391	0.000014229405026	0.210698057169234
137.667163	144.300333	150.933503	0.000032962006538	0.000000082643790	0.000010611507980	0.194635746102919
150.883125	158.540000	166.196875	0.000271917325865	0.000000175086903	0.000025169208024	0.109276066810395
166.143933	175.023333	183.902733	0.000453194133818	0.000000209137766	0.000030857897547	0.016171229730914
183.832982	194.285667	204.738352	0.000152531109353	0.000000140688835	0.000014416536665	0.124373199524737
204.656313	217.099333	229.542353	0.000120928585691	0.000000129601838	0.000011263087003	0.285727812975916
229.426902	244.483667	259.540432	0.000025852168547	0.000000059892110	0.000004533111482	0.516044776446773

Table A.XI.8. Proton Yields from Hydrogen 400 MeV/n on 40 g/cm^2 Aluminium at30.0 deg

KE_left(MeV)	KE_mid(MeV)	KE_right(MeV)	Norm_Cts(#/SP*ster*MeV)	Y_stat(#/SP*ster*MeV)	Y_syst_tot(#/SP*ster*MeV)	X_tot(MeV)
44.956473	46.636533	48.316593	0.000118068724476	0.000000051941379	0.000033707345528	0.691424351993043
48.316573	49.996633	51.676693	0.000130817786903	0.000000056756479	0.000030962783419	0.991981447950515
51.601202	53.368067	55.134932	0.000134000686853	0.000000056548498	0.000030112623467	0.423273263350805
55.210462	57.309667	59.408872	0.000171803490596	0.000000067223296	0.000034751634569	0.437891949150701
59.408895	61.508100	63.607305	0.000162217181058	0.000000068123786	0.000030964185897	0.684490235121729
63.495500	65.823900	68.152300	0.000176614739576	0.000000072268781	0.000032094762781	0.547757988651010
68.264120	70.786700	73.309280	0.000174348182162	0.000000079838194	0.000031402300148	0.583925402890643
73.198155	75.955100	78.712045	0.000185225442051	0.000000081289355	0.000030219785893	0.558598221108875
78.823182	81.771567	84.719952	0.000184543345514	0.000000091264532	0.000030714617532	0.552540278501034
84.710833	88.078633	91.446433	0.000190669260586	0.000000095984934	0.000029296329682	0.614699578059071
91.363042	95.038167	98.713292	0.000248428883122	0.000000112339589	0.000032444377442	0.541614414714934
98.700032	102.772667	106.845302	0.000249302249692	0.000000118478632	0.000031004505761	0.508532367568673
106.854445	111.395000	115.935555	0.000210028633525	0.000000116099710	0.000026790933574	0.507659405709182
115.907473	121.035333	126.163193	0.000147145845587	0.000000099288649	0.000019694363618	0.422839506859281
126.162742	131.965667	137.768592	0.000023178866568	0.000000046238862	0.000007136414226	0.377327129916469
137.741303	144.372333	151.003363	0.000005003134703	0.000000027462748	0.000003493056139	0.314093701097300
150.963263	158.582333	166.201403	0.000044612097959	0.000000054779104	0.000007607962999	0.173281757789013
166.178332	175.045667	183.913002	0.000047406416566	0.000000058292634	0.000007269555927	0.066587693708447
183.835123	194.263333	204.691543	0.000010162329476	0.000000028221002	0.000002672545849	0.163911269032547
204.579567	216.990667	229.401767	0.000006137126278	0.000000028519298	0.000002248769769	0.473206089527597
229.562775	239.227000	248.891225	0.000003462668751	0.000000019281995	0.000001376822831	0.645190486740156

Table A.XI.9. Proton Yields from Hydrogen 400 MeV/n on 40 g/cm^2 Aluminium at27.2 deg

KE_left(MeV)	KE_mid(MeV)	KE_right(MeV)	Norm_Cts(#/SP*ster*MeV)	Y_stat(#/SP*ster*MeV)	Y_syst_tot(#/SP*ster*MeV)	X_tot(MeV)
44.781017	46.363733	47.946449	0.000204709847626	0.000000059126206	0.000037679190064	0.217933173619552
48.040828	49.884133	51.727438	0.000165553932413	0.000000058970633	0.000034991660655	0.805162198495434
51.727428	53.570733	55.414038	0.000214239102527	0.000000070531737	0.000038683461506	0.731763001639875
55.385268	57.257333	59.129398	0.000236016129593	0.000000076423307	0.000040715630518	0.372277414505970
59.158188	61.419933	63.681678	0.000257656402497	0.000000085153145	0.000041181061454	0.559806717853582
63.681688	65.943433	68.205178	0.000269086909661	0.000000089316351	0.000040522641238	0.756877531381399
68.119187	70.685067	73.250947	0.000292148974920	0.000000098522360	0.000041253231150	0.422187449340930
73.336947	76.020267	78.703587	0.000342439637206	0.000000111819593	0.000044779854213	0.667707608084557
78.670477	81.744867	84.819257	0.000383691852747	0.000000126052925	0.000045456915844	0.509679476914659
84.737008	88.048133	91.359258	0.000386527601116	0.000000131167273	0.000043849925623	0.553168409551739
91.386902	95.041067	98.695232	0.000470753119234	0.000000152230122	0.000047825274538	0.538286243061255
98.697037	102.774667	106.852297	0.000544786646625	0.000000169758154	0.000049235453526	0.511624336335753
106.834432	111.399667	115.964902	0.000562422073912	0.000000184943131	0.000049284232614	0.519269741156752
115.960103	121.066333	126.172563	0.000654119978678	0.000000214677392	0.000052837170844	0.479408968488284
126.145898	131.971333	137.796768	0.000699583408681	0.000000244241731	0.000054606526454	0.384512296257220
137.753702	144.380667	151.007632	0.000499326810297	0.000000212215535	0.000040580444735	0.329936683401528
150.990333	158.612333	166.234333	0.000785651801013	0.000000264193642	0.000060921099622	0.225598095218023
166.171813	175.047333	183.922853	0.000767101336596	0.000000273497808	0.000057380158332	0.071684161796732
183.877942	194.286667	204.695392	0.000503965186906	0.000000224629804	0.000039320028105	0.117756685627356
204.613105	217.041000	229.468895	0.000169769812857	0.000000132740896	0.000016006572122	0.388621953210315
229.325437	244.351667	259.377897	0.000017506146497	0.000000046706048	0.000003778050861	0.743547580057255

Table A.XII.1. Deuteron Yields from Hydrogen 400 MeV/n on 60 g/cm^2 Aluminium at12.7 deg

KE_left(MeV)	KE_mid(MeV)	KE_right(MeV)	Norm_Cts(#/SP*ster*MeV)	Y_stat(#/SP*ster*MeV)	Y_syst_tot(#/SP*ster*MeV)	X_tot(MeV)
43.807814	45.143500	46.479185	0.000032878187317	0.000000023384347	0.000018879976617	22.158447836663044
46.479181	47.814867	49.150552	0.000027570842693	0.000000020021584	0.000016117211773	0.576991752310204
49.150548	50.486233	51.821919	0.000072721569979	0.000000038186213	0.000031525578472	0.293697331131371
51.796897	53.492167	55.187437	0.000057362589155	0.000000021301132943	0.000021301132943	0.354863395723044
55.212462	56.932767	58.653072	0.000055388733293	0.000000035485254	0.000022902413596	0.774732808749571
58.650972	60.373367	62.095762	0.000089767691970	0.000000039655644	0.000026498288482	0.421115928828393
62.097835	64.200700	66.303565	0.000059566781230	0.000000035400355	0.000018984240262	0.379210765147879
66.303535	68.406400	70.509265	0.000036452759133	0.000000032620013	0.000016830478778	0.589121377485149
70.445252	72.866467	75.287682	0.000055769333814	0.000000037624931	0.000017524213345	0.321781572477356
75.304805	77.837400	80.369995	0.000049493937700	0.000000037406908	0.000016579043152	0.429933288799553
80.416930	83.287300	86.157670	0.000035844733978	0.000000032071250	0.000012379262524	0.361327710768217
86.078895	89.229900	92.380905	0.000046022158571	0.000000039541248	0.000014192299472	0.331955711332099
92.357245	95.829900	99.302555	0.000037460534263	0.000000034623289	0.000011258040822	0.257860818291884
99.299982	103.162667	107.025352	0.000011233775064	0.000000023015997	0.000006337865694	0.194501254389374
107.063890	109.890500	112.717110	0.000002107123651	0.000000008738298	0.000002175480215	0.073228711871574

Table A.XII.2. Deuteron Yields from Hydrogen 400 MeV/n on 60 g/cm^2 Aluminium at10.0 deg

KE_left(MeV)	KE_mid(MeV)	KE_right(MeV)	Norm_Cts(#/SP*ster*MeV)	Y_stat(#/SP*ster*MeV)	Y_syst_tot(#/SP*ster*MeV)	X_tot(MeV)
43.683256	45.060600	46.437944	0.000098528853597	0.000000037927374	0.000031456374164	22.045173283770509
46.437923	47.815267	49.192610	0.000195720092787	0.000000055998071	0.000049465766440	0.574426164437171
49.192623	50.569967	51.947310	0.000612119154280	0.000000105679352	0.000113019443467	0.418642362502889
51.850085	53.446900	55.043715	0.000699311314548	0.000000122239803	0.000120965589416	0.248187658618877
55.140912	56.901567	58.662222	0.000663621049893	0.000000123527364	0.000110256729699	0.720242010184771
58.662212	60.422867	62.183522	0.000642522824075	0.000000118375963	0.000104269550691	0.492925066307243
62.109435	64.156600	66.203765	0.000416867997758	0.000000095937440	0.000070323127994	0.307745439317693
66.277863	68.420133	70.562403	0.000204218165760	0.000000072102016	0.000042740287098	0.608944724805134
70.474057	72.860767	75.247477	0.000145698947394	0.000000065873020	0.000034026082224	0.309365148736893
75.335857	77.860267	80.384677	0.000171791655317	0.000000068377296	0.000034971249226	0.463992407901250
80.373340	83.270600	86.167860	0.000114148417495	0.000000059401793	0.000024904273591	0.333863090802203
86.084563	89.225733	92.366903	0.000083046390445	0.000000052782536	0.000020138314880	0.326508477637258
92.359997	95.830067	99.300137	0.000062303945647	0.000000046171035	0.000015541140556	0.255924420415481
99.298490	103.164000	107.029510	0.000047673454177	0.000000040686381	0.000012252831814	0.194118456299884
107.066285	109.887500	112.708715	0.000008609893202	0.000000015127087	0.000003949407107	0.079581498570773

Table A.XII.3. Deuteron Yields from Hydrogen 400 MeV/n on 60 g/cm^2 Aluminium at7.20 deg

KE_left(MeV)	KE_mid(MeV)	KE_right(MeV)	Norm_Cts(#/SP*ster*MeV)	Y_stat(#/SP*ster*MeV)	Y_syst_tot(#/SP*ster*MeV)	X_tot(MeV)
46.381999	47.791633	49.201267	0.000235144790360	0.000000063855756	0.000056143877057	0.532776986712076
49.201233	50.610867	52.020501	0.000962176778360	0.000000137459945	0.000162773566772	0.483484729815741
51.939601	53.464467	54.989333	0.001535681497446	0.000000179190496	0.000228753189910	0.245518916853671
55.070240	56.862200	58.654160	0.001482213362667	0.000000191200530	0.000215354346622	0.653220654948234
58.654173	60.446133	62.238093	0.001622022129030	0.000000194381031	0.000223866155258	0.527203460229540
62.139727	64.144467	66.149207	0.001143196167336	0.000000174515237	0.000164712397246	0.274246695239596
66.247597	68.420467	70.593337	0.000559019262138	0.000000119020144	0.000090648914715	0.608212168116522
70.488070	72.849500	75.210930	0.000255706372070	0.000000080649781	0.000047871776483	0.304727900573430
75.316200	77.870700	80.425200	0.000205544720946	0.000000079816241	0.000040656963586	0.480253666728324
80.369640	83.252400	86.135160	0.000189006429763	0.000000076675637	0.000034864520519	0.306644115066636
86.084005	89.218300	92.352595	0.000160576981609	0.000000070117359	0.000029328007696	0.320353896548801
92.368045	95.836700	99.305355	0.000111242189010	0.000000062849279	0.000022755176459	0.263142612843302
99.301800	103.170000	107.038200	0.000052462764453	0.000000046405146	0.000014000149204	0.198443452380873
107.066565	109.884000	112.701435	0.000012043363548	0.000000016081264	0.000004148224094	0.087883594216840

Table A.XII.4. Proton Yields from Hydrogen 400 MeV/n on 60 g/cm^2 Aluminium at12.7 deg

KE_left(MeV)	KE_mid(MeV)	KE_right(MeV)	Norm_Cts(#/SP*ster*MeV)	Y_stat(#/SP*ster*MeV)	Y_syst_tot(#/SP*ster*MeV)	X_tot(MeV)
44.679506	46.130933	47.582360	0.000176458564683	0.000000062418788	0.000050901596160	0.312167288470397
47.559808	49.445033	51.330258	0.000140683378032	0.000000058970445	0.000037831575082	0.350840759608938
51.352843	53.260633	55.168423	0.000175948748227	0.000000070240764	0.000045028823374	0.929674397843137
55.168410	57.076200	58.983990	0.000205213677428	0.000000076662900	0.000050200759467	1.014553402364804
58.856687	61.002067	63.147447	0.000223158956070	0.000000082858671	0.000049883005170	0.396383197272538
63.274770	65.647200	68.019630	0.000220343771913	0.000000089789415	0.000048789155455	0.741181794547060
67.966492	70.392067	72.817642	0.000294747444668	0.000000099729575	0.000057235901294	0.772118513890841
72.870773	75.708533	78.546293	0.000280858240276	0.000000106568333	0.000053424399805	0.664287499211749
78.447587	81.426167	84.404747	0.000288094294951	0.000000111340247	0.000053915340321	0.706847169132055
84.503445	87.807300	91.111155	0.000355929482860	0.000000131787624	0.000061438987369	0.694722503244281
91.045938	94.752333	98.458728	0.000363668842650	0.000000137135319	0.000059670906073	0.693106104896646
98.420440	102.508400	106.596360	0.000351343681870	0.000000144432344	0.000056735442156	0.669841826231387
106.594968	111.153333	115.711698	0.000352053313892	0.000000156071572	0.000056302435526	0.637539829395780
115.710738	120.830333	125.949928	0.000309853031296	0.000000153409896	0.000048818095880	0.561362413429150
125.941238	131.796333	137.651428	0.000197965685970	0.000000127321109	0.000032820225649	0.509137440550192
137.581287	144.231667	150.882047	0.000140667230777	0.000000111626638	0.000024204595637	0.394012133800471
150.862787	158.517667	166.172547	0.000079762978711	0.000000084582966	0.000014748232400	0.274501475659057
166.231705	172.011500	177.791295	0.000029155173550	0.000000041021307	0.000005577047391	0.055908575918637

Table A.XII.5. Proton Yields from Hydrogen 400 MeV/n on 60 g/cm^2 Aluminium at10.0 deg

KE_left(MeV)	KE_mid(MeV)	KE_right(MeV)	Norm_Cts(#/SP*ster*MeV)	Y_stat(#/SP*ster*MeV)	Y_syst_tot(#/SP*ster*MeV)	X_tot(MeV)
44.798992	46.326367	47.853742	0.000200752260365	0.000000066094284	0.000052560499125	0.601536808855451
47.763277	49.409267	51.055257	0.000243944284600	0.000000074291911	0.000057640506888	0.223497278234904
51.145710	53.131500	55.117290	0.000222716562113	0.000000078497564	0.000050763642733	0.729944611419935
55.117277	57.103067	59.088857	0.000224277395533	0.000000079309797	0.000051273249685	1.048506231999601
59.063252	61.074667	63.086082	0.000282173893016	0.000000085608571	0.000057650191728	0.537638343992502
63.111685	65.561200	68.010715	0.000222466162477	0.000000089971588	0.000047883892418	0.613969548806779
68.010685	70.460200	72.909715	0.000247078081422	0.000000095536107	0.000051773886726	0.878243300551163
72.824507	75.637367	78.450227	0.000254291019327	0.000000099913628	0.000049541818772	0.548783111596011
78.514068	81.449333	84.384598	0.000304157652589	0.000000109426839	0.000054691010762	0.748017041626727
84.405993	87.785133	91.164273	0.000349002696620	0.000000126520252	0.000059218041419	0.657218865332547
91.058592	94.743567	98.428542	0.000512406007097	0.000000173266876	0.000080491222016	0.670313712261654
98.404168	102.486433	106.568698	0.000616560101655	0.000000190549807	0.000089742573364	0.634796846680101
106.571193	111.135333	115.699473	0.000591719683629	0.000000196102921	0.000084451860373	0.610687948242799
115.722423	120.835333	125.948243	0.000620504897806	0.000000207284249	0.000084751662782	0.568949205105342
125.923103	131.774333	137.625563	0.000518111139303	0.000000204757059	0.000071060006636	0.472359568860418
137.574910	144.219000	150.863090	0.000522909263222	0.000000218595814	0.000068959521941	0.376330181728758
150.838463	158.500333	166.162203	0.000656820891816	0.000000267173636	0.000082229370085	0.250173294253423
166.112738	175.006333	183.899928	0.000566844237148	0.000000265265253	0.000075983417560	0.051742508236942

Table A.XII.6. Proton Yields from Hydrogen 400 MeV/n on 60 g/cm^2 Aluminium at7.20 deg

KE_left(MeV)	KE_mid(MeV)	KE_right(MeV)	Norm_Cts(#/SP*ster*MeV)	Y_stat(#/SP*ster*MeV)	Y_syst_tot(#/SP*ster*MeV)	X_tot(MeV)
44.801742	46.388967	47.976192	0.000280153558153	0.000000079057053	0.000064075979007	0.701725018198012
47.976208	49.563433	51.150658	0.000247505428362	0.000000070510245	0.000056888290544	0.482919930581665
51.062683	52.998033	54.933383	0.000248051288363	0.000000084643884	0.000056440352158	0.520189075657111
55.021392	57.067767	59.114142	0.000239662205555	0.000000083532357	0.000053172614143	0.981917510839378
59.114158	61.160533	63.206908	0.000282071981374	0.000000090931316	0.000059199120875	0.667620651848039
63.112048	65.491233	67.870418	0.000323193469613	0.000000103596284	0.000061960398530	0.495524701771768
67.965250	70.474600	72.983950	0.000332608665346	0.000000111378435	0.000063024951274	0.899731178825098
72.860622	75.618067	78.375512	0.000331888574383	0.000000116681619	0.000061291474433	0.516073454800768
78.498842	81.471767	84.444692	0.000346486868823	0.000000122674802	0.000061666774200	0.786715481456289
84.376755	87.746400	91.116045	0.000410521367123	0.000000144077277	0.000067994022426	0.596898375344581
91.054483	94.725133	98.395783	0.000639466989181	0.000000190342112	0.000096206728252	0.640226768129856
98.414688	102.494233	106.573778	0.001011384685027	0.000000247026968	0.000138492195277	0.641768490363932
106.566383	111.136333	115.706283	0.001031701705556	0.000000262993459	0.000138869292779	0.608411345487574
115.705093	120.830333	125.955573	0.001006064430276	0.000000263732198	0.000130766327763	0.561612068149359
125.917347	131.750667	137.583987	0.000881610357202	0.000000269104332	0.000114148245481	0.434881756079742
137.579645	144.220000	150.860355	0.000759500282220	0.000000261783517	0.000097658127609	0.375956789353511
150.817123	158.485333	166.153543	0.000862012095747	0.000000314132871	0.000106116062961	0.230138994340572
166.123378	175.011333	183.899288	0.000847299677868	0.000000323209737	0.000107933175478	0.061848668163914

Table A.XII.7. Proton Yields from Hydrogen 400 MeV/n on 60 g/cm^2 Aluminium at32.7 deg

KE_left(MeV)	KE_mid(MeV)	KE_right(MeV)	Norm_Cts(#/SP*ster*MeV)	Y_stat(#/SP*ster*MeV)	Y_syst_tot(#/SP*ster*MeV)	X_tot(MeV)
43.867467	45.677367	47.487267	0.000109109749872	0.000000055859536	0.000034783222910	0.231018444566379
47.487300	49.297200	51.107100	0.000096804569499	0.000000055774971	0.000034215682272	0.851047840872650
51.107100	52.917000	54.726900	0.000116707831864	0.000000053170794	0.000033618563990	0.929335918477813
54.710225	56.536800	58.363375	0.000140873246577	0.000000059217072	0.000038228008037	0.362269672871040
58.380050	60.680000	62.979950	0.000115571974583	0.000000067047266	0.000033322834536	0.318740896692109
62.979850	65.279800	67.579750	0.000154475275041	0.000000070236314	0.000036354414043	0.761408113383355
67.462162	69.951667	72.441172	0.000145279487369	0.000000080983353	0.000037793449926	0.409468337579354
72.558780	75.348600	78.138420	0.000170431925449	0.000000081678487	0.000036053758721	0.520929657202390
78.012593	81.016733	84.020873	0.000175971406129	0.000000083546885	0.000034766115877	0.500549325114918
84.146678	87.425933	90.705188	0.000178898798251	0.000000096995067	0.000036462696782	0.496445927127014
90.662980	94.390100	98.117220	0.000236913259061	0.000000115673181	0.000041378803665	0.514610450001746
98.051153	102.151633	106.252113	0.000223540921975	0.000000114620820	0.000037248544201	0.490247733255341
106.245097	110.819667	115.394237	0.000215703410653	0.000000119000394	0.000035083371976	0.478155810598386
115.411817	120.537667	125.663517	0.000233729298002	0.000000129565509	0.000035493203025	0.424258516903315
125.641503	131.525333	137.409163	0.000228616949520	0.000000138542993	0.000033601756893	0.363127777242392
137.351850	144.022000	150.692150	0.000228868973990	0.000000149068739	0.000032412779635	0.291236077167648
150.658075	158.361000	166.063925	0.000173817855319	0.000000142383235	0.000025825725757	0.187515621044781
166.043488	174.976333	183.909178	0.000147171899076	0.000000132764940	0.000021002921272	0.067843690875202
183.854778	194.406333	204.957888	0.000165180762788	0.000000146759105	0.000021508168466	0.200338366960126
194.241930	201.696000	209.150070	0.000025612295475	0.000000044796160	0.000004727970694	0.256295827340205

Table A.XII.8. Proton Yields from Hydrogen 400 MeV/n on 60 g/cm^2 Aluminium at30.0 deg

KE_left(MeV)	KE_mid(MeV)	KE_right(MeV)	Norm_Cts(#/SP*ster*MeV)	Y_stat(#/SP*ster*MeV)	Y_syst_tot(#/SP*ster*MeV)	X_tot(MeV)
44.595672	46.187967	47.780262	0.000142098455887	0.000000056716900	0.000040782680211	0.888202449455641
47.780272	49.372567	50.964862	0.000133243812327	0.000000054524629	0.000038634662300	0.957767108258057
50.849218	52.738133	54.627048	0.000143635566931	0.000000064796376	0.000040795536287	0.615968904101498
54.742680	56.817600	58.892520	0.000175471361955	0.000000071680812	0.000041407517397	0.758758474239333
58.892513	60.967433	63.042353	0.000150539092065	0.000000071301772	0.000039846092999	0.760925332426908
62.908437	65.228667	67.548897	0.000192778348607	0.000000079809986	0.000042108619242	0.689244032750375
67.682815	70.243000	72.803185	0.000237520658938	0.000000097058798	0.000047454773787	0.886609578780311
72.701510	75.405000	78.108490	0.000235879149111	0.000000099219173	0.000046384751308	0.616878259687436
78.210145	81.255100	84.300055	0.000234723869910	0.000000105293897	0.000044435728241	0.910378570033917
84.182323	87.520933	90.859543	0.000239943071238	0.000000110695750	0.000043431143431	0.666434082606074
90.882622	94.534367	98.186112	0.000284595411214	0.000000122034050	0.000046211006999	0.777919143072080
98.218485	102.297200	106.375915	0.000268586220961	0.000000122305720	0.000041855446564	0.740322764113734
106.354842	110.945667	115.536492	0.000249614323055	0.000000130463577	0.000038836059539	0.687536009807486
115.507158	120.677333	125.847508	0.000293688654325	0.000000148683073	0.000041781311555	0.662834773147124
125.842303	131.647333	137.452363	0.000266344330767	0.000000143920096	0.000036679654586	0.572654997723760
137.436265	144.130000	150.823735	0.000199974916633	0.000000131577197	0.000028319959506	0.473380325502655
150.769423	158.440333	166.111243	0.000088897798968	0.000000093655259	0.000015749360968	0.306528912667305
166.053658	175.009333	183.965008	0.000036742235876	0.000000060329441	0.000007846893345	0.139470547839642
183.877760	194.383000	204.888240	0.000020040651147	0.000000046576444	0.000005092518445	0.239906483141265
191.045185	198.268000	205.490815	0.000001901496542	0.000000013941308	0.000001366694346	0.262776157581334

Table A.XII.9. Proton Yields from Hydrogen 400 MeV/n on 60 g/cm^2 Aluminium at27.2 deg

KE_left(MeV)	KE_mid(MeV)	KE_right(MeV)	Norm_Cts(#/SP*ster*MeV)	Y_stat(#/SP*ster*MeV)	Y_syst_tot(#/SP*ster*MeV)	X_tot(MeV)
44.043503	45.742933	47.442364	0.000227574349140	0.000000069834537	0.000055018192937	0.214036792869357
47.539835	49.375700	51.211565	0.000222327365022	0.000000071616206	0.000049968424436	0.988979905682618
51.211535	53.047400	54.883265	0.000210306227737	0.000000071240099	0.000044178469958	1.150220167542284
54.883235	56.719100	58.554965	0.000209436540841	0.000000069475788	0.000043382950435	0.625987491435731
58.505832	60.774267	63.042702	0.000194607281919	0.000000076335362	0.000042725941321	0.469147888192455
63.091792	65.409367	67.726942	0.000248404978646	0.000000088359425	0.000046684288145	0.985910907677768
67.621325	70.095200	72.569075	0.000281743086329	0.000000094643129	0.000047333206943	0.650317126235347
72.674692	75.474067	78.273442	0.000360954028034	0.000000111940338	0.000055463764784	0.737536831382677
78.153378	81.152433	84.151488	0.000397248836078	0.000000125070259	0.000056030557959	0.734052316156008
84.271573	87.552733	90.833893	0.000522478746680	0.000000149691033	0.000067856305390	0.715740698019192
90.792043	94.514133	98.236223	0.000486415648986	0.000000157957375	0.000063389918943	0.728859951190899
98.173632	102.270567	106.367502	0.000504377602377	0.000000170589583	0.000063592835374	0.694349356892480
106.362120	110.931000	115.499880	0.000539349292832	0.000000180273501	0.000063169944023	0.667131629321381
115.516727	120.633667	125.750607	0.000651155669274	0.000000210253592	0.000069471552347	0.589510608876549
125.734923	131.617333	137.499743	0.000739341032837	0.000000233827021	0.000075538822366	0.520540268130142
137.420447	144.084667	150.748887	0.000763072499633	0.000000249820999	0.000073354169687	0.401348903804408
150.727928	158.414333	166.100738	0.000675064404172	0.000000253184344	0.000062437661245	0.272607060674077
166.060497	174.983667	183.906837	0.000811676552099	0.000000300738567	0.000066618161681	0.082770635342554
183.853142	194.376667	204.900192	0.000346970430732	0.000000208744607	0.000034521418203	0.257607553138180
194.214375	201.645000	209.075625	0.000032288403941	0.000000055379098	0.000006146850394	0.335313920319452

Table A.XIII.1. Deuteron Yields from Hydrogen 800 MeV/n on 20 g/cm^2 Aluminium at12.7 deg

KE_left(MeV)	KE_mid(MeV)	KE_right(MeV)	Norm_Cts(#/SP*ster*MeV)	Y_stat(#/SP*ster*MeV)	Y_syst_tot(#/SP*ster*MeV)	X_tot(MeV)
44.276238	45.497400	46.718562	0.000039942810126	0.000000016368589	0.000014225778734	0.141179851673707
46.762649	48.211100	49.659551	0.000031258264192	0.000000018365962	0.000013359160112	0.163807235297529
49.659549	51.108000	52.556451	0.000019054667998	0.000000013736133	0.000009987346571	0.317316039665504
52.487751	54.050033	55.612315	0.000032661310261	0.000000018435669	0.000012456443111	0.057630784782527
55.681028	57.406433	59.131838	0.000025990476864	0.000000017960932	0.000010972271317	0.168327974570420
59.075710	60.875200	62.674690	0.000049377854786	0.000000021567632	0.000012869953931	0.182364960268825
62.730765	64.738800	66.746835	0.000027323608124	0.000000018079124	0.000009515907196	0.143426585530159
66.667922	68.823967	70.980012	0.000052775086229	0.000000025899202	0.000012824291108	0.108725444271426
71.045278	73.355633	75.665988	0.000026194538277	0.000000019764977	0.000009050782052	0.105848529299466
75.679668	78.271233	80.862798	0.000030773439816	0.000000022761564	0.000009288052303	0.112382267981875
80.808248	83.637933	86.467618	0.000049729912225	0.000000027444083	0.000010363714444	0.102154002970907
86.456720	89.563900	92.671080	0.000032512898057	0.000000021686432	0.000007330542939	0.098921607541376
92.673107	96.103567	99.534027	0.000036445348323	0.000000028144544	0.000008732638820	0.071534607096065
99.525370	103.349000	107.172630	0.000039375564191	0.000000032190769	0.000008973822304	0.056075962935304
107.164458	111.459333	115.754208	0.000031477588647	0.000000029119407	0.000007229256567	0.030908642381426
115.715352	120.521667	125.327982	0.000030467750733	0.000000029097944	0.000006529714519	0.031943571845991
125.326357	130.768667	136.210977	0.000019474629129	0.000000025863607	0.000004995974051	0.044646859311872
136.178630	142.393000	148.607370	0.000026722529306	0.000000032273699	0.000005448144417	0.074707273603177
148.590180	155.705000	162.819820	0.000032570152615	0.000000036156869	0.000005456782663	0.115959327027713
162.794725	171.066000	179.337275	0.000015037433546	0.000000027081493	0.000003534648138	0.139933969783287
179.409385	185.697000	191.984615	0.000004940863956	0.000000012024054	0.000001336064496	0.181184987228523
198.874835	202.473000	206.071165	0.000001490542442	0.000000006462450	0.000000628597000	0.176093000000000

Table A.XIII.2. Deuteron Yields from Hydrogen 800 MeV/n on 20 g/cm^2 Aluminium at10.0 deg

KE_left(MeV)	KE_mid(MeV)	KE_right(MeV)	Norm_Cts(#/SP*ster*MeV)	Y_stat(#/SP*ster*MeV)	Y_syst_tot(#/SP*ster*MeV)	X_tot(MeV)
44.343166	45.538567	46.733968	0.000062333631448	0.000000021253170	0.000018821433823	0.107609504650839
46.721542	48.175500	49.629458	0.000061392168386	0.000000022827039	0.000016645236430	0.152458011605065
49.641890	51.108300	52.574711	0.000056337367624	0.000000022538509	0.000016302651683	0.314465361763422
52.520145	54.057967	55.595789	0.000062038586049	0.000000026541579	0.000018452110256	0.067559729223647
55.650355	57.393400	59.136445	0.000043176973777	0.000000020340747	0.000012362956312	0.154316134969549
59.095755	60.879500	62.663245	0.000052284447000	0.000000023623727	0.000014014711717	0.203812685611102
62.703965	64.729400	66.754835	0.000033560585072	0.000000022654637	0.000011806356522	0.136549823472057
66.682508	68.828633	70.974758	0.000037368955448	0.000000025656526	0.000012611477288	0.114388194335124
71.047045	73.360900	75.674755	0.000034714483149	0.000000021115909	0.000009662009329	0.112139344765073
75.665617	78.265067	80.864517	0.000040694365589	0.000000024344061	0.000009931240787	0.100176950826625
80.812620	83.639700	86.466780	0.000043627030281	0.000000027643768	0.000010351370578	0.098785843505130
86.456708	89.563733	92.670758	0.000041828378242	0.000000029807413	0.000010179588389	0.096668492549744
92.673460	96.105700	99.537940	0.000031763375099	0.000000029508304	0.000009008312232	0.069103184610245
99.534687	103.349667	107.164647	0.000028390745121	0.000000025268974	0.000006962113305	0.058290175109533
107.159668	111.460333	115.760998	0.000046019288902	0.000000034002184	0.000008438406779	0.035782752616392
115.724358	120.528333	125.332308	0.000052674258643	0.000000035649841	0.000007972599252	0.032364352567910
125.329777	130.772667	136.215557	0.000061819538692	0.000000048502812	0.000009535724592	0.038472248278857
136.179427	142.396667	148.613907	0.000134271591521	0.000000079825182	0.000014050872024	0.068381959556377
148.599440	155.715000	162.830560	0.000295602196778	0.000000121782562	0.000020378498336	0.098677961952049
162.804447	171.076667	179.348887	0.000155341008789	0.000000091639195	0.000012885742299	0.121200138780572
179.264635	188.961000	198.657365	0.000085050130383	0.000000072236485	0.000008360379768	0.226306261962766
198.893195	202.490000	206.086805	0.000009382624997	0.000000013673600	0.000001340620000	0.159006000000000

Table A.XIII.3. Deuteron Yields from Hydrogen 800 MeV/n on 20 g/cm^2 Aluminium at7.20 deg

KE_left(MeV)	KE_mid(MeV)	KE_right(MeV)	Norm_Cts(#/SP*ster*MeV)	Y_stat(#/SP*ster*MeV)	Y_syst_tot(#/SP*ster*MeV)	X_tot(MeV)
44.351284	45.555833	46.760383	0.000062600643196	0.000000022068286	0.000019389802684	0.104898386094020
46.720193	48.155400	49.590608	0.000055330834297	0.000000020732812	0.000015191244238	0.156493343255304
49.630817	51.106200	52.581584	0.000045523965929	0.000000019337537	0.000013873573342	0.309526541133390
52.533986	54.059900	55.585814	0.000049883481035	0.000000022530204	0.000015744853690	0.085782542151011
55.633402	57.385267	59.137132	0.000044003862011	0.000000022040014	0.000013320128506	0.146442989078651
59.112910	60.889000	62.665090	0.000064399429707	0.000000025187062	0.000015029540047	0.209436897199705
62.689280	64.723400	66.757520	0.000063054328707	0.000000025988650	0.000013617796563	0.132818330589009
66.689790	68.831100	70.972410	0.000050225189957	0.000000026541579	0.000013259718723	0.119020988313238
71.040150	73.362600	75.685050	0.000051841626909	0.000000028726749	0.000013128437271	0.114672002687055
75.664612	78.261267	80.857922	0.000043884501941	0.000000026654521	0.000010902811729	0.093727402676378
80.814078	83.639933	86.465788	0.000058029670690	0.000000031315772	0.000011857249002	0.097580974352637
86.456157	89.563167	92.670177	0.000051624994423	0.000000032177292	0.000010931556338	0.095853152997124
92.673248	96.106433	99.539618	0.000055018412940	0.000000032490348	0.000010121924779	0.068412282048986
99.542588	103.353333	107.164078	0.000060153311307	0.000000036829119	0.000010309793696	0.056227796045195
107.157077	111.460667	115.764257	0.000052265254517	0.000000037788734	0.000009344632234	0.038608298233273
115.728792	120.531667	125.334542	0.000058354248792	0.000000043431887	0.000009682555101	0.034714803234707
125.331770	130.775000	136.218230	0.000067210520173	0.000000049599962	0.000009711188455	0.035990364470230
136.181623	142.400333	148.619043	0.000268873547863	0.000000109071279	0.000020360049884	0.060997462040482
148.602343	155.720333	162.838323	0.000309555747324	0.000000124550277	0.000021150661280	0.089504661916238
162.811912	171.082667	179.353422	0.000214100388107	0.000000105969894	0.000015093428145	0.111068394840702
179.270095	188.969000	198.667905	0.000189873040499	0.000000110919338	0.000013675748334	0.212895983629189
198.902820	202.499000	206.095180	0.000026480734532	0.000000025448900	0.000002522820000	0.149778000000000

Table A.XIII.4. Proton Yields from Hydrogen 800 MeV/n on 20 g/cm^2 Aluminium at12.7 deg

KE_left(MeV)	KE_mid(MeV)	KE_right(MeV)	Norm_Cts(#/SP*ster*MeV)	Y_stat(#/SP*ster*MeV)	Y_syst_tot(#/SP*ster*MeV)	X_tot(MeV)
46.580420	48.257000	49.933580	0.000084133698688	0.000000033691386	0.000021381817835	0.292910677775666
49.933520	51.610100	53.286680	0.000131858691228	0.000000038229382	0.000024578499910	0.125746068589559
53.276110	55.264100	57.252090	0.000106346516525	0.000000041287311	0.000022252489165	0.291773016111731
57.262700	59.261300	61.259900	0.000116002240508	0.000000042126427	0.000022648914502	0.271969971779974
61.191563	63.425233	65.658903	0.000125117235721	0.000000048321610	0.000023533354427	0.129480104434780
65.727258	68.055933	70.384608	0.000125144718935	0.000000047189434	0.000021877043252	0.298018458731150
70.360050	73.000600	75.641150	0.000150591997500	0.000000055932494	0.000023101146604	0.178409131738148
75.575060	78.397800	81.220540	0.000125429505494	0.000000055044787	0.000021118031903	0.206846920725255
81.246545	84.331600	87.416655	0.000155819984506	0.000000062175815	0.000022020425367	0.195175574520097
87.425507	90.836867	94.248227	0.000138501631329	0.000000061947181	0.000019844855467	0.175412367112385
94.236825	98.027800	101.818775	0.000149638285440	0.000000069217501	0.000020044816417	0.164960325216580
101.796430	106.013000	110.229570	0.000152245259382	0.000000073442153	0.000019230848271	0.190180406725193
110.235348	114.918333	119.601318	0.000136907360010	0.000000077202467	0.000018158533810	0.149321155574353
119.589197	124.923667	130.258137	0.000111882814833	0.000000069348414	0.000014341590625	0.137333606825824
130.201480	136.228000	142.254520	0.000068394737330	0.000000056346699	0.000010196429274	0.102285953136978
142.240653	149.116333	155.992013	0.000034268972151	0.000000041700125	0.000006473322881	0.074609085296966
155.965995	163.935000	171.904005	0.000021289346153	0.000000031674034	0.000004270577040	0.060864855642727
171.848398	181.109333	190.370268	0.000006805650706	0.000000022721304	0.000002633563404	0.014432054259671
190.303953	201.246333	212.188713	0.000006244593491	0.000000018066735	0.000001741835399	0.068901198214980
212.077642	225.164667	238.251692	0.000005381826089	0.000000020247619	0.000001666596211	0.154814018239499
238.421210	248.657000	258.892790	0.000001376649001	0.000000008780641	0.000000610147257	0.185375081917716

Table A.XIII.5. Proton Yields from Hydrogen 800 MeV/n on 20 g/cm^2 Aluminium at10.0 deg

KE_left(MeV)	KE_mid(MeV)	KE_right(MeV)	Norm_Cts(#/SP*ster*MeV)	Y_stat(#/SP*ster*MeV)	Y_syst_tot(#/SP*ster*MeV)	X_tot(MeV)
46.520592	48.230967	49.941342	0.000117354970975	0.000000039576457	0.000024793122224	0.249647018436031
49.941358	51.651733	53.362108	0.000123725898254	0.000000042677890	0.000026721574132	0.169861616050390
53.294268	55.230633	57.166998	0.000163649325820	0.000000051099860	0.000028738241992	0.227319871666099
57.234830	59.267300	61.299770	0.000158457831198	0.000000049866999	0.000026603897072	0.276102271357915
61.209432	63.410667	65.611902	0.000159862599350	0.000000053292501	0.000026460968028	0.111142285028561
65.702265	68.064600	70.426935	0.000188762327984	0.000000060086160	0.000027801210743	0.302126418472467
70.363673	72.984433	75.605193	0.000161645785407	0.000000060179965	0.000025085234661	0.153968744552036
75.592603	78.404533	81.216463	0.000164818392624	0.000000061466119	0.000024070042818	0.222093673307503
81.252078	84.332833	87.413588	0.000143694128755	0.000000062412301	0.000022023119952	0.198634393972947
87.430420	90.842400	94.254380	0.000156647542133	0.000000065944463	0.000021236057192	0.182789549865412
94.225180	98.020600	101.816020	0.000181855015111	0.000000074261395	0.000021801403316	0.154331510823616
101.787582	106.011667	110.235752	0.000155390707480	0.000000071967285	0.000018829760040	0.182398274418811
110.225657	114.918667	119.611677	0.000179077646549	0.000000081477003	0.000019550594648	0.150382789012107
119.593030	124.921000	130.248970	0.000151498437760	0.000000079540858	0.000016716357579	0.135240703993472
130.205367	136.231667	142.257967	0.000149307592495	0.000000085574091	0.000015940983662	0.106458352772622
142.242785	149.123000	156.003215	0.000188232263918	0.000000101264406	0.000016916433876	0.086395252947196
155.966457	163.932667	171.898877	0.000207877691114	0.000000112679516	0.000016602129907	0.057615390723834
171.845372	181.109667	190.373962	0.000171943318050	0.000000108825397	0.000013663332284	0.010388288784251
190.311752	201.254667	212.197582	0.000170450894492	0.000000123803703	0.000013264852224	0.057818926192035
212.089648	225.177333	238.265018	0.000143802378821	0.000000128620186	0.000011695201998	0.132545399718474
238.437680	248.674500	258.911320	0.000033326210541	0.000000054869479	0.000003981701526	0.161108835890525

Table A.XIII.6. Proton Yields from Hydrogen 800 MeV/n on 20 g/cm^2 Aluminium at7.20 deg

KE_left(MeV)	KE_mid(MeV)	KE_right(MeV)	Norm_Cts(#/SP*ster*MeV)	Y_stat(#/SP*ster*MeV)	Y_syst_tot(#/SP*ster*MeV)	X_tot(MeV)
46.483020	48.210300	49.937580	0.000121578671295	0.000000038368096	0.000023865773184	0.216865057824561
49.937587	51.664867	53.392147	0.000130295765538	0.000000040507548	0.000025214112780	0.187100647149495
53.310397	55.221967	57.133537	0.000145098162404	0.000000045600248	0.000026166445735	0.195211661494799
57.215262	59.264667	61.314072	0.000134347572856	0.000000045934176	0.000024185611790	0.269935398992055
61.232010	63.417700	65.603390	0.000138664138314	0.000000050620816	0.000024945094714	0.101805646729895
65.685450	68.064600	70.443750	0.000165371240485	0.000000057378736	0.000026211565003	0.298422227158099
70.371847	72.983167	75.594487	0.000164103178846	0.000000057967424	0.000024353332994	0.144040793028225
75.597888	78.404733	81.211578	0.000181930923711	0.000000065372399	0.000025514138486	0.228318786587963
81.258407	84.337267	87.416127	0.000138253762337	0.000000058883428	0.000020845382458	0.203562024907914
87.430453	90.842933	94.255413	0.000172344356030	0.000000071526821	0.000023069264070	0.184622644846075
94.224110	98.021900	101.819690	0.000176019444554	0.000000075593429	0.000022036194554	0.154374458433544
101.781378	106.009333	110.237288	0.000181348029031	0.000000078010890	0.000020633578429	0.176796768785207
110.219208	114.917333	119.615458	0.000198241979355	0.000000085690782	0.000020681246443	0.149722208865085
119.593453	124.918333	130.243213	0.000189075156611	0.000000092087830	0.000019478803147	0.133450043633564
130.207023	136.233333	142.259643	0.000206208321927	0.000000096636293	0.000018540769086	0.108344925694977
142.244415	149.127000	156.009585	0.000253174971163	0.000000117397481	0.000020224506010	0.093301970083220
155.966403	163.931333	171.896263	0.000253312135659	0.000000130322546	0.000019479964470	0.055670738791667
171.843920	181.110000	190.376080	0.000188945225434	0.000000115900417	0.000014788395983	0.008273366785130
190.316033	201.259333	212.202633	0.000107352450178	0.000000101038553	0.000010373870639	0.052890424725941
212.095875	225.184000	238.272125	0.000096940916281	0.000000106113403	0.000009386936277	0.120791085614502
238.446580	248.684000	258.921420	0.000014260609035	0.000000036398923	0.000002583200209	0.148131825473664

Table A.XIII.7. Proton Yields from Hydrogen 800 MeV/n on 20 g/cm^2 Aluminium at32.7 deg

KE_left(MeV)	KE_mid(MeV)	KE_right(MeV)	Norm_Cts(#/SP*ster*MeV)	Y_stat(#/SP*ster*MeV)	Y_syst_tot(#/SP*ster*MeV)	X_tot(MeV)
46.320611	47.984067	49.647523	0.000059124076999	0.000000029309985	0.000016662374191	0.091048810299421
49.738572	51.565167	53.391762	0.000048581379574	0.000000028681215	0.000014098899769	0.235269166763709
53.391772	55.218367	57.044962	0.000053721508103	0.000000030500893	0.000014789724144	0.398633704539644
56.982570	59.076200	61.169830	0.000043180342071	0.000000030732961	0.000013024733833	0.150608875406099
61.232197	63.399367	65.566537	0.000060934754011	0.000000036292309	0.000014601885558	0.260468261715319
65.494848	67.909533	70.324218	0.000074676795950	0.000000042319362	0.000015781388352	0.238923557819232
70.375600	72.910100	75.444600	0.000064211452892	0.000000038549543	0.000012823826984	0.216718854717350
75.464920	78.331600	81.198280	0.000060209998029	0.000000040964659	0.000012484094957	0.279168242658437
81.121235	84.234200	87.347165	0.000066516479970	0.000000045601507	0.000012665351609	0.237661111956184
87.326355	90.742300	94.158245	0.000074548575593	0.000000050664341	0.000012518016509	0.220141811498952
94.156243	97.937133	101.718023	0.000067484126364	0.000000049773714	0.000011011995391	0.207066198192752
101.730877	105.928667	110.126457	0.000072602755791	0.000000053792504	0.000010605077542	0.221628081605288
110.098675	114.818000	119.537325	0.000073844004514	0.000000059843141	0.000010457459797	0.162438420080103
119.544775	124.851000	130.157225	0.000072689327353	0.000000062868625	0.000009530423585	0.158237793346501
130.139513	136.177333	142.215153	0.000079636134095	0.000000070133039	0.000009224107944	0.149478701372604
142.176457	149.072667	155.968877	0.000079246735117	0.000000073049989	0.000008281375834	0.090960940240798
155.943415	163.914000	171.884585	0.000062969105514	0.000000073015301	0.000007031529445	0.059915740102748
171.832433	181.109333	190.386233	0.000080499184905	0.000000089571091	0.000007490658679	0.021852730364227
190.312152	201.271667	212.231182	0.000153135597279	0.000000125972533	0.000010433820397	0.109909028995165
212.120000	225.231000	238.342000	0.000090249070629	0.000000112364708	0.000006830930891	0.205771842142311
238.196260	254.130000	270.063740	0.000060408902629	0.000000102417468	0.000004852417278	0.354560566118118
269.848850	289.609000	309.369150	0.000043960462284	0.000000093310986	0.000003838863893	0.573482314546839
309.033400	334.198000	359.362600	0.000037382169982	0.000000097830667	0.000003163800176	0.870917136495201
358.780017	391.862667	424.945317	0.000025515909879	0.000000092498650	0.000002429386086	1.335764756132606
423.893600	469.390000	514.886400	0.000014766912924	0.000000072251822	0.000001681664337	2.083266962777455
512.681700	579.456000	646.230300	0.000006536654617	0.000000055089985	0.000000905592975	3.436384162255437
637.986600	712.390500	786.794400	0.000004635674906	0.000000046337101	0.000000454074303	4.514593443545055

Table A.XIII.8. Proton Yields from Hydrogen 800 MeV/n on 20 g/cm^2 Aluminium at30.0 deg

KE_left(MeV)	KE_mid(MeV)	KE_right(MeV)	Norm_Cts(#/SP*ster*MeV)	Y_stat(#/SP*ster*MeV)	Y_syst_tot(#/SP*ster*MeV)	X_tot(MeV)
46.530305	48.127400	49.724495	0.000062657652554	0.000000030292705	0.000016842848168	0.234378155561669
49.641727	51.432367	53.223007	0.000071146947841	0.000000035134242	0.000017964658229	0.081864980816608
53.305780	55.234300	57.162820	0.000056392517420	0.000000031669009	0.000014823681502	0.430443507777734
57.124202	59.091367	61.058532	0.000080897133248	0.000000034617170	0.000015319361964	0.200989849254526
61.097170	63.365800	65.634430	0.000072385758808	0.000000038833136	0.000015860703705	0.223373274647819
65.573225	67.910100	70.246975	0.000071926916131	0.000000043863107	0.000015813967817	0.289951151655050
70.308170	72.923000	75.537830	0.000079268012439	0.000000045342909	0.000015322929684	0.232582664506622
75.457087	78.298667	81.140247	0.000066454862634	0.000000043970246	0.000013517120393	0.223807590626413
81.139865	84.230800	87.321735	0.000087844544151	0.000000047631996	0.000013356526138	0.221749875612141
87.333493	90.744633	94.155773	0.000071327894648	0.000000047187175	0.000011947652552	0.207811020805466
94.150242	97.939467	101.728692	0.000065925369153	0.000000047767654	0.000010816488961	0.205651867579752
101.708863	105.925333	110.141803	0.000094294628227	0.000000061619361	0.000012510456698	0.221881619387817
110.152553	114.839333	119.526113	0.000087655797152	0.000000062490857	0.000011393300889	0.195724529045927
119.513358	124.855333	130.197308	0.000077236693245	0.000000058411859	0.000009406691247	0.166972674937698
130.139740	136.174000	142.208260	0.000057194685579	0.000000051783812	0.000007588113941	0.141340411118724
142.192462	149.082667	155.972872	0.000033714315451	0.000000041070225	0.000005157792236	0.106739980879753
155.931767	163.909667	171.887567	0.000013213392608	0.000000027297688	0.000003071551203	0.056532329312439
171.828220	181.111000	190.393780	0.000008942869495	0.000000026415385	0.000002480297891	0.010789756949779
190.332148	201.295333	212.258518	0.000013153148487	0.000000031832381	0.000002883486801	0.076283588373057
212.154302	225.266667	238.379032	0.000005310729812	0.000000021722826	0.000001583758514	0.144674115669183
238.238755	254.181000	270.123245	0.000002464862641	0.000000015473714	0.000000983276124	0.266351660880874
269.910650	289.691000	309.471350	0.000000903593971	0.000000014271785	0.000000572166214	0.430560903897463
309.131083	334.314333	359.497583	0.000000705244903	0.000000012529645	0.000000432474732	0.668431258958616
379.736200	402.866500	425.996800	0.000000977153248	0.000000010315054	0.000000302869167	0.894639103725072
425.669100	454.250500	482.831900	0.000000371688235	0.000000008431376	0.000000157222918	1.202431306979322
517.359150	536.636000	555.912850	0.000000358350080	0.000000005514330	0.000000100225000	1.255010000000000
638.996500	713.108500	787.220500	0.000000146484391	0.000000010151002	0.000000088549568	3.493433638542459

Table A.XIII.9. Proton Yields from Hydrogen 800 MeV/n on 20 g/cm^2 Aluminium at27.2 deg

KE_left(MeV)	KE_mid(MeV)	KE_right(MeV)	Norm_Cts(#/SP*ster*MeV)	Y_stat(#/SP*ster*MeV)	Y_syst_tot(#/SP*ster*MeV)	X_tot(MeV)
46.480030	48.153100	49.826170	0.000093898776103	0.000000036125267	0.000021138106606	0.270885923065411
49.826130	51.499200	53.172270	0.000117909108684	0.000000038341747	0.000022593444180	0.135864563076080
53.156920	55.146500	57.136080	0.000092282422017	0.000000040272424	0.000019618664963	0.308546194251363
57.151455	59.156400	61.161345	0.000090169253174	0.000000035578212	0.000017445696657	0.274311567816598
61.083535	63.307900	65.532265	0.000100001116392	0.000000042160245	0.000019113282742	0.137589103351610
65.610077	67.954667	70.299257	0.000107743588786	0.000000046324140	0.000019175353865	0.334408736454358
70.241543	72.873833	75.506123	0.000109104865891	0.000000051871590	0.000019227813718	0.178594426475241
75.483860	78.297000	81.110140	0.000126338675279	0.000000054421237	0.000018831279436	0.241401090759528
81.153087	84.231567	87.310047	0.000114920391825	0.000000057408071	0.000018544875743	0.223776232976717
87.334892	90.745467	94.156042	0.000110546535061	0.000000058691549	0.000017119640060	0.205037994957032
94.131570	97.929400	101.727230	0.000120232225822	0.000000063602348	0.000016563283553	0.188037725061116
101.687988	105.920333	110.152678	0.000138688601279	0.000000070798361	0.000016491042187	0.205805458717596
110.127077	114.835667	119.544257	0.000138799016120	0.000000075945115	0.000016020850855	0.197907584030123
119.516332	124.842667	130.169002	0.000137406878997	0.000000080897857	0.000014776814617	0.155856910659746
130.142800	136.176000	142.209200	0.000142053333264	0.000000089264526	0.000014508453785	0.144766398963434
142.193547	149.093667	155.993787	0.000180961578298	0.000000104760472	0.000014288882268	0.124164473993208
155.930600	163.902000	171.873400	0.000123764574011	0.000000090172558	0.000010973496356	0.042835672283409
171.823317	181.113667	190.404017	0.000114282171385	0.000000089240204	0.000010124623994	0.017053466926405
190.351813	201.316333	212.280853	0.000138665051455	0.000000109225707	0.000010859185383	0.038044062563876
212.182940	225.297000	238.411060	0.000117467863270	0.000000110026583	0.000009266279189	0.090587524619839
238.265557	254.214667	270.163777	0.000092145796656	0.000000108700369	0.000007634886918	0.207574054481768
269.954717	289.750667	309.546617	0.000056712553459	0.000000096147591	0.000005348869239	0.326915631408166
309.200783	334.398333	359.595883	0.000033001975205	0.000000081180334	0.000003452984449	0.521067796522679
359.023200	392.169000	425.314800	0.000021562915124	0.000000072645529	0.000002378444193	0.801290814005752
424.259083	469.868333	515.477583	0.000013026874866	0.000000065992535	0.000001591347243	1.248736962564575
513.254883	580.240333	647.225783	0.000003344528808	0.000000041900249	0.000000706585751	2.063450901258375
639.751550	713.645500	787.539450	0.000000899340996	0.000000023025385	0.000000226417698	2.730371393437164

Table A.XIV.1. Deuteron Yields from Hydrogen 800 MeV/n on 40 g/cm^2 Aluminium at12.7 deg

KE_left(MeV)	KE_mid(MeV)	KE_right(MeV)	Norm_Cts(#/SP*ster*MeV)	Y_stat(#/SP*ster*MeV)	Y_syst_tot(#/SP*ster*MeV)	X_tot(MeV)
44.124919	45.392100	46.659281	0.000044513625180	0.000000018915113	0.000016079215890	0.231593858478587
46.659219	47.926400	49.193581	0.000069286307723	0.000000025290214	0.000021716908881	0.111573120719150
49.136906	50.681600	52.226295	0.000043954617938	0.000000019906641	0.000014134809956	0.216029945114676
52.282970	53.885900	55.488830	0.000055392029735	0.000000026464316	0.000017880599626	0.260077514897001
55.488870	57.091800	58.694730	0.000043794186119	0.000000024085321	0.000016173954204	0.115305603993822
58.679217	60.603767	62.528317	0.000063703686792	0.000000026932817	0.000015516578050	0.259160844390525
62.543827	64.483867	66.423907	0.000049632947994	0.000000029023853	0.000016154207288	0.217462283786614
66.361427	68.567067	70.772707	0.000061160045017	0.000000030007601	0.000015146038379	0.133752102466204
70.817417	73.114967	75.412517	0.000054954524522	0.000000031060447	0.000014799766639	0.230152088245230
75.430245	78.053400	80.676555	0.000053567606837	0.000000033326671	0.000013938564845	0.145750975122844
80.594417	83.434667	86.274917	0.000065196397280	0.000000035340808	0.000013857845773	0.110405715843583
86.269022	89.386567	92.504112	0.000064600699654	0.000000037328100	0.000013390145438	0.107168350261120
92.507917	95.964867	99.421817	0.000053247692614	0.000000036171298	0.000011705279118	0.063726691358017
99.410178	103.258333	107.106488	0.000048839743635	0.000000036061449	0.000010287435269	0.063922405519035
107.117840	111.402000	115.686160	0.000055857500432	0.000000040290682	0.000010534996892	0.011863637679127
115.664282	120.523667	125.383052	0.000045739434239	0.000000037308907	0.000008577629000	0.080814546174064
125.358585	130.832000	136.305415	0.000029157363422	0.000000032708378	0.000006597227891	0.110437217091386
136.283153	142.538333	148.793513	0.000043800855740	0.000000045671410	0.000008096378813	0.188991034396053
148.770737	155.952667	163.134597	0.000053622001926	0.000000050449439	0.000008331891507	0.257576931005088
163.078690	171.415000	179.751310	0.000019473773207	0.000000032126976	0.000004269794046	0.403950595000181
179.704848	189.468333	199.231818	0.000015449746328	0.000000028674456	0.000003254631434	0.542979294114426
199.146278	210.742333	222.338388	0.000004329599508	0.000000016690247	0.000001560709802	0.732316176416307
222.637250	226.981000	231.324750	0.000000513682557	0.000000004670590	0.000000376453000	0.523136000000000

Table A.XIV.2. Deuteron Yields from Hydrogen 800 MeV/n on 40 g/cm^2 Aluminium at10.0 deg

KE_left(MeV)	KE_mid(MeV)	KE_right(MeV)	Norm_Cts(#/SP*ster*MeV)	Y_stat(#/SP*ster*MeV)	Y_syst_tot(#/SP*ster*MeV)	X_tot(MeV)
44.089655	45.384467	46.679279	0.000083433411649	0.000000028558583	0.000024130947288	0.216103044650000
46.679288	47.974100	49.268912	0.000090722695327	0.000000028134738	0.000023979088132	0.189120551884241
49.182206	50.663700	52.145194	0.000068127001402	0.000000026834169	0.000020394744894	0.154369635186781
52.231908	53.861733	55.491558	0.000067696089608	0.000000031083648	0.000020779585888	0.219355779271940
55.491542	57.121367	58.751192	0.000067599418688	0.000000029196558	0.000019610764896	0.135069444387137
58.687055	60.573200	62.459345	0.000079711707131	0.000000032065671	0.000019195835032	0.213011307136898
62.523487	64.489867	66.456247	0.000083370604143	0.000000034302747	0.000019343343083	0.220880134736015
66.377312	68.559267	70.741222	0.000076982601232	0.000000035933701	0.000018546060378	0.101862736170624
70.820138	73.125833	75.431528	0.000084017802279	0.000000038212540	0.000018499227982	0.231167052532233
75.409432	78.036067	80.662702	0.000077069918067	0.000000037202471	0.000016020175796	0.132080897404135
80.591658	83.424333	86.257008	0.000076826062137	0.000000041549505	0.000016316612551	0.122383296345539
86.271452	89.386267	92.501082	0.000075330295759	0.000000040571161	0.000014624067440	0.109451129082938
92.503602	95.961467	99.419332	0.000087984557456	0.000000046326840	0.000015328029454	0.056193619880107
99.406762	103.258667	107.110572	0.000065151032533	0.000000038409064	0.000011414260468	0.048562875191961
107.108467	111.398667	115.688867	0.000076028666295	0.000000042318739	0.000011497391671	0.019426744282378
115.661652	120.513667	125.365682	0.000063189093585	0.000000043253556	0.000010163777480	0.101551409896909
125.360470	130.832000	136.303530	0.000081321161345	0.000000051873306	0.000011282266527	0.110692901357433
136.280580	142.538000	148.795420	0.000173804114871	0.000000085472354	0.000018881138608	0.188452013739015
148.765590	155.953000	163.140410	0.000490448164119	0.000000165203575	0.000040018745118	0.257551124437460
163.075360	171.412000	179.748640	0.000204764726807	0.000000109494936	0.000019790353866	0.408763910629351
179.710050	189.472000	199.233950	0.000150415401321	0.000000103849440	0.000014850919467	0.536328127402433
199.152507	210.752667	222.352827	0.000133813658203	0.000000102281620	0.000012848088569	0.713970156839906
222.643235	226.991000	231.338765	0.000031674715862	0.000000026334100	0.000002428670000	0.512400000000000

Table A.XIV.3. Deuteron Yields from Hydrogen 800 MeV/n on 40 g/cm^2 Aluminium at7.20 deg

KE_left(MeV)	KE_mid(MeV)	KE_right(MeV)	Norm_Cts(#/SP*ster*MeV)	Y_stat(#/SP*ster*MeV)	Y_syst_tot(#/SP*ster*MeV)	X_tot(MeV)
44.056671	45.369867	46.683063	0.000053261417473	0.000000023775986	0.000019497966407	0.190953069752754
46.683037	47.996233	49.309429	0.000088149470999	0.000000029146475	0.000024348424050	0.227597538183083
49.229645	50.670733	52.111821	0.000072192861099	0.000000025796541	0.000019866963286	0.179509922497365
52.191632	53.839367	55.487102	0.000085012110739	0.000000030771332	0.000020808432100	0.183847254877521
55.487065	57.134800	58.782535	0.000081247352504	0.000000029840558	0.000020129139013	0.148522465957242
58.704423	60.565933	62.427443	0.000076035543392	0.000000031699359	0.000018691177310	0.174965156727569
62.505585	64.489500	66.473415	0.000096245440967	0.000000037074053	0.000020978025290	0.217448537842865
66.383682	68.550467	70.717252	0.000099867707952	0.000000038877574	0.000020545905848	0.096847393011118
70.806973	73.129933	75.452893	0.000084730894660	0.000000039721222	0.000019033183317	0.229250781826998
75.404670	78.022200	80.639730	0.000092582188345	0.000000040483011	0.000017783561513	0.126117617725558
80.595370	83.423300	86.251230	0.000077971415300	0.000000036133258	0.000014515926990	0.127228115456451
86.271313	89.384533	92.497753	0.000080732916022	0.000000043371245	0.000015778988589	0.112183883023231
92.499488	95.958133	99.416778	0.000087760871074	0.000000047161088	0.000015582633257	0.054271607882022
99.403440	103.258000	107.112560	0.000101474901138	0.000000050655967	0.000015255373301	0.039026494671907
107.101635	111.396000	115.690365	0.000067955112070	0.000000046256070	0.000012216538393	0.029413327401629
115.659670	120.507000	125.354330	0.000076111972154	0.000000050822497	0.000012020145740	0.115404453042073
125.362525	130.833000	136.303475	0.000101496659504	0.000000059914192	0.000013221608599	0.110984391520884
136.279253	142.538333	148.797413	0.000358409660033	0.000000133258429	0.000032922426507	0.187252708686523
148.763113	155.954333	163.145553	0.000519452971204	0.000000167940820	0.000042627876435	0.255633535004702
163.074925	171.412000	179.749075	0.000276284095401	0.000000127968593	0.000024039558188	0.409286489613327
179.715128	189.476333	199.237538	0.000376863642531	0.000000162052566	0.000029917484445	0.528479109835952
199.159168	210.762333	222.365498	0.000294713176527	0.000000156698061	0.000024219420708	0.697434704890716
222.651500	227.002000	231.352500	0.000039968451315	0.000000035481100	0.000003222130000	0.502299000000000

Table A.XIV.4. Proton Yields from Hydrogen 800 MeV/n on 40 g/cm^2 Aluminium at12.7 deg

KE_left(MeV)	KE_mid(MeV)	KE_right(MeV)	Norm_Cts(#/SP*ster*MeV)	Y_stat(#/SP*ster*MeV)	Y_syst_tot(#/SP*ster*MeV)	X_tot(MeV)
46.121355	47.823300	49.525245	0.000164038152540	0.000000047299908	0.000032370741469	0.257527113855998
49.525255	51.227200	52.929145	0.000158936849568	0.000000049639376	0.000033476784537	0.337823797592769
52.824907	54.705367	56.585827	0.000195020505568	0.000000059913061	0.000037879088205	0.248831334941964
56.690040	58.794600	60.899160	0.000162684979232	0.000000054074830	0.000030303274846	0.295710494859415
60.899173	63.003733	65.108293	0.000227461287324	0.000000063999192	0.000037048774003	0.226608644220405
65.063250	67.530100	69.996950	0.000195562162351	0.000000066650850	0.000032616752644	0.330627246129898
70.042000	72.553900	75.065800	0.000210314822543	0.000000071922571	0.000034706320691	0.270008974590550
75.048250	77.953100	80.857950	0.000190669259915	0.000000071710679	0.000030317265025	0.333556485030647
80.771707	83.867467	86.963227	0.000236423292094	0.000000082787912	0.000033991830640	0.210855490580634
87.004195	90.403200	93.802205	0.000248498225625	0.000000086847797	0.000033416250221	0.305051920223837
93.832375	97.618700	101.405025	0.000212919639154	0.000000089930901	0.000030142714041	0.261509606731760
101.373243	105.613333	109.853423	0.000242633662247	0.000000096599811	0.000030509660690	0.231592549783019
109.821225	114.570000	119.318775	0.000252116374924	0.000000104044301	0.000030387404582	0.247665701268868
119.311470	124.616000	129.920530	0.000203907555586	0.000000096408019	0.000024769246497	0.210041513011119
129.904748	135.982333	142.059918	0.000115303340816	0.000000075699852	0.000015776311128	0.184664937976894
142.008192	148.932667	155.857142	0.000074581268068	0.000000065116576	0.000011304162759	0.127069459341299
155.804698	163.814333	171.823968	0.000039401895791	0.000000047553447	0.000007041664966	0.060474873597718
171.774785	181.108000	190.441215	0.000013134830397	0.000000029899108	0.000003503069181	0.027818680149755
190.378578	201.381333	212.384088	0.000009771824489	0.000000026022670	0.000002562643648	0.120821022069878
212.290755	225.483000	238.675245	0.000008742002246	0.000000026757161	0.000002203750478	0.243057834839776
238.524583	254.558333	270.592083	0.000006299843912	0.000000023919762	0.000001669522641	0.433896676158046
270.372700	290.284000	310.195300	0.000002065945287	0.000000016651111	0.000000893660911	0.711040415630504
310.824450	318.570000	326.315550	0.000001771621058	0.000000007944990	0.000000365652000	0.547014000000000

Table A.XIV.5. Proton Yields from Hydrogen 800 MeV/n on 40 g/cm^2 Aluminium at10.0 deg

KE_left(MeV)	KE_mid(MeV)	KE_right(MeV)	Norm_Cts(#/SP*ster*MeV)	Y_stat(#/SP*ster*MeV)	Y_syst_tot(#/SP*ster*MeV)	X_tot(MeV)
45.992980	47.746300	49.499620	0.000160245564453	0.000000047919477	0.000031737919669	0.159983046566544
49.499647	51.252967	53.006287	0.000200240351638	0.000000056536395	0.000037898428027	0.381781585263093
52.978120	54.759600	56.541080	0.000213462187760	0.000000061163776	0.000040403318738	0.370762217778511
56.569285	58.725100	60.880915	0.000223532416995	0.000000066332686	0.000037555824693	0.187516522440024
60.880885	63.036700	65.192515	0.000263946481864	0.000000072010211	0.000041411871361	0.270872431027966
65.095688	67.503433	69.911178	0.000240219442765	0.000000071101877	0.000036926658521	0.256555487530476
70.008022	72.570667	75.133312	0.000289261086592	0.000000081890342	0.000041217461043	0.283741678611021
75.053520	77.923500	80.793480	0.000270533609781	0.000000080997769	0.000037336878418	0.284709558743643
80.792528	83.869633	86.946738	0.000231701099718	0.000000081325780	0.000033608265059	0.221626089221215
87.021905	90.413500	93.805095	0.000262363465452	0.000000092118210	0.000035466275328	0.308930955647051
93.810502	97.613767	101.417032	0.000268187171110	0.000000097031831	0.000034291314393	0.258372471706817
101.378747	105.609667	109.840587	0.000264338018771	0.000000097703633	0.000031844812447	0.228634265784921
109.794355	114.555000	119.315645	0.000262704839749	0.000000105099314	0.000030937452780	0.222438516372502
119.285645	124.606000	129.926355	0.000282257727409	0.000000115883054	0.000031307898865	0.193062008436771
129.901022	135.970667	142.040312	0.000277782621083	0.000000121199924	0.000029470509663	0.164721968179141
141.999652	148.925667	155.851682	0.000318605190977	0.000000136725171	0.000031184530204	0.117320836939991
155.808592	163.808667	171.808742	0.000371309151680	0.000000159033719	0.000033825690044	0.043141818914598
171.774052	181.108667	190.443282	0.000302007943573	0.000000148792642	0.000026699917568	0.027260351023785
190.368115	201.373000	212.377885	0.000322900713708	0.000000175216553	0.000027955238386	0.137120101684691
212.283662	225.478667	238.673672	0.000317735506907	0.000000191175808	0.000027024782446	0.249916069523350
238.519448	254.552333	270.585218	0.000229935811193	0.000000185910431	0.000020944725476	0.444472981361072
270.368233	290.284333	310.200433	0.000045426205767	0.000000090018100	0.000006076025255	0.710135906106711
310.485900	326.656500	342.827100	0.000006741896776	0.000000027887315	0.000001306414326	0.823091324671206

Table A.XIV.6. Proton Yields from Hydrogen 800 MeV/n on 40 g/cm^2 Aluminium at7.20 deg

KE_left(MeV)	KE_mid(MeV)	KE_right(MeV)	Norm_Cts(#/SP*ster*MeV)	Y_stat(#/SP*ster*MeV)	Y_syst_tot(#/SP*ster*MeV)	X_tot(MeV)
45.882457	47.670067	49.457677	0.000172390494380	0.000000053018539	0.000034423585690	0.142374418186097
49.457657	51.245267	53.032877	0.000184453825777	0.000000056039801	0.000036457841082	0.371676813481821
53.032890	54.820500	56.608110	0.000231273597702	0.000000061428431	0.000041057106092	0.462868799666817
56.540655	58.662400	60.784145	0.000207461984893	0.000000061200944	0.000035070961473	0.119033064458116
60.851597	63.041567	65.231537	0.000247246855009	0.000000068446148	0.000038641983963	0.277374080861929
65.126140	67.496800	69.867460	0.000251770982896	0.000000070633817	0.000037870858413	0.241628471097675
69.972827	72.569267	75.165707	0.000226747493300	0.000000072728217	0.000034882333197	0.276834876738824
75.067603	77.915833	80.764063	0.000242019758474	0.000000079070838	0.000035579738535	0.253644560420305
80.802572	83.868267	86.933962	0.000283671659844	0.000000087780488	0.000037819333529	0.229284985229387
86.993562	90.412767	93.831972	0.000266302783460	0.000000089977876	0.000034960210783	0.303067877378979
93.800112	97.604567	101.409022	0.000291273816742	0.000000100588095	0.000036239858698	0.251184523597773
101.392708	105.602333	109.811958	0.000325811099663	0.000000111729921	0.000037746729668	0.223776394093211
109.778262	114.541667	119.305072	0.000306287217951	0.000000116773005	0.000035198492820	0.201594489681638
119.266472	124.597667	129.928862	0.000331282853614	0.000000125045160	0.000035120233614	0.180932409231320
129.895513	135.960333	142.025153	0.000354656655732	0.000000134775367	0.000035407222670	0.150077554023145
141.997595	148.925000	155.852405	0.000415645704162	0.000000160222874	0.000038972671885	0.116221935788946
155.811890	163.806000	171.800110	0.000444048340424	0.000000174070411	0.000039357803380	0.039094951652355
171.773115	181.109000	190.444885	0.000341165612741	0.000000167837560	0.000030394907272	0.026619144288651
190.360435	201.372000	212.383565	0.000289703201058	0.000000170336180	0.000025885833240	0.140057306369750
212.284685	225.477000	238.669315	0.000208208892644	0.000000159155463	0.000019441557746	0.252121675599303
238.517573	254.550333	270.583093	0.000127074608060	0.000000136977901	0.000013463681841	0.447370913928253
270.368383	290.288333	310.208283	0.000017604231954	0.000000054816753	0.000003302189488	0.703707489729930
310.496450	326.669500	342.842550	0.000004485851196	0.000000023314755	0.000001074080743	0.804975564073842

Table A.XIV.7. Proton Yields from Hydrogen 800 MeV/n on 40 g/cm^2 Aluminium at32.7 deg

KE_left(MeV)	KE_mid(MeV)	KE_right(MeV)	Norm_Cts(#/SP*ster*MeV)	Y_stat(#/SP*ster*MeV)	Y_syst_tot(#/SP*ster*MeV)	X_tot(MeV)
45.912420	47.418000	48.923580	0.000114071655355	0.000000042223129	0.000024859496447	0.247569957844242
48.912485	50.825700	52.738915	0.000124528419836	0.000000041152052	0.000024260912266	0.365475153208806
52.750065	54.674400	56.598735	0.000105436818706	0.000000046905689	0.000023093565000	0.421308770306292
56.598698	58.523033	60.447368	0.000132665010241	0.000000052888198	0.000025761182054	0.226948566481240
60.389205	62.681800	64.974395	0.000114584986273	0.000000055287312	0.000023912069625	0.377678162580205
65.032563	67.383333	69.734103	0.000104596853631	0.000000051619538	0.000021024195785	0.439923746567516
69.632297	72.249567	74.866837	0.000133701480417	0.000000061095873	0.000022671853651	0.210616154884330
74.968627	77.748367	80.528107	0.000116361906299	0.000000060100486	0.000020489635115	0.446042343484338
80.480870	83.644700	86.808530	0.000138407240143	0.000000064937976	0.000020703787108	0.297779186650108
86.736037	90.161567	93.587097	0.000135613709693	0.000000071333262	0.000020302261945	0.331667536682881
93.609902	97.400167	101.190432	0.000146962480665	0.000000075794373	0.000019912057393	0.328225216650092
101.188222	105.421667	109.655112	0.000140140458981	0.000000078027569	0.000018259907409	0.308747352055042
109.633187	114.372667	119.112147	0.000131921681973	0.000000083499832	0.000017134476424	0.282613820399852
119.118792	124.439667	129.760542	0.000146512138445	0.000000090736499	0.000016926853187	0.251784549285694
129.755107	135.839667	141.924227	0.000126822722606	0.000000095289853	0.000015100583128	0.225503077741502
141.880110	148.827000	155.773890	0.000144350561743	0.000000105683276	0.000015257953973	0.154465775401705
155.715780	163.752000	171.788220	0.000150113728074	0.000000113755438	0.000014529776786	0.073167919282565
171.743715	181.109000	190.474285	0.000137459212964	0.000000116074777	0.000012305923129	0.029897999364840
190.400347	201.450667	212.500987	0.000223605382129	0.000000154245890	0.000016017854156	0.172225657763325
212.407195	225.658000	238.908805	0.000136480045428	0.000000137473486	0.000010899654225	0.345370459844208
238.753217	254.860667	270.968117	0.000104558738224	0.000000137059337	0.000008225279329	0.624368703938626
270.757950	290.790000	310.822050	0.000103336807611	0.000000155748572	0.000007646741312	0.979170699768432
310.467983	335.997333	361.526683	0.000053380571242	0.000000124461977	0.000004616556388	1.514980128597732
360.932683	394.578333	428.223983	0.000034463115767	0.000000110161952	0.000003116651324	2.338117839481150
427.131133	473.551333	519.971533	0.000015734747852	0.000000080628632	0.000001883553274	3.686566271613736
517.654983	586.120333	654.585683	0.000010724695813	0.000000077228553	0.000001377381313	6.144864704816534
658.444650	689.232000	720.019350	0.000014027340800	0.000000058819122	0.000000761160852	5.102150000000000

Table A.XIV.8. Proton Yields from Hydrogen 800 MeV/n on 40 g/cm^2 Aluminium at30.0 deg

KE_left(MeV)	KE_mid(MeV)	KE_right(MeV)	Norm_Cts(#/SP*ster*MeV)	Y_stat(#/SP*ster*MeV)	Y_syst_tot(#/SP*ster*MeV)	X_tot(MeV)
46.076507	47.756567	49.436627	0.000102696412280	0.000000037440522	0.000022424284605	0.839289013646670
49.436607	51.116667	52.796727	0.000129262585177	0.000000046658837	0.000025450402365	0.889911380151417
52.685987	54.592567	56.499147	0.000123026133601	0.000000048543783	0.000026121699396	0.292968834280440
56.609928	58.709133	60.808338	0.000108910803719	0.000000048749922	0.000022387070722	0.542293253687523
60.808362	62.907567	65.006772	0.000127227653746	0.000000054338742	0.000024509541735	0.696184891902288
64.953708	67.423233	69.892758	0.000123306517803	0.000000057438961	0.000022767856015	0.499020208394410
69.945820	72.468400	74.990980	0.000133402692298	0.000000058788515	0.000022389828246	0.569691490655249
74.941520	77.840400	80.739280	0.000145540017057	0.000000065847176	0.000023158453574	0.594425386634016
80.696580	83.778700	86.860820	0.000147275444483	0.000000069619373	0.000021926905680	0.504851532399378
86.942655	90.329900	93.717145	0.000146779074714	0.000000070690084	0.000020474731627	0.606089947768481
93.727375	97.536100	101.344825	0.000144907832883	0.000000078719143	0.000020174563075	0.567572746599940
101.315628	105.536333	109.757038	0.000156429635332	0.000000086893977	0.000020215846809	0.510061966317819
109.708708	114.478333	119.247958	0.000159511167573	0.000000092696116	0.000019177858838	0.463711612907203
119.205230	124.546000	129.886770	0.000139736852154	0.000000089567465	0.000016361838526	0.430217766832101
129.841503	135.908333	141.975163	0.000094864714315	0.000000079509121	0.000012164669943	0.343724360862014
141.955843	148.892333	155.828823	0.000048035873393	0.000000056068889	0.000007179111240	0.272517803574372
155.812253	163.801333	171.790413	0.000032715617078	0.000000047694701	0.000005204897473	0.148110212974832
171.764100	181.111000	190.457900	0.000015159878482	0.000000034556027	0.000003157267511	0.052141990928809
190.358295	201.400000	212.441705	0.000024448018158	0.000000043291980	0.000004169720322	0.272208496699221
212.339675	225.525000	238.710325	0.000011935400248	0.000000033597080	0.000002664205561	0.580126247946945
238.564343	254.628333	270.692323	0.000003918330239	0.000000021033001	0.000001223559101	1.028587264284368
270.467967	290.398667	310.329367	0.000001646821514	0.000000015261516	0.000000669514055	1.661570116810302
309.989167	335.380667	360.772167	0.000000842089473	0.000000014621551	0.000000450848869	2.589538392262219
360.178250	393.609000	427.039750	0.000000375702826	0.000000011815570	0.000000264243203	4.027674590356078
425.961150	472.017000	518.072850	0.000000469238533	0.000000012417422	0.000000228264520	6.368234070611726
518.738200	560.595500	602.452800	0.000000208041420	0.000000008745559	0.000000148362393	7.801113661683184
710.440350	751.826000	793.211650	0.000000303052800	0.000000008421712	0.000000071586925	42.633600000000001

Table A.XIV.9. Proton Yields from Hydrogen 800 MeV/n on 40 g/cm^2 Aluminium at27.2 deg

KE_left(MeV)	KE_mid(MeV)	KE_right(MeV)	Norm_Cts(#/SP*ster*MeV)	Y_stat(#/SP*ster*MeV)	Y_syst_tot(#/SP*ster*MeV)	X_tot(MeV)
45.745552	47.464200	49.182849	0.000158353187449	0.000000047642488	0.000030312168660	0.381475835716877
49.269695	51.113000	52.956305	0.000149720539703	0.000000047521358	0.000027712963177	0.862577975970868
52.956295	54.799600	56.642905	0.000161710537036	0.000000052627996	0.000029519918620	0.643385945629060
56.540322	58.551867	60.563412	0.000144877633608	0.000000051585335	0.000027532036475	0.275419959594888
60.666022	62.927767	65.189512	0.000160761320747	0.000000056893807	0.000026593615574	0.744082145622377
65.166437	67.451267	69.736097	0.000161114558870	0.000000059756397	0.000026880146916	0.576741706354760
69.759180	72.442500	75.125820	0.000154491435739	0.000000063856437	0.000024827881198	0.536704215084995
75.042580	77.834200	80.625820	0.000186655888505	0.000000071157982	0.000026402503026	0.596565511729433
80.709058	83.816533	86.924008	0.000183906137890	0.000000073032894	0.000024977162952	0.569015307640313
86.849475	90.303000	93.756525	0.000196377687713	0.000000080984111	0.000025419012686	0.547813329270108
93.727373	97.525133	101.322893	0.000197513890482	0.000000083578923	0.000023841796394	0.543609681838909
101.318738	105.541333	109.763928	0.000200591618877	0.000000087587331	0.000022478990603	0.519792928237774
109.780275	114.492000	119.203725	0.000224523521748	0.000000098762163	0.000023837260989	0.485931301858606
119.178992	124.542667	129.906342	0.000220337205281	0.000000106962103	0.000021978273161	0.429714964540450
129.885962	135.932667	141.979372	0.000215480310746	0.000000111020498	0.000020328304658	0.384271029463581
141.955592	148.901667	155.847742	0.000257305484097	0.000000130129690	0.000021101300781	0.286581630232993
155.805050	163.826000	171.846950	0.000321623821020	0.000000158495008	0.000023007546773	0.195722889436187
171.765423	181.113333	190.461243	0.000186686469756	0.000000122852747	0.000015913889735	0.045805018693807
190.410297	201.442667	212.475037	0.000209710731670	0.000000136806583	0.000017701392037	0.192351744906694
212.364377	225.567667	238.770957	0.000199201779944	0.000000151157896	0.000017028950858	0.505422762389072
238.640617	254.714667	270.788717	0.000158423535962	0.000000147096436	0.000013719779634	0.879344649175737
270.562333	290.517333	310.472333	0.000098893756584	0.000000134071611	0.000009240148577	1.456027017412108
310.123733	335.538333	360.952933	0.000058027833049	0.000000111541763	0.000005849320236	2.313747073558387
360.373433	393.864333	427.355233	0.000032945085876	0.000000094818387	0.000003662364636	3.583993620111509
426.264000	472.409000	518.554000	0.000019562056696	0.000000085641174	0.000002337483486	5.682662091036208
516.276117	584.212667	652.149217	0.000005791273511	0.000000055815416	0.000001000124207	9.484550403413964
648.351050	719.726500	791.101950	0.000001603691238	0.000000032044011	0.000000327885636	42.220322313560089

Table A.XV.1. Deuteron Yields from Hydrogen 800 MeV/n on 60 g/cm^2 Aluminium at12.7 deg

KE_left(MeV)	KE_mid(MeV)	KE_right(MeV)	Norm_Cts(#/SP*ster*MeV)	Y_stat(#/SP*ster*MeV)	Y_syst_tot(#/SP*ster*MeV)	X_tot(MeV)
43.807814	45.143500	46.479185	0.000053464722715	0.000000021745276	0.000018394660900	22.158447836663044
46.479181	47.814867	49.150552	0.000057359931133	0.000000022647126	0.000019347260977	0.576991752310204
49.150548	50.486233	51.821919	0.000056604157140	0.000000021945546	0.000018647028969	0.293697331131371
51.796897	53.492167	55.187437	0.000058059785281	0.000000026890387	0.000018139491366	0.354863395723044
55.212462	56.932767	58.653072	0.000069337754431	0.000000028890460	0.000019621268418	0.774732808749571
58.650972	60.373367	62.095762	0.000053235066658	0.000000024665323	0.000016385434597	0.421115928828393
62.097835	64.200700	66.303565	0.000072832727195	0.000000034882286	0.000019489981492	0.379210765147879
66.303535	68.406400	70.509265	0.000070016102935	0.000000033595295	0.000018843257485	0.589121377485149
70.445252	72.866467	75.287682	0.000066450301027	0.000000031796155	0.000015902814346	0.321781572477356
75.304805	77.837400	80.369995	0.000060760866077	0.000000034123578	0.000015771396462	0.429933288799553
80.416930	83.287300	86.157670	0.000083065236659	0.000000038322439	0.000016640654501	0.361327710768217
86.078895	89.229900	92.380905	0.000068062981376	0.000000036376063	0.000014266188219	0.331955711332099
92.357245	95.829900	99.302555	0.000064160584889	0.000000039034391	0.000013669397521	0.257860818291884
99.299982	103.162667	107.025352	0.000086919969554	0.000000045556187	0.000015230794769	0.194501254389374
107.040355	111.349000	115.657645	0.000054191115955	0.000000040170940	0.000011300419554	0.107161110978797
115.627452	120.503667	125.379882	0.000059386978991	0.000000043167609	0.000011132181461	0.087967072321977
125.391312	130.884667	136.378022	0.000031202013429	0.000000034207970	0.000007216618849	0.191604021238178
136.365072	142.655667	148.946262	0.000048651659607	0.000000046140950	0.000009391450965	0.382945558220748
148.886205	156.129000	163.371795	0.000058662976029	0.000000054369299	0.000009842948188	0.649180440602611
163.339633	171.715333	180.091033	0.000025366555844	0.000000034486329	0.000005220051625	0.954719410443718
180.025143	189.868333	199.711523	0.000007526998582	0.000000018965735	0.000002201930436	1.428011797322767
199.614927	211.282667	222.950407	0.000002573670681	0.000000013451305	0.000001271709176	2.006213034076890

Table A.XV.2. Deuteron Yields from Hydrogen 800 MeV/n on 60 g/cm^2 Aluminium at10.0 deg

KE_left(MeV)	KE_mid(MeV)	KE_right(MeV)	Norm_Cts(#/SP*ster*MeV)	Y_stat(#/SP*ster*MeV)	Y_syst_tot(#/SP*ster*MeV)	X_tot(MeV)
43.683256	45.060600	46.437944	0.000063746026924	0.000000023212599	0.000019480796686	22.045173283770509
46.437923	47.815267	49.192610	0.000080866854281	0.000000026230172	0.000022469878586	0.574426164437171
49.192623	50.569967	51.947310	0.000074866849552	0.000000028016047	0.000023359526591	0.418642362502889
51.850085	53.446900	55.043715	0.000091289137120	0.000000030707237	0.000023137553926	0.248187658618877
55.140912	56.901567	58.662222	0.000092079940228	0.000000035960427	0.000024280133200	0.720242010184771
58.662212	60.422867	62.183522	0.000090523500839	0.000000032968468	0.000022438956602	0.492925066307243
62.109435	64.156600	66.203765	0.000089567586708	0.000000035386914	0.000021504432314	0.307745439317693
66.277863	68.420133	70.562403	0.000090219703941	0.000000035874838	0.000020481236743	0.608944724805134
70.474057	72.860767	75.247477	0.000102460087362	0.000000039716304	0.000021261572691	0.309365148736893
75.335857	77.860267	80.384677	0.000079025170353	0.000000039133234	0.000018700240599	0.463992407901250
80.373340	83.270600	86.167860	0.000094733568260	0.000000042869249	0.000018635607994	0.333863090802203
86.084563	89.225733	92.366903	0.000092904143197	0.000000046444870	0.000018431988141	0.326508477637258
92.359997	95.830067	99.300137	0.000083356477165	0.000000046855201	0.000016756395490	0.255924420415481
99.298490	103.164000	107.029510	0.000087844925268	0.000000049715288	0.000016307896112	0.194118456299884
107.032658	111.348333	115.664008	0.000088069881056	0.000000050874807	0.000015162568744	0.114417094568644
115.643688	120.506333	125.368978	0.000083075846572	0.000000052811501	0.000014010718514	0.077379361189532
125.373443	130.882333	136.391223	0.000098646466680	0.000000061359437	0.000015179516135	0.195463236985091
136.371482	142.661667	148.951852	0.000207908379529	0.000000101179159	0.000028318933354	0.370035715836999
148.900158	156.134333	163.368508	0.000547903822997	0.000000180422138	0.000061231533435	0.638734055375944
163.353028	171.729333	180.105638	0.000288157719986	0.000000135277744	0.000036524117387	0.930605030482857
180.037972	189.888667	199.739362	0.000157392631803	0.000000106834038	0.000019404732604	1.392354179923341
199.631687	211.304667	222.977647	0.000095267780510	0.000000089144403	0.000013861760297	1.967101558486496

Table A.XV.3. Deuteron Yields from Hydrogen 800 MeV/n on 60 g/cm^2 Aluminium at7.20 deg

KE_left(MeV)	KE_mid(MeV)	KE_right(MeV)	Norm_Cts(#/SP*ster*MeV)	Y_stat(#/SP*ster*MeV)	Y_syst_tot(#/SP*ster*MeV)	X_tot(MeV)
46.381999	47.791633	49.201267	0.000082341845104	0.000000027642494	0.000023049439720	0.532776986712076
49.201233	50.610867	52.020501	0.000079118073635	0.000000026847664	0.000022331000903	0.483484729815741
51.939601	53.464467	54.989333	0.000102067061448	0.000000033198251	0.000025977973047	0.245518916853671
55.070240	56.862200	58.654160	0.000070155012611	0.000000028793624	0.000018956495307	0.653220654948234
58.654173	60.446133	62.238093	0.000109788561822	0.000000039206832	0.000026460451528	0.527203460229540
62.139727	64.144467	66.149207	0.000095301492742	0.000000035953419	0.000021878474634	0.274246695239596
66.247597	68.420467	70.593337	0.000105371596782	0.000000041020351	0.000023308788176	0.608212168116522
70.488070	72.849500	75.210930	0.000092713685402	0.000000040423514	0.000020860186637	0.304727900573430
75.316200	77.870700	80.425200	0.000101264162600	0.000000045582847	0.000022267240312	0.480253666728324
80.369640	83.252400	86.135160	0.000105651734698	0.000000044353751	0.000019940807628	0.306644115066636
86.084005	89.218300	92.352595	0.000092080500491	0.000000043706404	0.000017821940845	0.320353896548801
92.368045	95.836700	99.305355	0.000089128856438	0.000000048664651	0.000017606295545	0.263142612843302
99.301800	103.170000	107.038200	0.000104782489199	0.000000049863287	0.000017241529452	0.198443452380873
107.025107	111.346667	115.668227	0.000095234485962	0.000000054246573	0.000016277877195	0.121981216540581
115.666927	120.519667	125.372407	0.000095781959528	0.000000058731387	0.000015916178534	0.052004689449510
125.371063	130.892333	136.413603	0.000111293143079	0.000000063417503	0.000016433398156	0.176082119580297
136.378292	142.668667	148.959042	0.000456926079524	0.000000151898393	0.000054641022588	0.357205067067924
148.919855	156.148000	163.376145	0.000726885522077	0.000000202096775	0.000078425109331	0.613895096724188
163.360917	171.744667	180.128417	0.000370647967394	0.000000155556279	0.000041874526581	0.904967108363061
180.058588	189.909333	199.760078	0.000445121168956	0.000000178857496	0.000048328895916	1.355654923859682
199.653498	211.331333	223.009168	0.000212442108898	0.000000138446010	0.000028352742034	1.920486410808470

Table A.XV.4. Proton Yields from Hydrogen 800 MeV/n on 60 g/cm^2 Aluminium at12.7 deg

KE_left(MeV)	KE_mid(MeV)	KE_right(MeV)	Norm_Cts(#/SP*ster*MeV)	Y_stat(#/SP*ster*MeV)	Y_syst_tot(#/SP*ster*MeV)	X_tot(MeV)
45.553250	47.134233	48.715216	0.000159183105538	0.000000048152075	0.000038957308020	0.146870924607073
48.809110	50.716900	52.624690	0.000158880358278	0.000000049879192	0.000034538018275	0.546086803959773
52.624677	54.532467	56.440257	0.000185826006185	0.000000057426462	0.000040006517818	1.096452535817670
56.440277	58.348067	60.255857	0.000231656831823	0.000000060467759	0.000045058112717	0.770172266795553
60.183707	62.483967	64.784227	0.000219016619237	0.000000065976001	0.000041188125997	0.438557082560526
64.856370	67.228800	69.601230	0.000223234422712	0.000000066095113	0.000040880860090	0.841461727502802
69.480148	72.060833	74.641518	0.000216277262299	0.000000072209715	0.000040181121192	0.658594227237075
74.762607	77.600367	80.438127	0.000213219089895	0.000000075670936	0.000039254383174	0.716003211680646
80.329722	83.463667	86.597612	0.000286769715264	0.000000088160769	0.000046793932408	0.699549405110175
86.623822	90.018367	93.412912	0.000240020526251	0.000000090069732	0.000041028451811	0.642109632453836
93.492327	97.266767	101.041207	0.000279583269169	0.000000098753550	0.000044403669665	0.704783790693288
101.043315	105.286000	109.528685	0.000284949078791	0.000000104055477	0.000043089404241	0.668111382934014
109.464487	114.244667	119.024847	0.000314183802354	0.000000114400981	0.000045792380206	0.607269702772994
118.975515	124.350000	129.724485	0.000230173306419	0.000000104157608	0.000034213502306	0.572470588389482
129.686355	135.754000	141.821645	0.000159574529524	0.000000090145650	0.000024361235414	0.478071943140360
141.814160	148.775000	155.735840	0.000086079051383	0.000000071530945	0.000014586985786	0.354108448617087
155.683288	163.741333	171.799378	0.000042316373550	0.000000051560313	0.000008246512016	0.223398627936722
171.725473	181.107333	190.489193	0.000019607348296	0.000000034488049	0.000004408372979	0.076660808230021
190.425298	201.498333	212.571368	0.000013224426436	0.000000031139318	0.000003301100881	0.366737488360544
212.491170	225.757000	239.022830	0.000011802742435	0.000000032124037	0.000002857327563	0.759219065517983
238.863950	255.011000	271.158050	0.000005785760240	0.000000026112668	0.000001865175978	1.386275451548501
270.937883	290.989333	311.040783	0.000002731043336	0.000000018159758	0.000000990162220	2.272745210290850
311.323400	327.616000	343.908600	0.000000868060254	0.000000008837984	0.000000400187861	2.734387257229670

Table A.XV.5. Proton Yields from Hydrogen 800 MeV/n on 60 g/cm^2 Aluminium at10.0 deg

KE_left(MeV)	KE_mid(MeV)	KE_right(MeV)	Norm_Cts(#/SP*ster*MeV)	Y_stat(#/SP*ster*MeV)	Y_syst_tot(#/SP*ster*MeV)	X_tot(MeV)
45.817258	47.344633	48.872008	0.000235608781142	0.000000059020785	0.000051006575207	0.467663749312473
48.758705	50.557500	52.356295	0.000244885779708	0.000000063103390	0.000050882162286	0.269794843053773
52.469577	54.455367	56.441157	0.000247764869842	0.000000066860099	0.000048142802127	0.976817052683357
56.441143	58.426933	60.412723	0.000303928719587	0.000000072115458	0.000055162538528	0.887858295079795
60.301143	62.467133	64.633123	0.000290874190306	0.000000074950372	0.000052655670860	0.401761756780060
64.744685	67.194200	69.643715	0.000304299494022	0.000000084698321	0.000053182284485	0.791551962356231
69.589923	72.093233	74.596543	0.000303356746987	0.000000083839073	0.000052379626092	0.734680966467759
74.650360	77.564200	80.478040	0.000300095204221	0.000000090806343	0.000050407128204	0.660658138868356
80.367502	83.457867	86.548232	0.000267225113453	0.000000088107323	0.000044886988546	0.694529761199619
86.658760	90.037900	93.417040	0.000329056553660	0.000000102608247	0.000051868104522	0.672277482938407
93.411410	97.252100	101.092790	0.000338728257496	0.000000108575534	0.000051559749635	0.674359210324883
101.021130	105.260000	109.498870	0.000281356010643	0.000000107168022	0.000043112290549	0.626072032780574
109.503247	114.230667	118.958087	0.000339778704323	0.000000119938730	0.000049018708919	0.582511217057663
118.934025	124.330000	129.725975	0.000320665215789	0.000000128504573	0.000045103009512	0.541771438913127
129.696802	135.749667	141.802532	0.000329075214553	0.000000132402248	0.000044804457023	0.470696222705260
141.793598	148.758333	155.723068	0.000418234437984	0.000000158080966	0.000053119970390	0.324619422291705
155.653088	163.720333	171.787578	0.000410946377251	0.000000171217600	0.000051140100646	0.189485178309809
171.729737	181.108667	190.487597	0.000382097641326	0.000000173038788	0.000045093136244	0.080596061200284
190.406602	201.490667	212.574732	0.000395661162424	0.000000193056577	0.000046219594839	0.384913829994455
212.489680	225.745000	239.000320	0.000430954973408	0.000000221816355	0.000049927031026	0.779640911266847
238.850300	255.006000	271.161700	0.000264758533132	0.000000192743126	0.000033186615701	1.395501370647123
270.931183	290.985333	311.039483	0.000051209923691	0.000000090702489	0.000007957250394	2.279726712503058
311.323950	327.618000	343.912050	0.000011486948204	0.000000035621547	0.000001987487320	2.730798209535081

Table A.XV.6. Proton Yields from Hydrogen 800 MeV/n on 60 g/cm^2 Aluminium at7.20 deg

KE_left(MeV)	KE_mid(MeV)	KE_right(MeV)	Norm_Cts(#/SP*ster*MeV)	Y_stat(#/SP*ster*MeV)	Y_syst_tot(#/SP*ster*MeV)	X_tot(MeV)
45.859908	47.447133	49.034358	0.000214671435252	0.000000054817391	0.000045986106222	0.634119554179651
48.992350	50.621600	52.250850	0.000260703136291	0.000000062603252	0.000052900667323	0.373134790879918
52.292892	54.339267	56.385642	0.000262915345623	0.000000068399675	0.000049188592267	0.798368448435307
56.385658	58.432033	60.478408	0.000269672680300	0.000000070866364	0.000051116065382	0.889498917785739
60.454232	62.524767	64.595302	0.000293534660984	0.000000074272539	0.000053147897758	0.514727988636717
64.619450	67.128800	69.638150	0.000252134480756	0.000000077800962	0.000045780205620	0.694497623037689
69.638150	72.147500	74.656850	0.000312131878448	0.000000083920625	0.000053221129306	0.811517960414309
74.595897	77.507867	80.419837	0.000288326881101	0.000000088621492	0.000048837779054	0.577268712380985
80.400212	83.460067	86.519922	0.000321941988222	0.000000097006333	0.000052229369162	0.713856555676979
86.600523	90.038133	93.475743	0.000306051987400	0.000000095703819	0.000048090459957	0.673356712776371
93.397857	97.224067	101.050277	0.000354575624582	0.000000113129971	0.000054011865507	0.626801449450302
101.029960	105.266000	109.502040	0.000380114384156	0.000000118846791	0.000054998531661	0.629656871050416
109.508067	114.235667	118.963267	0.000394069140983	0.000000128984178	0.000055744485212	0.586040124843001
118.932572	124.306667	129.680762	0.000435987310581	0.000000144098361	0.000058173645715	0.506524482096374
129.674363	135.740333	141.806303	0.000424887563725	0.000000152947149	0.000056514057875	0.456508886141332
141.787325	148.757000	155.726675	0.000540056793252	0.000000183246841	0.000067999121450	0.318905099120412
155.658602	163.709667	171.760732	0.000559709126850	0.000000197311573	0.000067060230712	0.167118607528246
171.732330	181.110000	190.487670	0.000425524917109	0.000000184171369	0.000049920885415	0.082859489454860
190.396152	201.489667	212.583182	0.000349689902950	0.000000182371885	0.000041359859075	0.388298691103897
212.487200	225.740000	238.992800	0.000326770524289	0.000000194614503	0.000038722463612	0.788221492265975
238.850467	255.009667	271.168867	0.000131215570764	0.000000134008803	0.000019041815862	1.389641969268703
270.933867	290.991667	311.049467	0.000027977164301	0.000000066063705	0.000004936492336	2.268918008236525
311.339450	327.636000	343.932550	0.000005922668342	0.000000025724971	0.000001318828172	2.705560550052429

Table A.XV.7. Proton Yields from Hydrogen 800 MeV/n on 60 g/cm^2 Aluminium at32.7 deg

KE_left(MeV)	KE_mid(MeV)	KE_right(MeV)	Norm_Cts(#/SP*ster*MeV)	Y_stat(#/SP*ster*MeV)	Y_syst_tot(#/SP*ster*MeV)	X_tot(MeV)
45.074100	46.884000	48.693900	0.000125358133875	0.000000042799064	0.000028735428409	0.367873013919027
48.693900	50.503800	52.313700	0.000122715527122	0.000000043152410	0.000028209032519	1.007928101892690
52.313700	54.123600	55.933500	0.000151828602854	0.000000045844188	0.000030993567341	0.755077916839050
55.819042	57.808967	59.798892	0.000172256433811	0.000000055825383	0.000035199903130	0.159140314261283
59.913317	62.213267	64.513217	0.000163757209581	0.000000056248681	0.000031038847605	0.475598060234690
64.513150	66.813100	69.113050	0.000189637083994	0.000000060751697	0.000033627926346	0.755662106887066
69.012972	71.665767	74.318562	0.000162346326198	0.000000059082524	0.000029019225821	0.331940093904006
74.418680	77.208500	79.998320	0.000170100348059	0.000000062465154	0.000029608918923	0.573023854072411
79.906582	83.073867	86.241152	0.000168383228512	0.000000067255898	0.000027983383546	0.467815597714527
86.237990	89.638400	93.038810	0.000204354968243	0.000000074597898	0.000031746161851	0.484969793725341
93.130390	96.903000	100.675610	0.000187861714229	0.000000079759326	0.000029934951595	0.495991780829078
100.678875	104.940000	109.201125	0.000183517318509	0.000000082434136	0.000027459283717	0.493803519601673
109.146358	113.924333	118.702308	0.000186228460198	0.000000087153321	0.000027016019376	0.459349338548560
118.650682	124.055667	129.460652	0.000196053332738	0.000000094907065	0.000026680339798	0.422067024506772
129.442078	135.514333	141.586588	0.000192315790555	0.000000096781154	0.000025096914236	0.364753144898026
141.575117	148.582667	155.590217	0.000207051305050	0.000000108440166	0.000025637227491	0.252942918730689
155.515247	163.612667	171.710087	0.000214141102579	0.000000116337520	0.000024794644620	0.136895504691060
171.683017	181.110667	190.538317	0.000197344196231	0.000000117949920	0.000021683827018	0.079327750169849
180.007365	190.213000	200.418635	0.000195286849079	0.000000131148742	0.000021411797583	0.198862376287623
212.671163	226.031333	239.391503	0.000177622219921	0.000000141327940	0.000020074305711	0.644343735530966
239.258967	255.540667	271.822367	0.000166393521260	0.000000148013986	0.000018092074269	1.122590908242624
271.595450	291.846000	312.096550	0.000119138519698	0.000000137360838	0.000013490560848	1.846253219963340
311.739883	337.588333	363.436783	0.000070159333589	0.000000121037681	0.000008256538325	2.905470298006847
362.826617	396.941667	431.056717	0.000039640091417	0.000000100171030	0.000004932405766	4.586469237757951
429.924833	477.111333	524.297833	0.000013308617465	0.000000066902290	0.000002076278612	7.380691654641860
524.976250	568.045500	611.114750	0.000001279306026	0.000000016213379	0.000000302761219	9.164344936660775

Table A.XV.8. Proton Yields from Hydrogen 800 MeV/n on 60 g/cm^2 Aluminium at30.0 deg

KE_left(MeV)	KE_mid(MeV)	KE_right(MeV)	Norm_Cts(#/SP*ster*MeV)	Y_stat(#/SP*ster*MeV)	Y_syst_tot(#/SP*ster*MeV)	X_tot(MeV)
45.657205	47.249500	48.841795	0.000147742148472	0.000000043507059	0.000032669121724	0.919826569578201
48.841805	50.434100	52.026395	0.000181104823340	0.000000047622727	0.000036711367417	0.888842921770208
52.001243	54.051033	56.100823	0.000161074016227	0.000000052331357	0.000032037836026	0.624490507970297
56.125980	58.200900	60.275820	0.000186374913219	0.000000052889428	0.000032941871137	0.771325419903947
60.275780	62.350700	64.425620	0.000185109293568	0.000000058434221	0.000034889040562	0.700737403323099
64.347415	66.829400	69.311385	0.000175516340936	0.000000059668513	0.000030800101090	0.800235304123731
69.389615	71.949800	74.509985	0.000228193284529	0.000000067689628	0.000035735770704	0.820183048660480
74.396087	77.261167	80.126247	0.000174809494387	0.000000066109748	0.000029602415354	0.677697031693367
80.240112	83.285067	86.330022	0.000194212722799	0.000000077112774	0.000033152290035	0.845682832810268
86.300267	89.800567	93.300867	0.000180817278711	0.000000076039233	0.000029370010199	0.780594252499338
93.209038	97.022933	100.836828	0.000191766801190	0.000000079034385	0.000029123412409	0.704720509675999
100.829037	105.070667	109.312297	0.000207256871722	0.000000087554253	0.000030082932165	0.719111078296670
109.306240	114.061000	118.815760	0.000214782031545	0.000000092947899	0.000029177068009	0.682629953299736
118.843675	124.179000	129.514325	0.000195011317821	0.000000091067148	0.000025242323169	0.632897340443140
129.492225	135.623000	141.753775	0.000151656747580	0.000000083834858	0.000019689306270	0.551817831472489
141.688475	148.672000	155.655525	0.000086154383806	0.000000065771082	0.000012469069378	0.408506209485241
155.636090	163.700000	171.763910	0.000044957235357	0.000000046669883	0.000007282653921	0.271898584634051
171.688288	181.114333	190.540378	0.000020046051592	0.000000031472791	0.000004150030230	0.112415890153038
180.574002	190.823667	201.073332	0.000007889620496	0.000000023801022	0.000002441968227	0.305113336131019
212.616718	225.958333	239.299948	0.000005079745506	0.000000018947619	0.000001646795693	0.773060079347653
239.135150	255.363000	271.590850	0.000002923019353	0.000000014622822	0.000001076146476	1.432573056417717
271.369217	291.540667	311.712117	0.000002340108993	0.000000015330181	0.000000853486424	2.379255616195956
311.358000	337.079000	362.800000	0.000000691233373	0.000000012898546	0.000000532857256	3.794325381329335
362.204667	396.140667	430.076667	0.000000603065173	0.000000010897082	0.000000342846977	5.986907267872119
445.076750	476.418500	507.760250	0.000000438661882	0.000000009571942	0.000000218256091	7.948364050306202
524.894350	544.785000	564.675650	0.000000169182720	0.000000003829520	0.000000067928500	7.666090000000000

Table A.XV.9. Proton Yields from Hydrogen 800 MeV/n on 60 g/cm^2 Aluminium at27.2 deg

KE_left(MeV)	KE_mid(MeV)	KE_right(MeV)	Norm_Cts(#/SP*ster*MeV)	Y_stat(#/SP*ster*MeV)	Y_syst_tot(#/SP*ster*MeV)	X_tot(MeV)
45.092002	46.927867	48.763732	0.000147431317354	0.000000045815650	0.000034937514244	0.443347462950720
48.763735	50.599600	52.435465	0.000224686852772	0.000000054403299	0.000040604002747	1.175399142232544
52.435435	54.271300	56.107165	0.000172563246140	0.000000052084411	0.000033033129100	1.004202950016081
56.016472	57.963767	59.911062	0.000205230850085	0.000000058584019	0.000037035970530	0.400438677485629
60.001725	62.319300	64.636875	0.000243887113971	0.000000063032155	0.000039605655859	0.657751669561545
64.636858	66.954433	69.272008	0.000234064706205	0.000000066070717	0.000037754156888	0.996951440361064
69.163492	71.797967	74.432442	0.000240756402756	0.000000071475583	0.000037100107494	0.556388447388153
74.540958	77.340333	80.139708	0.000248862602315	0.000000076515800	0.000038860364671	0.801377626724131
80.045683	83.205333	86.364983	0.000241530020285	0.000000078368910	0.000034180271399	0.694618637360818
86.365683	89.765933	93.166183	0.000288106227668	0.000000083127426	0.000037779137419	0.705439891243046
93.249595	97.023400	100.797205	0.000274779996824	0.000000089953630	0.000035230795504	0.703683958144564
100.807052	105.055667	109.304282	0.000276153990783	0.000000096379895	0.000034274972440	0.693341359041850
109.247310	114.031000	118.814690	0.000309320664225	0.000000103765389	0.000035066446455	0.640789862779523
118.761422	124.154667	129.547912	0.000322355252343	0.000000115379983	0.000035314122484	0.591310167689513
129.522223	135.594333	141.666443	0.000310698993161	0.000000117492502	0.000032683904711	0.502729913808598
141.661275	148.640000	155.618725	0.000389323088589	0.000000141908901	0.000036710535323	0.354536332999877
155.557057	163.653667	171.750277	0.000449291255395	0.000000165336331	0.000039171416069	0.207461790203329
171.697257	181.109667	190.522077	0.000269064301960	0.000000124571806	0.000027872144939	0.093822234155023
180.008803	190.190333	200.371863	0.000070601939645	0.000000066456066	0.000008862024964	0.255291128380913
212.617528	225.937333	239.257138	0.000029180443686	0.000000053050745	0.000005111326576	0.810130083165043
239.116300	255.360000	271.603700	0.000019016550677	0.000000041583960	0.000003274011189	1.437282909975973
271.367100	291.549000	311.730900	0.000009153590420	0.000000036103150	0.000002109214142	2.365704330659264
311.376450	337.121000	362.865550	0.000007838791304	0.000000038183945	0.000001744211768	3.720641858940470
362.270900	396.230000	430.189100	0.000003647426002	0.000000027540471	0.000000953888295	5.828599712400913
429.069817	475.994667	522.919517	0.000001038491804	0.000000016357213	0.000000399313426	9.329526791831405
523.594850	566.380000	609.165150	0.000000370014216	0.000000009516777	0.000000164600878	11.528223535766472

APPENDIX B

PHITS INPUT SCRIPT

The following script was used as an input deck for the PHITS Monte Carlo particle transport code to calculate the nuclear attenuation correction factors. The execution of this code was automated using a series of bash scripts that pulled in the particle type (proton, deuteron, triton, helion, alpha) and particle energy (in MeV/n) from a text file. The output was a histogram of counts across an energy spectrum (representing energy deposition).

Input Script:

```
file = AUTO.inp
[ T i t l e ]
NaI Detector efficiency calculation with mono-energetic VARIABLE MeV VARIABLE Source


[ P a r a m e t e r s ]
 icntl = 0                  # (D=0) 3:echo 5:noRxn 6:source 7,8:gshow 11:3dshow 12:dump
 itall = 1
 maxcas = 1000               # (D=10) number of particles per one batch
 maxbch = 100             # (D=10) number of batches

 emin(1) = 0.9           # (D=1.0) cut-off energy of proton (MeV)
 emin(2) = 0.9           # (D=1.0) cut-off energy of neutron (MeV)
 dmax(2) =  1.          # (D=emin(2)) data max. energy of neutron (MeV)
 emin(12) = 0.9          # (D=1.d9) cut-off energy of electron (MeV)
 dmax(12) = 1.0E4        # (D=emin(12)) data max. energy of electron (MeV)
 emin(13) = 0.9          # (D=1.d9) cut-off energy of positron (MeV)
 dmax(13) = 1000.        # (D=emin(13)) data max. energy of positron (MeV)
 emin(14) = 0.9          # (D=1.d9) cut-off energy of photon (MeV)
 dmax(14) = 1000.        # (D=emin(14)) data max. energy of photon (MeV)
 emin(15) = 0.9          # (D=1.0) cut-off energy of deuteron (MeV/u)
 emin(16) = 0.9          # (D=1.0) cut-off energy of triton (MeV/u)
 emin(17) = 0.9          # (D=1.0) cut-off energy of 3He (MeV/u)
 emin(18) = 0.9          # (D=1.0) cut-off energy of Alpha (MeV/u)
 emin(19) = 0.9          # (D=1.0) cut-off energy of Nucleus (MeV/u)

 igamma = 2                 # (D=0) 0:No, 1:Old, 2:EBITEM, 3:EBITEM+Isomer
 ipnint = 1                 # (D=0) 0: no, 1: consider photo-nuclear reaction
 negs = 0                   # (D=0) =1 EGS photon and electron
 e-mode = 0                 # (D=0) 0: Normal, 1: Event generator mode

 file(6) = phits.out        # (D=phits.out) general output file name
 file(7)=/Applications/phits/data/xsdir.jnd    # path to xs library


[ S o u r c e ]
 s-type = 1.           # mono-energetic point source     (look at gaus. dist?)
 dir = 1.0             # z-direction of beam [cos(0)]
 r0 = 0.              # radius [cm]
 x0 = 0.               # x-position[cm]
 y0 = 0.               # y-position[cm]
 z0 = -5.             # minimum position of z-axis [cm]  (flat disk)
 z1 = -5.             # maximum position of z-axis [cm]
 infl: {particle.tmp}         # incident particle is written in particle.tmp
 infl: {energy.tmp}            # energy of beam [AMeV]


[ M a t e r i a l ]
 mat[1] 27Al   1.0            $ Aluminum, 2.699 g/cm3

 mat[2] 23Na   0.4999999    $ NaI 3.667 g/cm3
        127I    0.5000001

```

```
54
55 [ Mat Name Color ]
56  mat   name     color
57  1     Al       pastelviolet
58  2     NaI      pastelblue
59
60
61 [ S u r f a c e ]
62  11  so    50.                                $ air
63
64 107 pz 20
65 108 pz 20.1016                          $ finish Al casing front, front detector
66 109 pz 30.2616                          $ finish NaI front detector
67 110 pz 30.3632                          $ finish Al casing back, front detector
68 111 pz 30.4648                          $ finish Al casing front, back detector
69 112 pz 40.6248                          $ finish NaI back detector
70 113 pz 40.7263                          $ finish Al casing back, back detector
71 114 py -5.08
72 115 py 5.08
73 116 px -20.32
74 117 px 20.32
75
76
77 [ C e l l ]
78  100    1  -2.699  107 -108 114 -115 116 -117 $ ALUMINUM front, front
79  101    2  -3.667  108 -109 114 -115 116 -117 $ NaI front
80  102    1  -2.699  109 -110 114 -115 116 -117 $ ALUMINUM front, back
81  103    1  -2.699  110 -111 114 -115 116 -117 $ ALUMINUM back, front
82  104    2  -3.667  111 -112 114 -115 116 -117 $ NaI front
83  105    1  -2.699  112 -113 114 -115 116 -117 $ ALUMINUM back, back
84
85  111    0          (-107:113:-114:115:-116:117) -11        $ air
86  999    -1 11                      $ outer region
87
88
89 [ T - D e p o s i t ]
90 file = deposit.out
91 mesh = reg
92 reg = 101
93 unit = 3
94 part = all
95 deposit = 1
96 axis = eng
97 output = deposit
98 e-type = 2
99 ne = 1200
100 emin = 0.
101 emax = 800.
102 ginfo = 1
103
104 [ E n d ]
```

APPENDIX C

ADDITIONAL MCNP COMPARISONS

The plots presented in Section 5.5.4 showed comparisons between the experimental data and simulations for the Fe 400 MeV/n data set. The figures presented here show the remaining comparisons.

Figures C.I.1-8 – Fe 800 MeV/n

Figures C.II.1-4 – He 400 MeV/n

Figures C.III.1-3 – H 400 MeV/n

Figures C.IV.1-3 – H 800 MeV/n

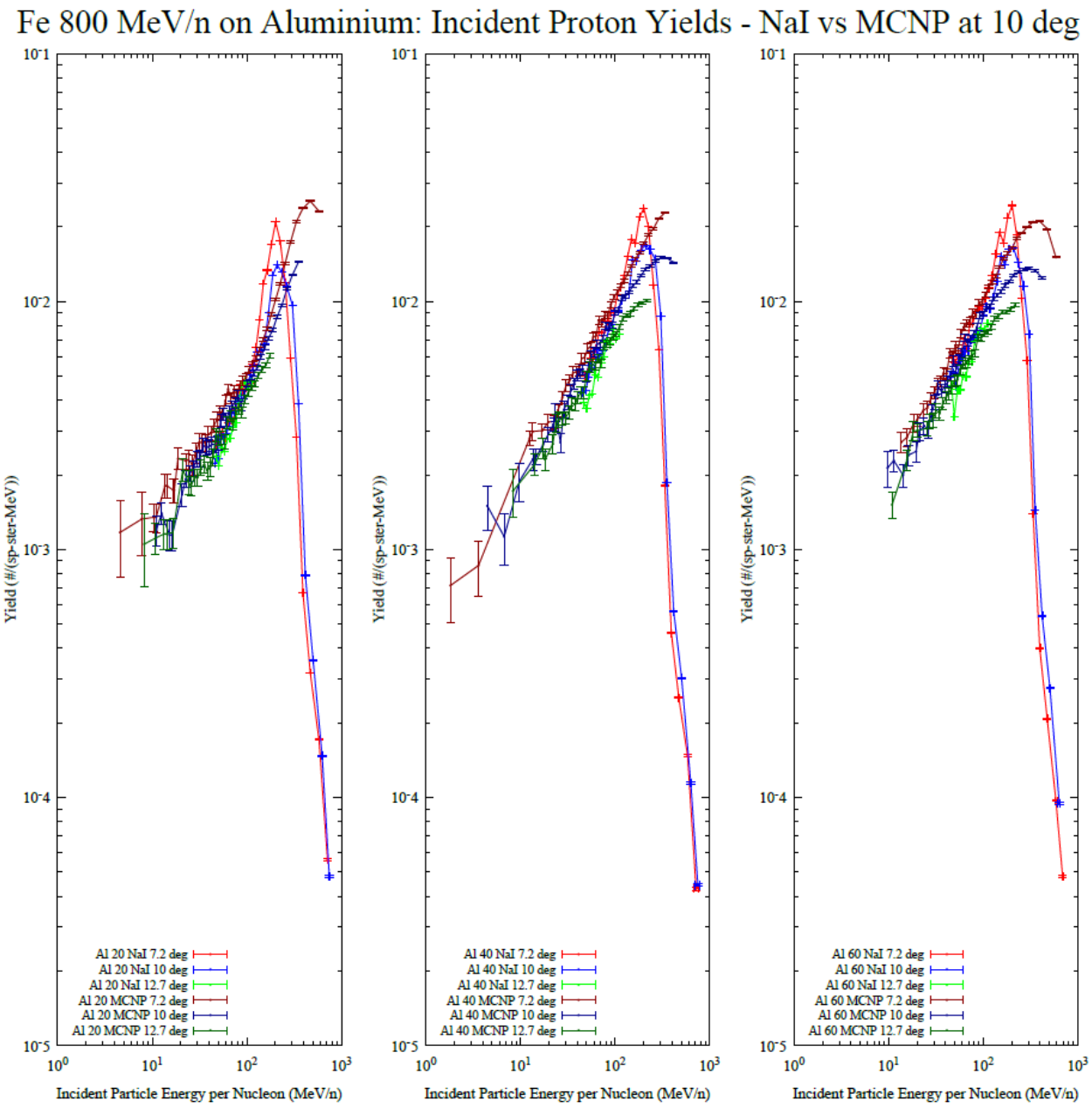


Figure C.I.1. Comparison of proton yields at 10 deg NaI detector array with MCNP simulated yields at same angles from 800 MeV/n iron nuclei incident upon 20 g/cm^2 (left), 40 g/cm^2 (middle), and 60 g/cm^2 (right) Aluminium shielding

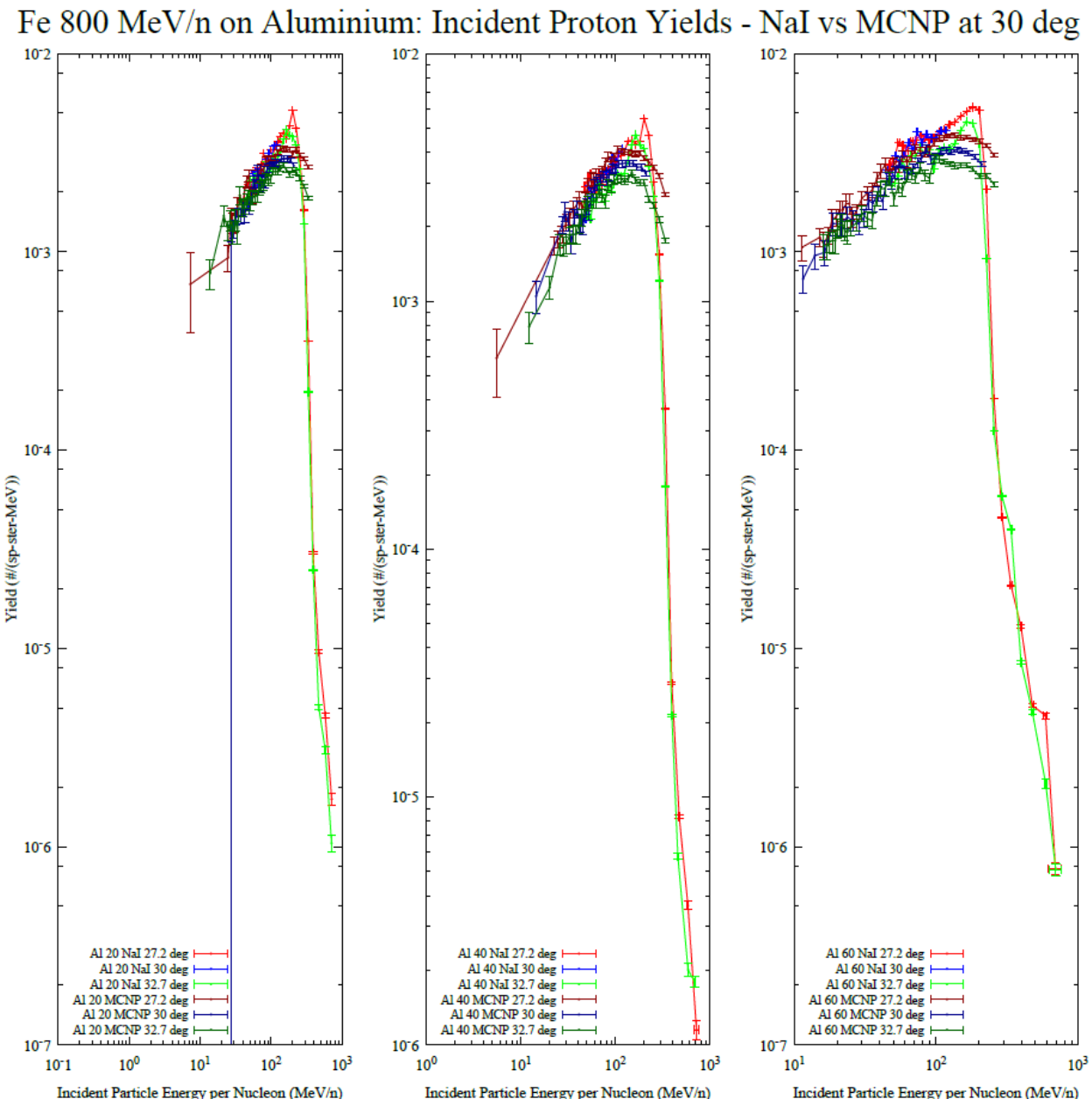


Figure C.I.2. Comparison of proton yields at 30 deg NaI detector array with MCNP simulated yields at same angles from 800 MeV/n iron nuclei incident upon 20 g/cm^2 (left), 40 g/cm^2 (middle), and 60 g/cm^2 (right) Aluminium shielding

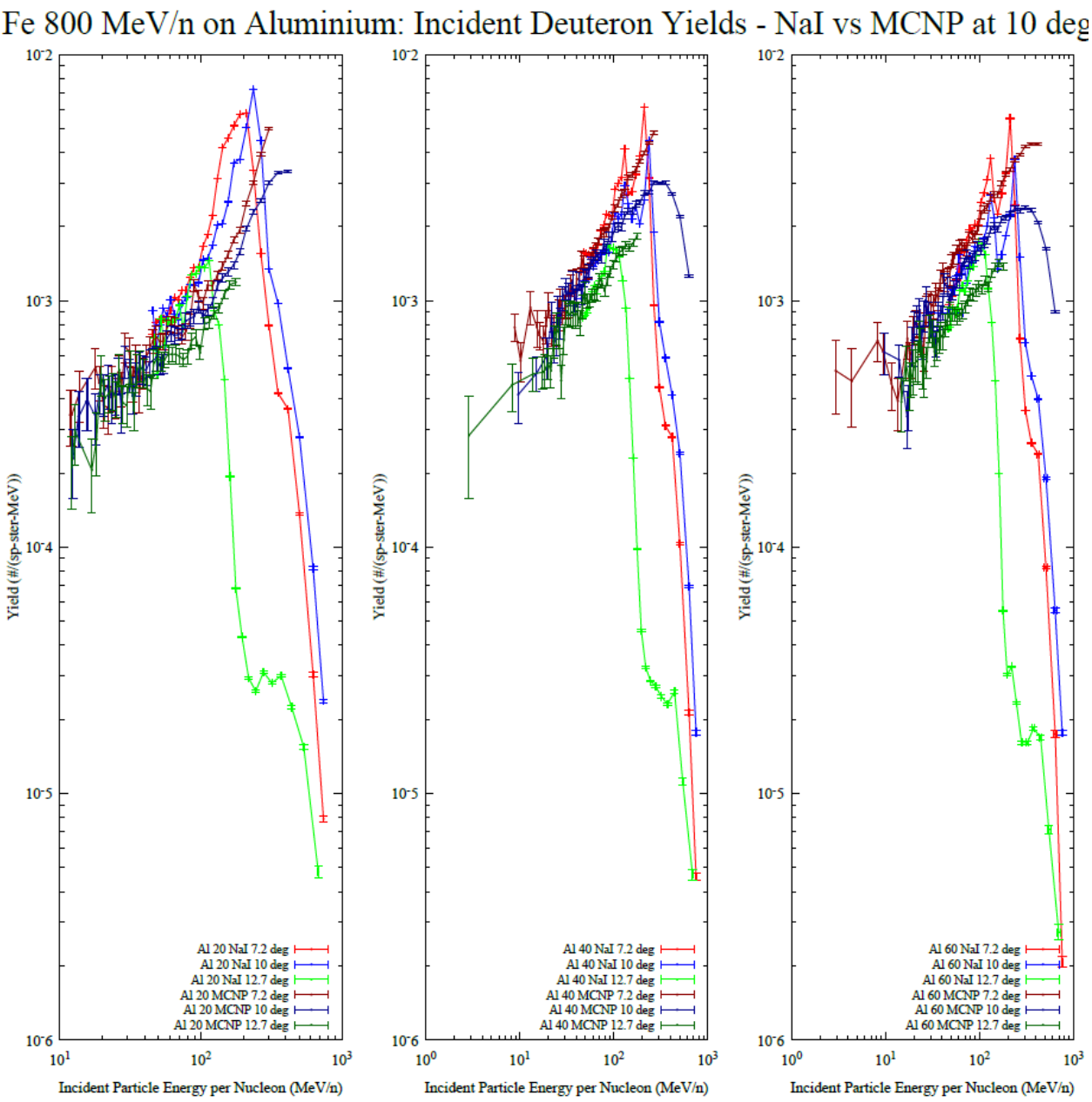


Figure C.I.3. Comparison of deuteron yields at 10 deg NaI detector array with MCNP simulated yields at same angles from 800 MeV/n iron nuclei incident upon 20 g/cm^2 (left), 40 g/cm^2 (middle), and 60 g/cm^2 (right) Aluminium shielding

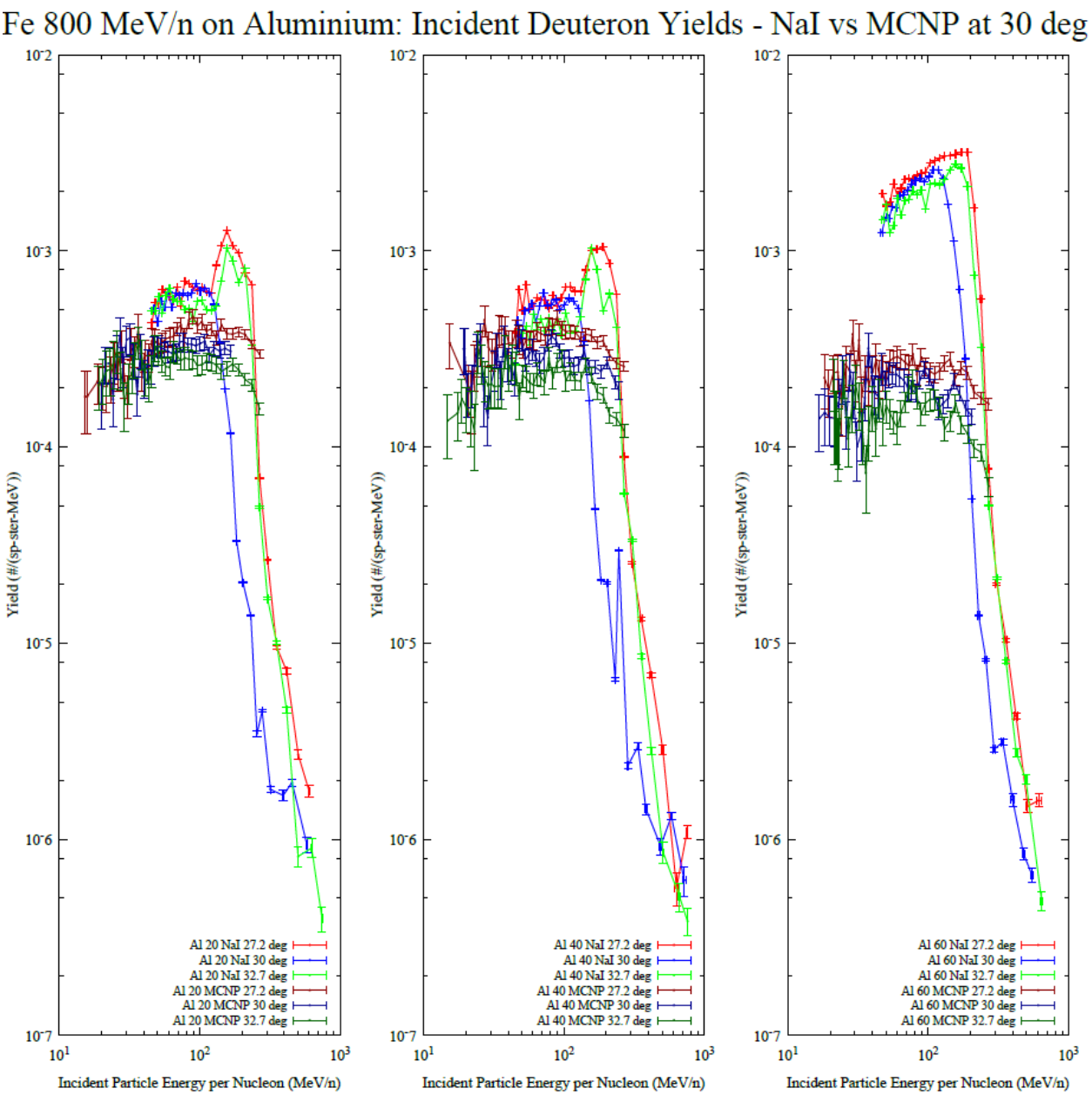


Figure C.I.4. Comparison of deuteron yields at 30 deg NaI detector array with MCNP simulated yields at same angles from 800 MeV/n iron nuclei incident upon 20 g/cm^2 (left), 40 g/cm^2 (middle), and 60 g/cm^2 (right) Aluminium shielding

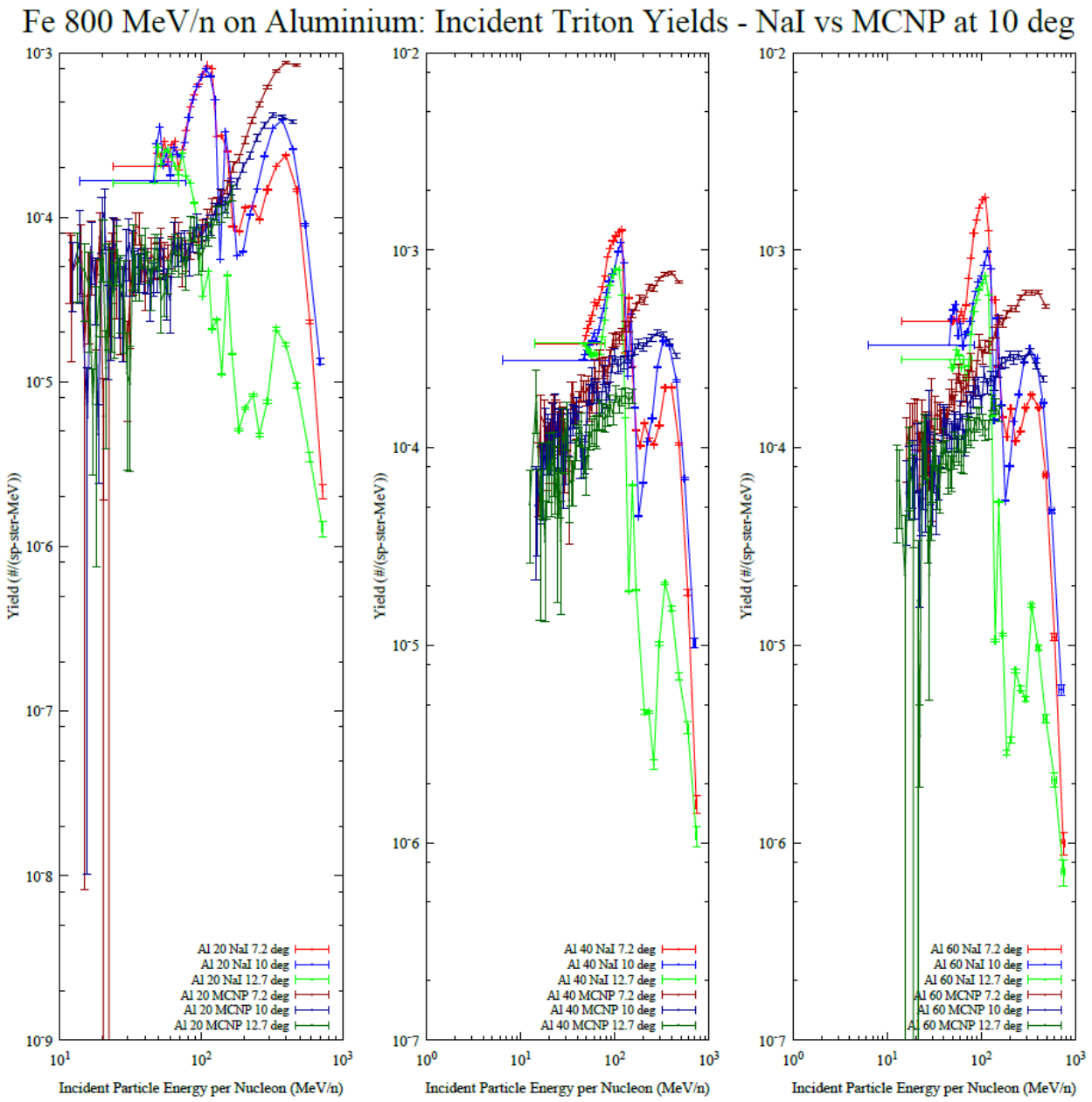


Figure C.I.5. Comparison of triton yields at 10 deg NaI detector array with MCNP simulated yields at same angles from 800 MeV/n iron nuclei incident upon 20 g/cm^2 (left), 40 g/cm^2 (middle), and 60 g/cm^2 (right) Aluminium shielding

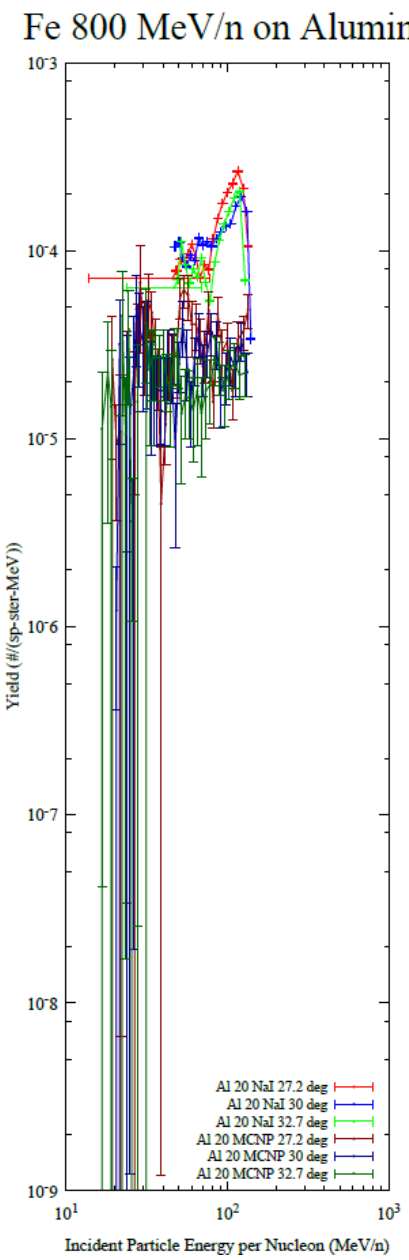


Figure C.I.6. Comparison of triton yields at 30 deg NaI detector array with MCNP simulated yields at same angles from 800 MeV/n iron nuclei incident upon 20 g/cm^2 (left), 40 g/cm^2 (middle), and 60 g/cm^2 (right) Aluminium shielding

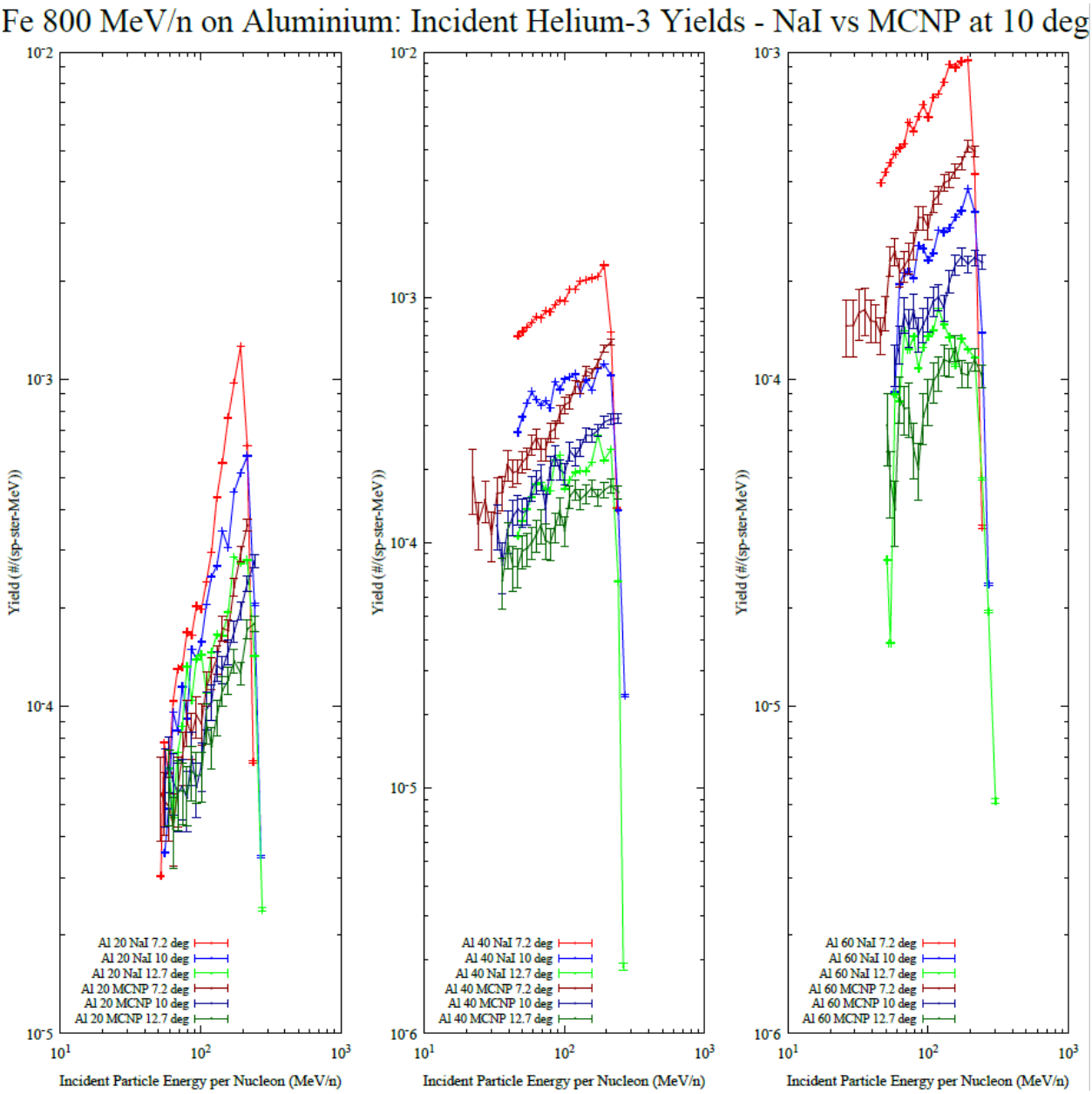


Figure C.I.7. Comparison of helion yields at 10 deg NaI detector array with MCNP simulated yields at same angles from 800 MeV/n iron nuclei incident upon 20 g/cm^2 (left), 40 g/cm^2 (middle), and 60 g/cm^2 (right) Aluminium shielding

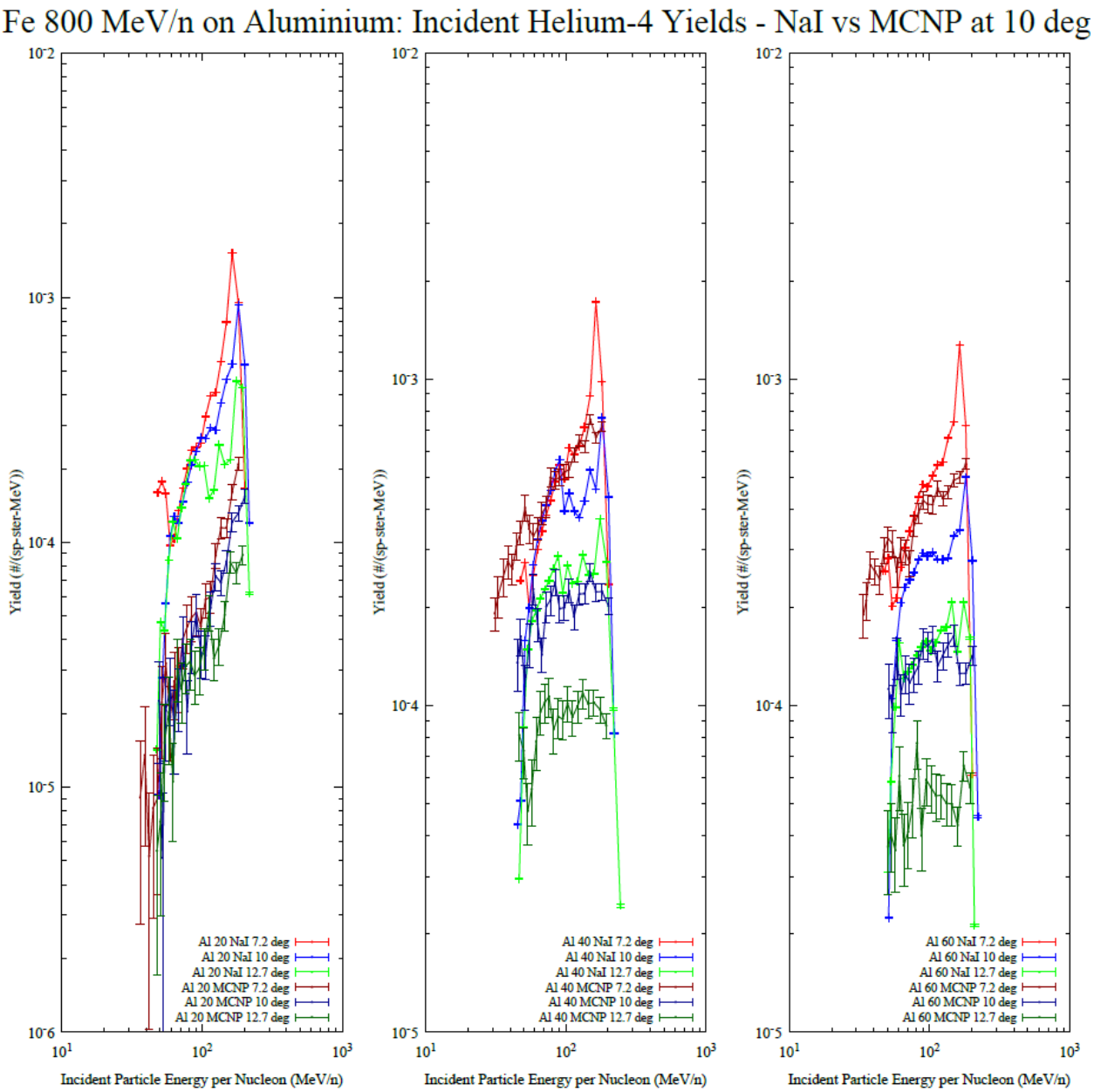


Figure C.I.8. Comparison of alpha yields at 10 deg NaI detector array with MCNP simulated yields at same angles from 800 MeV/n iron nuclei incident upon 20 g/cm^2 (left), 40 g/cm^2 (middle), and 60 g/cm^2 (right) Aluminium shielding

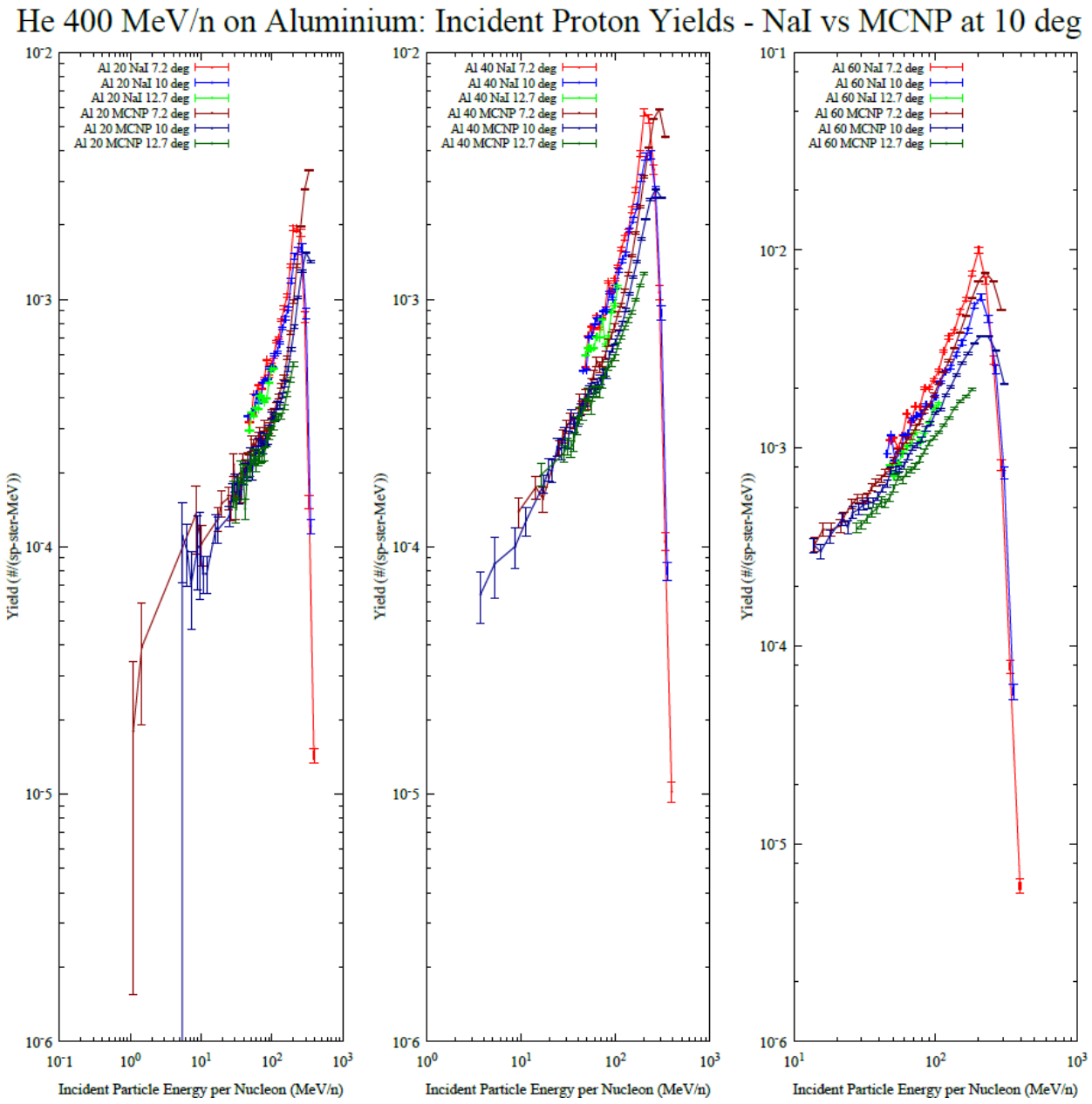


Figure C.II.1. Comparison of proton yields at 10 deg NaI detector array with MCNP simulated yields at same angles from 400 MeV/n helium nuclei incident upon 20 g/cm^2 (left), 40 g/cm^2 (middle), and 60 g/cm^2 (right) Aluminium shielding

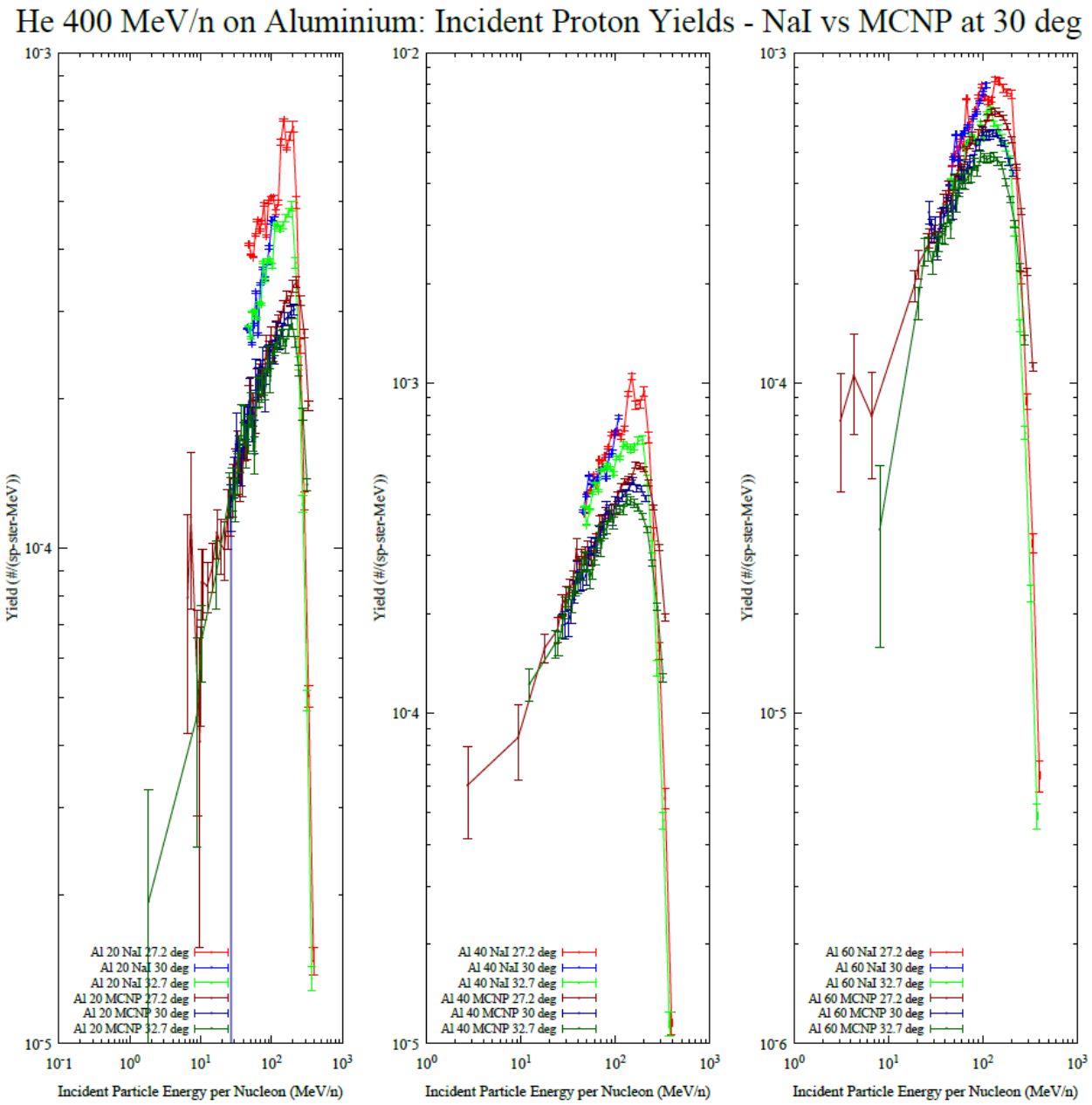


Figure C.II.2. Comparison of proton yields at 30 deg NaI detector array with MCNP simulated yields at same angles from 400 MeV/n helium nuclei incident upon 20 g/cm^2 (left), 40 g/cm^2 (middle), and 60 g/cm^2 (right) Aluminium shielding

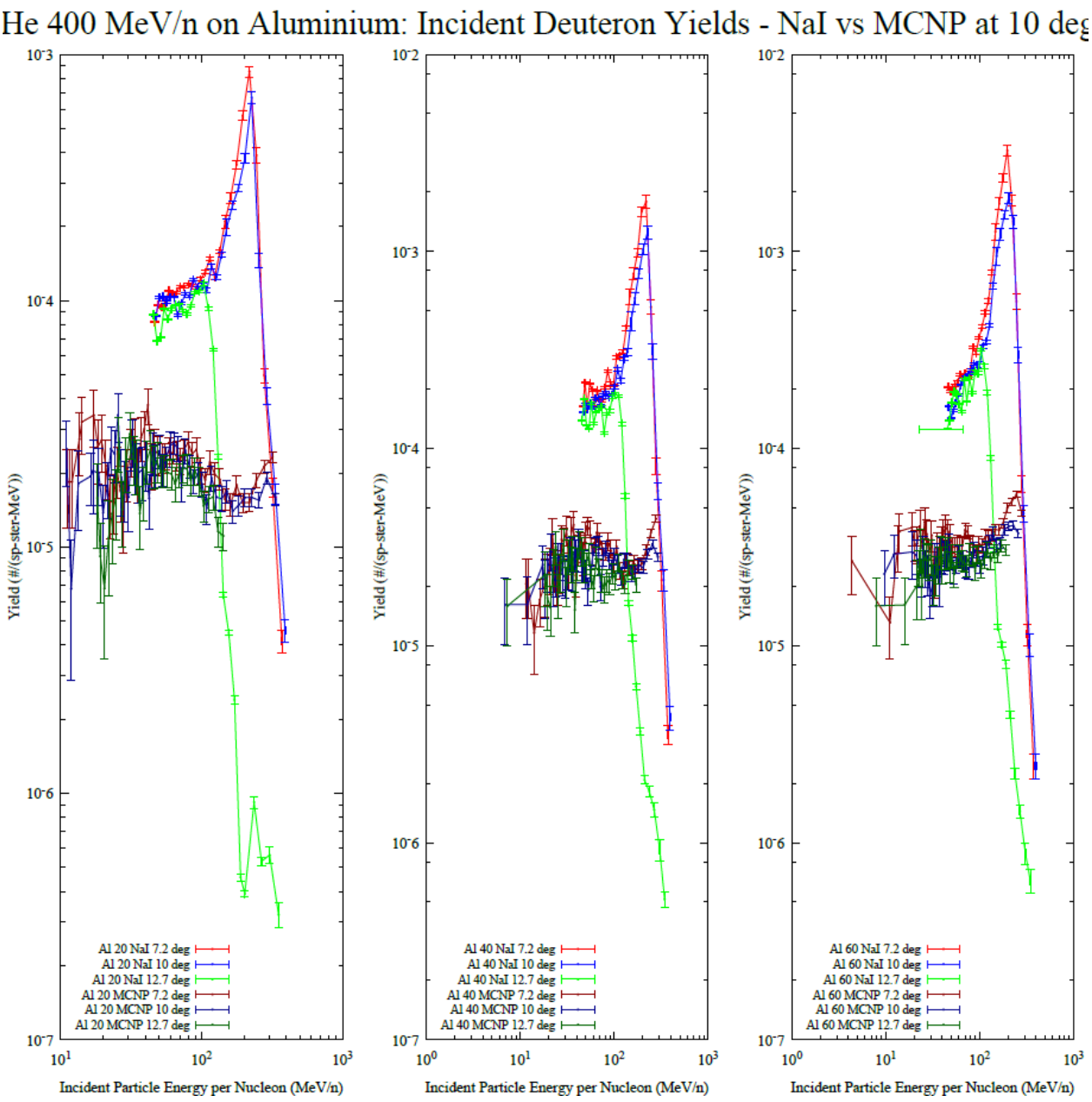


Figure C.II.3. Comparison of deuteron yields at 10 deg NaI detector array with MCNP simulated yields at same angles from 400 MeV/n helium nuclei incident upon 20 g/cm^2 (left), 40 g/cm^2 (middle), and 60 g/cm^2 (right) Aluminium shielding

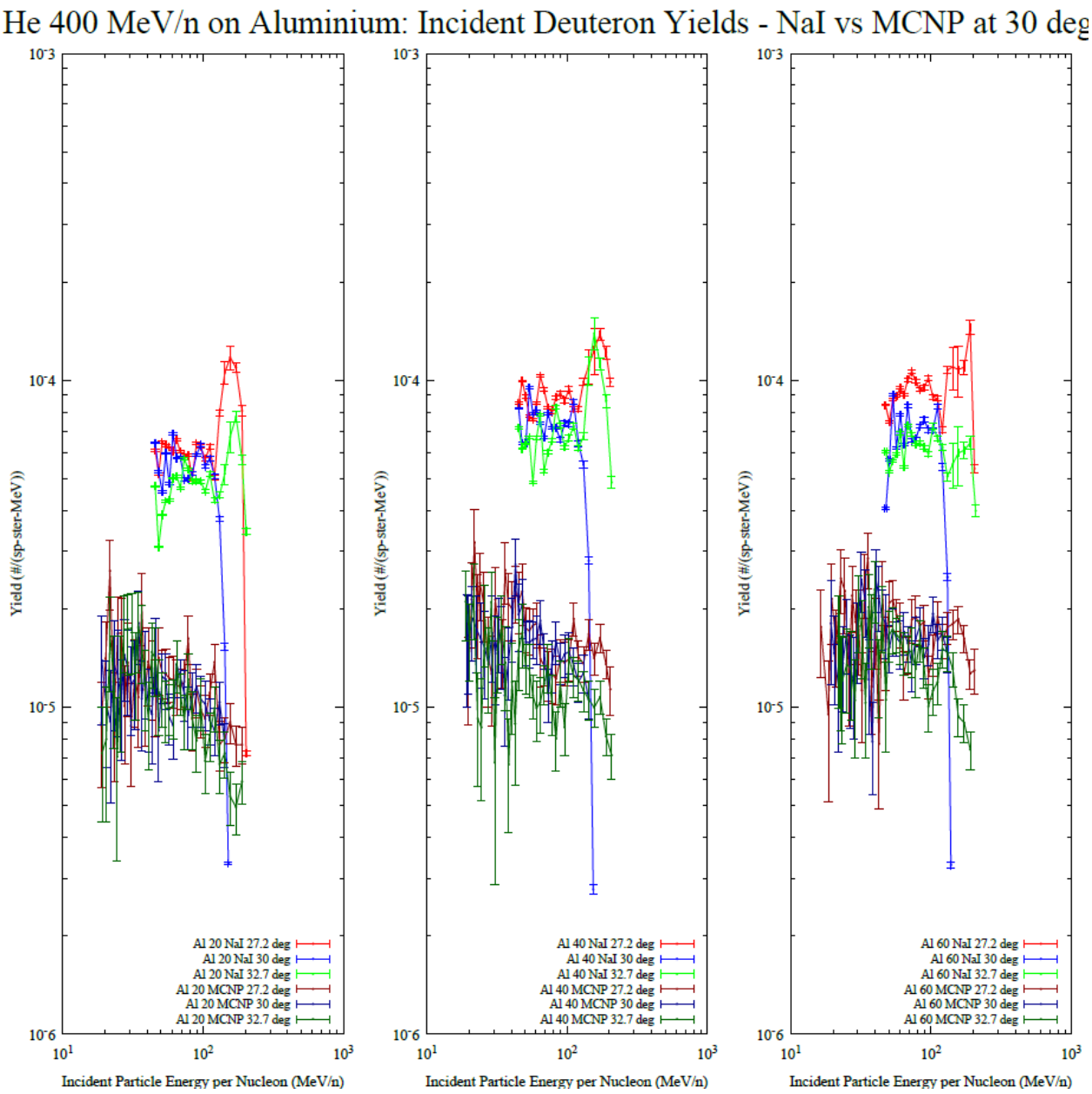


Figure C.II.4. Comparison of deuteron yields at 30 deg NaI detector array with MCNP simulated yields at same angles from 400 MeV/n helium nuclei incident upon 20 g/cm^2 (left), 40 g/cm^2 (middle), and 60 g/cm^2 (right) Aluminium shielding

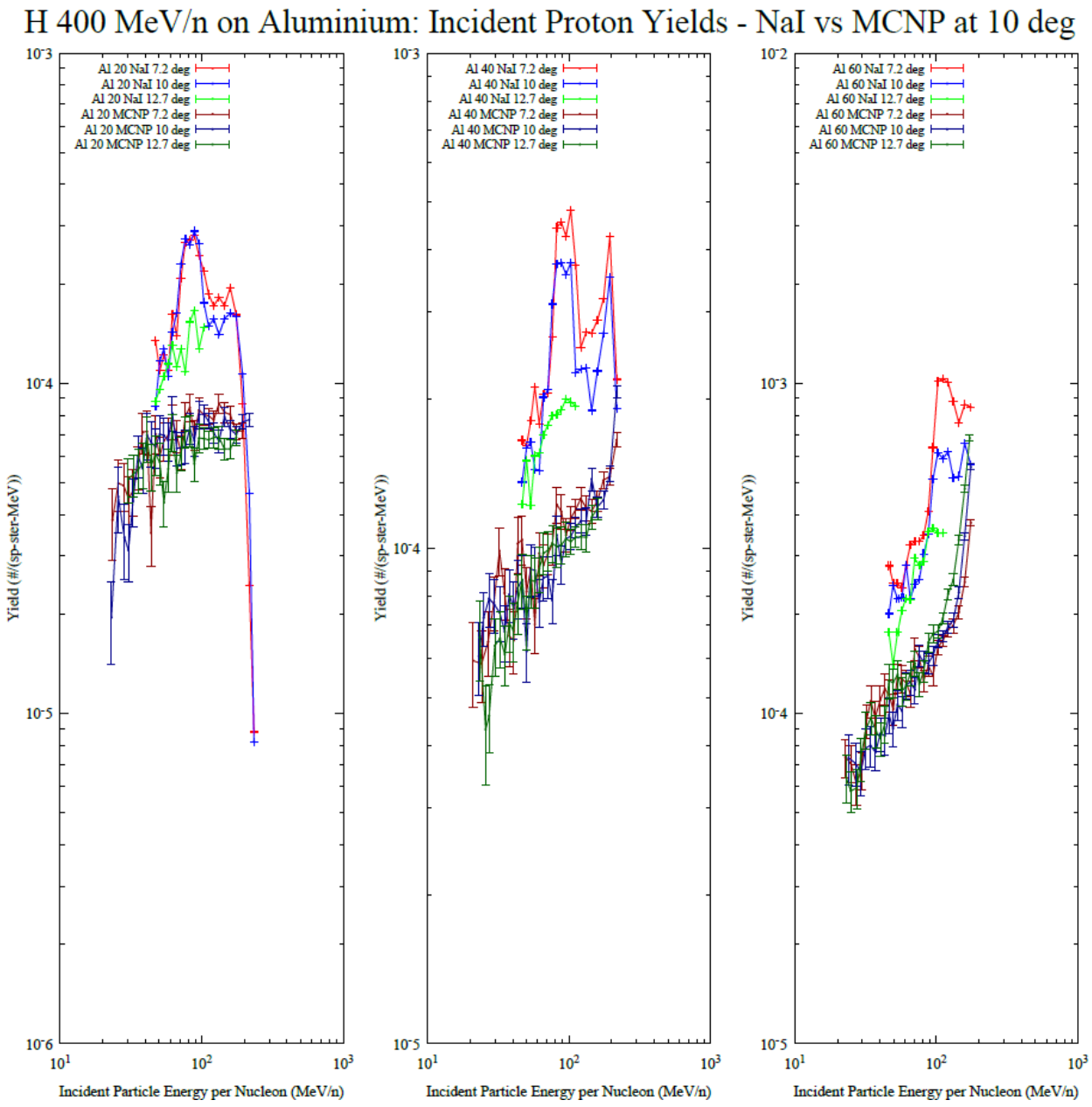


Figure C.III.1. Comparison of proton yields at 10 deg NaI detector array with MCNP simulated yields at same angles from 400 MeV/n hydrogen nuclei incident upon 20 g/cm^2 (left), 40 g/cm^2 (middle), and 60 g/cm^2 (right) Aluminium shielding

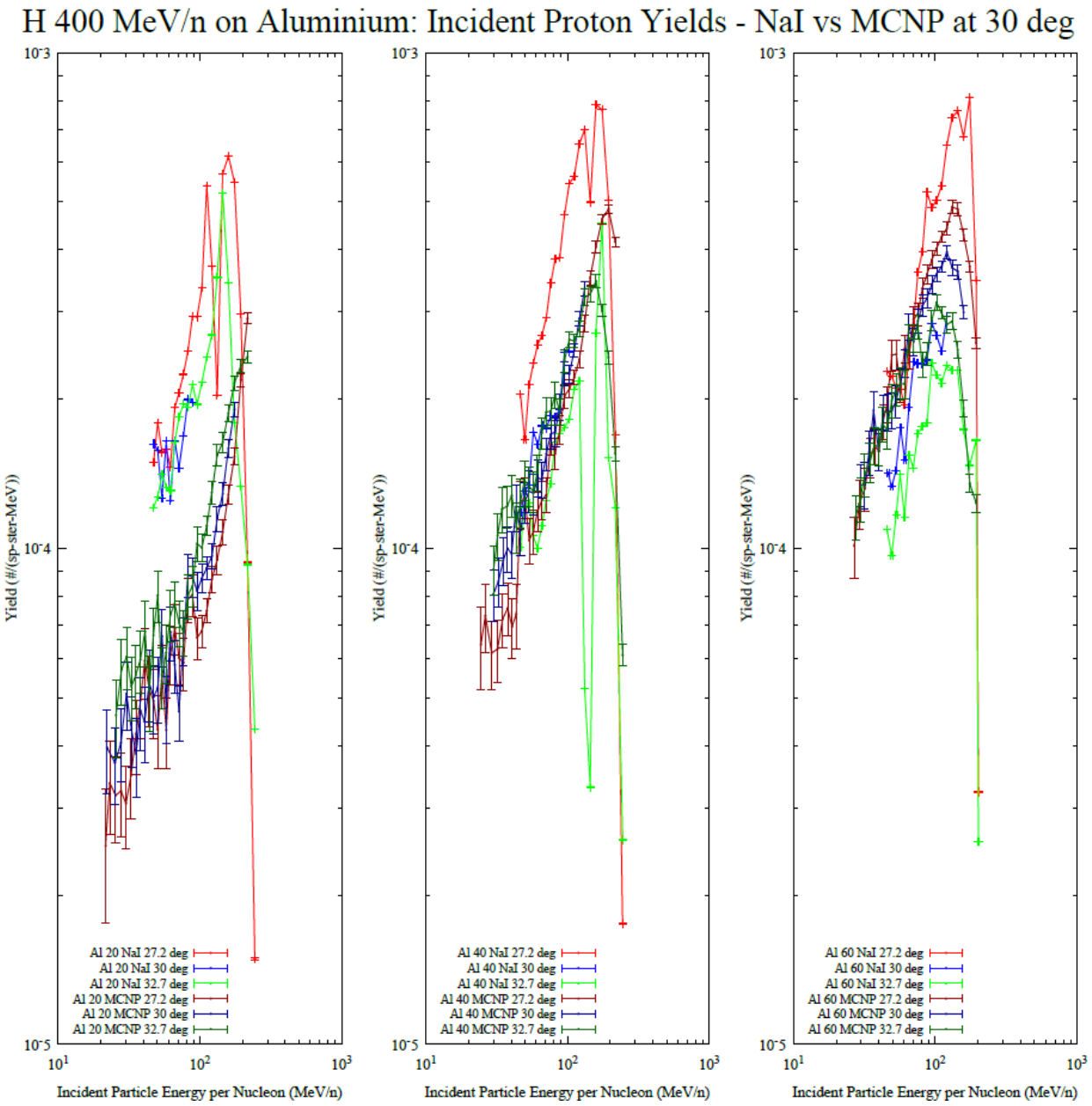


Figure C.III.2. Comparison of proton yields at 30 deg NaI detector array with MCNP simulated yields at same angles from 400 MeV/n hydrogen nuclei incident upon 20 g/cm^2 (left), 40 g/cm^2 (middle), and 60 g/cm^2 (right) Aluminium shielding

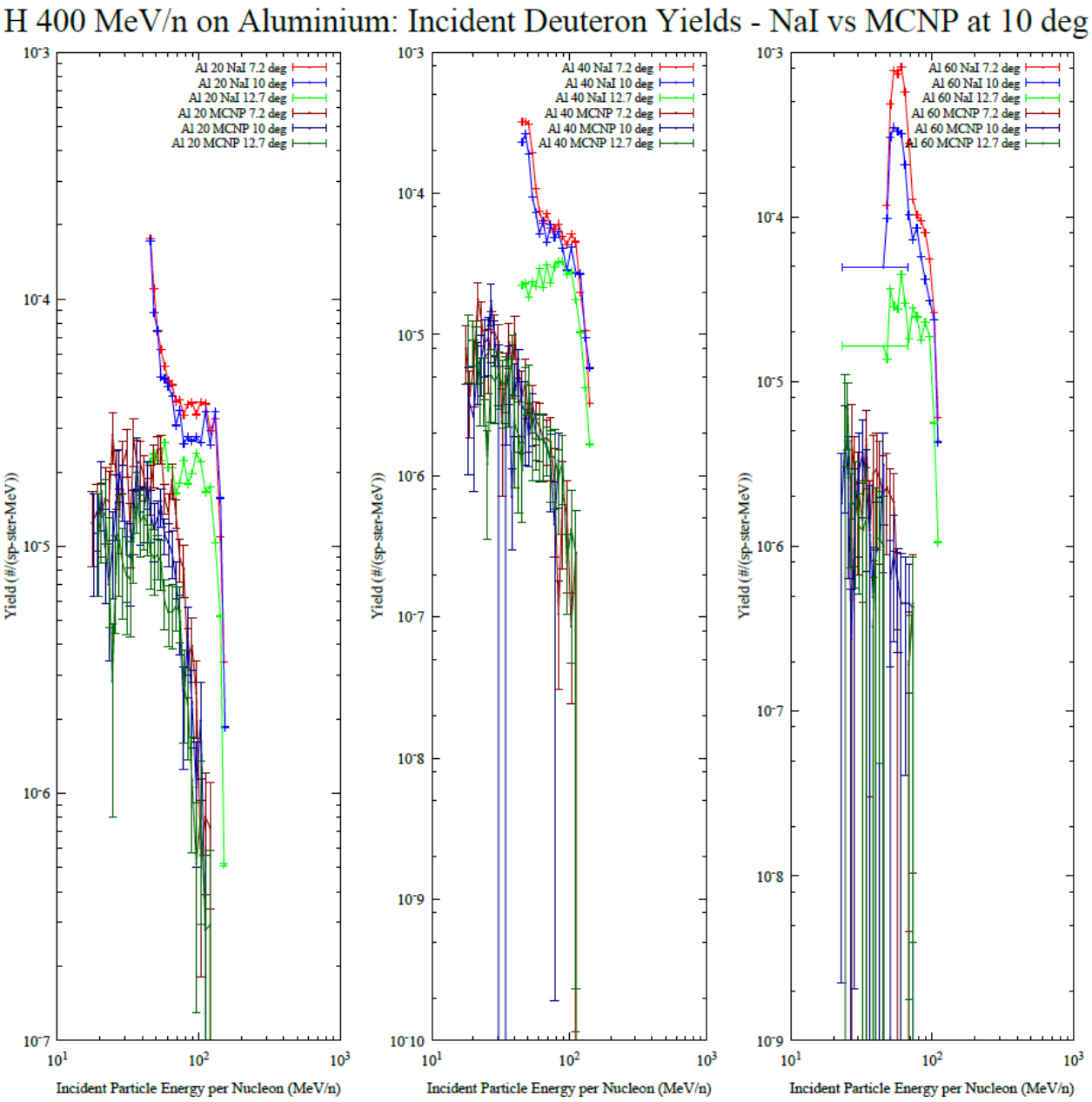


Figure C.III.3. Comparison of deuteron yields at 10 deg NaI detector array with MCNP simulated yields at same angles from 400 MeV/n hydrogen nuclei incident upon 20 g/cm^2 (left), 40 g/cm^2 (middle), and 60 g/cm^2 (right) Aluminium shielding

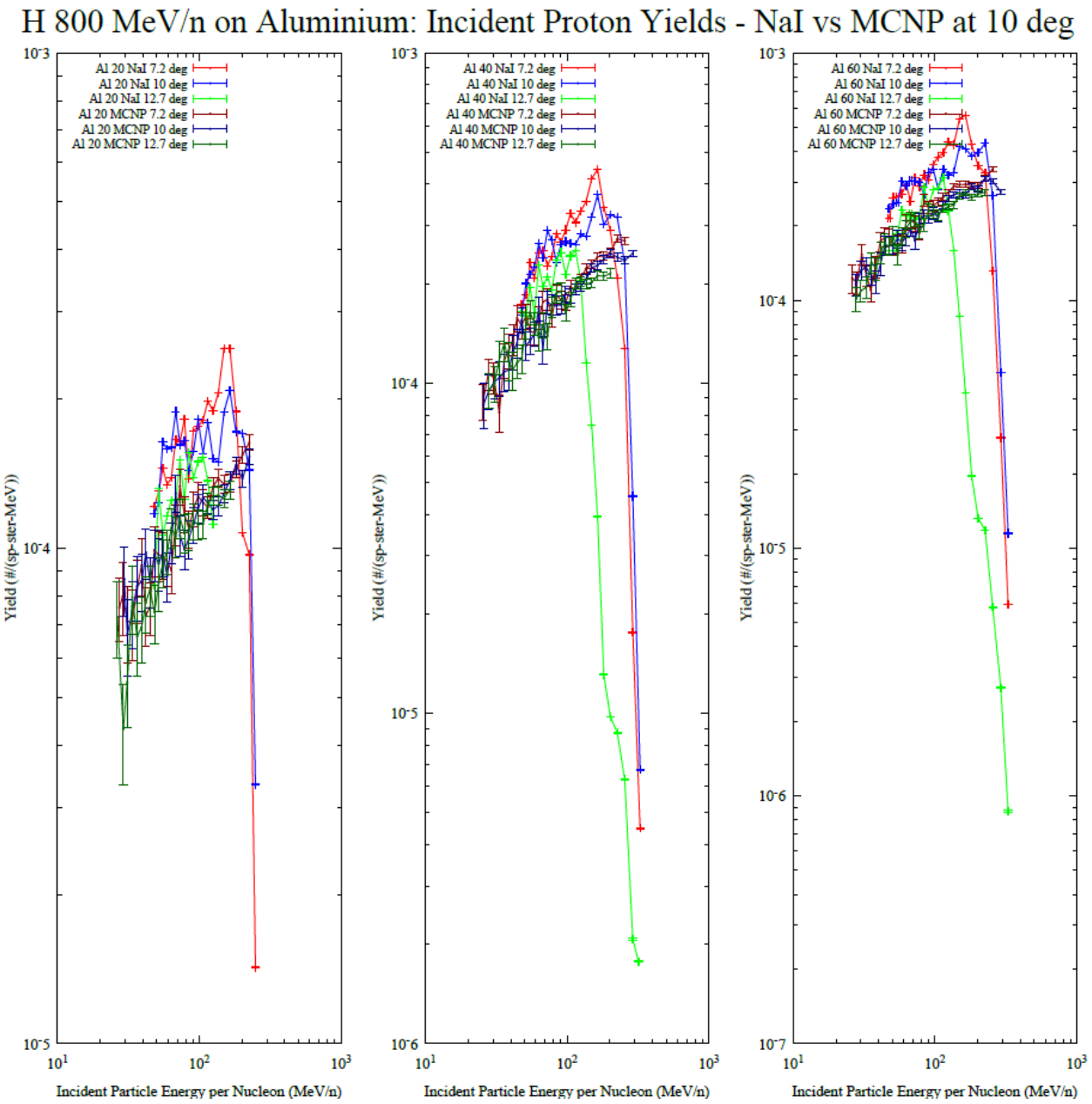


Figure C.IV.1. Comparison of proton yields at 10 deg NaI detector array with MCNP simulated yields at same angles from 800 MeV/n hydrogen nuclei incident upon 20 g/cm^2 (left), 40 g/cm^2 (middle), and 60 g/cm^2 (right) Aluminium shielding

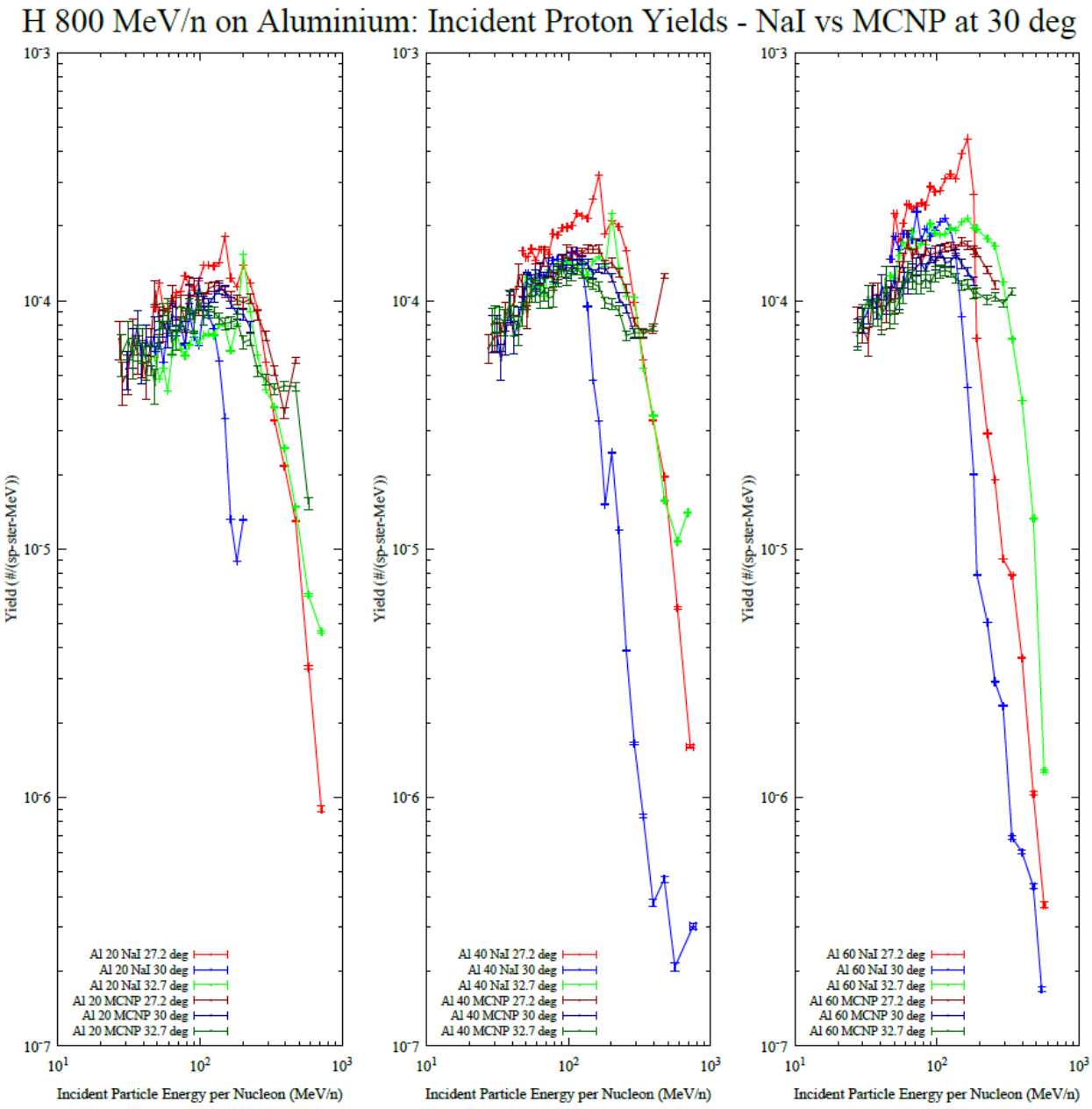


Figure C.IV.2. Comparison of proton yields at 30 deg NaI detector array with MCNP simulated yields at same angles from 800 MeV/n hydrogen nuclei incident upon 20 g/cm^2 (left), 40 g/cm^2 (middle), and 60 g/cm^2 (right) Aluminium shielding

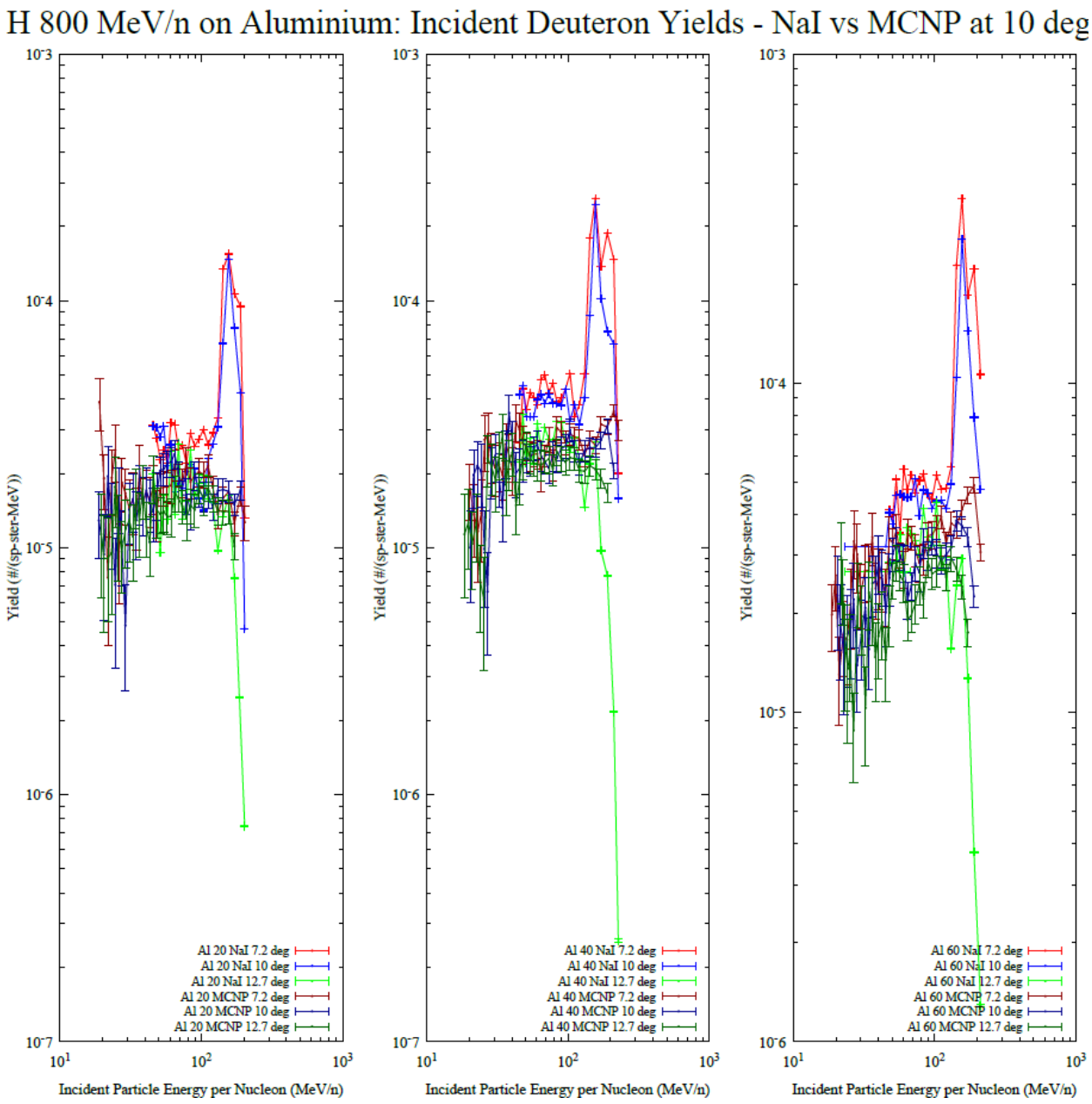


Figure C.IV.3. Comparison of deuteron yields at 10 deg NaI detector array with MCNP simulated yields at same angles from 800 MeV/n hydrogen nuclei incident upon 20 g/cm^2 (left), 40 g/cm^2 (middle), and 60 g/cm^2 (right) Aluminium shielding

APPENDIX D

ADDITIONAL OLS COMPARISONS

The plots presented in Section 5.5.3 showed comparisons between the experimental data from the sodium iodide (NaI) detectors and previously completed work from the organic liquid scintillators (OLS) data sets. The figures presented here show the remaining comparisons.

Figures D.I.1-5 – Fe 800 MeV/n

Figures D.II.1-5 – He 400 MeV/n

Figures D.III.1-2 – H 400 MeV/n

Figures D.IV.1-2 – H 800 MeV/n

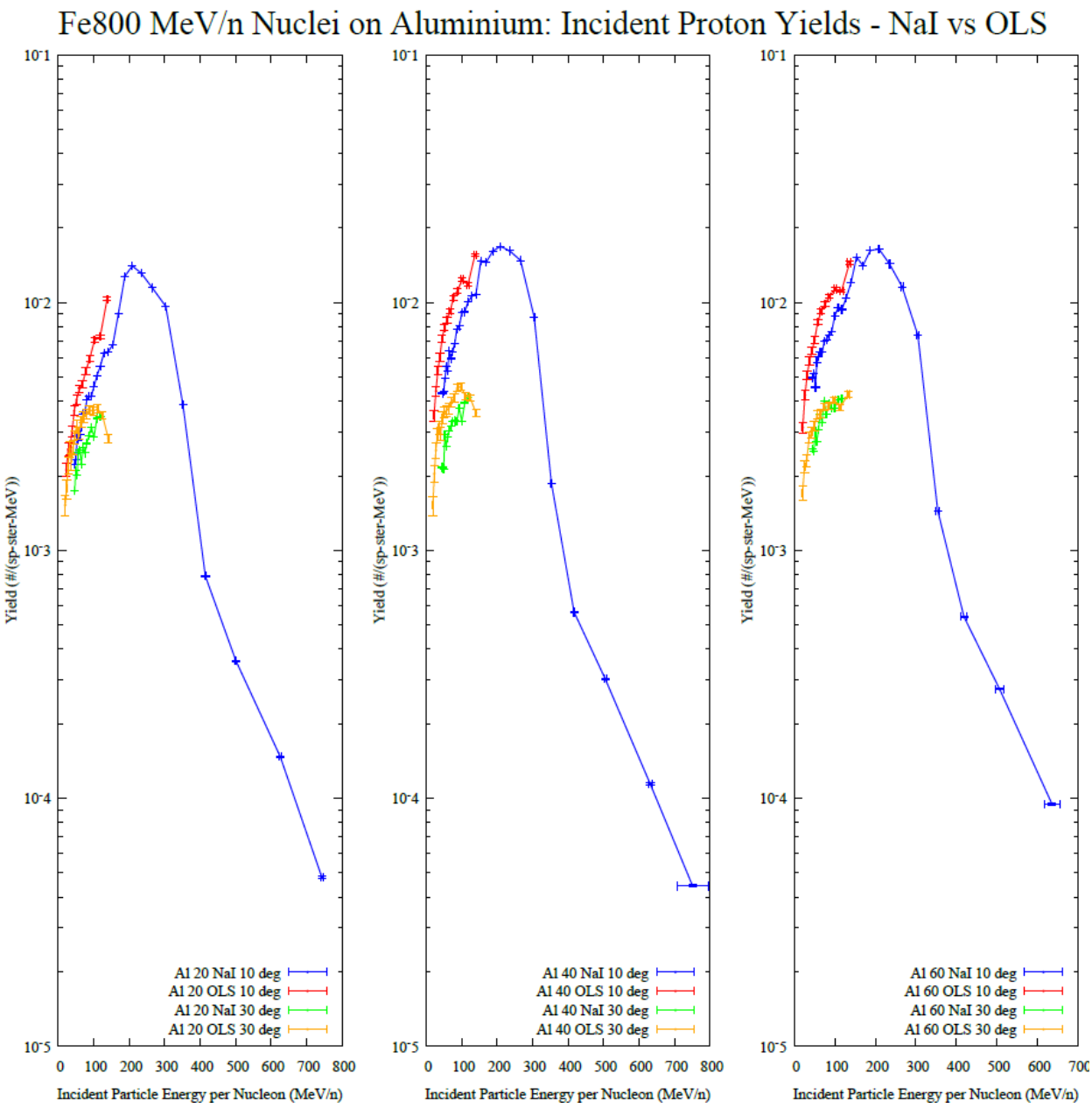


Figure D.I.1. Proton Double Differential Yields as a function of incoming energy per nucleon from the 800 MeV/n Iron beam on the 20g/cm^2 (left), 40 g/cm^2 (middle), and 60 g/cm^2 (right) Aluminium shielding thicknesses detected at 10° and 30° NaI and OLS detectors

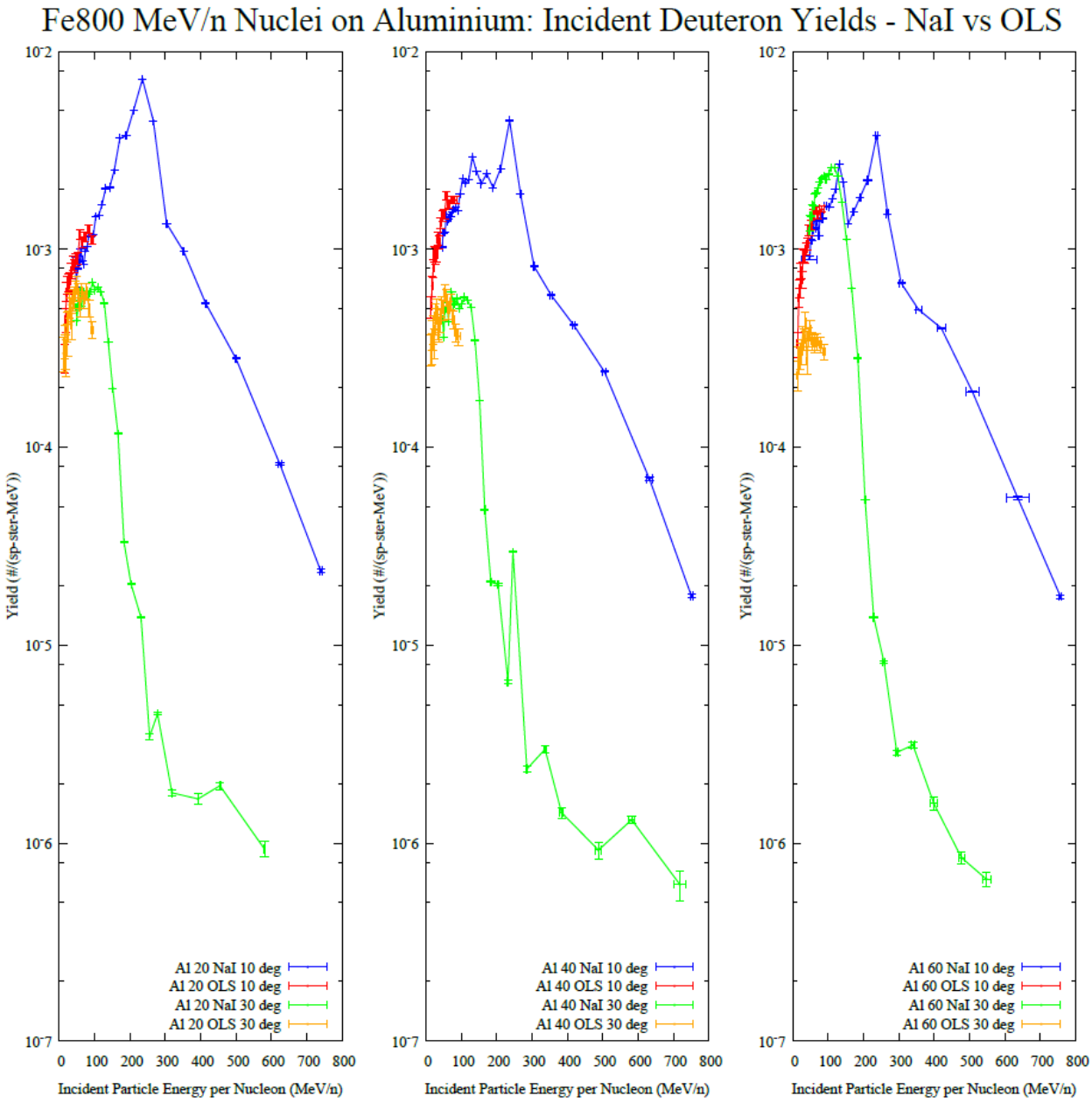


Figure D.I.2. Deuteron Double Differential Yields as a function of incoming energy per nucleon from the 800 MeV/n Iron beam on the 20g/cm^2 (left), 40 g/cm^2 (middle), and 60 g/cm^2 (right) Aluminium shielding thicknesses detected at 10° and 30° NaI and OLS detectors

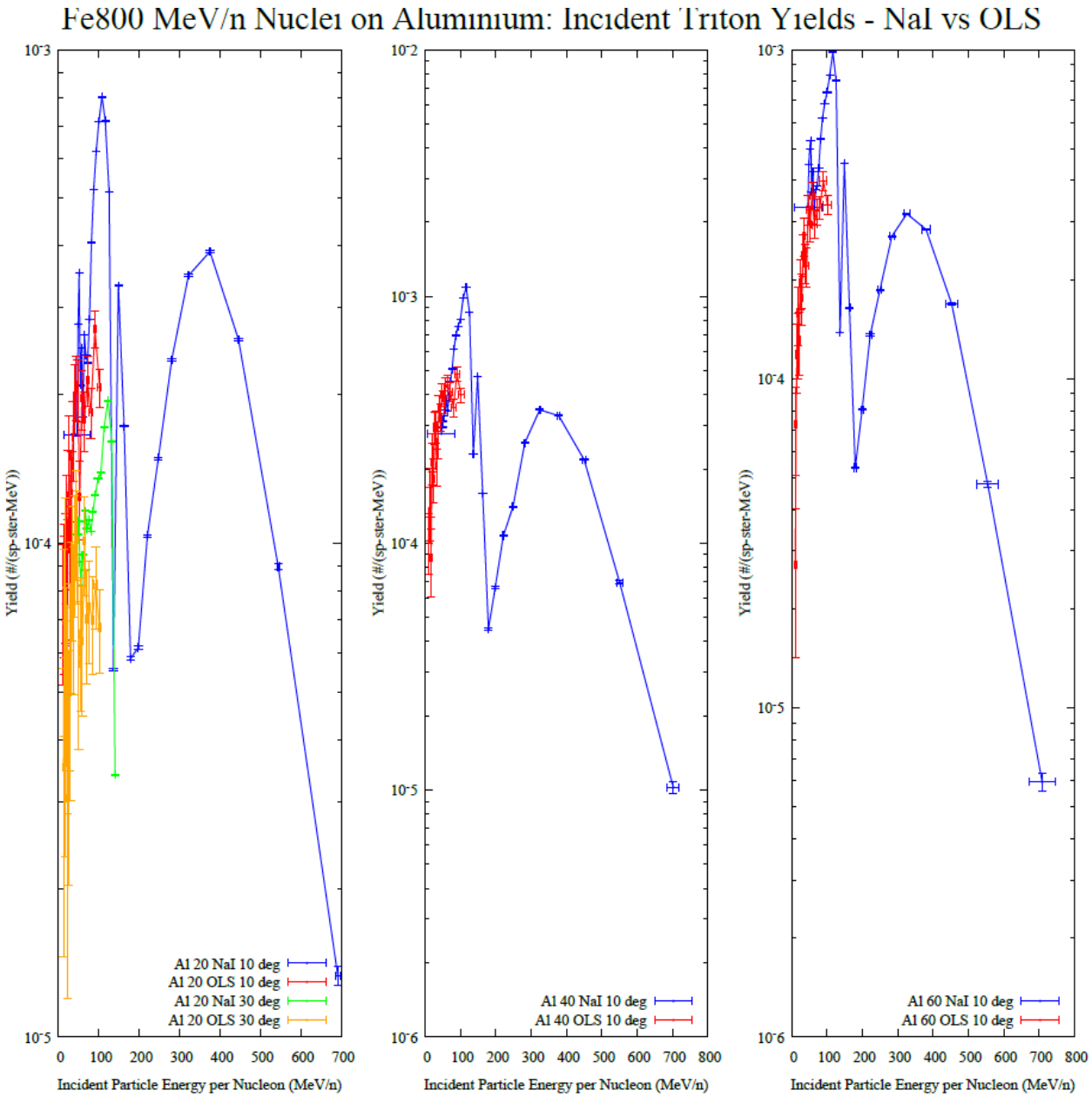


Figure D.I.3. Triton Double Differential Yields as a function of incoming energy per nucleon from the 800 MeV/n Iron beam on the 20g/cm^2 (left), 40 g/cm^2 (middle), and 60 g/cm^2 (right) Aluminium shielding thicknesses detected at 10° and 30° NaI and OLS detectors

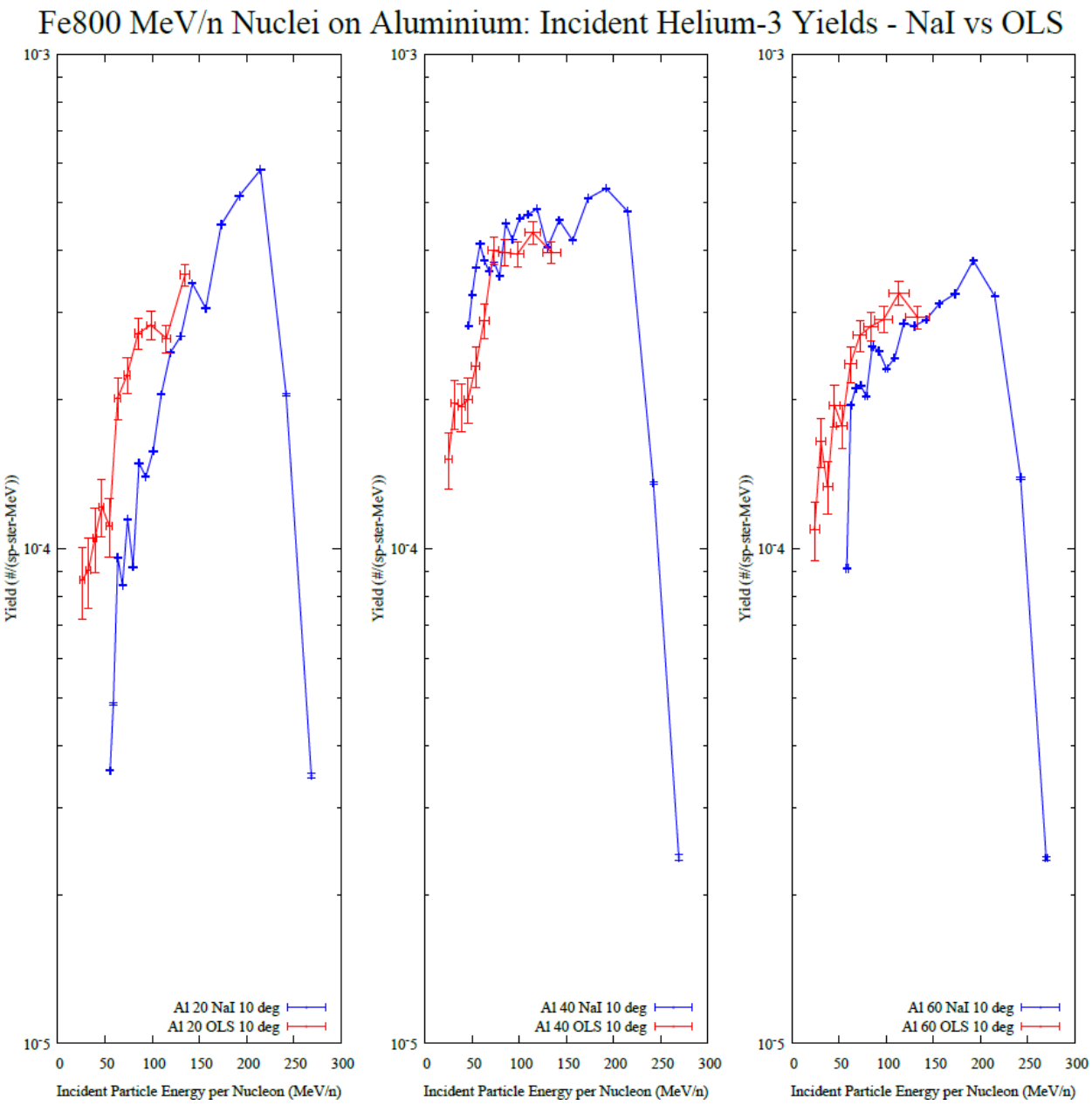


Figure D.I.4. Helion Double Differential Yields as a function of incoming energy per nucleon from the 800 MeV/n Iron beam on the 20g/cm^2 (left), 40 g/cm^2 (middle), and 60 g/cm^2 (right) Aluminium shielding thicknesses detected at 10° and 30° NaI and OLS detectors

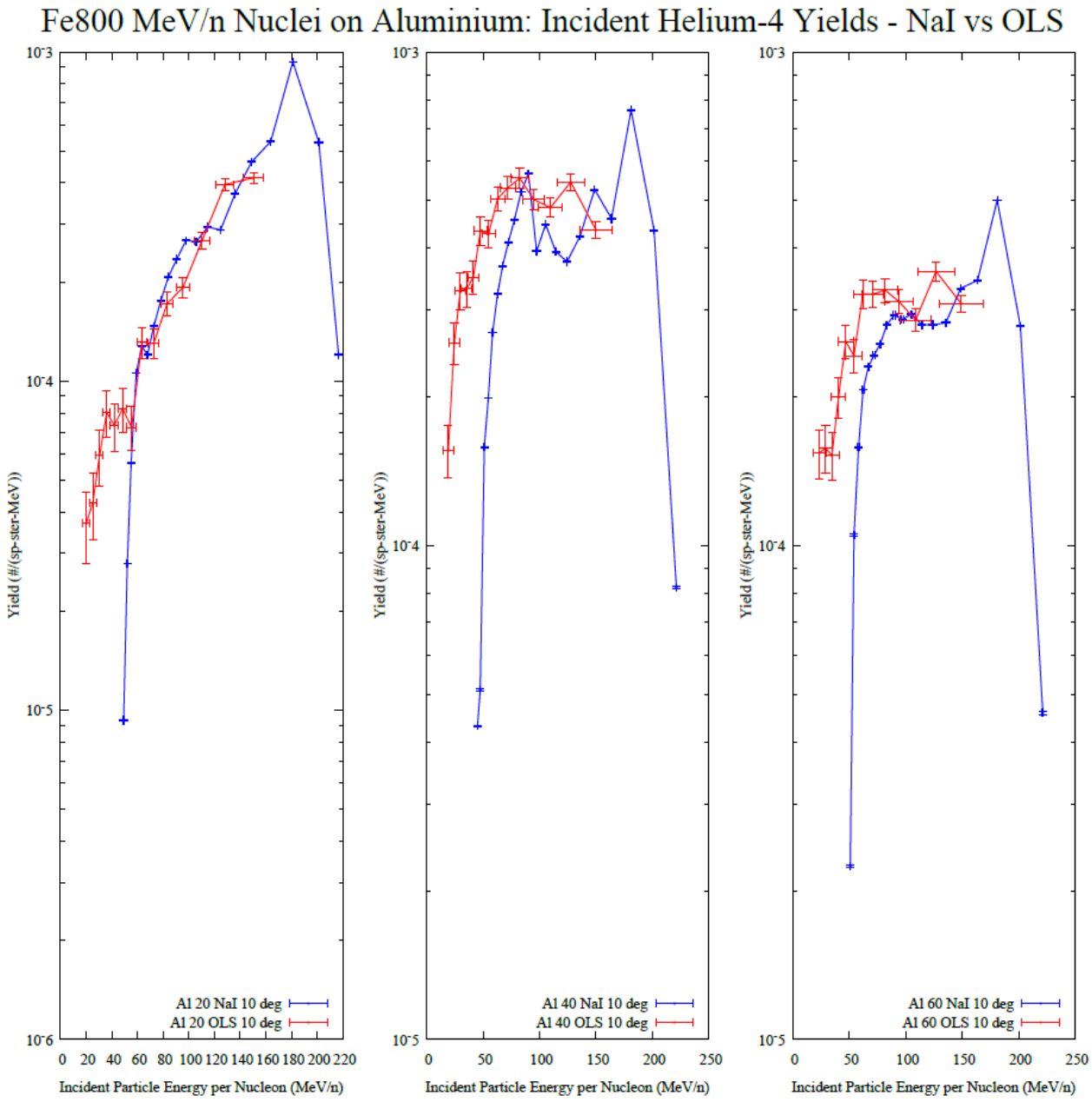


Figure D.I.5. Alpha Double Differential Yields as a function of incoming energy per nucleon from the 800 MeV/n Iron beam on the 20g/cm^2 (left), 40 g/cm^2 (middle), and 60 g/cm^2 (right) Aluminium shielding thicknesses detected at 10° and 30° NaI and OLS detectors

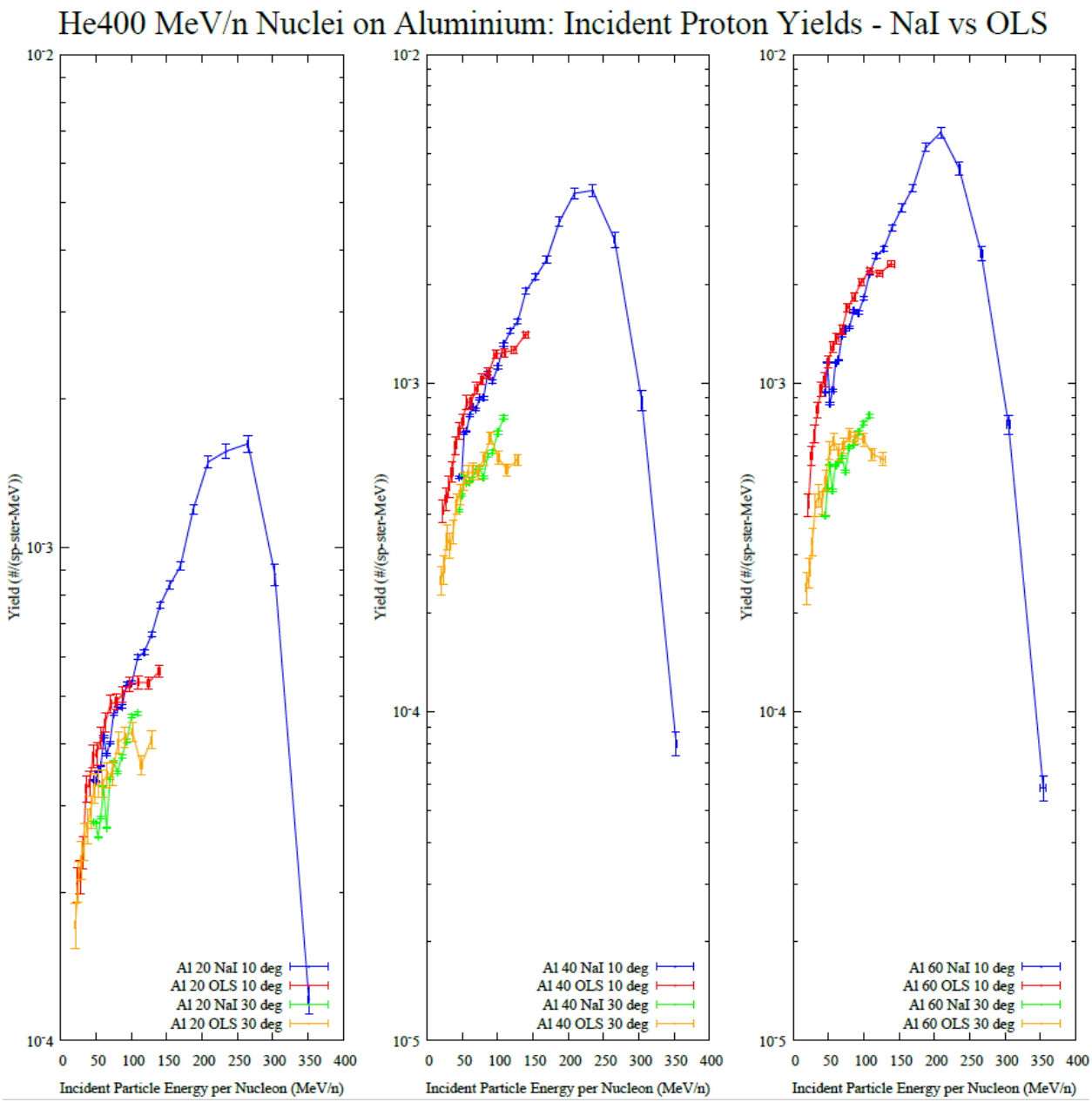


Figure D.II.1. Proton Double Differential Yields as a function of incoming energy per nucleon from the 400 MeV/n Helium beam on the 20g/cm^2 (left), 40 g/cm^2 (middle), and 60 g/cm^2 (right) Aluminium shielding thicknesses detected at 10° and 30° NaI and OLS detectors

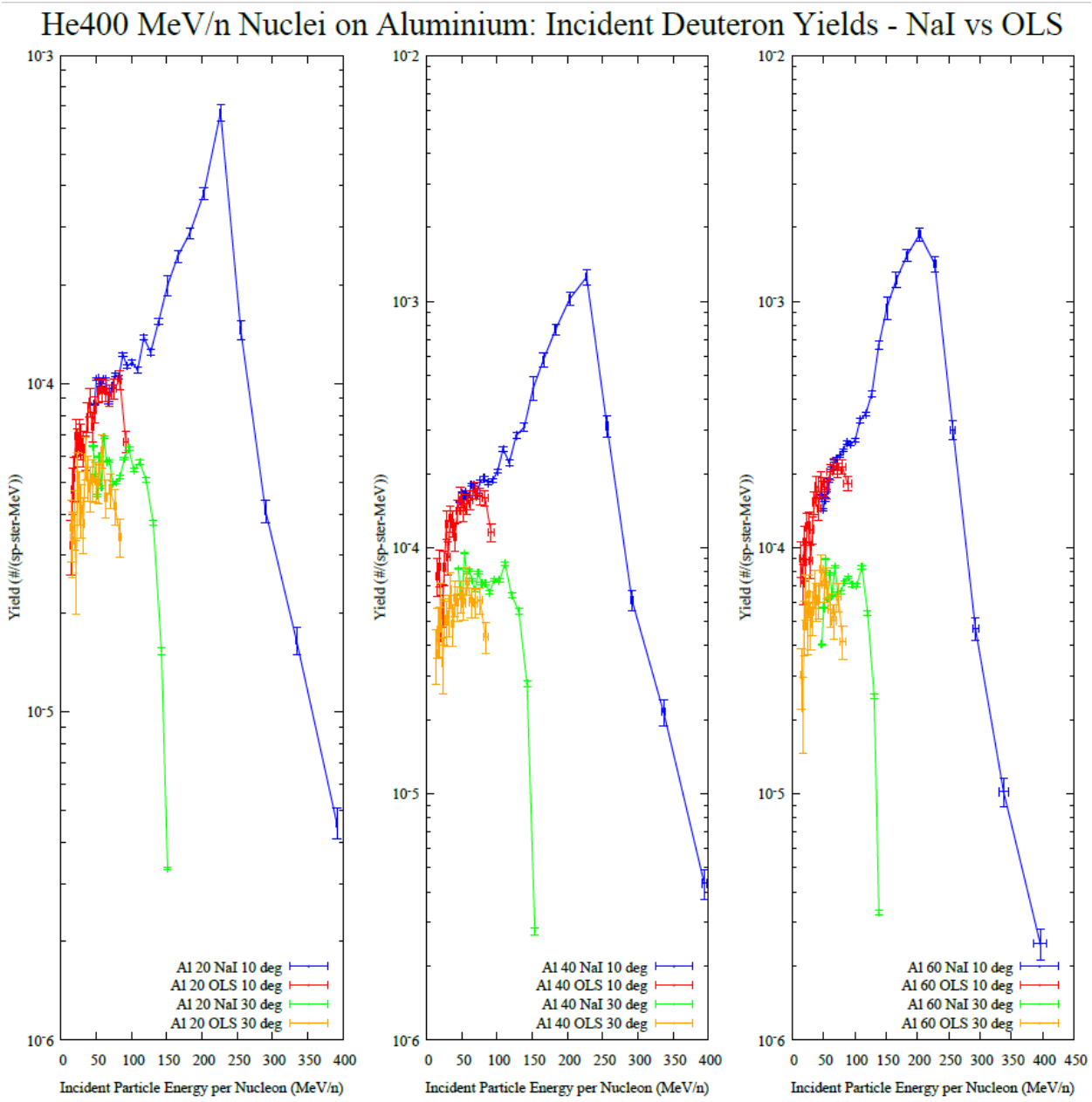


Figure D.II.2. Deuteron Double Differential Yields as a function of incoming energy per nucleon from the 400 MeV/n Helium beam on the 20g/cm^2 (left), 40 g/cm^2 (middle), and 60 g/cm^2 (right) Aluminium shielding thicknesses detected at 10° and 30° NaI and OLS detectors

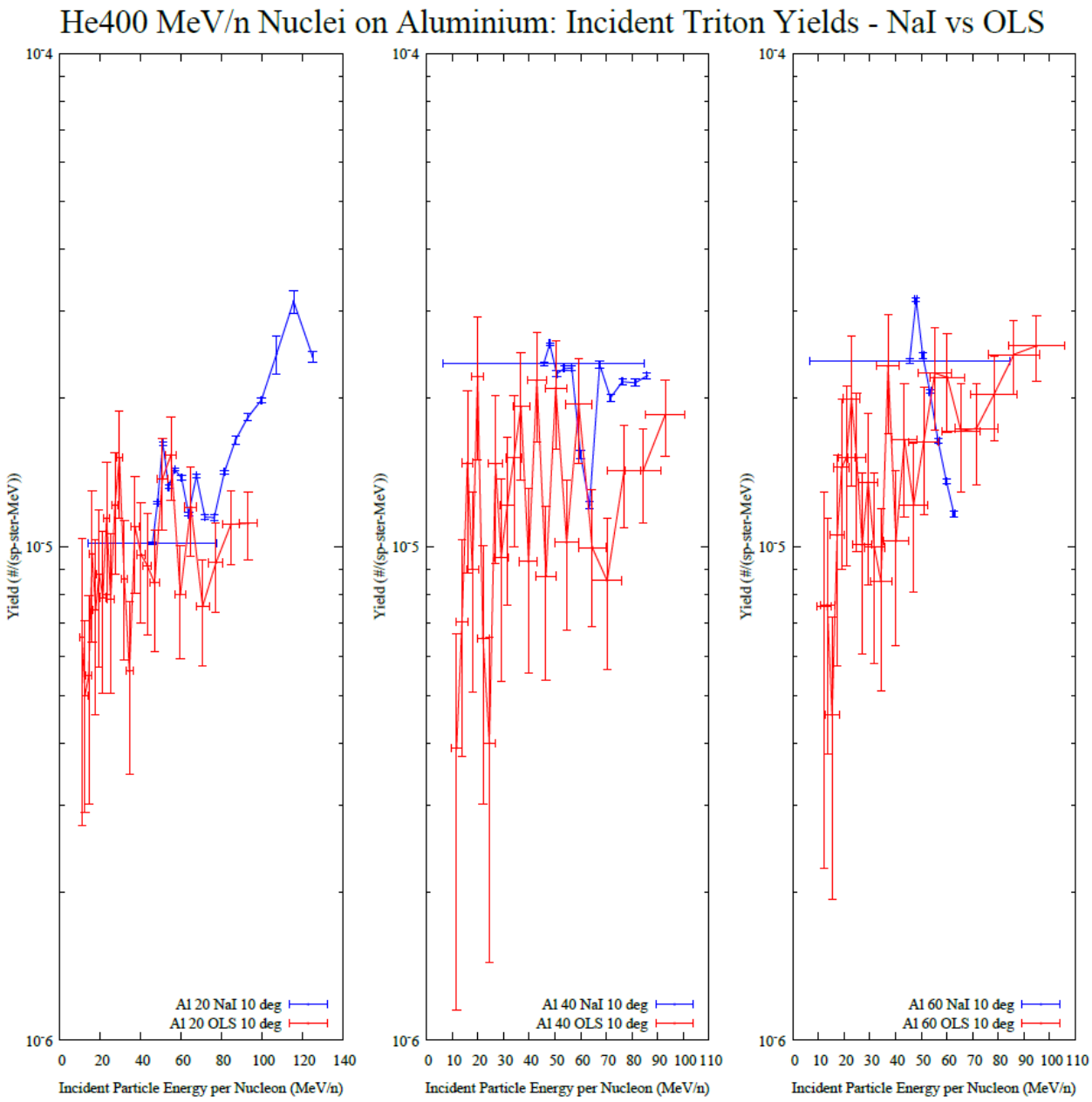


Figure D.II.3. Triton Double Differential Yields as a function of incoming energy per nucleon from the 400 MeV/n Helium beam on the 20g/cm^2 (left), 40 g/cm^2 (middle), and 60 g/cm^2 (right) Aluminium shielding thicknesses detected at 10° and 30° NaI and OLS detectors

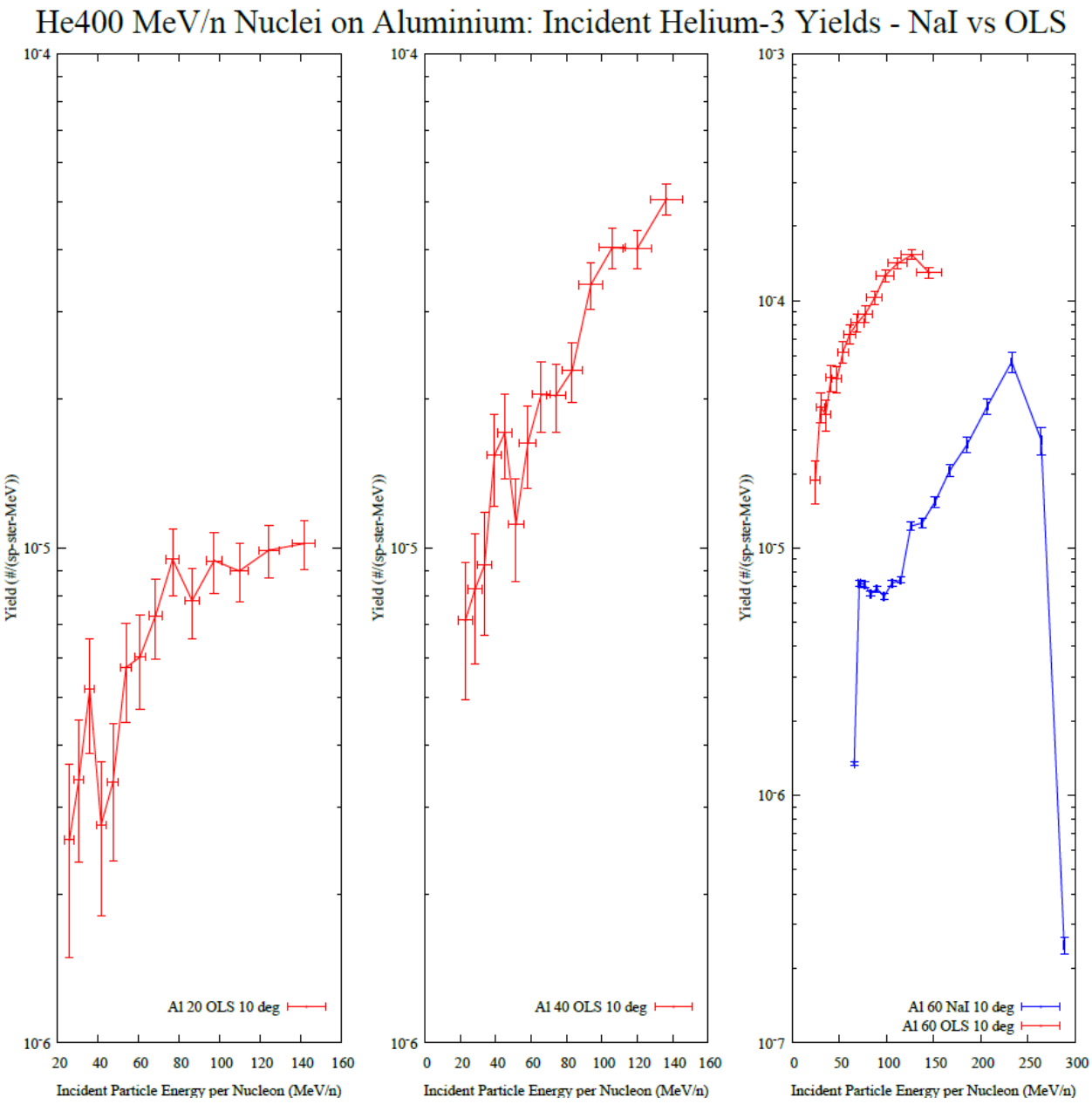


Figure D.II.4. Helion Double Differential Yields as a function of incoming energy per nucleon from the 400 MeV/n Helium beam on the 20g/cm^2 (left), 40 g/cm^2 (middle), and 60 g/cm^2 (right) Aluminium shielding thicknesses detected at 10° and 30° NaI and OLS detectors

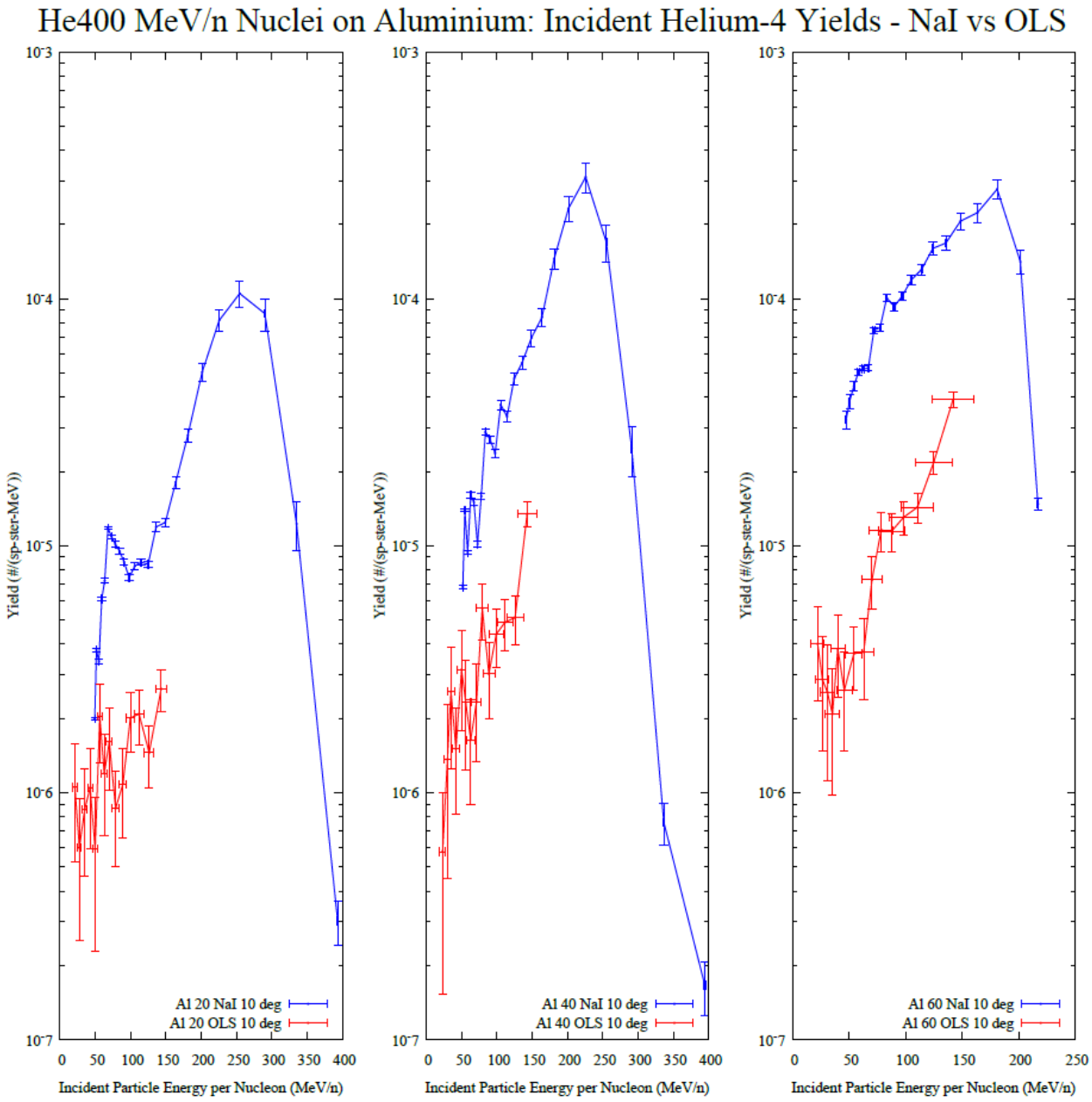


Figure D.II.5. Alpha Double Differential Yields as a function of incoming energy per nucleon from the 400 MeV/n Helium beam on the 20g/cm^2 (left), 40 g/cm^2 (middle), and 60 g/cm^2 (right) Aluminium shielding thicknesses detected at 10° and 30° NaI and OLS detectors

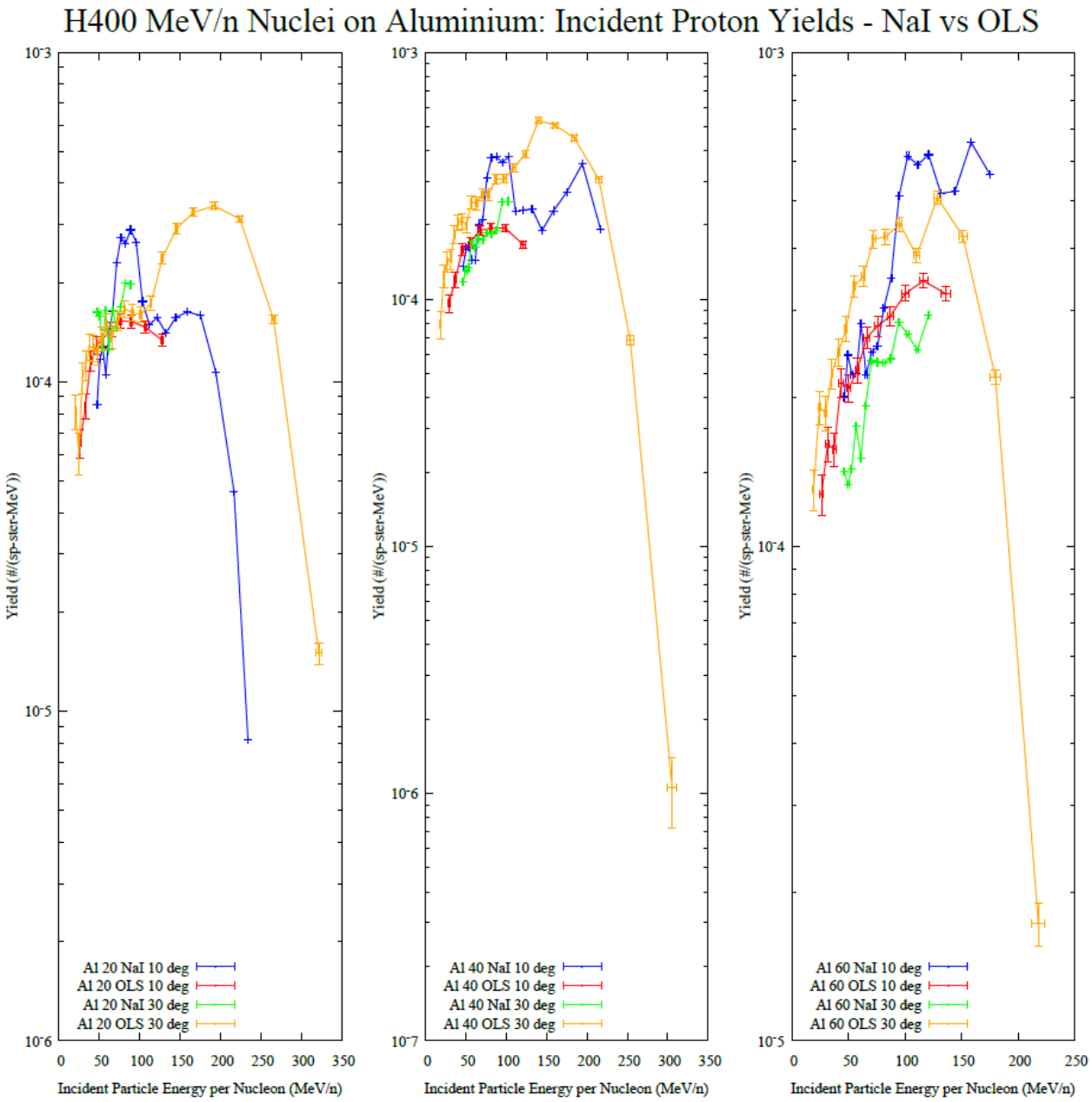


Figure D.III.1. Proton Double Differential Yields as a function of incoming energy per nucleon from the 400 MeV/n Hydrogen beam on the 20g/cm^2 (left), 40 g/cm^2 (middle), and 60 g/cm^2 (right) Aluminium shielding thicknesses detected at 10° and 30° NaI and OLS detectors

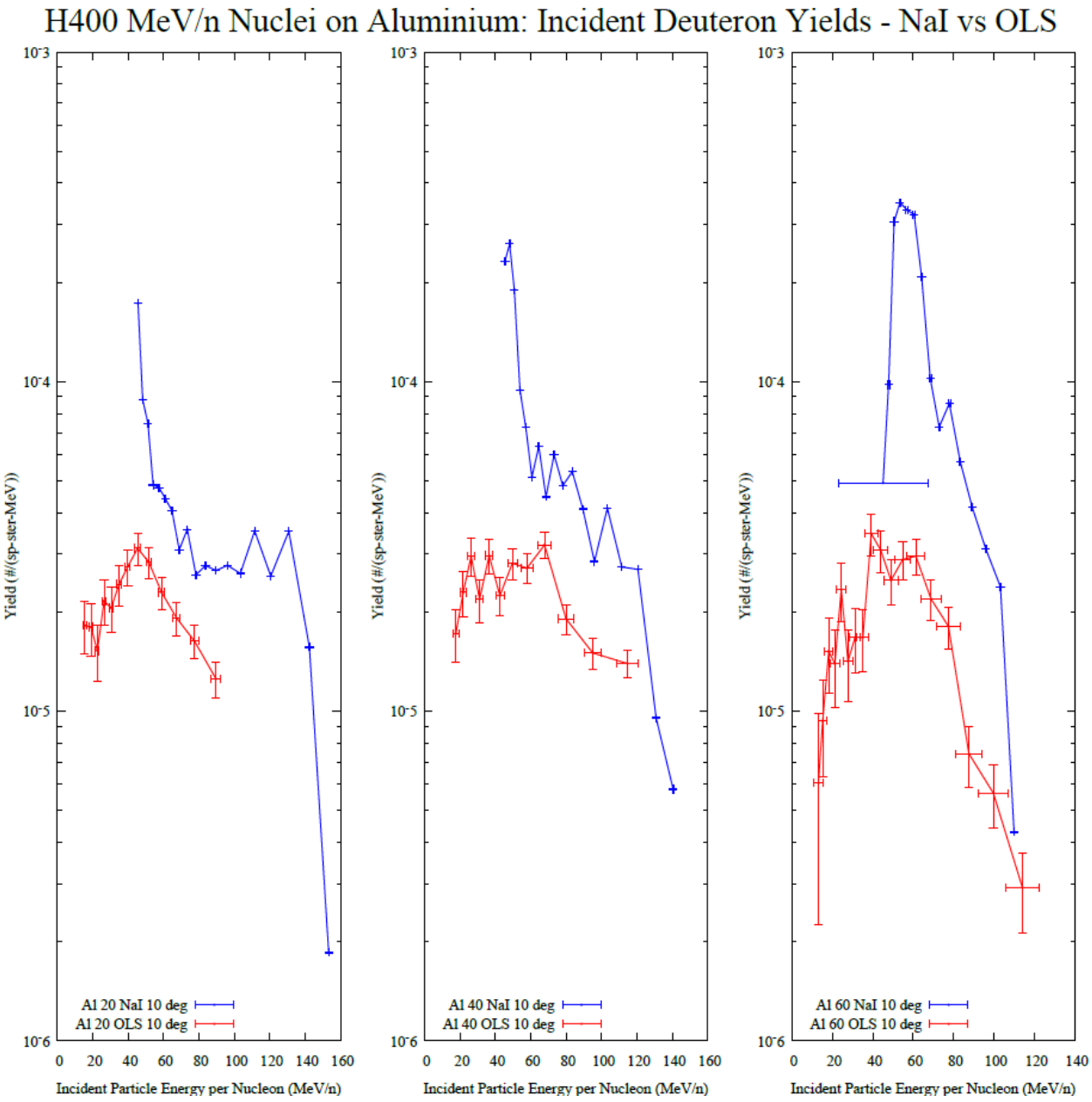


Figure D.III.2. Deuteron Double Differential Yields as a function of incoming energy per nucleon from the 400 MeV/n Hydrogen beam on the 20g/cm^2 (left), 40 g/cm^2 (middle), and 60 g/cm^2 (right) Aluminium shielding thicknesses detected at 10° and 30° NaI and OLS detectors

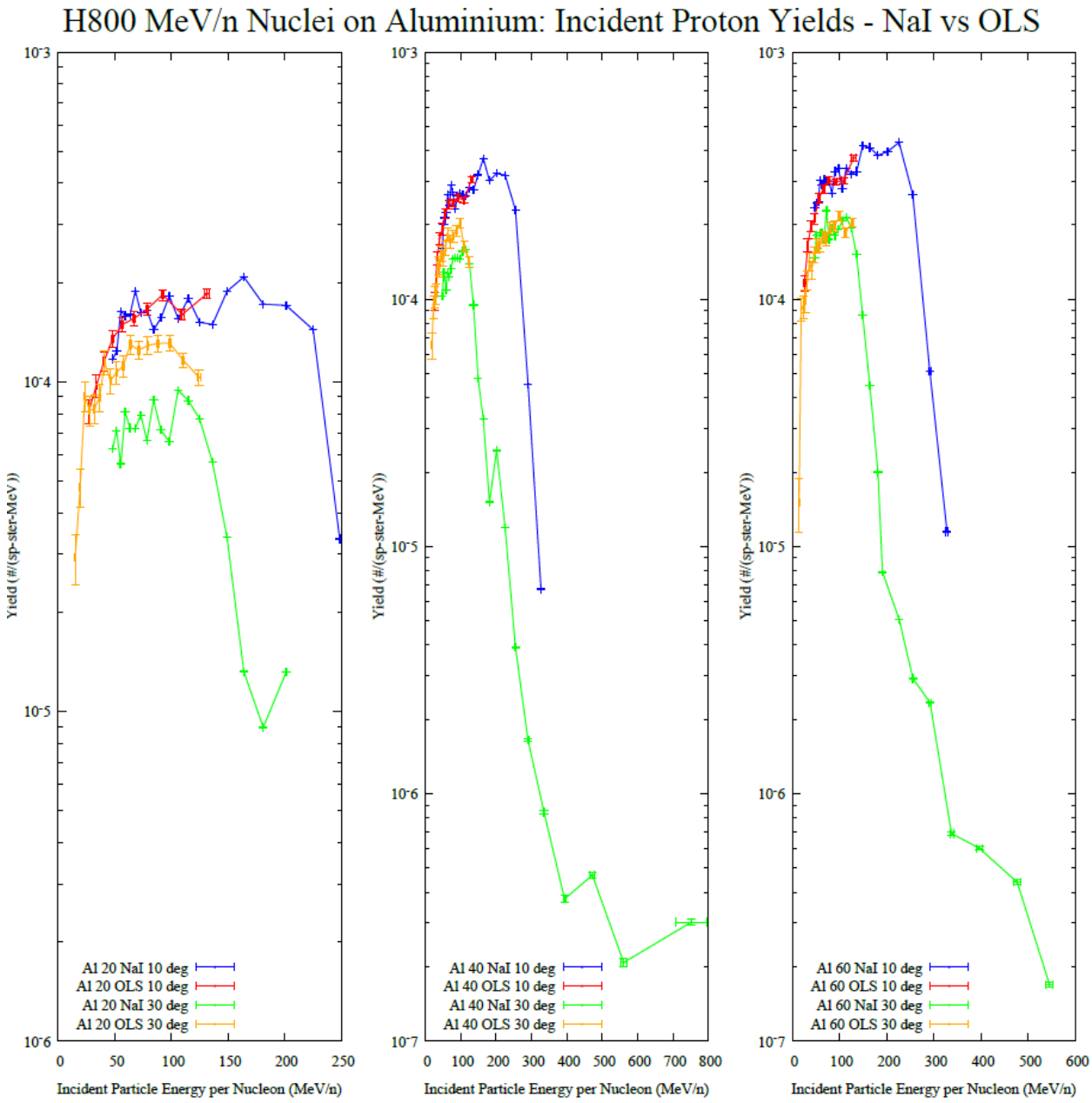


Figure D.IV.1. Proton Double Differential Yields as a function of incoming energy per nucleon from the 800 MeV/n Hydrogen beam on the 20g/cm^2 (left), 40 g/cm^2 (middle), and 60 g/cm^2 (right) Aluminium shielding thicknesses detected at 10° and 30° NaI and OLS detectors

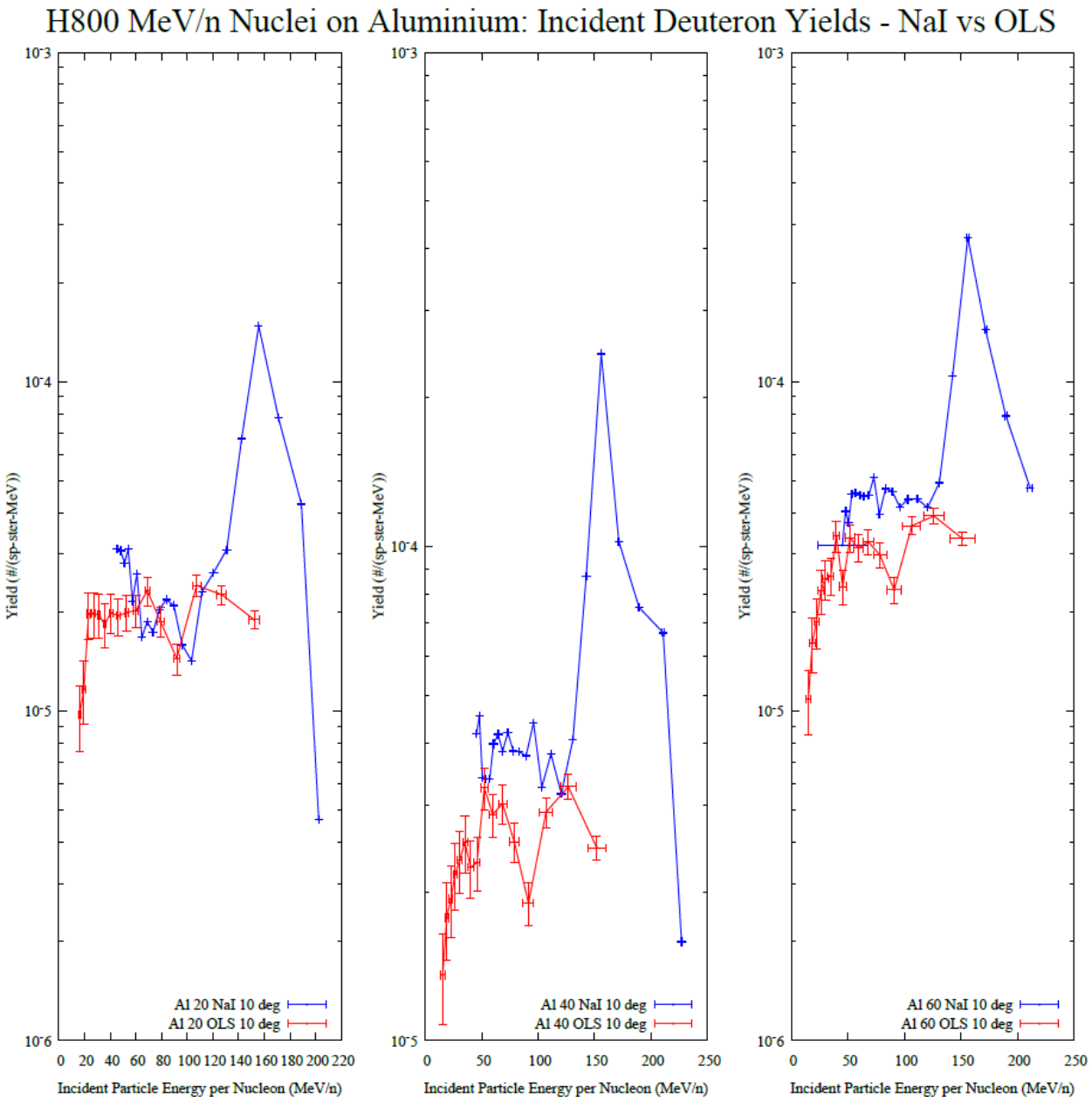


Figure D.IV.2. Deuteron Double Differential Yields as a function of incoming energy per nucleon from the 800 MeV/n Hydrogen beam on the 20g/cm^2 (left), 40 g/cm^2 (middle), and 60 g/cm^2 (right) Aluminium shielding thicknesses detected at 10° and 30° NaI and OLS detectors

VITA

Ashwin Paul Srikrishna is from Raleigh, NC. He graduated from North Carolina State University with a B.S. in Chemical and Biomolecular Engineering with a focus on nanoscience and a minor in Nuclear Engineering in 2013. He moved to Knoxville to attend the University of Tennessee to work on research related to nuclear engineering fields for the purpose of achieving a Ph.D. in the field. In addition to the research presented here, he also worked on the development of a post-processing code for MCNP for the sake of Inverse Kinematics calculations and simulations. After graduation, he hopes to continue working in radiation transport and detection, especially as it relates to space exploration.